



# *University of* **HUDDERSFIELD**

## **University of Huddersfield Repository**

Agater, Irena Barbara

Applications of permanganate chemiluminescence to the analysis of food components

### **Original Citation**

Agater, Irena Barbara (1999) Applications of permanganate chemiluminescence to the analysis of food components. Doctoral thesis, University of Huddersfield.

This version is available at <http://eprints.hud.ac.uk/id/eprint/5955/>

The University Repository is a digital collection of the research output of the University, available on Open Access. Copyright and Moral Rights for the items on this site are retained by the individual author and/or other copyright owners. Users may access full items free of charge; copies of full text items generally can be reproduced, displayed or performed and given to third parties in any format or medium for personal research or study, educational or not-for-profit purposes without prior permission or charge, provided:

- The authors, title and full bibliographic details is credited in any copy;
- A hyperlink and/or URL is included for the original metadata page; and
- The content is not changed in any way.

For more information, including our policy and submission procedure, please contact the Repository Team at: [E.mailbox@hud.ac.uk](mailto:E.mailbox@hud.ac.uk).

<http://eprints.hud.ac.uk/>

# **Applications of Permanganate Chemiluminescence to the Analysis of Food Components**

By

Irena Barbara Agater B.Sc. CChem MRSC

A thesis submitted to the University of Huddersfield in partial fulfilment of the requirement for the award of Doctor of Philosophy

Department of Chemical and Biological Sciences  
The University of Huddersfield  
Queensgate  
Huddersfield  
West Yorkshire  
HD1 3DH

January 1999



# Acknowledgement

I would like to thank the academic and technical staff of the Department of Chemical and Biological Sciences for their help during this work. In particular I am grateful to my Director of Studies, Dr Roger Jewsbury, for his expertise, encouragement and advice during the project.

I am grateful to the University of Huddersfield, for funding this research, to Chemlab Ltd for loan of equipment and provision of samples and to the Analytical Division of Royal Society of Chemistry for financial support to attend conferences.

In addition I would like to acknowledge Dr Terry Gough, Dr Neil Crosby and my former colleagues at the Laboratory of the Government Chemist for my training and experience in analytical chemistry.

Finally I would like to thank my colleagues in the research group, Neil Kearney, Stephane Clerc, Zuotao Zeng, Nadia Mahmood, Hazel Waller, Lisa Jeffries, Sze Tai Yau, Amal Abdel-Mageed and the BScIV, MSc and DUT students for their help and friendship which made my time in the department very enjoyable.

# Abstract

Chemiluminescent oxidations with manganese reagents have been investigated using flow and spectroscopic techniques.

An assay has been developed for ascorbic acid using the chemiluminescent oxidation of ascorbic acid with permanganate in acid medium. The assay has a linear range of  $5 \times 10^{-7}$  to  $1 \times 10^{-3}$  mol dm<sup>-3</sup> and has been applied to a range of food supplements and fruit juices.

The addition of a manganese (II) catalyst extends the applicability of acid permanganate to the determination of sugars and polyhydric alcohols. The reaction has been optimised for the determination of mono and disaccharides in a flow injection system.

Development of a reagent based on manganese (III), in a methanol and sulphuric acid solution, has further extended the scope of the reaction enabling the determination of fructose in the range  $1 \times 10^{-7}$  to  $1 \times 10^{-3}$  mol dm<sup>-3</sup>. The reagent has successfully been used in post column detection with HPLC.

It has been established that the light emission occurs after manganese (VII) has been reduced and appears to be connected with the production and disappearance of Mn (III). Chemiluminescence spectroscopy has shown that the spectra are the same for a large number of aliphatic and aromatic polyhydroxy compounds. The spectrum remains the same whether the oxidising reagent is Mn (VII), Mn (IV) or Mn (III), indicating that the same emitting species is involved in all these reactions and that it involves Mn(III) and/or Mn(II).



# CONTENTS

## Chapter 1 Introduction to the Research Programme

1.1 Introduction to the Research	1
1.2 Aims of the Research Programme	3
1.3 Analytical Techniques Selected for the Research Programme	3
1.4 Chemiluminescent Systems Included in the Research Programme	4

## Chapter 2 Introduction to Analytical Methods

2.1 Luminescence	6
2.1.1 Historical Perspective	6
2.1.2 Types of Luminescence	10
2.1.2.1 Luminescence Induced by Absorption of Radiation	10
2.1.2.2 Luminescence in Hot materials	10
2.1.2.3 Luminescence due to Vibration	10
2.1.2.4 Luminescence Produced in a Chemical Reaction	11
2.1.3 Photoluminescence	11
2.1.4 Generation of Chemiluminescence	12
2.1.5 Quantum Efficiency	14
2.1.6 Types of Chemiluminescence Reactions	16
2.1.7 Gas Phase Reactions	16
2.1.8 Reactions in Solution - Bioluminescence	17
2.1.9 Reactions in Solution - Chemiluminescence	18
2.1.9.1 Luminol	19
2.1.9.2 Polyphenols	20
2.1.9.3 Peroxyoxalate (PO-CL)	21
2.1.9.4 Ruthenium and Electrochemiluminescence	24
2.1.9.5 Singlet Oxygen	25
2.2 Flow Analysis	27
2.2.1 Flow Injection Analysis	27
2.2.2 Sequential Flow Injection Analysis	31
2.2.3 Post Column Applications	31
2.2.4 Instrumentation for Flow Injection Analysis	32
2.2.4.1 Pumps	32
2.2.4.2 Injection systems	32
2.2.4.3 Manifold design	33

2.2.4.4 Detection systems	34
2.2.5 Flow Injection with Chemiluminescence Detection	35
2.2.5.1 Photomultipliers	35
2.2.5.2 Photodiode systems	38
2.2.5.3 Photographic systems	38
2.5.5.4 Charge Coupled Devices (CCD)	38
<b>2.3 Stopped Flow Technique</b>	39
2.3.1 Principle of Stopped Flow Technique	39
2.3.2 Application of Stopped-Flow to Spectroscopic Studies	41
2.3.3 Application of Stopped-Flow to Chemiluminescence	41
2.3.4 Stopped-Flow in Flow Injection	42
<b>2.4 Permanganate Oxidations</b>	44
2.4.1 Chemiluminescence from Permanganate Reactions	51
<b>2.5 The Use of Flow Injection and Chemiluminescence in Food Analysis</b>	56
 <b>Chapter 3 Methods and Materials</b>	
<b>3.1 Chemicals</b>	60
<b>3.2 Preparation of Solutions</b>	64
3.2.1 Potassium Permanganate Solutions	64
3.2.2 Manganese sulphate(III)/ sulphuric acid	64
3.2.3 Manganese (III) reagent – Aqueous Formulation	64
3.2.4 Manganese (III) reagent – Methanol Formulation	64
3.2.5 Ascorbic acid Solutions	65
3.2.5.1 Aqueous	65
3.5.5.2 Phosphate stabilised	65
<b>3.3 Samples</b>	66
3.3.1 Samples for Vitamin C Analysis	66
3.3.2 Beers	66
3.3.3 Brewing Materials	66
<b>3.4 Instrumentation and Equipment</b>	67
3.4.1 Volumetric Equipment	67
3.4.2 Weighing	67
3.4.3 Batch Counter	67
3.4.4 Fluorescence Spectrophotometer	67
3.4.5 Stopped-Flow Measurements	68
3.4.6 UV-visible Spectrophotometry	68
3.4.7 Flow Injection Analysis	68
3.4.7.1 Pump	68
3.4.7.2 Injection Valve	68
3.4.7.3 Detectors	68



3.4.7.4 Manifolds	69
3.4.7.5 Chart Recorder	69
3.4.7.6 Data Capture	69
3.4.8 Cyclic Voltammetry	69
3.4.9 pH Measurement	69
3.4.10 HPLC Equipment	69
3.4.11 Data Handling	70
<b>3.5 Calibration Procedures</b>	71
3.5.1 Peristaltic Pumps	71
3.5.2 Air Displacement pipettes	71
3.5.3 Flow Injection Sample Loop	71
3.5.4 UV- Visible Spectrophotometers	72
3.5.5 Fluorescence Spectrophotometer	72
3.5.5.1 Fluorescence Mode	72
3.5.5.2 Chemiluminescence Mode	72
3.5.6 Stopped-Flow Equipment	74
3.5.7 Batch Counting System	76
<b>3.6 Experimental Procedures</b>	77
3.6.1 Flow Injection Experiments	77
3.6.2 Chemiluminescence Time Course Experiments	78
3.6.3 Batch Counting System	79
3.6.4 Fluorescence Spectrophotometer	79
3.6.5 Chemiluminescence Spectrophotometry	80
3.6.5.1 Batch Procedure	80
3.6.5.2 Semi-flow Procedure	80
3.6.5.3 Continuous flow Procedure	80
3.6.5.4 Stopped flow Procedure	80
3.6.6 Consumption of Permanganate	81
3.6.7 Determination of Vitamin C	81
 <b>Results and Discussion</b>	
 <b>Chapter 4 Permanganate Chemiluminescence</b>	
<b>4.1 Oxidation of Food Systems</b>	82
4.1.1 Oxidation of Beer by Various Oxidising Systems	83
4.1.1.1 Batch Experiments	83
4.1.1.2 Preliminary Flow Injection Studies	84
4.1.1.3 Batch Experiments with Permanganate and Peroxide	85
<b>4.2 Oxidation of Carbohydrates by Permanganate</b>	87
4.2.1 Batch Experiments	87
4.2.2 Flow Experiments	94

4.2.2.1	Photomultiplier Voltage	94
4.2.2.2	Sulphuric Acid Concentration	94
4.2.2.3	Manganese Sulphate Concentration	95
4.2.2.4	Optimisation of Permanganate Concentration	97
4.2.2.5	Optimisation of Flow Rate	97
4.2.2.6	Replication of Calibration	98
4.2.2.7	Calibration Lines for Sugars and Related Compounds	98
4.2.2.9	Relationship Between Saccharide Structure and Chemiluminescence	101
4.2.3	Data Handling for Flow Injection Analysis	107
4.2.3.1	Flow Injection Analysis of Carbohydrate Mixtures	110
4.2.4	Spectroscopic Investigations	114
4.2.4.1	Problems with Recording Spectra	116
4.2.4.2	Inner Filter Effect	120
4.2.5	Investigation of Phosphate Effects on Spectra	120
4.3	Investigation of Permanganate Reduction	127
4.4	Summary	135
 <b>Chapter 5 Determination of Ascorbic Acid</b>		
5.1	Determination of Ascorbic Acid	136
5.2	Reasons for Determination of Ascorbic Acid	136
5.3	Methods of Determination	137
5.4	Development of a Flow Injection- Chemiluminescence Assay	138
5.4.1	Optimisation of Flow Rate	138
5.4.2	Optimisation of Acid Concentration	139
5.4.3	Optimisation of Permanganate Concentration	141
5.4.4	Effect of Modifiers	141
5.4.5	Preparation of Standard Solutions	143
5.4.6	Assessment of Interferences	144
5.4.6.1	Inorganic	144
5.4.6.2	Organic	145
5.4.7	Other Compounds Related to Ascorbic Acid	146
5.4.8	Analysis of Real Samples	147
5.4.8.1	Statistical Comparison	147
5.5	Batch Studies	148
5.6	Spectroscopic Studies	149
5.6.1	Batch Studies	149
5.6.2	Stopped Flow Studies	149
5.7	Summary	151



## **Chapter 6 Development of a Manganese (III) Reagent for Chemiluminescence**

<b>6.1 Reasons for Using Other Manganese Species</b>	153
<b>6.2 Manganese (IV) Oxide</b>	154
6.2.1 Studies with Prepared Manganese Dioxide Solid	154
6.2.2 Studies with Manganese Dioxide Sol	154
6.2.3 Flow Studies with Manganese Dioxide Sol	155
6.2.4 Spectroscopic Studies with Manganese Dioxide Sol	158
6.2.4.1 Chemiluminescence Spectrophotometry	158
6.2.4.2 Absorbance Spectrophotometry	162
<b>6.3 Manganese (III) Acetate</b>	162
6.3.1 Spectroscopic Studies	162
<b>6.4 Manganese (III) Sulphate</b>	167
6.4.1 Manganese (III)/Manganese(II) Reagents Flow Studies	167
6.4.1.1 Effect of Manganese(III) Concentration	167
6.4.1.2 Effect of Manganese(II) Concentration	170
6.4.1.3 Effect of Phosphates	172
6.4.2 Spectroscopic Studies with Glucose	175
6.4.3 Flow Studies with Phenolic Compounds	181
6.4.4 Further Flow Studies with Prepared Manganese (III) Reagents	182
6.4.4.1 Investigation of the Manganese(III) Reagent in a Post-Column Format	182
6.4.4.2 Effect of Manganese(III) and Acid Concentrations	183
6.4.4.3 Effect of Manganese(II) Concentration	185
6.4.4.4 Comparisons for Different Saccharides and Related Compounds	186
6.4.5 Effects of Organic Solvents on Chemiluminescence Signal	189
6.4.5.1 Effect of Methanol in the Carrier	189
6.4.5.2 Effect of Methanol in the Reagent	190
6.4.5.3 Preparation of an Improved Manganese(III) Reagent	191
6.4.5.4 Effect of the Ratio of Carrier to Reagents	193
6.4.5.5 Further Attempts to Prepare Stronger Manganese(III) Reagents	195
6.4.5.6 Flow Studies using Ribose and Inositol	197
6.4.6 Kinetic Studies Using Batch Mode	200
6.4.7 Chemiluminescence Spectroscopy Using Stopped-Flow	206
<b>6.5 Electrochemical Generation of Manganese(III)</b>	209
<b>6.6 Summary</b>	210

<b>Chapter 7 Applications of Manganese (III) Reagent in HPLC with Chemiluminescence Detection</b>	
<b>7.1 Chromatographic Analysis of Carbohydrates</b>	211
7.1.1 Choice of Chromatographic System	211
7.1.2 Detection Systems	212
<b>7.2 Linking the Permanganate Chemiluminescence System to a Chromatograph</b>	213
<b>7.3 Linking the Manganese(III) CL System to a Chromatograph</b>	214
7.3.1 Separation System	214
7.3.2 Optimisation of Post-Column Parameters	218
7.3.3 Calibration for Glucose	219
<b>7.4 Summary</b>	220
 <b>Chapter 8 Summary and Conclusions</b>	
<b>8.1 Summary of the Project</b>	222
8.1.1 Permanganate Chemiluminescence	222
8.1.2 Manganese (III) Chemiluminescence	222
8.1.3 Chemiluminescence Spectroscopy	223
<b>8.2 Analytical Applications</b>	223
<b>8.3 Future Work</b>	223
 <b>References</b>	225



## Abbreviations

ADC	Analog-digital converter
ATP	Adenosine triphosphate
CL	Chemiluminescence
CCD	Charge coupled device
CIEEL	Chemically initiated electron exchange luminescence
EDTA	Ethylenediamine tetracetic acid
EMG	Exponentially modified Gaussian
FIA	Flow injection analysis
HPLC	High-performance liquid chromatography
KOT	Knitted open tubular
OVAT	One variable at a time
PAH	Polycyclic aromatic hydrocarbon
PMT	Photomultiplier tube
PTFE	Polytetrafluorethane
R	Coefficient of regression
RSD	Relative standard deviation
SIA	Sequential injection analysis
UV	Ultra violet

# CHAPTER 1

## INTRODUCTION TO THE RESEARCH PROBLEM

### 1.1 Introduction to the Research

Chemiluminescence as an analytical tool has been the subject of considerable interest since the discovery, at the end of the last century, of luminescent chemicals such as luminol and lophine. The popularity and potential of the technique is shown by the large number of publications on the subject. These include books, journal articles, reviews<sup>1,2,3,4,5,6,7</sup> and articles in the technical<sup>8</sup> and popular press.

In the absence of noise, even very low levels of light are readily measured with simple instrumentation. In chemiluminescent reactions the only source of radiation is the chemical reaction. As no external light source or wavelength restriction is required the system is inherently sensitive. Most chemiluminescent reactions in solution are fast and proceed at room temperature and are therefore readily linked with systems such as flow injection<sup>9</sup> and immunoassay.<sup>10,11</sup>

Wide linear ranges can be achieved; up to five orders of magnitude. This makes the techniques particularly suitable for determinations where analyte concentration can vary greatly. The simplicity of the equipment makes the technique attractive for field applications. The development of miniature photomultiplier tubes and rugged photodiode systems makes field systems even more attractive. The rapid response of many chemiluminescence systems suggests applications in process control, where analytical results are used to monitor streams and to initiate processes.

Most reported analytical applications of chemiluminescence have been in the medical and environmental sectors. More applications are now appearing in the area of food analysis.<sup>12</sup> The determination of ATP is the most widely used application of



bioluminescence in the food industry and luminol is probably the most frequently used chemiluminescent reagent. The use of peroxyoxalate chemiluminescence is gaining popularity, particularly as a detection system for HPLC or other separation techniques. Solvents often used in HPLC are compatible with peroxyoxalate reagents. Gas phase chemiluminescence, particularly determination of nitric oxide is used, often with gas chromatography, in environmental and food analysis.

There are relatively few reactions which generate chemiluminescence, and most of them are oxidations. Foods contain many components which are readily oxidised. Polyhydroxy compounds, for example simple sugars and polysaccharides, which are the structural and storage materials in plants are readily oxidised. Many minor components of foods also contain multiple hydroxy groups. Examples are ascorbic acid and vitamins with anti-oxidant and other metabolic functions. Foods can also contain undesirable components, such as toxic metabolites of fungal or bacterial origin, metals and residues of agricultural chemicals, which can be oxidised by simple oxidising agents to yield chemiluminescence.

Direct chemiluminescence, in which the oxidation of analyte is the source of luminescence, has the advantage of needing only simple reagents and avoids the cost and toxic hazards associated with some chemiluminescent reagents and their solvent systems. Selectivity can be introduced through separation systems such as HPLC and affinity chromatography. In some cases additional specificity can be achieved by exploiting differences in rates of the reaction of the oxidising agents with different components in the sample mixture.

## **1.2 Aims of the Research Programme**

The aims of this project were to investigate oxidation reactions of food components which give direct chemiluminescence, and to use these reactions to develop analytical methods suitable for use in process analysis and control. The studies were also designed to increase the understanding of the mechanisms of the reactions.

## **1.3 Analytical Techniques Selected for the Research Programme**

Many chemiluminescent reactions are known to be fast. Techniques applicable to fast reactions in solution were selected for the studies. These were flow injection, continuous flow methods and stopped-flow techniques.

Flow injection analysis is based on the dispersion of a sample in a flowing carrier stream. The size of sample and rate of dispersion were readily controlled and varied enabling different points of the reaction to be sampled by the detection system. Continuous flow and stopped-flow methods enabled complete mixing of reagents. In continuous flow, as in flow injection, different points in the reaction could be sampled by controlling the speed at which the mixed stream passed through the flow cell. An increased flow rate decreased the time interval between mixing and sampling by the detector. The stopped flow technique allowed the reaction to be monitored throughout the reaction time.

While most chemiluminescent reactions are fast, some of those studied were found to take several minutes to reach maximum emission. Batch techniques were applied to these systems. Emitted light was measured using a liquid scintillation counter modified to act as a photon counter.

For both fast and slow reactions, where the emission was sufficiently intense, studies of the chemiluminescence emission spectra were undertaken using a fast scanning



fluorimeter. An extended range photomultiplier was used in the fluorimeter to measure wavelengths over 650nm. Complementary studies were undertaken using UV-visible absorbance spectroscopy to investigate the fates of oxidising species in the reactions.

The detection systems used were photomultiplier and photodiode based. These were selected for ease of use and low cost. Principles of the analytical techniques selected are discussed in Chapter 2.

#### **1.4 Chemiluminescent Systems Included in the Research Programme**

Direct chemiluminescence was selected for study as the reagents are simple, readily available, and low cost when compared with many specific chemiluminescence and bioluminescence reagents. Oxidation reactions which give direct chemiluminescence are known; some have been studied extensively. For most of these reactions the mechanisms are not fully understood. Several oxidation systems were investigated to establish whether light was emitted during oxidation of food components. Of the systems examined, oxidation with permanganate showed the greatest potential and was selected for detailed study.

Permanganate oxidations have been studied for some considerable time and the production of chemiluminescence with a range of organic compounds has been reported. A survey of analytical applications of permanganate chemiluminescence is presented in Chapter 2. Chemiluminescence from the permanganate oxidation of carbohydrates was identified and investigated. This class of compound was not previously reported to give chemiluminescence in this type of system. The reaction was investigated and methods were developed for the determination of sugars and related carbohydrates in solution; the results are described in Chapter 4. A related

reaction was identified and developed for the determination of trace levels of ascorbic acid, a water-soluble vitamin; this is described in Chapter 5.

Investigation of the permanganate oxidation with sugars indicated the involvement of intermediate manganese oxidation states in the reactions. Reports by other workers have also indicated this. A novel reagent for chemiluminescence, based on manganese (III), is described in Chapter 6. The application of the new reagent to the chromatography of carbohydrates is reported in Chapter 7.

## CHAPTER 2

### INTRODUCTION TO ANALYTICAL METHODS

#### 2.1 Luminescence

##### 2.1.1 Historical Perspective<sup>13</sup>

The phenomenon of luminescence, of light being produced in the absence of heat, has been known throughout history. The first true luminescences observed was bioluminescence in luminous organisms including insects, fungi and the bacteria on rotting wood and flesh. Electroluminescence was observed as the aurora borealis and ignis lambens, a silent electric discharge observed under some atmospheric conditions. The earliest written reference to luminescent animals is in Chinese poetry of around 1500BC and there are other references in ancient writings from Japan and India.

The Greek philosopher Aristotle (384-322BC) gave the first recorded detailed description of luminescent animals and other luminescence phenomena in *De Anima*. This discussed the differences between luminescence and items which have colour and are seen in daylight. In the first century AD Caius Plinius Secundus, Pliny the Elder, described luminous glow-worms, fungus, lantern fish and jellyfish in *Historia Naturalis*. During the Middle Ages various authors including St Isidore of Seville, in the 6<sup>th</sup> century, Rabanus Maurus, Archbishop of Mainz in the 9<sup>th</sup> century and Hildegard of Bingen in the 12<sup>th</sup> century made references to luminous insects and other luminescence phenomena.



The first book totally devoted to luminescence was published at Zurich, in 1555, by Conrad Gesner. Generally referred to as *De Luminariis* it was titled, in translation, *A short commentary on rare and marvellous plants that are called lunar either because they shine at night or for other reasons; and also on other things that shine in darkness*. It drew on the ancient authors, describing luminous plants and animals, also luminous stones, and included Gesner's own ideas on the subject.

Ancient and medieval authors on luminescence had been mainly concerned with describing luminescent objects. From the beginning of the 17<sup>th</sup> century more attempts were being made to explain these phenomena. Francis Bacon (1561-1626) wrote several works on light and luminescence including *The Advancement of Learning* (1605), *Topica Inquisitionis de Luce at Lumine* (published before 1612) and *Sylva Sylvarum or A Natural History in Ten Centuries* (published 1627). The latter describes sixteen experiments with shining wood, fish and flesh. At about the same time an Italian, Vincenzo Cascariolo of Bologna, found that a local mineral consisting of native barium sulphate could be made to phosphoresce; this was the Bolognian phosphor or Lapis Bononiensis. Other inorganic luminescences were then discovered; the most important being that of phosphorus, first prepared in 1669 by Hennig Brandt. Thermoluminescence in certain types of fluorspar, which emit light when warmed slightly, was recognised as a separate form of luminescence in 1676 by Johan Sigmund Elsholtz.

Robert Boyle made an extended study of the properties of luminescing materials. His first studies were into diamond and were reported in 1663. Diamond can display phosphorescence, thermoluminescence, electroluminescence and also triboluminescence, which is the property of emitting light for a short while when broken. Preparing phosphorus independently of Brandt, Boyle's work on the element was published in 1680 as *The Aerial Noticula*. His best known studies into luminescence related to shining flesh and wood and the effects of air on these.



These experiments were made possible by the vacuum pump invented by Otto von Guericke in 1650 and improved by Boyle and Hooke in the 1660s. The results were reported in the *Philosophical Transactions*, on December 16 1672 as “Some Observations about Shining Flesh”. Reports of these experiments appear to have circulated widely. In the play “The Virtuoso”, a satire on the Royal Society, written in 1676 by Thomas Shadwell for the Dukes Company, a character described the essential features of these experiments:

*“There was a lucid sirloin of beef in the Strand. Foolish people thought it burned when it only became lucid and crystalline by the coagulation of the aqueous juice of the beef by the corruption that invaded it. ‘Tis frequent. I myself have read a Geneva Bible by a leg of pork.... ‘tis the finest light in the world. But for all that, I could eclipse the leg of pork in my receiver by pumping out the air. But immediately upon the appulse of the air let in again, it becomes lucid as before.”<sup>14</sup>*

At this time many philosophers, including Isaac Newton (1642-1727) and Robert Hooke (1635-1702), considered that the emission of light was connected with vibrations in the emitting object. Newton considered that the light was propagated in the form of a stream of particles while Hooke and Christian Huygens (1629-1695) supported the wave theory of propagation. Hooke also made a number of studies of luminescence phenomena.

During the 18<sup>th</sup> century many materials were found to be luminescent, including several observed by Jacopo Bartolomeo Beccari and co-workers in Bologna. These workers developed a classification of luminescence by the method of excitation. They did not use modern terminology, but otherwise the classification is very similar to those in current use.

By the early 19<sup>th</sup> century the wave theory of light became more widely supported due to the work on diffraction by Thomas Young (1773-1829) and Augustin Fresnel (1778-

1827). In 1802 the first spectrometer to use a slit was proposed by Hyde Wollaston enabling the first good spectra of phosphors to be observed. In the 1850's publications by Edmond Becquerel (1820-1891) described the composition of the exciting light, and later the emitted light of fluorescent materials.

Several new inorganic luminescent systems were reported in the 18<sup>th</sup> century, including the white flash observed when lime is mixed with a strong acid. In 1877 Bronislaus Radziszewski synthesised lophine, a triphenylimidazole, and found that it emits light when dissolved in an alkaline solution of alcohol and shaken with air. This discovery essentially founded the science of solution chemiluminescence. In 1888 the term chemiluminescence was proposed by Eilhard Wiedeman (1852-1928) to describe light emission occurring as a result of chemical processes.

The next major discovery in solution chemiluminescence was that of pyrogallol, described by J. M. Eder in 1887, and studied in detail by Trautz and Shorin in 1905. In 1887 Raphael Dubois demonstrated that light is emitted from the mixture of a luciferin and luciferase in the presence of oxygen and discovered the chemiluminescence from aesculin, a glucosidic compound present in horse-chestnut bark. Several more chemiluminescent compounds were discovered in the early part of this century. These included lucigenin by K. Gleu and P. Petsch in 1935 and luminol, which was discovered by H.O. Albrecht in 1928. Luminol is still the most widely used chemiluminescent compound for analytical applications.



### **2.1.2 Types of Luminescence**

Luminescence is the emission of radiation, particularly in the ultraviolet, visible or infrared parts of the spectrum, by atoms or molecules, which occurs when the species in an electronically excited state returns to its ground state.

There is a range of luminescence phenomena, which can be classified in various ways. The following classification uses the mechanism by which the emission is initiated.

#### **2.1.2.1 Luminescence Induced by the Absorption of Radiation**

- Photoluminescence: from the absorption of visible, ultra-violet or infrared radiation.
  - Fluorescence
  - Phosphorescence
- Radioluminescence: from the absorption of X-rays or  $\gamma$ -rays.
- Anodoluminescence : from interaction with alpha particles
- Cathodoluminescence : from interaction with beta particles

#### **2.1.2.2 Luminescence in Hot Materials**

- Pyroluminescence : from metals in flames
- Candoluminescence from incandescent solids
- Thermoluminescence : from mild heating of solids

#### **2.1.2.3 Luminescence due to Vibration**

- Triboluminescence : from rearrangements in solids subject to pressure
- Sonoluminescence : from exposure to ultrasonic sound waves in solution

#### **2.1.2.4 Luminescence where the Excited state is Produced in a Chemical Reaction**

- Chemiluminescence: the excited state is produced in a chemical reaction
- Bioluminescence: the excited species is formed in an enzyme mediated reaction.
- Electrogenenerated chemiluminescence: the excited species is formed in a reaction at an electrode surface.

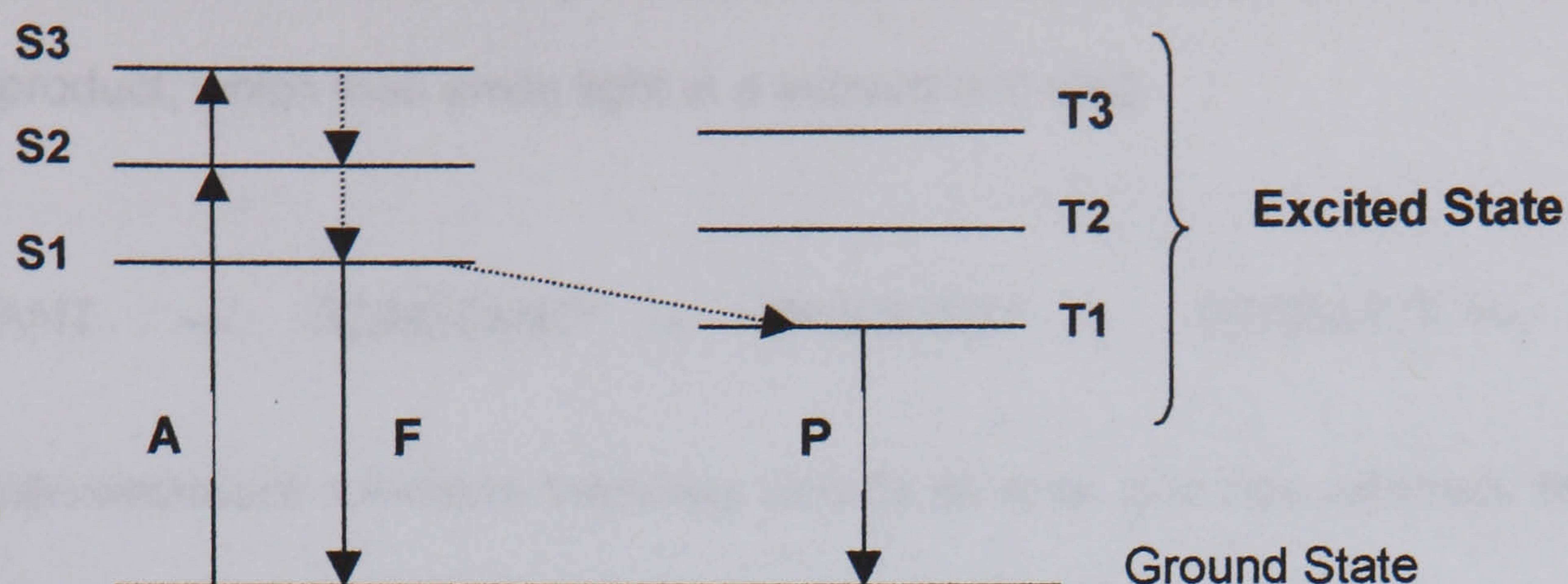
All these forms of light emission are distinct from the light emitted by hot bodies, which is termed incandescence and where the colour and intensity are dependent on the temperature of the emitting body, according to the Kirchoff and Stephan-Boltzmann laws.

Analytically fluorescence, bio- and chemiluminescence have the widest application.

#### **2.1.3 Photoluminescence**

For a singlet ground state molecule photoluminescence is either short-lived fluorescence from a singlet excited state or phosphorescence from a triplet state. This is shown in Figure 2.1. Energy is absorbed by a molecule and raises the energy to an excited singlet state S<sub>2</sub> or S<sub>3</sub>. By means of internal conversions the species falls to the lowest singlet excited state and then returns to the ground state emitting fluorescence of longer wavelength than the exciting light. The lifetime of the process is short, less than 10<sup>-5</sup> sec. Where intersystem crossing occurs a triplet energy state can be achieved, the decay of which is slower than the singlet state, yielding phosphorescence, which can continue for seconds or minutes after illumination ceases. Intersystem crossing is strictly a 'forbidden electronic transition', therefore phosphorescence is considerably less intense and less common than fluorescence.



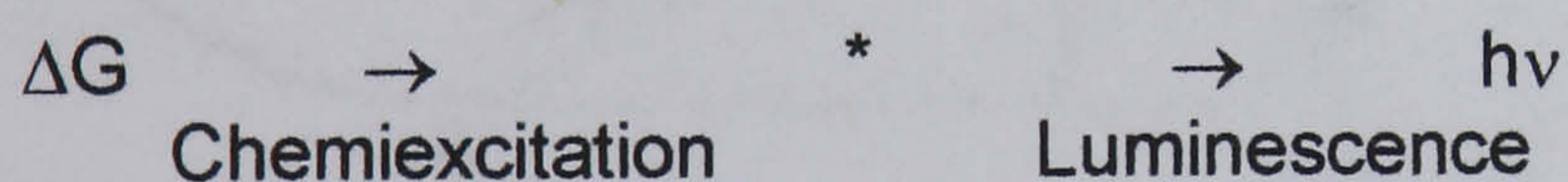


**Figure 2.1 Energy states in Photoluminescence**

A Absorption F Fluorescence Emission P Phosphorescent Emission

#### 2.1.4 Generation of Chemiluminescence

For chemiluminescence the source of excitation energy is a chemical reaction and occurs when a large fraction of the exothermicity of the reaction is converted into excitation energy. The second step is a luminescence step as described above.



Chemiluminescence reactions are described as direct or sensitised. In direct chemiluminescence the reaction generates an excited state molecule which emits the light. In a sensitised reaction the energy from the primary excited product is transferred by one of a number of mechanisms to a fluorescent acceptor molecule. This then loses energy by emitting light at its own characteristic fluorescence wavelength. This mechanism is also known as energy transfer chemiluminescence.



Additional classification into adiabatic and non-adiabatic chemiluminescence has been made<sup>15</sup> but is of limited usefulness. Adiabatic chemiluminescence describes

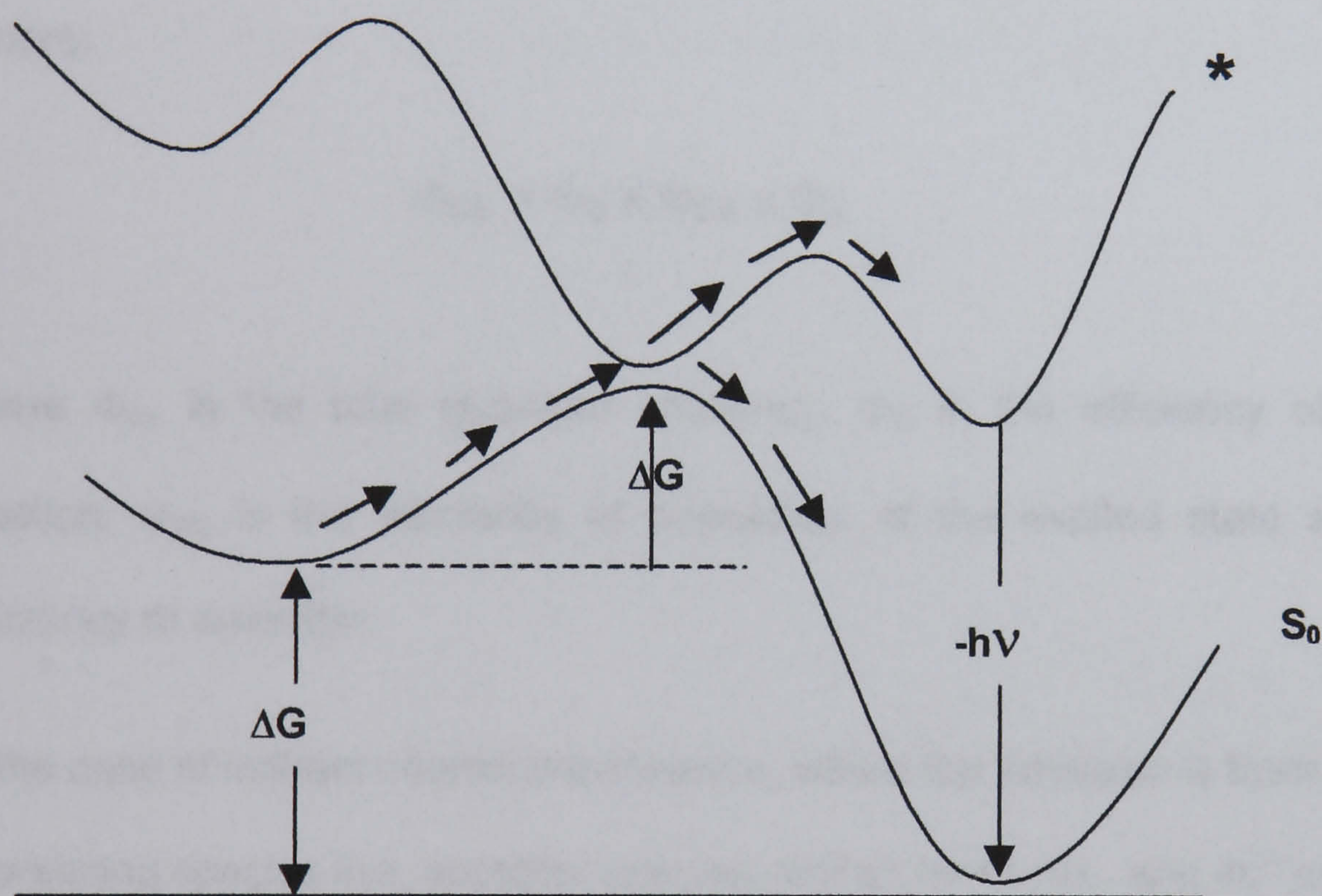


reactions where an electronically excited reactant reacts to give an electronically excited product, which then emits light in a subsequent step.



All chemiluminescent reactions therefore include at least one non-adiabatic step as electronically excited species eventually result in ground state products.

For chemiluminescence to occur reactions must be exothermic and a large fraction of the energy must be converted into electronic excitation energy.



**Figure 2.2 Schematic of a Chemiluminescent Organic Reaction**

\* is the potential energy surface for the excited state and  $S_0$  is the surface for the ground state.



For the reaction to be chemiluminescent in the visible region (400-750nm) the energy required is in the range  $160\text{-}300\text{kJ mol}^{-1}$ , as derived from the combined Planck-Einstein equations:



$$E = hc/\lambda$$

The energy generated in the reaction can be lost as vibrational and rotational energy (heat). If a suitable pathway exists, as shown in Figure 2.2, an excited species can be produced and the energy, if not lost in non-radiative processes, can be emitted as a photon either directly or after transfer to a suitable fluorophore.

### 2.1.5 Quantum Efficiency

The chemiluminescence efficiency of a chemiluminescent reaction depends on three factors:

$$\Phi_{CL} = \Phi_C \times \Phi_{EX} \times \Phi_e$$

where  $\Phi_{CL}$  is the total quantum efficiency,  $\Phi_C$  is the efficiency of the chemical reaction,  $\Phi_{EX}$  is the efficiency of population of the excited state and  $\Phi_e$  is the efficiency of emission.

In the case of indirect chemiluminescence, where the emission is from a second fluorescing species the, acceptor species, further terms,  $\Phi_T$ , and  $\Phi_e^A$  are added. The term  $\Phi_T$  describes the efficiency of energy transfer and  $\Phi_e^A$  relates to efficiency of emission from the acceptor molecule.

$$\Phi_{CL} = \Phi_C \times \Phi_{EX} \times \Phi_T \times \Phi_e^A$$

Quantum efficiencies of many chemiluminescent reactions are low, those used analytically are typically in the range 0.001 to 0.1 and up to 0.5 for peroxyoxalate systems. Reactions with lower quantum efficiencies, down to  $10^{-15}$ , often called

ultraweak can also be used analytically,<sup>16,17,18,19,20</sup> particularly when the time of emission is relatively long.

Some reactions have particularly high quantum efficiencies, approaching 1. These are mainly bioluminescent reactions, where the presence of other biological molecules such as proteins is believed to protect emitting species from loss of energy by interaction with solvent or other molecules. Natural selection, during the course of evolution selects for the most efficient luminescence systems for particular environments resulting in the high quantum efficiencies and spectral characteristics. In marine environments luminescent species typically emit green light. Terrestrial species emit blue light to enabling it to be seen from the maximum distance.



### 2.1.6 Types of Chemiluminescence Reactions

The majority of chemiluminescent reactions involve oxidation of a substrate and all systems used analytically are of this type. Other chemiluminescent reactions include electron transfer, fragmentation and pericyclic rearrangements.

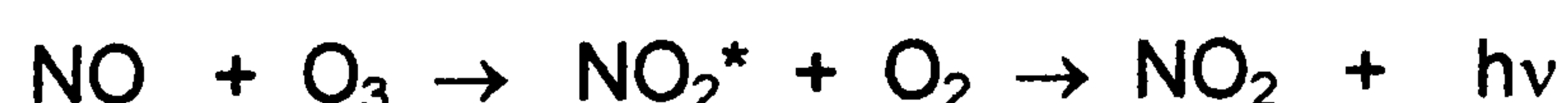
### 2.1.7 Gas Phase Reactions

Chemiluminescence in the gas phase is common, for example, the air afterglow in the upper atmosphere. This is due to the recombination of reactive species formed by the action of ultraviolet radiation from the sun, and includes red and green emissions from atomic oxygen and other inorganic species.

The luminescence of nitric oxide is used analytically as the basis for commercial NO<sub>x</sub> monitors and in the gas chromatographic determination of volatile N-nitrosamines.<sup>21</sup>

These are suspected carcinogens, produced during cooking of foods containing nitrite and nitrate preservatives.

The effluent from the gas chromatograph is passed into a heated reactor containing a catalyst of tungsten oxides where the weak N-NO bonds are cleaved giving a nitrosyl and an organic radical. Reaction of the nitrosyl radical with low pressure ozone forms excited nitric oxide which rapidly decays back to the ground state emitting in the near infra-red at 1200nm.



An optical, filter absorbing light below 600nm, eliminates chemiluminescence from the reaction of ozone compounds such as hydrocarbons and carbon monoxide. The detector has a linear range of five orders of magnitude and a detection limit of less than one nanogram. The gas phase chemiluminescent reactions of ozone with

hydrocarbons at atmospheric pressure and of sodium vapour with nitrous oxide are also used as sensitive detectors for gas chromatography.<sup>22,23</sup>

The reaction of metal vapours with halogens is often chemiluminescent. For example the reaction of manganese vapour as atoms and small molecules with chlorine or fluorine gives complex chemiluminescence spectra.<sup>24</sup> The spectra include both sharp bands and broad emissions, possibly from  $Mn_2$  and  $Mn_2X$  species. Thermally induced low-pressure gas phase decomposition of nitrate esters and nitramines gives blue-green chemiluminescence. This has been used for detection of explosives directly, or after gas chromatographic separation.<sup>25</sup>

#### **2.1.8 Reactions in Solution- Bioluminescence**

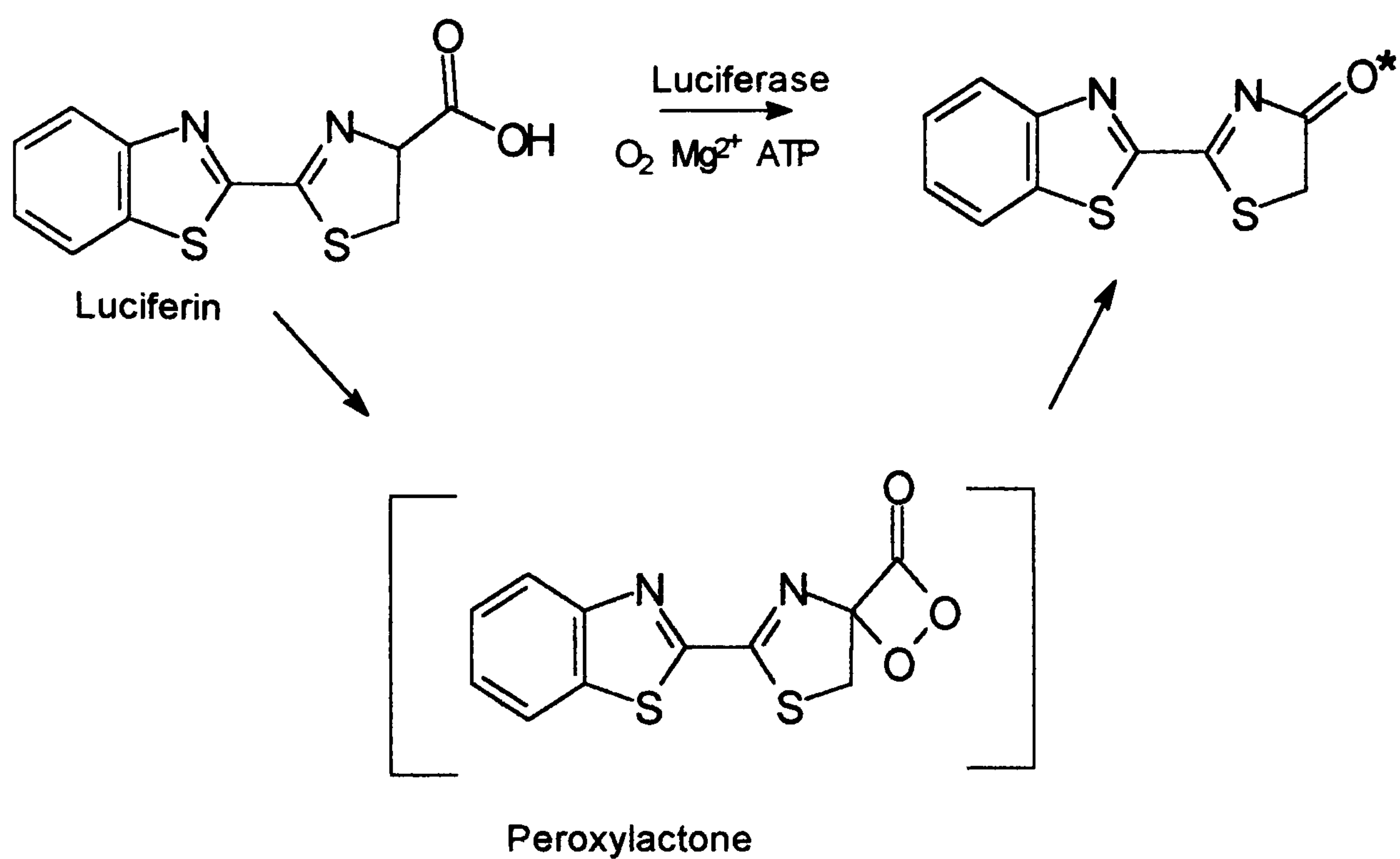
This type of chemiluminescence is derived from reactions in organisms including bacteria, fungi and insects. It is due to the oxidation of certain substrates in the presence of enzymes and cofactors such as ATP and flavin mono- and dinucleotides. Firefly (*Photinus pyralis*) bioluminescence<sup>26</sup> involves the oxidation of the luciferin shown in Scheme 2.1.

The enzymes (luciferases) responsible have been isolated from luminous organisms and are widely used in analysis.<sup>27</sup> As the intensity of luminescence is proportional to the amount of co-factor the above reaction can be used to measure ATP as follows:



Using this system very low levels of ATP can be detected, down to  $10^{-17}$  mol.<sup>28</sup> This reaction forms the basis of a very widely used technique of hygiene assessment in the food processing industry in both continuous flow<sup>29</sup> and batch<sup>30</sup> formats.

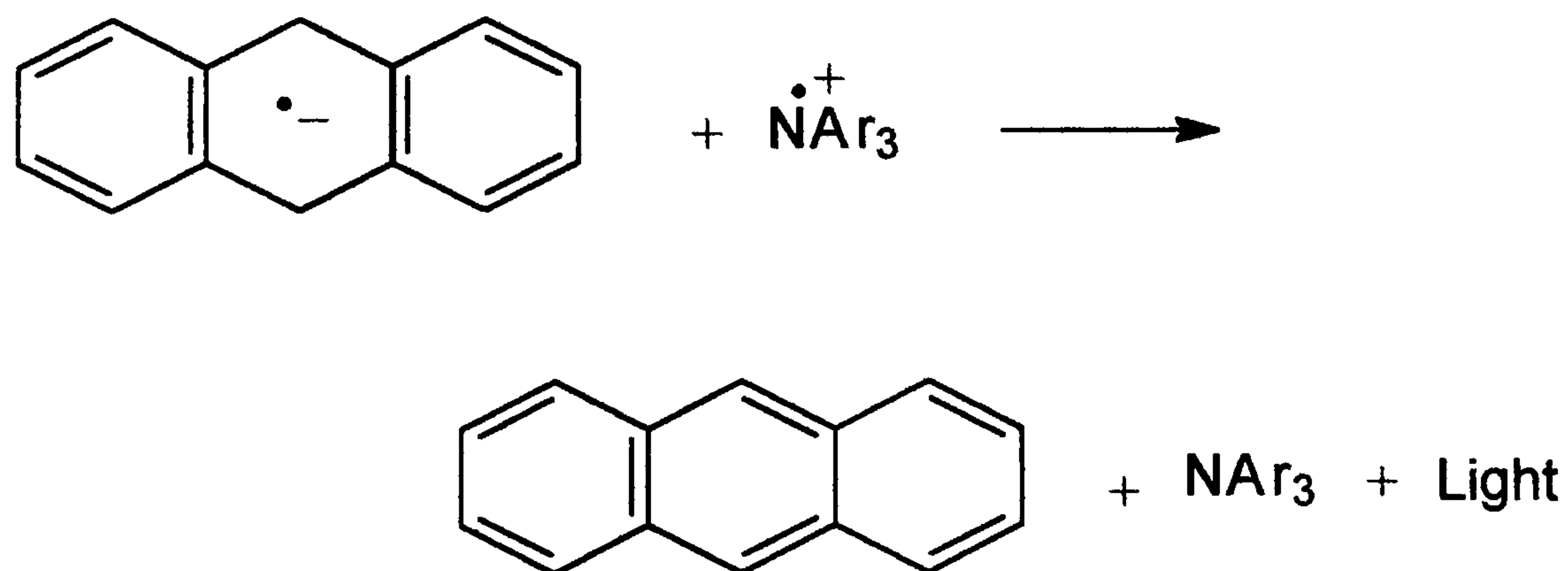




**Scheme 2.1 Mechanism for the Bioluminescence from Firefly**

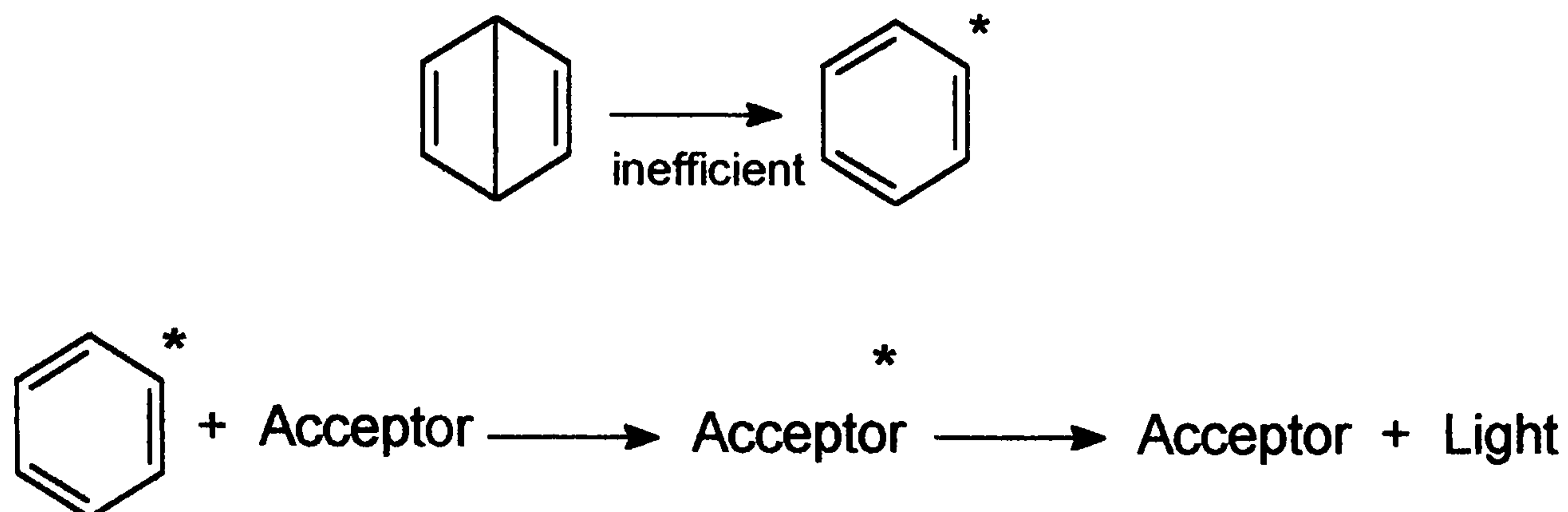
### 2.1.9 Reactions in Solution - Chemiluminescence

Chemiluminescent reactions which do not involve oxidations are rare, however an examples is reactions of radical anions with aromatic amines<sup>31</sup> (Scheme 2.2).



**Scheme 2.2**

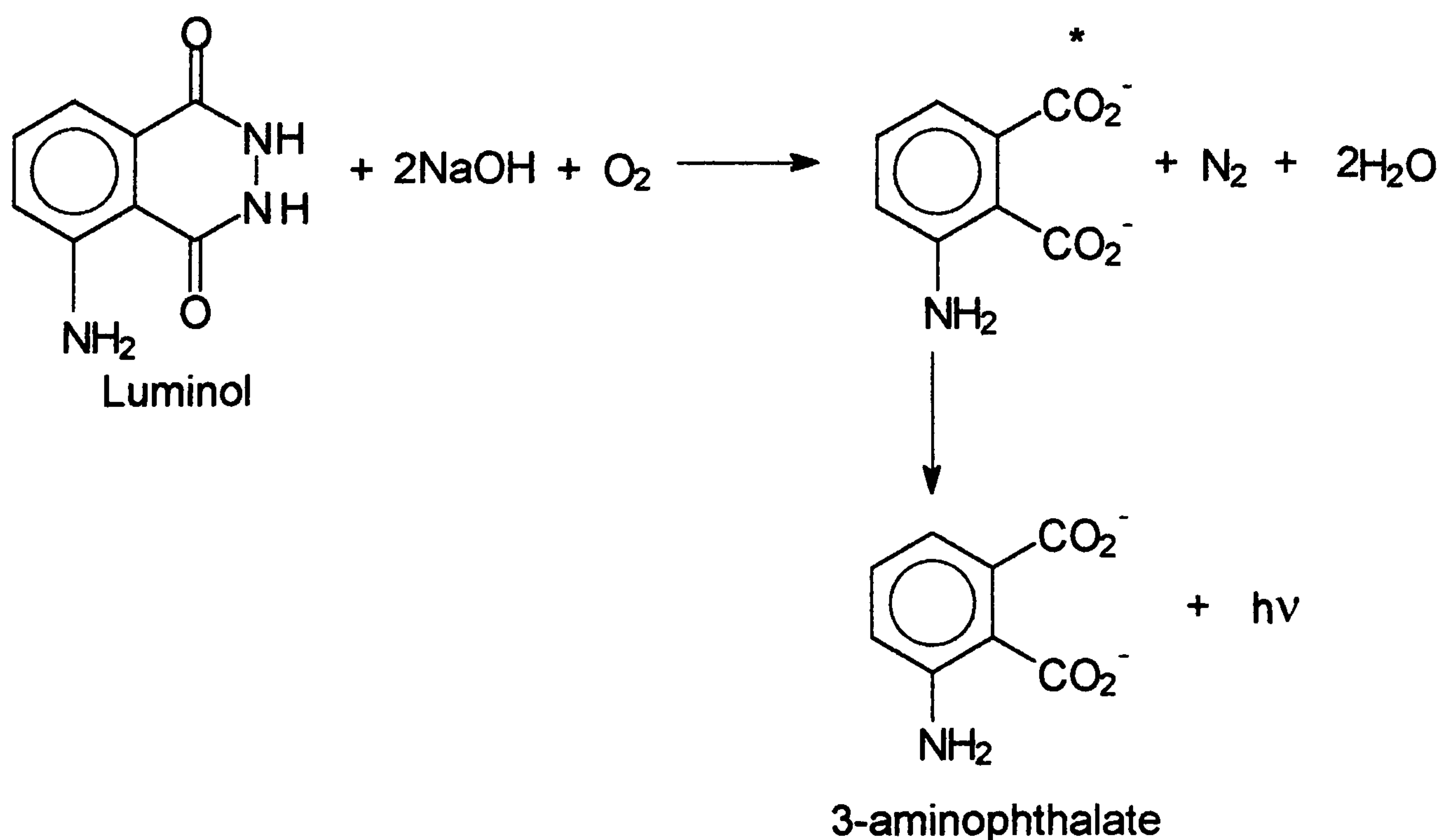
The rearrangement of Dewar benzene to benzene (Scheme 2.3) is another example. In this case the emission is weak and an efficient acceptor is required as a sensitiser.<sup>32</sup>



**Scheme 2.3**

#### 2.1.9.1 Luminol

Perhaps the most widely used chemiluminescent reaction is that of luminol (5-aminophthalhydrazide). Blue luminescence with a  $\lambda_{\text{max}}$  of 425nm is produced when luminol reacts with a wide range of strong oxidants, including molecular oxygen, in alkaline solution.



**Scheme 2.4**

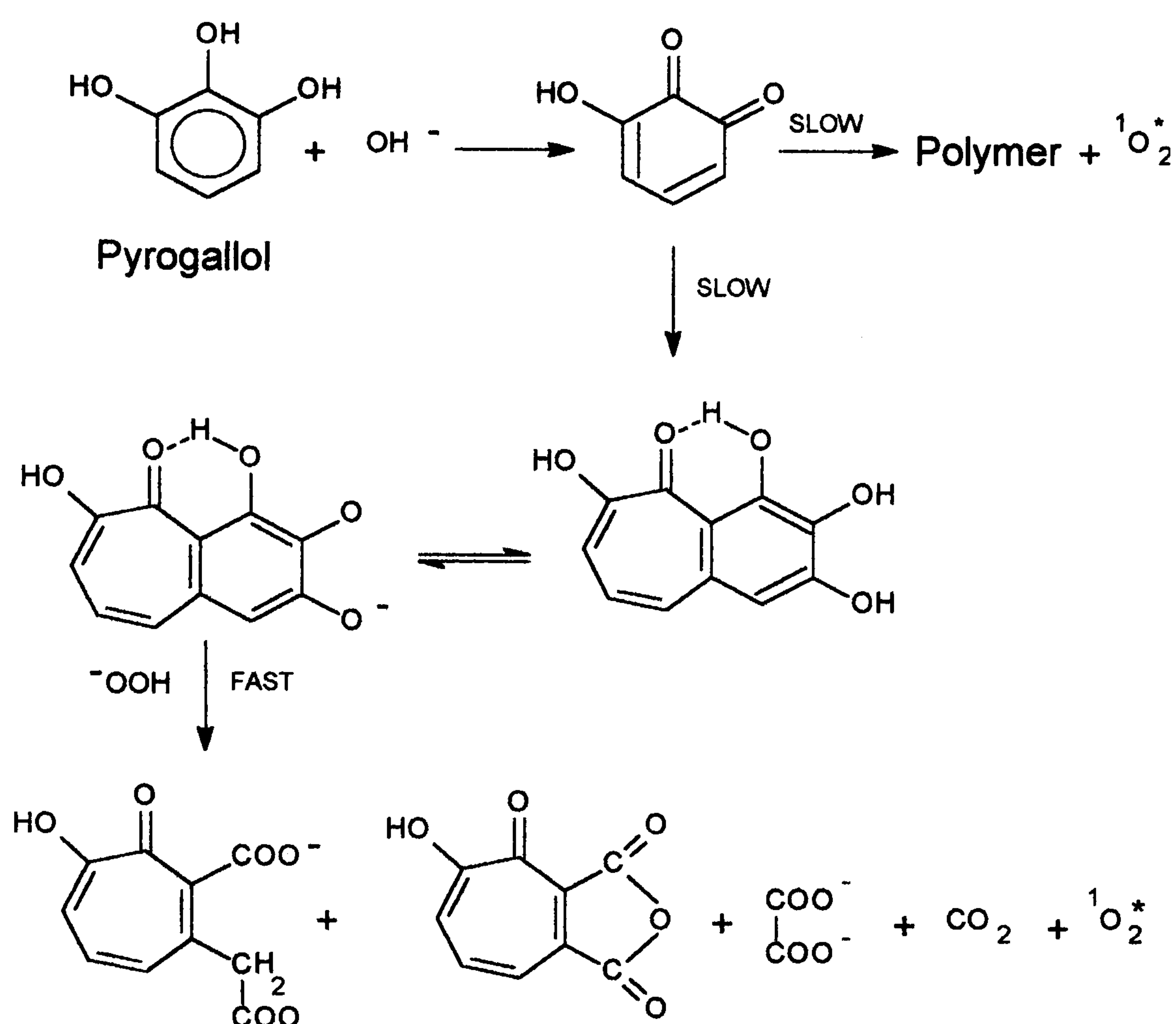
The excited species is considered to be the 3 aminophthalate.<sup>33,34</sup> In dimethyl sulphoxide the quantum yield is approximately 5% and is reduced to less than 1% in protic solvents. In analytical applications the most frequently used oxidant is hydrogen peroxide. This reaction is catalysed by a variety of metal ions and haem containing enzymes. The reaction with haem is the basis of the application luminol in locating blood stains in forensic investigations. Metal ions including Co(II), Cu(II), Fe(II), Cr(III) and Ti(III) have been determined to pg levels. The reaction with luminol has also been used to determine enzymatically generated peroxide. The reaction of sulphite with immobilised sulphite oxidase gives hydrogen peroxide, which can be determined by luminol chemiluminescence. This technique has been used as a very sensitive assay for sulphite in environmental samples.<sup>35</sup> The application of luminol chemiluminescence has been reviewed.<sup>9</sup>

Several inorganic and organic materials can inhibit Luminol chemiluminescence. The suppression of the signal is dependent on the concentration of inhibitor and can be used analytically, for example in the determination of sulphite in wine.<sup>36</sup>

#### **2.1.9.2 Polyphenols**

Pyrogallol, gallic acid and related polyhydroxybenzenes react with oxidants including molecular oxygen and hydrogen peroxide in the presence of a metal catalyst.. The chemiluminescence is red, has a spectral maximum  $\lambda_{\text{max}}$ , in the region of 600nm and depends on the phenol used. At high pH autoxidation of the phenol occurs. After a period of autoxidation reaction with hydrogen peroxide yields blue chemiluminescence with  $\lambda_{\text{max}} \approx 480\text{nm}$ .<sup>37</sup> A mechanism, which includes singlet oxygen, has been proposed for the red chemiluminescence produced.<sup>38</sup> As the maximum is significantly below 633nm, where singlet oxygen emits, and depends on the phenol singlet oxygen cannot be the major emitting species.



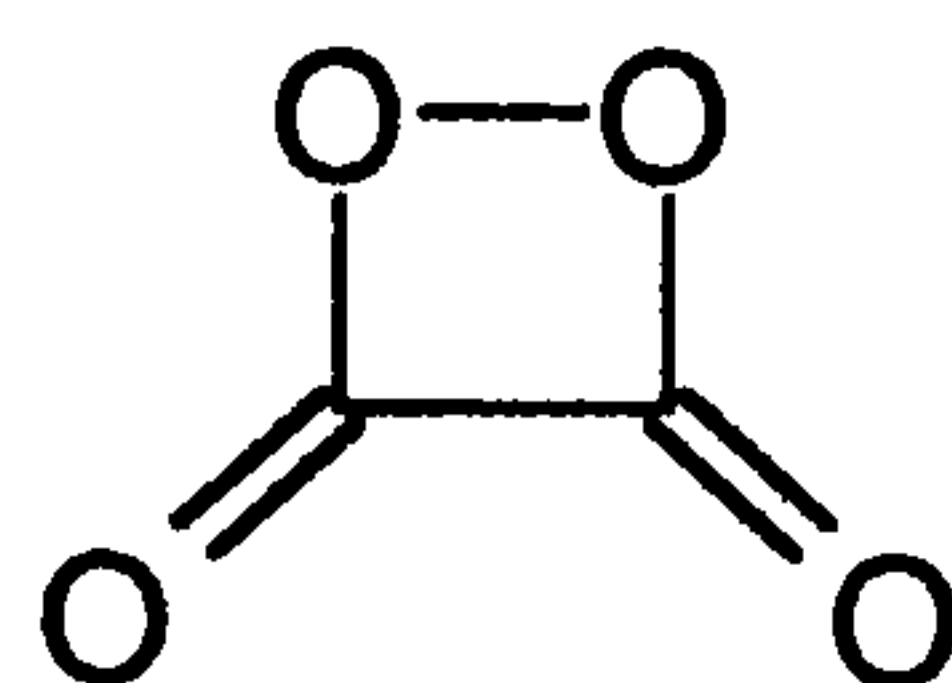


**Scheme 2.5**

### 2.1.9.3 Peroxyoxalate

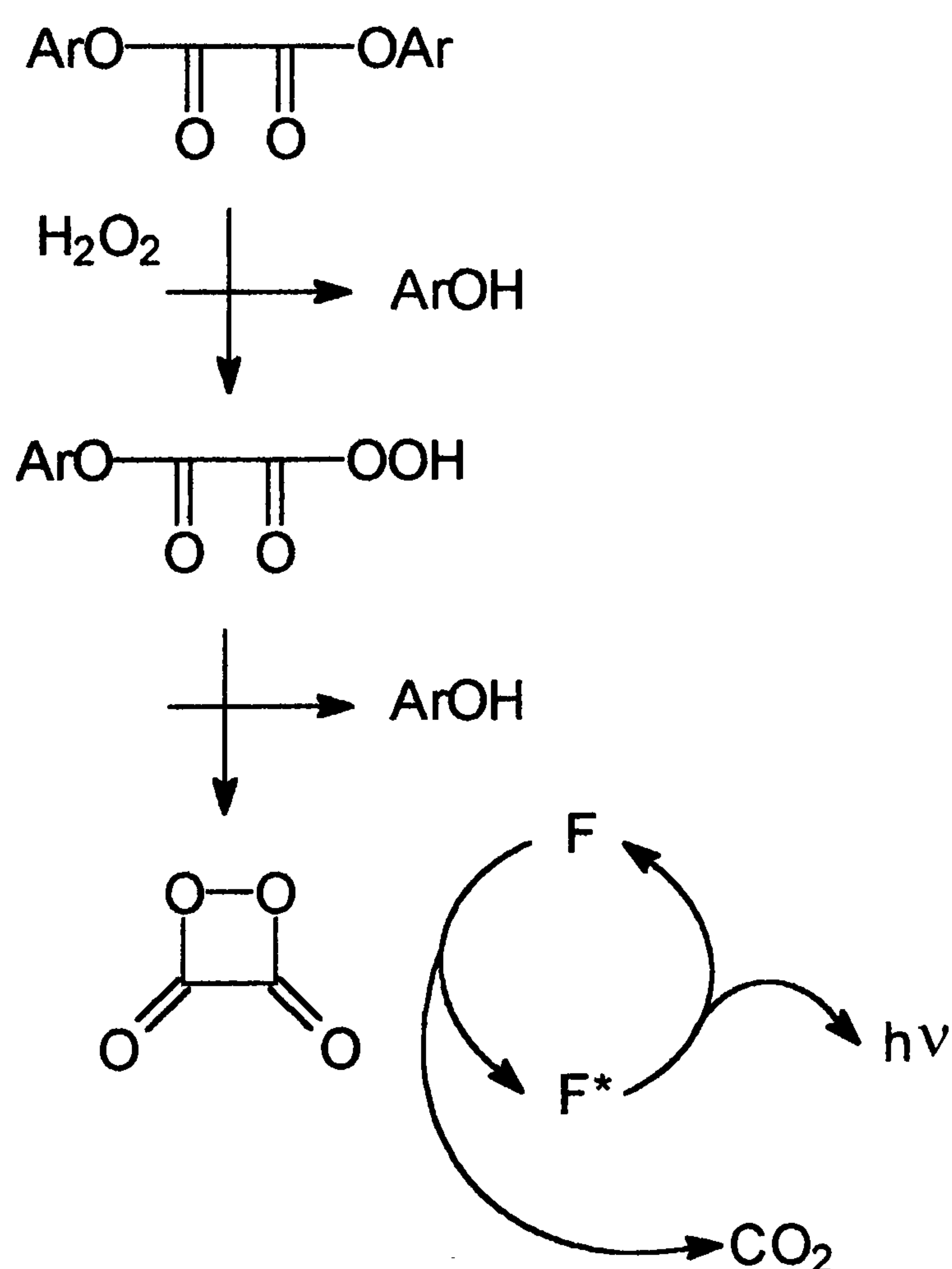
With quantum yields of up to 0.5, the most efficient non-enzymatic chemiluminescent reactions are those based on peroxyoxalate. These reactions are the basis of the light sticks used in emergency lighting. The chemiluminescence is indirect; an oxalate ester reacts with hydrogen peroxide producing a high-energy intermediate which can excite a wide range of acceptor molecules.<sup>39</sup> Radiative decay of the excited fluorescent molecules emits light of spectrum identical to the fluorescence spectrum of the acceptor molecule. A wide range of fluorscers can be used, for example the xanthene dyes fluourescein (yellow/green) and rhodamine (red). A base catalyst, generally imidazole, is used to increase the reaction rate.

The nature of the intermediate responsible for exciting the fluorophore has been proposed as 1,2 dioxetanedione.



1,2- dioxetanedione

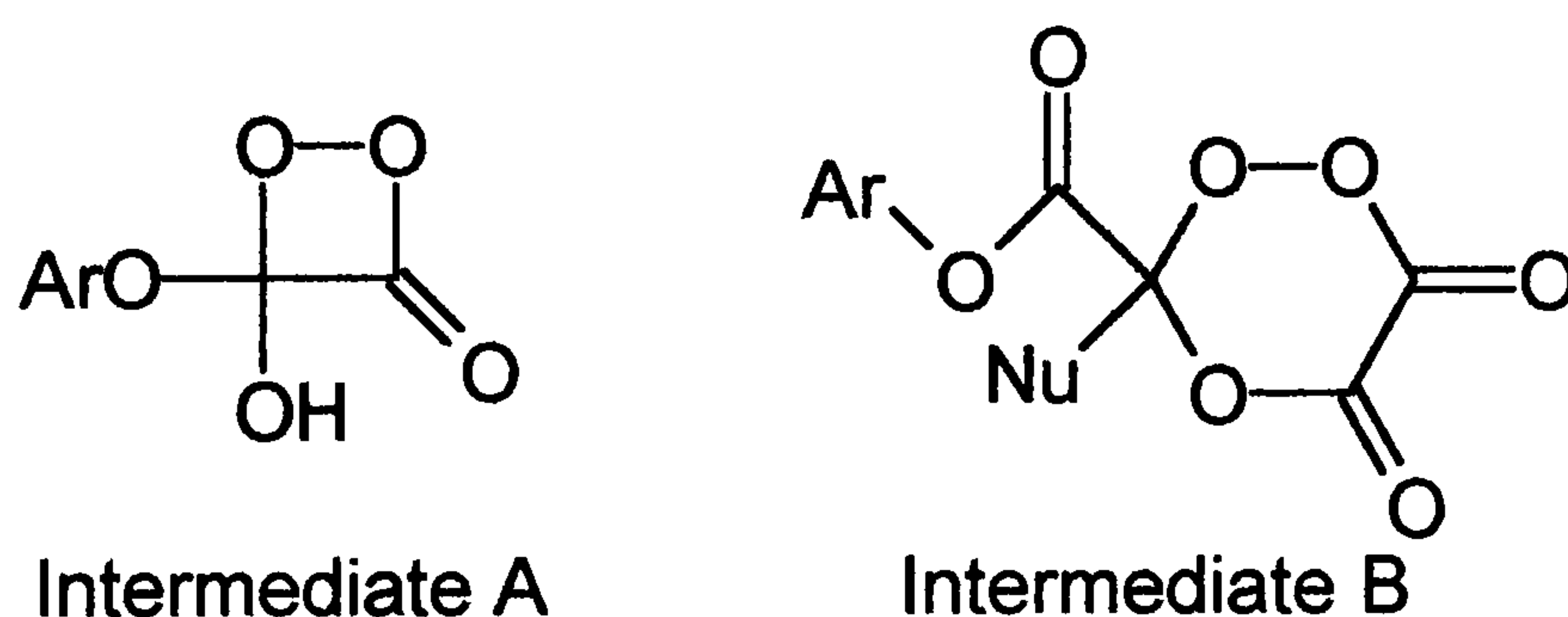
It was found<sup>40</sup> that oxalate esters with electronegative substituents have the largest chemiluminescent efficiencies. The presence of electronegative substituents on the aromatic rings makes the O-Ar better leaving groups increasing the reaction rate. This is consistent with the scheme proposed by Rauhut.<sup>41</sup> In this scheme the reaction is initiated by the nucleophilic attack of hydrogen peroxide on one of the carbonyls of the ester followed by ring formation in which the OOH substituted in the first stage displaces the second OAr giving the dioxetanedione intermediate. This is shown in Scheme 2.6.



Scheme 2.6

Chemiluminescence from dioxetanes and dioxetanones, which are structurally related to the proposed dioxetanedione intermediate, is postulated to proceed thorough a chemically initiated electron exchange luminescence (CIEEL) mechanism.<sup>42</sup> McCapra<sup>43</sup> incorporated the CIEEL mechanism into the peroxyoxalate mechanism. He postulated a short-lived charge transfer complex between the dioxetanedione intermediate and the fluorophore. The return of the electron to the fluorophore is sufficiently energetic to leave the fluorophore in the excited state. Many attempts have been made to explain the strong dependence of the chemiluminescence efficiency on the structure of the aryl group.

Several other intermediates have been proposed. Catterall<sup>44</sup> proposed a cyclic high-energy intermediate in which the aryl group stabilises the formation of charge transfer complexes with the fluorophore. The proposed structure is shown as intermediate A below. Milofsky<sup>45</sup> postulated intermediate B. Multiple pathways might also be involved.



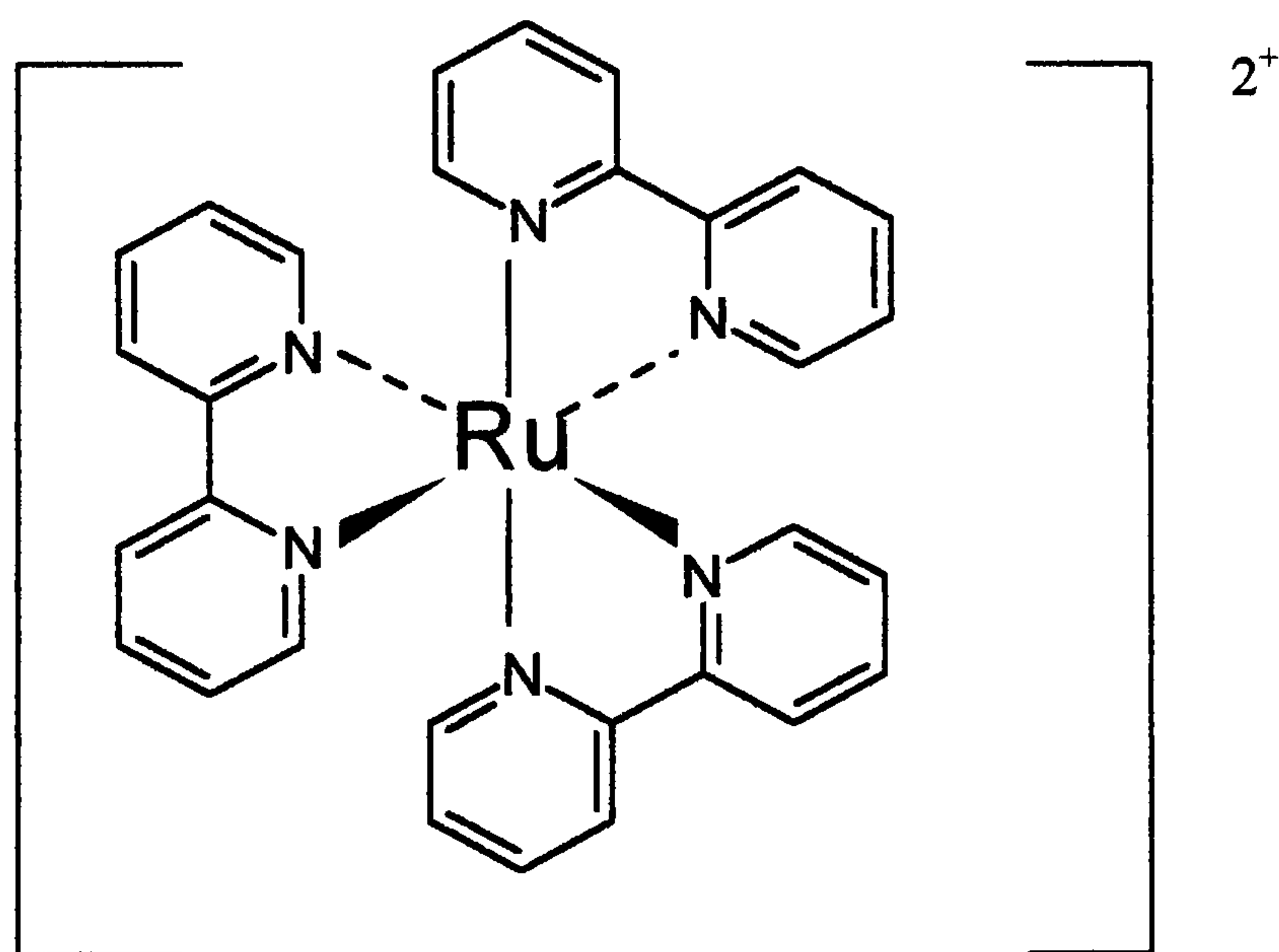
Analytically peroxyoxalate chemiluminescence can be used to measure any of the reagents involved in the reaction, that is fluorophore, base catalyst, peroxide or oxalate. Most commonly the fluorophore is the analyte and a 100-fold increase in sensitivity over conventional fluorescence measurement can be achieved. Peroxyoxalate chemiluminescence is widely used as a post column detection system for HPLC of environmentally important fluorescent materials such as carcinogenic polyaromatic hydrocarbons (PAHs).<sup>46</sup> It is also widely applicable in trace analysis of



analytes such as amino acids, which can be readily derivatised with fluorescent reagents such as dansyl chloride. Determinations in the fm range have been reported.<sup>47</sup> Some readily oxidised non-fluorescing compounds can quench the peroxyoxalate signal. As there are relatively few of these in biological samples this can be a selective technique.<sup>48</sup> The main limitation of the use of peroxyoxalate systems is the incompatibility of aryl oxalate esters with water and their limited solubility in the organic solvents, such as acetonitrile, generally used in HPLC.

#### 2.1.9.4 Ruthenium and Electrochemiluminescence

Many systems are being developed that are based on the chemiluminescence of Tris(2,2'-bipyridyl)ruthenium ( $\text{Ru}(\text{bpy})_3^{2+}$ ).



Chemiluminescence from  $\text{Ru}(\text{bpy})_3^{2+}$  was first described in 1966.<sup>49</sup> It is produced when various oxidants or reductants react with the oxidised or reduced forms of  $\text{Ru}(\text{bpy})_3^{2+}$  giving the excited species which emits at 610nm. Chemically generated  $\text{Ru}(\text{bpy})_3^{2+}$  has been used with chromatographic systems and recently with capillary electrophoresis.<sup>50</sup> The oxidised and reduced forms can also be generated electrochemically where an annihilation reaction between reduced and oxidised forms generated gives the excited species. The original  $\text{Ru}(\text{bpy})_3^{2+}$  species is regenerated.



Applications for  $\text{Ru(bpy)}_3^{2+}$  ECL in flow injection, HPLC and biosensors have been described.<sup>51</sup> Electrogenerated chemiluminescence is increasingly used as an analytical technique. It has the advantage that the reacting species are produced in situ from stable precursors allowing use of unstable reagents. The systems are more complex than those using chemiluminescent reagents. Electrochemical cells are required which can be subject to problems such as fouling of electrodes. Electrode cleaning protocols are often required to achieve adequate repeatability.<sup>52</sup>

#### 2.1.9.5 Singlet Oxygen

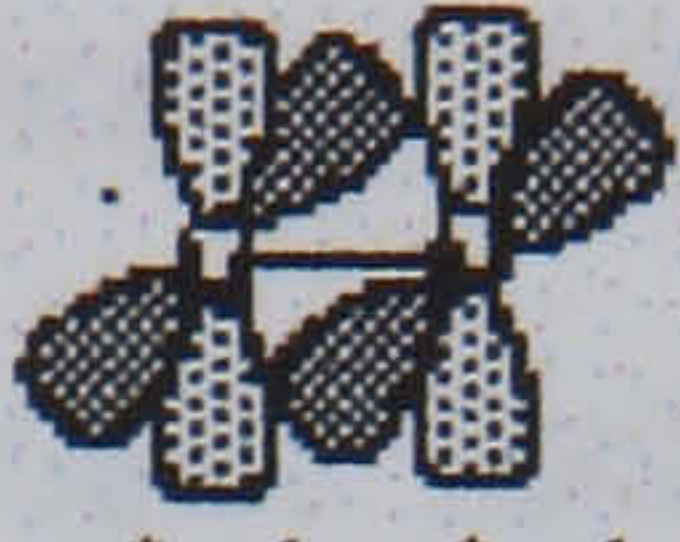

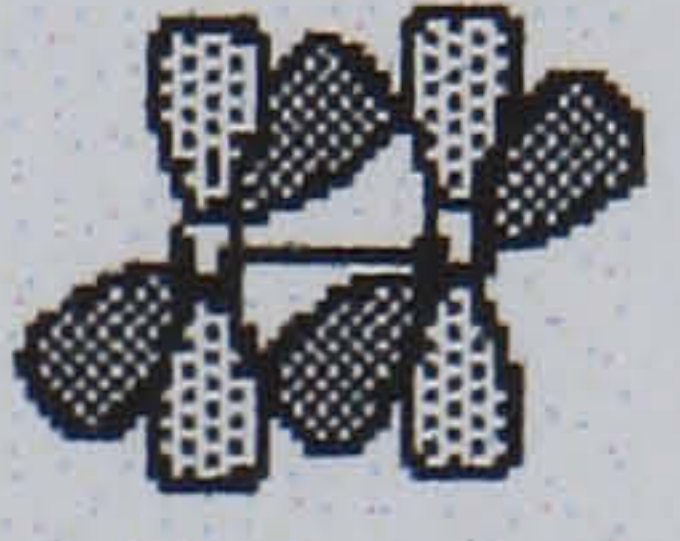
A species considered responsible for chemiluminescence in a range of reactions is singlet oxygen. Singlet oxygen is produced in many inorganic reactions in solution for example the reaction of hydrogen peroxide with hypochlorite. This reaction is accompanied by the evolution of large amounts of gas.



The orbital configurations of the three lowest states are shown in table 2.1<sup>15</sup>



**Table 2.1 Electronic Orbital Configurations of Molecular Oxygen**

State	Orbital Occupancy	Spectral Designation	Lewis Structure	Orbital Description
$S_2$	$\uparrow \quad \downarrow$	$^1\Sigma_g$	O-O ..	 $(\pi_x^*)^1(\pi_y^*)^1$
$S_1$	$\uparrow\downarrow \quad \text{—}$	$^1\Delta_g$	O=O	 $(\pi_x^*)^2$
$T_0$	$\uparrow \quad \uparrow$	$^3\Sigma_g$	O-O .	 $(\pi_x^*)^1(\pi_y^*)^1$

The emission spectrum shows sharp bands characteristic of gas phase emissions with energies as shown in table 2.2

**Table 2.2 Emission Bands from Singlet Oxygen**

Transition	Energy $\text{kJmol}^{-1}$	$\lambda_{\text{max}}$ nm
$^1\Delta_g \rightarrow ^3\Sigma_g$	94	1268
$^1\Sigma_g \rightarrow ^3\Sigma_g$	157	762
$^1\Delta_g \rightarrow ^1\Delta_g \rightarrow 2^3\Sigma_g$	189	634 $v=0$
		703 $v=1$
$^1\Delta_g \rightarrow ^1\Sigma_g \rightarrow 2^3\Sigma_g$	250	478

The strongest bands are the two from the  $^1\Delta_g \rightarrow 2^3\Sigma_g$  transition arising from the first two vibrational levels of the singlet state dimol.<sup>53</sup> Singlet oxygen has been suggested as the emitting species in reactions such as peroxide oxidation of formaldehyde.<sup>54</sup>



## **2.2 Flow Analysis**

### **2.2.1 Flow Injection Analysis**

The technique of flow injection analysis (FIA) was introduced in 1975 by Ruzicka and Hansen<sup>55</sup> and has become one of the most widely used techniques in routine analysis. Up to 1997 over 7000 papers were published on this technique. It is a continuous method of analysis in which samples are injected into a flowing stream contained in a narrow tube. This allows dispersion of the injected solution in a controlled manner.

Prior to the introduction of FIA, continuous flow methods based on the work of Skeggs<sup>56,57</sup> were in wide use. The Skeggs system, which was commercialised in the Technicon Autoanalyser systems, used bubbles of air or nitrogen to segment the flowing streams to reduce carry over between samples. The first continuous flow systems were developed for the determination of urea and glucose in blood and had the advantage over automated batch reactors of lower reagent consumption and mechanically simpler equipment. The factors controlling dispersion in segmented streams were studied by many groups<sup>58</sup> in order to optimise flow, segmentation and frequency for any tubing system.

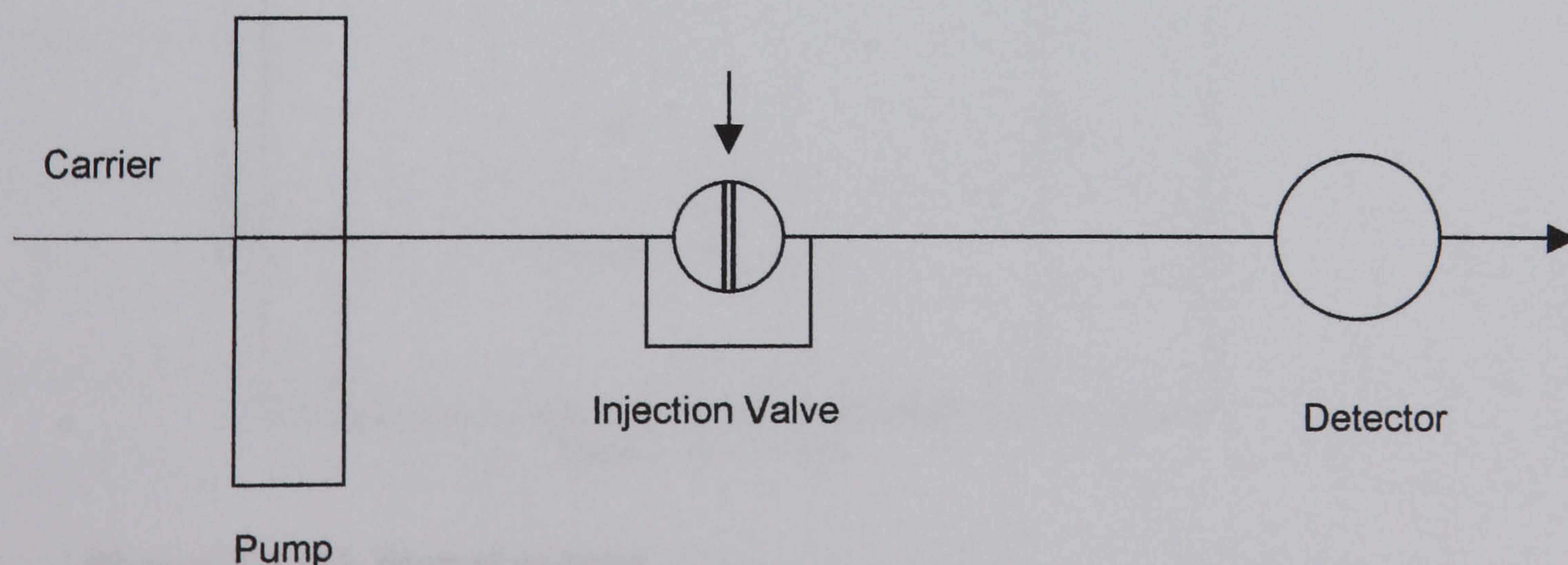
In a flow injection system the reagent stream is unsegmented and continuous. The sample is injected as a zone, which is transported towards a detector, which continuously records a physical parameter such as absorbance or electrode potential. During the passage towards the detector the sample zone disperses in a reproducible way and reacts with the reagents in the carrier stream. As there is no requirement to remove gas bubbles, design of the detector is simpler than for segmented flow. A comparison of the parameters for segmented and flow injection analysis in Table 2.3 shows the advantages of the FIA system over segmented flow systems.



**Table 2.3 Comparison of Segmented Flow and Flow Injection Analysis**

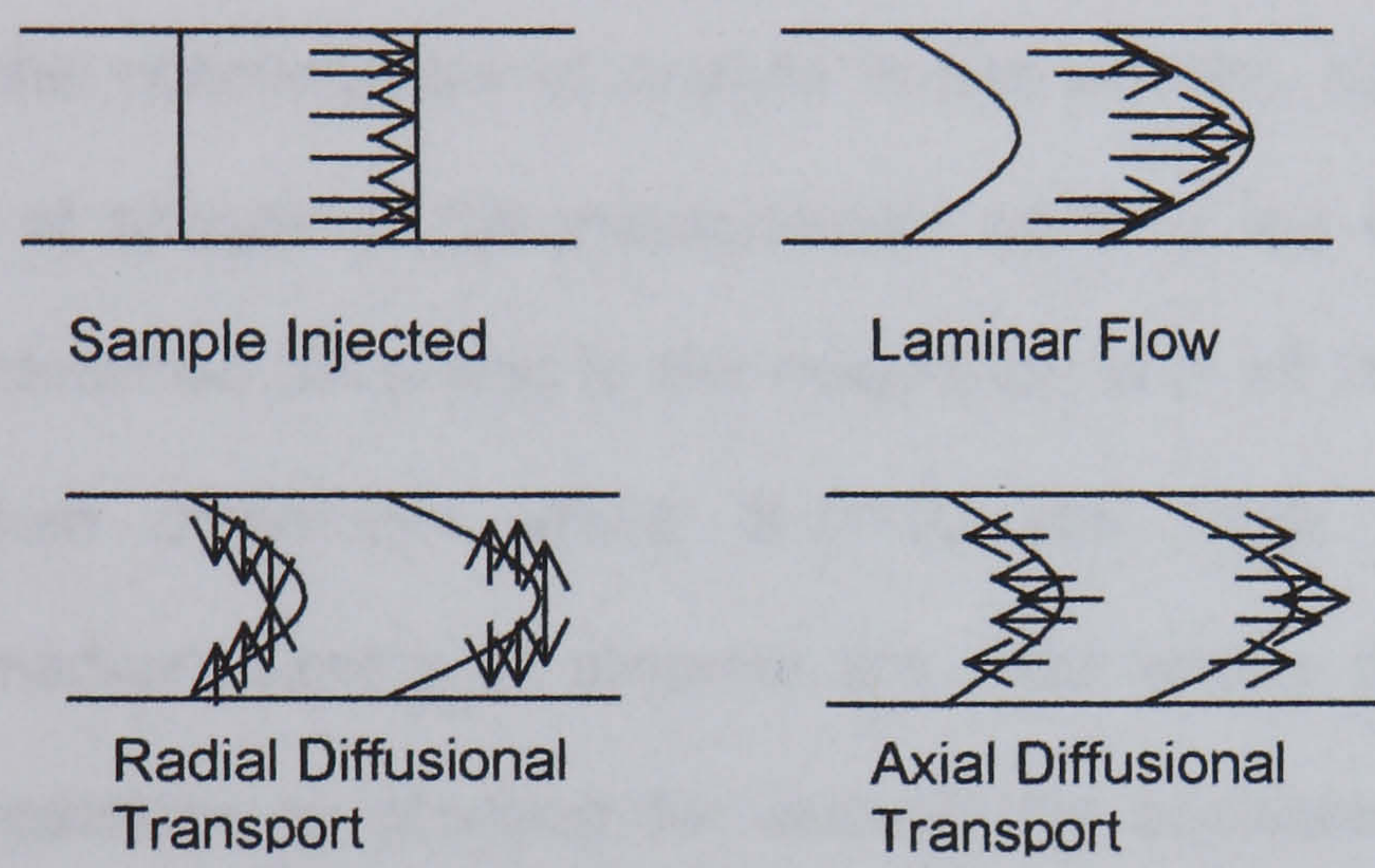
	Segmented Flow	Flow Injection
Sample Introduction	Aspiration	Injection
Sample Volume/ $\mu\text{L}$	200 to 2000	10 to 100
Response Time/sec	120 to 2000	3 to 60
Tubing i.d./mm	2	0.5 to 0.7
Detection	Equilibrium homogeneity	Controlled partial dispersion
Throughput/samples $\text{hr}^{-1}$	80	300
Precision/%	1	1
Reagent consumption	High	Low
Washout Cycle	Essential	None
Kinetic Analysis	Not Possible	Possible
Data	Peak Height	Peak Height Peak Area Peak Width Peak-Peak Distance Data from doublets

In its simplest form, as shown in Figure 2.3, a pump propels the carrier stream through a tube and a specific, reproducible volume of sample is injected. After a period of dispersion, during which chemical reactions may occur, the sample passes through a detector.

**Fig 2.3 Single Line FIA Manifold**

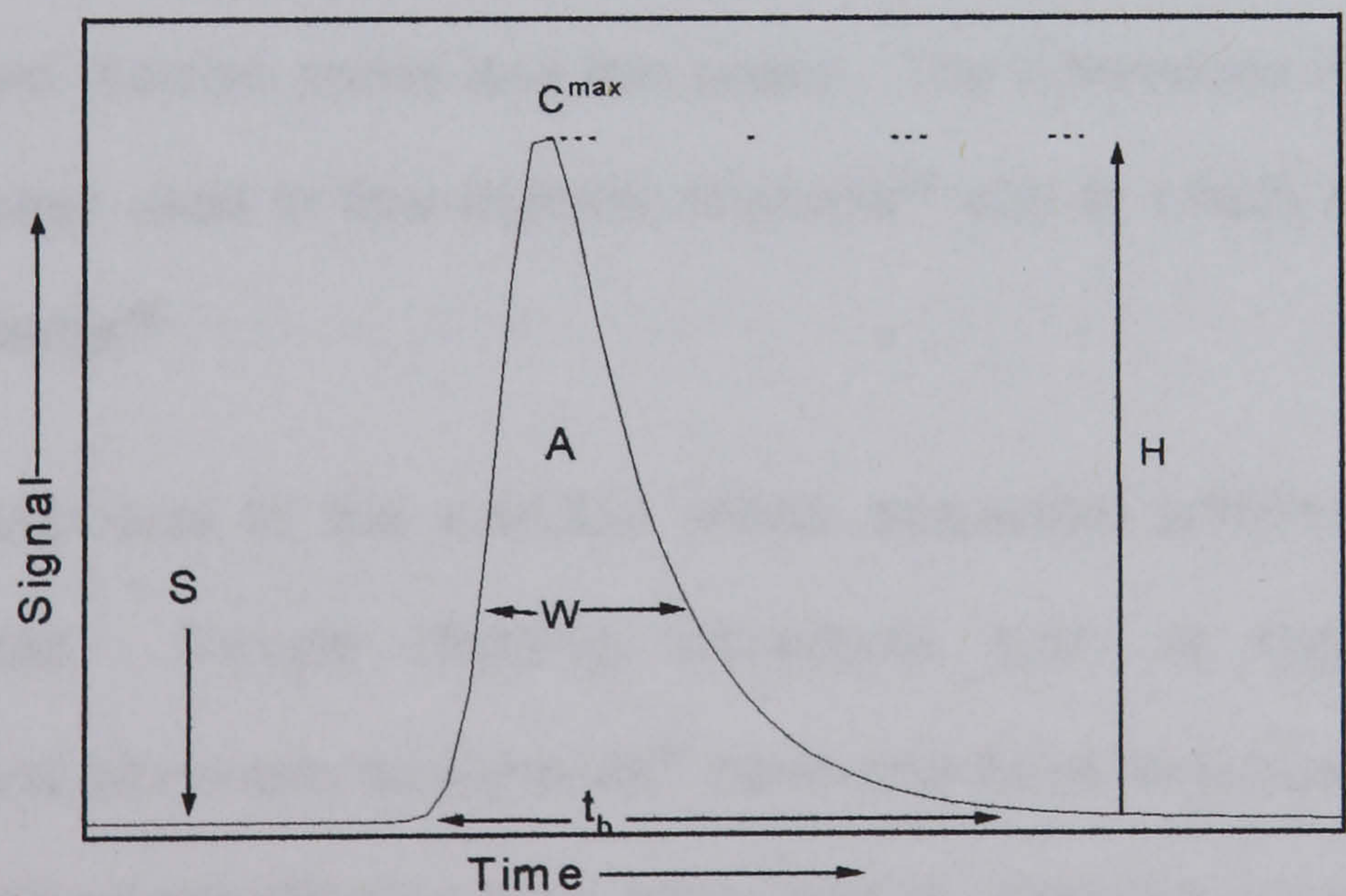


In an ideal injection system the sample is injected as a plug. In narrow tubing blocks of fluid move more quickly in the centre of the tube than near the walls giving the parabolic profile of laminar flow. In addition diffusion occurs axially and radially between the blocks of fluid. This secondary movement of fluid results in a washout effect accounting for the low mutual contamination of successive samples.



**Fig 2.4 Convective and Diffusional Transport in Flow Injection Analysis**

Output to a chart recorder the detector response is in the form of a peak Figure 2.5



**Figure 2.5 FIA Signal output**

S- Injection point, H-Peak height, A- Peak Area, W -Peak Width,  $t_b$ -Peak Width at baseline  $C^{max}$ -maximum concentration of analyte



Height, area and width<sup>59,60</sup> can all be used quantitatively, however peak height is most commonly used. The peak height is related to the concentration of the injected solution by dispersion D as follows:

$$D = C^0 / C^{\max}$$

Where  $C^0$  is the concentration of analyte in the solution injected and  $C^{\max}$  is the concentration of analyte at the measurement point or top of the analytical peak. Systems are classified according to the magnitude of D as limited dispersion where  $1 > D > 3$ , medium dispersion where  $3 > D > 10$  and large dispersion for  $D > 10$ . Analytically, medium dispersion systems are most widely used as sufficient time elapses for reactions to proceed far enough for accurate measurement of the reaction products. In the case of fast chemiluminescent reactions limited dispersion systems are often appropriate.

The factors affecting dispersion have been reviewed.<sup>61,62,63</sup> Where a relatively large sample volume is injected little or no mixing occurs in the middle of the sample zone resulting in two reaction zones and two peaks. The differences in peak heights or areas have been used in flow injection titrations<sup>64</sup> and to obtain kinetic data<sup>65</sup> and stability constants.<sup>66</sup>

Addition of elements to the manifold allows sequential addition of reagents as merging zones. Sample clean-up procedures such as dialysis, liquid-liquid extraction<sup>67</sup> and enzymatic conversions<sup>68</sup> have also been developed. Flow injection methods based on gas diffusion have been used, for example in the determination of ammonia from protein digests. The acid digest is injected into a carrier stream which is merged with a stream containing excess hydroxide. Ammonia gas is generated which diffuses across a gas permeable membrane into an acceptor stream containing an indicator.<sup>69</sup> A particular advantage of flow injection systems is the

possibility of using unstable reagents, which are formed in the manifold immediately prior to reaction with the analyte. Examples are strongly reducing agents, which are unstable to atmospheric oxidation. Unstable chromium (II) has been generated in a flow system and used immediately.<sup>70</sup> Partial re-oxidation can occur but is reproducible and therefore does not affect precision.

### **2.2.2 Sequential Flow Injection Analysis**

A recent development, which uses the principles of controlled dispersion, is sequential injection analysis (SIA). Introduced by Ruzicka and Marshall,<sup>71</sup> it involves aspiration of sequential aliquots of sample reagents and carrier solutions into a holding coil. Reversing the flow direction allows dispersion and reaction, as in conventional flow injection. The flow then proceeds to the detector. Recently a new SIA system has been proposed and applied to the determination of phosphate by the molybdenum blue reaction. In this system the sample forms the carrier and reagents are sequentially injected. This system corresponds to reverse flow injection and is particularly applicable to process control systems.<sup>72</sup> SIA has the advantage that a single manifold can be applied to many systems and that reagent and sample consumption are very low. The requirement for accurate timing of valve and pump movements, hence computer control, makes the system more expensive to set up.<sup>73</sup>

### **2.2.3 Post Column Applications**

Flow injection principles have wide application as post column systems in chromatography. The analyte is separated from other components in the sample in the chromatographic column, where it also undergoes dispersion. Reagents are added to the column eluate to derivatise the analyte or to modify the mobile phase, to facilitate detection by an appropriate detector. As with classical FIA, non-segmented systems have replaced earlier segmented systems.



## 2.2.4 Instrumentation for Flow Injection

### 2.2.4.1 Pumps

Peristaltic pumps, commonly used in FIA, have the advantage of low cost and reliability. Pump tubes of different materials make these pumps compatible with a wide range of solvents and reagents. The direction of flow can be easily changed for SIA applications. Peristaltic pumps can be subject to considerable pulsation, particularly where significant back-pressure is introduced by manifold components. Wear of pump tubes can result in gradual changes in flow rate and hence slow drift of the analytical signal. Reciprocating pumps are less suitable as they require pulse damping and cannot be reversed. They are most often used in post column applications in chromatography, where high back-pressures may be present. Syringe pumps provide smooth pulse-less and reversible flow and are the pumps of choice for SIA. They are expensive and have limited capacity, requiring refilling between experiments. The use of a diaphragm micropump has been reported where the rapid oscillation of the diaphragm at 50-60Hz results in very little flow pulsation.<sup>74</sup>

### 2.2.4.2 Injection Systems

Precision in FIA is dependent on accurate and reproducible injection. The system most often used consists of a loop injection valve as used in HPLC.

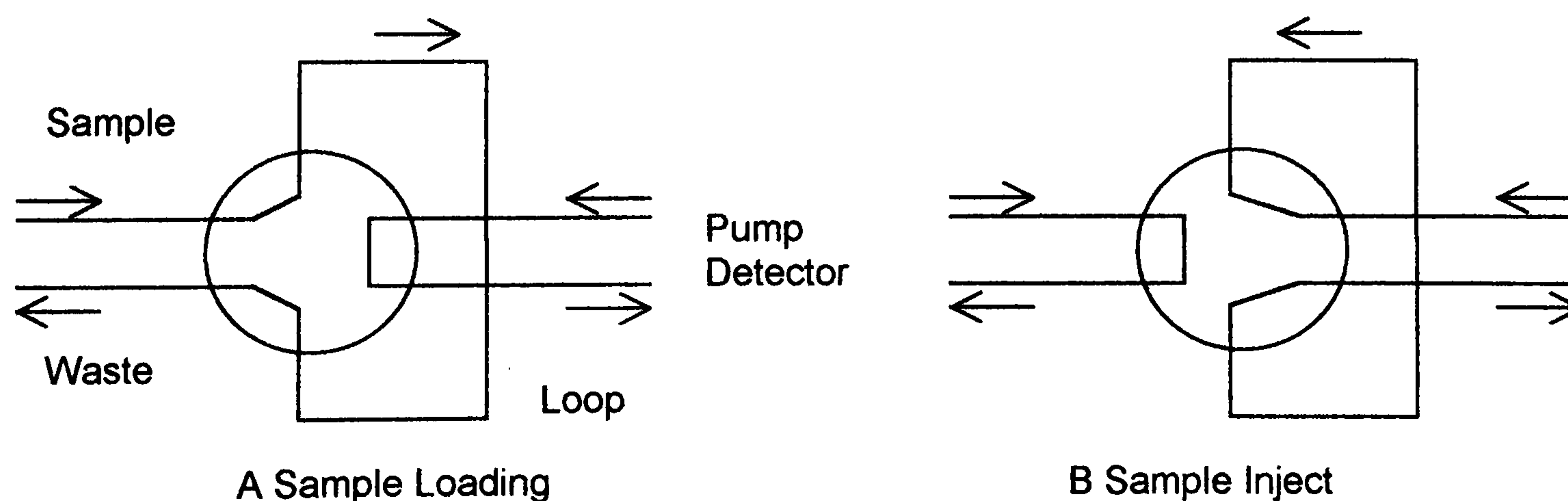


Figure 2.6 Loop injection valve for FIA



Ideally the carrier flow should not be disturbed, however as the valve is turned all the channels are temporarily closed giving in a rise in back pressure, then a pulse on reaching the inject position. It is important that the valve is actuated quickly and reproducibly, therefore motor and pneumatic actuators are often used. Valve injection is also appropriate for sequential systems in which case a multi-port valve is used, with each reagent/carrier/sample delivered through adjacent ports.

#### **2.2.4.3 Manifold Design**

The simplest manifold design is the single line system described above. The tubing in which dispersion occurs is typically 0.5 to 1mm internal diameter, of a chemically stable material such as PTFE. Mixing of reagents is achieved using Y or T pieces of inert material. For chemiluminescence applications, where limited dispersion is required, the narrower tubing diameters, up to 0.5mm id are preferred. Where delays are required, for a slow reaction to take place, delay coils of dispersion tubing are used. Generally reactor tubing is wound in coils, however more complex formats such as knitted open tubular (KOT) reactors have been recommended, in order to reduce dispersion while achieving adequate radial mixing.<sup>75</sup> FIA systems are generally low pressure and push fittings are often sufficient for linking tubes, however flanged and ferrule joints are also used. Joints must be smooth to avoid disturbances of laminar flow.

For many applications the analyte is injected into the stream of carrier. FIA systems, in which a reagent is injected into a stream containing the analyte, are generally called reverse FIA. These are widely where the analyte stream is taken from a process or the reagent is expensive or hazardous.



#### 2.2.4.4 Detection Systems

Spectrophotometry is the most widely used detection system and many reactions giving products which absorb light in the visible or ultraviolet, or are fluorescent, have been automated in flow injection format. Examples of analytes include cations,<sup>76,77,78</sup> anions,<sup>79, 80</sup> and organic species such as glucose.<sup>81</sup> Metals are also commonly detected by atomic absorption spectrometry.<sup>59</sup>

Electrochemical detectors based on potentiometric, amperometric and conductimetric measurement are used. An alternative to conventional conductimetry is the bulk acoustic wave impedance sensor (BWIAS), which does not suffer from high background signals; it has recently been described for use in FIA systems.<sup>82</sup>

Flow injection incorporating gravimetric determination has been described.<sup>83</sup> A precipitate of cuprous oxide is formed from the reaction of reducing sugars with Fehling's solution and is gathered on a glass sinter suspended under an analytical balance. Good repeatability was reported demonstrating the repeatability of a flow injection format. The time-consuming washing and drying stages of classical gravimetry were not required.

Recently flow injection has been used to deliver samples to biosensors. Biosensors are analytical devices consisting of a transducing element covered by an appropriate layer of a recognition material, which is brought into contact with the sample. Transducers are commonly electrochemical or optical. Recognition elements consist of one or more enzymes immobilised in a membrane or layer, or immunological components, for example antibodies. Whole cells or tissues can also be used.<sup>84</sup> The performance of biosensors is generally diffusion controlled, particularly in the case of electrochemical transducers. Flow injection, which has strictly reproducible timing of events in the assay cycle, is particularly appropriate. In a flow injection system the



time of exposure of analyte to the recognition layer, and hence the amount of analyte converted, can be readily controlled by variation of flow rate. The analytical range of the assay can be controlled in this way. The time of exposure can be used to discriminate between analyte and interfering species, which may diffuse at different rates in membranes.<sup>85</sup> FIA/biosensor applications have been reviewed by Hansen.<sup>86</sup>

### **2.2.5 Flow Injection with Chemiluminescence Detection**

Many chemiluminescent reactions are fast and are therefore particularly suited to FIA systems. Applications of chemiluminescence in flow injection have been reviewed.<sup>9</sup> All the major solution reactions, discussed in section 2.2.1, have been used in FIA. In particular a large number of applications use luminol chemiluminescence to determine metals. A wide range of transition metals is known to enhance luminol chemiluminescence.<sup>87</sup>

Chemiluminescence has several features, which make it particularly suitable for use in flow injection. The reactions are often fast therefore the limited dispersion of flow injection results in sharp peaks and high sampling rate. As no external light source is required the detection of chemiluminescence is limited only by the sensitivity of the light detector used. No scattering is present in the detector eliminating a major source of noise in fluorescence systems.

The most commonly used detector is the photomultiplier (PMT). Diode systems, charge-coupled devices (CCD) and photographic methods are also used. Systems available for detection of chemi- and bioluminescence have been reviewed.<sup>88 89</sup>

#### **2.2.5.1 Photomultipliers**

A PMT consists of an evacuated tube containing a photosensitive cathode consisting of two or more alkali metals, a chain of electrodes called dynodes and an anode.



When a photon strikes the photocathode a photoelectron is ejected as a result of the photoelectric effect. The photoelectron is focused towards the first dynode where it causes emission of a number of secondary electrons. These are accelerated and hit the next dynode each releasing a further number of electrons. Further multiplications occur along the dynode chain resulting in a pulse, typically 5 ns long, at the anode. This is output to a recorder or data capture device, via a signal amplifier if necessary. Amplifications of  $10^6$  are typical. In order to cause the photoelectric effect the wavelength of the light must be below a critical level, which depends on the photocathode material.

The kinetic energy  $E_{\text{kin}}$  of the photoelectron is given by :

$$E_{\text{kin}} = h\nu - W$$

Where  $W$  is the 'work function' of the photosensitive material,  $h$  is the Planck constant and  $\nu$  is the frequency of the light.<sup>90</sup> The threshold of the photoelectric effect corresponds to  $h\nu = W$  for which the velocity of emitted electrons is 0. While the photocathode has good sensitivity in the UV, in practice, the PMT range depends on the material of the window, generally optical glass, or silica. Photomultipliers commonly used for FIA/chemiluminescence systems have good sensitivity in the range 300 to 600nm, which is appropriate for the luminol  $\lambda_{\text{max}}$  at 425nm. Other PMTs can detect light in the near IR up to 1200nm but the quantum efficiency is lower.

For high sensitivity and low limit of detection it is necessary to achieve a high signal to noise ratio. This can be done by increasing the signal or decreasing the noise. If another signal is present it may be possible to identify and correct for it. Random noise is generally of a physical, often thermal, nature and can be characterised by frequency spectrum, amplitude distribution and the mechanism responsible for its generation. Contributors to the total include<sup>91</sup> Johnson noise generated by any



resistor across its terminals and is an example of white noise. It depends on the resistance and temperature, is irreducible and increases linearly with frequency. Shot noise is a consequence of the charge quantum nature of electric current. Flicker noise depends on the construction of the resistor, its material and connections and has a spectrum approximating to the reciprocal of frequency ( $1/f$ ).

For a PMT “dark noise” is that produced when the photocathode is shielded from external optical radiation. Wright<sup>92</sup> has reviewed the factors affecting the noise in a PMT. Dark current is dependent on temperature and cooling the photocathode to around 0°C can reduce noise significantly. Other sources of noise are Cerenkov radiation from cosmic rays, from radio-isotopes, such as <sup>40</sup>K, present in the glass of the tube, dust and potential gradients in the tube envelope. Residual gas molecules can be ionised near the anode, light emission can occur resulting in optical feedback to the photocathode. If photocathode material is deposited on dynodes in manufacture the dynodes can behave as weak photocathodes giving a pre-pulse at. After pulses are probably due to ionisation of residual gas between the cathode and the first dynode. These can be, in the order of 1% per photoelectron, but can be reduced by the use of suitable focusing before the first dynode. Exposing the photocathode to quite low levels of ambient light increases dark noise and it can take up to several days for the dark noise to reach equilibrium after exposure. Noise can be minimised by keeping the PMT clean, cooling and shielding from radiation. Spikes, or burst noise, can be caused by temporary breakdown of capacitors.

In addition to the noise arising from the PMT, noise can arise from amplifier components and recording equipment, resulting in little gain in S/N on amplification. While photomultipliers are sensitive and versatile, a problem is reproducibility of signal, which can be poor. It is necessary to calibrate PMTs with appropriate standards on each use. Miniature PMTs are now available which can be powered by 12V supplies, enabling development of small systems for field use.



### **2.2.5.2 Photodiode Systems**

These form the basis of many commercial luminometers and chromatographic detectors. The wavelength range depends on the diode material and most systems have a range up to 1500 nm making them particularly useful in the near infra red, for example the gas phase emission of nitrogen dioxide. Diode array and intensified diode array systems have been used to collect chemiluminescence spectra.<sup>93</sup> Diode systems are robust and can be connected to fibre-optic systems for remote sensing.

### **2.2.5.3 Photographic Systems**

Photographic systems have long been used for visualising chemiluminescent reactions and are very sensitive as long exposure times can be used. They have been used to image ultraweak chemiluminescence<sup>94</sup> and that from living cells. A widely used application of photographic systems is molecular biology for DNA studies where labelled probes with specific probe binding are detected by the use of chemiluminescent substrates and autoradiography. These probes typically have the same sensitivity as radioactive labels and need shorter exposure times.<sup>95</sup>

### **2.2.5.4 Charge Coupled Devices (CCD)**

With similar applications to photography, CCD systems have the advantage of electronic storage of images, and have been used in systems for quantification of protein and nucleotide blots and micro-titre plates. The systems have high sensitivity and good resolution but are expensive and require extensive data handling capacity. As with autoradiographic systems, the data is recorded in two dimensions<sup>96</sup> and spectral information can also be obtained.



## 2.3 Stopped-flow Techniques

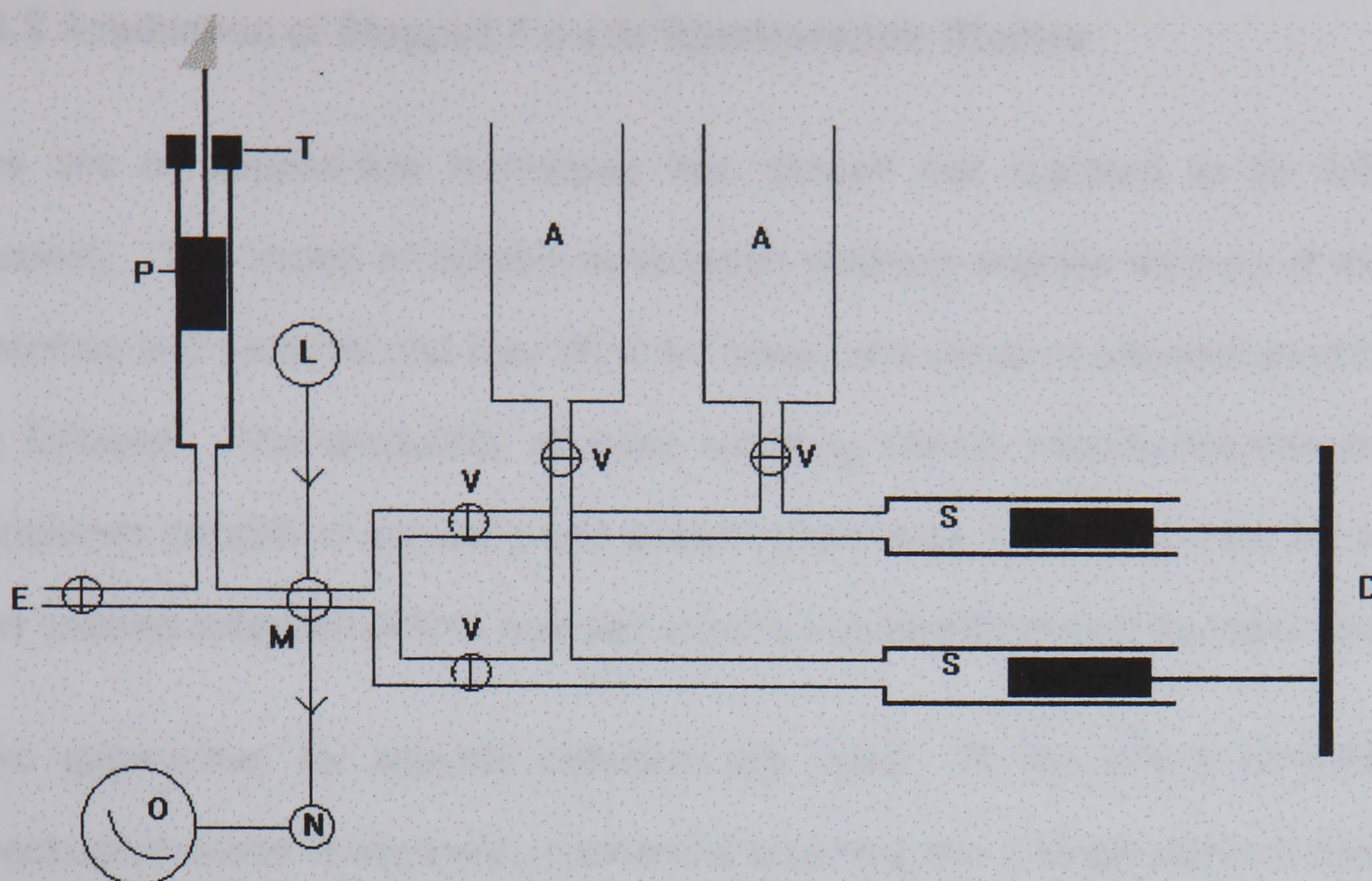
### 2.3.1 Principle of the Stopped Flow technique

The stopped-flow technique, introduced by Chance in 1940,<sup>97,98</sup> was developed to study the kinetics of fast reactions. The technique has been reviewed by Crouch<sup>99</sup> and GomezHenz.<sup>100</sup>

The basic instrumentation consists of a mixing chamber, into which two reagents are rapidly delivered. The flow is stopped suddenly so that the solution comes to rest in a very short time, of the order of a few milliseconds. An observation point is present after the mixing chamber where measurements are made on a stationary element of mixed solution. The reaction is followed using a rapid technique such as absorbance or fluorescence spectrophotometry, thermal measurements or electrochemistry.

Most systems are based on the design introduced by Gibson<sup>101,102</sup> which was developed for the study of enzyme kinetics. In this system the flow through the observation chamber is stopped by a small piston which is pushed along by the reaction mixture until it reaches an external stop. This brings a portion of mixed reactants to an almost instantaneous stop in the observation chamber. The syringe can be arranged to contact a microswitch and so initiate data capture by associated equipment. Figure 2.7 shows a typical system. The system can be actuated manually or, by means of a pneumatically driven piston. The key features of the system are the syringes, the mixing system and the observation point. The drive and stopping syringes need to move smoothly and now typically consist of smooth bore glass with Teflon tipped plungers.<sup>103</sup> To enable fast reactions to be observed the mixing of reagents must be accomplished, within 1-2ms To minimise dead time, the distance between the mixing point and the observation point must be short. Dead time has been defined as the time taken by the solution to flow from the mixer to a point half way through the observation cell.<sup>100</sup>





**Figure 2.7 Schematic of a Gibson Stopped Flow system:**

A sample reservoirs, V valves, T seating, P stopping piston, S drive syringes, D drive plate, E exhaust valve, L light source, M mixing point, N photomultiplier, O oscilloscope

Simple stopped-flow systems such as the system of HiTech Scientific Ltd,<sup>104</sup> use T piece mixing where one reagent flows at right angles into the other. This is adequate for reactions with half times of 10 msec or more. More complicated mixing systems have been proposed, including jets arranged semi-tangentially, to impart a rotary motion to the liquid, giving effectively complete mixing within one or two msec. Detectors must be capable of following signal change in the millisecond range. UV-visible spectrophotometry is the most often used. Electrochemical and more recently mass spectrometric detectors<sup>105</sup> have been used. As reaction rates are strongly dependent on temperature accurate thermostating is recommended.

Stopped flow technique has been most used to obtain rate information on fast reactions but is becoming more used in routine analytical applications.<sup>106</sup>



### **2.3.2 Application of Stopped Flow to Spectroscopic Studies**

The use of stopped-flow techniques has allowed fast reactions to be followed precisely. The choice of suitable observation methods enables tracking of starting materials and products and may allow formation and decay of transient products to be followed. The availability of rapid scanning UV-vis spectrophotometers and computers capable of acquiring and analysing the large volumes of data generated has enabled collection of time resolved spectra and identification of transient species.

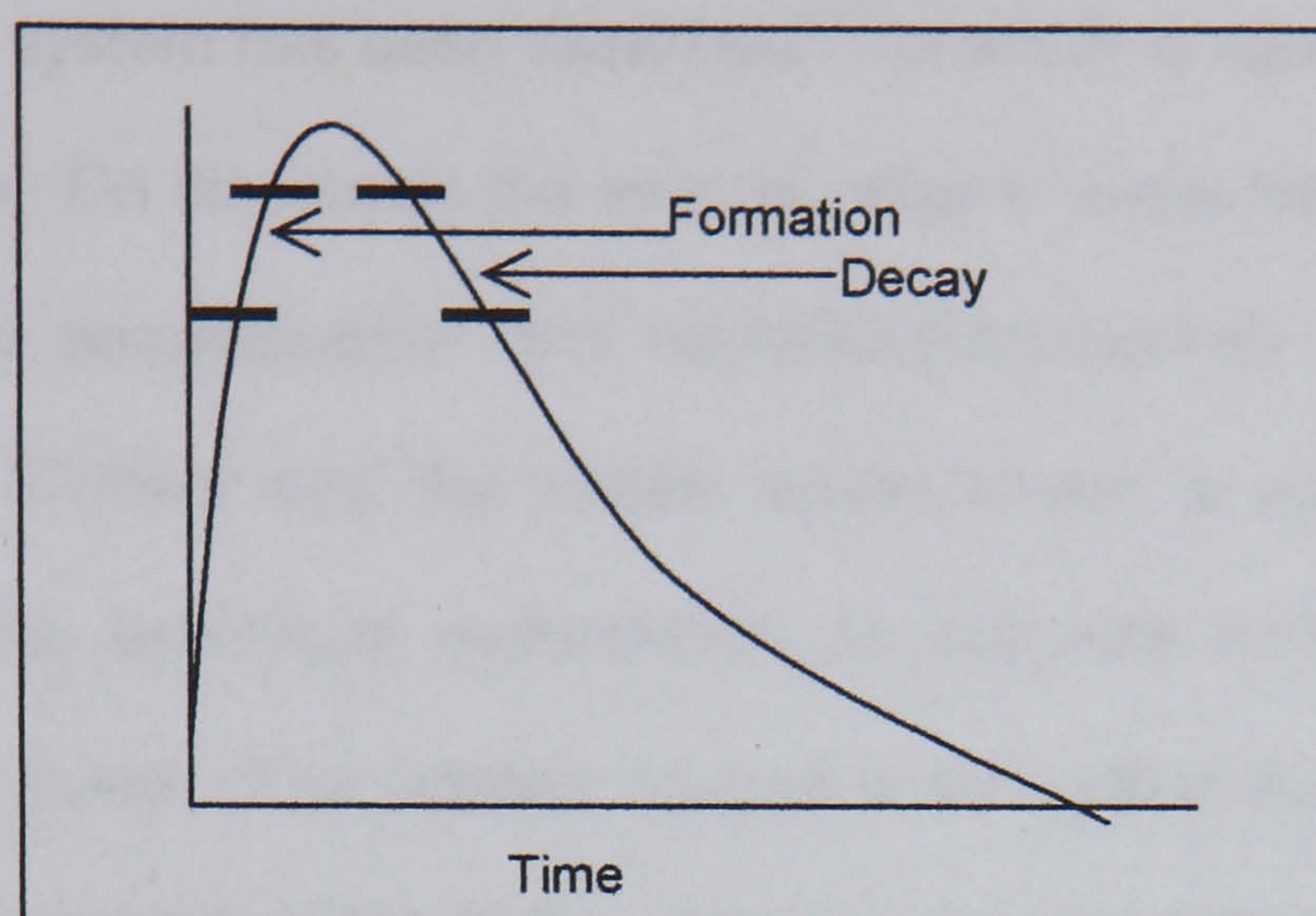
Two approaches for spectral collection are used. In the first a conventional spectrophotometer is used with mechanical scanning and a single element detector. The signal is sampled at a high rate relative to the scan rate. Alternatively a diode array system can be used with full spectrum illumination of sample. Post-sample the light is dispersed in a polychromator and collected on a linear diode array, spectra being formed from the individual elements of the array. In each case the data is acquired as a three-dimensional data-set with absorbance as a function of wavelength and time. The technique has been applied in studies of transition states in enzyme reactions.<sup>107</sup>

### **2.3.3 Application of Stopped Flow to Chemiluminescence**

Stopped-flow technique was applied to chemiluminescence by Chance et al<sup>108</sup> who looked at the kinetics of light production from the reaction of luciferin/luciferase/oxygen. Using photographic recording of a cathode ray oscilloscope the decay was found, in some cases, to be exponential. Repeatability was poor, probably due to the use of crude extracts of luciferase. Many stopped-flow systems have used luminol as the chemiluminescent reagent. Perez-Bendito and co-workers have used the maximum of the time/luminescence profile<sup>109</sup> and rates of chemiluminescence generation and decay.<sup>110,111,112</sup>



A typical intensity time profile is shown in Figure 2.8



**Figure 2.8 Intensity-Time profile for a Stopped-flow Experiment Showing Zones used for Determination of Rates of Formation and Decay.**

Wide dynamic ranges have been achieved using the measurement techniques, peak height, peak area and rates of formation and decay. Hydrogen peroxide in the range  $5 \times 10^{-5}$  to  $1 \times 10^{-8}$  mol dm<sup>-3</sup> was measured using the luminol-peroxide-cobalt system.<sup>110</sup>

#### **2.3.4 Stopped-flow in Flow Injection**

In addition to stopped-flow as described above, analytical, particularly kinetic data can be obtained by stopped flow injection.<sup>113,114</sup> A conventional flow injection system is used, in which the analyte is injected into a stream of carrier. In the dispersed zone a concentration gradient of analyte in carrier is formed and after a determined time the flow is stopped and dispersion ceases. The change in signal of the element of solution in the detector then depends on the rate of the reaction. By selection of the interval between injection and stop time different points on the dispersion gradient, corresponding to different analyte concentrations can be observed. Both single line manifolds and merging zones have been used and permanganate oxidations have been studied by this technique.<sup>115</sup> Doubly stopped flow systems, have been described.<sup>116</sup> More than one aliquot of sample is injected and each is treated in a different way before being stopped in the observation cell.



Additional modifications can be used to increase selectivity in stopped-flow injection. A chasing zone system has been described<sup>117</sup> in which a second reagent is injected after the sample. On dispersion the second reagent reacts with the dispersion tail of the sample, the sample/carrier and sample/carrier/second reagent elements are stopped in the detector and the kinetic measurement is undertaken. Successful application of this technique depends on accurate timing and instantaneous response of the pump. The reaction mixture is stopped in the observation chamber by stopping the pump in front of the chamber, in contrast with the Gibson system where the flow is stopped after the observation point. Stopped-flow injection is not applicable to the very fast reactions, which can be examined by conventional stopped-flow.



2.4 Permanganate Oxidations

Oxidation reactions with permanganate ion in acid solution have been known for a long time and have been thoroughly reviewed.<sup>118</sup> Despite well over a century of study the mechanisms are still not fully understood.

The highest oxidation state of manganese is permanganate, Mn (VII),an ion with tetrahedral geometry.<sup>119</sup> The standard reduction potentials for manganese species in acid and base medium are shown below:

Table 2.4 Standard Redox Potentials for Manganese Species				
Oxidation State	Acid	Reduction Potential/V	Base	Reduction Potential /V
0	Mn		Mn	
		-1.19		-1.55
I				
II	Mn <sup>2+</sup>		Mn <sup>2+</sup>	
		+1.51		-0.20
III	Mn <sup>3+</sup> ( aq)D		Mn(OH) <sub>3</sub>	
		+0.95		+0.1
IV	MnO <sub>2</sub>		MnO <sub>2</sub>	
		+2.26		+0.93
V			MnO <sub>4</sub> <sup>3-</sup> D	
				+0.27
VI	HMnO <sub>4</sub> <sup>-</sup> D		MnO <sub>4</sub> <sup>2-</sup>	
		+0.56		+0.56
VII	MnO <sub>4</sub> <sup>-</sup>		MnO <sub>4</sub> <sup>-</sup>	

D Disproportionates

The first systematic study of the kinetics of the reaction between permanganate and oxalate was made by Harcourt and Esson in 1866.<sup>120</sup> Using iodometric methods, they studied the effects of permanganate and oxalic acid concentrations. The stoichiometry is precise and is used to standardise volumetric MnO<sub>4</sub><sup>-</sup> solutions.





It was also observed that addition of manganese sulphate at the start of the reaction increases the rate of reaction with the rate increasing up to the permanganate: manganese sulphate ratio of 2:3. The reaction was initially suggested to proceed by the initial formation of manganese dioxide and subsequent reaction of manganese dioxide with oxalic acid.

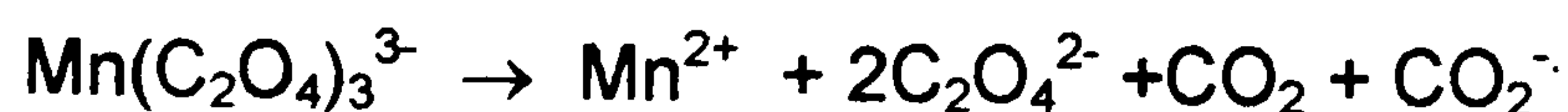
The reaction is autocatalytic in nature. Manganese (II), produced in the reaction can react with permanganate ion producing manganese (III) which is stabilised by complexation with oxalate.<sup>121</sup> The permanganate/ oxalate/ acid reaction was reported to yield chemiluminescence by Stauff and Bergman<sup>122</sup>, who reported blue and yellow/green emissions. These workers also suggested that when manganese (II) was present at the start of the reaction red emission occurs in addition to the blue and yellow/green emissions.

Manganese (III), disproportionates rapidly in water<sup>123</sup> as follows :



but can be stabilised by a range of inorganic and organic ligands including fluoride<sup>124</sup>, pyrophosphate,<sup>125</sup> azide<sup>126</sup> or a large excess of manganese(II). Complexes are readily broken down on heating, for example the manganese (III)-trioxalato complex is rapidly broken down at 60°. A mechanism involving a radical anion intermediate<sup>127</sup> has been proposed. The formation of this complex is the reason that permanganate/ oxalate titrations are normally carried out at elevated temperatures. The use of surfactants or crown ethers<sup>128</sup> has been proposed to prevent formation of the trioxalato complex and so increase the rate of reaction in oxalate/permanganate titrations.





Koupparis and co-workers<sup>129</sup> used stopped-flow to follow the disappearance of permanganate ion at 525 nm, in the first step of the reaction. They found that the reaction is first order in permanganate and Mn (II) and second order in oxalate ion. They used this relationship as the basis of a kinetic measurement of Mn(II).

Manganate (Mn VI) is stable in very basic solutions but in solutions less than 1mol dm<sup>-3</sup> in hydroxide concentration disproportionation occurs:



Manganate oxidations tend to be much slower than permanganate oxidations and oxidation with manganese V (hypomanganate) is even slower. In solutions lower than 4mol dm<sup>-3</sup> in hydroxide ion, disproportionation occurs rapidly:



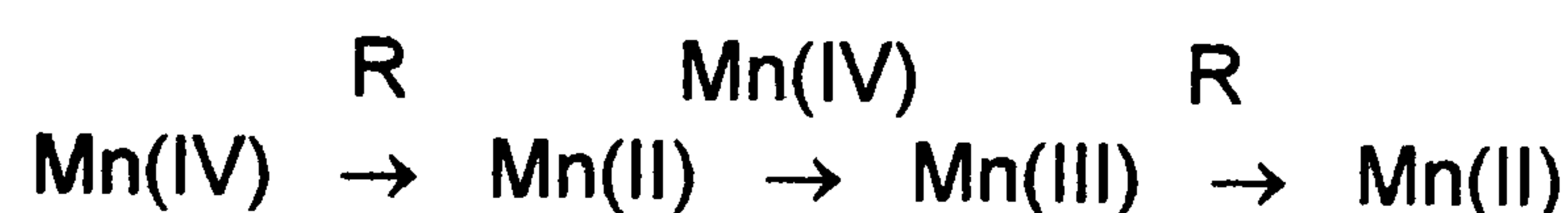
Manganese (V) is an intermediate in the reaction between hydrogen peroxide and permanganate in strongly basic solution, however no chemiluminescence has been reported for permanganate oxidation in alkaline medium.

Manganese (IV), as manganese dioxide, is one of the products of the above disproportionation reactions and is usually formed as a black/brown insoluble solid. The reaction of permanganate with thiosulphate to give manganese dioxide is well known,<sup>130</sup> however if dilute neutral solutions are mixed in stoichiometric ratio colloidal sols can be prepared.<sup>131</sup> These can be used as oxidising agents without the normal solubility problems associated with manganese dioxide.





The colloidal sols are stable, probably due to anions on the surface of the colloidal particles. In mildly acid solutions (pH 4-5) the manganese dioxide sol is reduced by oxalic acid and the following reduction sequence has been proposed where R is the reductant:



Early workers suggested that manganese (II) is formed directly in the first step, and when sufficient has formed, reacts with more Mn(IV) giving Mn(III), which then reacts with more reductant. Other workers have suggested that Mn(III) is formed directly.<sup>132</sup> The formation and reduction of colloidal manganese dioxide has been suggested as an explanation<sup>133</sup> for the apparent oscillatory kinetics in the permanganate oxalate reaction.<sup>134,135</sup>

Most permanganate oxidation reactions utilise potassium permanganate, however copper permanganate<sup>136,137</sup> has been used to improve specificity of some oxidations. Aqueous potassium permanganate solutions are reasonably stable if kept in the dark but undergo photochemical decomposition with evolution of oxygen and precipitation of manganese dioxide. The photochemical reaction is catalysed by manganese dioxide. It has been suggested that the reaction occurs by light induced formation of a Mn(V) peroxo complex which then undergoes reductive elimination<sup>138</sup> giving products. Acid or alkaline solutions of potassium permanganate are much less stable than neutral solutions.

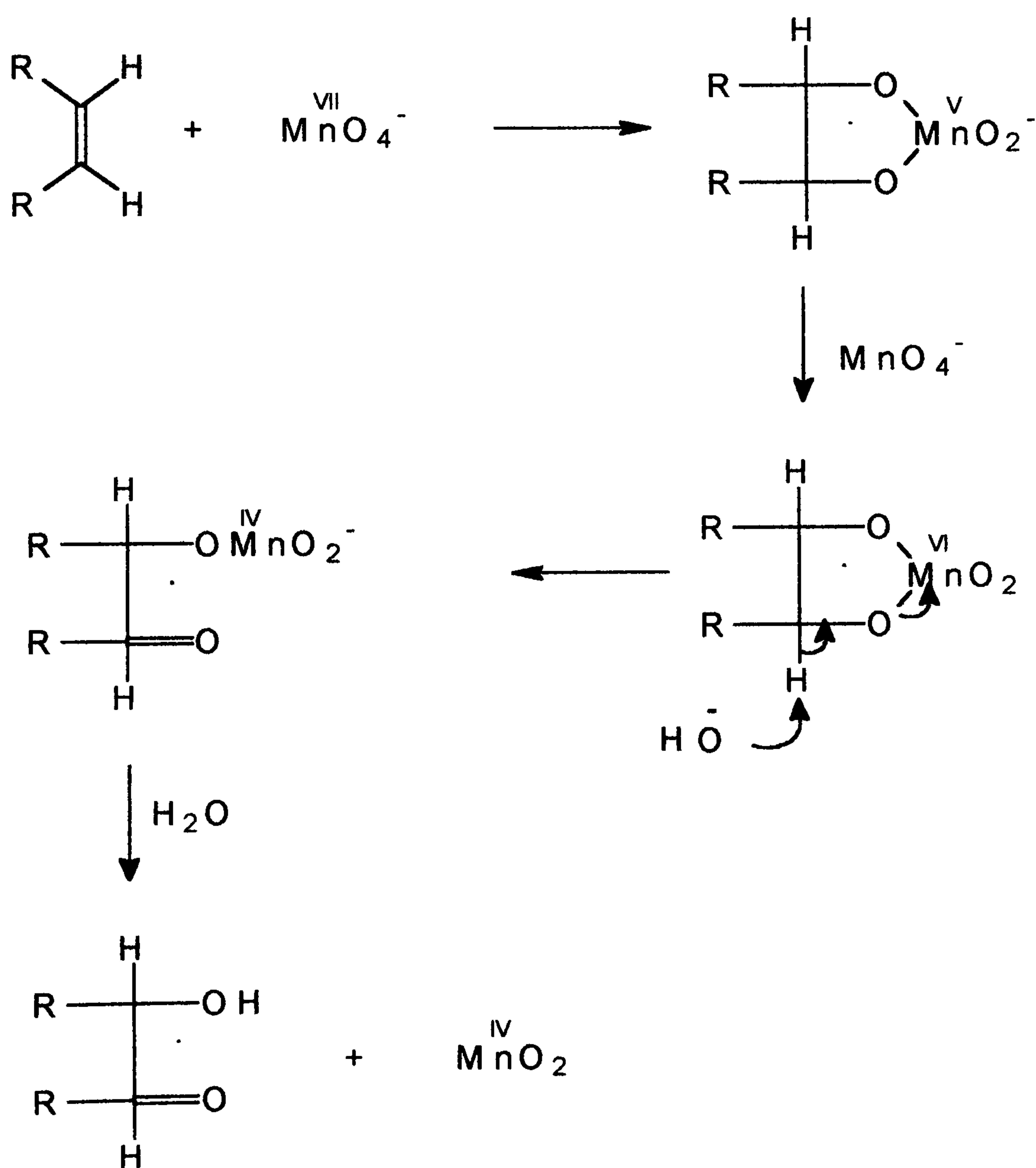
With prolonged heating, most organic compounds are degraded by permanganate to carbon dioxide, however in basic solution oxalate can be a major product. The broad reactivity of permanganate with organic compounds is used in the preparation of pure water, where distillation from permanganate results in water free from organic contaminants. The reaction is also used in methods for chemical oxygen demand, or permanganate index<sup>139</sup> in waters. Some regulatory authorities, including the EU,



consider that the reaction is too general and methods based on dichromate are preferred. Permanganate time in spiritous preparations<sup>140</sup> and solvents is used as a quality measure for high purity solvents for applications such as HPLC.

Monohydric alcohols are reasonably stable to neutral and mildly acid permanganate but are readily oxidised in basic and strongly acid solution.

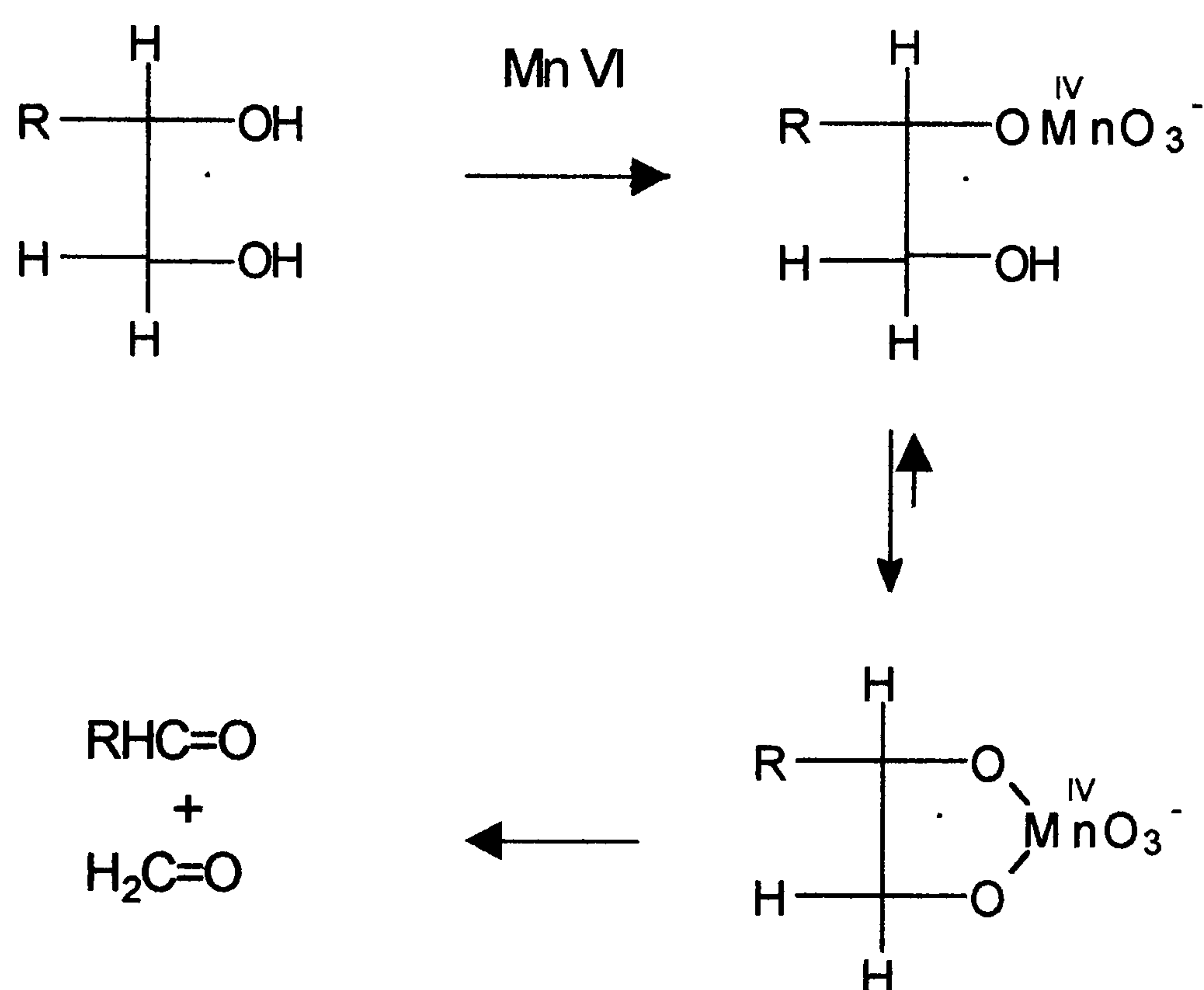
Oxidation of alkenes involves the formation of a cyclic manganese ester<sup>118,141,142,143</sup> with, at high pH, formation of glycols. At low hydroxyl ion concentration  $\alpha$ -hydroxy ketones are formed (Scheme 2.7 ).



**Scheme 2.7**



Studies of the reaction of unstable Mn(V), produced from permanganate and arsenic(III) with vicinal diols found the same products as in the reaction of permanganate with the parent olefin. This suggested the formation of a manganese(V) ester prior to the formation of the cyclic manganese ester shown below. In the presence of excess substrate and a suitable complexing agent, such as pyrophosphate, the main manganese species is manganese (III).<sup>144</sup> If the oxidising species is Mn(VI) however, C-C bond cleavage is present to some extent as shown in Scheme 2.8.



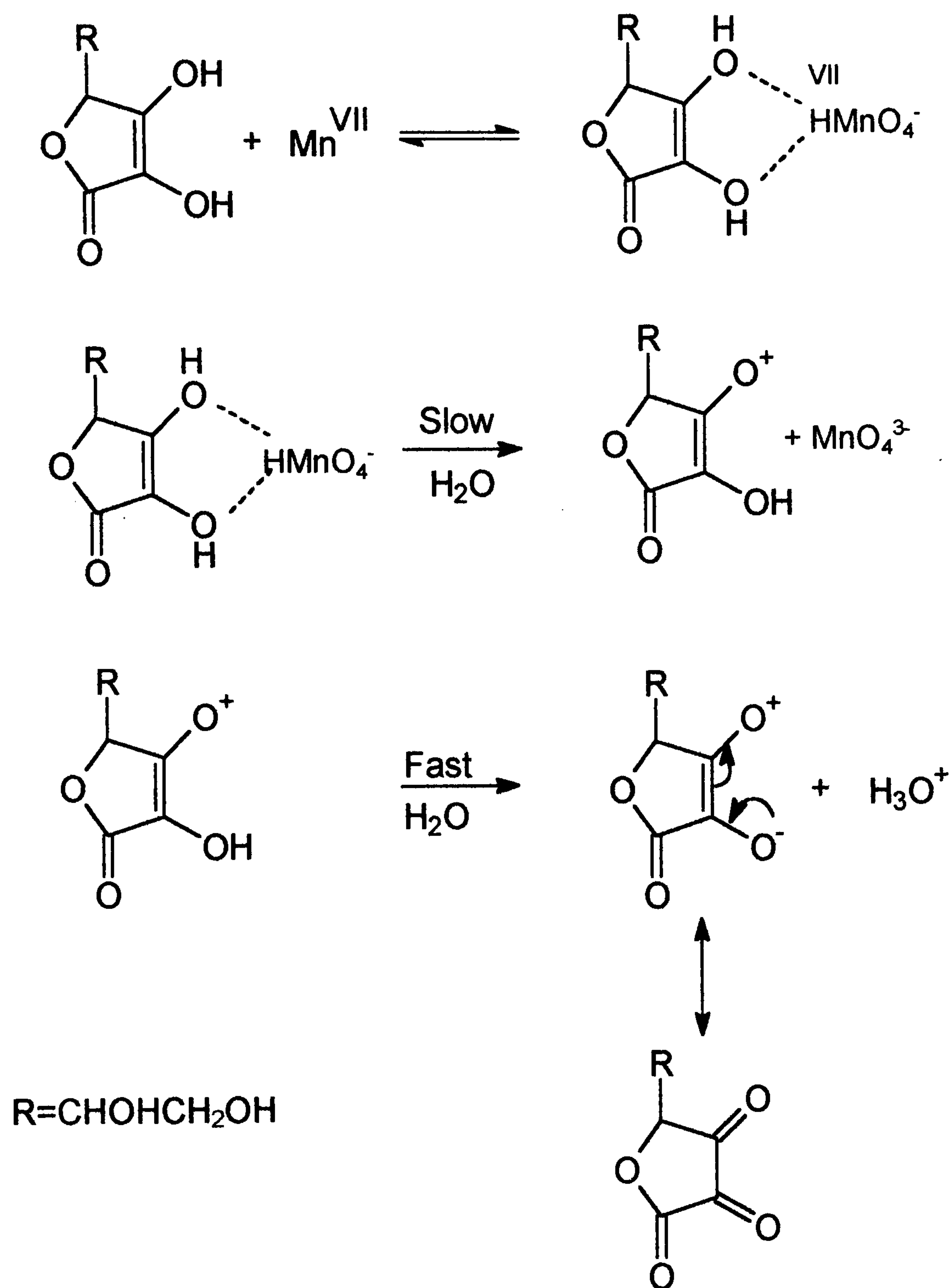
**Scheme 2.8**

Permanganate oxidations of many other classes of organic compounds have been studied including aromatic acids and polyphenols,<sup>145 146</sup> aldehydes,<sup>147</sup> amino acids<sup>148</sup> and carbohydrates.<sup>149,150,151,152</sup> In the case of ascorbic acid a mechanism has been proposed in which the principal oxidising species is manganese (VII),<sup>153</sup> as shown in Scheme 2.9.

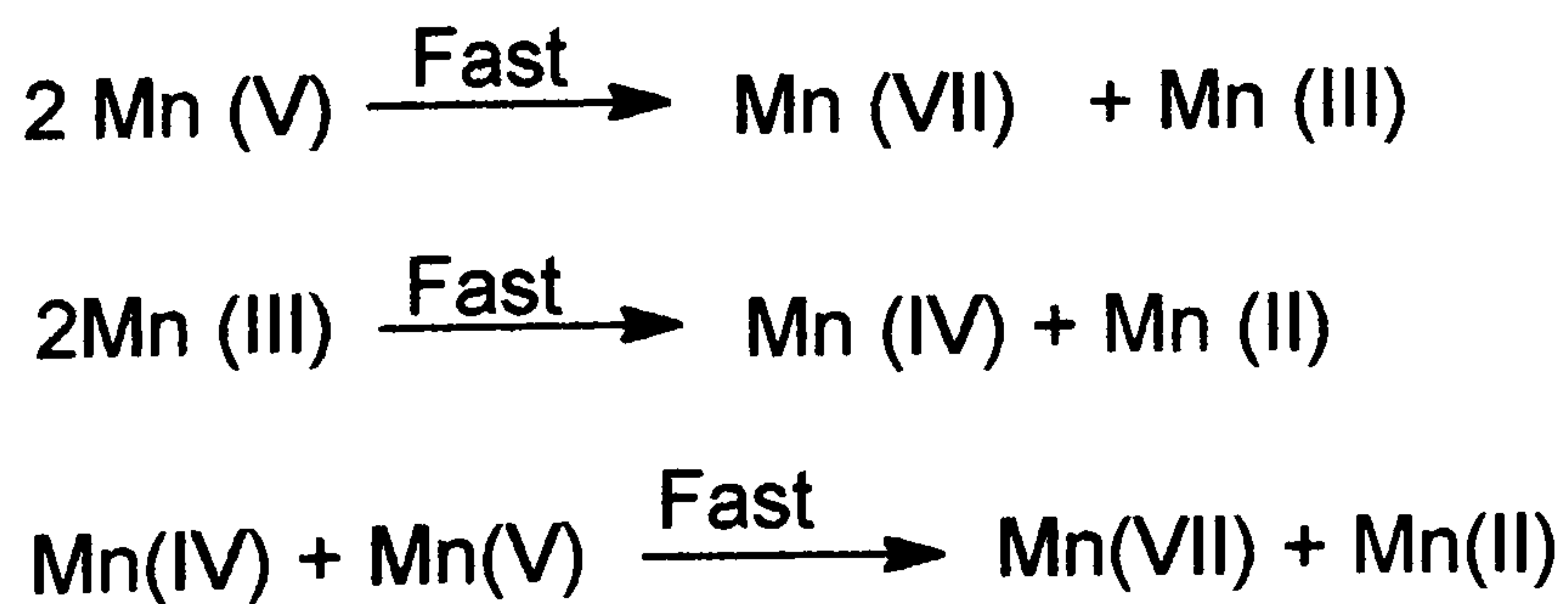
As discussed above, manganese (III) can be stabilised and as such used directly as an oxidant. It is milder and often more specific than permanganate.<sup>154,155</sup> In addition



to the use of stabilised forms, Mn(III) oxidations are carried out using Mn(III) electrochemically generated from Mn(II).<sup>156</sup>



**Scheme 2.9(a)**



**Scheme 2.9 (b)**

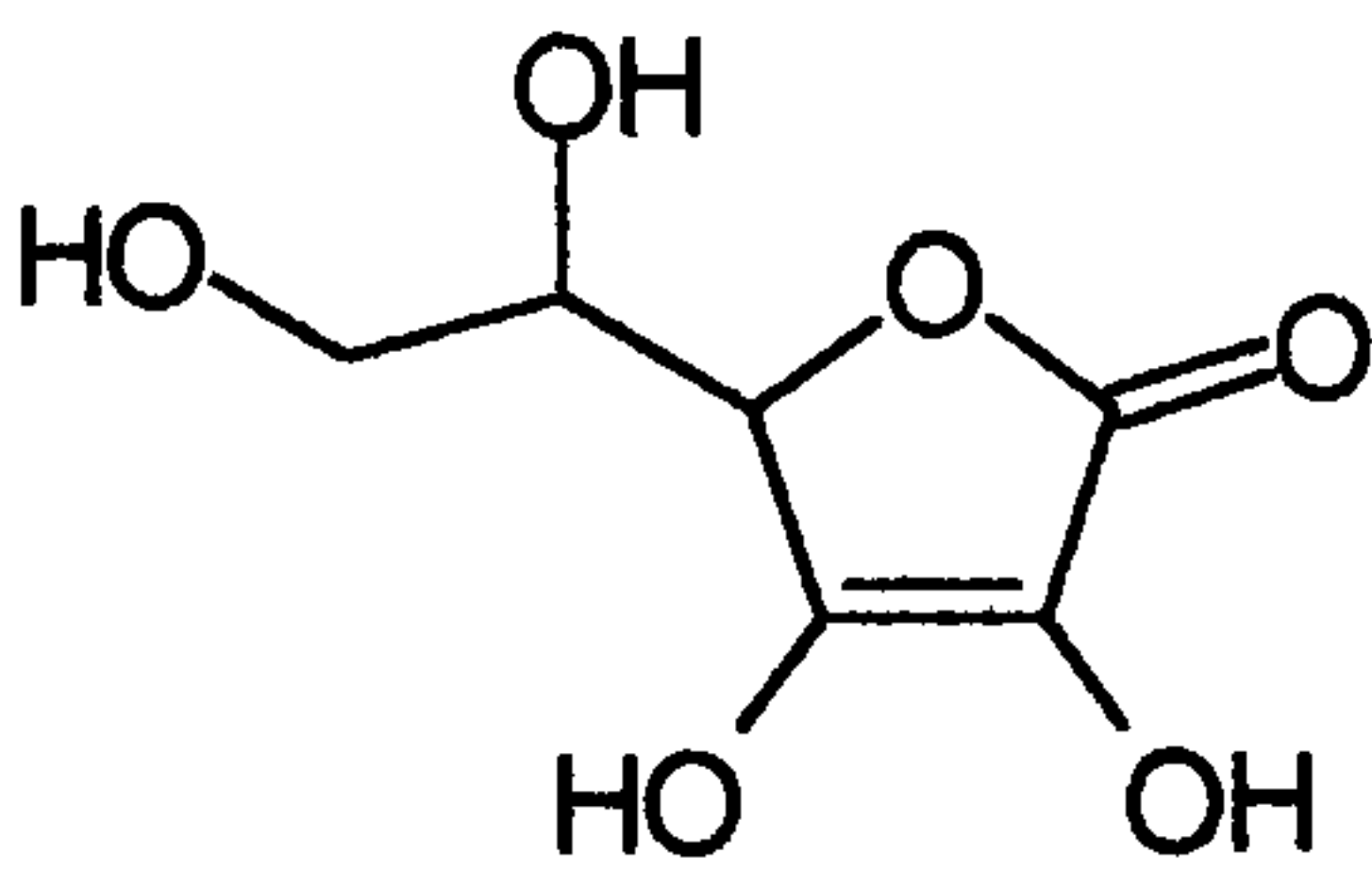
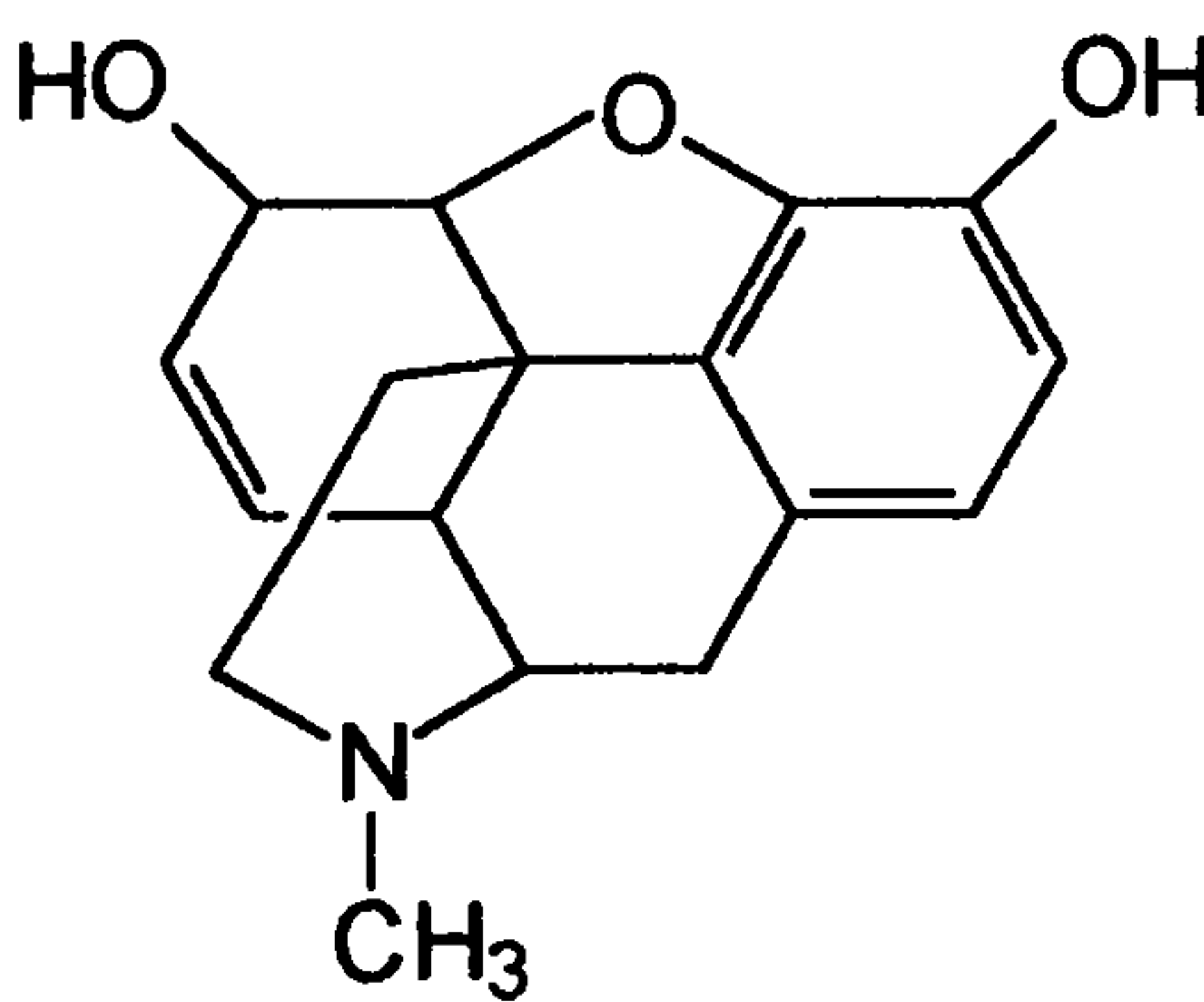


## 2.4.1 Chemiluminescence from Permanganate Reactions

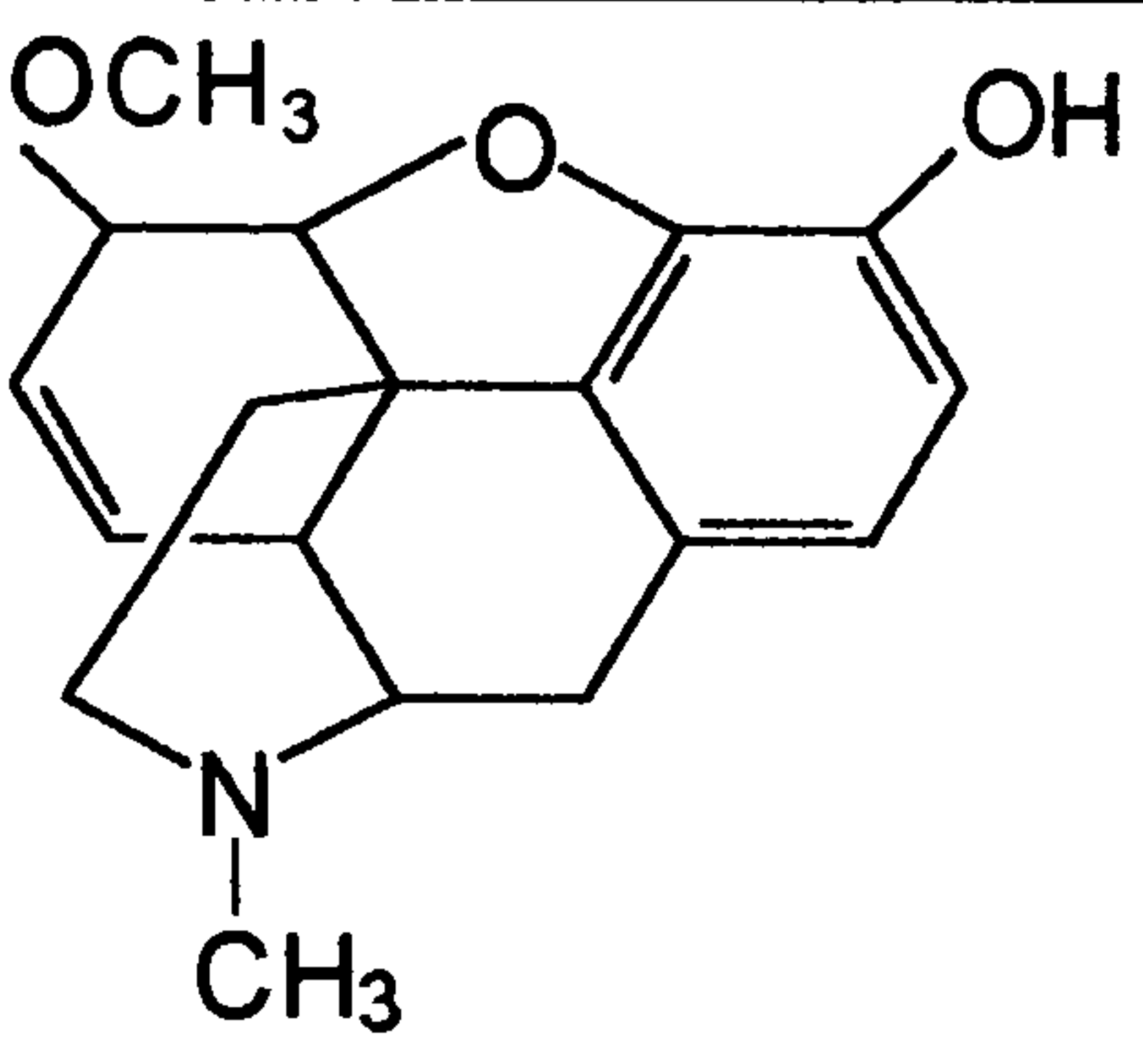
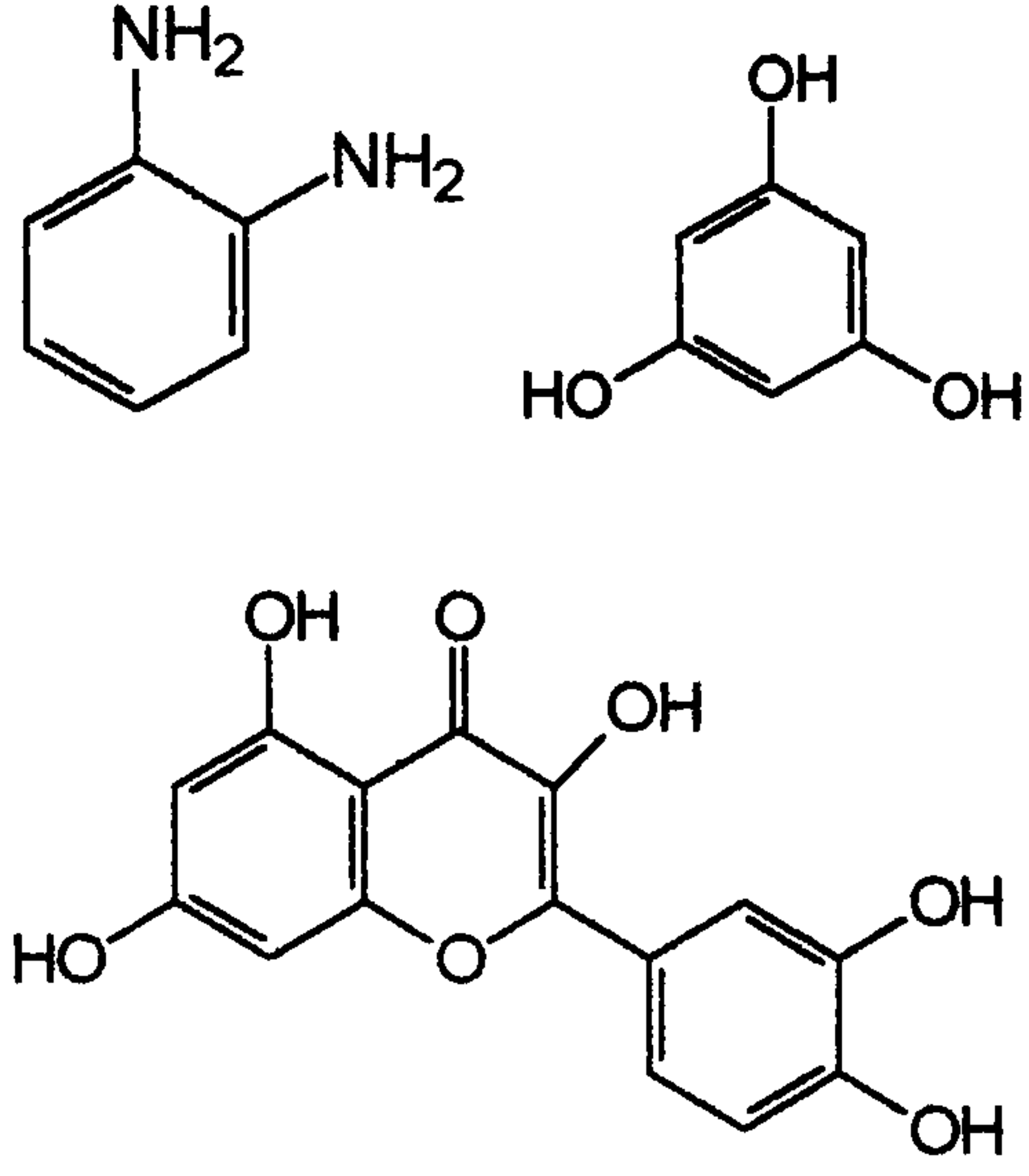
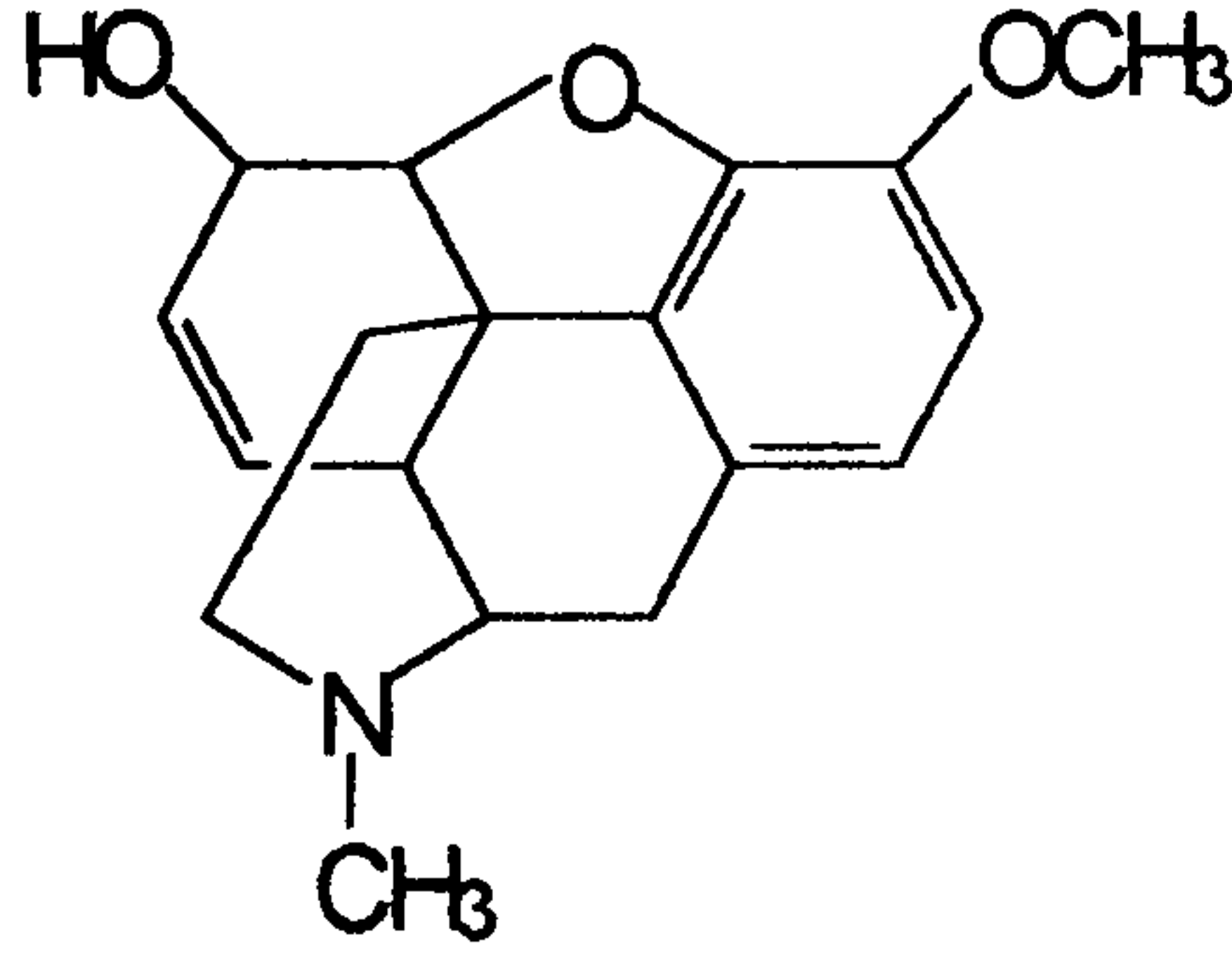
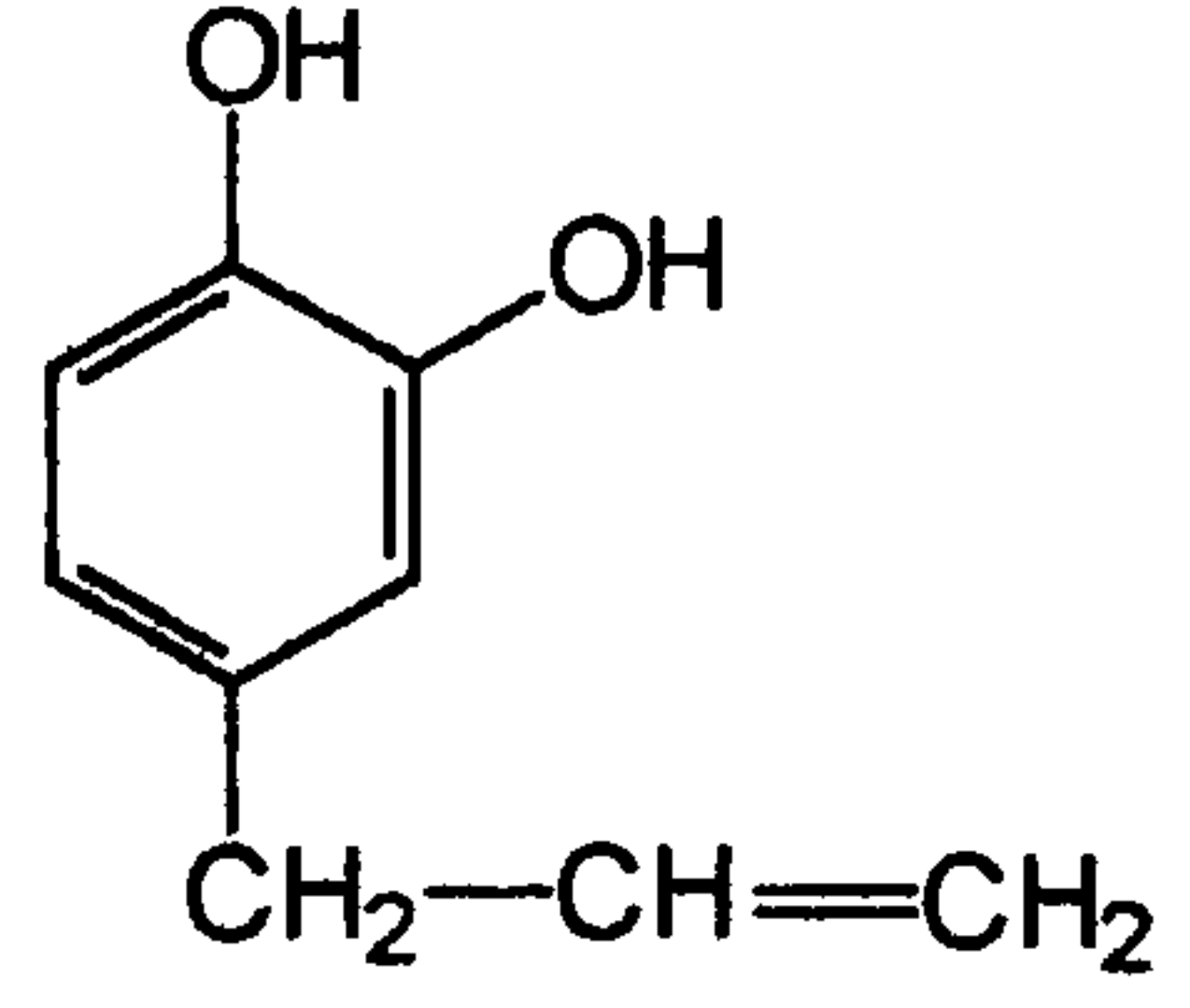
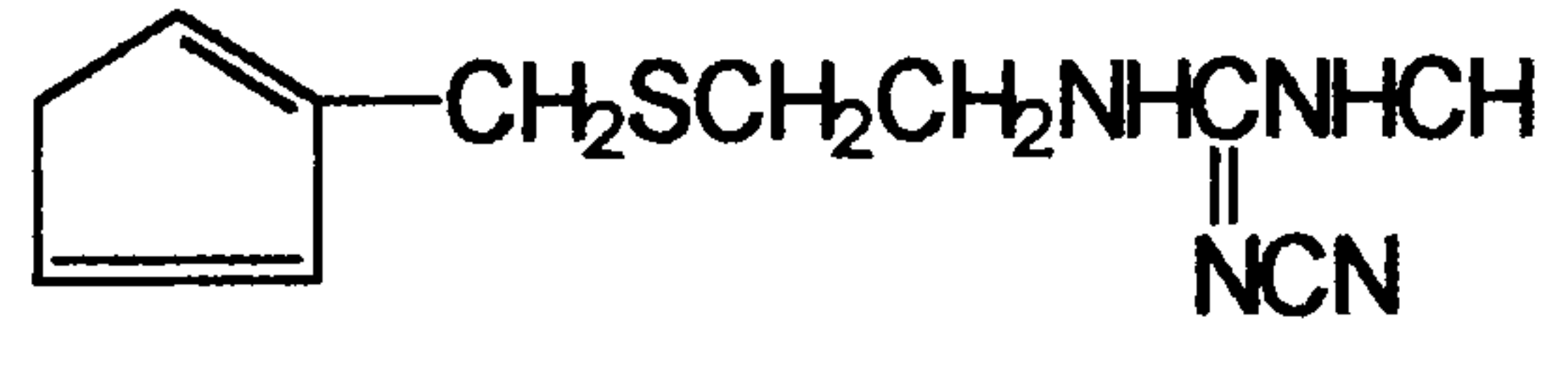
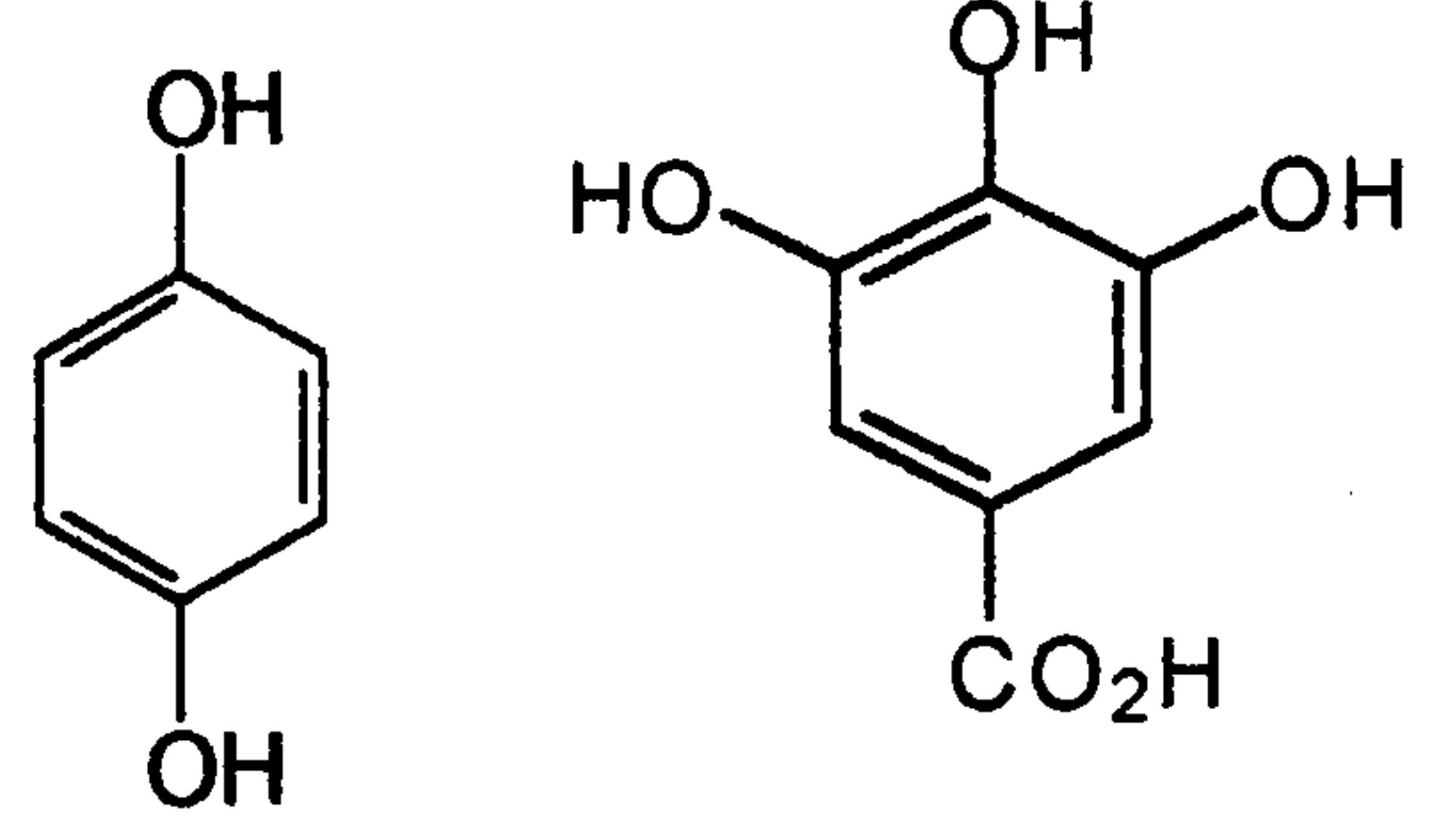
Chemiluminescence from the reaction of inorganic compounds and permanganate has been used analytically.<sup>157</sup> For example the reaction of permanganate with sulphite gives luminescence which is thought to be due to excited SO<sub>2</sub>. It is weak and riboflavin or 3-cyclohexylammoniumpropane sulphonic acid is used as a sensitiser. Bile acids such as cholic acid can also act as sensitisers in this reaction which has been used for their determination.<sup>158</sup> Stronger chemiluminescence is observed when permanganate is mixed with a sodium carbonate/potassium hydroxide solution. It has been suggested that the chemiluminescence is due to singlet oxygen.<sup>159</sup>

A large number of permanganate oxidations of organic compounds are known to give direct chemiluminescence. Most of these reactions are in acid medium. The following table shows some of the compounds determined by permanganate chemiluminescence. Limits of detection and relative intensities were determined using both batch and flow methods.

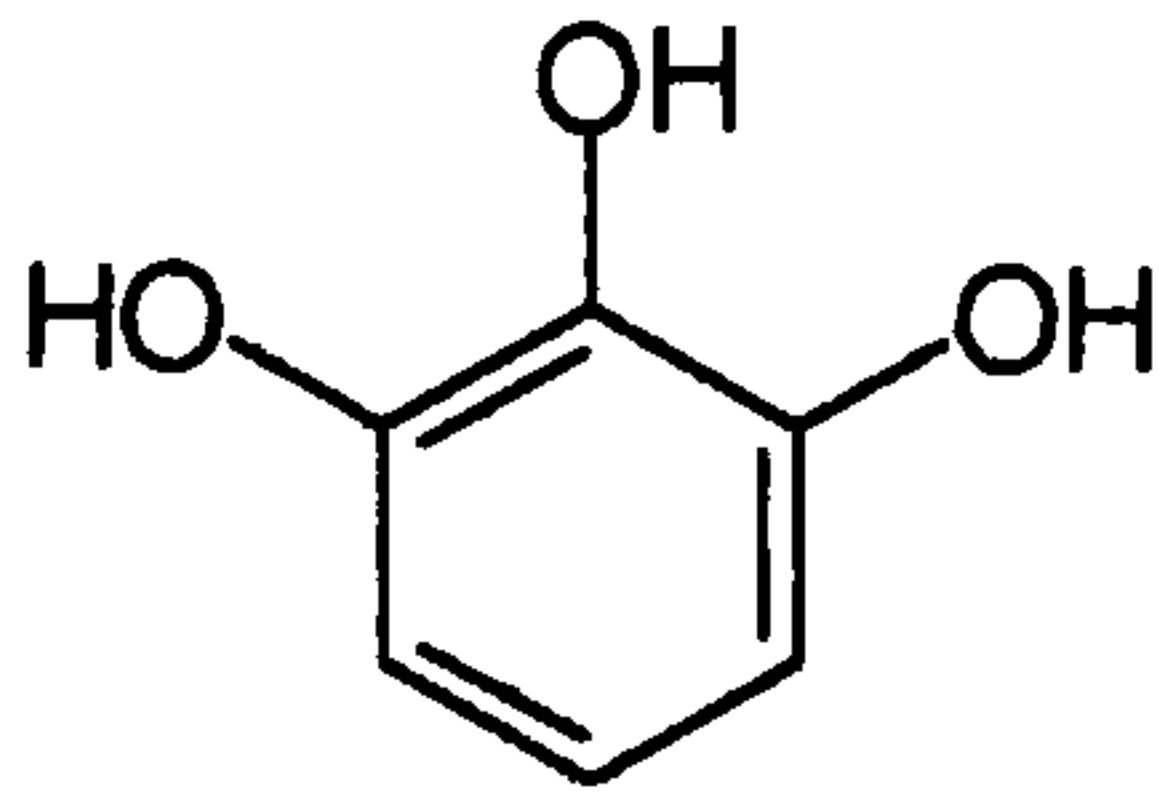
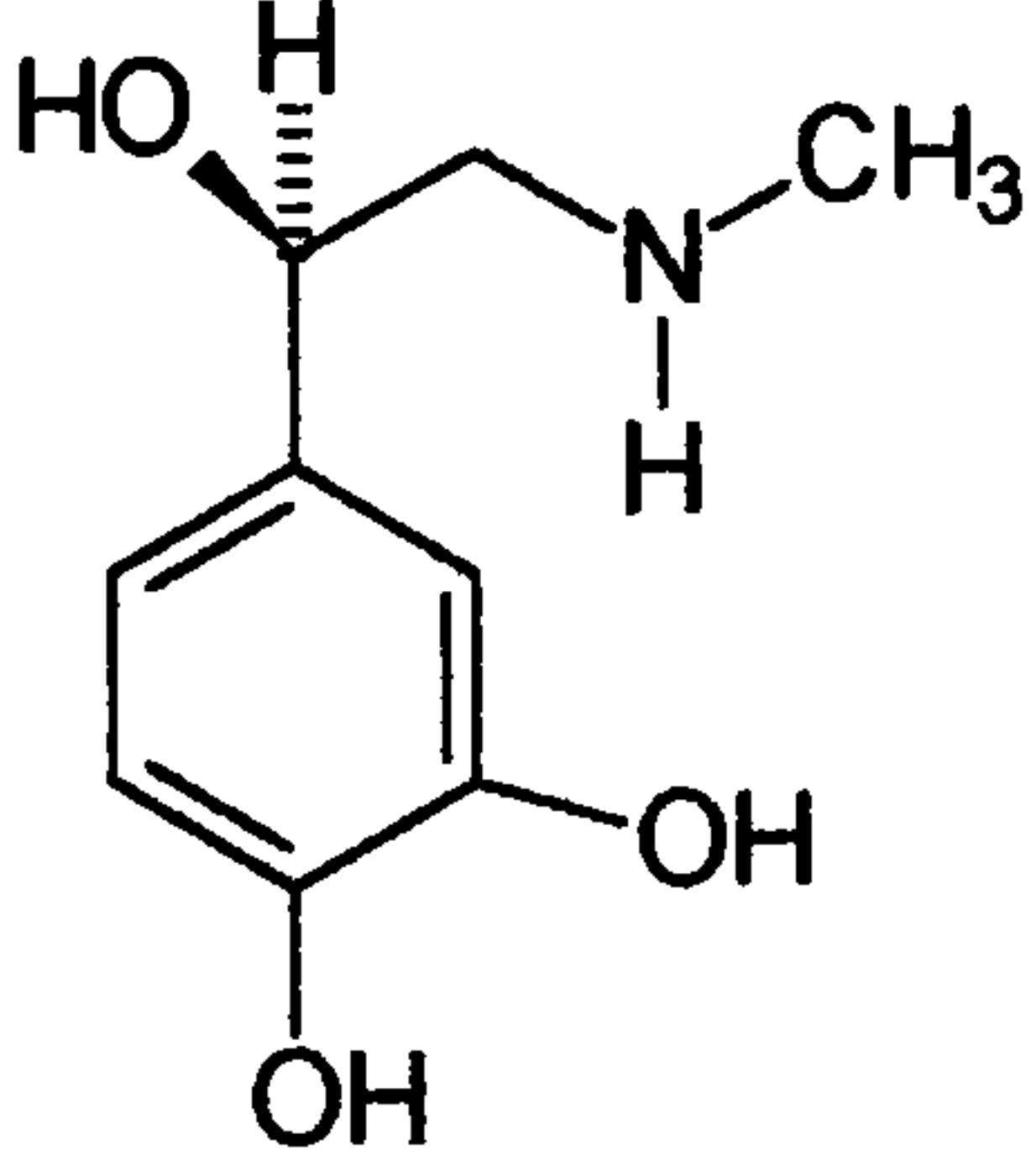
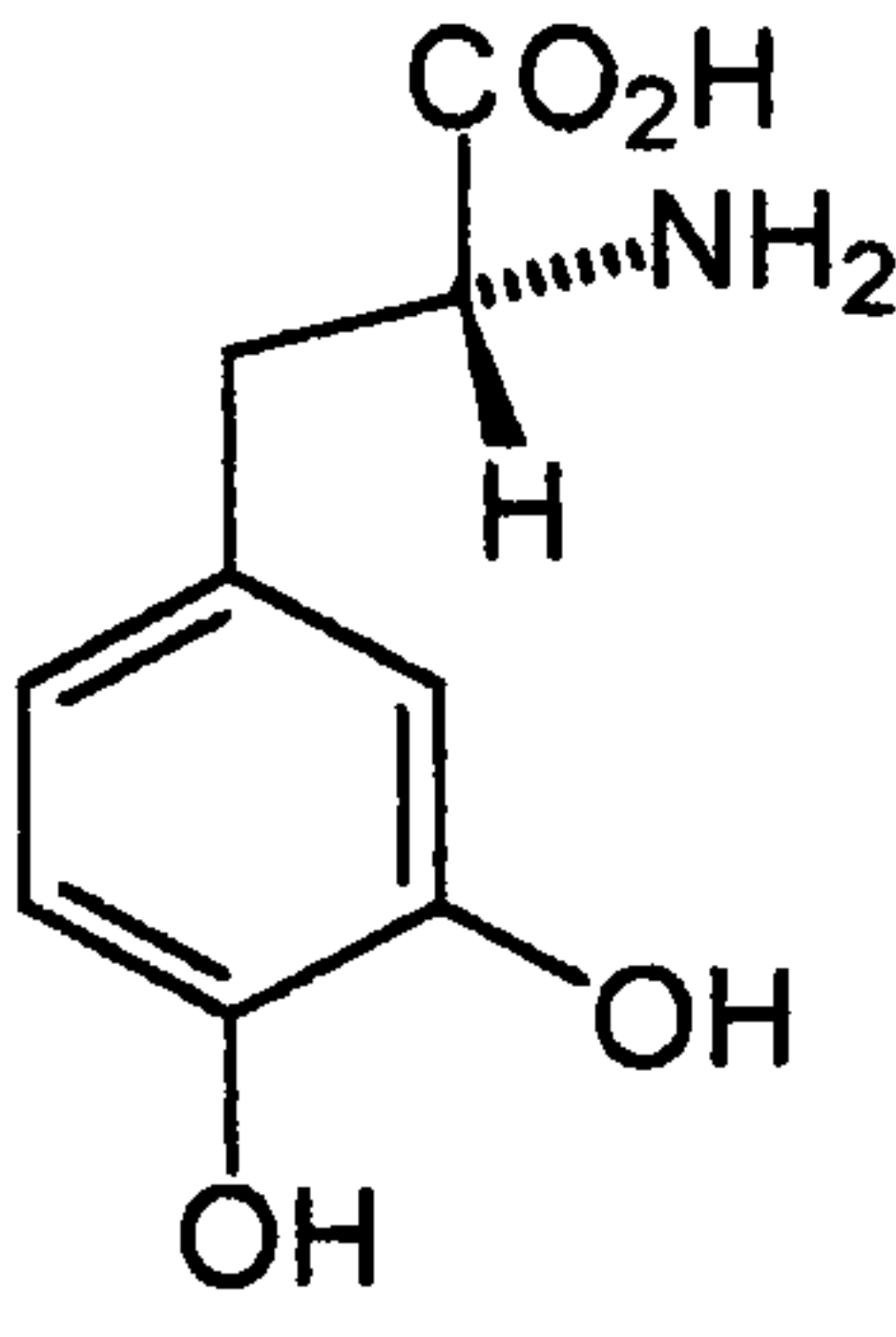
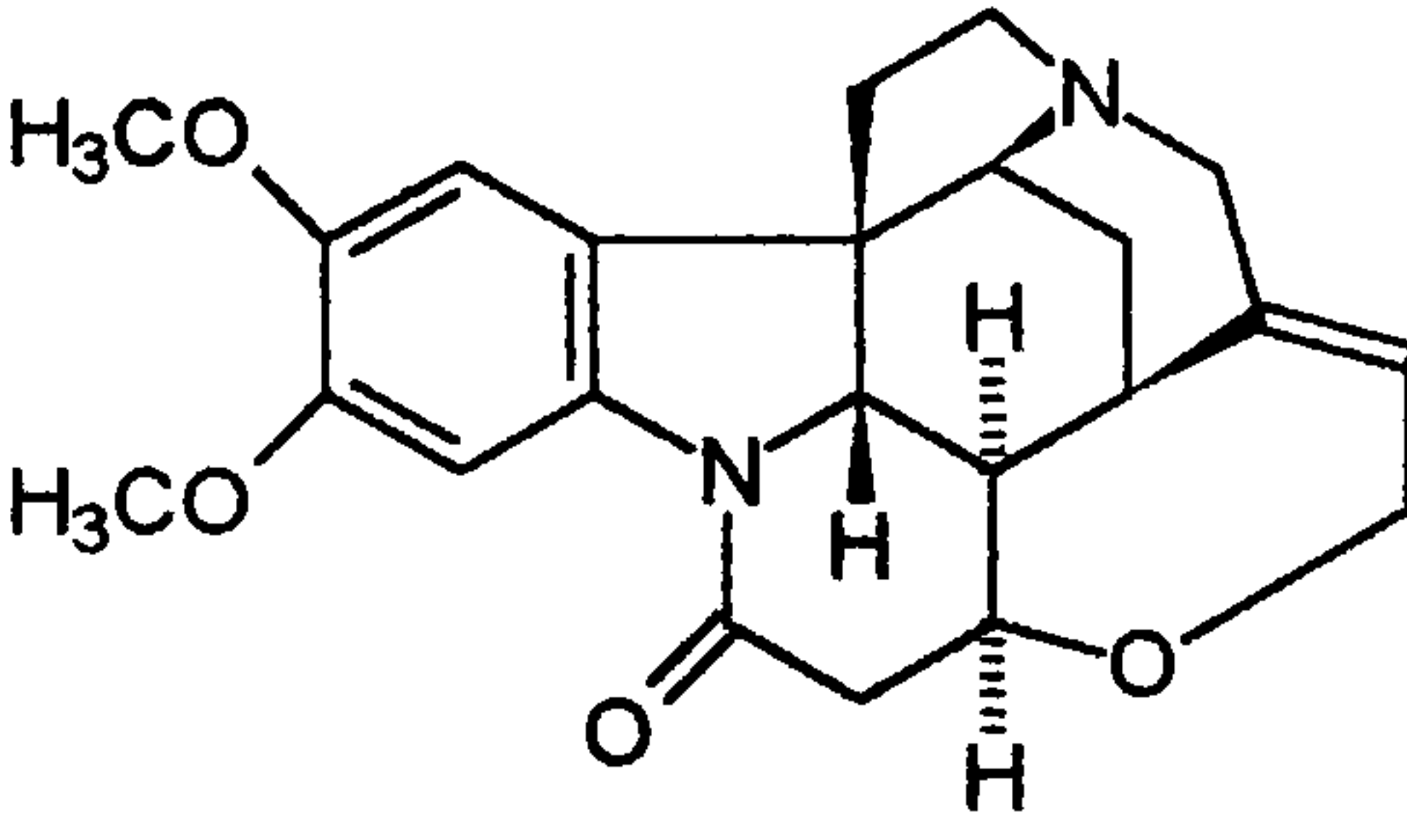
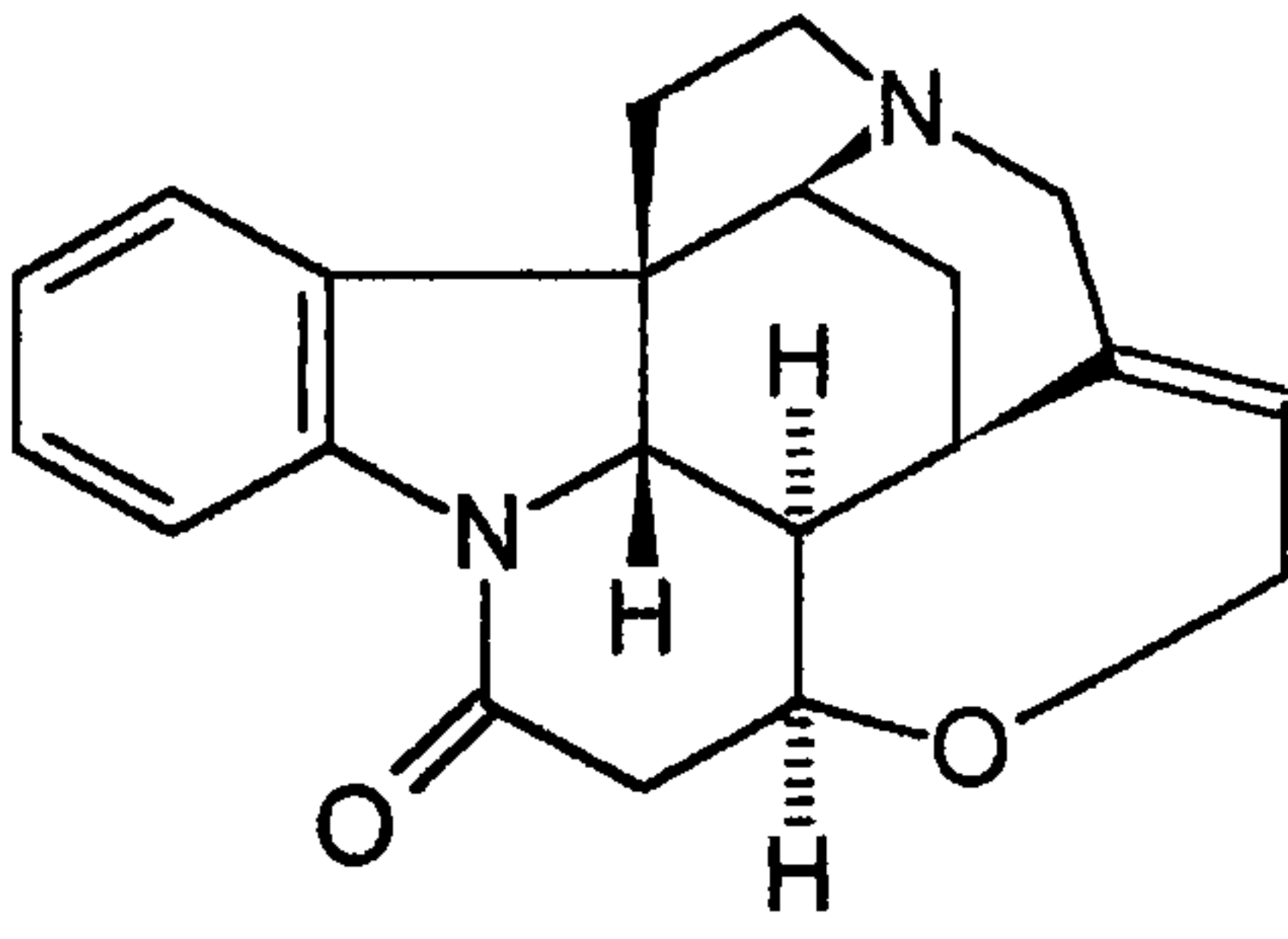
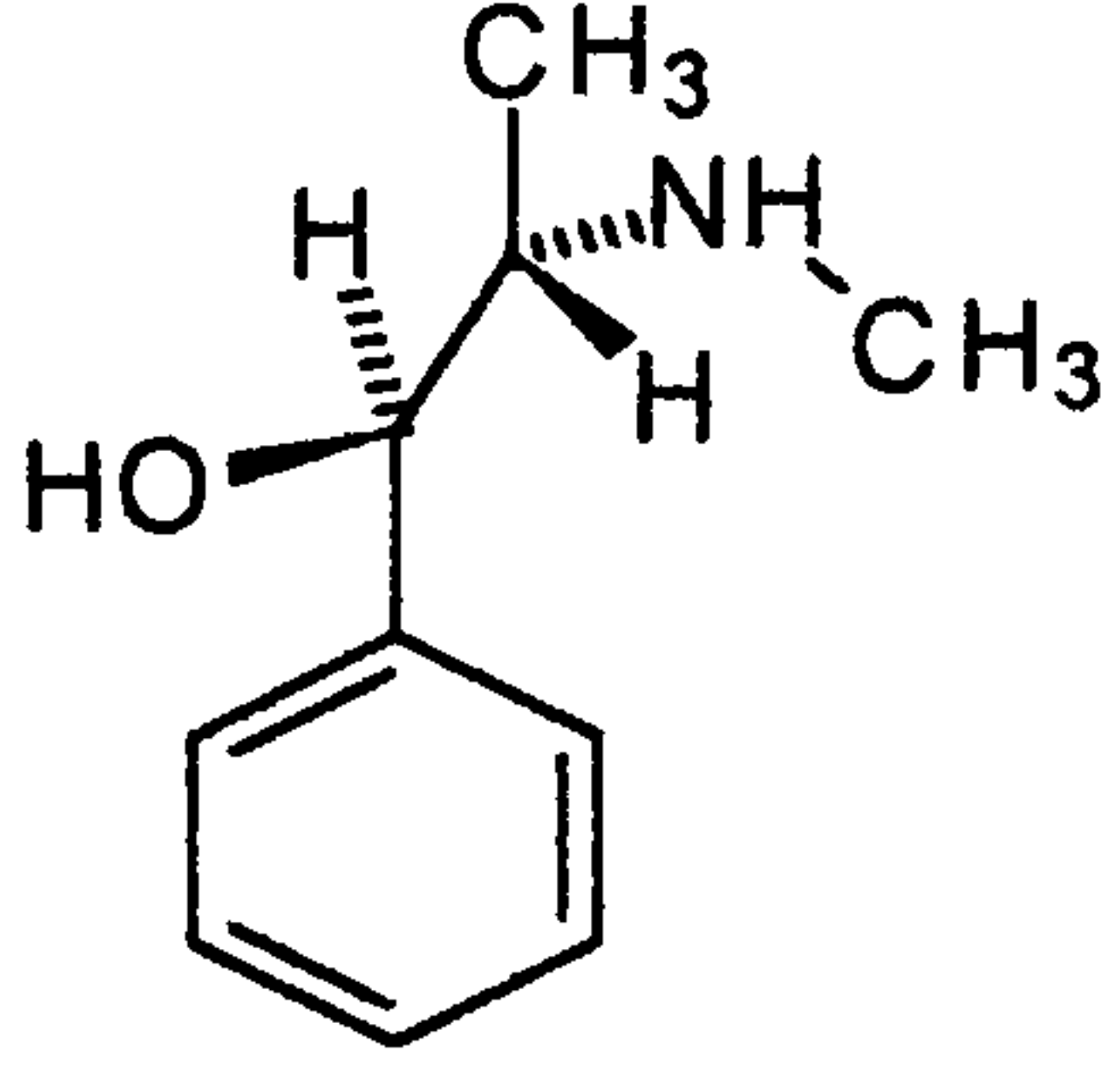
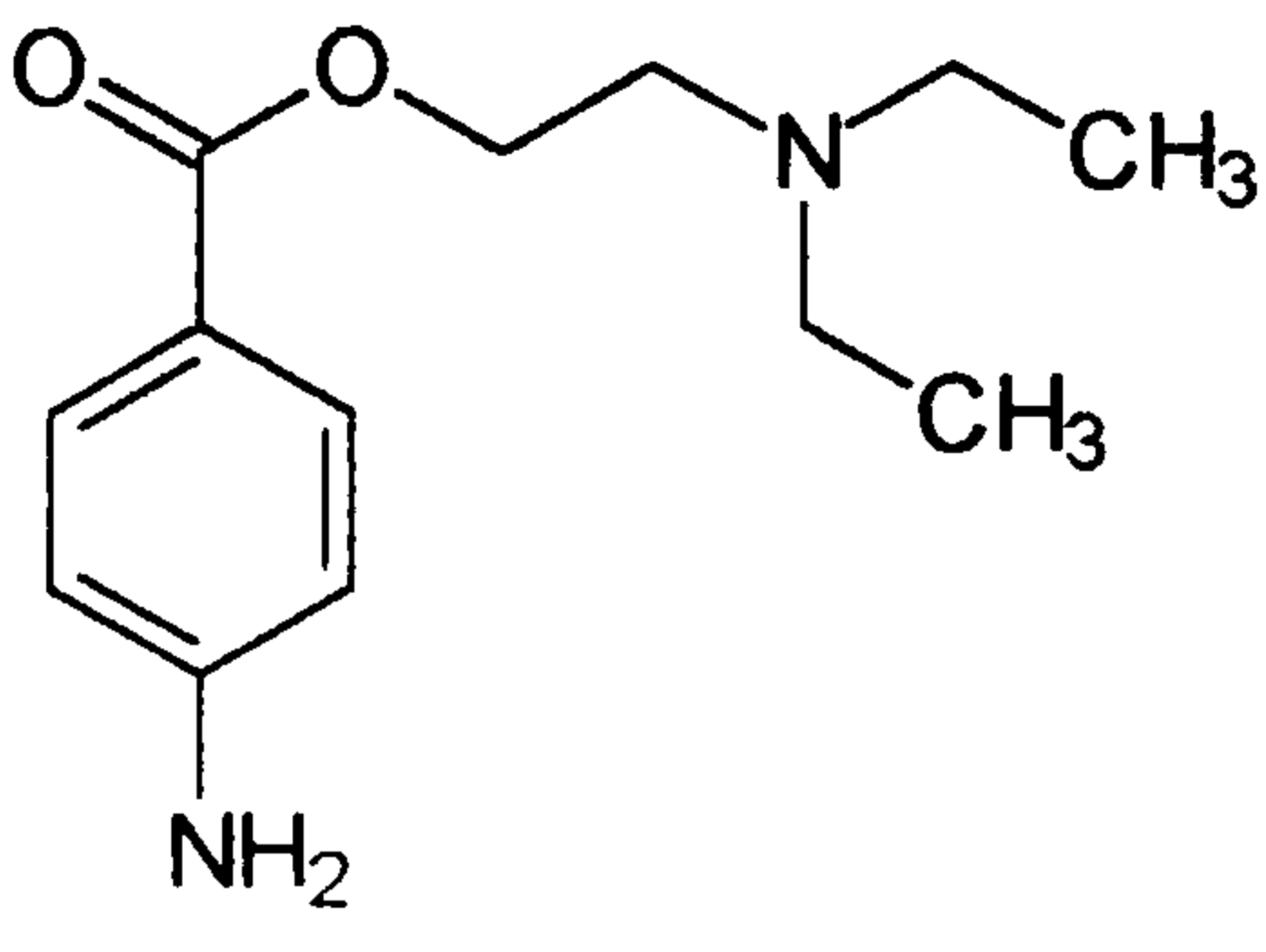
**Table 2.5 Analytes Investigated by Permanganate Chemiluminescence**

Compound Investigated	Examples of Structures	Sensitivity	Reference
Ethanol‡	CH <sub>3</sub> CH <sub>2</sub> OH	1%	Montalvo <sup>160</sup>
Ascorbic acid‡		0.3 x 10 <sup>-6</sup> M	Zhu <sup>161</sup>
Morphine‡		1x10 <sup>-10</sup> M	Abbott <sup>162</sup> Abbott <sup>163</sup> Barnett <sup>164</sup> Barnett <sup>165</sup>

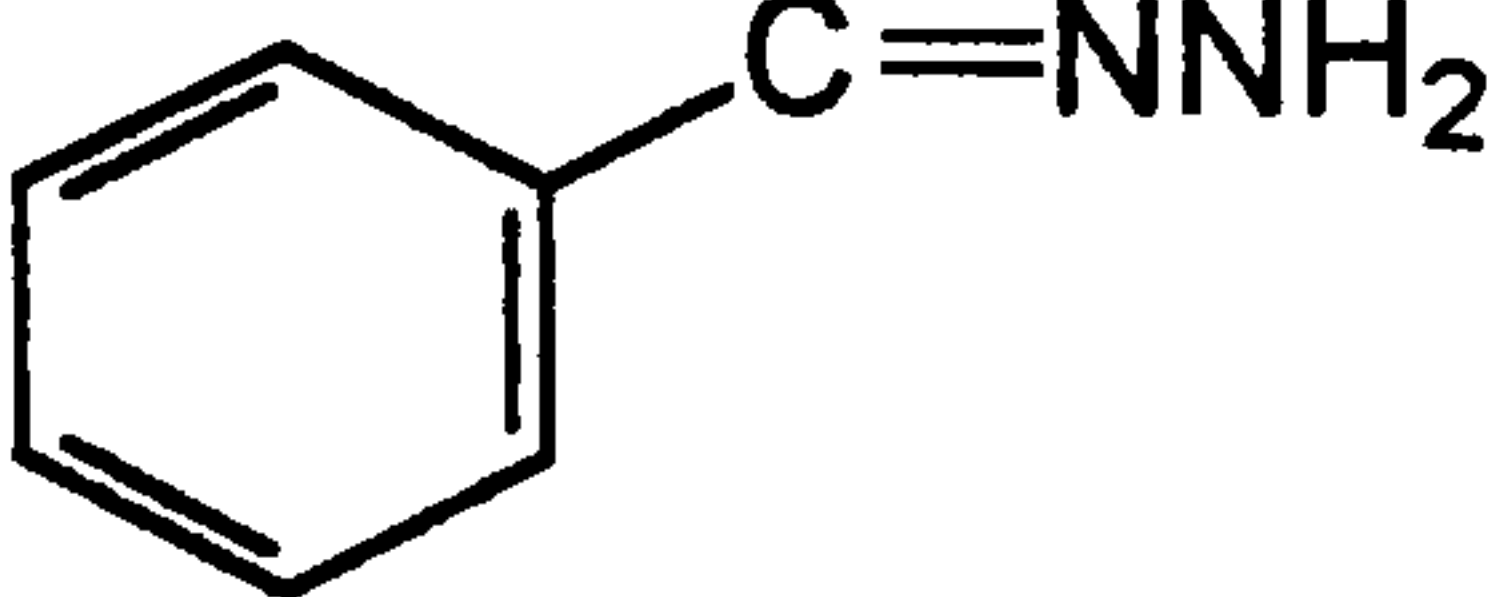
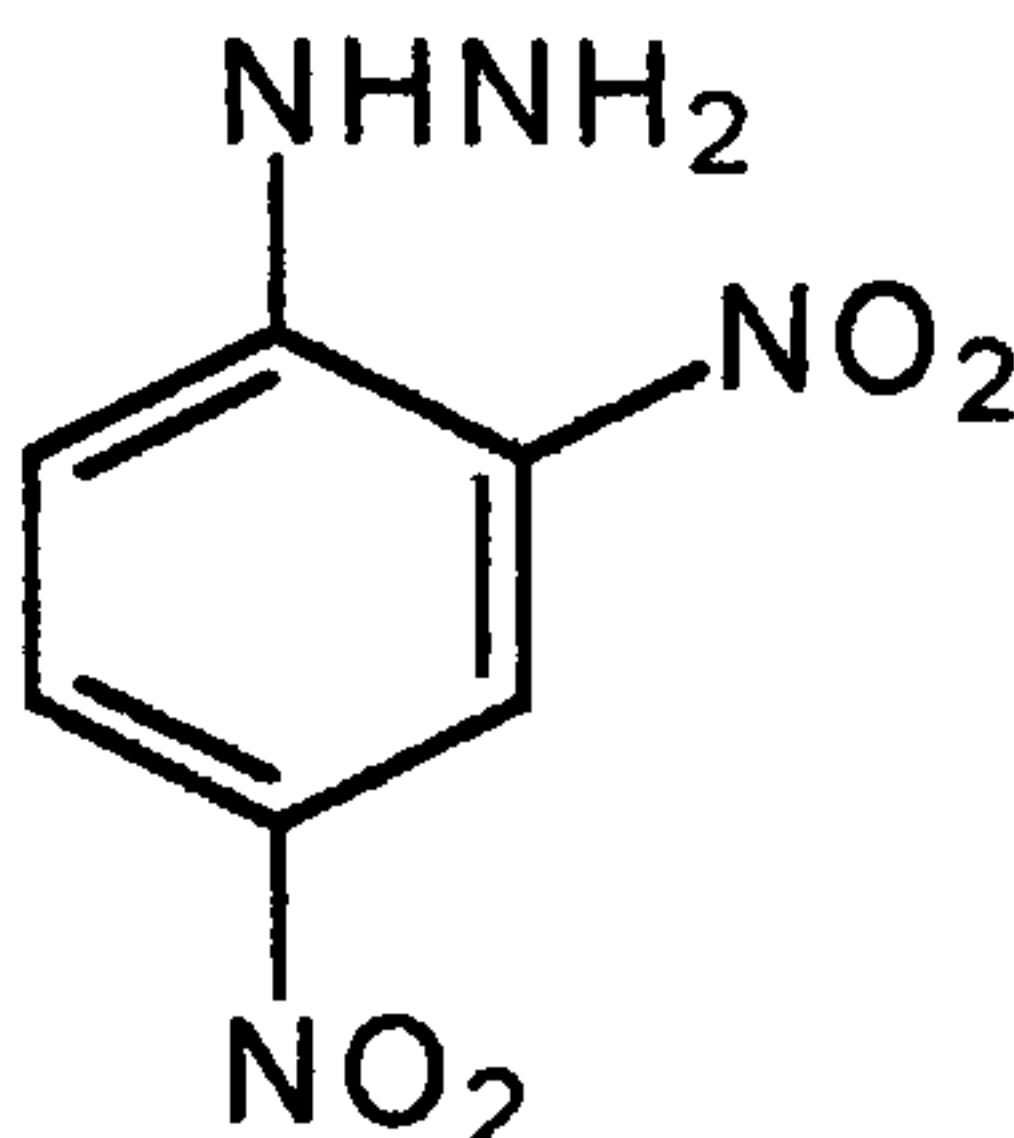
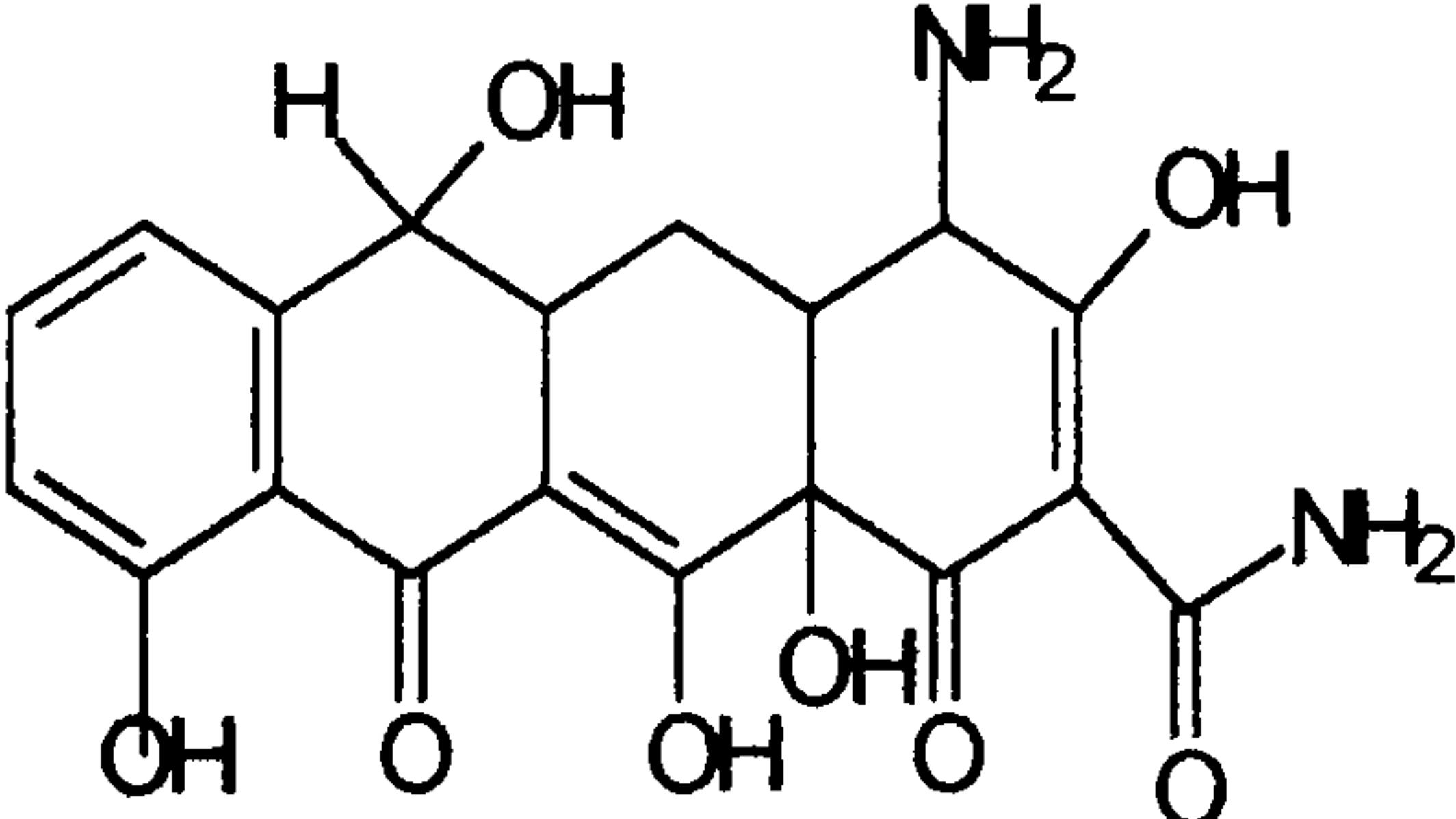
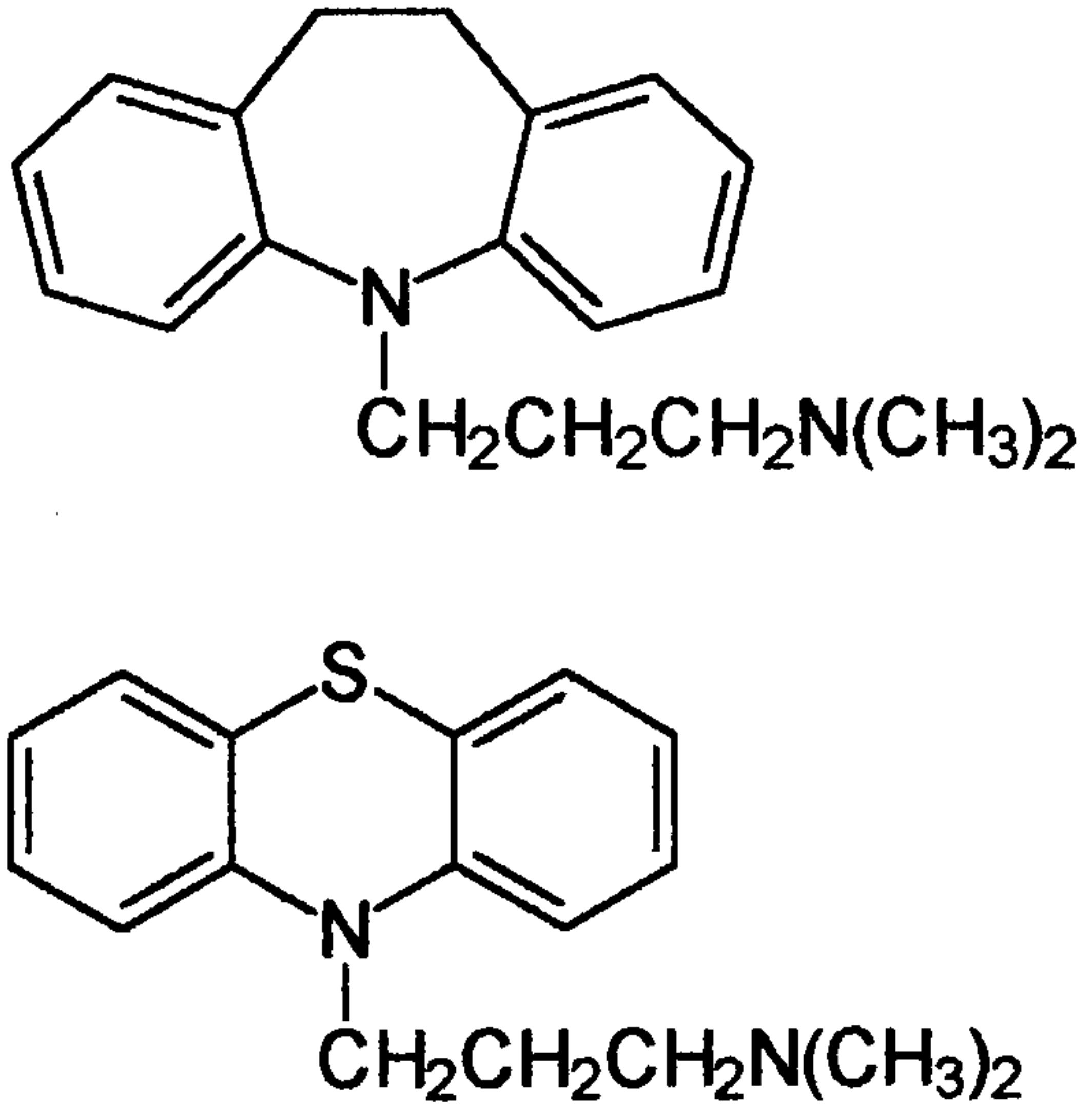
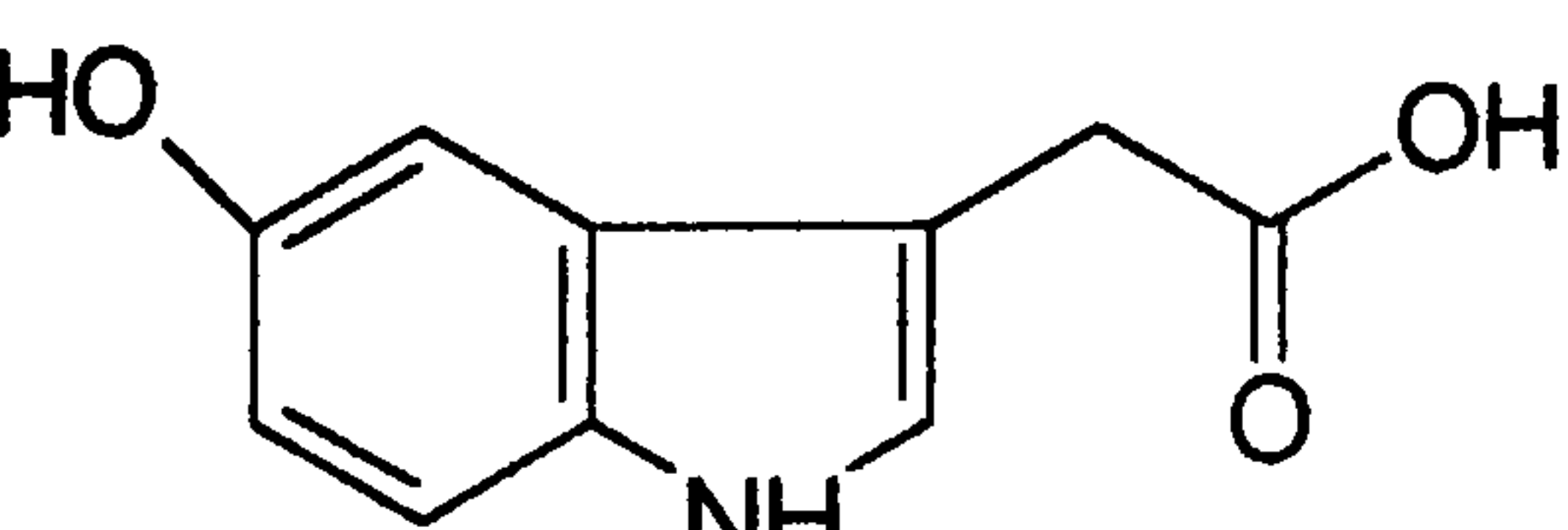
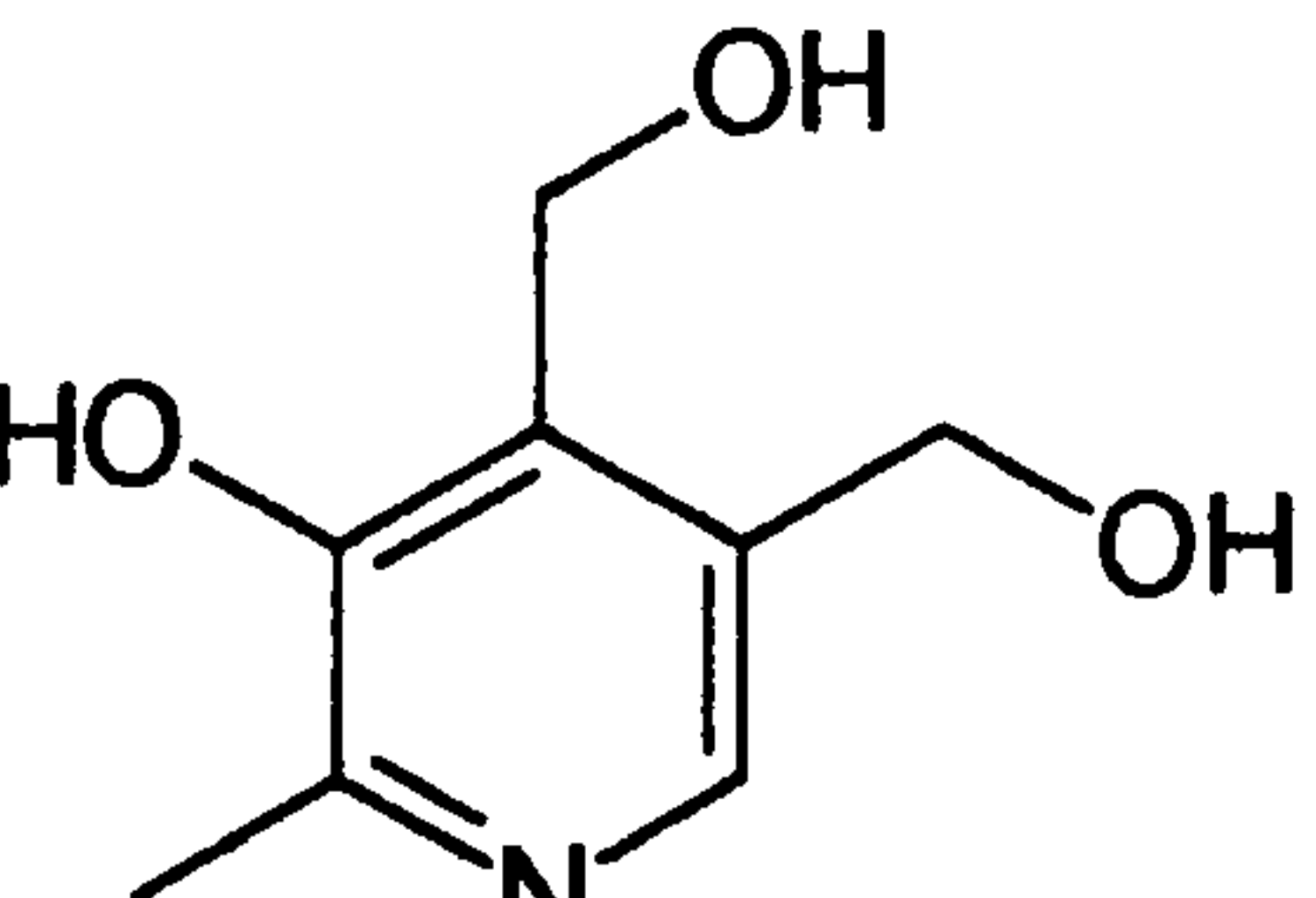


Morphine Oripavine‡ Pseudomorphine (dimer of morphine)		morphine $5 \times 10^{-8}$ M oripavine 0.71 re morphine pseudomorphine 0.29 re morphine	Barnett <sup>166</sup>
Morphine Hydroquinone N-phenylenediamine‡ Ascorbic acid Metol Floroglucinol‡ Thymol Rutin Quercetin‡		Relative to Morphine 1.0 0.1 0.11 0.11 0.04 0.08 0.004 0.004 0.001	Tsaplev <sup>167</sup>
Codeine‡		$3 \times 10^{-7}$ M	Christie <sup>168</sup>
Eugenol‡ Isoeugenol Caffeic Acid   Cimetidine‡	 	$1 \times 10^{-5}$ M $1 \times 10^{-4}$ M 20 $\mu$ g/mL	Mitsana-Papazoglou <sup>169</sup>
Catecholamines and Polyhydroxy- benzenes Including Adrenaline Hydroquinone‡ Pyrogallol Gallic Acid‡		Relative to Adrenaline Pyrogallol 2.9 Gallic Acid 0.4	Ikkai <sup>170</sup>

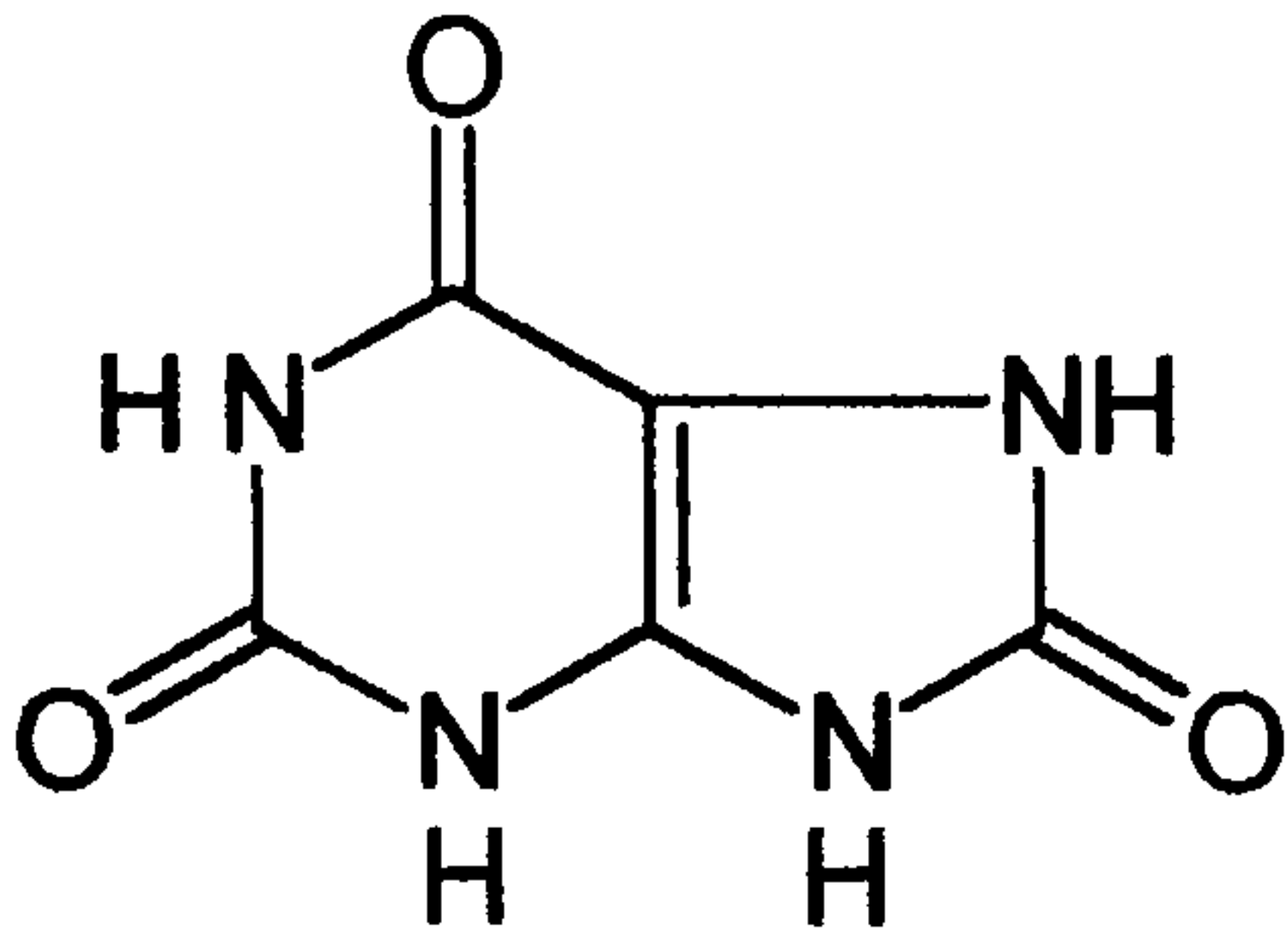
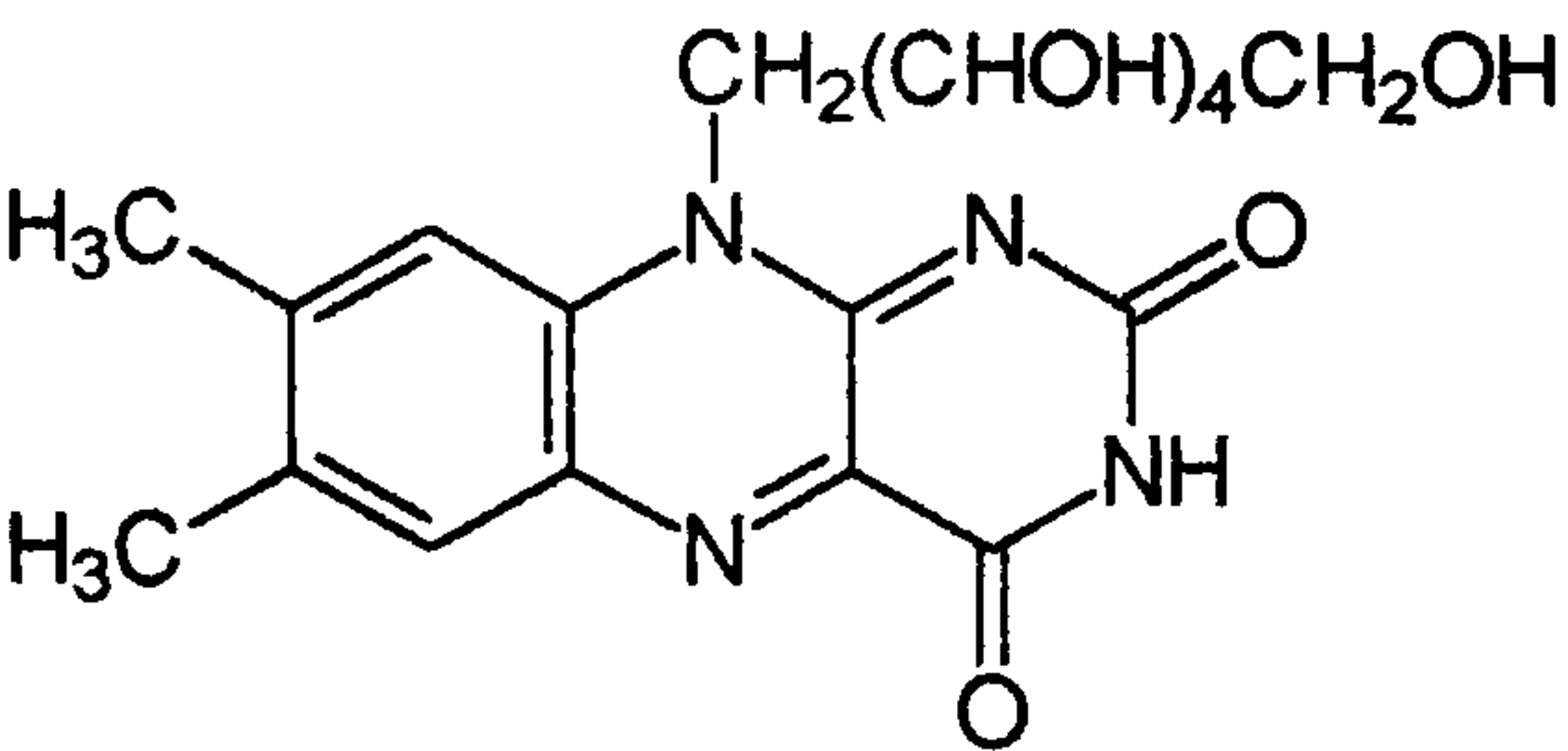
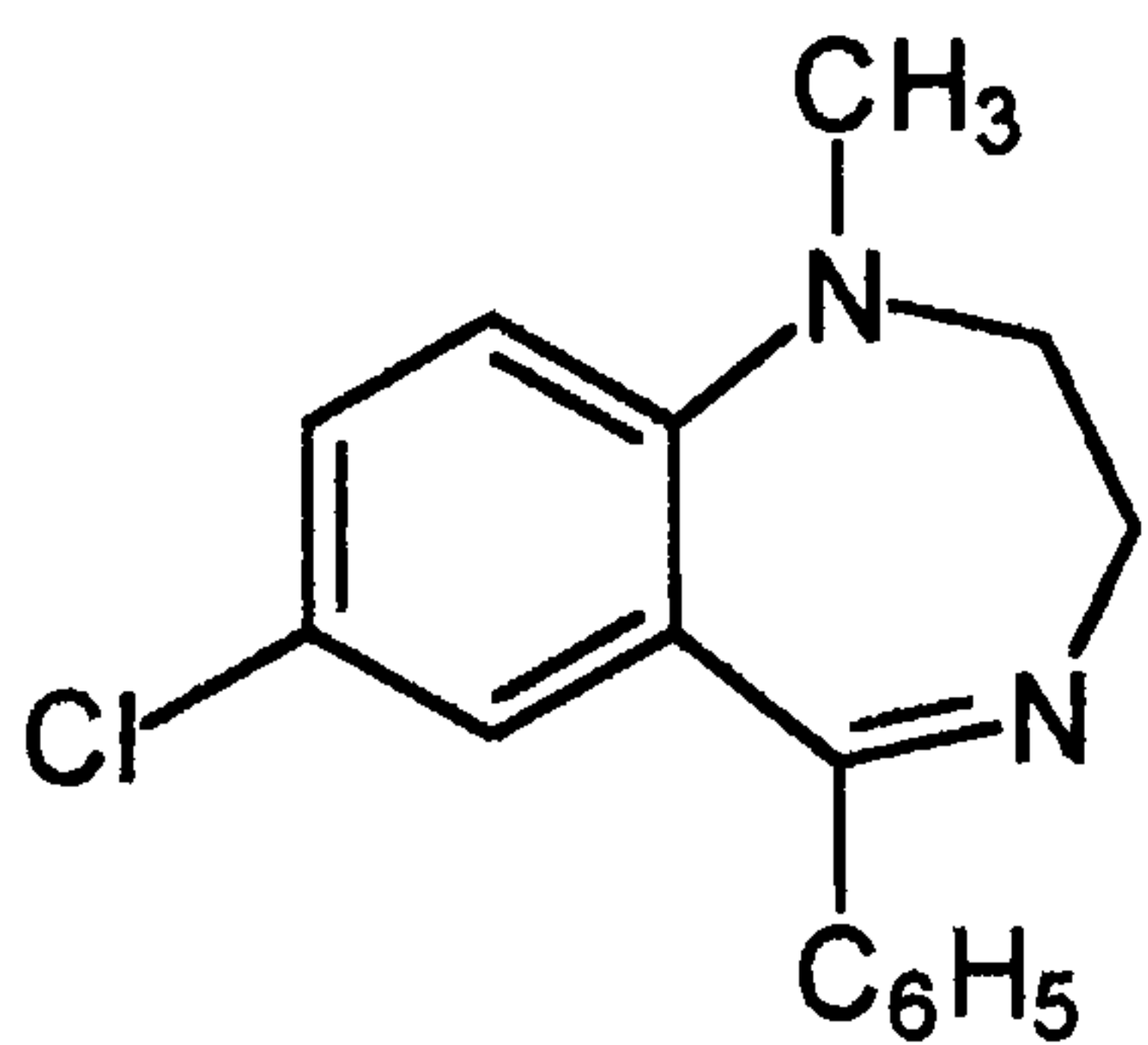
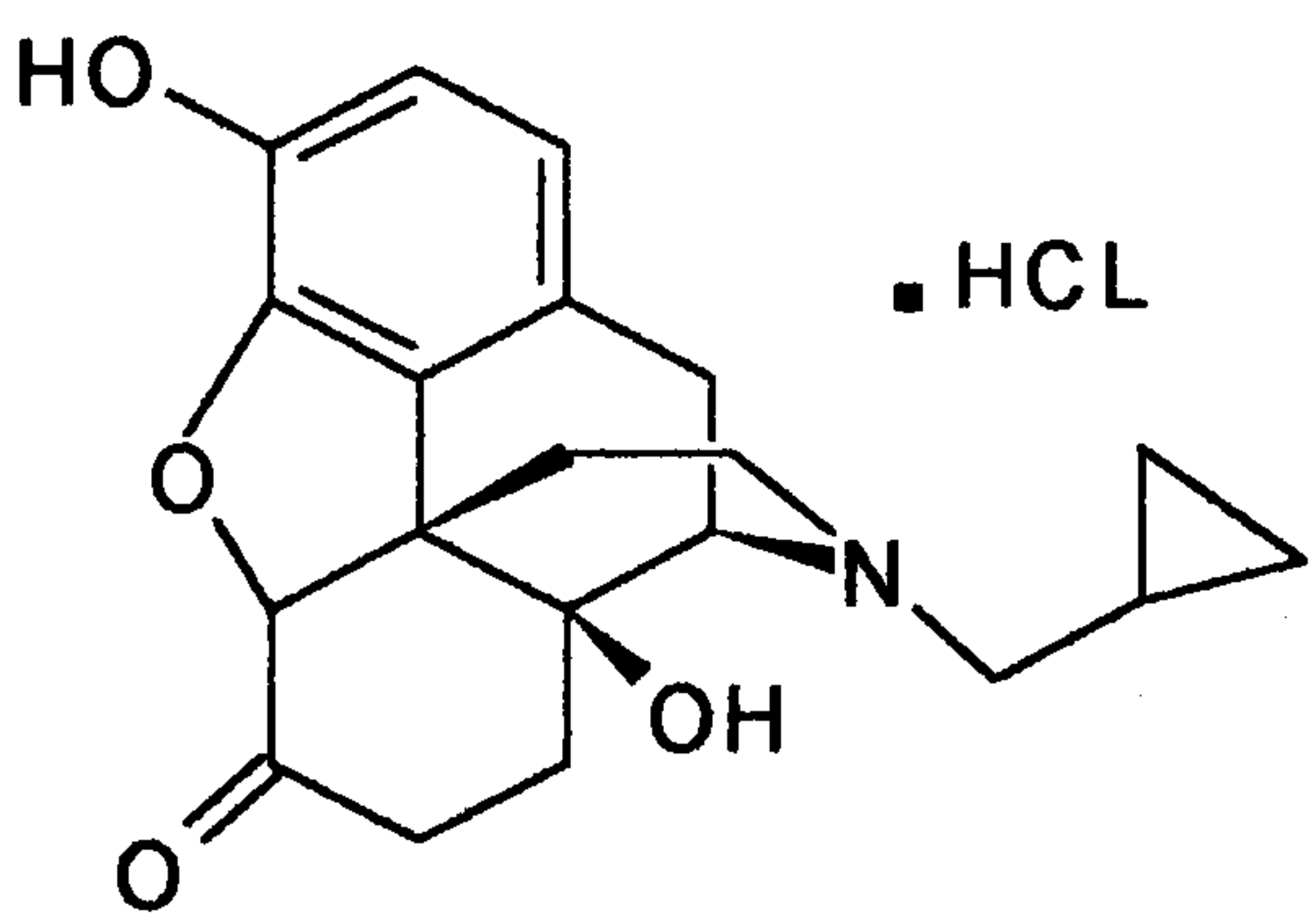


Pyrogallol*		$1 \times 10^{-4} \text{ M}$	Evmiridis <sup>171</sup>
Epinephrine‡ Norepinephrine Dopamine L-Dopa		0.03 to 0.05 μg/mL	Defteros <sup>172</sup>
L-dopa‡		62 μg/L	Yang <sup>173</sup>
Brucine‡		$1.5 \times 10^{-9}$	Qui <sup>174</sup>
Strychnine‡			Zhu <sup>175</sup>
Ephedrines‡			
Benzocaine Buticaine Butoform Procaine‡ Tetracaine		0.003-0.04 μg/mL	Zhang <sup>176</sup>



Humic acid	Complex polyhydroxy polyaromatic	0.7mg/L	Marino <sup>177</sup>
Hydrazones of Aromatic ketones Benzophenone hydrazone‡		$3 \times 10^{-6} \text{M}$ (Rhodamine sensitised)	Ahmed <sup>178</sup>
2,4 dinitrophenyl hydrazine*		$1 \times 10^{-7} \text{mol dm}^{-3}$	Townshend <sup>179</sup> Townshend <sup>180</sup>
Carbonyls by attenuation of 2,4 dinitrophenyl hydrazine	$\text{CH}_3(\text{CH}_2)_4\text{CHO}$	$2 \times 10^{-7} \text{mol dm}^{-3}$ for hexenal	Townshend <sup>181</sup>
Tetracycline‡ Oxytetracycline Chlortetracycline		$0.4 \mu\text{g/mL}$ $0.56 \mu\text{g/mL}$ $0.6 \mu\text{g/mL}$ (Sensitised)	Li <sup>182</sup>
Imipramine‡  Chlorpromazine‡		$5 \times 10^{-7} \text{mol dm}^{-3}$  $2 \times 10^{-6} \text{mol dm}^{-3}$	LopezPaz <sup>183</sup>
5-hydroxytryptamine (serotonin) 5-hydroxytryptophan 5-hydroxyindole-3- acetic acid‡		$2 \times 10^{-6} \text{mol dm}^{-3}$ $2 \times 10^{-6} \text{mol dm}^{-3}$ $2 \times 10^{-5} \text{mol dm}^{-3}$	Barnett <sup>184</sup>
Vitamin B6 (pyridoxine‡)		$58 \text{ng cm}^{-3}$	Li <sup>185</sup>



Uric Acid‡		55ng cm <sup>-3</sup>	Li <sup>186</sup>
Riboflavin‡		62 ng cm <sup>-3</sup>	Li <sup>187</sup>
Medazepam‡		1x10 <sup>-5</sup> mol dm <sup>-3</sup>	Sultan <sup>188</sup>
Naltrexone‡		2.5 ng cm <sup>-3</sup>	Campiglio <sup>189</sup>

‡Structures shown

In addition a recent publication has suggested the use of the reaction as a monitoring method for chemical pollutants. Gallic acid was used as a model compound.<sup>190</sup>

As can be seen from the above, a wide range of structures is capable of producing chemiluminescence on reaction with permanganate, although some of these need a sensitiser to achieve adequate sensitivity for trace analysis applications. There are no clear structural requirements for chemiluminescence. Adjacent hydroxy groups have been suggested as indicators for the potential for chemiluminescence<sup>169</sup> on permanganate oxidation, however it is clear that other features are significant.



## 2.5 The Use of Flow injection and Chemiluminescence in Food Analysis

Food production and processing form an important part of the UK economy, contributing significantly to exports both within the European Union and in the world market.

Production and sale of foods are regulated in the UK by the Food Safety Act 1990<sup>191</sup> and associated regulations. The food and agricultural sectors require a large number of analyses for various reasons including food safety, nutritional value, quality and reasons relating to international trade, where issues of authenticity and origin may have very large financial consequences. Together with control of weights and measures, regulations to ensure that food has not been '*rendered injurious to health*' and is '*of the nature and quality demanded by the purchaser*' were among the first statutory requirements which necessitated physical and chemical measurement to ensure compliance.

Food adulteration has been recorded since the since the Middle Ages. Statutes for particular foods including beer and wine were introduced, mainly to protect revenue. Lack of reliable methods of analysis meant that the consumer had little real protection. In 1860 an Act for Preventing the Adulteration of Food was passed, which established the appointment of Public Analysts bringing, for the first time, qualified analysts into the public regulation of food safety. The Sale of Food Act 1875, Food and Drugs Act 1955 and Food Act 1984 preceded the current Act which meets the requirement of the Directives of the European Union.<sup>192</sup>

Frequently results are required quickly, for example where perishable commodities are taken into a manufacturing line. Multiple analysis may be required as food products are typically inhomogeneous. While good sampling practice can reduce the uncertainty,<sup>193</sup> the analysis of many samples taken from different points in the bulk gives information on the level and distribution of the analytes. In process control both



fast and multiple analyses are required. For example in fermentations where the change of a parameter such as pH or sugar content is used to identify the need to start the next stage of processing.

As discussed in earlier sections the use of chemiluminescence detection, particularly with flow injection, answers both of the needs. The use of chemiluminescence in food analysis was reviewed<sup>12</sup> with a range of applications being described. The majority of chemiluminescence methods so far developed have been for water analysis rather than the more complex food matrices.

Determination of N-nitrosamines, using gas chromatography with chemiluminescent detection of nitric oxide, has been discussed in section 2.1.7. It is used for foods such as cured meats, which are likely to be subject to nitrosating conditions and with HPLC separation for non-volatile nitrosamines.<sup>194</sup>

Other than determination of ATP as an indicator of microbial contamination the most widely used chemiluminescence reagent used in food analysis is luminol. Reactions which produce hydrogen peroxide, such as oxidation of glucose by glucose oxidase, and catalysis of the luminol/hydrogen peroxide reaction by metal ions have been used in food analysis. Chromium (III) has been determined in a range of food products including bread and shrimp. Selectivity was achieved since complex formation of EDTA with chromium is slower than complex formation with other metal ions.<sup>195</sup> The enzymatic conversion of sucrose to glucose with invertase and mutarotase together, followed by reaction with glucose oxidase as above, has been used for analysis of soft drinks and cereals.<sup>196</sup> A similar system with galactosidase, in place of invertase has been used for determination of lactose in milk after dialysis in a flow injection system.<sup>197</sup> Enzyme reactors with luminol detection have been used to determine free amino acids in cheese<sup>198</sup> and soft drinks.<sup>199</sup> The luminol reaction has also been used to determine levels of lipid hydroperoxides formed during lipid



oxidation as an indication of oxidative rancidity.<sup>200</sup> A similar system has been used as an indicator for gamma irradiation of foodstuffs including milk meat and spices<sup>201</sup> and bones and seafood shells.<sup>202</sup>

The lucigenin reaction has been used to determine trace levels of cobalt in orchard leaves (a standard reference material).<sup>203</sup> A complex extraction system had to be used to avoid interference from iron and magnesium which are often present in biological systems at a great excess  $> 10^5$  over cobalt.

The measurement of chemiluminescence emitted directly from food samples, due to reactions within the food matrix or with atmospheric oxygen, is generally of low intensity, but has been used to monitor oxidation in oils and fats,<sup>16</sup> and after hydration, in cereals.<sup>204</sup> Attempts have been made to use the ultraweak chemiluminescence emission as an indicator for gamma irradiation. Peroxyoxalate methods have been used in conjunction with flow injection in determination of amines in fish.<sup>205</sup>

While a number of organic food constituents such as vitamins including thiamine,<sup>206</sup> folate<sup>207</sup> and riboflavin<sup>208</sup> have been determined by chemiluminescence these methods have been mainly applied to synthetic systems such as pharmaceutical preparations.

A major new application of chemiluminescence detection is in immunoassay, where chemiluminescent labels are replacing radiolabels as they do not have the health hazards and waste disposal problems encountered with radioactivity. A further advantage is the simple measuring equipment used, since no light source is required as in fluorescence or spectrophotometric measurement. Labels used include luminol and isoluminol derivatives such as aminobutylethylisoluminol, acridinium compounds,<sup>209</sup> oxalate esters and bioluminescent systems. The various labels and techniques have been reviewed.<sup>11,210,211</sup> Most applications are in medical



diagnostics, however there is scope for using chemiluminescent labels for the full range of immunoassays used in food analysis.

Many of the systems discussed above are or are potentially amenable to flow injection formats. Lopez-Fernandez et al have reviewed 200 methods using flow injection in food analysis including five luminescence methods and has developed a set of criteria to evaluate the quality of such methods.<sup>212</sup>

A more frivolous application of chemiluminescence in foods has recently been reported<sup>213</sup> in which it was proposed to use coelentraxine a luciferin produced in jellyfish in a luciferase system to produce glowing foods, beverages and cosmetics.



# CHAPTER 3

## METHODS AND MATERIALS

### 3.1 Chemicals

Chemicals were from the following sources. Reagents were of analytical grade, unless otherwise indicated.

#### **Acros, Loughborough, UK**

D- IsoAscorbic Acid  $C_6H_8O$

#### **Aldrich Chemical, Co UK**

Hydrogen Peroxide 30% stabilised  $H_2O_2$

#### **Avocado**

Luminol  $C_8H_7O_2N_3$

#### **BDH, Poole, UK**

Ethanal  $C_2H_4O$

Glucosamine  $C_6H_{13}NO_5$

Glycerol  $C_3H_8O_3$

Nicotinic acid  $C_6H_5O_2N$

Oxalic acid 98%  $C_2O_4H_2 \cdot 2H_2O$

Pyridoxine  $C_8H_{11}O_3N \cdot HCl$

Propan 1,2-diol  $C_3H_8O_2$

Propanone  $C_3H_6O$

Fluorescein  $C_{20}H_{12}O_5$

Rhodamine B  $C_{28}H_{31}O_3N_2$

Ribose  $C_5H_{10}O_5$



Trehalose  $C_{12}H_{22}O_{12}$

Aluminium chloride  $AlCl_3$

Ammonium nitrate  $NH_4NO_3$

Cobalt(II) chloride  $CoCl_2 \cdot 6H_2O$

Copper(II) sulphate  $CuSO_4 \cdot 5H_2O$

Metaphosphoric acid  $HPO_3$

Iron(III) chloride >95%  $FeCl_3$

Iron(II) sulphate 99%  $FeSO_4 \cdot 7H_2O$

Potassium bromide  $KBr$

Potassium chloride  $KCl$

Potassium iodide  $KI$

Potassium permanganate  $KMnO_4$

Sodium nitrite  $NaNO_2$

Sodium sulphite  $NaSO_3$

Tin(II) chloride  $SnCl_2 \cdot 2H_2O$

### **Breckland Scientific, Thetford UK**

Activated Charcoal

### **Fluka, Gillingham, UK**

Dehydro-L (+)-ascorbic acid, dimer >99%,  $C_{12}H_{12}O_{12}$

Methanal 36% (stabilised)  $CH_2O$

### **Fisher Scientific, Loughborough, UK**

Acetic acid  $C_2H_3O_2$

Hydrochloric acid SG 1.18  $HCl$

Nitric acid  $HNO_3$



Sulphuric acid SG 1.84  $\text{H}_2\text{SO}_4$

Sodium pyrophosphate  $\text{Na}_4\text{P}_2\text{O}_7 \cdot 10\text{H}_2\text{O}$

Tetrahydrofuran  $\text{C}_4\text{H}_8\text{O}$

**Sigma Chemical Company, Poole, UK**

Arabinose,  $\text{C}_5\text{H}_{10}\text{O}_5$

L+ Ascorbic acid  $\text{C}_6\text{H}_8\text{O}_6$

Cellobiose  $\text{C}_{12}\text{H}_{22}\text{O}_{12}$

D- Fructose <0.05% glucose  $\text{C}_6\text{H}_{12}\text{O}_6$

Dextran MW  $2 \times 10^6$

D+ Glucose >99.5%  $\text{C}_6\text{H}_{12}\text{O}_6$

D+ Galactose >98%  $\text{C}_6\text{H}_{12}\text{O}_6$

Lactose  $\text{C}_{12}\text{H}_{22}\text{O}_{12} \cdot \text{H}_2\text{O}$

Maltose 98%  $\text{C}_{12}\text{H}_{22}\text{O}_{12} \cdot \text{H}_2\text{O}$

D-Mannitol  $\text{C}_6\text{H}_{14}\text{O}_6$

Meso-Erythritol  $\text{C}_4\text{H}_{10}\text{O}_4$

Myo-inositol  $\text{C}_6\text{H}_{12}\text{O}_6$

D- Sorbitol  $\text{C}_6\text{H}_{14}\text{O}_6$

Sucrose >99.5%  $\text{C}_{12}\text{H}_{22}\text{O}_{12}$

Xylose,  $\text{C}_5\text{H}_{10}\text{O}_5$

2,6-Dichloro indophenol  $\text{C}_{12}\text{H}_5\text{O}_2\text{NCl}_2$

2,4 Dihydroxybenzoic acid  $\text{C}_7\text{H}_6\text{O}_4$

2,5 Dihydroxybenzoic acid  $\text{C}_7\text{H}_6\text{O}_4$

2,6 Dihydroxybenzoic acid  $\text{C}_7\text{H}_6\text{O}_4$

Flavin mononucleotide  $\text{C}_{17}\text{H}_{19}\text{N}_4\text{O}_9\text{PNa}_2$

o-Phenylenediamine  $\text{C}_6\text{H}_8\text{N}_2 \cdot 2\text{HCl}$

Pyridoxine  $\text{C}_7\text{H}_{11}\text{O}_3\text{N} \cdot \text{HCl}$



D-Saccharic acid potassium  $\text{C}_6\text{H}_9\text{O}_8\text{K}$

Thiamine  $\text{C}_{12}\text{H}_{16}\text{N}_4\text{OSCl.HCl}$

Manganese(III) acetate  $\text{Mn}(\text{C}_2\text{H}_3\text{O}_2)_3$

Manganese(IV) oxide  $\text{MnO}_2$

Manganese(II) sulphate  $(\text{MnSO}_4.\text{H}_2\text{O})$

Polyphosphoric acid  $\text{H}_2\text{PO}_3$

Trisodium Tripolyphosphate  $\text{Na}_3\text{P}_3\text{O}_{10}$

Sodium hydroxide  $\text{NaOH}$

Methanol  $\text{CH}_3\text{OH}$

Ethyl acetate  $\text{C}_4\text{H}_8\text{O}_2$

Ethanol  $\text{C}_2\text{H}_5\text{OH}$

Acetonitrile  $\text{CH}_3\text{CN}$



## **3.2 Preparation of solutions**

### **3.2.1 Potassium permanganate solutions**

Solutions were prepared by dissolving the required amount of potassium permanganate ( $M_r$  158) in deionised water, or the required strength of sulphuric acid.. Solutions in water of  $0.1 \text{ mol dm}^{-3}$  were stored refrigerated for up to 1 week. Working and acidic solutions or were prepared before use. Solutions were kept in the dark

### **3.2.2 Manganese sulphate (II)/ Sulphuric acid**

Manganese (II) sulphate monohydrate was dissolved in the required strength of sulphuric acid. Solutions were stored for up to 1 week.

### **3.2.3 Manganese (III) Reagent – Aqueous Final Formulation**

Manganese sulphate monohydrate, 1.5g, was dissolved in  $60 \text{ cm}^3$  water and  $20 \text{ cm}^3$  concentrated sulphuric acid was added with stirring. The mixture was cooled in an ice bath to below  $10^\circ$ . Potassium permanganate, 0.158 g, was dissolved in  $20 \text{ cm}^3$  water with stirring. The permanganate solution was added slowly to the manganese sulphate solution with constant stirring. Stirring was continued for 10 minutes and the solution was kept in ice during use. The solution was freshly prepared each day.

### **3.2.4 Manganese (III) Reagent – Methanol Final Formulation**

Manganese sulphate monohydrate, 1.5g, was dissolved in  $20 \text{ cm}^3$  water and  $10 \text{ cm}^3$  concentrated sulphuric acid was added with stirring. The mixture was cooled in an ice bath to below  $10^\circ$  and  $40 \text{ cm}^3$  methanol was added with stirring. The mixture was cooled again to below  $10^\circ$ . Potassium permanganate, 0.158 g, was dissolved in  $10 \text{ cm}^3$  water with stirring. The permanganate solution was added slowly to the



manganese sulphate solution with constant stirring. Stirring was continued for a further 10 minutes and the solution was kept in ice during use. The solution was freshly prepared each day.

### **3.2.5 Ascorbic Acid solutions**

#### **3.2.5.1 Aqueous**

Prepared daily, the required amount of ascorbic acid was dissolved in demineralised water (pH 4.8-5.5); dilutions were prepared in demin. water and stored in the dark.

#### **3.2.5.2 Phosphate Stabilised**

Solvent: Metaphosphoric acid, 20g, and glacial acetic acid 50cm<sup>3</sup> were dissolved in 1dm<sup>3</sup> demineralised water. The solution was kept refrigerated and in the dark for up to 4 weeks.

Standards: The required amount of ascorbic acid was dissolved in 100 cm<sup>3</sup> metaphosphoric/ acetic solvent. Dilutions were prepared in the same solvent.



### **3.3 Samples**

Samples were purchased locally or provided by Chemlab.

#### **3.3.1 Samples for Vitamin C analysis**

*Juice 1* Fruit juice concentrate, vitamin C declared greater than 45mg/100ml

*Juice 2* Fruit juice ready to drink, vitamin C declared greater than 15mg/100ml

*Tablet 1* 200mg vitamin C tablet, vitamin C declared 200mg/tablet sorbitol excipient

*Tablet 2* ADC multivitamin tablet, vitamin C declared 60mg/tablet lactose excipient

*Tablet 3* Multivitamin powder, vitamin C declared as 60mg/sachet includes vitamins ADE and water soluble vitamins in a base including citric acid and sucrose.

#### **3.3.2 Beers**

Bitter beer 1 -Parkins special, Sainsbury , 4% ABV

Bitter beer 2 -Traditional bitter, Sainsbury 3.4% ABV

Bitter beer 3 – Worthington best bitter 3.6% ABV

Stout 1 –Mackesons, 3% ABV

Stout 2 – Guinness Original, 4.3% ABV

Lager 1 – Skol, 3.4% ABV

Lager 2 – Carling Black Label, 4.1% ABV

#### **3.3.3 Brewing Materials**

Malt Extract 1- Amber malt extract (dry)

Malt Extract 2 - Munton's Dark malt extract (liquid)

Malt Extract 3 – Brupaks pale malt extract (liquid)

Malt Extract 4 – Edme DMS malt extract (liquid, high diastatic)

Isomerised hop pellets, Lupofresh

Dried hops variety Bramling cross

Brewcon isomerised hop extract.



## **3.4 Instrumentation and Equipment**

### **3.4.1 Volumetric Equipment**

Standard laboratory glassware, volumetric flasks, one mark and graduated pipettes, burettes, and air displacement pipettes (Gilson, Anachem).

### **3.4.2 Weighing**

Weighing was carried out using 2 place top pan (Salter BP2200) and 4 place (Precisa 120A) or 4/5 place (Precisa 405M-200A) analytical balances as appropriate.

### **3.4.3 Batch Counter**

Time courses of slow and low intensity chemiluminescence reactions were monitored using a liquid scintillation counter model (Packard 2002), from which the calibration source had been removed.

### **3.4.4 Fluorescence Spectrophotometry**

Fluorescence and chemiluminescence spectra were measured using a fast scanning fluorescence spectrophotometer, Hitachi model F-4500, (Hitachi Ltd, Japan) fitted with either standard or extended range PMT detectors. Data capture was using a Pentium PC with Hitachi software version 4.11

Fluorescence cuvettes, 10mm path length with four clear sides, from quartz, optical glass and polymethylmethacrylate.

For continuous flow – 10mm path length flow cell, optical glass (Hellma, Germany)



### **3.4.5 Stopped Flow Measurements**

Hitech SF20 rapid kinetic accessory, with pneumatic actuator. 10mm flow cell configured for Hitachi fluorimeter (Hi-Tech, Salisbury UK)

### **3.4.6 UV-Visible Spectrophotometry**

UV and visible spectra and UV-visible absorbance time courses of reactions were measured using scanning spectrophotometers, Shimadzu model 160A (Shimadzu corporation, Japan) and Unicam model Delta 2 (Unicam, Cambridge, UK ) Silica and optical glass cuvettes 10mm and 2mm path length.

### **3.4.7 Flow Injection Analysis**

#### **3.4.7.1 Pump**

Four-channel peristaltic pump, Ismatec model H07331 (Ismatec, Carshalton, UK), with minicartridges and three-stop tygon tubing of various internal diameters.

#### **3.4.7.2 Injection Valve**

Rheodyne model 5020 low-pressure loop injection valve with 0.8mm id flow passages and interchangeable loops (Rheodyne, Cotati, CA, USA) actuated by a Universal Valve switching module.

#### **3.4.7.3 Detectors**

**Photomultiplier** Thorn EMI blue sensitive bialkali (type 9813B) and red sensitive trialkali S20 (type 9816B) in Thorn EMI housing powered by a Thorne EMI type PM28B high voltage source (Thorn EMI Electron Tubes, Ruislip UK) used at 1.3kV unless otherwise indicated

**Photodiode detector** model CL1 (Chemlab, Great Dunmow, Essex, UK)



#### **3.4.7.4 Manifolds**

Various manifolds were constructed using 0.5mm id PTFE tubing with flanged connectors and 1.02mm id tygon tubing. Mixing was carried out in a low dead volume Kel-F T-piece, or nylon Y-piece as required.

#### **3.4.7.5 Chart Recorder**

BD40 and BD20 Chart recorders (Kipp and Zonnen, Delft, Netherlands)

#### **3.4.7.6 Data Capture**

Pico ADC 100 connected to 386PC (Pico Technology, Hardwick, UK)

#### **3.4.8 Cyclic Voltammetry**

Potentiostat - $\mu$ Autolab with Autolab software (Ecochemie).

#### **3.4.9 pH Measurement**

pH meter model 292 (Pye Unicam, Cambridge, UK) or hand held pH monitor were used depending on required accuracy, calibrated with pH 4, 7 and 9.2 buffers prepared from buffer tablets (BDH).

#### **3.4.10 HPLC Equipment**

Beckman System Gold 118 Solvent Module (Beckman, Fullerton, CA, USA)

Rheodyne 7125 loop injection valve (Rheodyne, Cotati, CA, USA)

Column 25 cm 4.6id containing 5 $\mu$ m Supersil aminopropyl silica packing (Supelco, Poole, UK)

Post column system consisting of : photodiode detector model CL1 (Chemlab, Great Dunmow, Essex, UK), Four-channel peristaltic pump Ismatec model H07331



(Ismatec, Carshalton, UK) supplied with minicartridges and three-stop tygon tubing 0.052mm id and low dead volume Kel-F T-piece (Supelco, Poole, UK).

### **3.4.11 Data Handling**

Chart recorder peaks were measured manually.

Batch counter output was recorded manually.

Results were entered into data analysis packages manually.

Data from the fluorescence spectrophotometer, Autolab potentiostat and ADC100 were converted into text files and imported into spreadsheets of data analysis packages.

Data analysis was undertaken using Origin version 4.1 (Microcal) and Excel versions 5.0 and '97(Microsoft).<sup>214</sup> Where error bars are shown in the graphs these are calculated as the sample standard deviation for the replicate measurements for that point. Unless otherwise indicated six replicate measurements were made for each point.

Coefficient of regression, calculated through the Origin programme. Unless otherwise indicated, error bars were not used to weight the regression .



## **3.5 Calibration procedures**

### **3.5.1 Peristaltic Pumps**

Pumps were calibrated for different pump tubes by weighing amounts of deionised water delivered in one minute at various pump rates. Repeatability for multiple aliquots was acceptable with RSDRs for 10 sequential measurements of less than 1%. Linear regression was used to calculate flow rates for intermediate speeds. Regression coefficients were good and better than 0.99.

### **3.5.2 Air-displacement Pipettes**

Volumes delivered were checked by weighing replicate aliquots of deionised water<sup>215</sup> and found to be within manufacturer's specifications.

### **3.5.3 Calibration of FIA Sample Loop**

The volume of sample delivered by the loop injector in was measured by spectrophotometry using a method based on that of van Straden.<sup>216</sup> Replicate injections of  $0.1\text{ mol dm}^{-3}$  potassium permanganate were made into a stream of deionised water flowing at  $2.5\text{ cm min}^{-1}$  in a single line manifold. The samples were collected in a  $50\text{ cm}^3$  volumetric flask and diluted to volume. The absorbance of the solutions was measured at 525nm. A calibration line over the range  $4\times 10^{-5}$  to  $2\times 10^{-4}$   $\text{mol dm}^{-3}$  was prepared from the same stock solution, using a previously calibrated air displacement pipette. The sample volume was found to be  $75.6\pm 0.9\text{ }\mu\text{L}$ . For larger volumes additional tubing, supplied with the injection valve, with stated volumes of  $100\mu\text{L}$  or  $500\mu\text{L}$  was inserted.



### **3.5.4 UV-Visible Spectrophotometers**

UV visible spectrophotometry was used to follow reactions of permanganate in the wavelength range 400 to 700nm. The peak maxima measured for dilute aqueous permanganate solutions agreed well with published data.

### **3.5.5 Fluorescence Spectrophotometer**

#### **3.5.5.1 Fluorescence Mode**

Using the manufacturer's instructions, accuracy of wavelength measurement, signal to noise and drift parameters were determined. Wavelength accuracy for excitation and emission monochromators was confirmed, by measuring the wavelength of a spectrum line for the xenon lamp source. In all cases the indicative peak was within the specification at  $451 \pm 1$  nm. Signal to noise and drift were determined by scanning for 10 minutes at the wavelength of the maximum Raman peak for water. The specification for signal to noise and drift was met or exceeded for the standard photomultiplier tube.

#### **3.5.5.2 Chemiluminescence Mode**

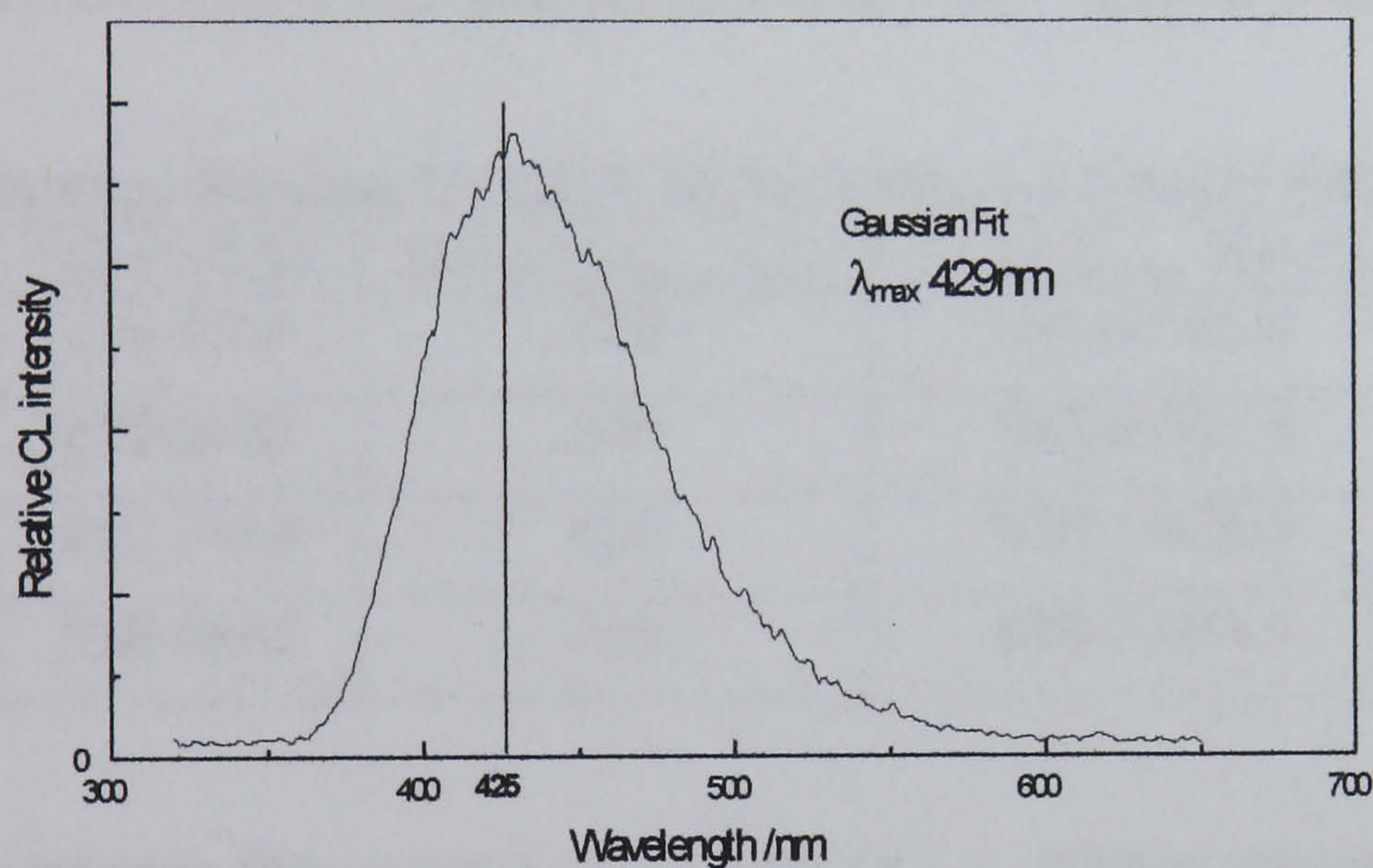
The accuracy of the wavelength measurement of the spectrofluorimeter was established using two well-characterised spectra. The emission from luminol was used for the low wavelength region, and that of singlet oxygen for the high wavelength region.

**a) Luminol Emission at 425nm** The luminol reaction, in aqueous solution, is known to have a wavelength maximum at 425nm.<sup>33</sup> A spectrum, run using continuous flow, has a  $\lambda_{\text{max}}$  consistent with literature values. An example is shown as Figure 3.1.

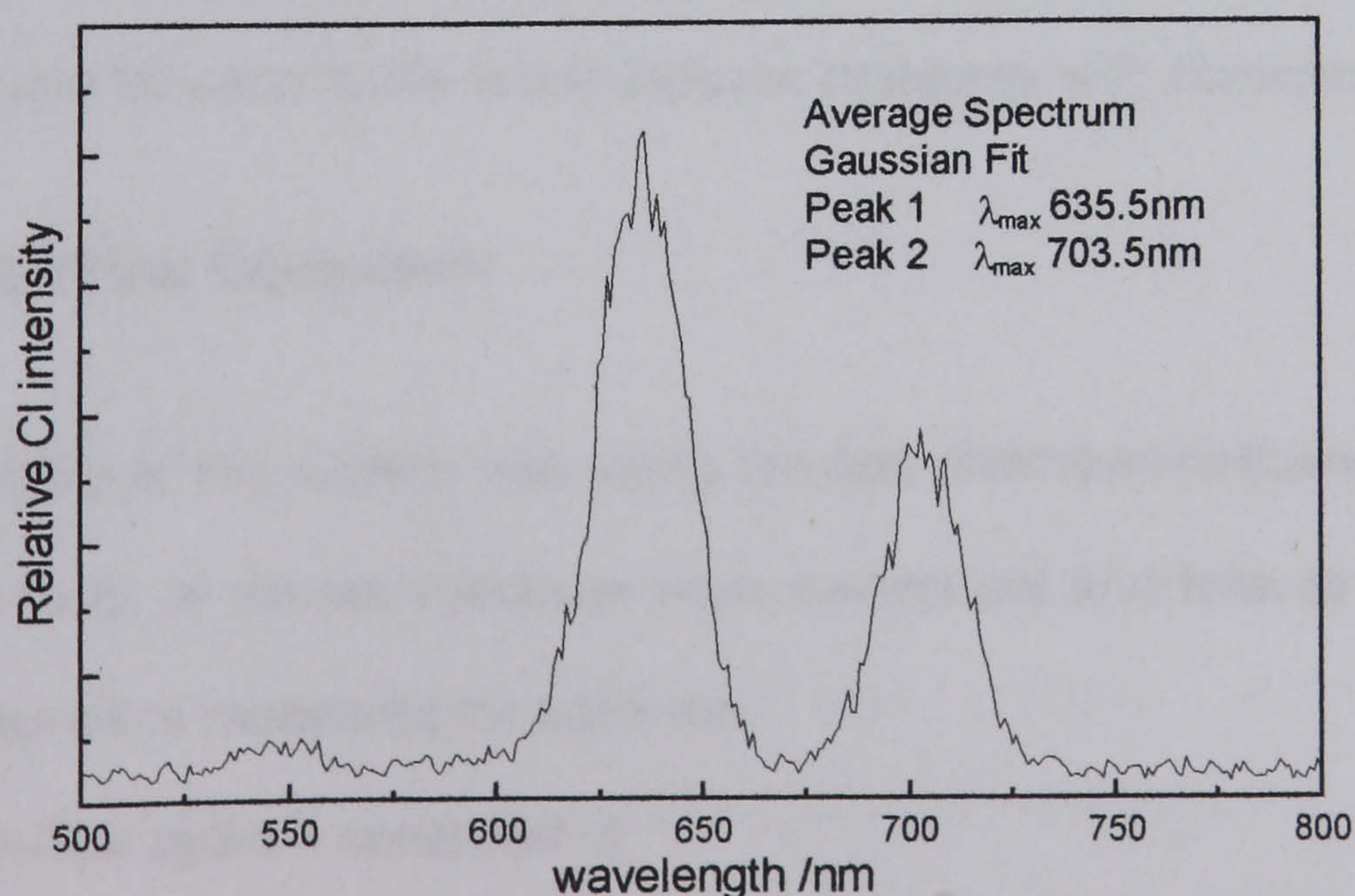


**b) Singlet Oxygen Emission at 633 and 704 nm** As discussed in section 2.1.9, singlet oxygen is known to emit as a number of sharp bands in the red and near-infrared. The reaction between peroxide and hypochlorite in alkaline solution is known to generate singlet oxygen. Due to the speed of the reaction and the short lifetime of singlet oxygen in an aqueous system it was not possible to use continuous flow and the semi-flow method was used. Individual spectra were noisy therefore replicate spectra were collected and averaged mathematically. The average from fifty runs consisted of two sharp peaks with maxima at 636 and 704nm. These maxima are consistent with literature values.<sup>53,93</sup> The spectrum is shown as Figure 3.2.

**Figure 3.1 Spectrum of Luminal Emission for Wide Range PMT**



**Figure 3.2 Emission Spectrum Singlet Oxygen Wide PMT**



The peak at approximately 550nm was observed in many systems and was considered to be an artefact, possibly due to reflections in the optical path.



Additional checks of wavelength precision were undertaken using a range of light emitting diodes (RS Components) connected to a 9V battery and resistor. Spectra were measured using various combinations of slit width (2.5, 5, 20nm), scan speed (30000, 2400, 240 nm sec<sup>-1</sup>), PMT voltage (400, 700 and 950V) and response time (0.004, 0.1 sec and Automatic).

For the fastest scan speed, the use of a response time of 0.1sec resulted in peaks with  $\lambda_{\text{max}}$  at approximately 10nm longer than when faster response rates were used. For fast scan speeds short response times, were used for collecting spectra although noise levels were high. The maximum wavelengths for LEDs were determined by fitting Gaussian functions to the spectral data and found to be as shown in Table 3.1:

**Table 3.1 Spectral Maxima for LEDs Determined on Hitachi F4500 Fluorimeter**

Colour	RS Part no	Nominal $\lambda_{\text{max}}$ $\lambda_{\text{max}}$	Found $\lambda_{\text{max}}$ 95%CI
Green	228 5427	565	565.3-565.9
Yellow	228 5433	590	580.8-581.8
Orange	227 5449	625	629.1-630.5
Red	228 5405	700	686.2-688.1

The deviation between the nominal and observed  $\lambda_{\text{max}}$  means that the diodes cannot be used to confirm wavelength accuracy but as their use is quick apparent changes in  $\lambda_{\text{max}}$  response for each diode would indicate problems with accuracy.

### 3.5.6 Stopped Flow Equipment

The repeatability of the system was using the fast chemiluminescence from luminol. Five sets (A to E) of eleven injections were carried out and time to peak maximum and peak area were measured for each run.

The stopped–flow system consisted of:

Syringe 1: Luminol 1x10<sup>-3</sup> mol dm<sup>-3</sup>, Co (II) 1x10<sup>-2</sup> mol dm<sup>-3</sup> in carbonate buffer pH 10 0.1 mol dm<sup>-3</sup>. Syringe 2: Hydrogen peroxide 0.03%. Drive pressure: 6 bar.



For the time to peak maximum there is a significant difference between the repeatability for individual syringe positions (injections) and the repeatability for injections from the same syringe filling (sets). The results are shown in Table 3.2.

Table 3.3 shows the results for the area measurement.

Table 3.2 Time to Peak Maximum

	Mean	SD	RSDR%
Injection			
1	115.8	1.79	1.54
2	117.6	2.61	2.22
3	119.4	1.34	1.12
4	122.0	2.83	2.32
5	126.8	2.17	1.71
6	128.2	2.17	1.69
7	134.0	4.80	3.58
8	134.8	4.15	3.08
9	137.4	3.65	2.65
10	140.4	3.78	2.69
11	144.4	2.19	1.52
Set			
A	129.7	10.77	8.30
B	131.2	11.37	8.66
C	128.7	9.41	7.31
D	129.0	9.38	7.27
E	127.2	9.11	7.16

Table 3.3 Peak Area

	Mean	SD	RSDR%
Injection			
1	68290	6156	9.01
2	56901	5430	9.54
3	54764	4477	8.18
4	58356	3319	5.69
5	59876	1968	3.29
6	61089	2041	3.34
7	58962	2948	5.00
8	57422	3181	5.54
9	57449	3585	6.24
10	56752	3060	5.39
11	59644	6588	11.04
Set			
A	56573	6093	10.77
B	57763	3421	5.92
C	61507	5356	8.71
D	61704	2588	4.20
E	57683	5422	9.40

The statistical significance was confirmed by carrying out the one way ANOVA<sup>217</sup>

Table 3.4 Analysis of Variance for Stopped-Flow replication

a) ANOVA for Time to Peak Maximum

Source of Variation	SS	df	F	P-value	F crit
Between Groups	4625.3	10	51.86	4.9E-21	2.054
Within Groups	392.4	44			
Total	5017.7	54			

b) ANOVA for Peak Area

Source of Variation	SS	df	F	P-value	F crit
Between Groups	6.23E+08	10	3.59	0.001525	2.054
Within Groups	7.64E+08	44			
Total	1.39E+09	54			



It can be seen that the F value exceeds the critical value showing that there is significant difference within the groups for time to peak maximum. A similar analysis for peak area also shows significant difference within the groups.

c) ANOVA for time to peak maximum for individual syringe points

Source of Variation	SS	df	F	P-value	F crit
Between Groups	93.9	4	0.233	0.919	2.56
Within Groups	5047.6	50			
Total	5141.53	54			

For precise work on fast reactions it was necessary to reload syringes between each injection in order to use the same syringe position for replicate experiments. As shown in table 3.4 c this gives satisfactory repeatability.

### 3.5.7 Batch Counting System

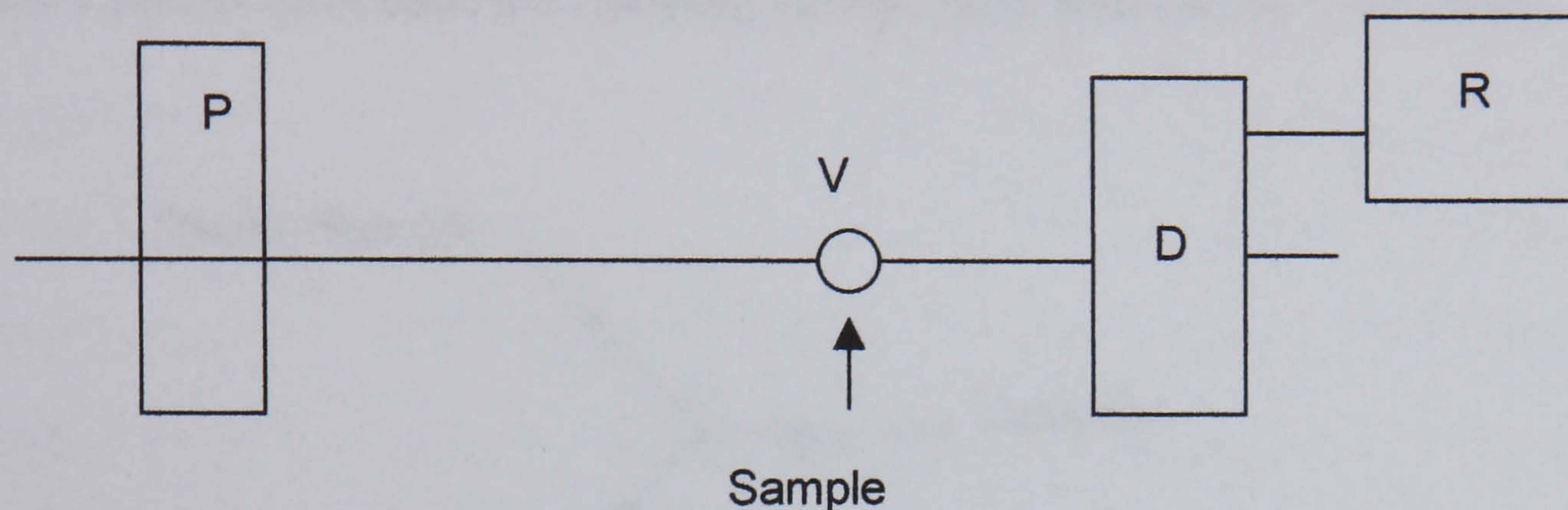
The modified liquid scintillation spectrophotometer had previously been calibrated using luminescence standards. It was found that, on average 6.7 photons were required per count. This equivalence was used to convert counts per counting interval (usually 12 sec) to photons/sec. As the emission spectrum of the luminescence standard has a maximum at around 440nm<sup>218</sup> the calibration is not strictly applicable at 700nm, the emission maximum of the reactions studied.



## 3.6 Experimental Procedures

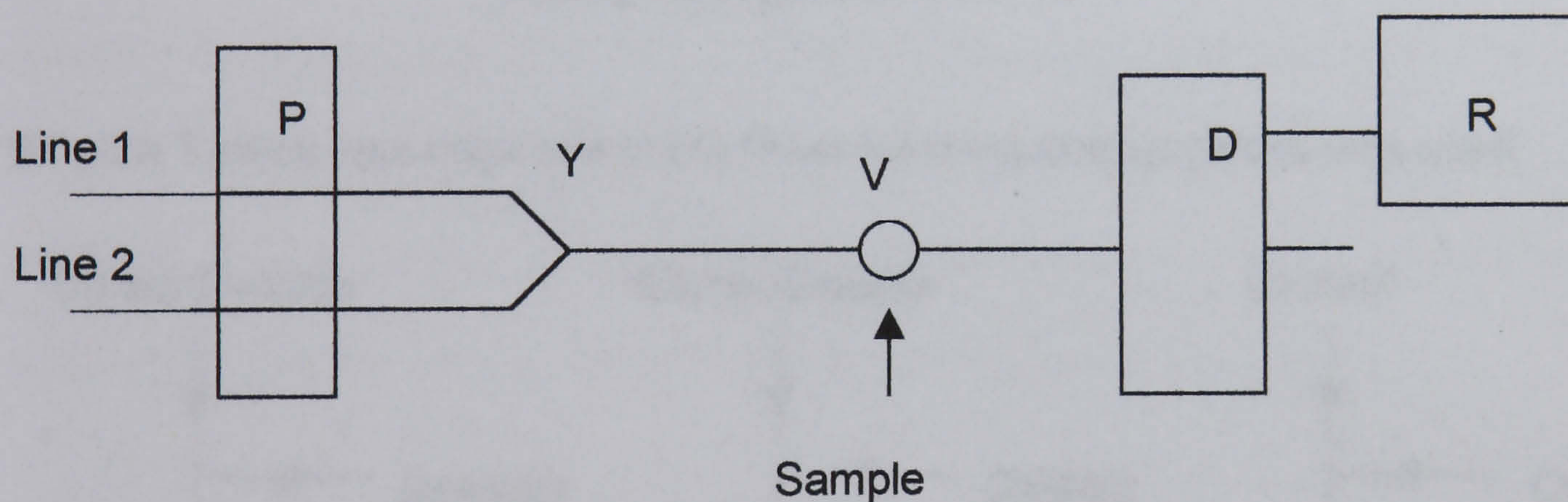
### 3.6.1 Flow Injection Experiments

Flow injection was studied using a number of different manifold designs using both single and multiple line manifolds and using both analyte and oxidant as injectant.



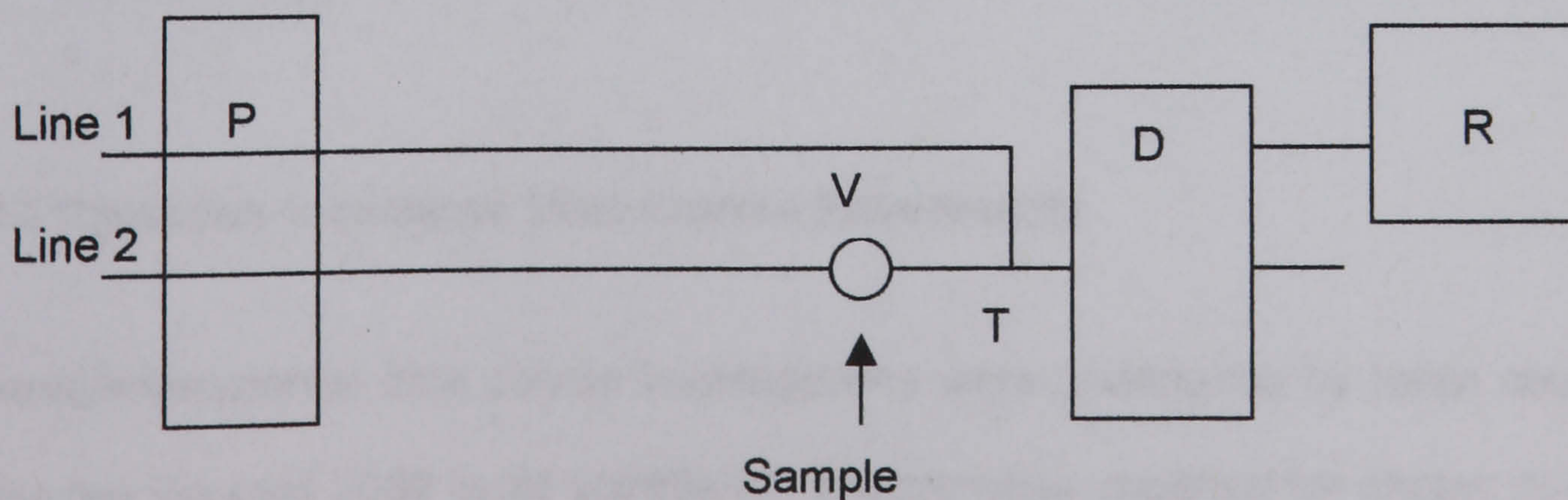
#### Manifold 1

P – Pump D – Detector R – Data recording V – Injection valve



#### Manifold 2

P – Pump D – Detector R – Data recording V – Injection valve Y – Y piece



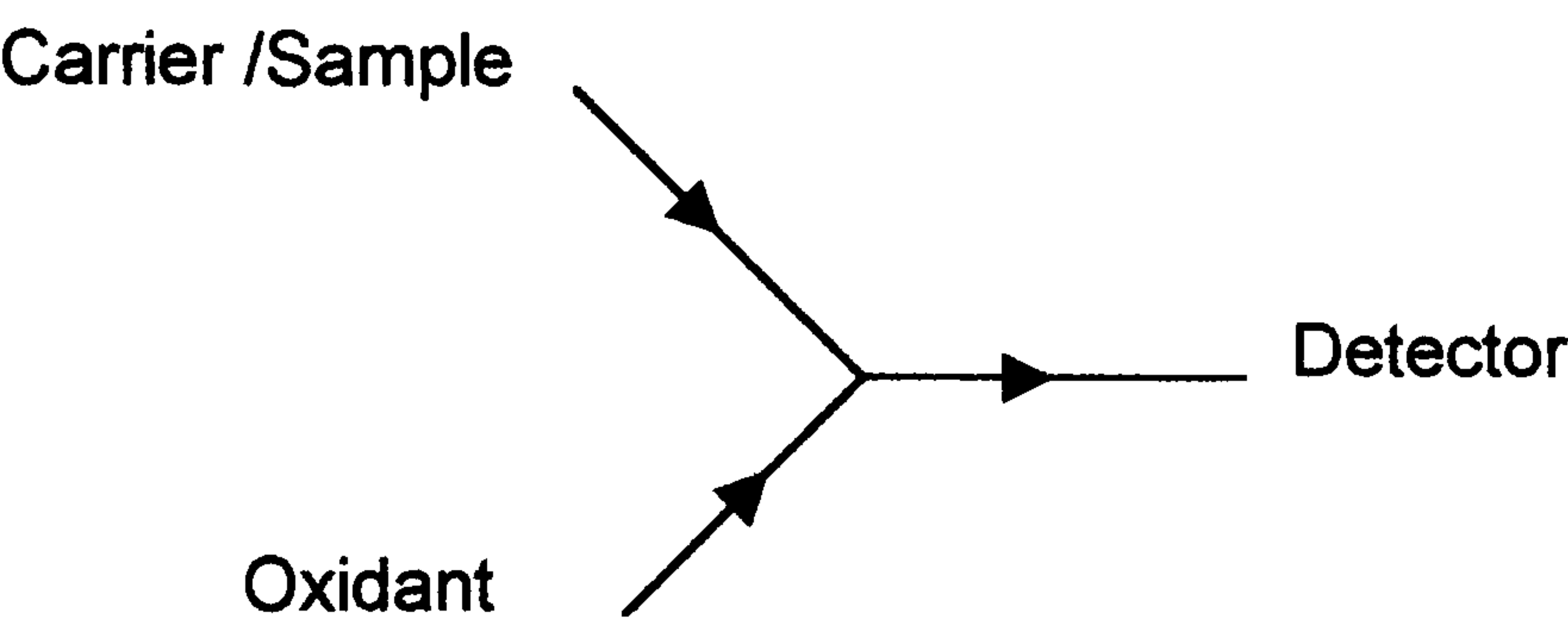
#### Manifold 3

P – Pump D – Detector R – Data recording V – Injection valve T – Y or T piece



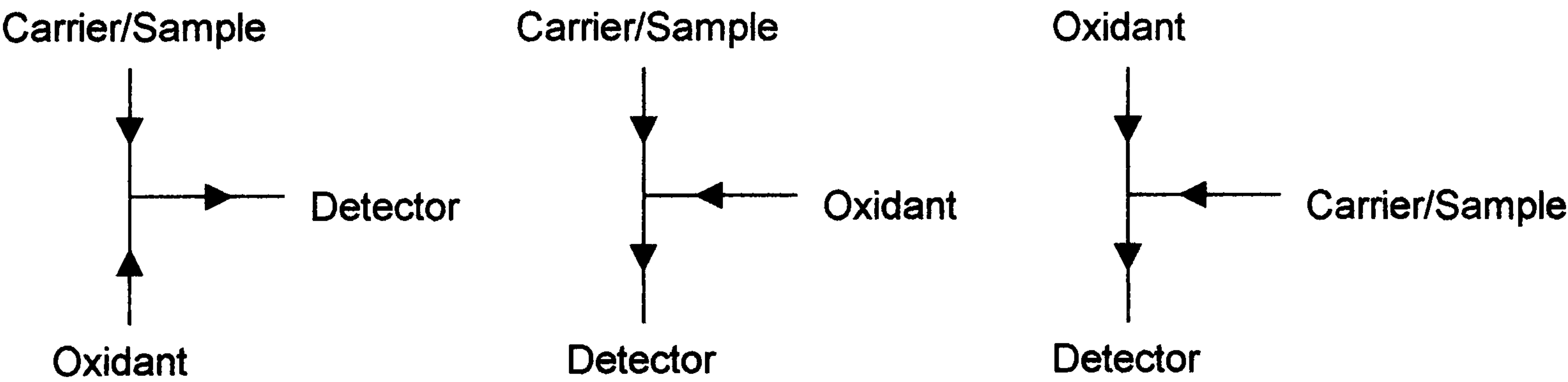
The detector, based on a published design,<sup>219</sup> consisted of a coiled tube of 0.5-mm id PTFE placed beneath the photocathode of the PMT inside the light tight housing. All experiments were undertaken at room temperature, except when the manganese (III) reagent was used which was kept in an ice bath at 2-5°C.

Where Y pieces were used the following configuration was applied in all cases:



**Mixing Configuration Y1**

When a T piece was used one of the three following configurations was used:



**Configuration T1**

**Configuration T2**

**Configuration T3**

### 3.6.2 Chemiluminescence Time Course Experiments

Chemiluminescence time course investigations were undertaken by batch counting, using the Packard 2002 liquid scintillation spectrometer, modified for photon counting and operating in coincidence mode. Where the emission was sufficiently intense the Hitachi fluorescence spectrophotometer was used with the source turned off.



3.6.3 Batch Counting

Aliquots of analyte and carrier solutions were introduced into a low-potassium glass liquid scintillation vial and mixed by swirling. The vial was closed with a resin screw cap and introduced into the sample chamber of the spectrometer. The spectrometer was started and the number of counts in 12 sec was determined to establish the background. The vial was removed from the spectrometer and an aliquot of oxidant was added, at the same time a stopwatch was started. The contents of the vial were mixed by swirling and the vial was returned to the spectrometer. After 15sec from the introduction of oxidant counting was started and counts recorded at 12 sec intervals until the count rate was typically less than 100 counts/12 sec.

3.6.4 Fluorescence Spectrophotometer

Aliquots of sample/carrier and oxidant were mixed using batch, semi-flow, continuous flow or stopped flow as required. The spectrometer was started as the final component was added and the luminescence was monitored at the required wavelength using the instrumental conditions in Table 3.5.

Table 3.5 Instrumental Parameters for Chemiluminescence Time-course Experiments

System	Data collection	Wavelength / nm	Slit Width / nm	PMT Voltage /V	Response /sec
Sugar/ Permanganate	Seconds	700	20	950	0.01
Ascorbic/ permanganate	Milliseconds	700	20	950	0.004
Sugar/ Mn(III)	Milliseconds	700	20	950	0.004
Sugar/ Peroxide	Milliseconds	440	20	950	0.004
Luminol/Co(II)/ Peroxide*	Milliseconds	425	10	700	0.004

\*System used to check stopped-flow performance



### **3.6.5 Chemiluminescence Spectrophotometry**

Chemiluminescence spectra were collected using the Hitachi fluorescence spectrophotometer by batch, semi-flow, continuous flow or stopped flow as required.

#### **3.6.5.1 Batch Procedure**

A fluorescence cuvette of optical glass, quartz or plastic was placed in the cell holder and reagents were added at timed intervals. The final solution was added quickly using an automatic pipette. After a previously established time the scan was started. For fast reactions the final solution was introduced using a syringe through a 0.5mm id PTFE tube and the scan started immediately.

#### **3.6.5.2 Semi-flow Procedure**

Reagents were added to a cuvette, as for the batch method. The final reagent, normally the oxidant, was pumped into the cuvette through a 0.5mm id PTFE tube by means of a peristaltic pump. Several spectra were collected a few seconds after starting the pump.

#### **3.6.5.3 Continuous-flow Procedure**

Reagents were pumped using a multi-channel peristaltic pump, mixed in Y fittings and passed through delay coils if required. The mixed solutions passed through a flow-cell in the fluorimeter. The flow rate and length of delay coil were adjusted to achieve maximum signal and spectra were collected.

#### **3.6.5.4 Stopped-flow Procedure**

Reagents were mixed using the stopped-flow accessory. For fast reactions timing was achieved by altering the scan range and for slow reactions the scan was collected after a time established in a time-course experiment. In all cases the



fluorimeter was operated in luminescence mode with the source turned off, a slit width of 20nm and response automatically set according to the scan speed. Other conditions were as shown in Table 3.6.

**Table 3.6 Instrumental Parameters for Collecting Chemiluminescence Spectra**

Type	Reaction type	Scan speed /nm min <sup>-1</sup>	Data collection
Batch	Slow	2400	Single scans
	Fast	30000	Repeat scans averaged
Semi-flow	Fast	30000	Repeat scans averaged
Continuous	Slow/fast	1200 30000	Single scans CAT(computerised averaging for transients)
Stopped flow	Slow/fast	30000	Repeat scans averaged

### 3.6.6 Consumption of Permanganate

The consumption of manganese species in oxidation reactions was followed by the change in absorbance at appropriate wavelengths. The same concentrations and volumes of solutions used for chemiluminescence measurements were mixed in a spectrophotometer cuvette and a time scan was started. Absorbance measurements were taken at intervals of 10 or 15 sec depending on the speed of the reaction.

### 3.6.7 Determination of Vitamin C

Ascorbic acid was determined in food supplements and fruit by titration with 2,6-dichlorophenol indophenol<sup>220</sup> and fluorimetrically after oxidation to dehydroascorbic acid and reaction with o-phenylamine diamine.<sup>221</sup>



# CHAPTER 4

## RESULTS AND DISCUSSION

### PERMANGANATE CHEMILUMINESCENCE

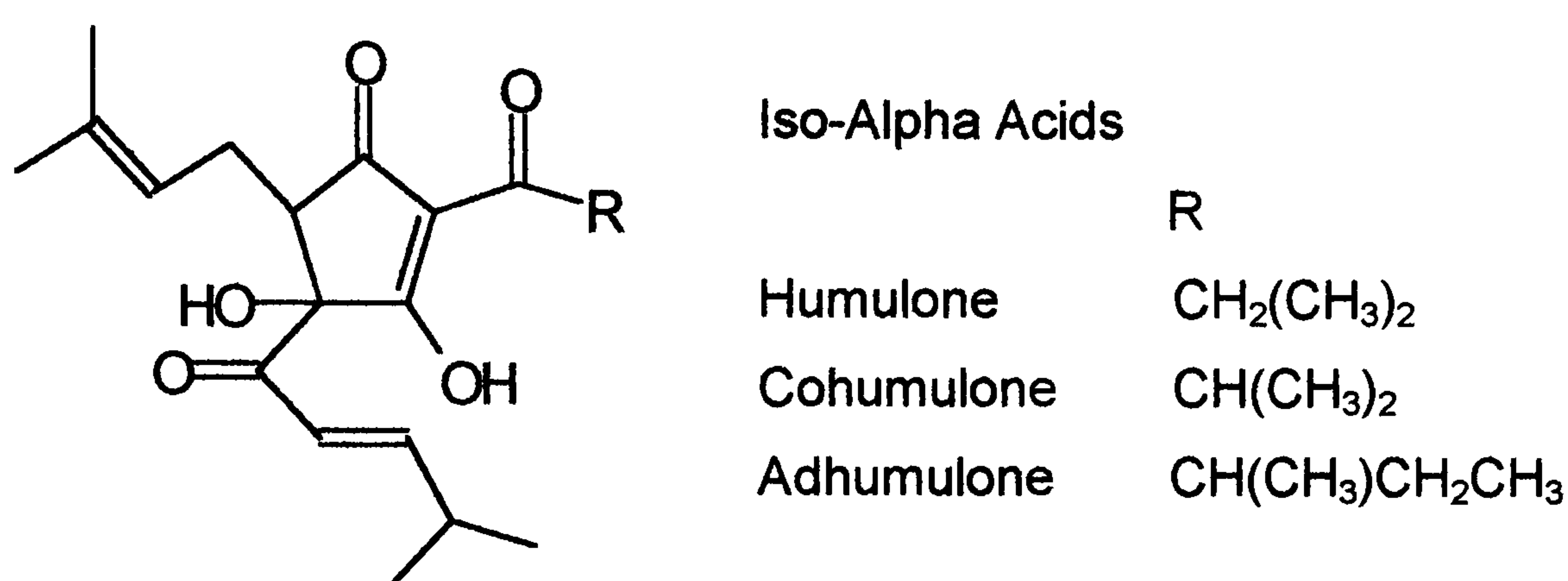
#### 4.1 Oxidation of Food Systems

As previously discussed, many food systems display chemiluminescence related to oxidative degradation of components such as oils and fats. Attempts have been made to relate the chemiluminescence to quality aspects such as beer staling<sup>18 19</sup> and oxidative rancidity of oils.<sup>16</sup> It has been suggested that the emitting species is an activated oxygen species such as singlet oxygen, a hydroxy- or hydroperoxy radical.

The mechanism of oxidative rancidity is complex and starts when oxygen is taken up by fats with formation of hydroperoxides, (ROOH). When the level of hydroperoxides reaches a certain point, after an induction period, the rate of oxidation accelerates and volatile products are formed. Peroxides may be further oxidised to diperoxides leading to polymer formation and fission reactions forming aldehydes, semi-aldehydes, aldehydo-glycerides, hydroxyl compounds and finally organic acids. Dehydration reactions give keto-glycerides, and oxidation of other double bonds forms epoxides, hydroxy- and dihydroxy-glycerides leading to off-flavour and odour in the food. Some specific unsaturated compounds, especially trans-2-nonenal are thought to be responsible for the 'cardboard' off flavour in beers. Maillard reactions, between carbohydrates and proteins, responsible for non-enzymic browning in foods, are known to give low levels of chemiluminescence.<sup>94</sup> In DMSO the chemiluminescence from Maillard reactions is sufficiently strong for a spectrum to be measured. A blue/green band was reported at 500nm and a red band at 695nm.



Beer was chosen for initial investigation as staling and deterioration are of considerable economic importance. Beers contain many hydroxy and polyhydroxy compounds which, as discussed in section 2.1.7.2, have long been known to give chemiluminescence on oxidation. Particularly important components of beer are the iso  $\alpha$ - and iso  $\beta$ - acids as shown in Scheme 4.1, compounds produced which are produced during boiling from the  $\alpha$ - and  $\beta$ - acids present in hops. The iso acids are responsible for the bitterness of beers and contribute to their stability.



**Scheme 4.1**

Free radicals generated during autoxidation are capable of degrading isohumulones yielding carbonyls including aldehydes which are responsible for off flavours. It was found that addition of metal ions and/or hydrogen peroxide to beer increased the amount of chemiluminescence observed.<sup>222</sup> Addition of EDTA or sulphite reduced the emission. This is consistent with the participation of free radicals in the mechanism. It was thought if oxidation of iso acids generated chemiluminescence it might be possible to develop an analysis for them in beers.

#### **4.1.1 Oxidation of Beer by Various Oxidising Species**

##### **4.1.1.1 Batch Experiments**

Initially chemiluminescence from a 5 cm<sup>3</sup> aliquot of a freshly opened sample of beer, (canned bitter beer, purchased locally) was counted for 2 minutes using the batch



counter. A fresh sample was heated to 65° and counted for 2 minutes. As expected from literature,<sup>17</sup> higher chemiluminescence was observed at higher temperatures.

**Table 4.1 Photon Emission by Fresh Beer Samples**

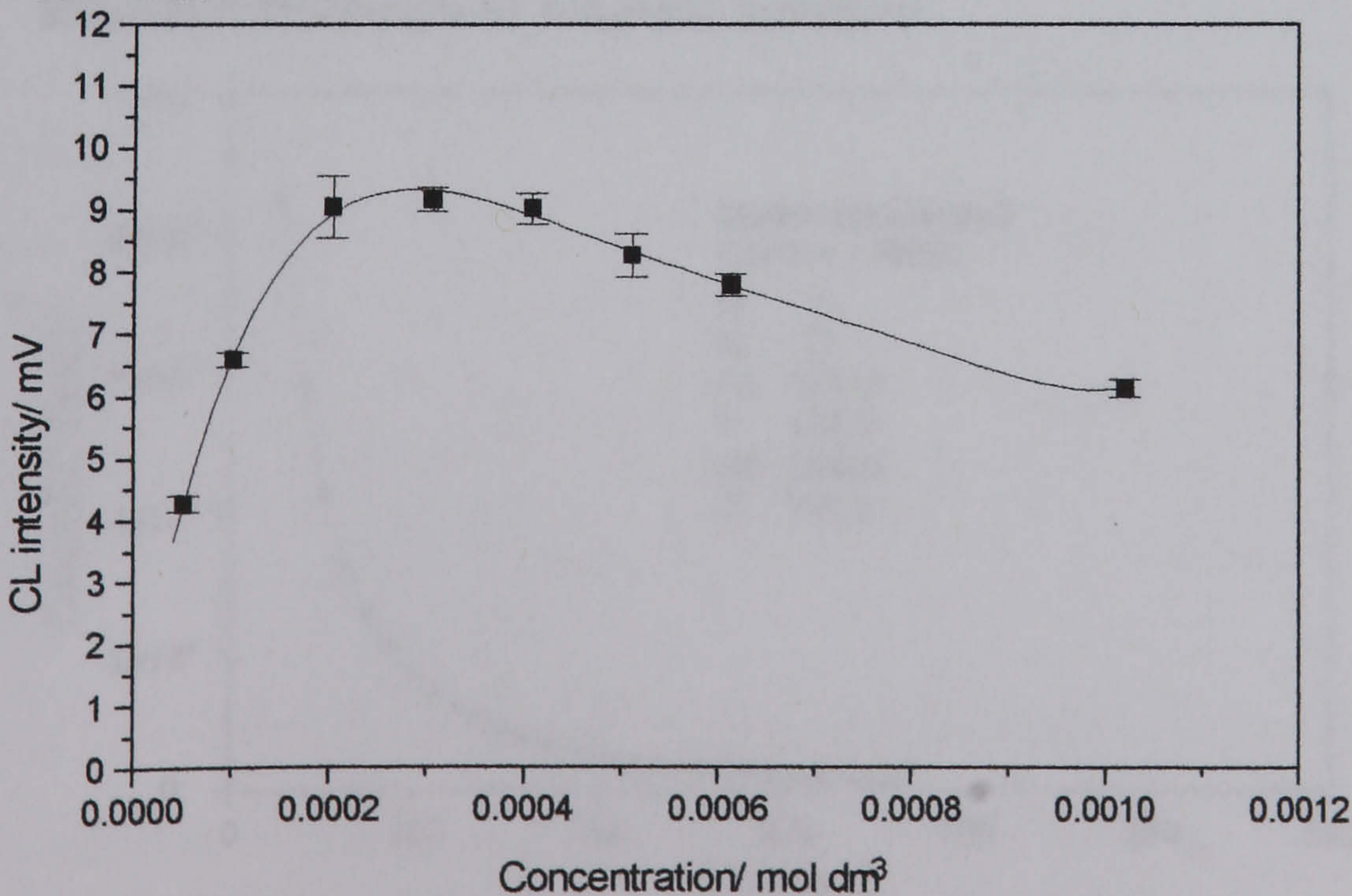
Temp/ C°	Photons/sec
10	100
40	210
60	550

**4.1.1.2 Preliminary Flow Injection Studies**

Using a single line flow injection manifold, the beer sample previously used was injected into carrier streams containing oxidants, known to give chemiluminescence. The oxidants were neutral periodate, acid permanganate, peroxide with copper in alkaline solution and cerium (IV) in acid solution. Only the permanganate and peroxide systems gave a signal with permanganate giving the higher signal.

Repeating the experiment using a photodiode detector confirmed that only permanganate and peroxide give a signal and suggested that the emission from the

**Figure 4.1 Effect of Permanganate Concentration on CL Signal from Bitter Beer**



Beer injected into a carrier of acid permanganate, concentration as shown  
Error bars represent standard deviation for 10 replicate injections

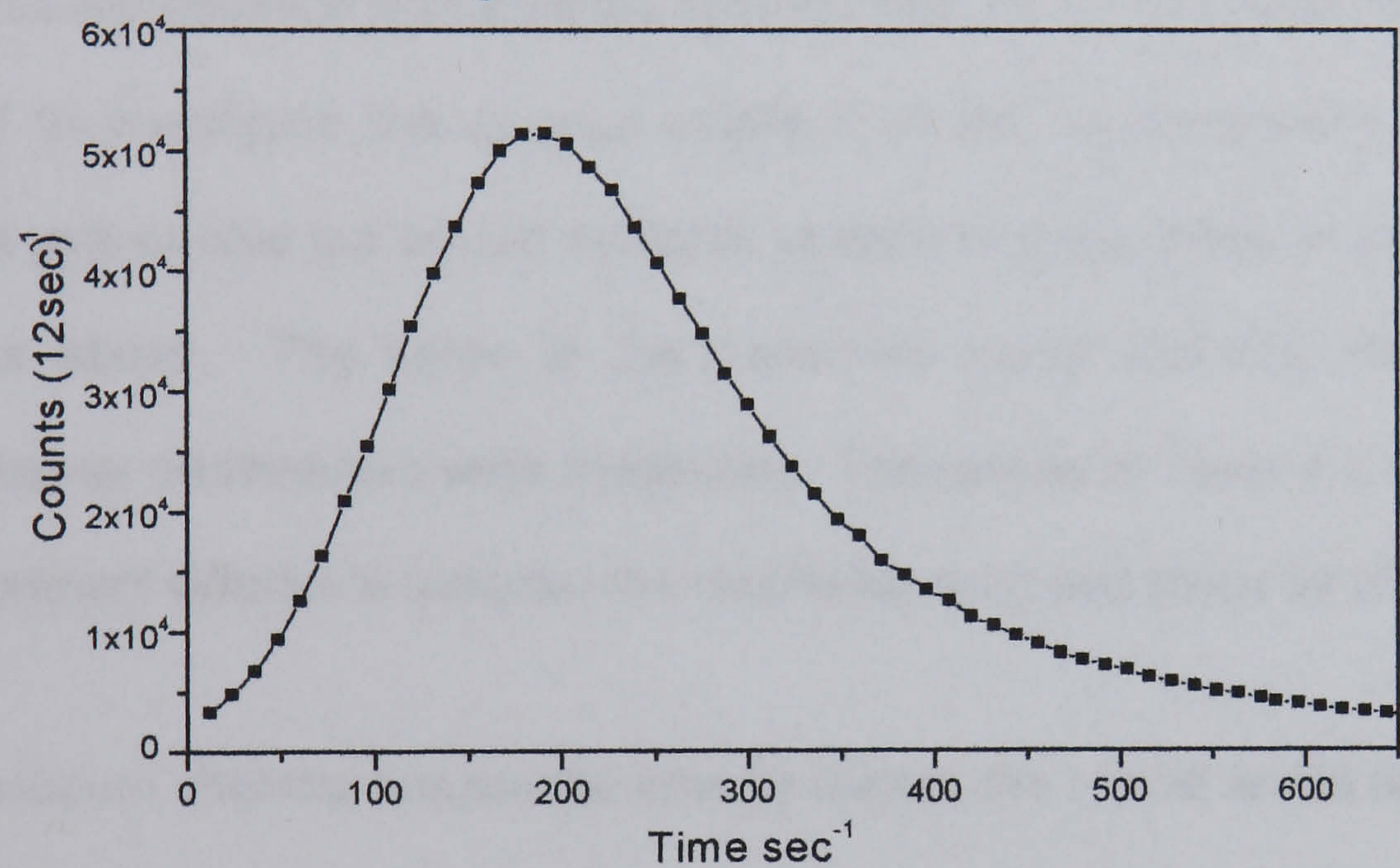


permanganate reaction was at longer wavelength than from the peroxide system.  
 The signal depended on the permanganate concentration as shown in Figure 4.1

### 4.1.1.3 Batch Experiments with Permanganate and Peroxide

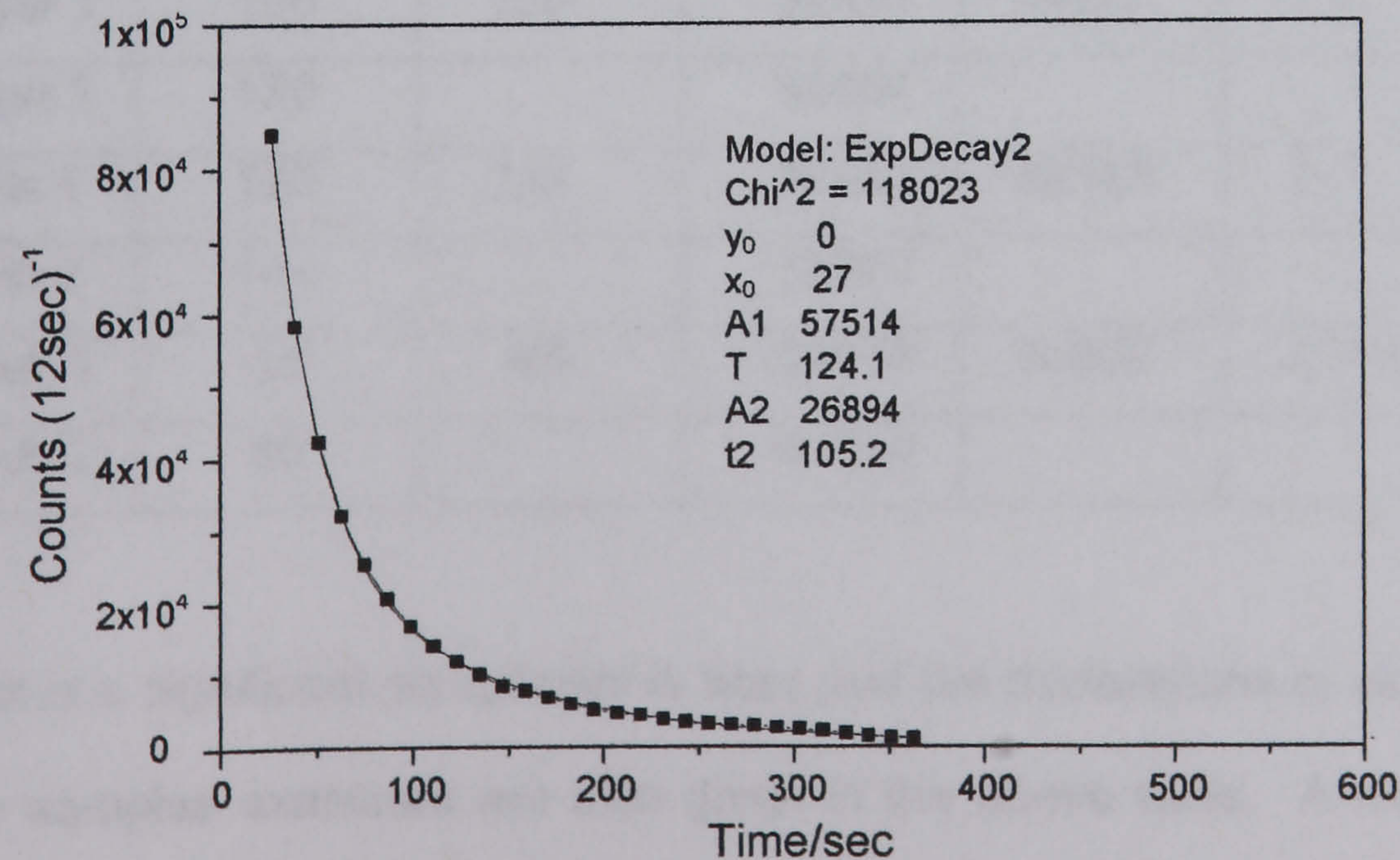
Batch experiments were undertaken where the beer sample was added to oxidant.  
 Emitted light was followed by batch counting until no more counts were observed.

**Figure 4.2 Chemiluminescence Time-course for the reaction of Beer and Permanganate in Acid solution**



0.5 cm<sup>3</sup> bitter beer, 5 cm<sup>3</sup> sulphuric acid 2 mol dm<sup>-3</sup>, reaction started by addition of 0.5cm<sup>3</sup> 0.022 mol dm<sup>-3</sup> permanganate, readings at 12 sec intervals

**Figure 4.3 Chemiluminescence Time-course for the Reaction of Beer and Peroxide in Alkaline solution**



2cm<sup>3</sup> bitter beer, 0.1cm<sup>3</sup> CoCl<sub>2</sub> 0.1 mol dm<sup>-3</sup>, 0.1 cm<sup>3</sup> KOH 1.0 mol dm<sup>-3</sup>  
 reaction started with 0.05 cm<sup>3</sup> 30% H<sub>2</sub>O<sub>2</sub>



Figures 4.2 and 4.3 show the chemiluminescence time courses for the reaction of beer with permanganate and peroxide.

It can be seen that the peroxide reaction is much faster than the permanganate reaction with much of the emission occurring in the 'dead time' of the spectrometer when no readings can be taken. The peroxide time course data fits well to an exponential function.

As chemiluminescence reactions are typically fast, as for the peroxide profile, it was decided to investigate the unusual profile from the permanganate reaction. The reaction was carried out on two samples of each of three types of beer. Conditions were as above. The times to the maximum signal and the maximum counts calculated as photons/sec were measured. The results in Table 4.2 show that there is a significant difference between the results for stout and those for lager and bitter.

The maximum chemiluminescence broadly follows the typical levels of free sugars in the beer types.

**Table 4.2 Chemiluminescence Time profiles for Different Beer Types**

Sample	Seconds to Max	Average	Maximum Phot/sec	Average	Typical Sugars g/100cm <sup>3</sup>	Declared Ethanol ABV
Lager 1	180	150	29447	39977	1.5	3.2
Lager 2	120		50507			
Bitter 1	120	132	56500	46550	2.3	3.1
Bitter 2	144		36600			
Stout 1	48	48	94033	94807	2.1-4.2	2.9-4.0
Stout 2	48		95580			

Ethanol is a significant component in beer and the declarations of alcohol by volume for the samples examined are also given in the above table. A method has been described for determination of ethanol of potable spirits (40 to 50% ABV), using the



chemiluminescence from permanganate oxidation.<sup>160</sup> To get a good signal the reaction was carried out in 95% nitric acid, which is difficult to use in a flow system. Reaction of ethanol with permanganate under the same conditions as for the beer samples gave only a very low signal.

The other major components of beers are water (90-95%), carbon dioxide (2-3%) and carbohydrates (2-5%) including free sugars and oligo- and polysaccharides. Several hundred minor components are also found in beers. These include higher alcohols, organic acids, nitrogenous compounds including free amino acids and proteins, esters, aldehydes, ketones, sulphur compounds, polyphenols, B-vitamins and inorganic salts present at levels from parts per million to 0.1%.<sup>223</sup>



## 4.2 Oxidation of Carbohydrates by Permanganate

### 4.2.1 Batch Experiments

It was decided to investigate the source of the permanganate chemiluminescence by examining materials used in beer production. Laboratory prepared hot water extracts of dried hops, iso hop pellets and malt extract were found to give similar chemiluminescence time profiles to those for beer samples.

A sample of commercial isomerised hop extract which contains high levels of iso alpha acids was diluted to the level which would be present in beer. The reaction with acid permanganate resulted in no emission, although as expected the permanganate was reduced, giving a colourless final solution. This shows that hop iso- acids are not responsible for the permanganate chemiluminescence of beers. Among the nitrogen containing components of beers are free amino acids and oligo-peptides. The amino acids alanine, lysine and cystine were examined as before. Permanganate was reduced but no signal was seen, showing that the main nitrogen components of beer are not responsible for the observed signal.

Glucose was previously reported to interfere in the chemiluminescence assay for various medicines, where it is be used as an excipient.<sup>183</sup> It was considered that the carbohydrates might be responsible for the chemiluminescence observed. Malted and unmalted barley and other cereals are the main carbohydrate source in beers. In commercial brewing the hot water extract of cereals, wort, is boiled with hops prior to fermentation with a selected yeast, *Saccharomyces cerevisiae* or *S. carlsbergensis*. If the hot water extract is concentrated by evaporation malt extract is produced which is widely used in domestic brewing and in production of foods such



as breakfast cereals. Malt extracts are readily available in different grades including those produced from highly roasted malt and types with high diastatic activity.

The major components are glucose, maltose and glucose oligosaccharides in proportions which depend on time and temperature of malting and post treatment.. Malt extract was used as a model for the carbohydrate component in beer and was found to give a chemiluminescence time profile similar to that for the beers. It was also found that glucose, a major component of malt extract gave the same profile.

The nutritionally important mono and disaccharides: glucose, fructose, galactose, maltose sucrose and lactose were selected for study in the reaction with permanganate. In each case excess substrate was used as indicated by the complete disappearance of the permanganate colour during the reaction.

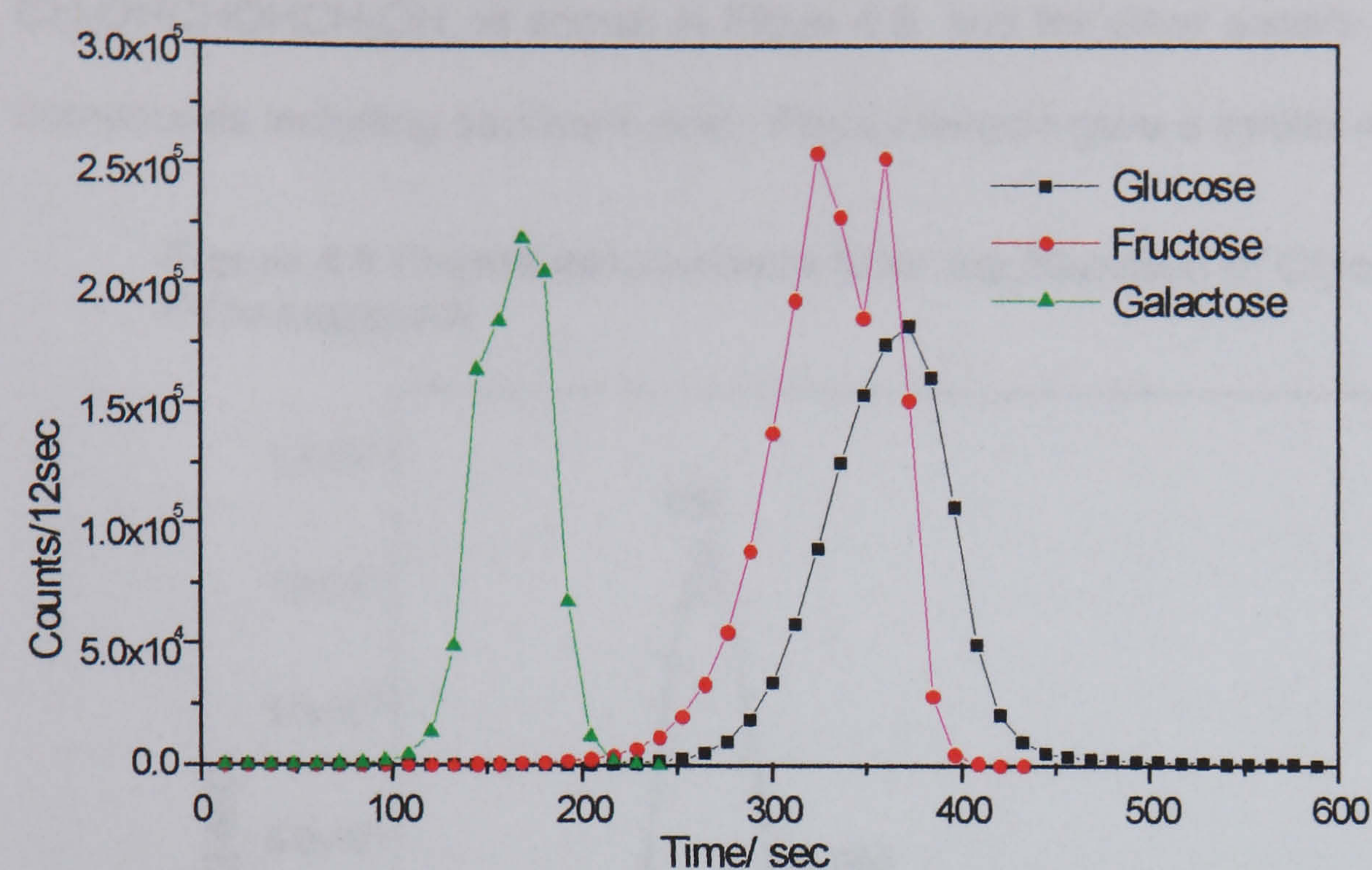
The reaction time courses, for equal concentrations of the mono and disaccharides are shown in figures 4.4 a and b.

It can be seen that both the rate of reaction and the size of the signal is different for each sugar. The double peak for fructose is probably due to saturation of the detector. The larger signals for disaccharides when mixed with sulphuric acid before addition of the permanganate are due to partial hydrolysis of the disaccharides to monosaccharides.

Using glucose as a representative sugar, glucose and permanganate concentrations were varied. An increase in glucose concentration resulted in a constant maximum signal with a decreasing time to reach the maximum signal while the total counts increased. An increase in permanganate concentration gave an initial increase in signal then a constant maximum while the total counts increased.

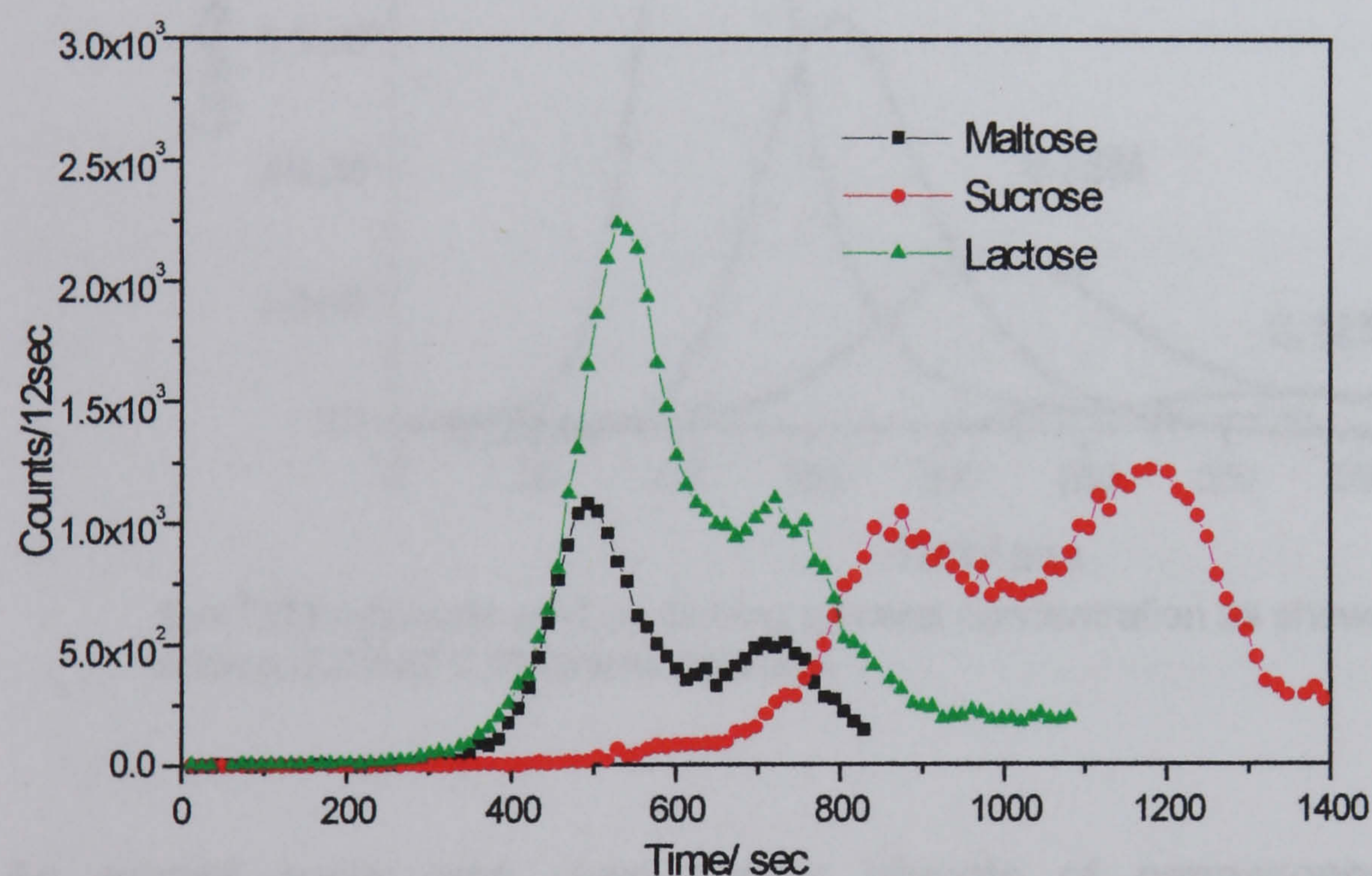


**Figure 4.4 Chemiluminescence Time-courses for the Permanganate Oxidation of Mono- and Disaccharides**



**a) Mono-saccharides**

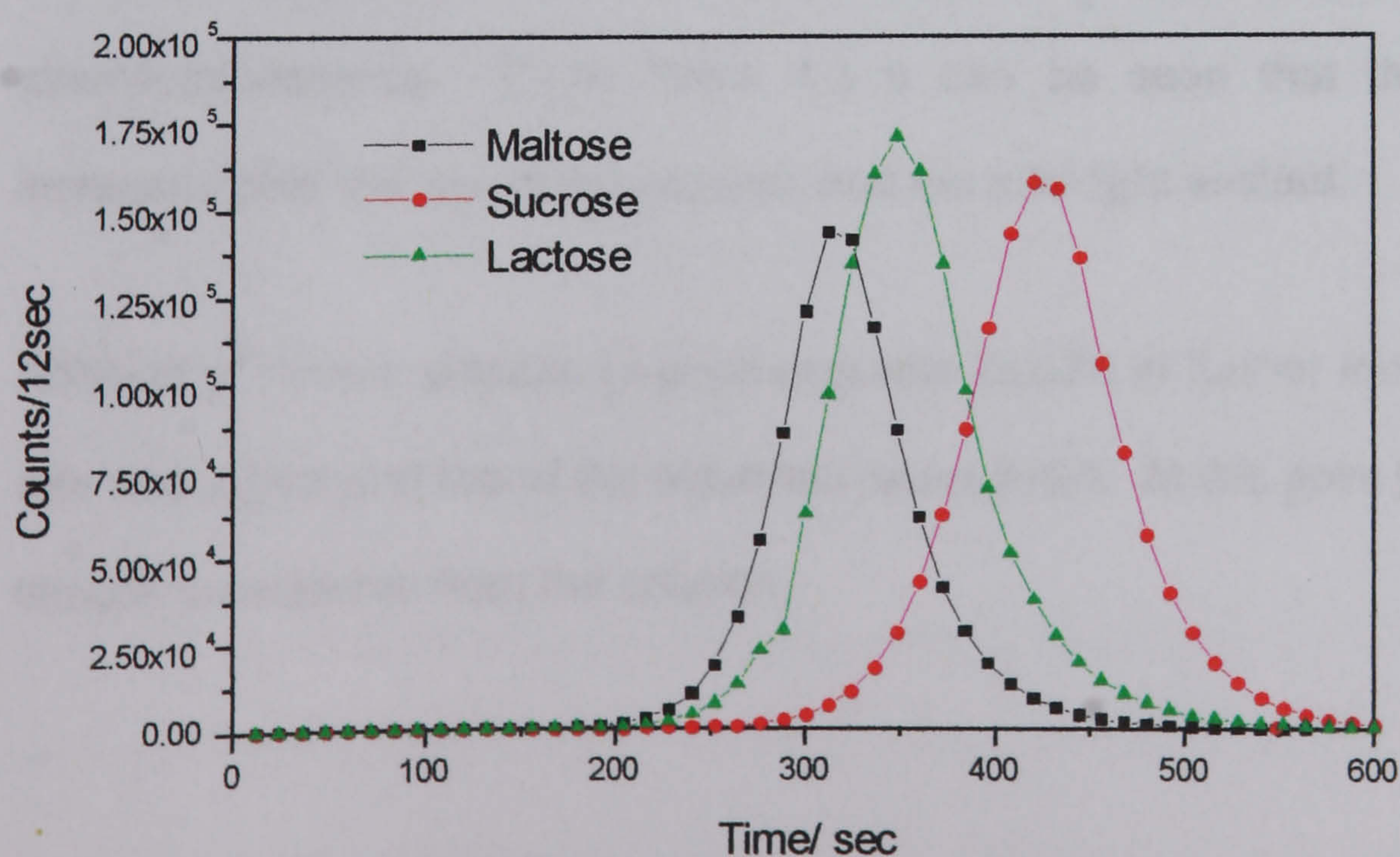
2cm<sup>3</sup> 2M  
sulphuric acid  
2cm<sup>3</sup> 0.02M  
permanganate  
1cm<sup>3</sup> 5%  
monosaccharide



**b) Disaccharides**

2cm<sup>3</sup> 2M  
sulphuric acid  
2cm<sup>3</sup> 0.02M  
permanganate  
1cm<sup>3</sup> 5%  
disaccharide

No hydrolysis



**c) Disaccharides**

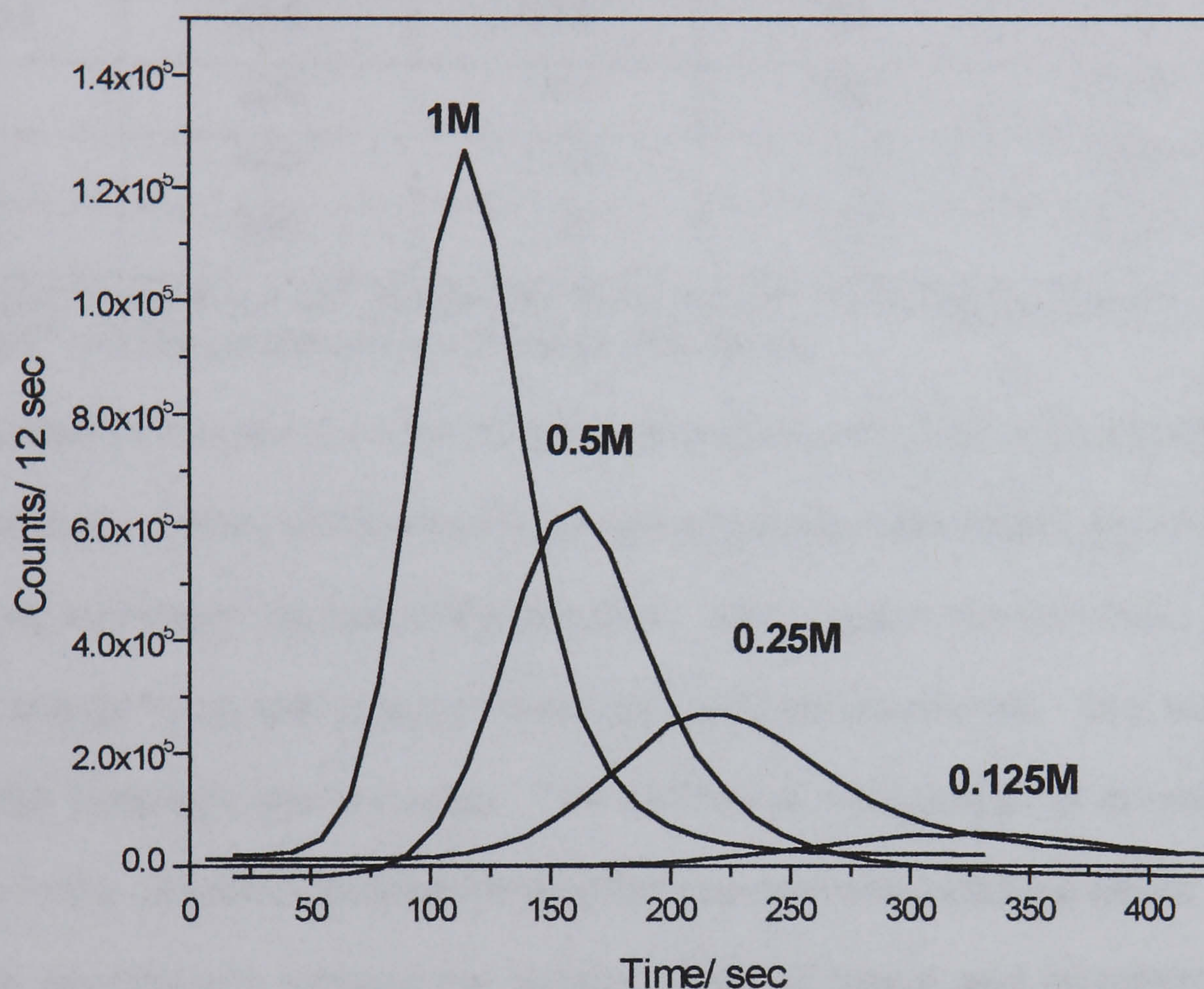
2cm<sup>3</sup> 2M  
sulphuric acid  
1cm<sup>3</sup> 5%  
disaccharide  
0.25cm<sup>3</sup> 0.1M  
permanganate

Hydrolysis



A similar pattern was observed for a simpler polyhydroxy compound, glycerol,  $\text{CH}_2\text{OHCHOHCH}_2\text{OH}$  as shown in Figure 4.5, and for other sugars and polyhydroxy compounds including saccharic acid. Formaldehyde gave a similar response.

**Figure 4.5 Chemiluminescence from the Reaction of Glycerol with Permanganate**



$2\text{cm}^3$  2M sulphuric acid containing glycerol concentration as shown reaction started by adding  $0.25\text{cm}^3$  0.1M permanganate

As excess sugar was used further aliquots of permanganate gave further chemiluminescence. From Table 4.3 it can be seen that the second aliquot increases both the rate of the reaction and the total light emitted.

Addition of further aliquots of permanganate results in further increases in reaction rate and signal until the all the substrate has reacted. At this point brown manganese dioxide precipitates from the solution.



**Table 4.3 Effect of Multiple Additions of Permanganate on Carbohydrate Chemiluminescence**

Sugar	Aliquot 1		Aliquot 2	
	Time to max / sec	Total Counts x10 <sup>-6</sup>	Time to max/ sec	Total Counts
Glucose	290	1.28	75	1.39
Fructose	255	1.19	50	1.22
Galactose	150	0.75	50	0.84
Maltose	330	1.01	100	1.31
Sucrose	450	1.34	90	1.96
Lactose	360	1.35	100	1.85

2.0ml sulphuric acid 2 mol dm<sup>-3</sup>, Sugar 0.5ml 0.28 mol dm<sup>-3</sup>, 0.25ml permanganate 0.1mol dm<sup>-3</sup>, permanganate addition repeated after 10 min

As discussed in Chapter 2.4, the oxidation of organic compounds by permanganate is autocatalytic. When further aliquots of permanganate were added the manganese (II) present increased the rate of the reaction. With a faster reaction there was less time for energy to be lost in ways other than chemiluminescence. This would also explain the increased total emission. The addition of manganese (II) as manganese sulphate to the sample increased the reaction rate and enhanced the signal. Results for batch experiments showed the enhancement of signal and increased rate of chemiluminescence production with increasing manganese (II) The results are shown in Table 4.4.

**Table 4.4 The Effect of Manganese(II) on the Chemiluminescence Signal**

Manganese(II)/ mol dm <sup>-3</sup>	Maximum Counts x10 <sup>-5</sup>	SD x10 <sup>-3</sup>	Time to Max /sec	SD
0	0.120	0.68	606	18
5x10 <sup>-4</sup>	1.199	3.57	104.7	3.5
1x10 <sup>-3</sup>	1.515	3.11	74.6	1.5

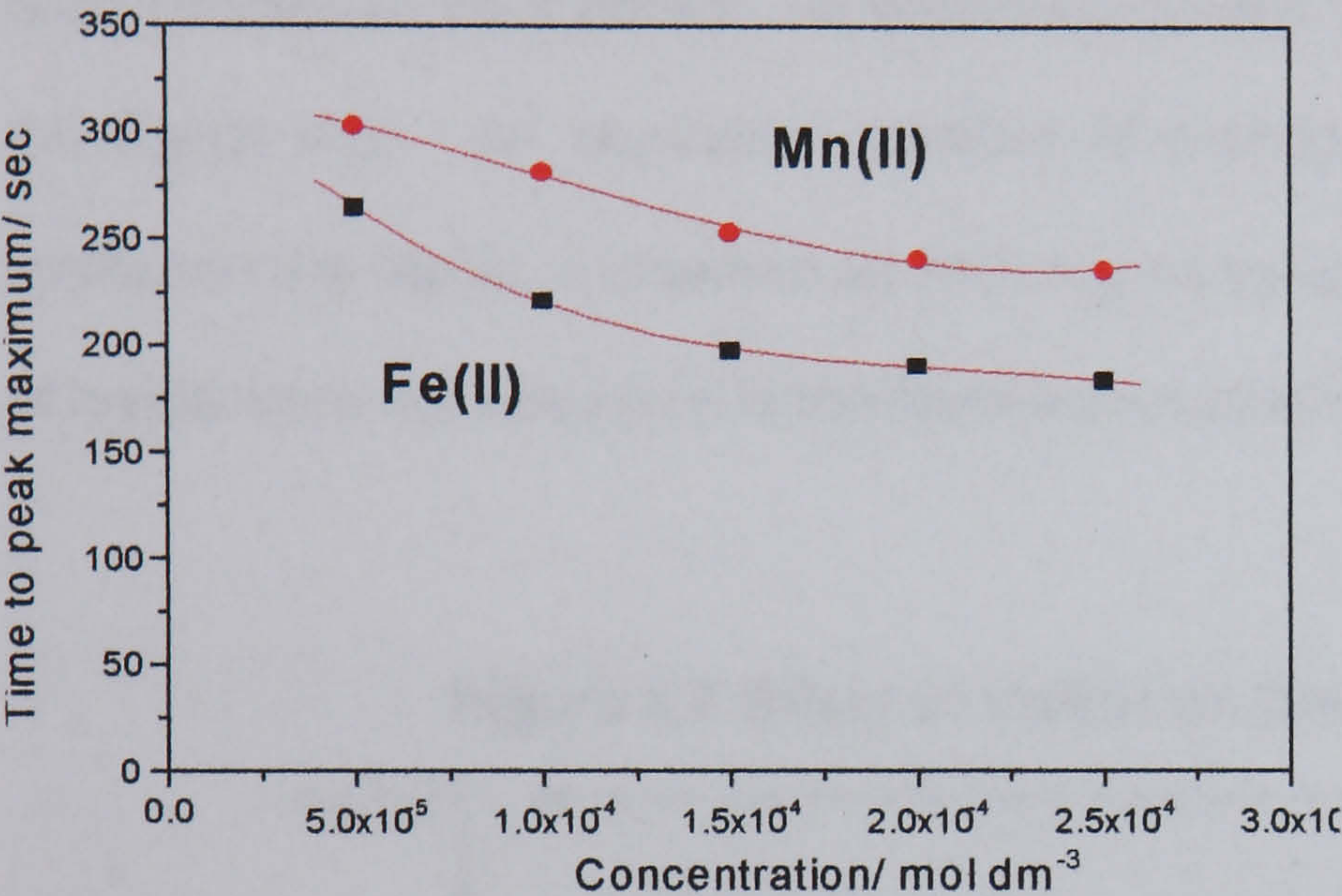
Reaction mixture: Sulphuric acid 0.75 mol dm<sup>-3</sup>, Glucose 0.05mol dm<sup>-3</sup>, permanganate 1.25x10<sup>-3</sup> mol dm<sup>-3</sup>, manganese sulphate as above

It was found that iron(II) sulphate also gave an increased signal and reaction rate, copper(II) and cobalt(II) had no effect on either the rate or the signal. Comparison of iron(II) ion with manganese(II) showed that both increase the rate of reaction. For



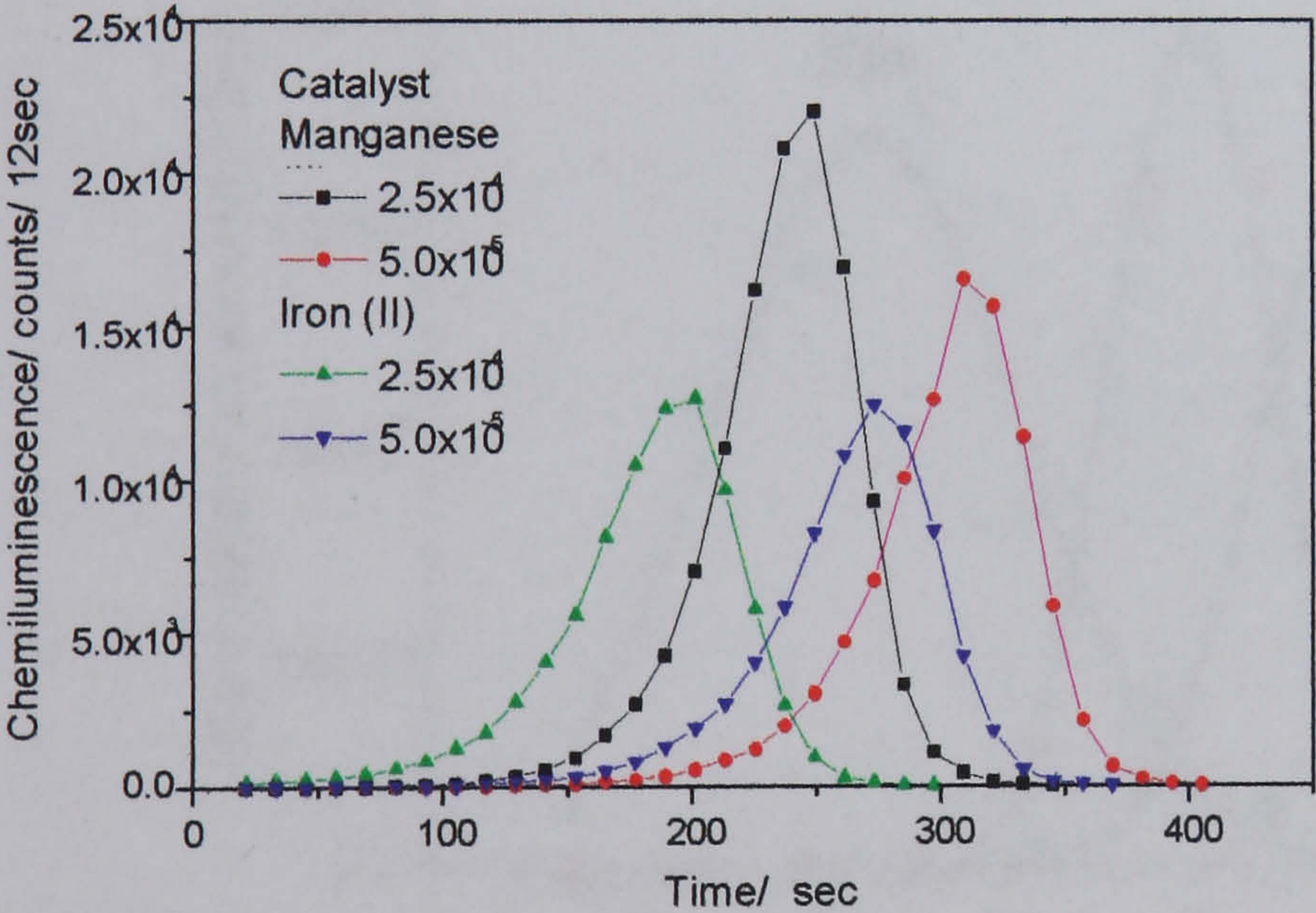
the same concentration of metal, the increase in emission due to manganese (II) is larger, and the signal continues to increase with increasing manganese (II) concentration. For iron (II) while the peak height, and total counts do not as shown in Figure 4.6 a, b and c.

Figure 4.6 Effect of Fe(II) and Mn(II) on Chemiluminescence Signal

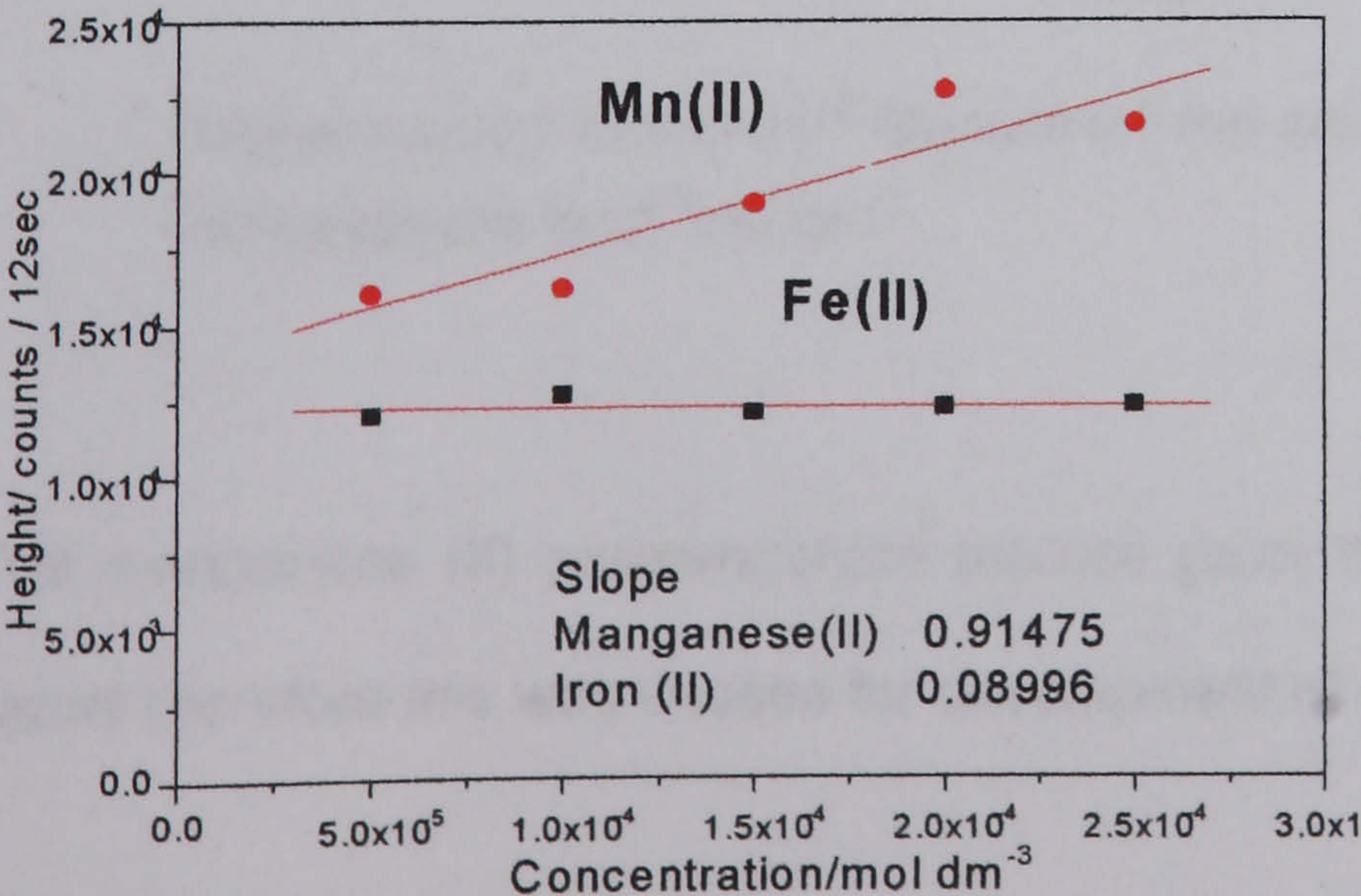


a)  
Effect on the rate of  
CL emission

Sulphuric acid 1.25 mol dm<sup>-3</sup>  
Glucose 0.1 mol dm<sup>-3</sup>  
Permanganate 4x10<sup>-3</sup> mol dm<sup>-3</sup>  
Manganese(II) and Iron(II) as  
on the figure



b) Chemiluminescence  
profiles



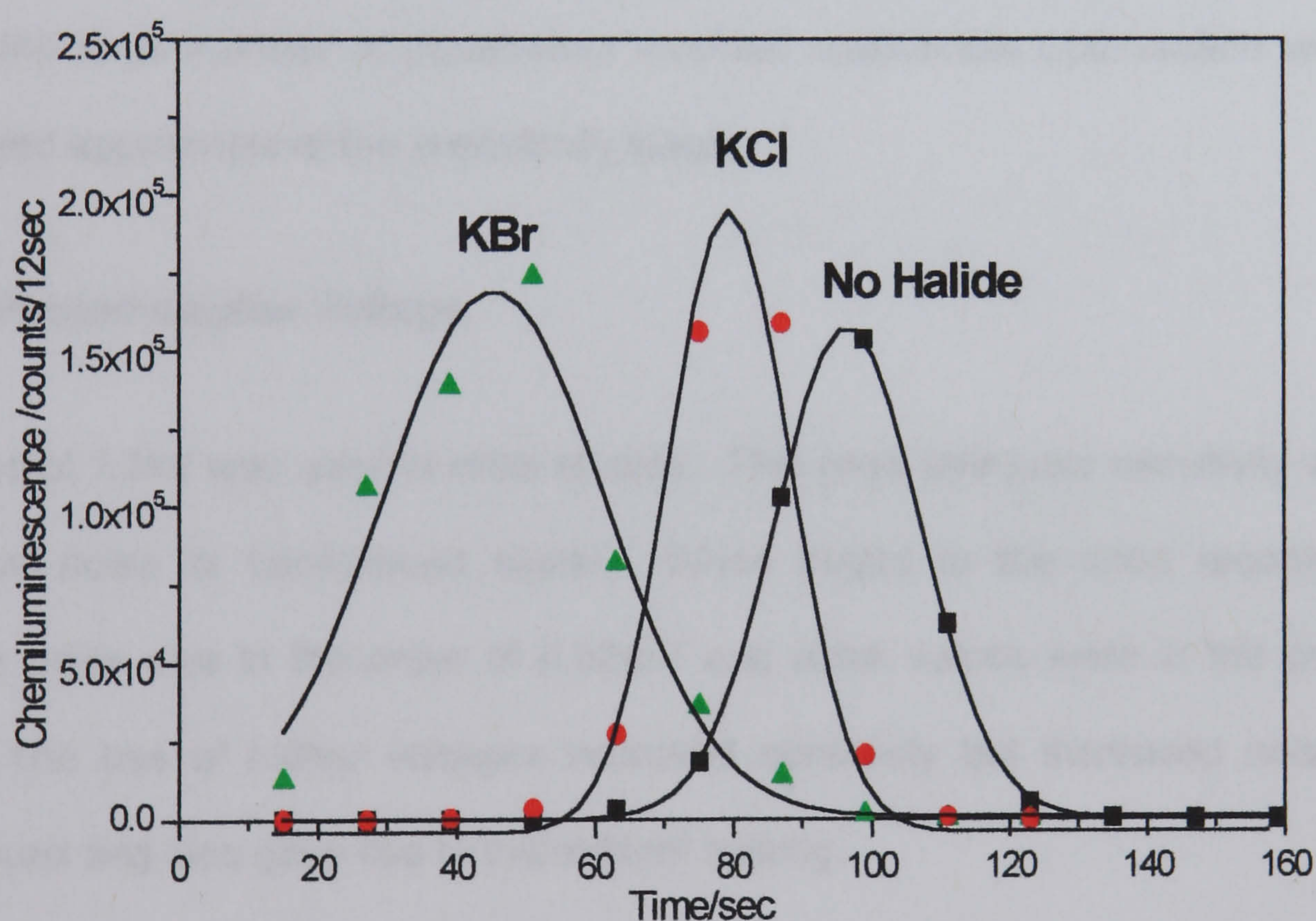
c)  
Effect on height of the CL  
peak



It has been reported<sup>224</sup> that manganese (III) species can form pseudohalide complexes. It was therefore decided to investigate the effect of chloride and bromide on the glucose/ sulphuric acid/ permanganate system.

Addition of  $0.01 \text{ mol dm}^{-3}$  chloride gave a slight increase in the rate of chemiluminescence emission, as shown in Figure 4.7, but had no significant effect on the signal size. An equivalent addition of bromide increased the rate more and increased the signal, expressed as total counts by approximately 50%. Higher levels of halide were not used due to the liberation of chlorine or bromine from the system.

**Figure 4.7 Effect of Halide on Chemiluminescence Signal**



Sulphuric acid  $1.25 \text{ mol dm}^{-3}$  Glucose  $0.1 \text{ mol dm}^{-3}$  Halide  $0.01 \text{ mol dm}^{-3}$   
 Permanganate  $4 \times 10^{-3} \text{ mol dm}^{-3}$

The manganese (II) permanganate mixture gave the greatest enhancement of the signal therefore this was chosen for development of a flow system.



### **4.2.2 Flow Experiments**

Flow experiments were carried out using reverse FIA. A dual line manifold was set up in which aqueous sample was mixed with sulphuric acid containing manganese sulphate in a Y piece. Permanganate was injected into the mixed stream. Earlier work had indicated that the emission was towards the red end of the spectrum; therefore a red sensitive photomultiplier tube was chosen as the detector. Some studies were also undertaken using a photodiode detector, which is sensitive up to 1100nm.

Optimisation was undertaken using a one variable at a time (OVAT optimisation). Due to the large number of parameters involved multivariate optimisation was not considered appropriate at the preliminary stage.

#### **4.2.2.1 Photomultiplier Voltage**

A voltage of 1.2kV was used in initial studies. This gave adequate sensitivity without excessive noise or background signal. When output to the chart recorder the baseline noise was in the order of 0.02mV and blank values were in the order of 0.2mV. The use of higher voltages improved sensitivity but increased noise and background and also gave rise to intermittent spiking.

#### **4.2.2.2 Sulphuric Acid Concentration**

An increase in acid concentration gave an increased signal. At concentrations above 2 mol dm<sup>-3</sup> increases were small. It was also found that concentrated acids were detrimental to materials used in the flow lines of the photodiode detector. The above concentration, corresponding to 1.0mol dm<sup>-3</sup> in the mixed sample/carrier stream was used for further work.



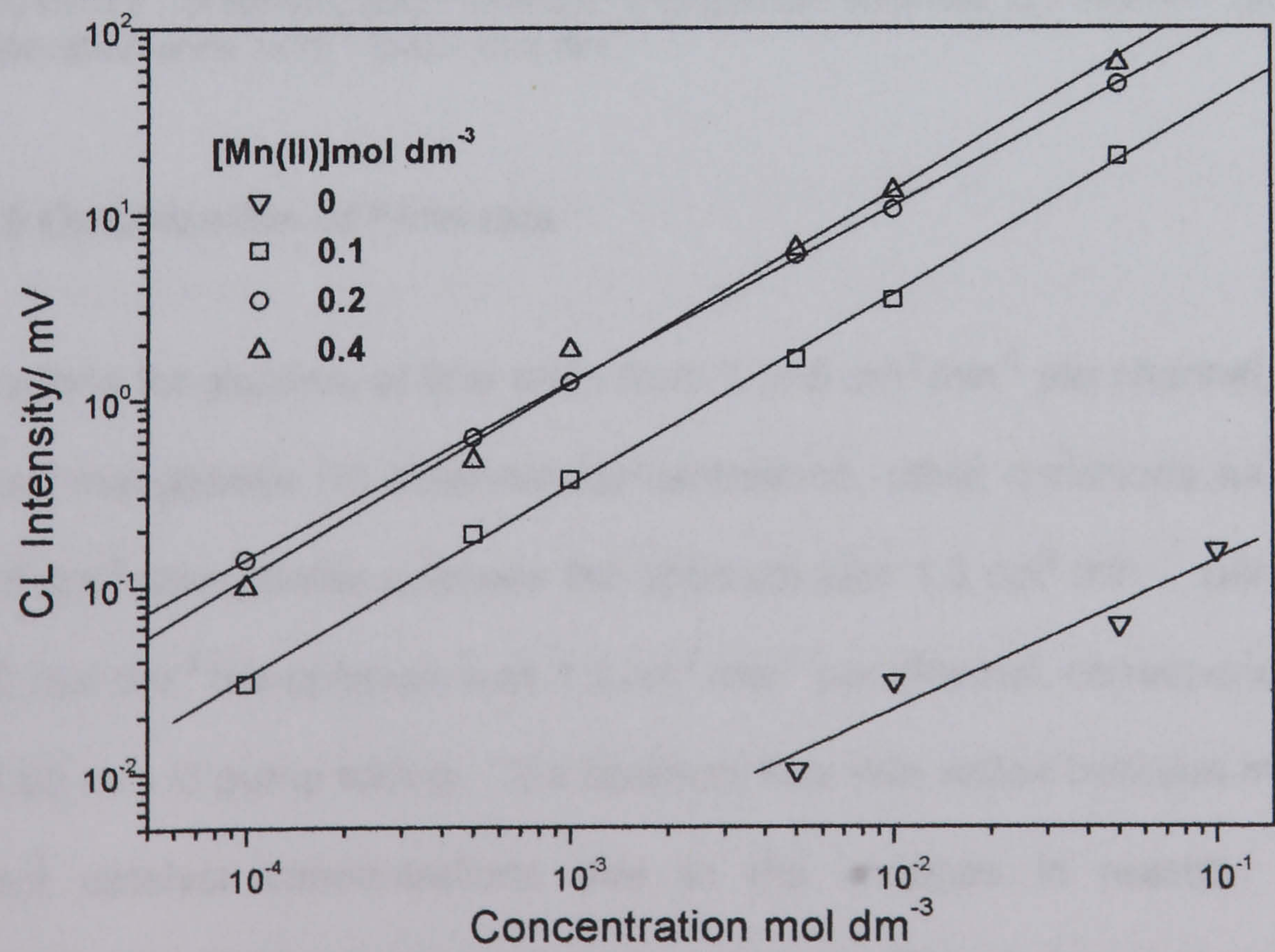
4.2.2.3 Manganese Sulphate Concentration

The signal was found to increase with increasing manganese sulphate concentration up to 0.5 mol dm<sup>-3</sup>. This was approximately the limit of solubility of manganese sulphate in strong acid. At concentrations above 0.2 mol dm<sup>-3</sup> the increase in signal was small and problems were found with manganese dioxide precipitation in the flow passages of the injection valve. Table 4.5 shows the parameters obtained by linear regression analysis. The results are also shown in Figure 4.8 using a log-log plot for clarity.

Table 4.5 Effect of Manganese Sulphate Concentration on Chemiluminescence

[MnSO <sub>4</sub> ] / mol dm <sup>-3</sup>	Slope / mV mol <sup>-1</sup> dm <sup>3</sup>	Intercept /mv	R
0	1.4	0.005	0.98400
0.1	402.7	0.061	0.99943
0.2	982.5	0.562	0.99978
0.4	1265.1	0.304	0.99993

Figure 4.8 Effect of Manganese Sulphate Concentration on Chemiluminescence of Glucose



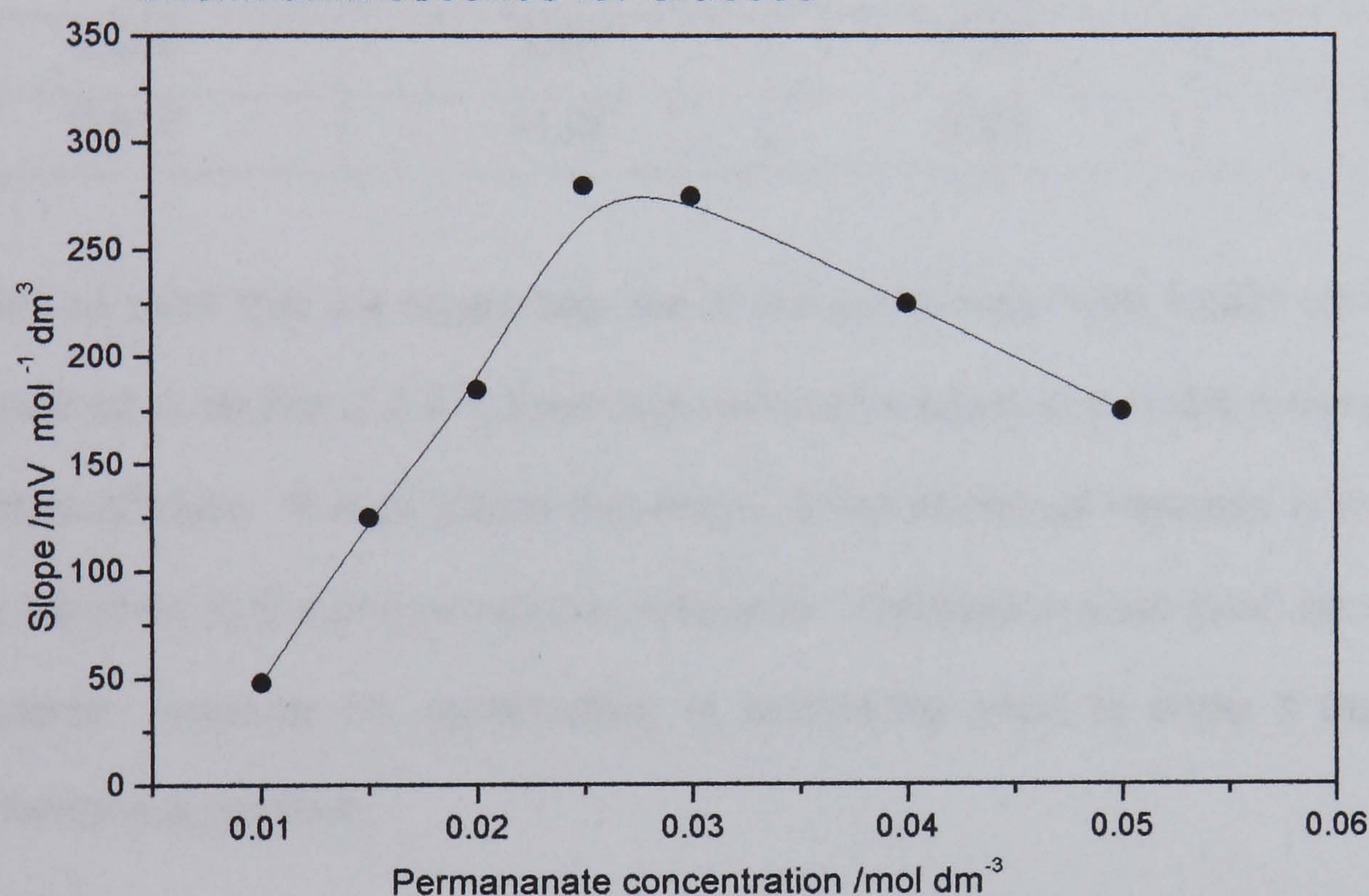
Manifold 2, Sulphuric acid 2 mol dm<sup>-3</sup> Permanganate 0.1 mol dm<sup>-3</sup> manganese sulphate concentration and glucose concentrations as indicated



#### 4.2.2.4 Optimisation of Permanganate Concentration

Potassium permanganate concentration was varied in the range  $0.01 - 0.05 \text{ mol dm}^{-3}$ . It was found that different sugars had different optimum concentrations, this is considered to be due to the different rates of reaction. The concentration used,  $0.025 \text{ mol dm}^{-3}$ , was the optimum for glucose. The variation is shown in Figure 4.9.

**Figure 4.9 Effect of Permanganate Concentration on Chemiluminescence for Glucose**



Manifold 2 Sulphuric acid  $2 \text{ mol dm}^{-3}$  Manganese sulphate  $0.2 \text{ mol dm}^{-3}$  glucose  
calibration lines  $1 \times 10^{-4}$  to  $0.1 \text{ mol dm}^{-3}$

#### 4.2.2.5 Optimisation of Flow rate

Calibrations for glucose, at flow rates from  $1$  to  $5 \text{ cm}^3 \text{ min}^{-1}$  per channel, were run for different manganese (II) sulphate concentrations, other conditions as above. For  $0.1 \text{ mol dm}^{-3}$  manganese sulphate the optimum was  $1.3 \text{ cm}^3 \text{ min}^{-1}$  per channel and for  $0.2 \text{ mol dm}^{-3}$  the optimum was  $1.9 \text{ cm}^3 \text{ min}^{-1}$  per channel, corresponding to 30rpm with 1.02 mm id pump tubing. The optimum flow rate varies between sugars and for different catalyst concentrations due to the changes in reaction rates. For comparisons the 30 rpm flow rate was adopted. The optimum also reduces with sugar concentration, however good linearity can still be achieved.



4.2.2.6 Replication of Calibration

Calibration lines for glucose under the above conditions were run seven times over a period of two weeks. Signals for three glucose concentrations were measured and corrected for the blank values. The statistical parameters are shown in Table 4.6.

Table 4.6 Statistical Evaluation of Repeatability of Glucose Calibration

[Glucose] /mol dm <sup>-3</sup>	Mean /mV	Standard deviation /mV	RSD /%
0.001	1.46	0.23	15.8
0.005	6.87	1.33	19.4
0.010	14.27	2.93	20.6

It can be seen that the responses are of the same order with RSDR up to 20%. As discussed in section 2.2.5.1, there are various factors that can affect the sensitivity of photomultipliers. It is probable that much of the observed variation is due to day to day variation in the photomultiplier response. Calibration lines must be run on each occasion, however the repeatability is sufficiently good to show if the system is performing acceptably.

4.2.2.7 Calibration Lines for Sugars and Related Compounds

Several sugars and related polyhydroxy compounds were examined over several days and regressions calculated. The results are shown in Table 4.7.

The comparatively poor signals for the disaccharides are consistent with the findings from the batch experiments. There is insufficient time during dispersion for significant hydrolysis to occur. A delay coil would improve the signal size, however for complete hydrolysis, at the acid strength, used heating would be necessary. Hydrolysis of sucrose at 100°C<sup>226</sup> in a flow system has been reported as have systems based on enzymic hydrolysis with immobilised invertase (EC 3.2.2.26).<sup>226</sup>



**Table 4.7 Calibration Parameters for Sugars and Polyhydroxy Compounds**

Compound	Slope /mV mol dm <sup>-3</sup>		Intercept /mV		R
	Value	SD ±	Value	SD ±	
Glucose	983	9	0.6	0.2	0.9998
Galactose	1787	22	-0.5	0.4	0.9996
Fructose	5062	9	1.3	0.6	0.9999
Arabinose	1557	15	0.6	0.3	0.9998
Xylose	1532	13	0.6	0.3	0.9998
Maltose	294	18	0.06	0.5	0.9981
Sucrose	222	16	0.16	0.07	0.9894
Lactose	840	1	0.15	0.02	1.0000
Mannitol	1461	18	1.2	0.7	0.9995
Glycerol	195	5	0.5	0.2	0.9984

In order to directly compare the responses for different sugars and related compounds 0.1 mol dm<sup>-1</sup> solutions of each sugar were injected, runs, on each of two days. The results, with 95% confidence intervals, are in Table 4.8.

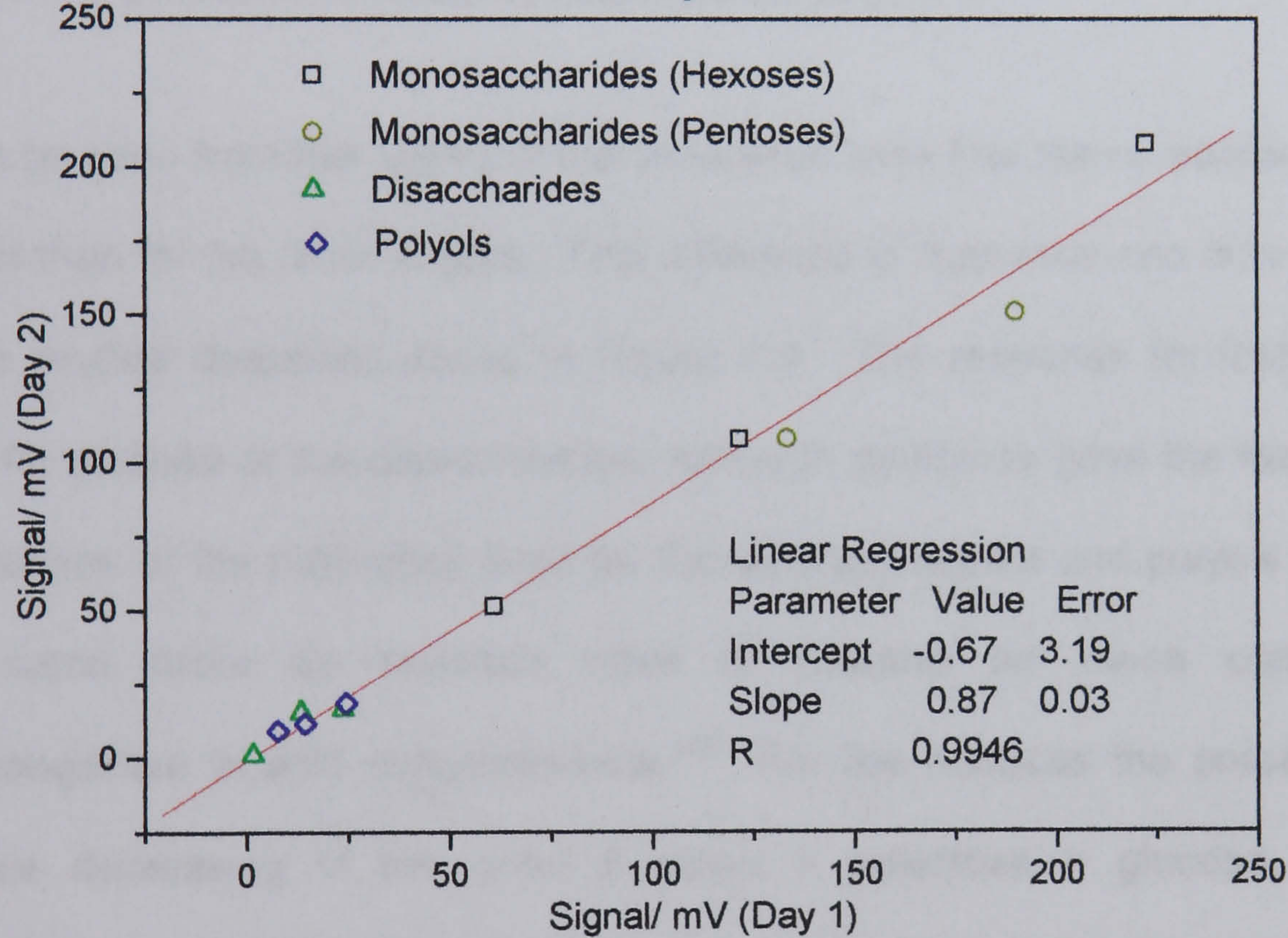
**Table 4.8 A Day to Day Reproducibility of Signal for Sugars and Polyols**

Compound	Day 1		Day 2		Residual
	mV	±	mV	±	
Glucose	60.7	0.957	51.3	0.98	-0.914
Galactose	121.3	3.32	107.8	2.99	2.79
Fructose	222.3	3.85	207.9	1.88	14.9
Arabinose	189.8	1.92	151.0	2.90	-13.7
Xylose	133.1	2.22	108.0	3.35	-7.30
Maltose	13.2	0.182	15.6	0.905	4.77
Sucrose	1.39	0.037	1.17	0.052	0.630
Lactose	23.5	0.646	16.67	0.408	-3.13
Mannitol			13.6	0.204	
Sorbitol			46.8	1.92	
Meso erythritol	24.3	0.498	18.8	0.683	-1.70
1,2 Propandiol	14.2	0.238	11.8	0.224	0.099
Glycerol	7.5	0.333	9.42	0.258	3.56



A plot of results for day 2 against results for day 1 has a regression coefficient of 0.9946, shown in Figure 4.10. Examination of the plot and the residuals, which are shown in the final column of Table 4.8, shows a fairly even distribution of points. The points for both the pentoses used have negative residuals and excluding these points gives a regression of 0.99875. These results tend to confirm that the major cause of day to day variation is the detector response, however the apparent differences between the pentoses and the other compounds suggest that kinetic or other effects may be also significant.

**Figure 4.10 Regression for Day to Day Variation in Signal for 0.1 mol dm<sup>-3</sup> Mono- and Disaccharides and Polyols**



Conditions as above

In addition to the polyhydric compounds shown above the monohydric alcohols methanol and ethanol were investigated. There was a slow reaction with the permanganate/ manganese (II), shown by the decrease in permanganate colour after several hours but no measurable light was emitted.

Some simple carbonyl compounds were examined under the same conditions. Glucose was run for comparison and the results are shown in Table 4.9. All reacted



with permanganate/ manganese(II) but only oxalic acid gave a significant amount of light. In the absence of manganese(II) the signal from ethanal was higher but the response for propanone was lower than that for a water blank.

**Table 4.9 Chemiluminescence Signal for 0.1 mol dm<sup>-3</sup> solutions of Simple Carbonyl Compounds**

Compound	Signal	
	mV	±
Glucose	53.41	0.525
Oxalic acid	7.81	1.622
Methanal	0.046	0.007
Ethanal	0.461	0.010
Propanone	0.011	0.003

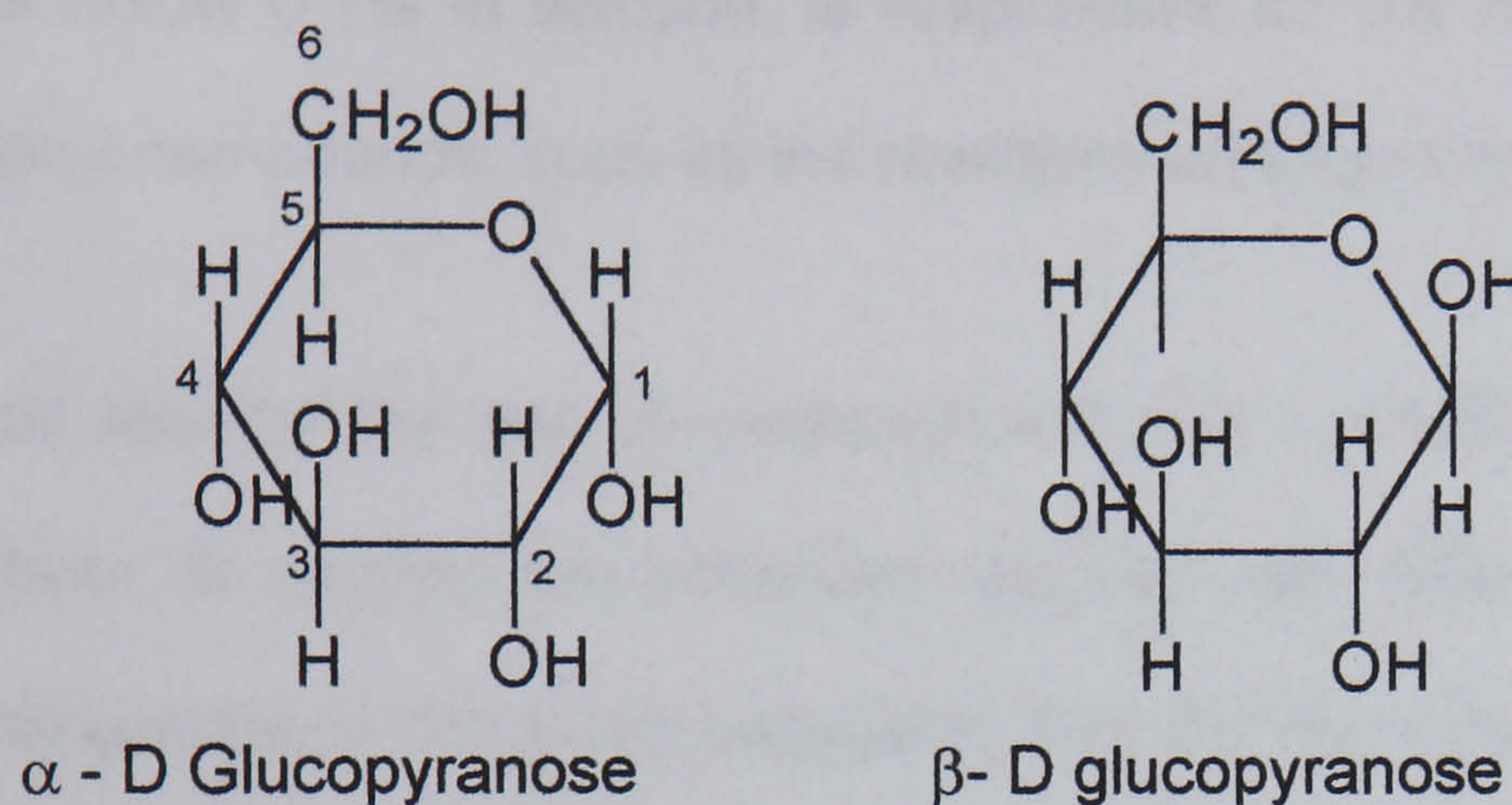
It can be seen from the slopes of the calibration lines that the response for fructose is higher than for the other sugars. This difference in response was also clear from the batch studies described above in Figure 4.4. The response for fructose is higher than for glucose or the disaccharides, although galactose gave the fastest emission. The slopes of the calibration lines for the different sugars and polyols are broadly in the same order as reported rates of reaction for these compounds with permanganate in acid pyrophosphate.<sup>148</sup> For the hexoses the present work gave signals decreasing in the order fructose > galactose > glucose, for pentoses arabinose > xylose and for polyols sorbitol > mannitol > erythritol > propan 1,2-diol > glycerol. For the saccharides the reported first order rate constants are in the same order. For mannitol and sorbitol the reported first order rate constants are almost identical whereas the signal observed is higher for sorbitol than for mannitol.

#### 4.2.2.9 Relationship between Saccharide Structure<sup>227</sup> and Chemiluminescence

Monosaccharides occur predominantly in ring forms as hemiacetals from the condensation of the carbonyl with a hydroxyl at the farther end of the chain. The size of ring formed depends on which hydroxyl group is involved in hemiacetal formation.

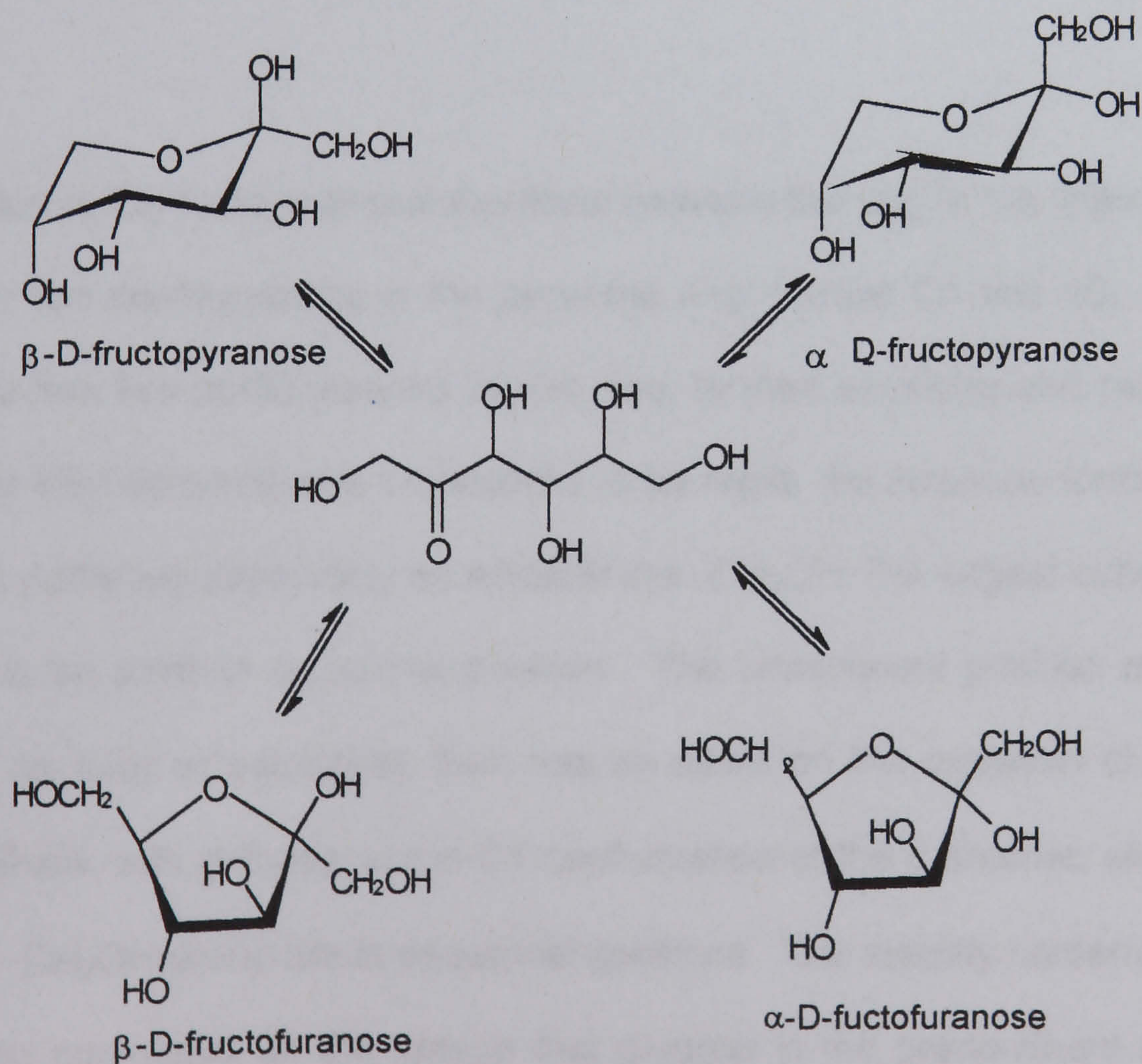


For pentoses and hexoses six member rings (pyranose forms) and five member rings (furanose forms) are possible. Two stereoisomeric forms, or anomers, are possible for each of the ring forms for example the Haworth representations for the  $\alpha$  - and  $\beta$ - anomers for the pyranose forms of glucose are shown as Scheme 4.2.



**Scheme 4.2**

In solution ring forms of monosaccharides are in equilibrium with the straight chain form. Ring and straight chain structures for fructose<sup>228</sup> are shown in Scheme 4.3.



**Scheme 4.3**

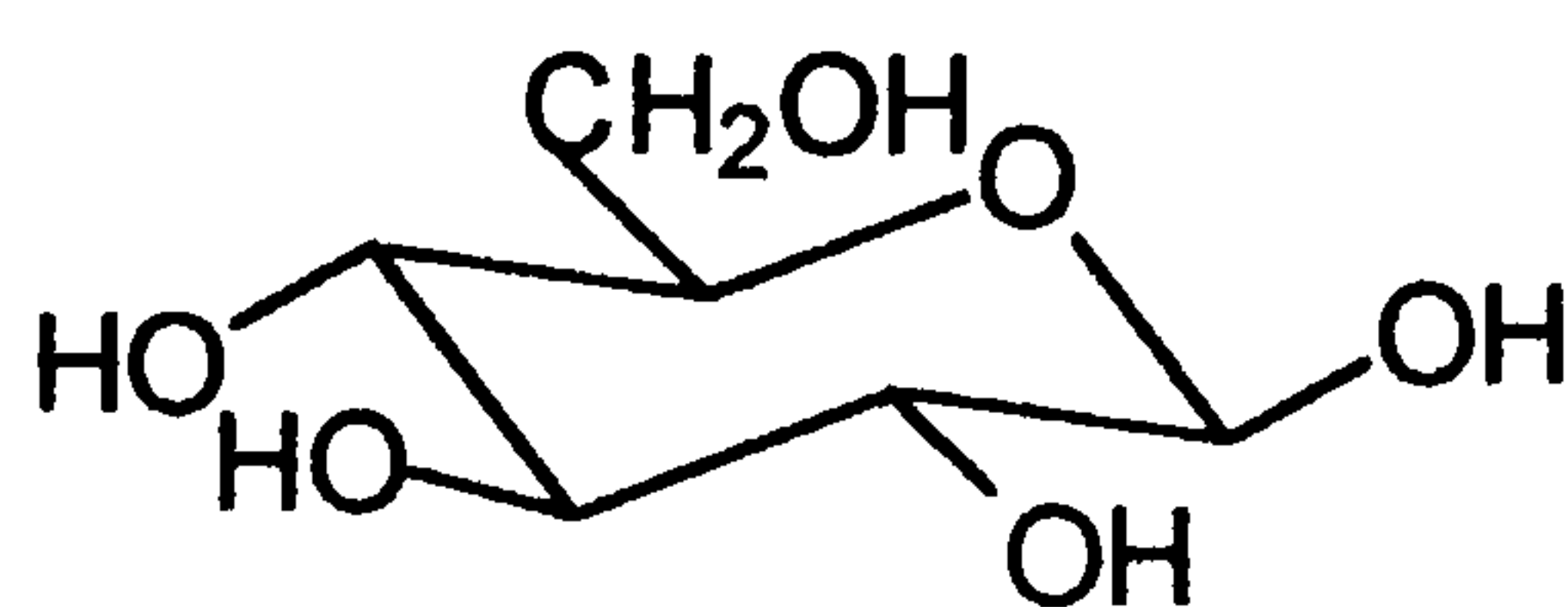


The move to equilibrium in solution is responsible for mutarotation, the change in specific rotation of a solution of one anomer to an equilibrium value. For glucose the equilibrium specific rotation is  $+52^\circ$ . The mutarotation can be acid, base or enzyme catalysed. The transition passes through the open chain form which, while present at levels below 0.1% in solution, is responsible for the reactions which are typical of carbonyl compounds, such as the reactions with Fehling's and Tollen's reagents.

In acid solution the rate of mutarotation is fast compared with the rate of oxidation. However, to explain the observed reaction rate differences in the oxidation with permanganate, it has been suggested that the first step of the reaction involves the ring forms. This is in contrast with oxidation with chromium (VI) and vanadium (V), in which the rate determining step is considered to be decomposition of an open chain metal saccharide complex.<sup>149</sup> Neither chromium nor vanadium have been found to give chemiluminescence under similar conditions to the present permanganate studies.

In addition to the mutarotational equilibria between the ring forms, there are equilibria between two conformations of the pyranose ring, termed C1 and 1C. The furanose ring also has two conformations for the ring, termed envelope and twist. While the furanose inter-conversion is considered to be rapid, the furanose forms clearly have different stabilities depending on whether the  $-\text{CH}_2\text{OH}$ , the largest substituent on the ring, is in an axial or equatorial position. The consequent position of the hydroxyl groups, as axial or equatorial, then has an effect on the oxidation of the molecule. For example, with glucose, in the C1 conformation of the  $\beta$  anomer, all the hydroxyls and the  $-\text{CH}_2\text{OH}$  group are in equatorial positions. The stability conferred in this state has been postulated as the reason that glucose is the predominant sugar in living systems, both as a structural element and metabolic intermediate.





C1 confirmation of β- D glucopyranose

Scheme 4.4

Studies using NMR,<sup>229,230</sup> and more recently chiral chromatographic techniques,<sup>231</sup> have determined the proportions of the conformations in various solutions. The equilibrium composition depends on temperature and solvent, however, for the hexoses and pentoses examined above, the proportions listed in Table 4.10 have been reported for aqueous solutions. The equatorial and axial confirmations of the hydroxyls in the C1 confirmation are also shown in Table 4.10.

**Table 4.10 Percentage of different Conformers in solution at Equilibrium  
Hexoses in Water and Pentoses Deuterium oxide**

Sugar	Hexose			Pentose	
	Glucose	Galactose	Fructose	Arabinose	Xylose
α Furanose	<1	<1	<1	2.5	<1
β Furanose	<1	<1	25	2	<1
α Pyranose	36	27	8	60	36.5
β Pyranose	64	73	67	35.5	63
Positional conformation for the β Pyranose form					
C1 hydroxyl	Equatorial	Equatorial	Equatorial	Equatorial	Equatorial
C2 hydroxyl	Equatorial	Equatorial	Equatorial	Equatorial	Equatorial
C3 hydroxyl	Equatorial	Equatorial	Equatorial	Equatorial	Equatorial
C4 hydroxyl	Equatorial	Axial	Axial	Axial	Equatorial

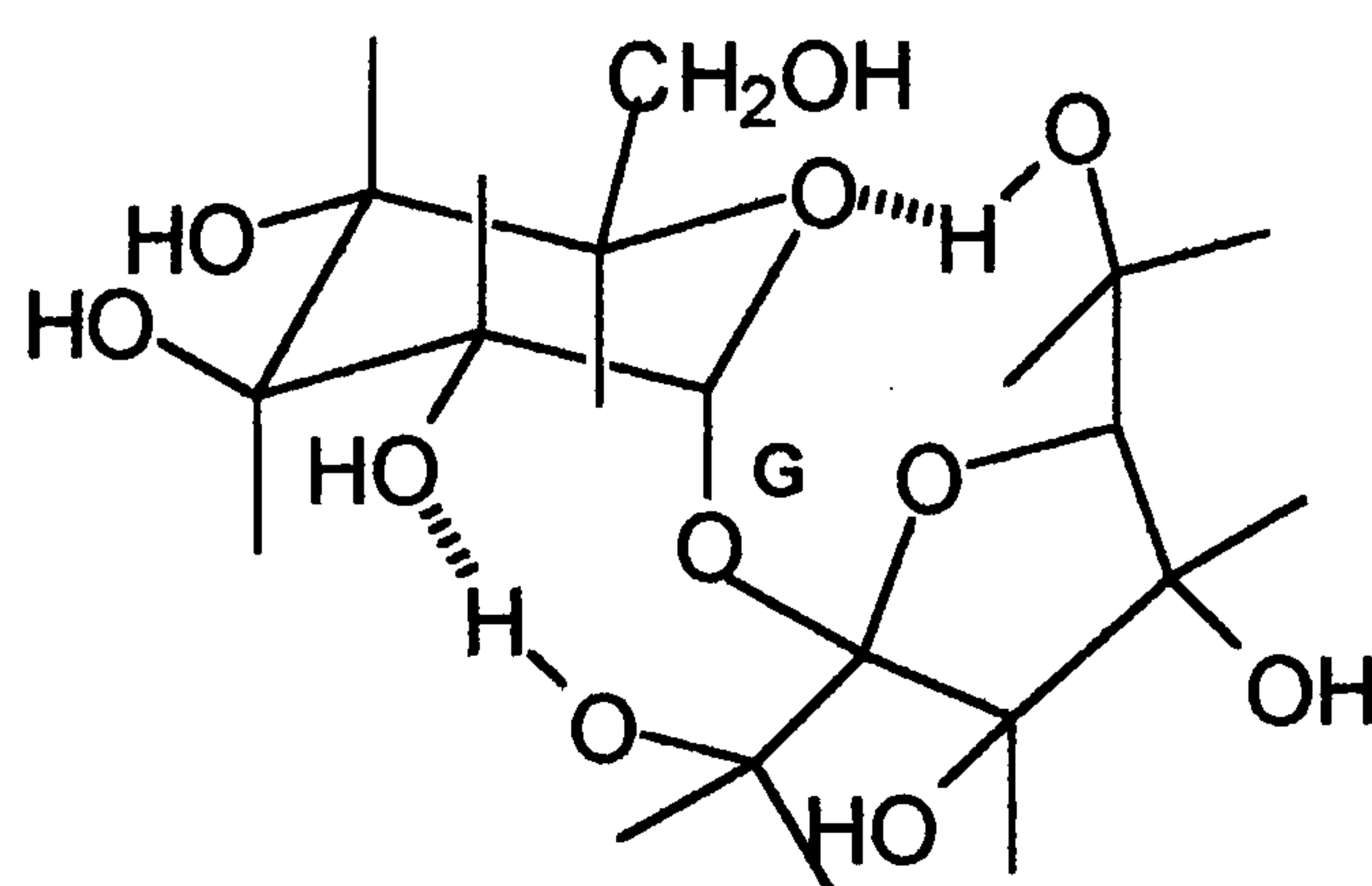
In the case of pentoses, there is no bulky -CH<sub>2</sub>OH substituent on C5 of the pyranose ring. The hydroxyl groups dictate the preferred conformation of the molecule.



Referring to Table 4.7, it can be seen that the presence of the furanose form and an axial-equatorial configuration about the C3-C4 bond gives higher chemiluminescence signals in both the hexose and pentose sets.

In the batch studies, the concentration of substrate sugar or sugar alcohol was in excess over the permanganate concentration. Under these conditions, the first oxidation product is a saccharide with one lower carbon number. In the case of glucose the smaller saccharide is the pentose arabinose. Formic acid is also produced in this reaction<sup>149</sup> and the final manganese species is Mn (II).

Disaccharides consist of monosaccharides linked through glycosidic linkages between the slightly acidic hydroxyl on the C1 in aldoses or C2 in ketoses with a hydroxyl on another sugar molecule. Where the hydroxyl of the second sugar is the C1 in aldoses, or C2 in ketoses, the resulting disaccharide is non-reducing. A non-reducing disaccharide will not undergo the reactions characteristic of the aldehyde group such as the reaction with Fehling's solution. In addition to the glycosidic linkage between two monosaccharides, hydrogen bonds can form between the sugars, as shown for sucrose in Scheme 4.5.



Conformational structure of Sucrose  
The glycosidic oxygen marked G.

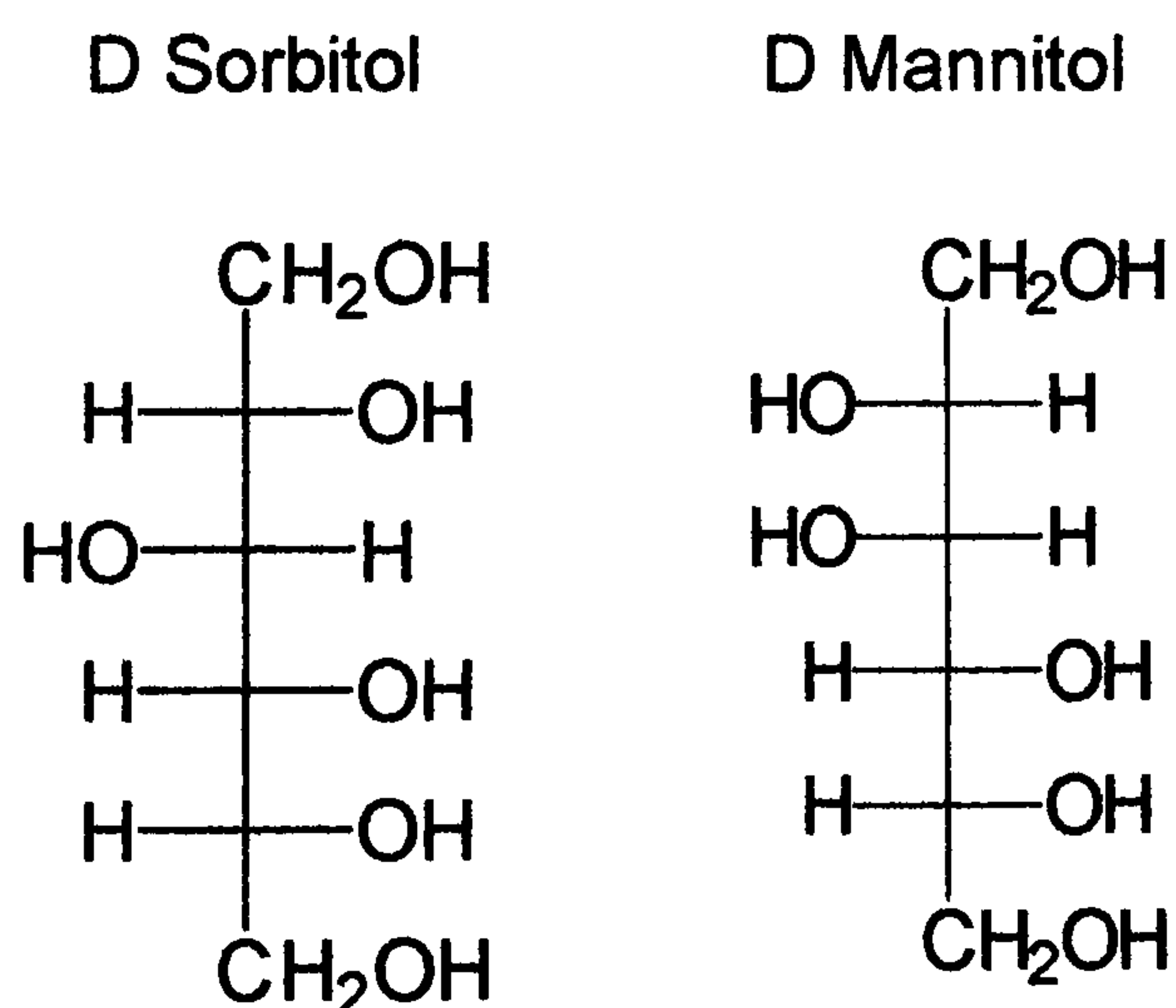
**Scheme 4.5**



As sugars possess more than one hydroxy group capable of linking through a glycosidic bond, a wide range of di- and oligosaccharides is possible. The saccharide unit linked through the C1 can no longer mutarotate, although the second saccharide can still mutarotate unless it is itself linked through its C1 hydroxyl.

Referring to Table 4.7, it is seen that the response for sucrose, a non-reducing disaccharide, is considerably smaller than for the reducing sugars. Other non-reducing sugars are not found at significant levels in foods; however trehalose, a disaccharide, where both glucose molecules are linked through C1, is found in edible mushrooms. Trehalose gives virtually no chemiluminescence with permanganate.

For the D-mannitol/ D-sorbitol pair of sugar alcohols, the signal for sorbitol is more than three times that for mannitol. The compounds, which are straight chain, differ in the position of one OH substituent as shown in Scheme 4.6.



**Scheme 4.6**

In the case of polyhydric alcohols, reduction results in carbonyl formation, as shown in Chapter 2 Scheme 2.8, and clearly there are no possible ring structures. The orientations of the hydroxyl group differ, with consequent differences in the ease of forming bridging complexes between manganese species and hydroxy groups. The ease of formation of complexes will also depend on the ionic size and the geometry of the manganese species, which is commonly octahedral for manganese (III) and manganese (IV) and tetrahedral for manganese (VII).



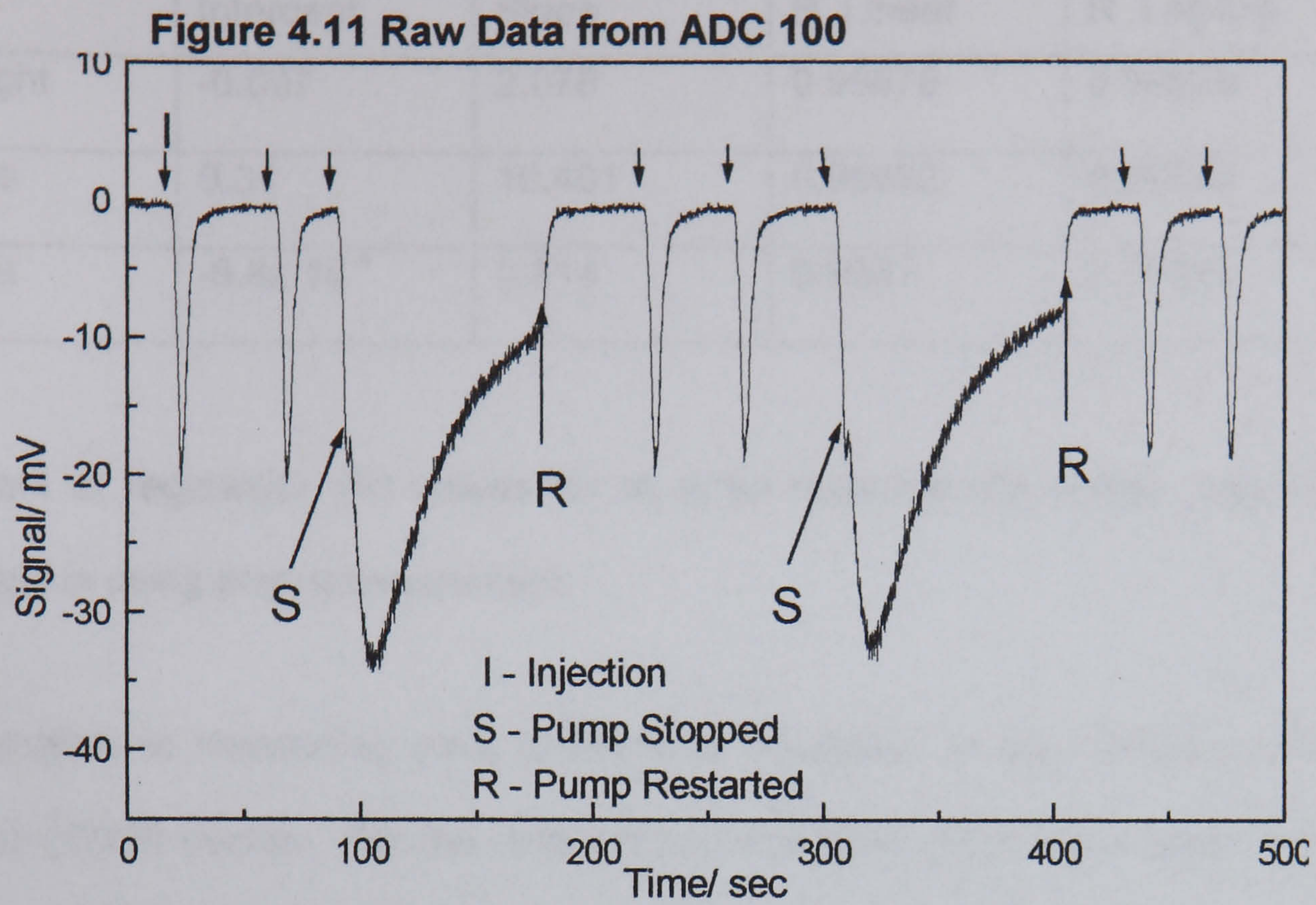
### 4.2.3 Data Handling for Flow Injection System

Data analysis for the flow injection experiments was by measurement of peak height on a chart recorder. Photomultiplier output is in the form of a current input into a chart recorder with high impedance, typically  $1\text{M}\Omega$ , giving a voltage response, which is recorded as a pen deflection. At a late stage in this project a data capture system ADC-PC with data logging software became available. As with the chart recorder, a high impedance, nominally  $1\text{M}\Omega$ , results in a voltage which can be converted into a digital signal. The ADC has variable, software selectable, input range from  $\pm 20\text{V}$  to  $\pm 50\text{mV}$ , and maximum data acquisition rate of  $1000\text{ points sec}^{-1}$ . There is also the facility for averaging data points during collection. High acquisition rates were not necessary and  $10\text{ points sec}^{-1}$  gave sufficient data for analysis of sharp FIA peaks. Data was stored as text files and input into the Origin data analysis package. In order to compare height, area and rate information a glucose calibration was carried out using conditions previously established. The ADC range was varied from  $1\text{V}$  for  $0.1\text{mol dm}^{-3}$  solutions to  $50\text{mV}$  for  $0.001\text{mol dm}^{-3}$  solutions.

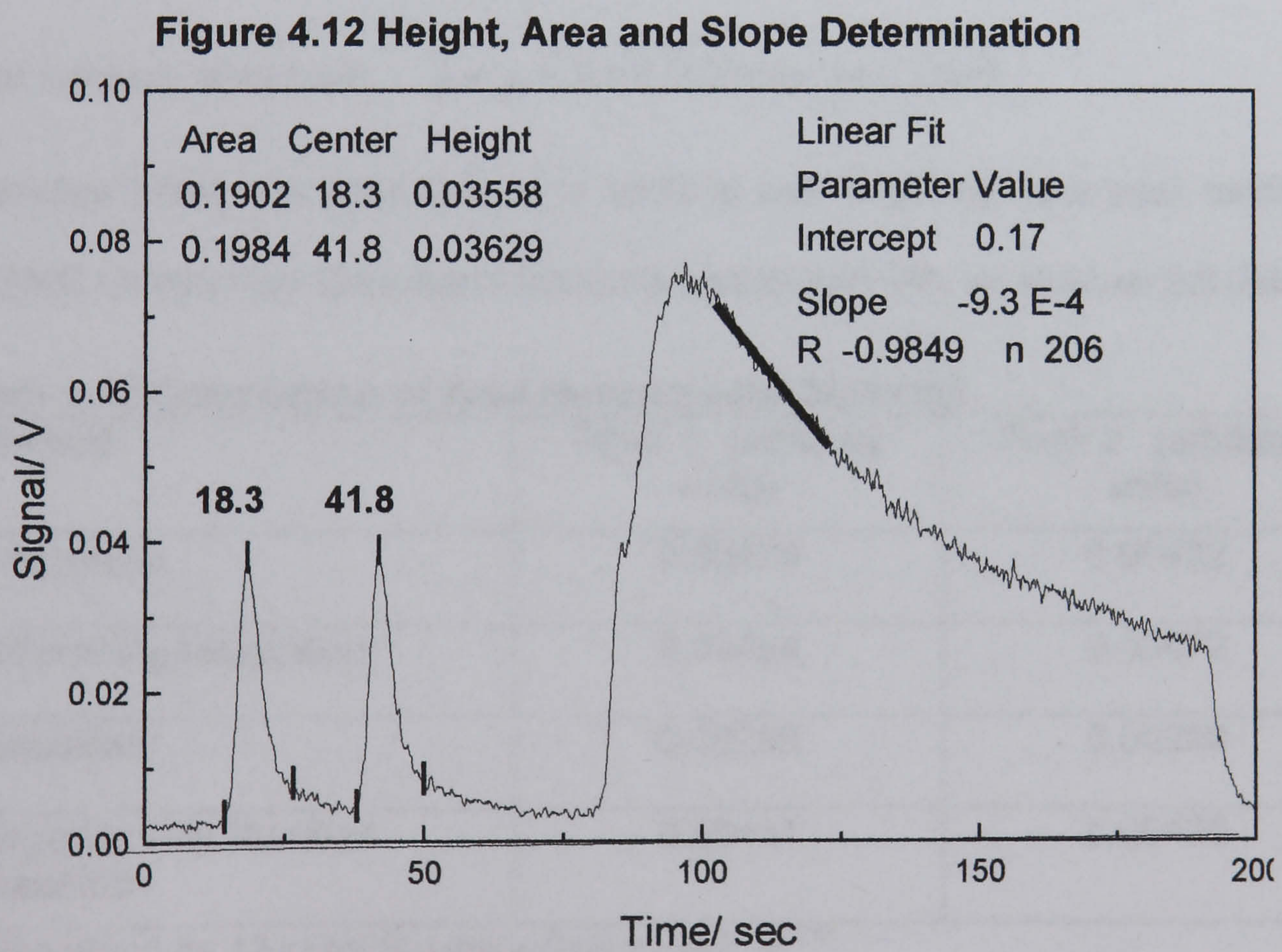
For rate determination stopped flow injection was used. Two injections were made under normal FIA conditions, a further injection was made and at the estimated top of the peak the pump was stopped. The signal was followed until the curve started to flatten and the pump was restarted. When the signal reached base line the set of three injections, was repeated. The raw data was as Figure 4.11.

The data was inverted, to give positive peaks, and area and height were measured. The decline in chemiluminescence fitted well to an exponential function. The rate was measured by fitting a linear function to the top part of the decline as shown in Figure 4.12. Approximately 200 data points were used to determine the slope and correlation coefficients were typically greater than 0.98.





Range 500mV Glucose 0.05 mol dm<sup>-3</sup>



Calibration lines for the three measurement methods were constructed and the parameters were as shown in Table 4.10.



**Table 4.11 Regression Parameters for Height, Area and Slope**

	Intercept	Slope	R Linear	R Log-log
Height	-0.007	2.078	0.99678	0.99825
Area	0.34	10.401	0.99682	0.99846
Rate	-6.6x 10 <sup>-4</sup>	0.814	0.9857	0.99980

Coefficient of regression (R) values for all three methods are similar, showing no advantage in using area measurement.

An alternative to measuring area is fitting to Gaussian or exponentially modified Gaussian (EMG) curves. For the data set both functions gave lower areas than the peak find method. Table 4.11 shows areas for the two peaks in Figure 4.13 by integration on raw and smoothed data and by Gaussian and EMG methods.

Gaussian function, area form :  $y = y_0 + A/(w\sqrt{\pi/2})\exp(-(x-x_c)^2/w^2)$

y<sub>0</sub> is baseline offset, A is peak area, w is width at half height and x<sub>c</sub> is peak centre

For the EMG function the Gaussian function is convoluted with an exponential decay.

**Table 4.12 Comparison of Area Measurement Methods**

Method	Peak 1 (arbitrary units)	Peak 2 (arbitrary units)
Integration	0.00470	0.00492
Smoothing/Integration *	0.00464	0.00472
Gaussian	0.00290	0.00289
Exponentially Modified Gaussian	0.00451	0.00436

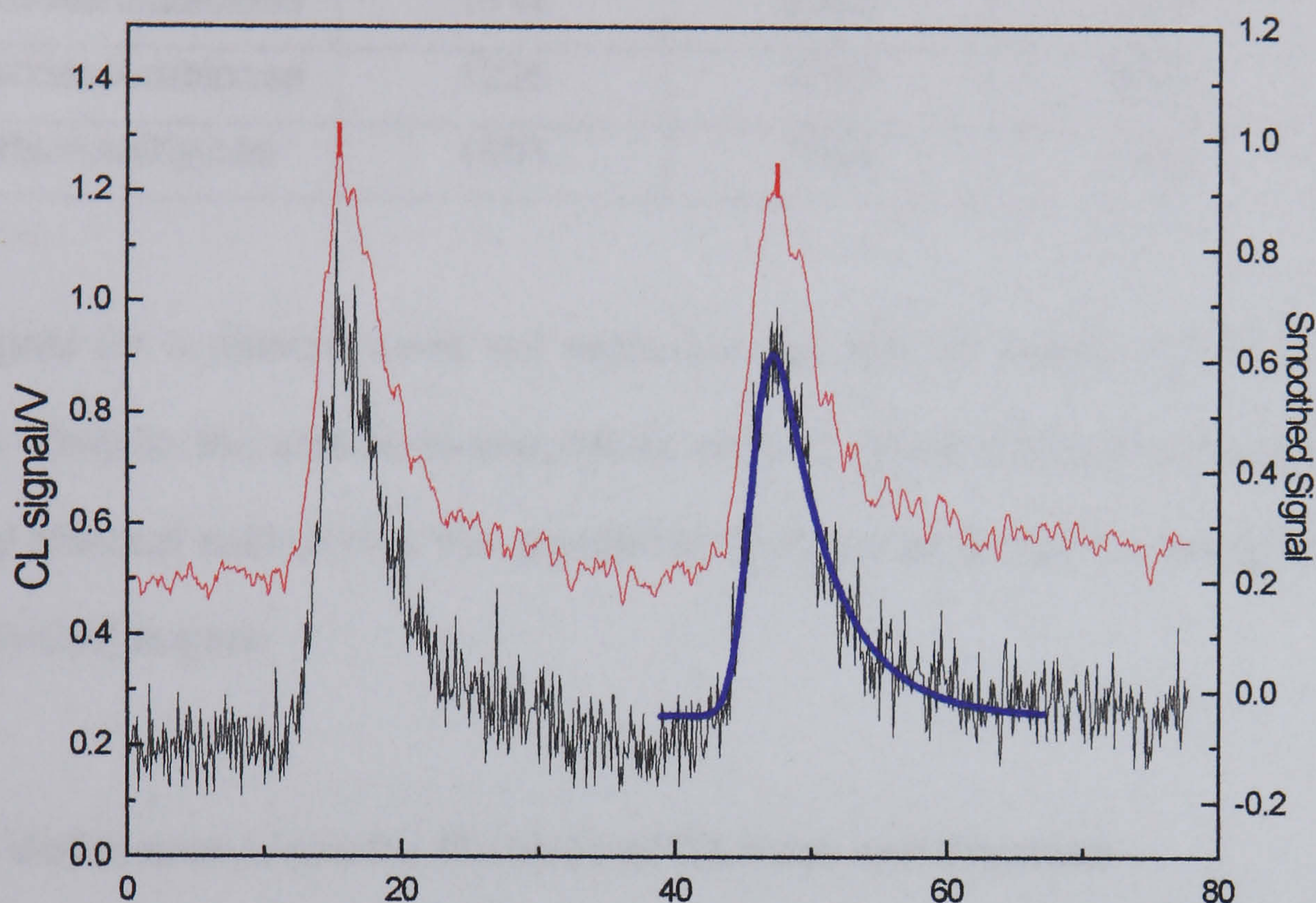
\*Smoothing by 13 point Savitzky-Golay method<sup>232</sup>

The EMG fit appears to give a good approximation of the experimental data. The smallest measurable signal for the ADC is 0.012 mV, however amplitude of the baseline noise is approximately 0.15mV. For S/N of 3 the limit of determination is



$2 \times 10^{-4} \text{ mol dm}^{-3}$  on a peak height basis. Using the chart recorder baseline noise is typically 0.02mV equivalent to a limit of detection of  $6 \times 10^{-5} \text{ mol dm}^{-3}$ .

**Figure 4.13 FIA Peaks used in Comparison**



Glucose  $0.001 \text{ mol dm}^{-3}$ , conditions as above  
 Raw data in black, offset smoothed data in red  
 Exponentially modified Gaussian fit in blue

#### 4.2.3.1 Flow Injection Analysis of Carbohydrate Mixtures

The differences in calibration parameters for different carbohydrates, shown in Table 4.6 above, mean that it is not possible to set up a simple calibration for total sugars. To investigate the possibility of applying the technique to mixtures of sugars equimolar mixtures of glucose with fructose, galactose and arabinose and a mixture of arabinose with xylose were run under the same conditions as above. For each pair calibrations for the individual sugars and for the mixture, over the range  $1 \times 10^{-4}$  to  $0.1 \text{ mol dm}^{-3}$  of individual or total sugar, were run at the same time and the calibration parameters were measured. The results are shown in Table 4.13.

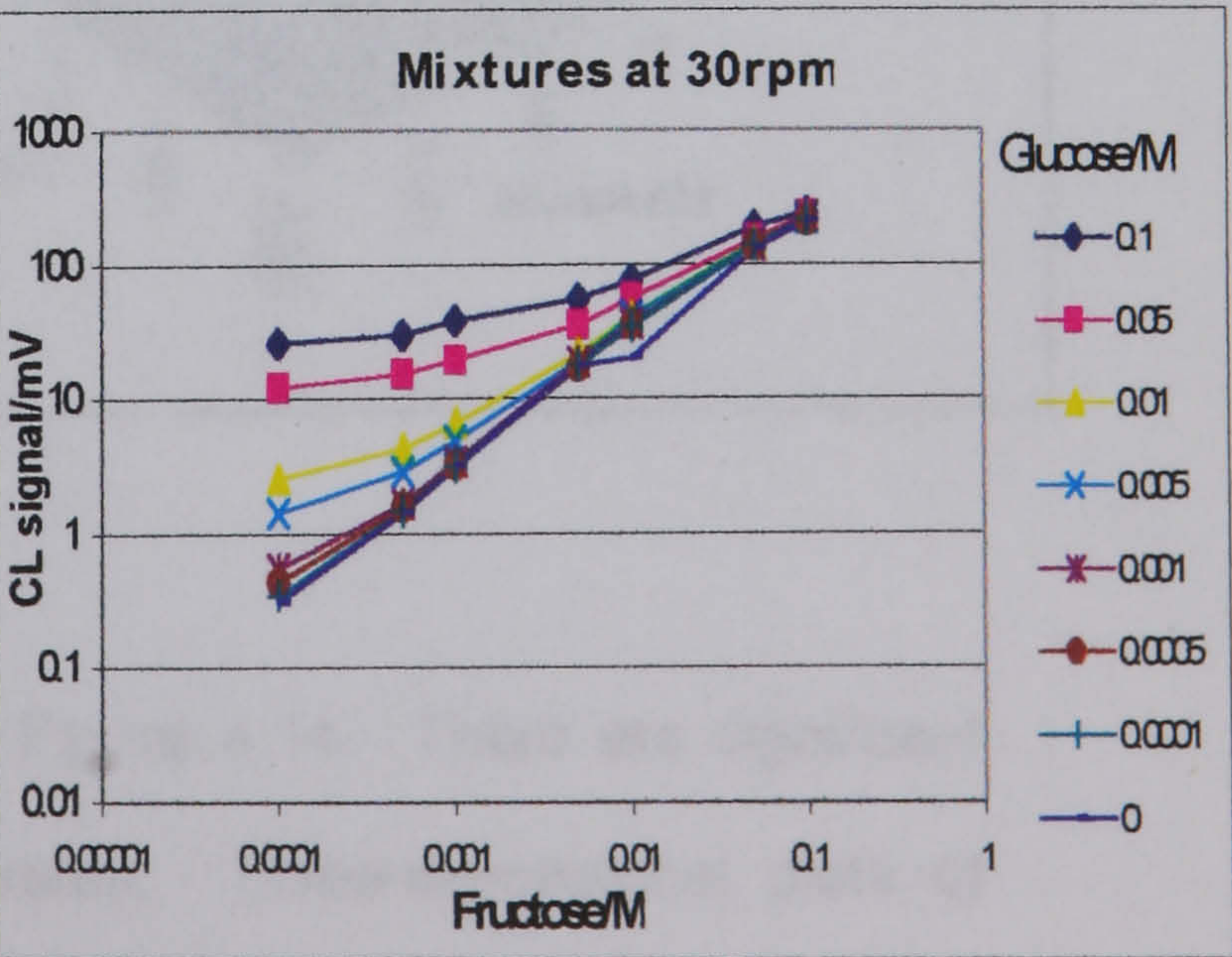
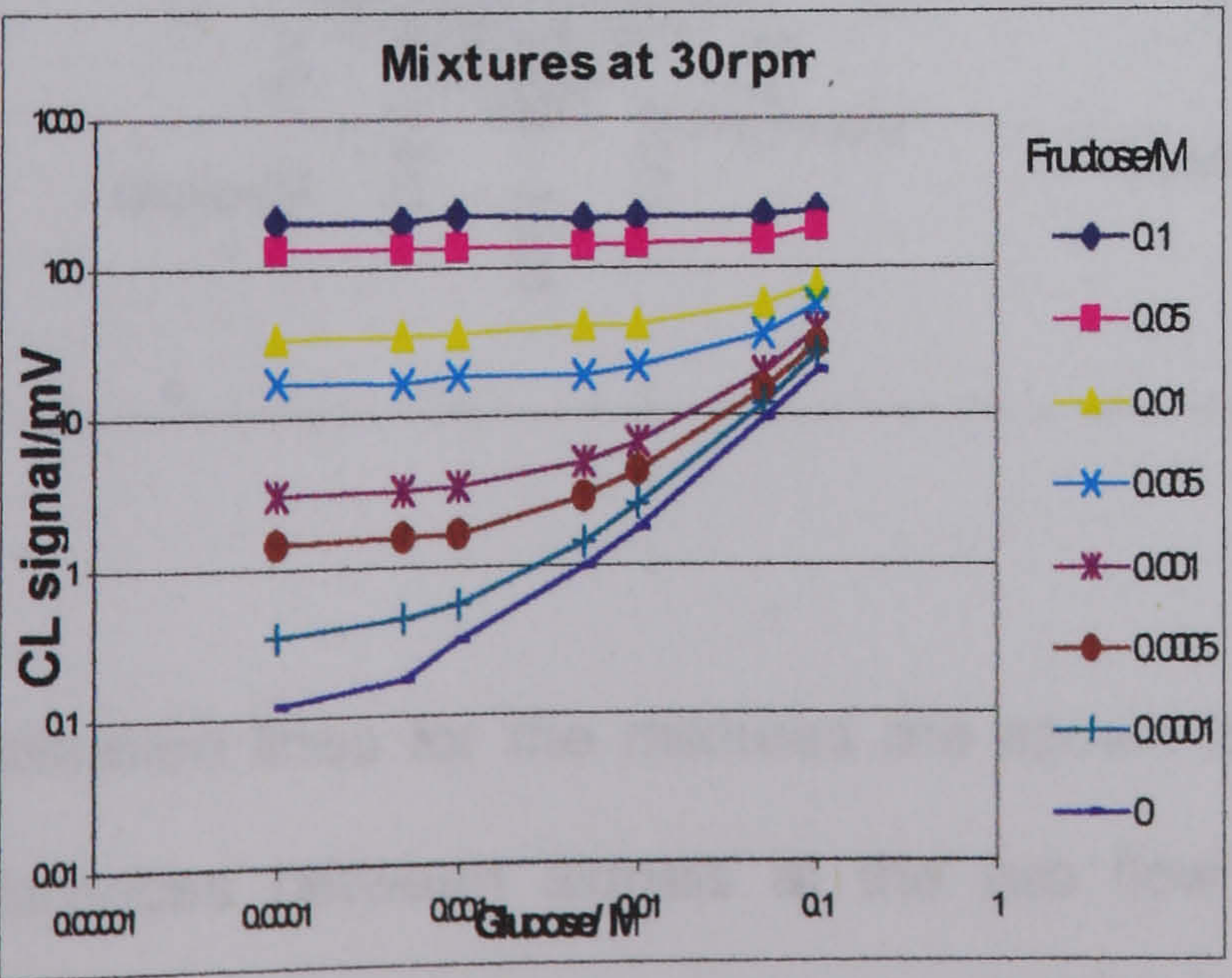
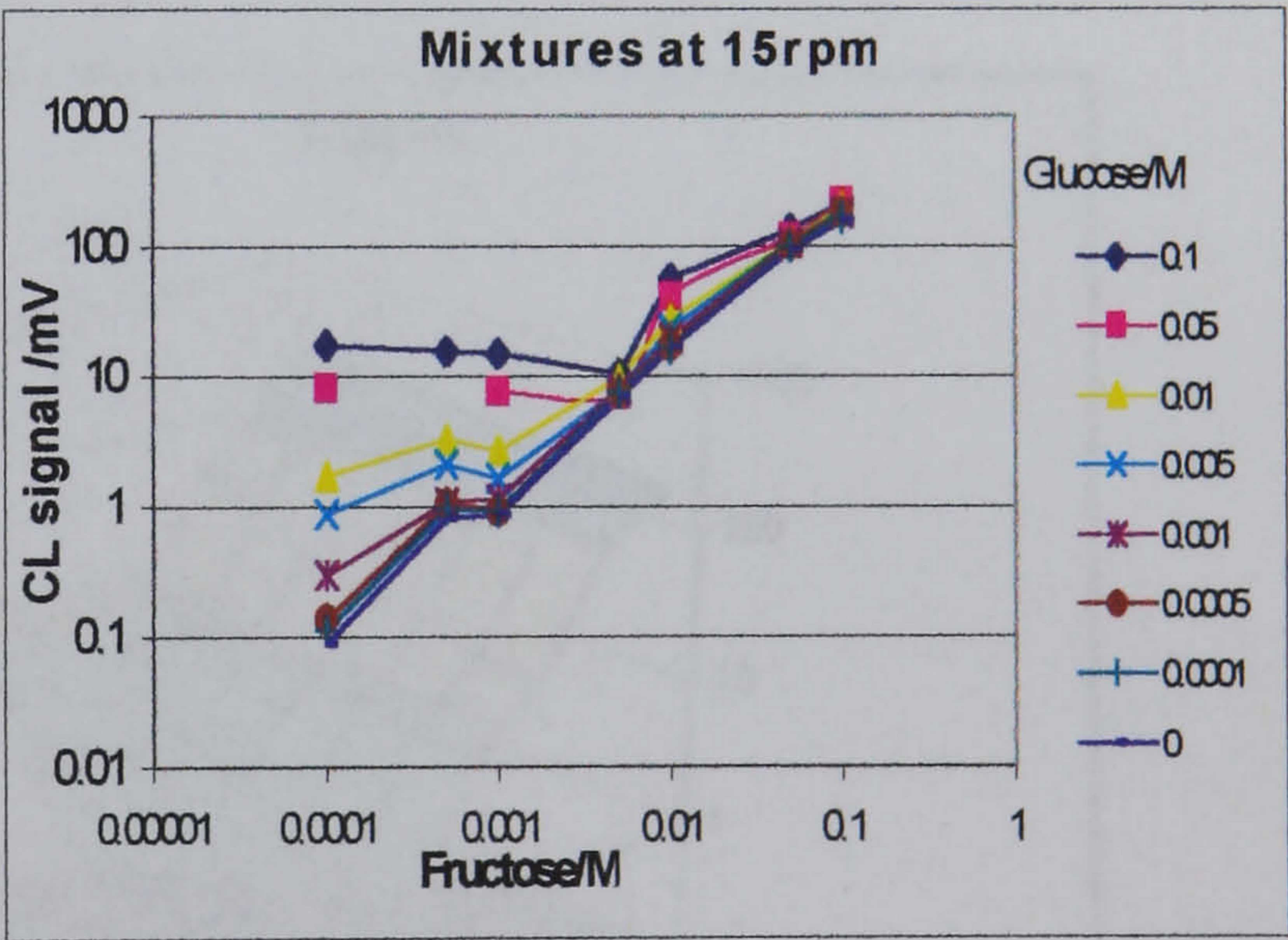
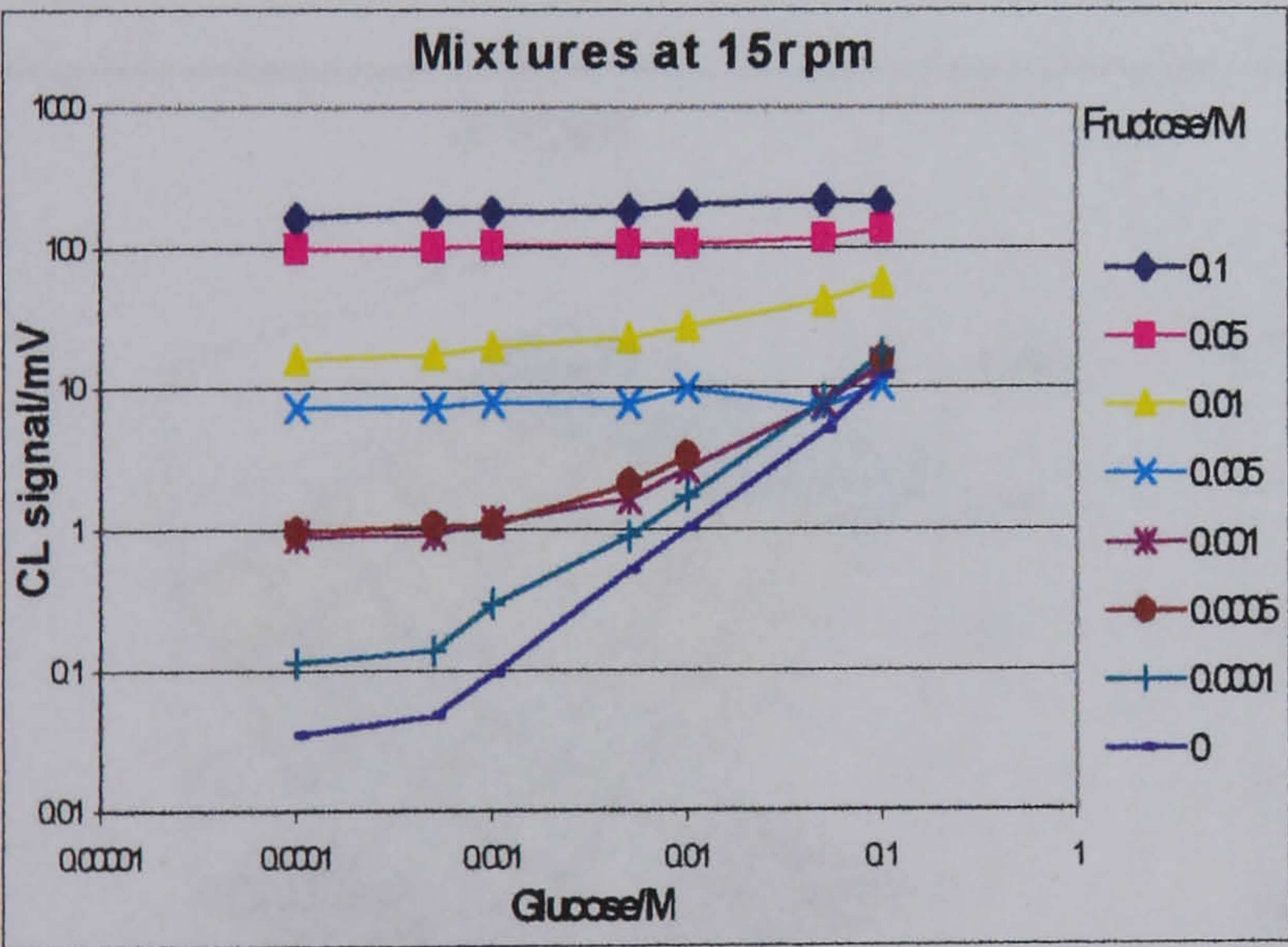


Table 4.13 Comparison of Calibration Parameters for Single Sugars and Mixtures

Sugar Mixture	Slope / mV mol <sup>-1</sup> dm <sup>3</sup> Sugar 1	Slope / mV mol <sup>-1</sup> dm <sup>3</sup> Sugar 2	Slope / mV mol <sup>-1</sup> dm <sup>3</sup> Mixture
Glucose/Fructose	1525	8438	6072
Glucose/Galactose	1514	2302	1151
Glucose/Arabinose	1225	4763	2381
Arabinose/Xylose	1601	1604	1340

The signal for a mixture does not represent the sum of signals for the individual sugars. Only for the arabinose and xylose mixture, where the individual sugars have virtually identical calibrations, the gradient for the mixture is close to the gradients for the individual sugars.

4.14 Calibration Lines for Mixtures of Glucose and Fructose

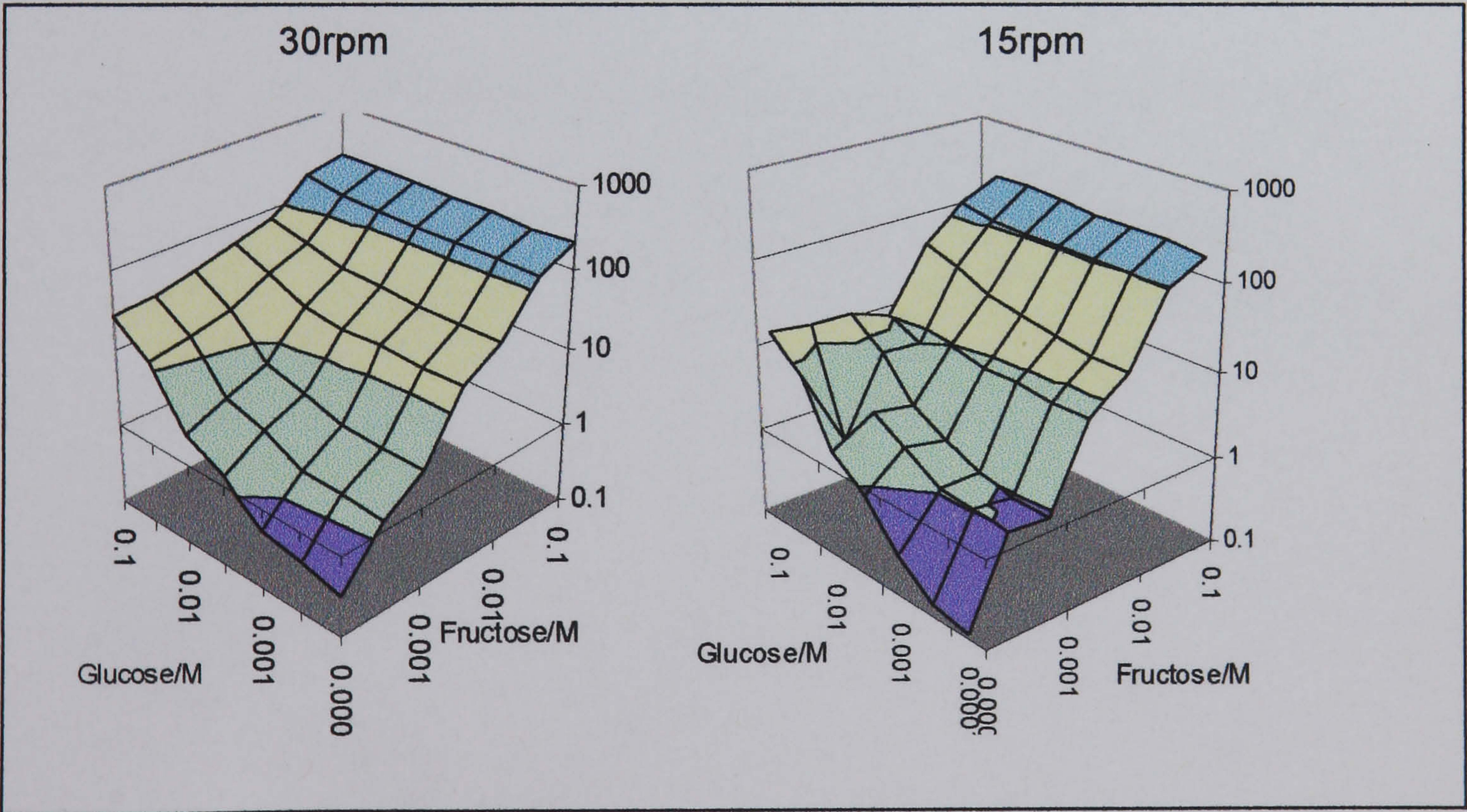




The difference in the response is partly due to the difference in rate between the reactions with the different sugars although this is clearly not the only factor. For equal concentrations of sugar, the reaction with galactose gives the fastest response, while the signal from the reaction with fructose gives the highest response.

It was considered that it could be possible to exploit the difference in reaction rates by measuring different points along the reaction profile. In order to investigate this mixtures of glucose and fructose were prepared to contain 0 to 0.1 mol dm<sup>-3</sup> of each sugar with two points for each decade giving a total of 64 points. Replicate injections were carried out for each point at two flow rates. Repeatability of injections was generally good with relative standard deviation below 5%.

**Figure 4.15 Three Dimensional Plots for Chemiluminescence of Glucose/Fructose Mixtures**



Calibration lines for the mixtures are shown in Figure 4.14. There are significant differences between signals at the two flow rates. Three-dimensional plots of glucose against fructose at the two flow rates again show distinct differences as



shown in Figure 4.15. This suggests that it may be possible to use chemometric techniques to predict concentrations of the individual sugars in mixtures by measuring the chemiluminescence at different flow rates. Alternatively using a detector array, it could be possible to measure the chemiluminescence at different times after mixing.

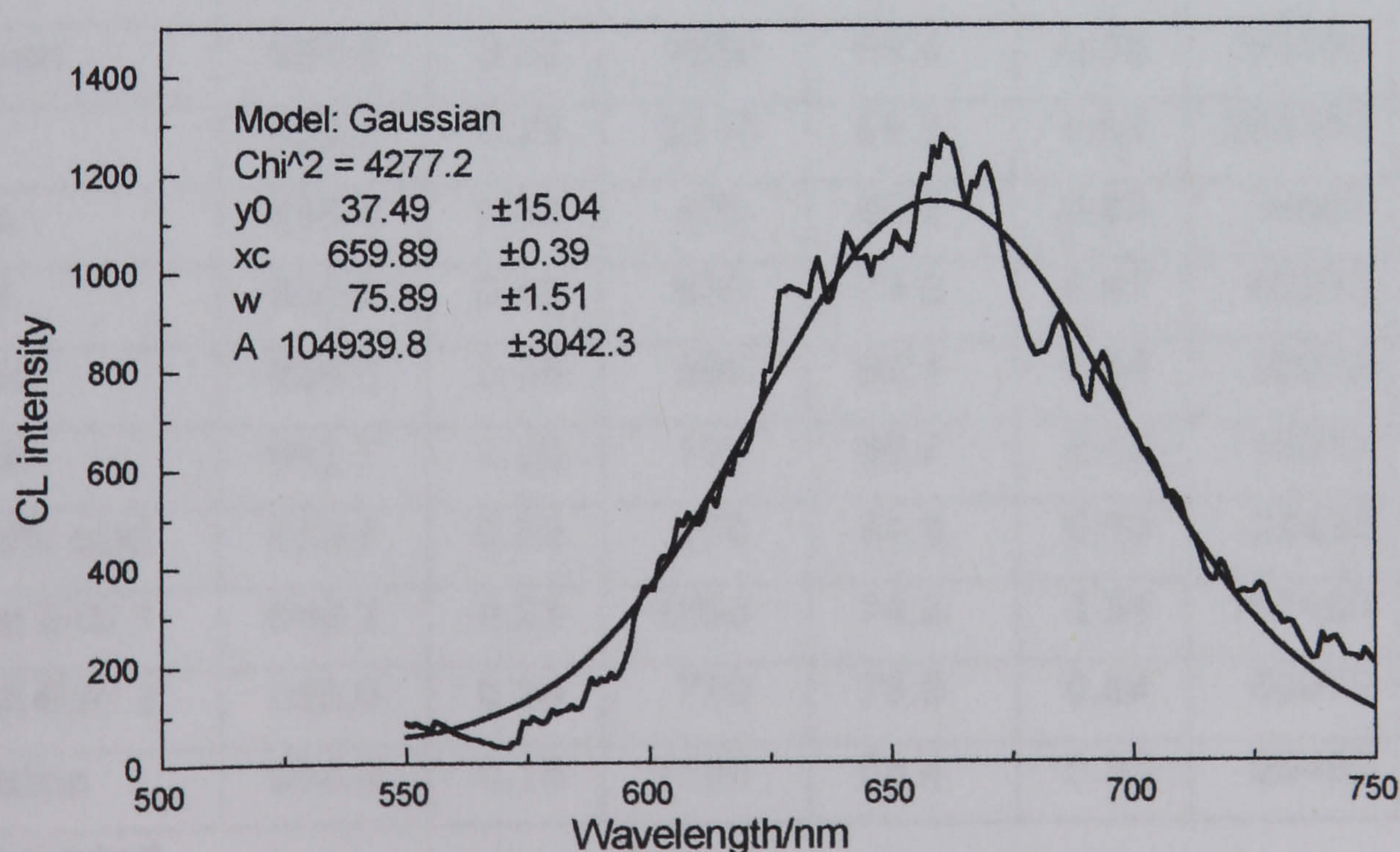


#### 4.2.4 Spectroscopic Investigations

In order to investigate the mechanism of the chemiluminescence from the reaction between permanganate and sugar, spectra of the emission were measured. Initial experiments were undertaken by the batch method. As there is a delay of several seconds, even in the presence of a catalyst, it was possible to mix the reagents and place the cuvette in the cell holder without loss of signal. Sugars were dissolved in acid containing manganese (II) sulphate. Permanganate was added and the solution mixed. After the required interval, estimated from the batch experiments, a spectrum was collected. High scan speeds were used to minimise the effects of the increase and decrease of total emission through the time of emission.

Initial experiments used the standard photomultiplier with low sensitivity for wavelengths above 600nm. A typical spectrum is shown in Figure 4.16.

**Figure 4.16 Chemiluminescence Spectrum for Permanganate Oxidation of Glucose**



Glucose 0.1g sulphuric acid 0.5 cm<sup>3</sup> 2 mol dm<sup>-3</sup>, permanganate 0.1cm<sup>3</sup>, 0.1 mol dm<sup>-3</sup>



Fitting of a Gaussian function gave a peak maximum at 651nm. Individual spectra were noisy and repeatability of intensity was poor. Repeatability of wavelength at maximum intensity and peak width were good as is shown in Table 4.14.

**Table 4.14 Parameters for 12 Spectra for Glucose-Permanganate Reaction**

	$\lambda$ Max nm	Width nm	Height	Area
Mean	658.9	71.36	1225	$1.434 \times 10^5$
Standard Deviation	1.83	5.47	697	$6.1 \times 10^4$
RSD %	0.28	7.7	56	55

Spectra for a range of sugars and carbohydrate rich food products were measured. The spectra were similar suggesting that the same emitting species is responsible for the emission. The results are shown in Table 4.15.

**Table 4.15 Parameters from Gaussian fit to Carbohydrate/Permanganate Spectra**

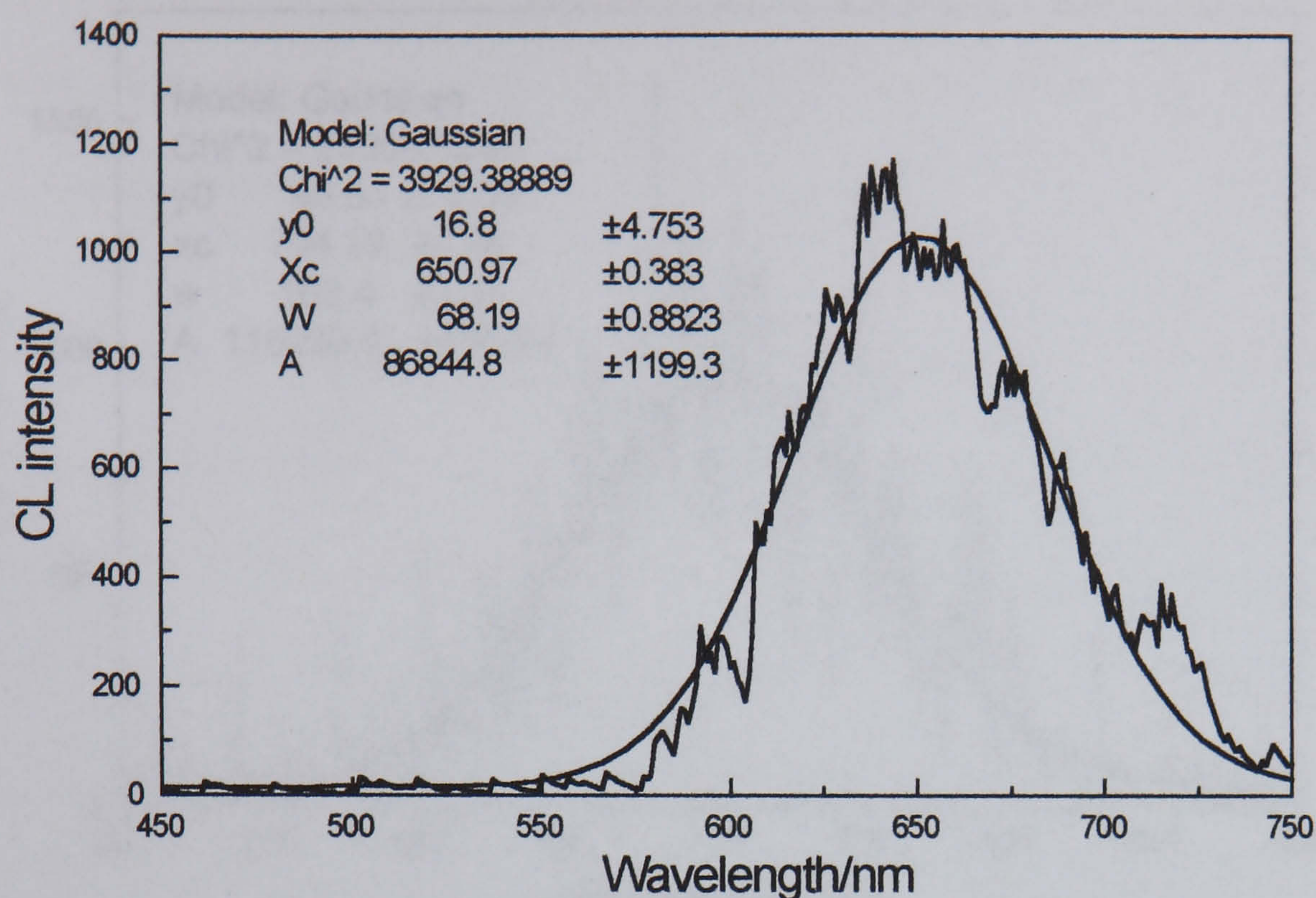
Sample	$\lambda$ Maximum nm $\pm$		Height at $\lambda_{max}$	Width nm $\pm$		Area $\pm$	
Glucose	658.7	0.24	1590	73.6	0.82	142814	2450
Galactose	655.4	0.24	1470	70.6	0.85	124205	2082
Fructose	657.4	0.24	1350	74.2	0.93	122885	2216
Arabinose	654.5	0.23	1650	69.4	0.55	150180	1245
Xylose	655.2	0.25	2310	69.9	0.56	202180	1693
Maltose	656.4	0.43	400	80.5	0.88	39897	374
Sorbitol	655.6	0.40	630	71.0	0.87	49250	589
Glycerol	656.8	0.26	690	62.4	0.54	50893	428
Formalin	653.7	1.08	195	85.7	2.45	18077	540
Saccharic acid	653.4	0.39	270	65.8	0.88	22438	310
Dry Malt Extr 1	660.2	0.23	1860	74.2	0.54	167450	1330
Dry Malt Extr 2	662.0	0.36	770	73.9	0.84	69073	844
Beer Solids	658.8	0.16	1150	68.4	0.36	95462	526

95% CI quoted

Spectra from second aliquots of permanganate, or from adding manganese (II) sulphate at the beginning of the reaction, did not alter the parameters for the spectrum. A glucose/ permanganate/ manganese(II) spectrum is in Figure 4.17.



**Figure 4.17 Chemiluminescence Spectrum for Permanganate Oxidation of Glucose with Manganese (II)**



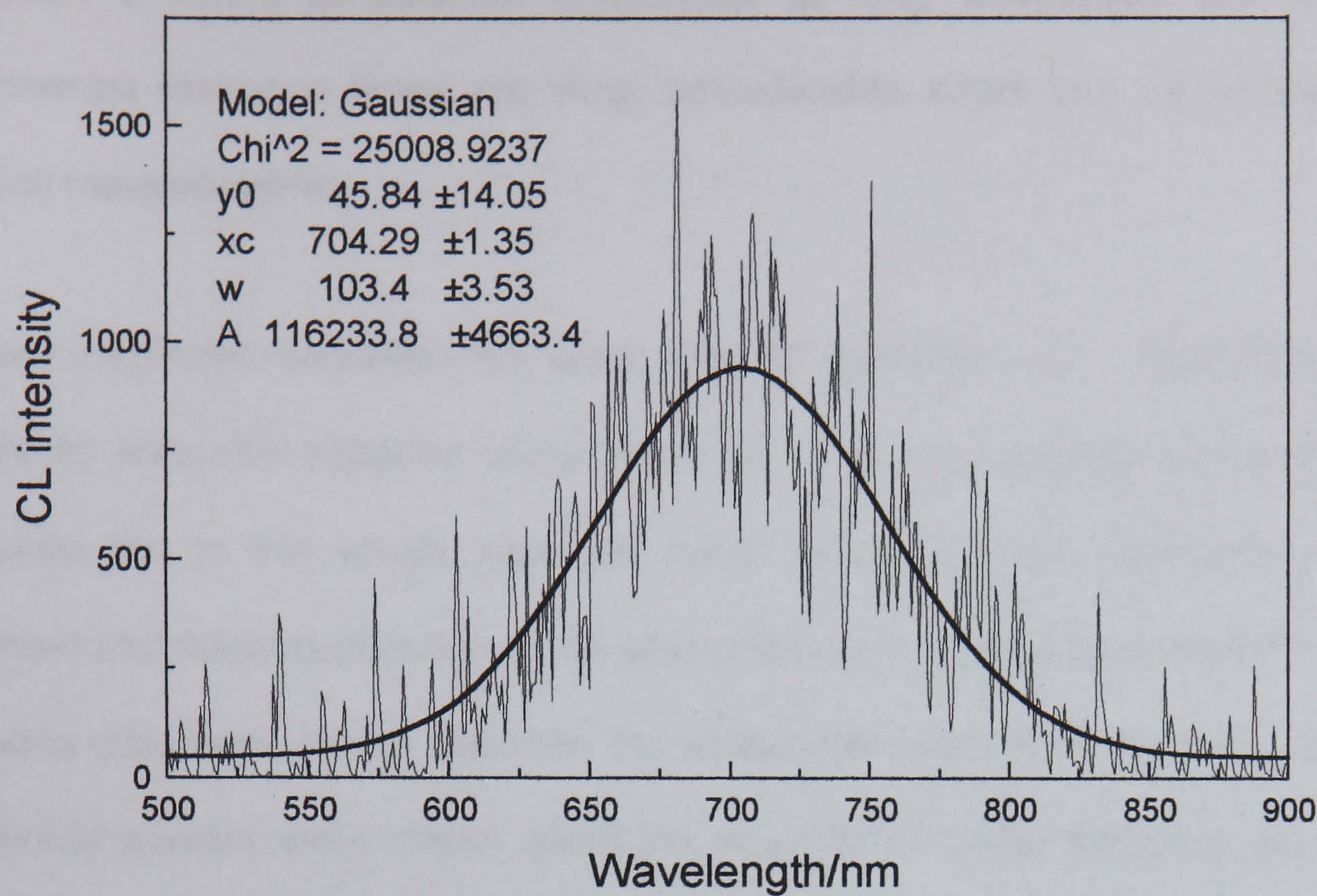
The spectral maxima were significantly higher than those reported for the permanganate oxidation of ethanol in gin,<sup>160</sup> at approximately 580nm. The maximum or for the permanganate oxidation of morphine and related alkaloids<sup>165</sup> was reported to be around 610nm.

#### 4.2.4.1 Problems with Recording Spectra

As discussed in 3.5.5.2 it was necessary to use the fastest response rate possible, resulting in a high level of noise. Most spectra required averaging and/or smoothing. It was also thought that the low efficiency of the standard PMT at wavelengths above 600nm could affect the observed  $\lambda_{\max}$ , therefore a PMT sensitive up to approximately 900nm was used for subsequent work. The wide range PMT has lower sensitivity in the region up to 500nm where many chemiluminescent emissions occur. A typical spectrum for the permanganate glucose reaction is shown in Figure 4.18

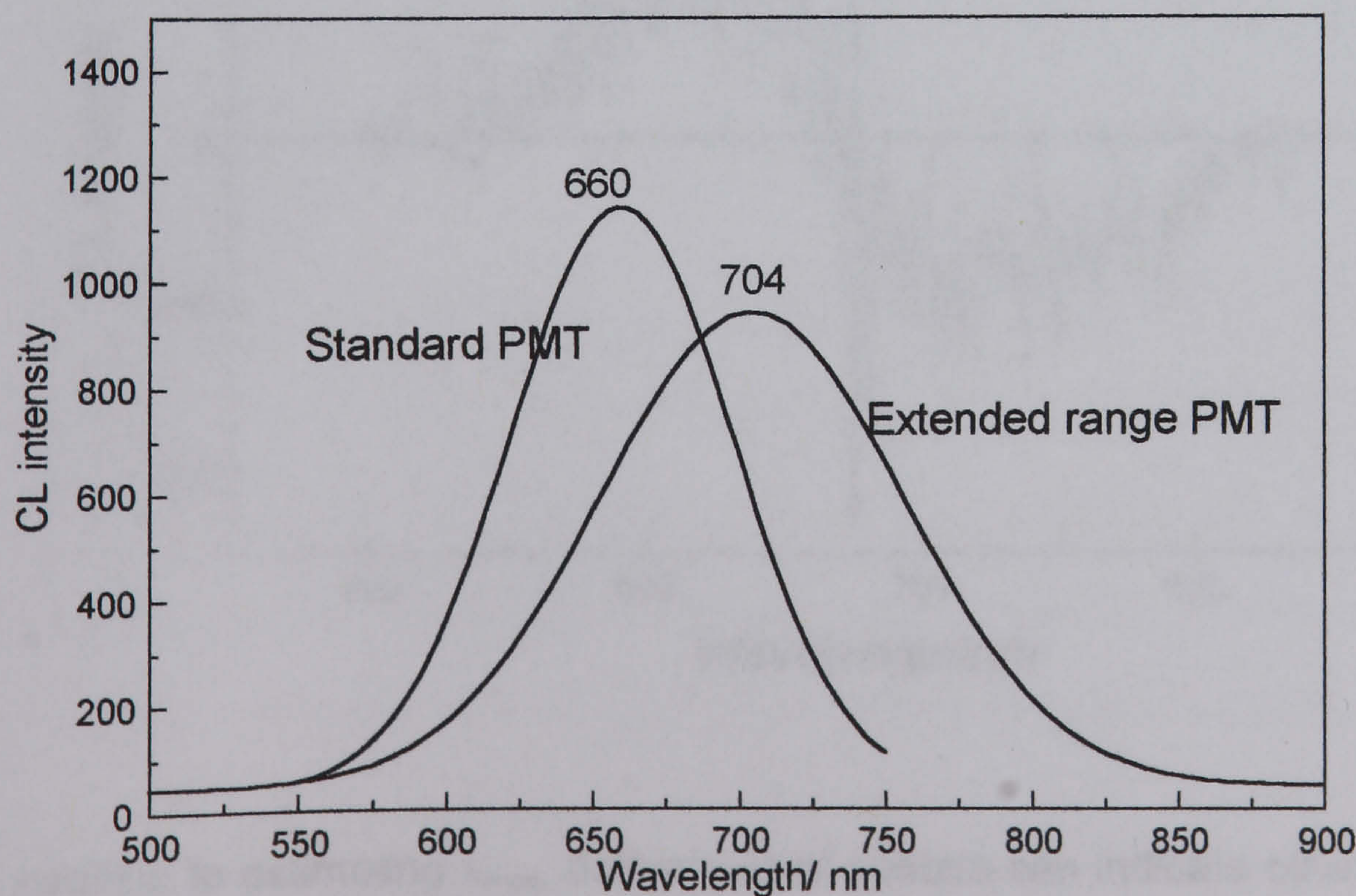


**Figure 4.18 Chemiluminescence Spectrum for Permanganate Oxidation of Glucose using a Wide-range PMT**



As can be seen in Figure 4.19 the maximum wavelength found using the extended range PMT is 40-50nm higher than the apparent maximum using the standard PMT.

**Figure 4.19 Comparison of Chemiluminescence Spectral Maxima for Permanganate Oxidation of Glucose using Standard and Wide-range PMT Using Gaussian Curves**



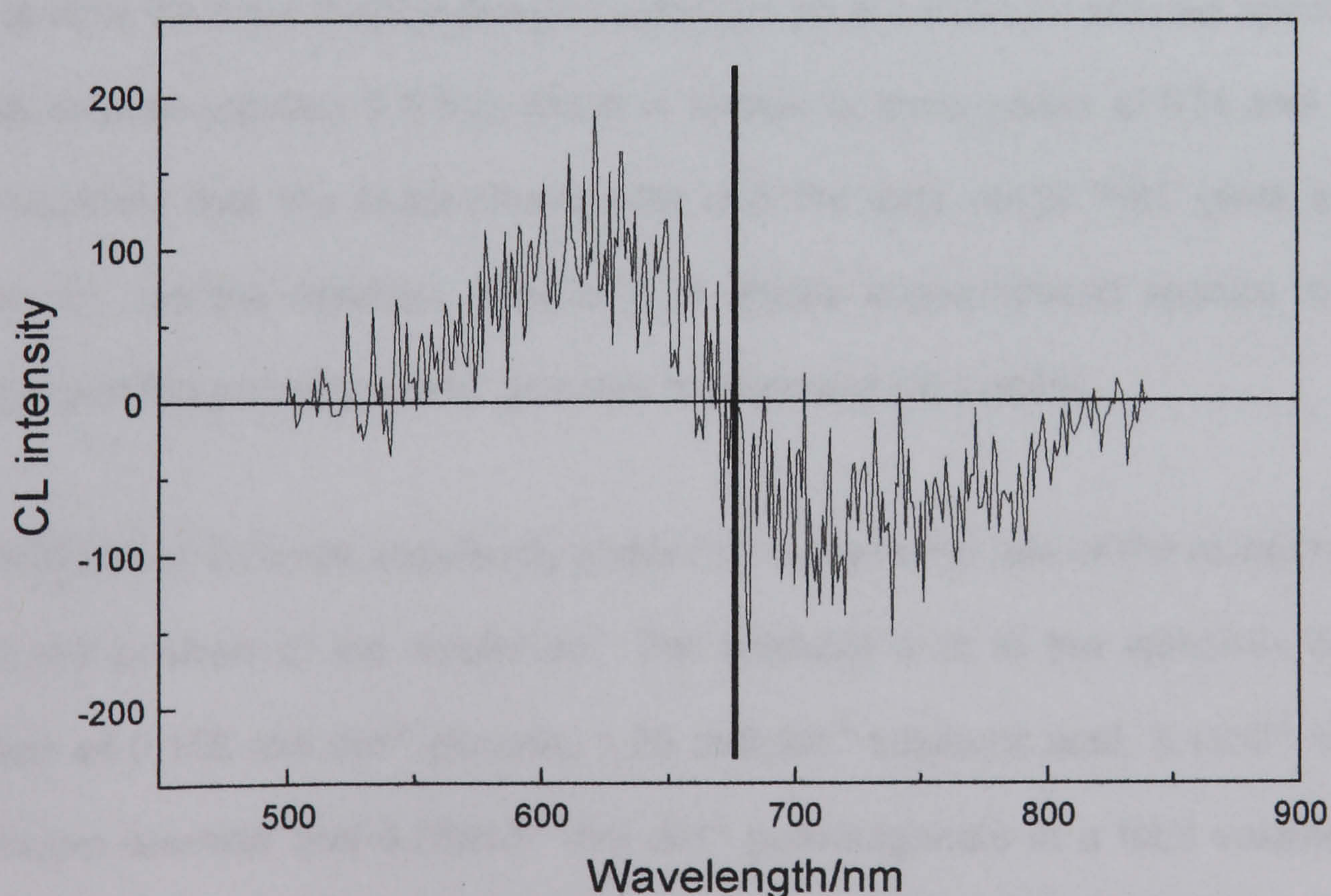
Glucose 0.1g sulphuric acid 0.5cm<sup>3</sup> 2 mol dm<sup>-3</sup> permanganate 0.1 cm<sup>3</sup> 0.1 mol dm<sup>-3</sup>



This probably explains the discrepancy between this work and the findings of other workers. If PMTs of different efficiencies at long wavelength are used, and instrumental response times are slow, considerable errors can be introduced into spectral measurements.

In most instances Gaussian fits were used to estimate  $\lambda_{\max}$ . Information on the bandwidth was also obtained using these fits. For asymmetrical bands the use of Gaussian fits to the whole data set could result in large differences between observed and calculated maxima. An alternative way of estimating the wavelength of the band maximum was to calculate the differential function of the data. Smoothed differential spectra were drawn using the spectrofluorimeter software, as shown in Figure 4.20. In this case the maximum wavelength from the Gaussian fit is nearly 30nm longer than estimated from the first derivative of the spectrum.

**Figure 4.20 First Derivative of Chemiluminescence Spectrum**

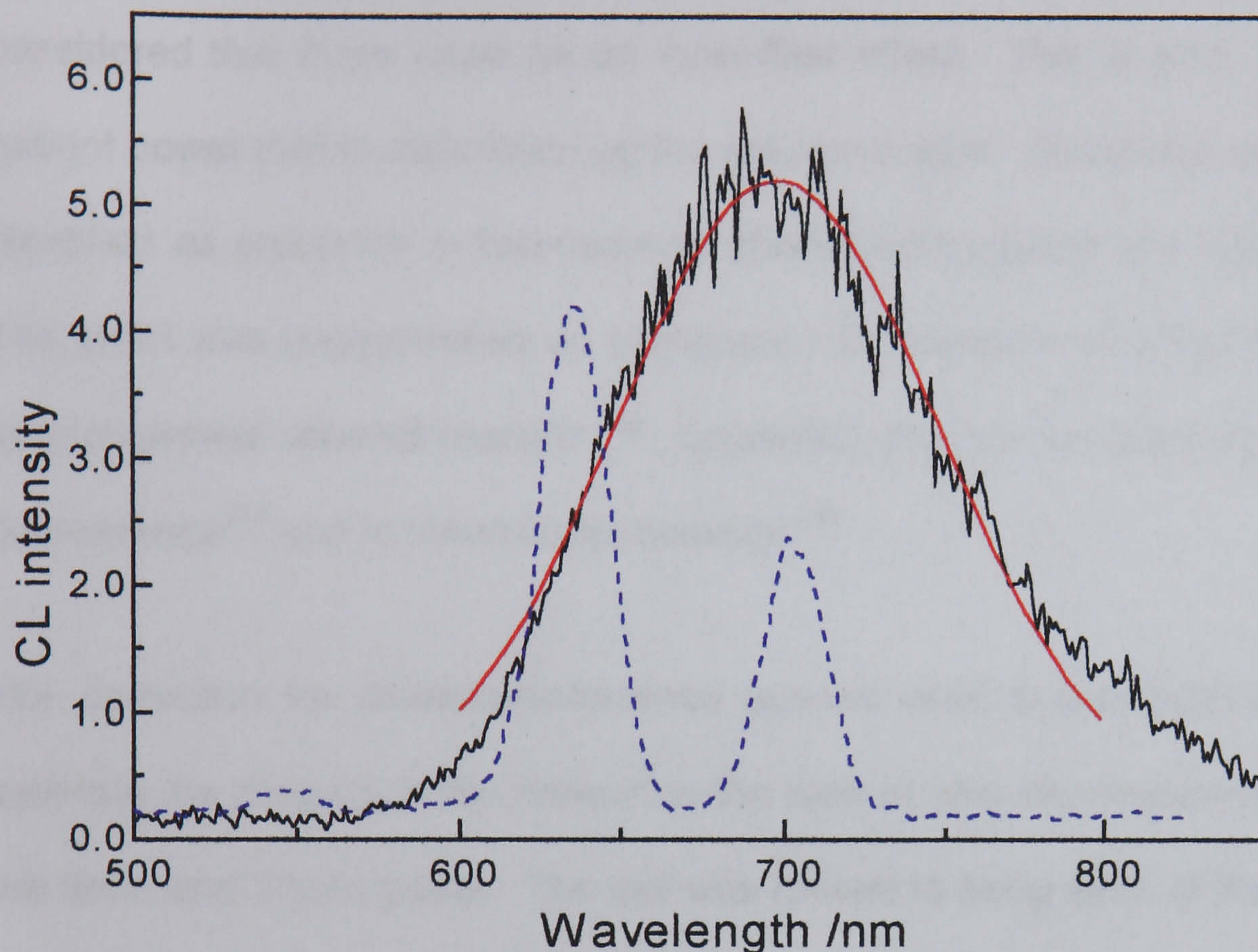


In addition to estimating  $\lambda_{\max}$ , derivatives of spectra can indicate other features such as hidden peaks. For a noisy spectrum, additional features are not readily observed.



Spectra generally had high noise levels and derivative spectra required considerable smoothing. Gaussian fitting was used unless secondary features were suspected.

**Figure 4.21 Comparison of Singlet Oxygen and Permanganate Spectra**



The spectra from the permanganate oxidations were compared with the spectrum for singlet oxygen (section 3.5.5.2) which is known to show peaks at 634 and 704nm. This confirms that the spectrofluorimeter with the long range PMT gives accurate values for spectral maxima. Figure 4.21 shows superimposed spectra of singlet oxygen and the permanganate/ glucose/ manganese (II) system.

The addition of bromide, previously shown to increase the rate of the reaction did not affect the position of the maximum. For example a fit to the spectrum from the reaction of  $0.156 \text{ mol dm}^{-3}$  glucose,  $1.25 \text{ mol dm}^{-3}$  sulphuric acid,  $3.1 \times 10^{-2} \text{ mol dm}^{-3}$  potassium bromide and  $6.25 \times 10^{-3} \text{ mol dm}^{-3}$  permanganate in a total volume of  $1.6 \text{ cm}^3$  using a moderate scan speed ( $12000 \text{ nm min}^{-1}$ ) gave the following parameters:  
 $\lambda_{\text{max}}$  704nm, band width 132 nm.



#### 4.2.4.2 Inner Filter Effect

As the emission from the permanganate reaction is in the red end of the spectrum, and both permanganate ion and manganese (III) absorb in this region, it was considered that there could be an inner-filter effect. This is attenuation of emitted radiant power due to absorption by the solution matrix. Inner filter effects have been identified as problems in fluorescence chemiluminescence and bioluminescence.<sup>233</sup> The effect was suggested as an explanation for variation of spectra with time in the permanganate/ ethanol reaction.<sup>160</sup> Correction procedures have been proposed for fluorescence<sup>234</sup> and for chemiluminescence.<sup>235</sup>

The correction for chemiluminescence spectra used a dual pathlength flowcell to estimate the magnitude by measuring the ratio of chemiluminescence intensity from the 5mm and 10mm paths. The cell was moved to bring each of the two light paths into line with a collimated monochromatic optical system at a frequency of 2 Hz. The two intensities were measured at different wavelengths. It was reported that the system could be used to correct spectra from apparently quenched reactions.

The ratio of intensity R is related to the absorbance by the expression:

$$R (\text{ratio of intensity}) = P_{b'}/P_b = (1 - e^{-2.303\epsilon b'c}) / (1 - e^{-2.303\epsilon bc})$$

Where  $b'$  and  $b$  are the two path lengths such that  $b' < b$ ,  $P_{b'}$  and  $P_b$  are the respective radiant powers,  $c$  is concentration and  $\epsilon$  is the molar absorptivity.

It was considered unlikely that permanganate ion would cause an inner filter effect, as the emission maximum is at a longer wavelength than the absorbance bands for permanganate at 525 and 545nm. Colloidal manganese dioxide could be formed during the reaction which has a broad absorbance profile extending into the red end of the spectrum.



A possible inner-filter effect was investigated for the galactose/ sulphuric acid/ permangante system. Chemiluminescence intensities were compared using 0.2 and 1cm pathlength cuvettes. If reabsorbtion of light is absent, or negligible, the intensity of light from 10mm should be five times that for the 2mm. It would be expected that any effect would be more marked for shorter than for longer wavelengths as any overlap between the absorbance and emission spectra would be greatest. Three wavelengths were used; the observed emission maximum of 700nm and points 50nm above and below this. At wavelengths around the maximum absorbance of permangante ion, 545nm, no emission was seen. Peak areas were measured for the three wavelengths and the two path lengths, 10mm and 2mm; replicate measurements were made at each point.

**Table 4.16 Relative Chemiluminescence Intensity for 1cm and 0.2cm Path lengths**

$\lambda$ /nm	Long path		Short path		Ratio
	Area	$\pm$	Area	$\pm$	
650	13247.98	532.05	2404.64	90.23	5.51
700	19374.19	777.94	3605.19	179.49	5.37
750	11226.30	478.17	2144.27	142.61	5.24

Table 4.16 shows the mean results for the areas and the ratios for each wavelength. The ratio was found to be greater than 5 at each point, possibly due to internal reflection from the back face of the cuvette. No inner filter effect was evident.

#### 4.2.5 Investigation of Phosphate Effects on Spectral Characteristics

Addition of high levels of phosphate to the batch glucose/ permanganate/ sulphuric acid reaction mixture prevented the oxidation reaction. This was shown by the persistence of the purple colour of permanganate, even after considerable periods.

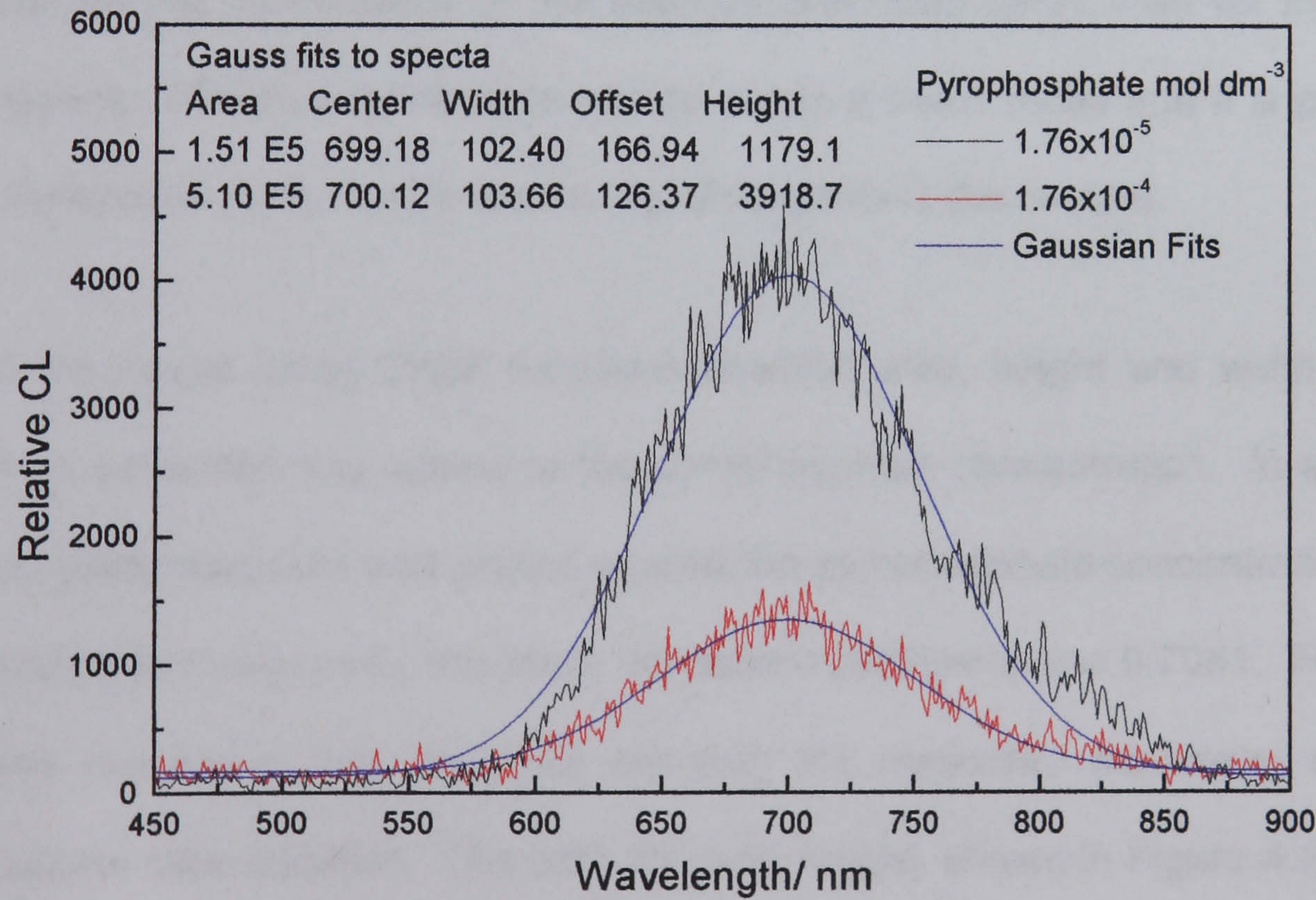
From FIA studies it had been shown that the presence of phosphate in the acid or sugar solutions resulted in a decrease in chemiluminescence. Many workers have



reported increased luminescence in the presence of phosphates, for example in assays for morphine.<sup>163,164</sup> It was decided to investigate the effect on the time course of the sugar/ permanganate reaction. Previous workers have used polyphosphates which have variable composition therefore pyrophosphate was selected as it was readily available and of known composition. Fructose was used as the model sugar due to the high signals observed even in the absence of added manganese (II)

Concentrations of pyrophosphate in the range  $4 \times 10^{-5}$  to  $4 \times 10^{-4}$  mol dm<sup>-3</sup>, in the sulphuric acid solution, were used. As expected the reaction was slower in the presence of pyrophosphate and the total light emitted decreased. The spectra were unchanged from those for the reaction in the absence of phosphate, as shown in Figure 4.22. Chemiluminescence was measured at maximum emission, 700nm.

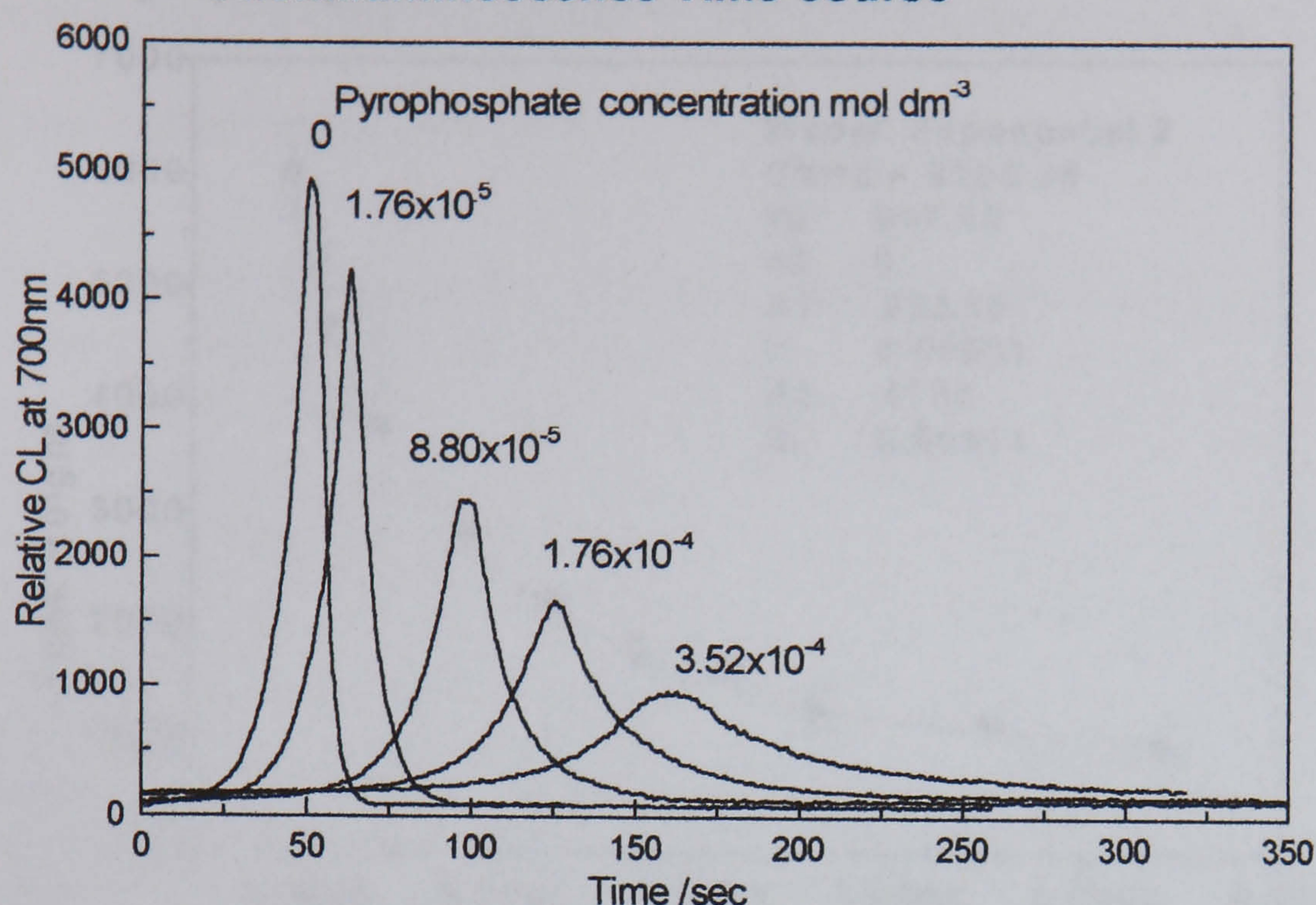
**Figure 4.22 Spectra for the Reaction of Fructose with acid Permanganate in the Presence of Pyrophosphate**



As expected, an increase in pyrophosphate concentration resulted in a slower reaction. Examples of average runs are shown in Figure 4.23.



**Figure 4.23 Effect of Pyrophosphate on Chemiluminescence Time-course**

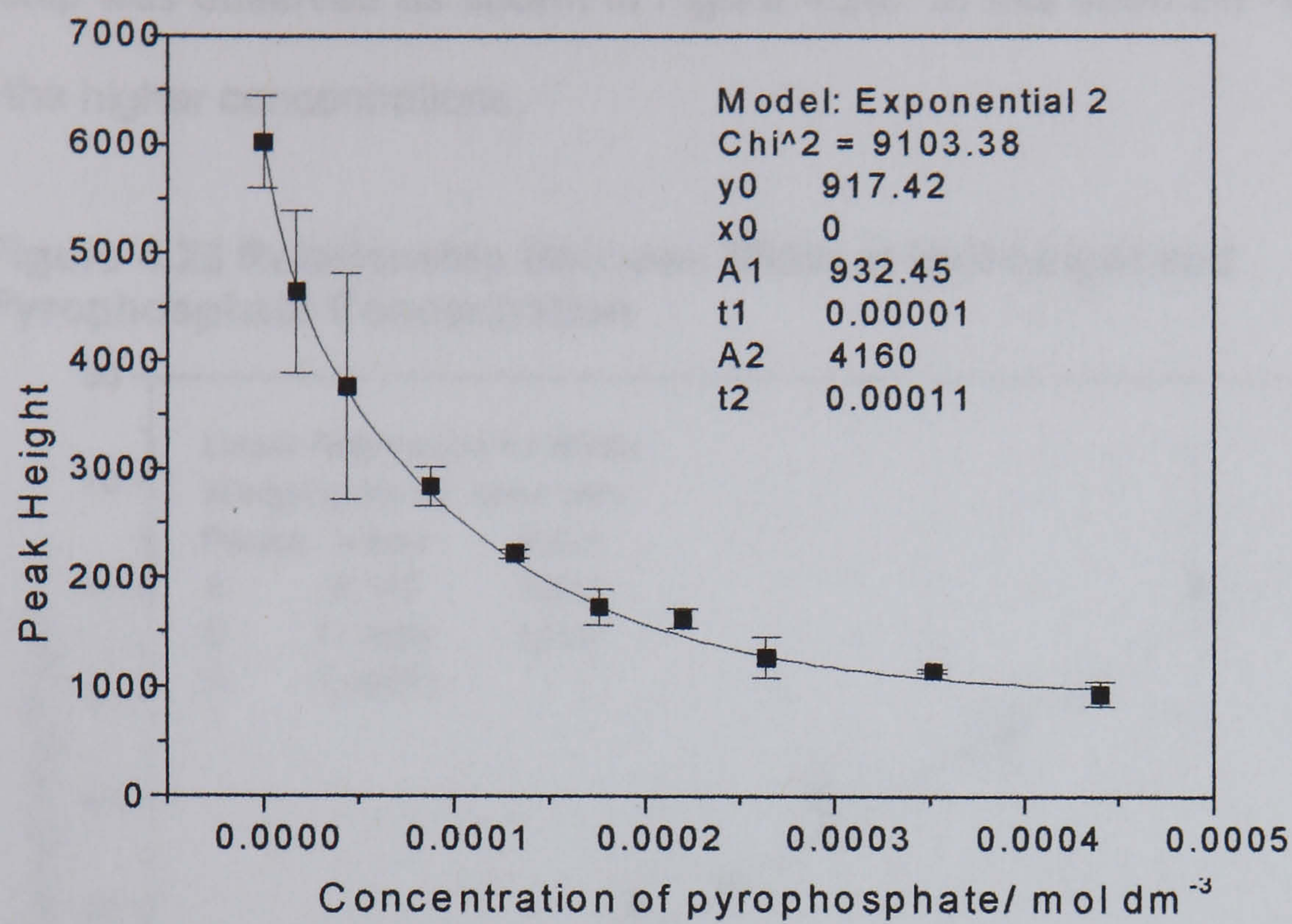


Only a limited range of phosphate concentrations could be run, as at high concentration the reaction profile was very broad and low. For the higher phosphate concentrations the repeatability of the determination was better than for the lower concentrations. Measurements were carried out in a batch mode and it is probable that the variation is partly due to the mixing of reagents in the cuvette.

Fitting of the peaks using Origin functions enabled area, height and width at half height to be estimated and related to the pyrophosphate concentration. In addition, the time to peak maximum was plotted against the pyrophosphate concentration. For area the correlation was poor, the linear regression coefficient was 0.7061. For other parameters correlation was observed between the measured parameter and the pyrophosphate concentration. The data for peak height, shown in Figure 4.24, fitted closely to a second order exponential decay. The large errors are due to mixing.

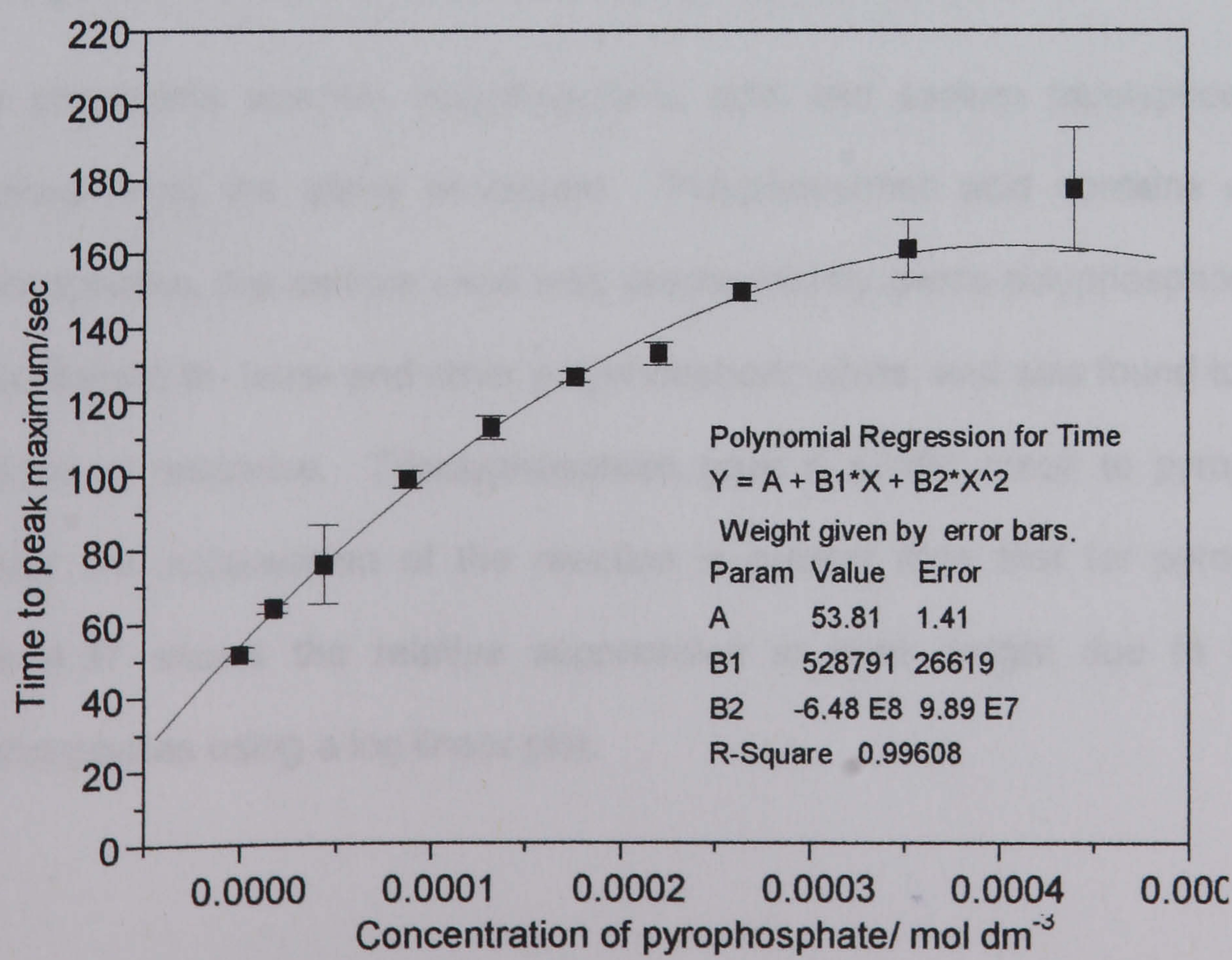


**Figure 4.24 Relationship Between Peak height and Pyrophosphate Concentration**



The time required to reach the peak maximum also shows a non-linear relationship with the pyrophosphate concentration, which fits to a second order polynomial as shown in Figure 4.25.

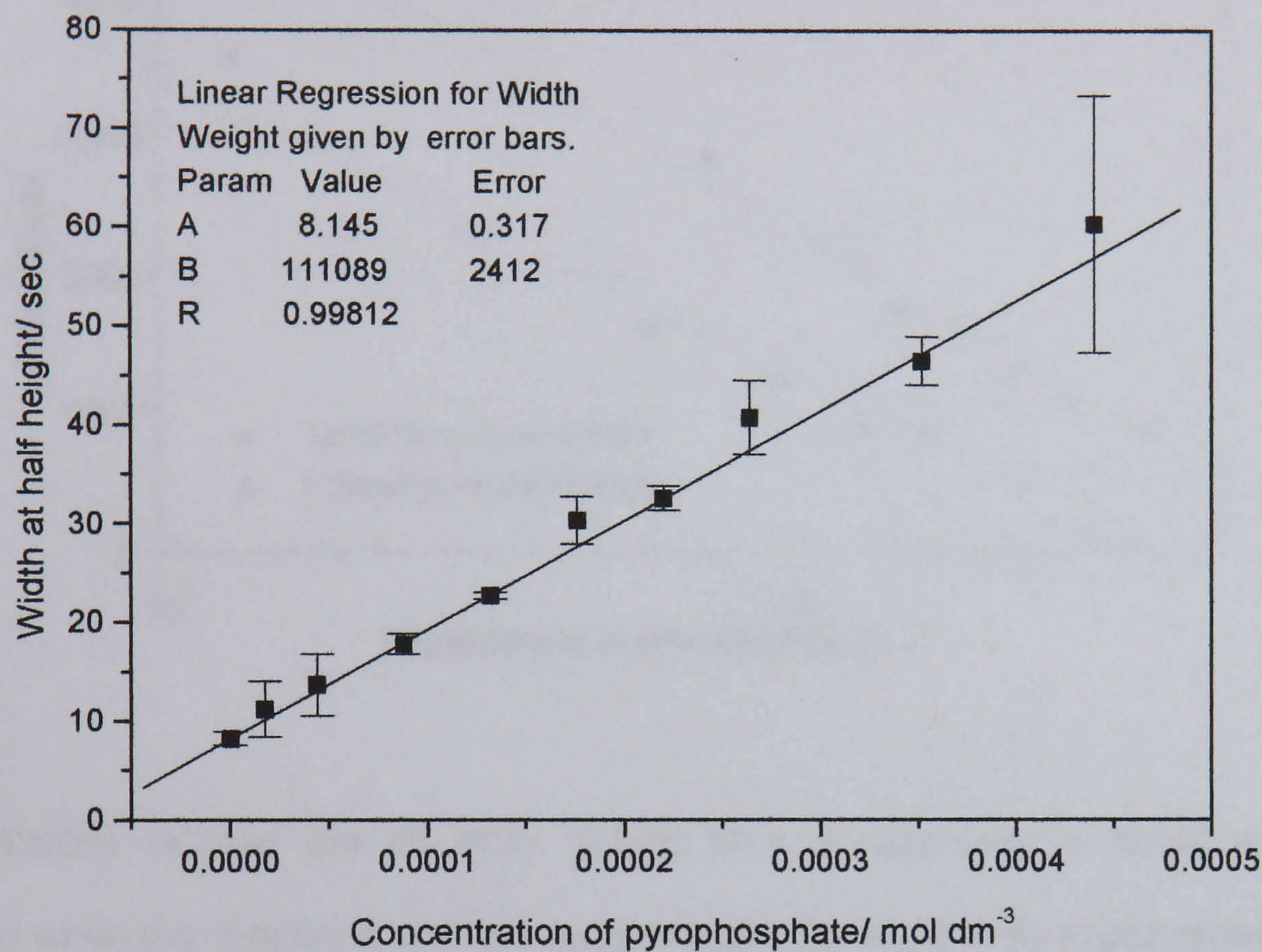
**Figure 4.25 Relationship Between Time to Reach Peak Maximum and Pyrophosphate Concentration**





The final parameter examined was width at half height. In this case a linear relationship was observed as shown in Figure 4.26. In this case the repeatability is poor at the higher concentrations.

**Figure 4.26 Relationship Between Width at Half-height and Pyrophosphate Concentration**

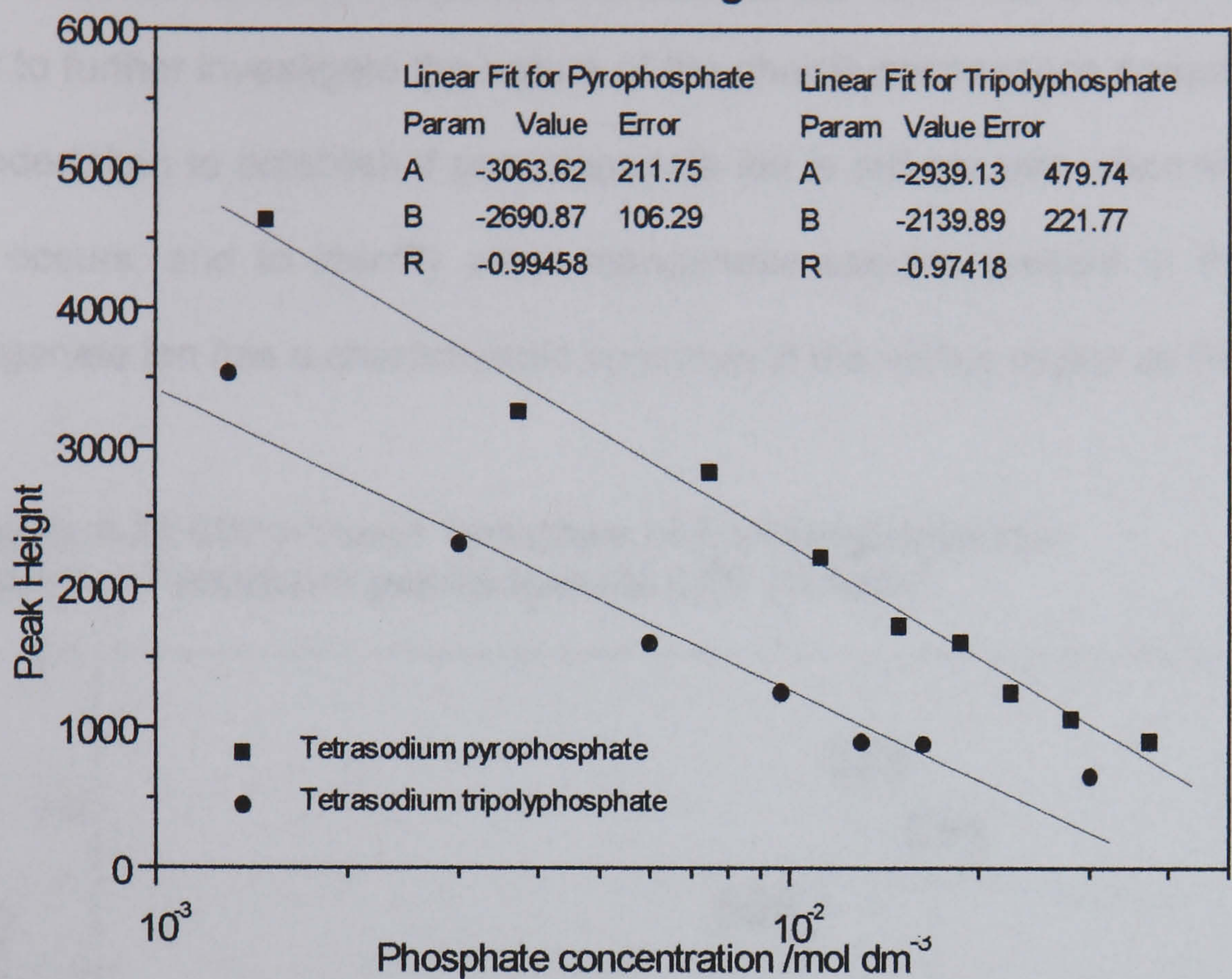


These relationships indicate the potential use of the inhibition of the sugar permanganate reaction in determination of phosphate concentrations.

Other phosphate species, polyphosphoric acid and sodium tripolyphosphate were examined using the same procedure. Polyphosphoric acid contains a range of polyphosphates, the sample used was predominantly penta-polyphosphoric acid but also contained tri- tetra- and other polyphosphoric acids, and was found to give large variations in response. Tripolyphosphate gave a similar result to pyrophosphate, however the suppression of the reaction is greater than that for pyrophosphate. Figure 4.27 shows the relative suppression in peak height due to tripoly and pyrophosphates using a log linear plot.



**Figure 4.27 Log-linear plot Showing the Effect of Phosphate Concentration on Glucose Permanganate Chemiluminescence**



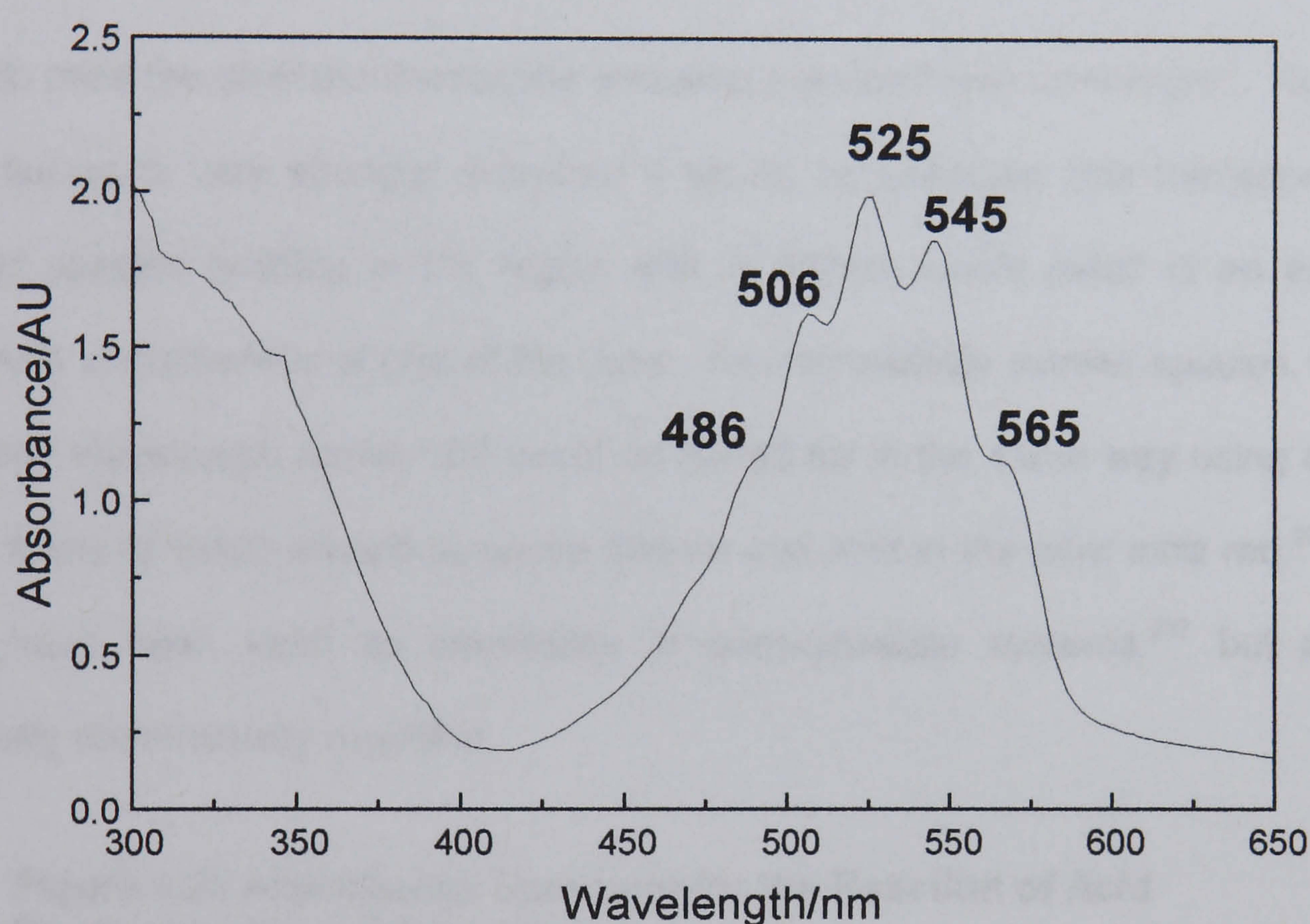
The reactions studied are all slow, taking tens of seconds to reach maximum, emission while the reactions with the compounds investigated by many other workers are fast. Pyro and polyphospates affect the reaction by stabilising manganese species, particularly manganese (III). The apparent enhancement of fast reactions may in fact be due to the phosphate slowing the reaction sufficiently to enable repeatable measurement in FIA systems. Little has been published about the rates of these reactions.



### 4.3 Investigation of Permanganate Reduction

In order to further investigate the nature of the chemiluminescence emission, studies were undertaken to establish if permanganate ion is still present when the emission of light occurs, and to identify other manganese species present in the reaction. Permanganate ion has a characteristic spectrum in the visible region as Figure 4.28.

**Figure 4.28 Absorbance Spectrum of Permanganate ion  
Aqueous Potassium permanganate 0.01 mol dm<sup>-3</sup>**



The emission maximum is at a longer wavelength than the absorbance bands for permanganate. The emitted light is not lost due to absorbance.

Fluorescence spectra were measured for the product of the permanganate reaction with a range of different carbohydrates; no fluorescence was observed at the 700nm for any excitation wavelength. An excited species can transfer energy, through non-radiative processes, to an accepting fluorophore which emits at its characteristic wavelength, as discussed in section 2 1.4. There is no indication that this happening in this reaction. If an original excited species, with a lower emission wavelength maximum was formed during the reaction, and not seen due to inner filter effect, it



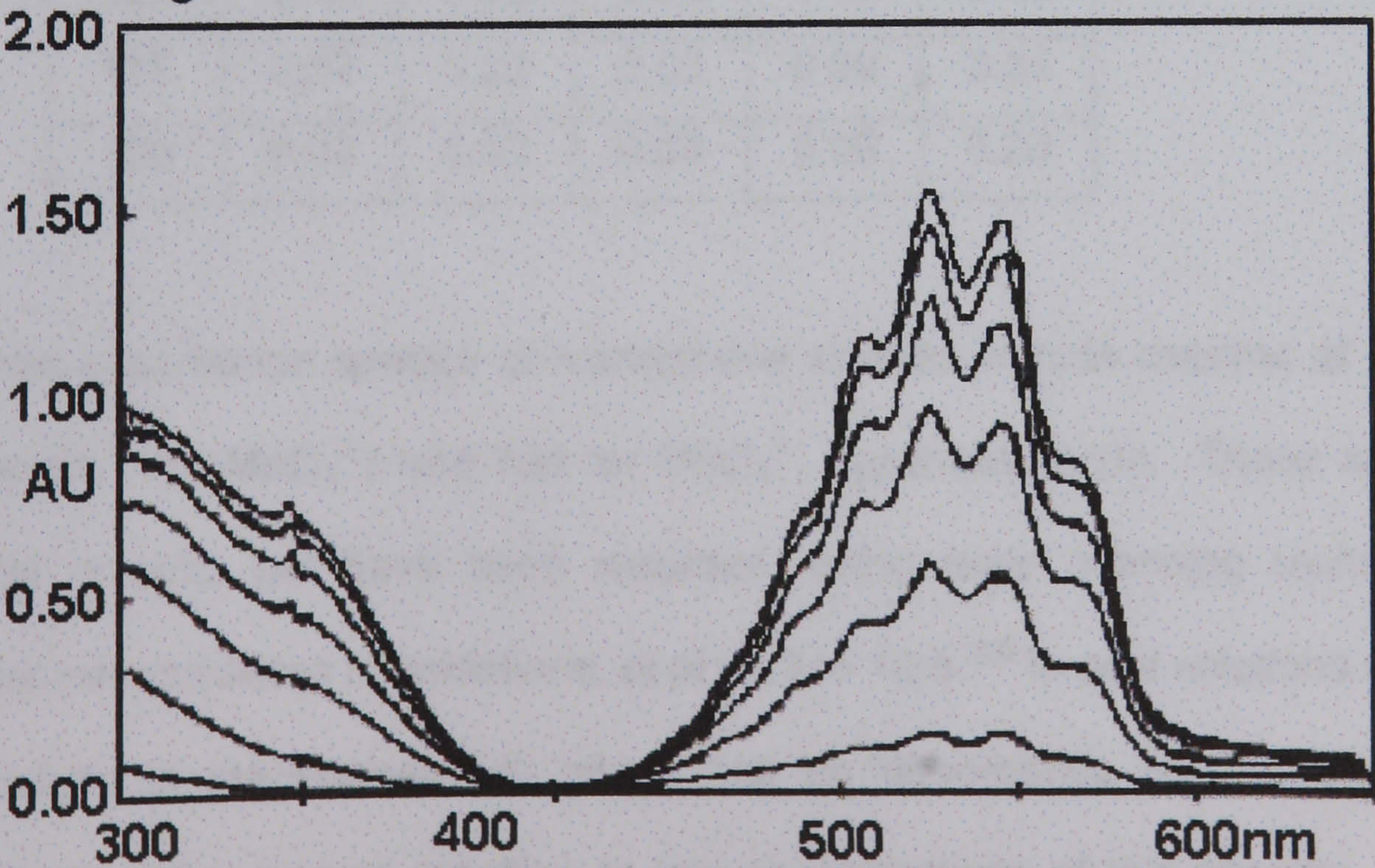
could transfer the energy to a suitable acceptor fluorophore. The use of rhodamine B as a sensitiser in permanganate chemiluminescence has been reported.<sup>178</sup> Fluorescent dyes, rhodamine B and fluorescein were added to permanganate/ glucose reactions. The excitation and emission maxima for are shown in Table 4.17.

**Table 4.17 Fluorescence Characteristics for Xanthene dyes**

Compound	$\lambda_{\text{max}}\text{Ex}$	$\lambda_{\text{max}}\text{Em}$
Fluorescein	450	525
Rhodamine B	510	585

In each case the chemiluminescence emission spectrum was unchanged. Xanthene dyes fluoresce very strongly; therefore it would be expected that formation of an excited species emitting in the region 400 to 550nm would result in an emission spectrum characteristic of one of the dyes. An intermediate excited species, with an emission wavelength above 550 could be tested for in the same way using cyanine dyes, many of which absorb at above 600nm and emit in the near infra red.<sup>236</sup> Such dyes have been used as sensitisers in peroxyoxalate systems,<sup>237</sup> but are not generally commercially available.

**Figure 4.29 Absorbance Spectrum for the Reaction of Acid Permanganate and Glucose**



Sulphuric acid 0.92mol dm<sup>-3</sup>, galactose 0.04 mol dm<sup>-3</sup>, permanganate 0.01 mol dm<sup>-3</sup>  
 Scans at 30 sec intervals



During the oxidation the permanganate spectrum can be seen to collapse uniformly over the range 500 to 650 as for the example of galactose in Figure 4.29.

Absorbance values for the collapse of the permanganate spectrum for a reaction mixture of sulphuric acid 0.92mol dm<sup>-3</sup>, glucose 0.1 mol dm<sup>-3</sup>, permanganate 0.01 mol dm<sup>-3</sup> and manganese sulphate 4x10<sup>-3</sup>, are shown in Table 4.18. For the three characteristic permanganate peaks 545, 525 and 506nm, there is a consistent decrease in absorbance. This suggests that no species which absorbs strongly in the range 500 to 545nm, other than permanganate ion, is being formed or removed.

**Table 4.18 Change of Absorbance with Time at Different Wavelengths Relative to Absorbance at 15 sec for Glucose/Permanganate/Manganese(II)**

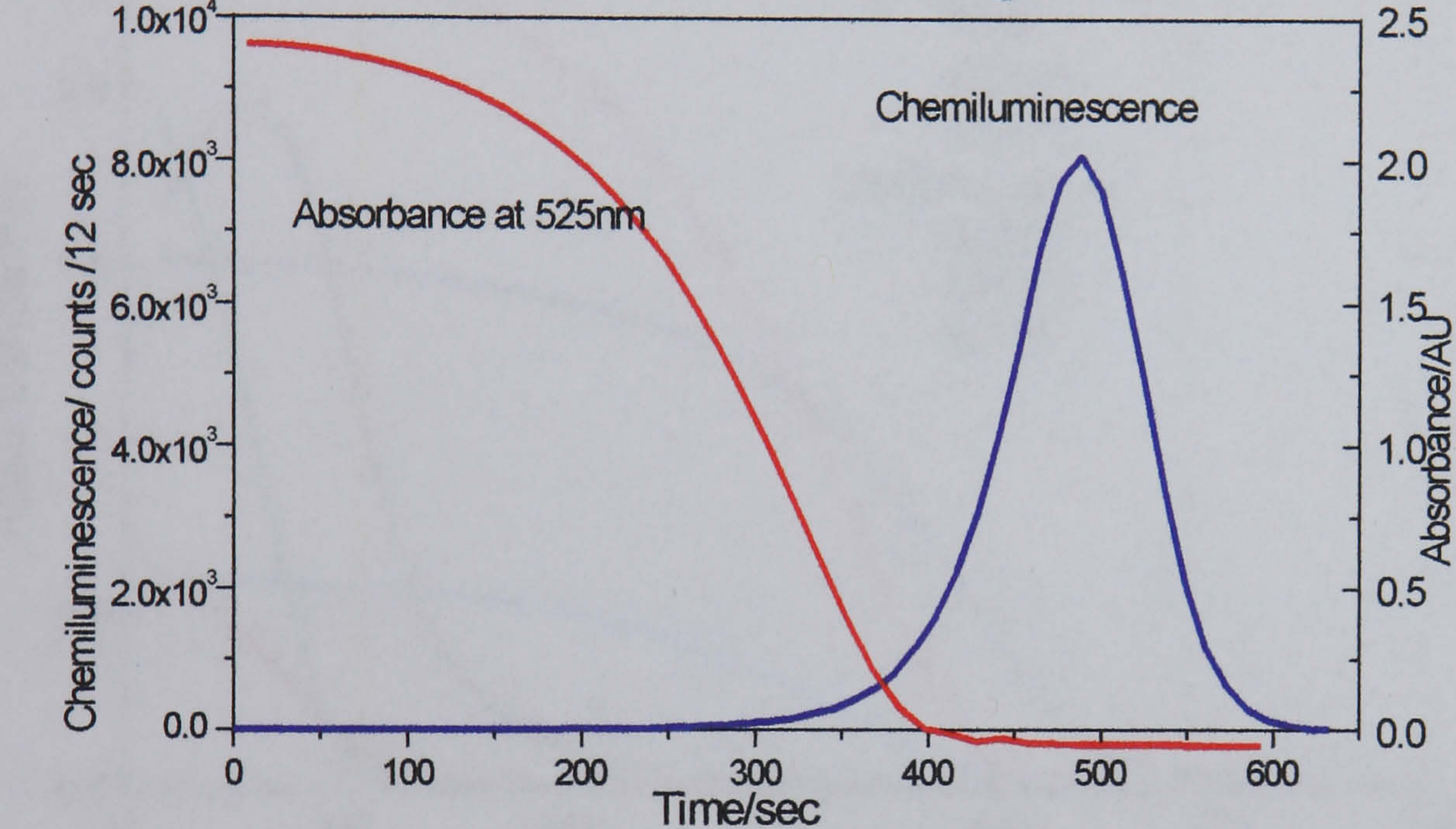
Time /sec	Wavelength/nm				
	545	525	506	475	450
15	1.00	1.00	1.00	1.00	1.00
30	0.89	0.87	0.87	0.92	1.01
45	0.71	0.68	0.68	0.78	1.00
60	0.46	0.43	0.45	0.60	0.95
75	0.22	0.21	0.23	0.41	0.81
90	0.07	0.08	0.10	0.26	0.61
105	0.03	0.04	0.06	0.17	0.42
120	0.02	0.03	0.04	0.12	0.30
135	0.02	0.02	0.03	0.09	0.24
150	0.02	0.02	0.03	0.08	0.20

Reported absorbance spectra of manganese species include maxima at 600nm for manganate (VI) (MnO<sub>4</sub><sup>2-</sup>) and 750 for MnO<sub>4</sub><sup>3-</sup>, hypomanganate. These species are unstable in acid, but have been recorded, using rapid scanning techniques, as transient intermediates in oxidations, at pH 9.3 to 12.5.<sup>238</sup> In acid solutions a probable intermediate is manganese (III) which has an absorbance maximum at 500nm. Disproportionation occurs resulting in low concentrations of this species. The final



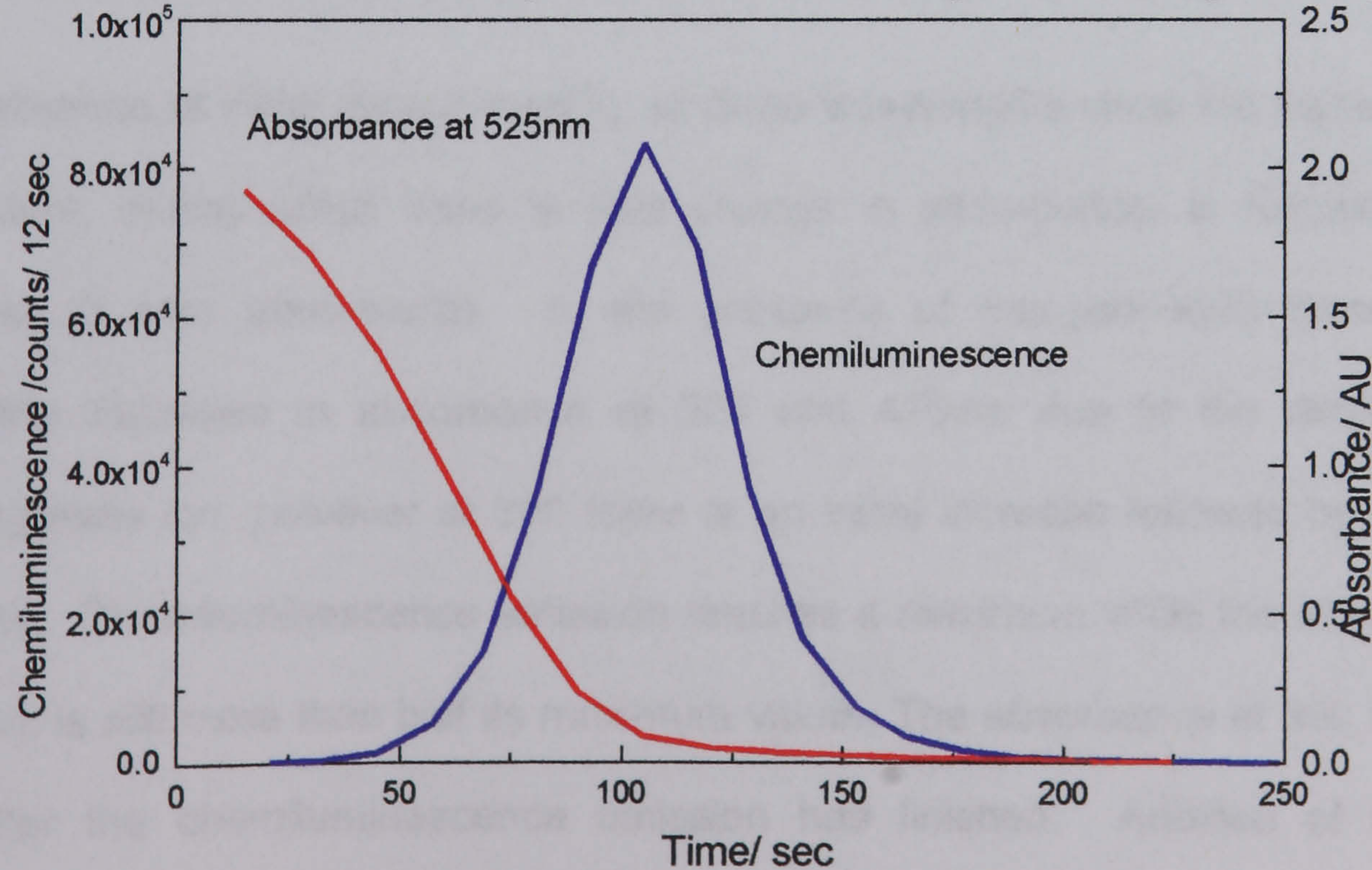
The final product of the reaction is manganese (II), which is very stable due to its  $3d^5$  configuration. The high spin hexaquo ion  $[\text{Mn}(\text{H}_2\text{O})_6]^{2+}$  is very pale pink and does not absorb significantly in the visible region. Using glucose as the model suga, the time course of emission was compared with the change in absorbance at 525, to follow the reduction of permanganate ion. The study was undertaken with and without the initial presence of manganese (II). The results are shown in Figures 4.30 and 4.31.

**Figure 4.30 Comparison of Absorbance and Chemiluminescence Time-course for Glucose/ Sulphuric acid/ Permanganate**



Sulphuric acid 1 dm<sup>-3</sup>, glucose 0.1 mol dm<sup>-3</sup>, permanganate 0.01 mol dm<sup>-3</sup>

**Figure 4.31 Comparison of Absorbance and Chemiluminescence Time courses for Glucose/ Sulphuric acid/ Permanganate/ Manganese (II)**

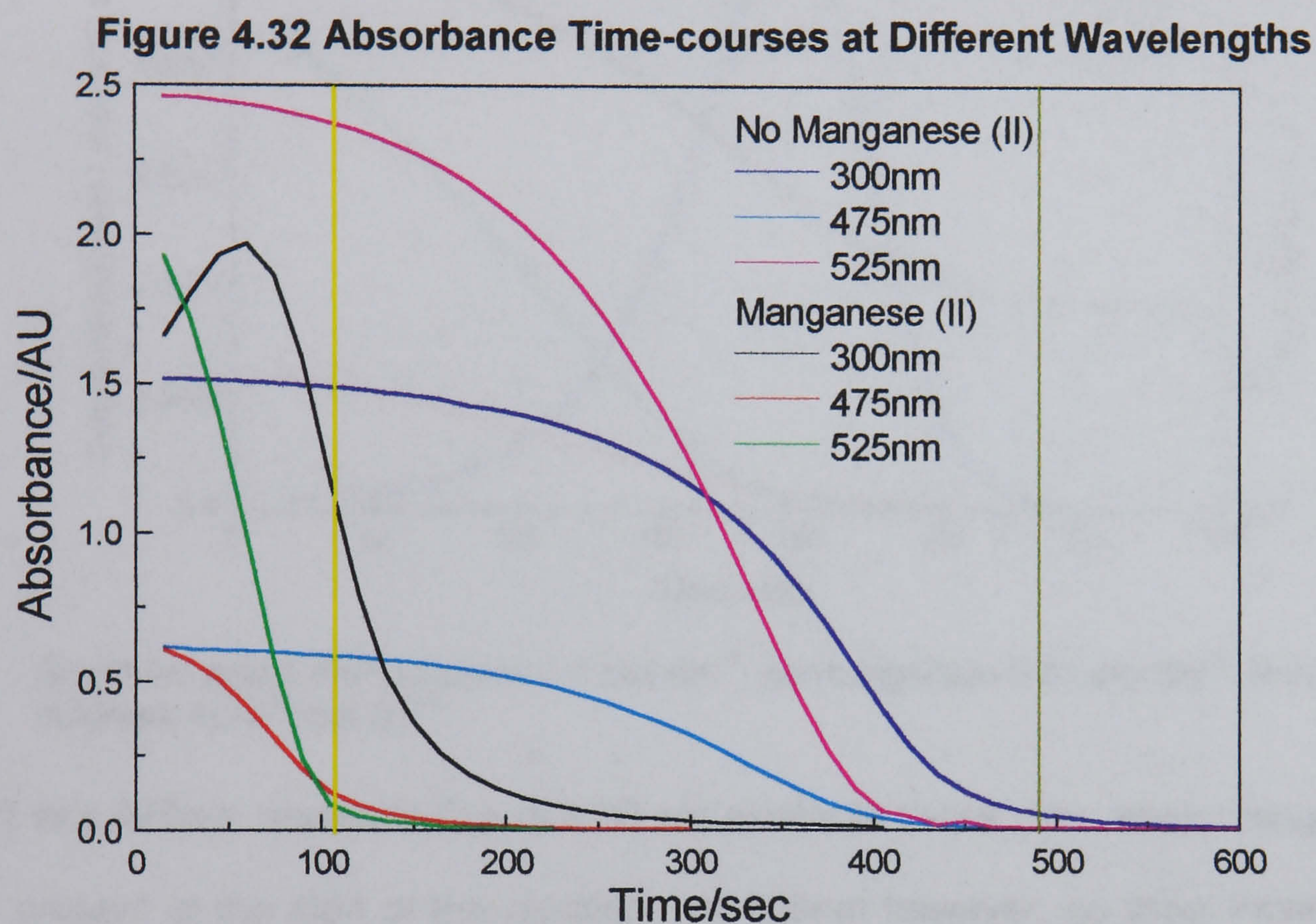


Sulphuric acid 0.92mol dm<sup>-3</sup>, glucose 0.1 mol dm<sup>-3</sup>, permanganate 0.01 mol dm<sup>-3</sup>  
manganese sulphate 4x10<sup>-3</sup> mol dm<sup>-3</sup>



The comparisons show that in the presence or absence of initial manganese (II) the emission of chemiluminescence takes place after most of the permanganate ion has been reduced. Earlier results showed that this is not due to internal filter effect.

Repeating the absorbance studies at different wavelengths, 525, 475 and 300nm, gave the time courses shown in Figure 4.32.



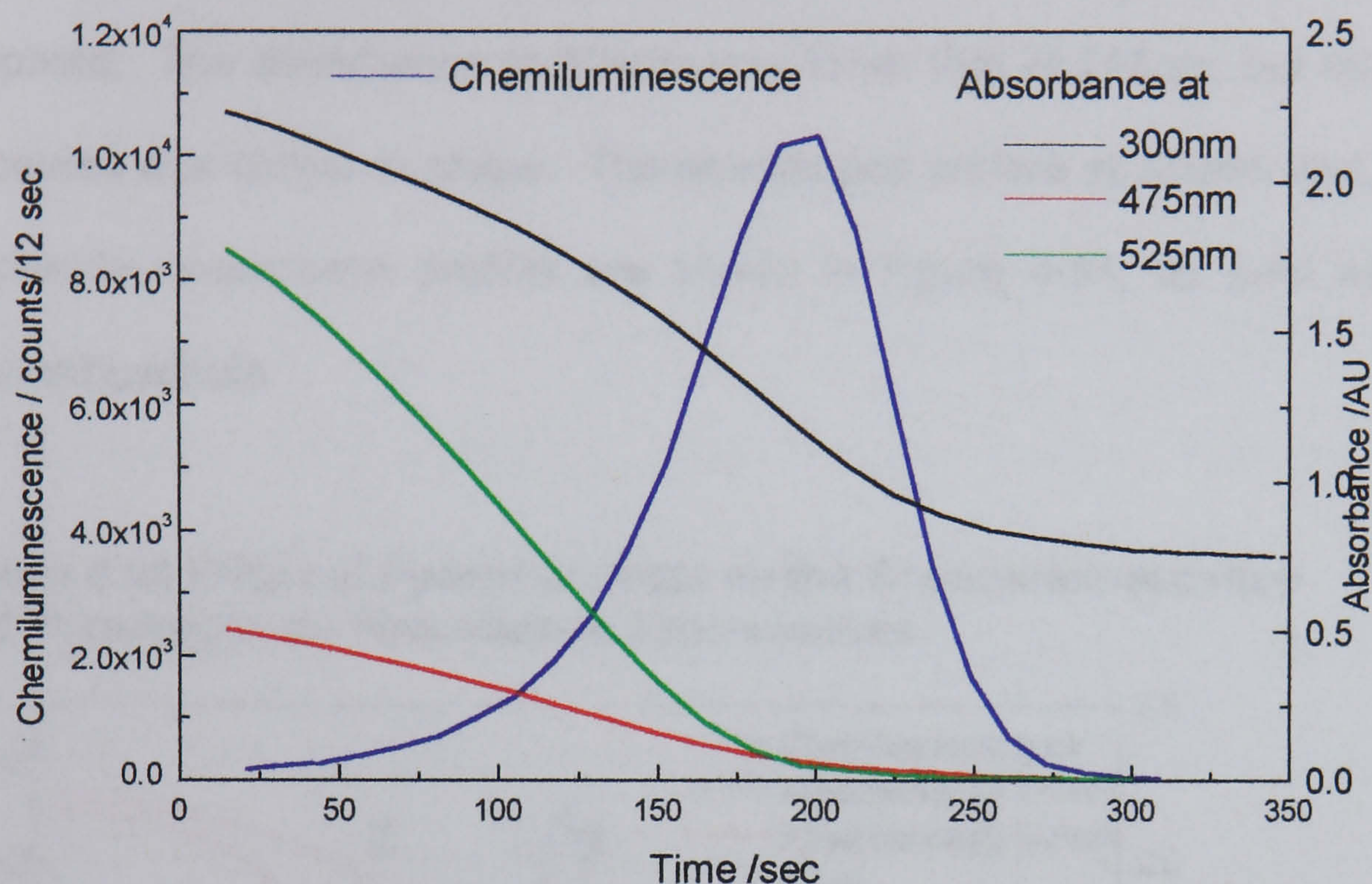
Concentrations as for figures 4.30 and 4.31, position of chemiluminescence maxima indicated by the vertical lines

In the absence of initial manganese(II), all three wavelengths show the same profile. A lag time, during which there is little change in absorbance, is followed by a decrease to zero absorbance. In the presence of manganese(II) there is an immediate decrease in absorbance at 525 and 475nm due to the decrease in permanganate ion, however at 300 there is an initial increase followed by a sharp decrease. Chemiluminescence emission reaches a maximum while the absorbance at 300nm is still more than half its maximum value. The absorbance at 300 reaches zero after the chemiluminescence emission has finished. Addition of iron (II) sulphate to the reaction increases the rate of disappearance of permanganate and



chemiluminescence emission. There is a fast reduction of permanganate to manganese(II) which can then catalyse the reaction. The absorbance time courses

**Figure 4.33 Comparison of Absorbance and Chemiluminescence Time- courses for Glucose/Sulphuric acid/Permanganate /Iron(II)**



Sulphuric acid  $1 \text{ dm}^{-3}$ , glucose  $0.1 \text{ mol dm}^{-3}$ , permanganate  $0.01 \text{ mol dm}^{-3}$ , ferrous sulphate  $4 \times 10^{-5} \text{ mol dm}^{-3}$

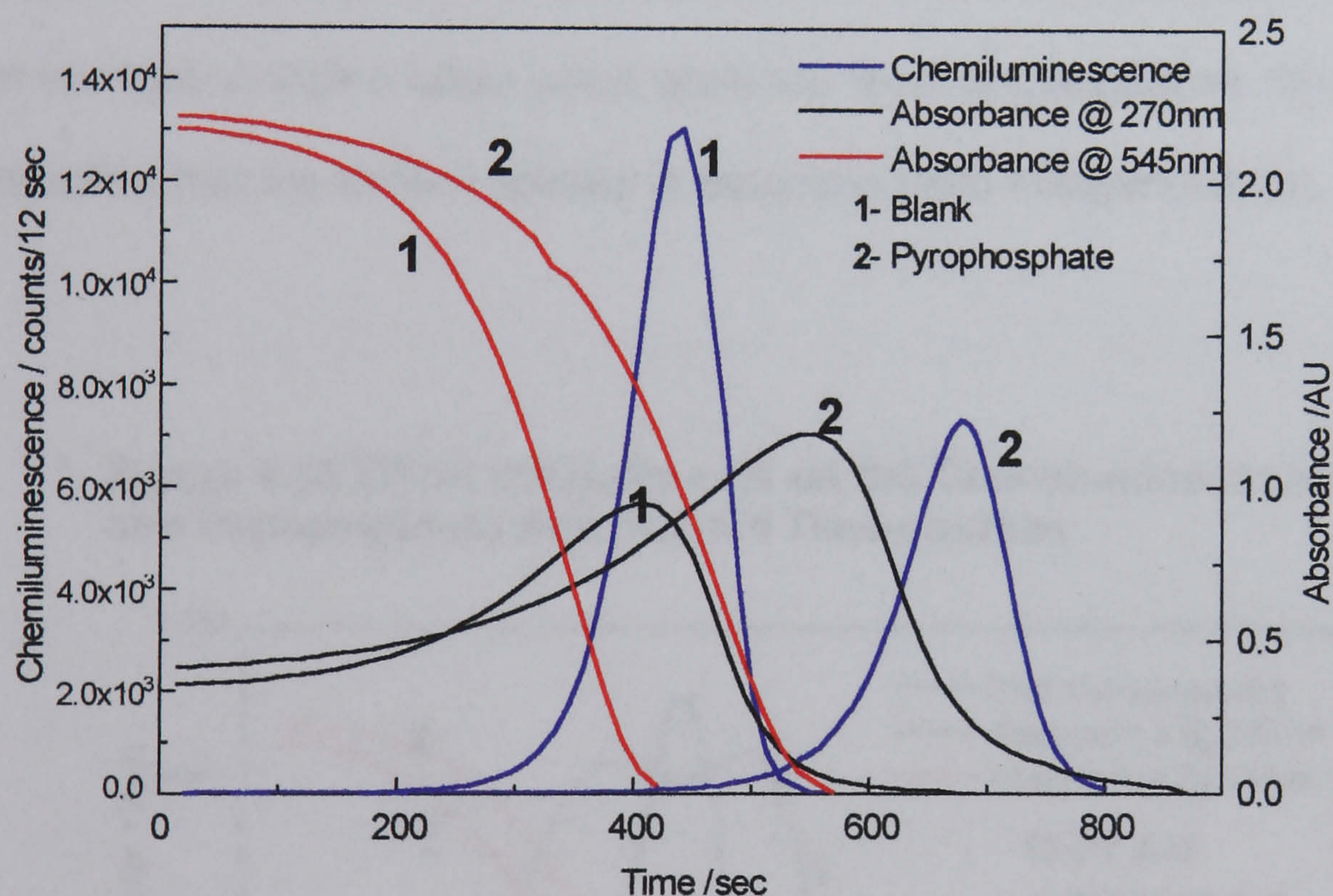
at 525 and 475nm, shown in Figure 4.33 are similar to those seen when manganese (II) is present at the start of the reaction. At 300nm however, no initial increase is seen and considerable absorbance is present after the light emission ceases, due to the presence of iron (III) complexes.

The most characteristic absorbance peak for manganese (III) is in the region of 500nm, depending on solvent. The molar absorptivity for this species is small compared with that for permanganate. It is therefore difficult to interpret absorbance changes at this wavelength. In the presence of manganese (II) an increase, due to manganese(III), can be observed at in the region of 300nm. In the absence of catalyst an isosbestic point appears to be present at 270nm during the early part of the reaction, therefore this wavelength was also monitored.



The addition of phosphates such as pyrophosphate results in an inhibition of the chemiluminescence, both in terms of the speed and the intensity of the emission. The generation of manganese (III) was followed at 270nm and 304nm and the loss of manganese (VII) was followed at 545nm as before, in the presence and absence of pyrophosphate. The absorbance at 304nm was lower than at 545nm, but otherwise the time course was similar in shape. The absorbance profiles at 270nm and 545nm and the chemiluminescence profiles are shown in Figure 4.34, for runs with and without pyrophosphate.

**Figure 4.34 Effect of Pyrophosphate on the Chemiluminescence and Permanganate Absorbance Time-courses**



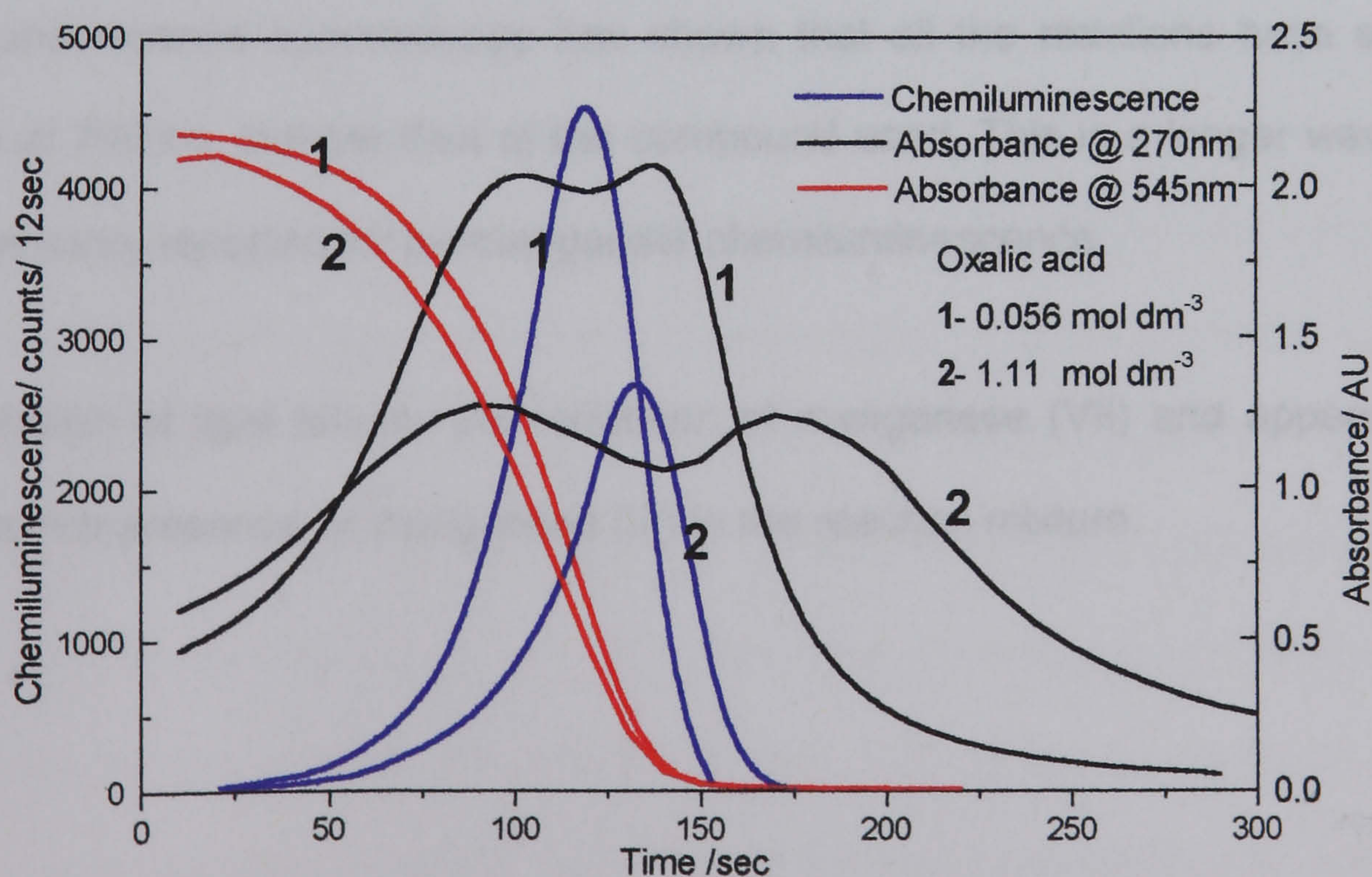
Chemiluminescence emission occurs after the majority of the permanganate has been reduced. Manganese (III) initially increases and the majority of the emission occurs while the level is at its highest. The stabilisation of manganese (III) by pyrophosphate is clear from the higher absorbance at 270nm. The emission takes place when the level of manganese (III) is high, strongly suggesting that a manganese (III) species is involved with the emitting species.



Another species known to form a complex with manganese (III), stabilising it in solution, is oxalate. A trioxalato complex  $\text{Mn}(\text{C}_2\text{O}_4)_3^{3-}$  is formed which is unstable to heat. Although chemiluminescence has been reported for the permanganate/oxalate reaction,<sup>122</sup> attempts to collect spectra were not successful. In the flow injection system, described above, oxalate was found to give one tenth of the peak height for glucose. The effect of oxalate on this system was investigated.

Oxalate increased the rate of reaction considerably, while inhibiting the chemiluminescence. Time profiles for two concentrations of oxalate are shown in Figure 4.35. At 304nm there were initially large increases in absorbance, followed by decreases to 0 AU after chemiluminescence emission was complete. It can be seen that the light emission takes place while the level of manganese (III) is high, again suggesting that the excited species is associated with manganese (III).

**Figure 4.35 Effect of Oxalic acid on the Chemiluminescence and Permanganate Absorbance Time-courses**





## 4.4 Summary

Investigations into the reaction between aliphatic polyhydroxy compounds and permanganate, in acid medium, have shown that the emitted chemiluminescence can be used analytically for their determination in solution.

The reactions are catalysed by the presence of manganese (II) and other reducing agents including iron (II) and halide ions. Only in the case of manganese (II) is there significant enhancement of the signal. The chemiluminescence intensity depends on the acid concentration, with sulphuric acid giving the highest signals.

The size of the chemiluminescent signal varies considerably with the nature of the polyhydroxy compound and appears to be related to the stereochemical configuration of the compound, in a way that is not yet fully understood.

For simple polyhydroxy compounds the trend shows an increase in chemiluminescence as the number of hydroxy groups increases.

Chemiluminescence spectroscopy has shown that all the reactions have emission maxima at 700nm, independent of the compound used. This is a longer wavelength than previously reported for permanganate chemiluminescence.

The emission of light follows the reduction of manganese (VII) and appears to be related to the presence of manganese (III) in the reaction mixture.



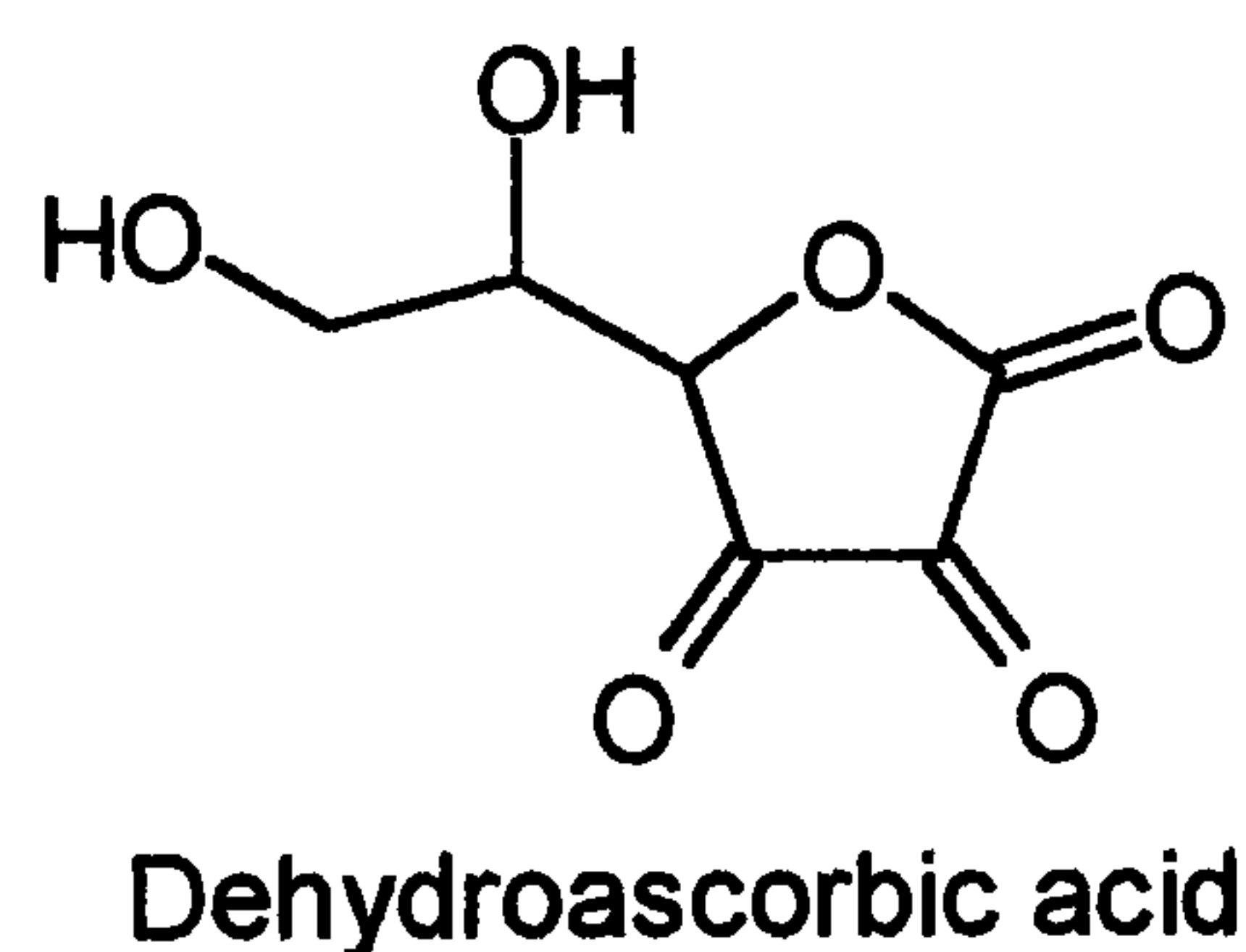
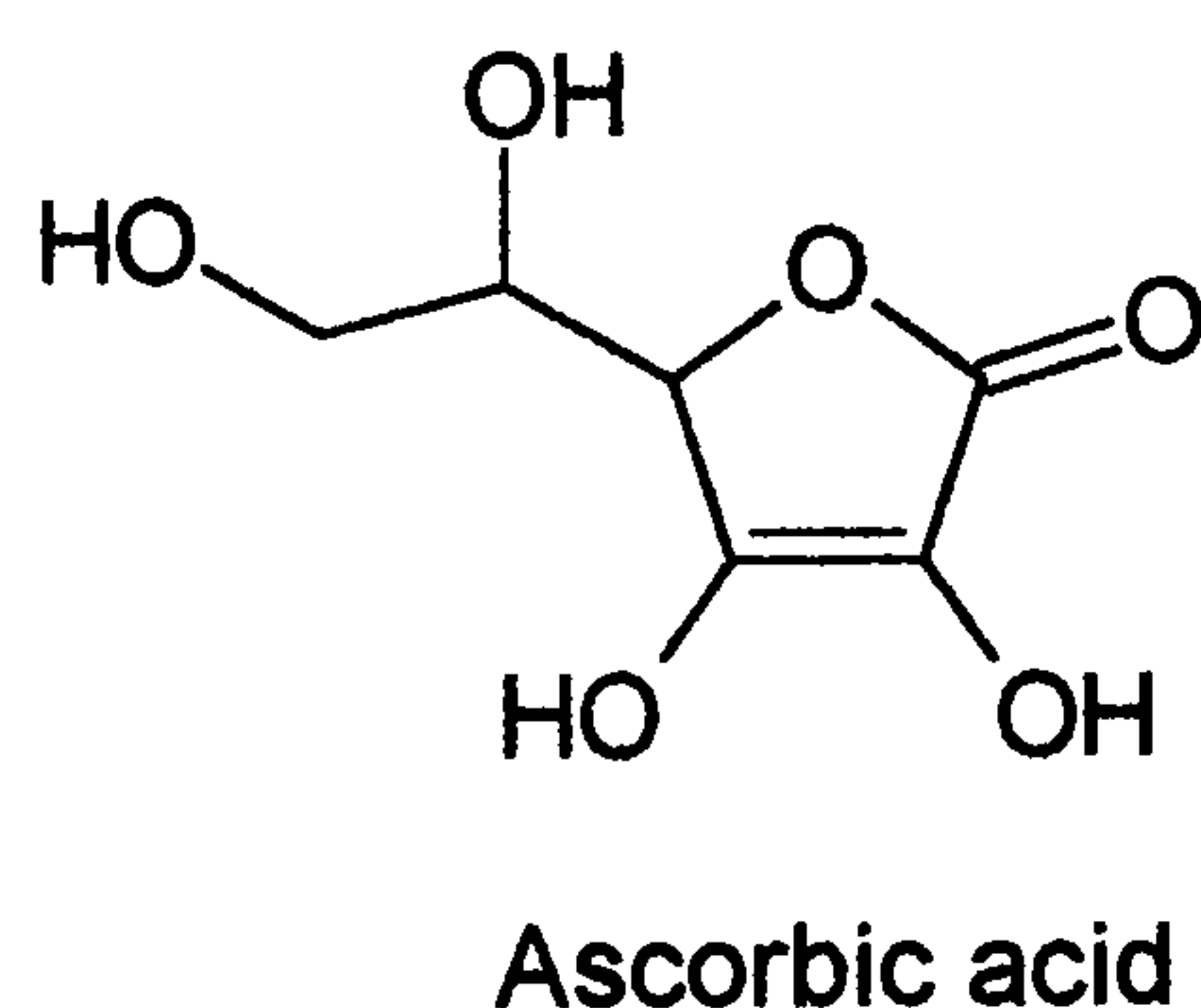
## CHAPTER 5

### DETERMINATION OF ASCORBIC ACID

#### 5.1 Determination of Ascorbic acid

Among compounds related to carbohydrates, it was found that the reaction of ascorbic acid with permanganate gave a more intense chemiluminescence than the carbohydrates already studied. It was decided to study this system in more detail, to optimise it and to investigate the application of the method to food supplements.

#### 5.2 Reasons for Determination of Ascorbic acid



Ascorbic acid (vitamin C) is a water-soluble anti-oxidant vitamin present naturally in a wide range of foods, particularly fruit and vegetables. It is an essential nutrient in mammals although most species can synthesise their own from glucose. In humans the absence of the enzyme L-gluconolactone oxidase means that sufficient Vitamin C must be obtained from the diet. The principal form of the vitamin is ascorbic acid; the first oxidation product, dehydro ascorbic acid has some physiological activity. Ascorbic acid has limited stability and is lost from foods during storage, preparation and cooking. Many foods are supplemented with the vitamin and nutritional supplements are available in which ascorbic acid is present alone or is formulated



with other micronutrients. Levels in supplements are from one, to many times the EU recommended daily allowance of 60mg for most individuals. It has been suggested that higher intakes can be beneficial in preventing and treating a range of diseases<sup>239</sup> and intakes of the order of several grams per day have been suggested.<sup>240 241</sup> Other workers consider that the high levels could be harmful.<sup>242</sup>

Ascorbic acid is used as an anti-microbial and antioxidant in foods and beverages, as an alternative to, or in conjunction with, nitrite or sulphite. Ascorbate is added to flour as an improver in breadmaking<sup>243</sup> in the widely used Chorleywood Bread Process (CBP). In this process ascorbic acid is oxidised to dehydroascorbic by the action of ascorbic acid oxidase, naturally present in flour. Dehydroascorbic acid oxidises glutathione to a dimeric form, which is inactive in the gluten disulphide exchange reactions of gluten development.

### 5.3 Methods of Determination

Ascorbic acid has been determined by a variety of methods, many based on its oxidation. Tillman's reagent, 2,6-Dichlorophenolindophenol is the most commonly used, in titrimetric<sup>220</sup> and spectrophotometric methods. Rate measurement using a stopped-flow method has also been described.<sup>244</sup> Direct titration is widely used for a range of foods but is subject to interference from reducing species such as sulphite.

A more specific method was developed by Deutch.<sup>221</sup> Ascorbic acid is oxidised to dehydroascorbic by atmospheric oxygen and an activated charcoal catalyst. Derivatisation of dehydroascorbic acid with o-phenylene diamine gives a fluorescent product. This method has been automated using a segmented flow system.

Flow injection systems have used spectrophotometric measurement after reaction with iodine<sup>245</sup> or the reduction of  $\text{Fe}^{3+}$  and formation of Prussian Blue.<sup>246</sup> Other



detection systems described recently have included amperometry<sup>247</sup> and potentiometry.<sup>248</sup> Methods using luminol chemiluminescence have been proposed, using oxidants including iron (III)<sup>249</sup> and hexacyanoferrate(III).<sup>250</sup> The reactions of ascorbic acid with many oxidising agents have high enthalpy changes. Reactions with iodine monochloride<sup>251</sup> and cerium (IV)<sup>252</sup> are used in thermometric methods

Permanganate is used as a titrimetric reagent for determination of ascorbic acid using both visual and potentiometric endpoints.<sup>253</sup> This reaction has been shown to give direct chemiluminescence. Since starting this study a batch method based on this has been reported.<sup>161</sup>

## **5.4 Development of a Flow Injection-Chemiluminescence Assay**

Initial investigations were made using a single line manifold (Manifold 1 section 4.3.2.1). To achieve the required flow rates the flow from two pump tubes, each pumping the same solution, was combined before the sample was injected.

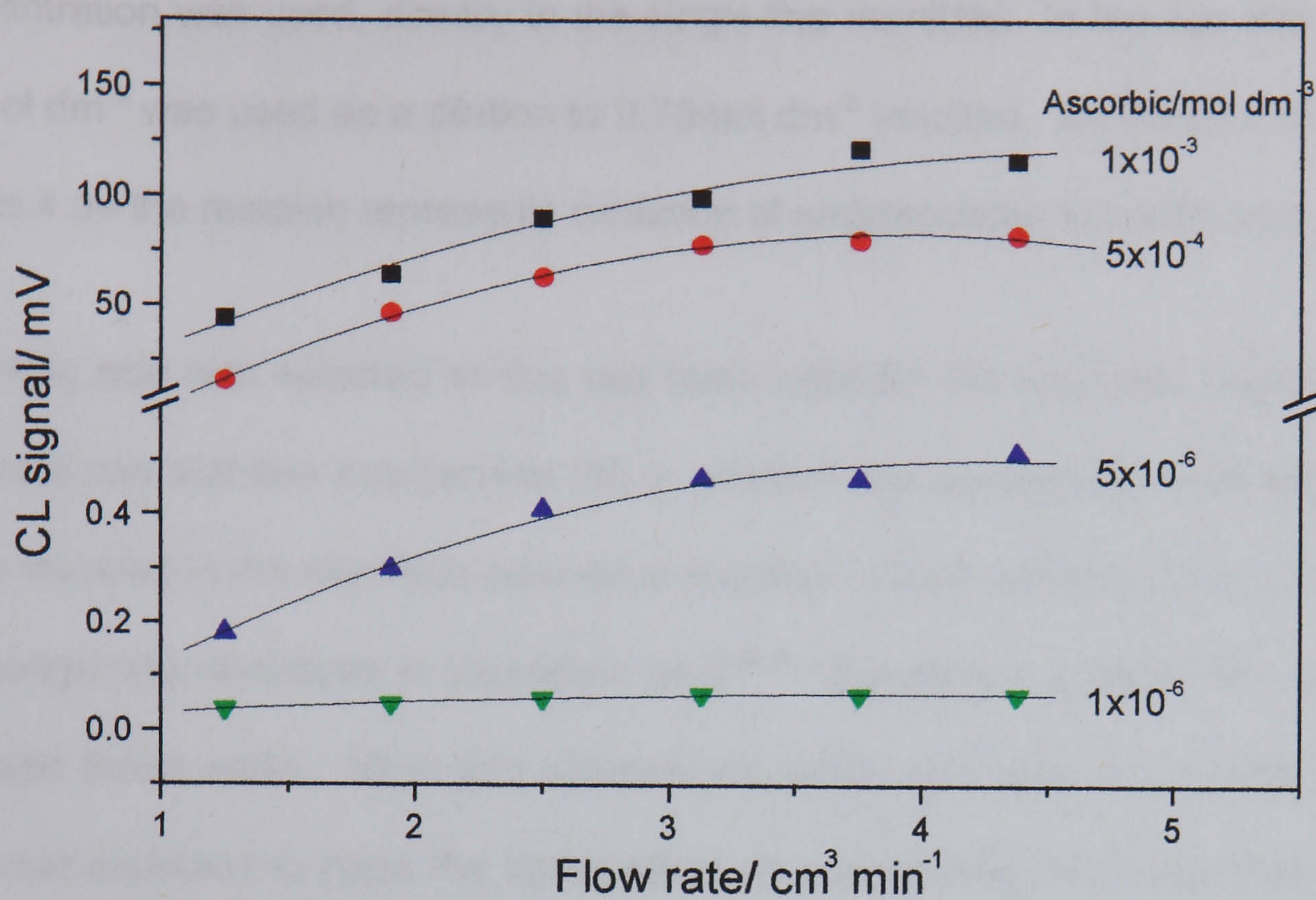
### **5.4.1 Optimisation of Flow-rate**

The reaction was found to be fast. The effect of flow rate was examined for an analyte range of  $1 \times 10^{-6}$  to  $5 \times 10^{-4}$  mol dm<sup>-3</sup> and  $1 \times 10^{-4}$  mol dm<sup>-3</sup> permanganate. The results are shown in Figure 5.1. The signal increased with increasing flow rate. At low ascorbic concentration the signal continued to increase up to the point where problems were found with leaking joints in the manifold. At higher ascorbic concentrations the optimum flow rate was found to be 4 cm<sup>3</sup> min<sup>-1</sup>.

At slow flow rates double peaks were observed for the  $1 \times 10^{-3}$  mol dm<sup>-3</sup> ascorbic acid. This shows that no reaction is occurring in the centre of the injected volume of 75 μL. At the higher flow rate single peaks were observed.



**Figure 5.1 The Effect of Flow Rate on CL Signal**



Ascorbic acid concentrations as shown permanganate  $1 \times 10^{-4} \text{ mol dm}^{-3}$

#### 5.4.2 Optimisation of Acid Concentration

Using  $2 \times 10^{-4} \text{ mol dm}^{-3}$  permanganate, calibration lines were run for ascorbic acid in the range  $1 \times 10^{-6}$  to  $1 \times 10^{-4} \text{ mol dm}^{-3}$ . The acid concentration varied from 0.1 to  $1.25 \text{ mol dm}^{-3}$ . Higher acid concentration gave in a higher signal as in Table 5.1:

**Table 5.1 Effect of Sulphuric Acid Concentration on CL Signal**

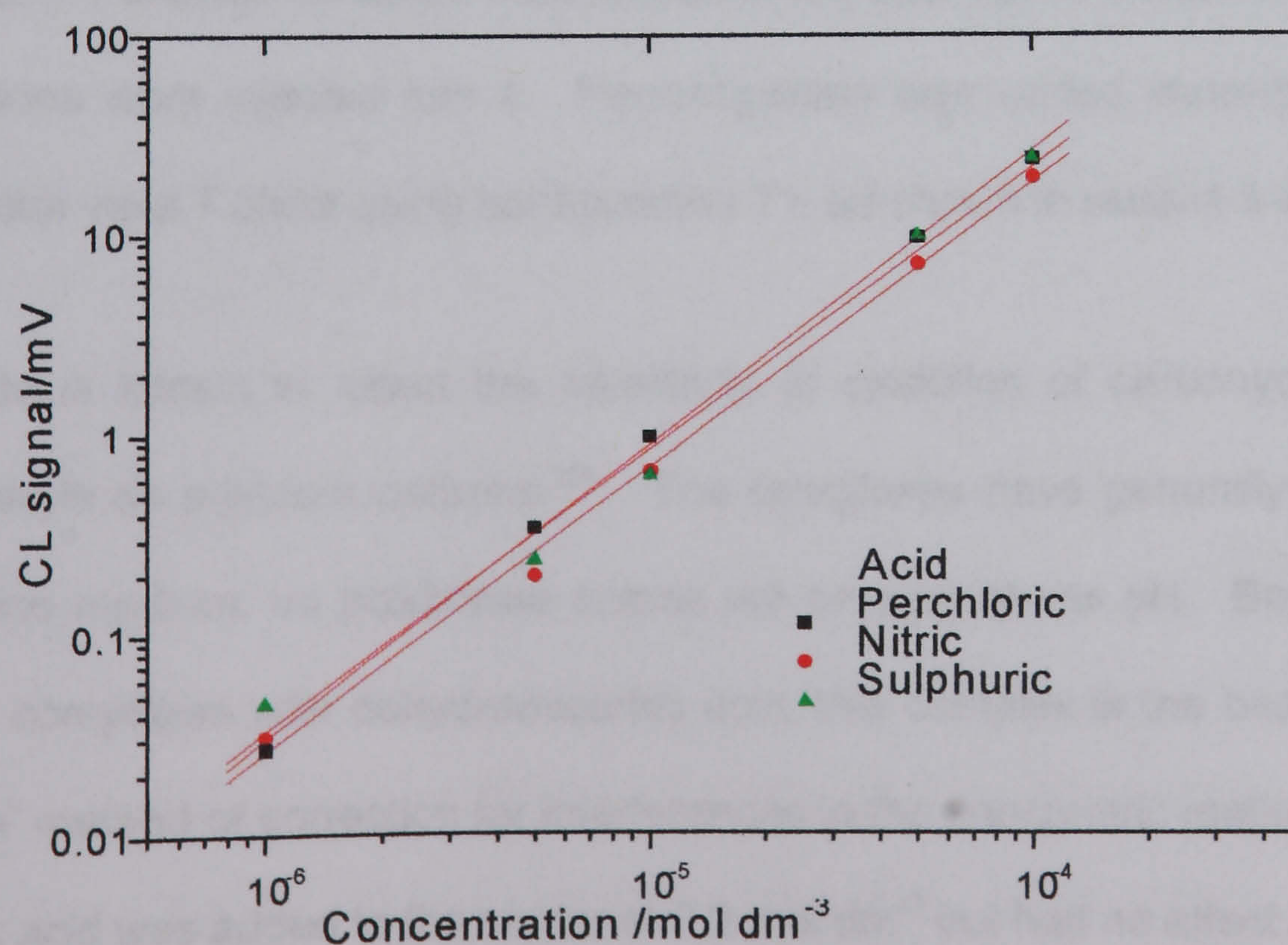
Sulphuric Acid /mol dm <sup>-3</sup>	Intercept/mV	Slope/ mV mol <sup>-1</sup> dm <sup>3</sup>	R
0.1	-0.61	$5.18 \times 10^4$	0.99889
0.25	-1.23	$8.26 \times 10^4$	0.99911
0.5	-1.41	$1.10 \times 10^5$	0.99902
0.75	-1.70	$1.21 \times 10^5$	0.99933
1.0	-2.33	$1.27 \times 10^5$	0.99936
1.25	3.07	$1.35 \times 10^5$	0.99908



Above  $0.75 \text{ mol dm}^{-3}$  sulphuric acid the increase in signal was small and this concentration was used, directly in the single line manifold. In the two line manifold  $1.5 \text{ mol dm}^{-3}$  was used as a dilution to  $0.75 \text{ mol dm}^{-3}$  resulted. As the  $\text{pK}_a$  of ascorbic acid is 4.04 the reaction represents oxidation of undissociated ascorbic acid.

Sulphuric acid was selected as this had been used for the work with carbohydrates. Sulphate can stabilise manganese (III) in solution and we consider that manganese (III) is involved in the chemiluminescence reaction. Other workers have investigated permanganate oxidations in perchloric acid<sup>151,254</sup> therefore a comparison was made between these acids. Nitric and hydrochloric acids were also investigated. These were not expected to have the same effect on manganese (III) in the system. The signals for sulphuric and perchloric acid carriers were very similar as in Figure 5.2. The slopes were  $2.41 \times 10^5$  and  $2.39 \times 10^5 \text{ mV mol}^{-1} \text{ dm}^3$  respectively. As expected nitric acid gave lower signals, with a slope of  $1.92 \times 10^5 \text{ mV mol}^{-1} \text{ dm}^3$ . Hydrochloric acid also gave a lower signal. The difference between sulphuric and perchloric acids was small; sulphuric acid was preferred for reasons of safety

**Figure 5.2 The Effect of Mineral Acid on CL Signal**





5.4.3 Optimisation of Permanganate Concentration

The effect of permanganate concentration was investigated. As shown in Table 5.2, linear range depends on the permanganate concentration. Higher permanganate concentrations are needed to extend the range to high ascorbic acid concentrations.

Table 5.2 Effect of Permanganate Concentration on CL Signal

Permanganate/ mol dm <sup>-3</sup>	Analyte range /mol dm <sup>-3</sup>	Intercept/ mV	Slope/ mV mol <sup>-1</sup> dm <sup>3</sup>	R
5x10 <sup>-5</sup>	1x10 <sup>-6</sup> to 1x10 <sup>-3</sup>	4.38	1.01x10 <sup>5</sup>	0.96940
	1x10 <sup>-6</sup> to 5x10 <sup>-4</sup>	1.88	1.46x10 <sup>5</sup>	0.99125
1x10 <sup>-4</sup>	1x10 <sup>-6</sup> to 1x10 <sup>-3</sup>	1.55	1.19x10 <sup>5</sup>	0.98893
	1x10 <sup>-6</sup> to 5x10 <sup>-4</sup>	-0.21	1.51x10 <sup>5</sup>	0.99954
5x10 <sup>-4</sup>	1x10 <sup>-6</sup> to 1x10 <sup>-3</sup>	-1.64	8.20 x10 <sup>4</sup>	0.99702
	1x10 <sup>-6</sup> to 5x10 <sup>-4</sup>	-1.66	8.23x10 <sup>4</sup>	0.98659
1x10 <sup>-3</sup>	5x10 <sup>-6</sup> to 1x10 <sup>-2</sup>	2.27	3.62x10 <sup>4</sup>	0.99828
	5x10 <sup>-6</sup> to 1x10 <sup>-3</sup>	-1.75	5.41x10 <sup>4</sup>	0.98049

5.4.4 Effect of Modifiers

A two-line manifold (manifold 3) was used to investigate the effect of modifiers on the system. Potential modifiers were added to the acid carrier stream and ascorbic acid solutions were injected into it. Permanganate was added immediately before the detector via a T piece using configuration T1, as shown in section 3.6.1.

Borate is known to affect the selectivity of oxidation of carbohydrates that have hydroxyls on adjacent carbons.<sup>255</sup> The complexes have generally been studied in alkaline medium, as polyborate anions are present at low pH. Borate is known to form complexes with dehydroascorbic acid, this complex is the basis of the ‘borate blank’ method of correction for interferences in the fluorimetric method of analysis.<sup>221</sup>

Boric acid was added to the carrier at 0.2 mol dm<sup>-3</sup> but had no effect on the signal.



As discussed earlier, phosphates are reported to increase chemiluminescence in some fast permanganate reactions; for example polyphosphoric acid has been used to enhance signals for codeine<sup>168</sup> and similar alkaloids. Polyphosphoric acid, metaphosphoric acid and trisodium tripolyphosphate were added to the carrier in the range 1 to 10% w/v. A slight increase in signal was observed but the linear ranges were shorter, giving no advantage over unmodified carriers.

Pyrophosphate was previously observed to significantly reduce the rate of emission form the reaction with carbohydrates, probably due to stable complexes formed with manganese (III). Low concentrations of pyrophosphate were added to the carrier. Results for additions up to 0.5% showed little change, however concentrations of 1 and 5% gave decreased gradients for the calibration lines, as expected from work with carbohydrates. The results are summarised in Table 5.3.

**Table 5.3 Effect of Pyrophosphate Addition to the Carrier**

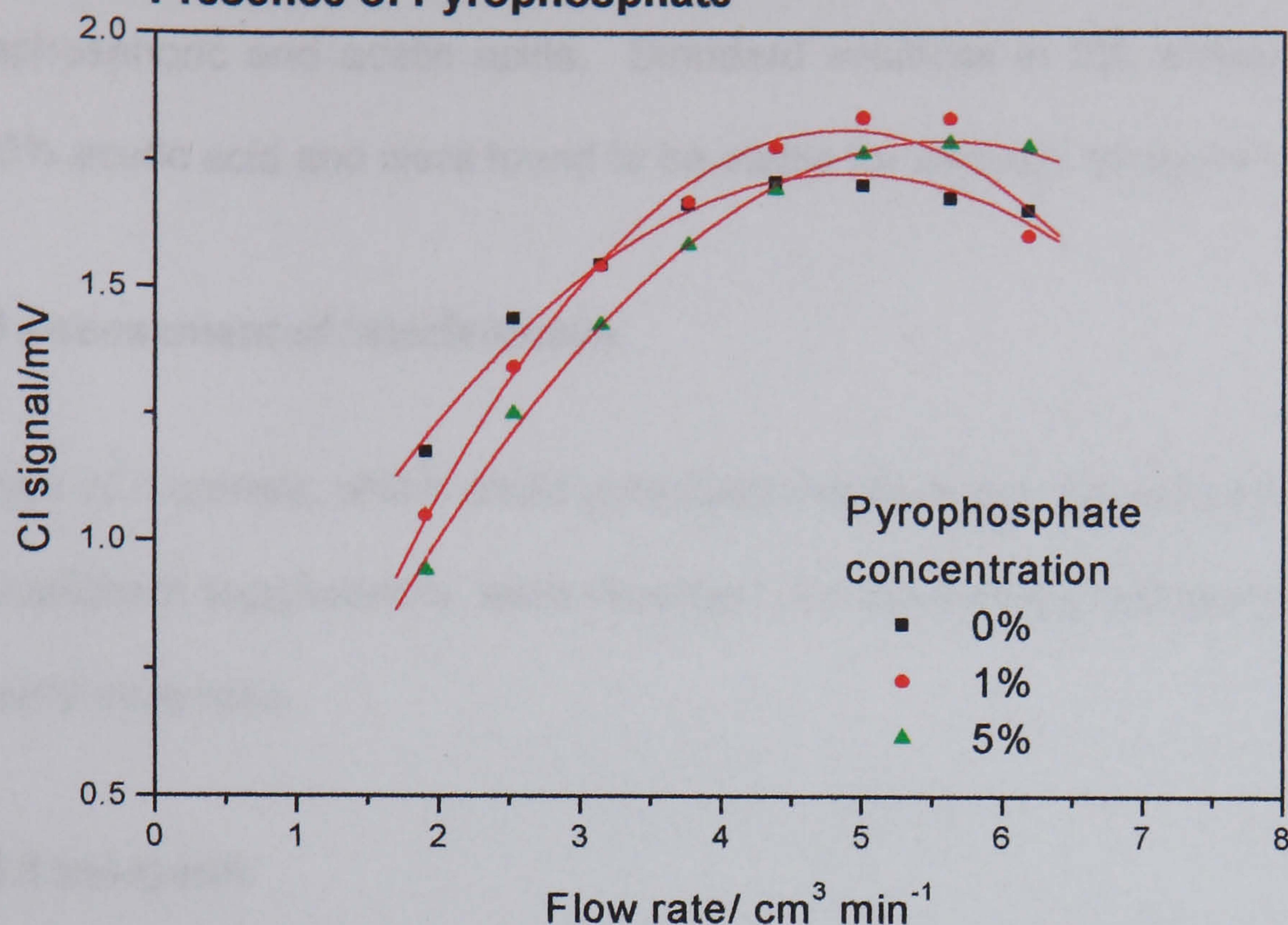
Pyrophosphate / %	Range/ mol dm <sup>-3</sup>	Intercept/ mV	Slope/mV mol <sup>-1</sup> dm <sup>3</sup>	R
0	1x10 <sup>-6</sup> to 5x10 <sup>-5</sup>	-1.19	5.07x10 <sup>5</sup>	0.99437
1	1x10 <sup>-6</sup> to 1x10 <sup>-4</sup>	-0.45	2.73x10 <sup>5</sup>	0.99919
5	1x10 <sup>-6</sup> to 1x10 <sup>-4</sup>	-0.41	2.27x10 <sup>5</sup>	0.99725

The effect of flow rate on the signal in the presence of pyrophosphate was examined for 1x10<sup>-5</sup> mol dm<sup>-3</sup> ascorbic acid. The effect is shown in Figure 5.3. Pyrophosphate results in a slight increase in signal for higher flow rates suggesting that the reaction is faster, consistent with the findings of other workers for fast reactions. As the increase is small and the linear range is reduced phosphate was not used.

Surfactants are known to enhance a range of chemiluminescent reactions, which may be due to energy transfer processes within the micelle.<sup>256</sup> The chemiluminescence from the oxidation of xanthene dyes is reported to be enhanced



**Figure 5.3 Effect of Flow rate on CL Signal in the Presence of Pyrophosphate**



using surfactants.<sup>257</sup> Other reasons for enhancement may be increased solubility or stabilisation of reacting species. It is known that the rate of the permanganate-oxalic acid reaction is increased in the presence of surfactants, dispensing with the requirement for carrying out the titrations at above 60°. <sup>258</sup> It was therefore decided to investigate the effect of an anionic surfactant, sodium dodecyl sulphate, and a cationic surfactant cetyltrimethylammonium bromide. Solutions of surfactant in the acid carrier were prepared at concentrations slightly above the critical micelle constant (CMC). Both surfactants resulted in inhibition of the signal, therefore the final system used an unmodified carrier.

#### 5.4.5 Preparation of Standard Solutions

In solution ascorbic acid is unstable to light and atmospheric oxygen. Initial work was carried out using aqueous ascorbic acid solution, kept in closed flasks in the dark. The oxidation is catalysed by metal ions, which may be present in the sample matrix, therefore ascorbic acid is generally extracted into an acid extracting solution. Various additives, including oxalic acid and EDTA,<sup>259</sup> have been proposed to minimise



interference from co-extractives. The most widely used extracting solutions contain metaphosphoric and acetic acids. Standard solutions in 2% metaphosphoric acid and 5% acetic acid and were found to be stable for 24hours refrigerated in the dark.

#### 5.4.6 Assessment of Interferences

A range of materials, which could potentially interfere with the determination in foods and nutritional supplements, were identified and assessed to establish the maximum tolerable mole ratio.

##### 5.4.6.1 Inorganic

Using a single line manifold a range of potentially interfering ions was examined, Reagent concentrations were  $1 \text{ mol dm}^{-3}$  sulphuric acid and  $1 \times 10^{-4} \text{ mol dm}^{-3}$  permanganate. Ion: ascorbic acid ratios up to 100:1 were used to establish the maximum ratio of interferent to ascorbic acid which gives less than 5% change in response compared with neat ascorbic acid. The species chosen were nutritional minerals, metals likely to come into contact with food such as tin and aluminium, and anions used as preservatives, nitrite and sulphite.

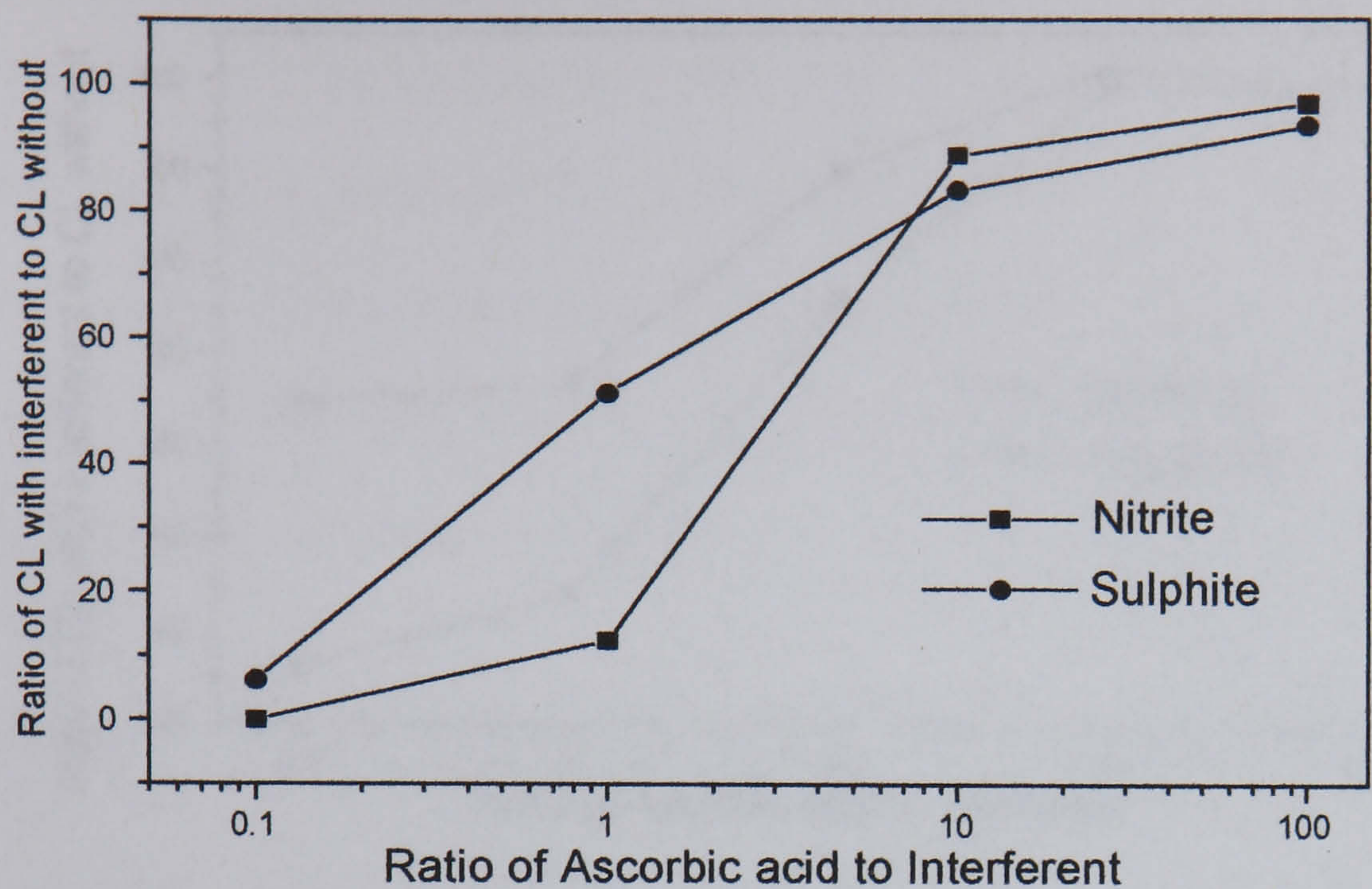
Interference was observed as a decrease in signal. Table 5.4 shows the maximum tolerable mole ratios and Figure 5.4 shows the effect of anion: ascorbic acid ratio on the signal.

**Table 5.4 Interference to Chemiluminescence Signal from Inorganic Species**

Species	Maximum Tolerable Mole Ratio
$\text{NH}_4^+$ , $\text{Co}^{2+}$ , $\text{Cr}^{3+}$ , $\text{Mg}^{2+}$ , $\text{Zn}^{2+}$	100
$\text{Al}^{3+}$ , $\text{Sn}^{2+}$ , $\text{Fe}^{3+}$ ,	10
$\text{Cu}^{2+}$	0.1
$\text{Mn}^{2+}$ , $\text{Br}^-$ , $\text{NO}_2^-$ , $\text{SO}_3^-$	0.01



Figure 5.4 Effect of Interfering Anions on the Chemiluminescence



5.4.6.2 Organic

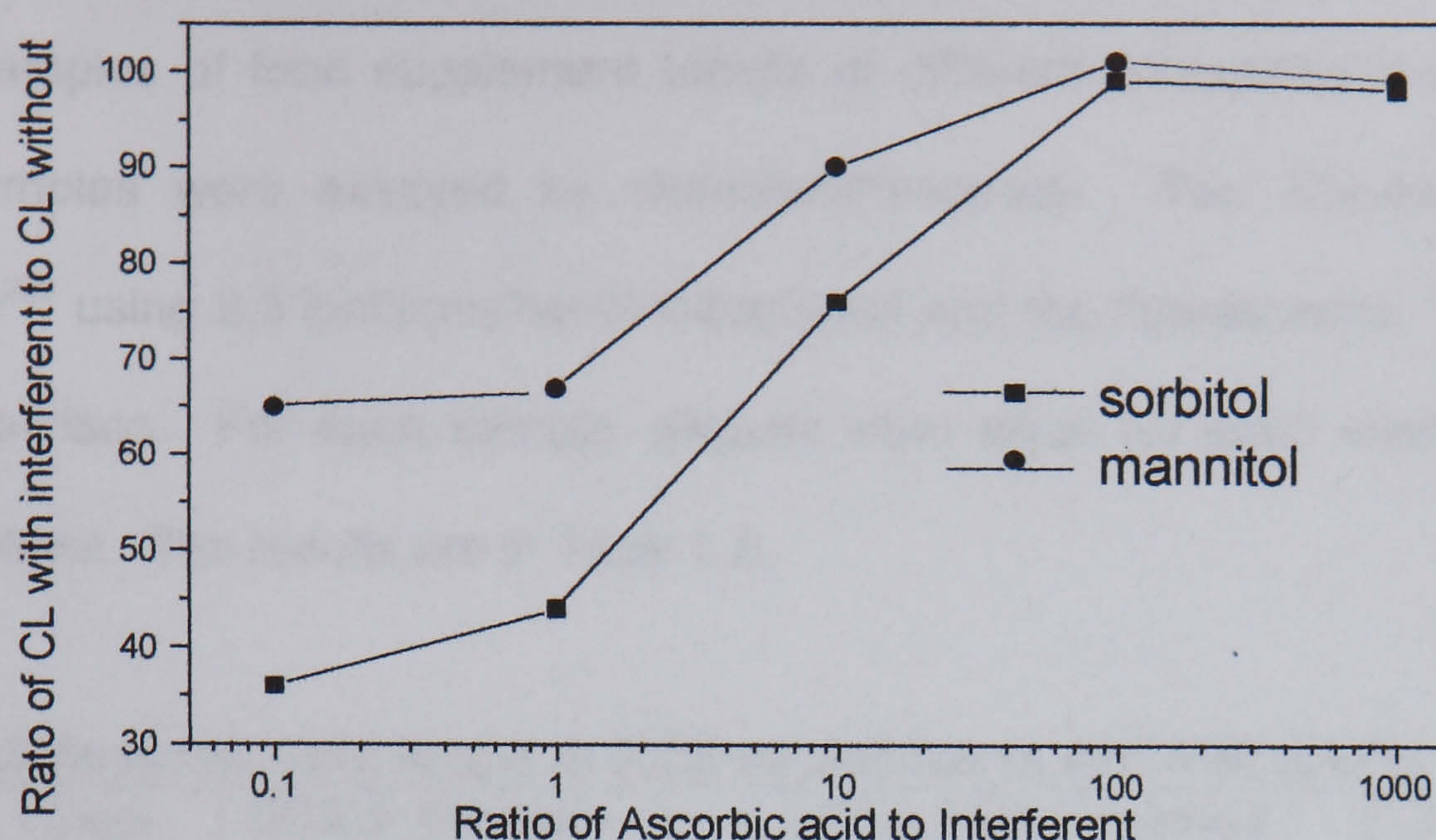
A range of organic compounds such as vitamins, carbohydrates and organic acids, which are likely to be present at significant concentrations in foods and food supplements were identified and examined as above. As for the inorganic materials, interference was observed as a decrease in signal. The maximum tolerable mole ratios for the organic compounds examined are shown in Table5.5. Figure 5.5 shows the effect of the polyols mannitol and sorbitol.

Table 5.5 Interference to Chemiluminescence Signal from Organic Species

Species	Maximum Tolerable Mole Ratio
Vitamin B1	100
Vitamin B2, Nicotinic Acid, Vitamin B6	10
Glucose, Fructose, Sucrose, Lactose	10
Mannitol Sorbitol	1



**Figure 5.5 Effect of Interfering Carbohydrates on the Chemiluminescence**



Typical ratios of the interfering species (total metal or vitamin) to ascorbic acid in common foodstuffs will not interfere in the assay<sup>260</sup>. It is possible that the high levels of mannitol or sorbitol, which are used as excipients in food supplement formulations, could limit the applicability of this method.

#### 5.4.7 Other Compounds Related to Ascorbic acid

The first oxidation product of ascorbic acid, dehydroascorbic acid can constitute 10 to 20% of the vitamin C content of fruits and vegetables.<sup>261</sup> In some fruits such as acerola cherry in excess of 50% of the vitamin is present as dehydroascorbic acid. A  $3 \times 10^{-4} \text{ mol dm}^{-3}$  solution of dehydroascorbic acid gave a peak height equivalent to 0.2% of that for the same concentration of ascorbic acid.

D-iso ascorbic acid (erythorbic acid) is not naturally present in foods and has little vitamin activity but is a permitted antioxidant in cooked meat products. As expected, the two isomers gave identical signals. The presence of erythorbic acid can be established by thin layer chromatography, if its presence is suspected in a sample.



5.4.8 Analysis of Real Samples

Three samples of food supplement tablets of different compositions and two fruit juice samples were assayed by chemiluminescence. Two standard methods, titrimetry<sup>220</sup> using 2,6 dichlorophenol indophenol and the fluorescence,<sup>221</sup> were used for comparison. For each sample, aliquots were taken for each method from the same extract. The results are in Table 5.6.

Table 5.6 Ascorbic acid found in food supplements and fruit drinks

Sample	Decl	DCICP titration			Fluorimetric method			Chemiluminescence		
	/mg	No	Mean /mg	SD/mg	No	Mean /mg	SD /mg	No	Mean /mg	SD /mg
Tablet 1	200	6	192.7	2.13	6	178.9	9.61	6	202.5	4.67
Tablet2	60	6	62.0	0.83	5	61.8	4.49	6	75.2	3.46
Powder	60	6	57.8	1.86	5	63.3	2.28	6	56.4	1.70
Juice1	>45	6	80.3	1.18	6	81.1	1.80	6	102.3	3.69
Juice2	>15	7	61.0	0.44	5	55.6	0.99	6	56.4	0.79

5.4.8.1 Statistical Comparison

Visual examination of results for individual samples showed a difference in variance between the methods with, generally, high variance for the fluorescence method. As the method is multistage, and was carried out manually, the higher variance was expected. Tablet 1 had a considerably higher level of ascorbic acid than the other samples and higher variances for all methods, although the relative standard deviations were similar to those for the other samples.



A paired t test for samples was used to compare methods. At the 95% confidence level there is no significant difference between any of the methods, as shown in Table 5.7.

**Table 5.7 t-Test: Paired Two Sample for Means**

	T vs F	F vs C	T vs F
Observations	5	5	5
Correlation coefficient	0.99704	0.98934	0.98711
df	4	4	4
t Statistic	0.7969	-1.533	-1.365
P(T<=t) two-tail	0.4702	0.2000	0.2440
t Critical two-tail	2.776	2.776	2.776
T- DCPIP titration, F –fluorescence, C – chemiluminescence			

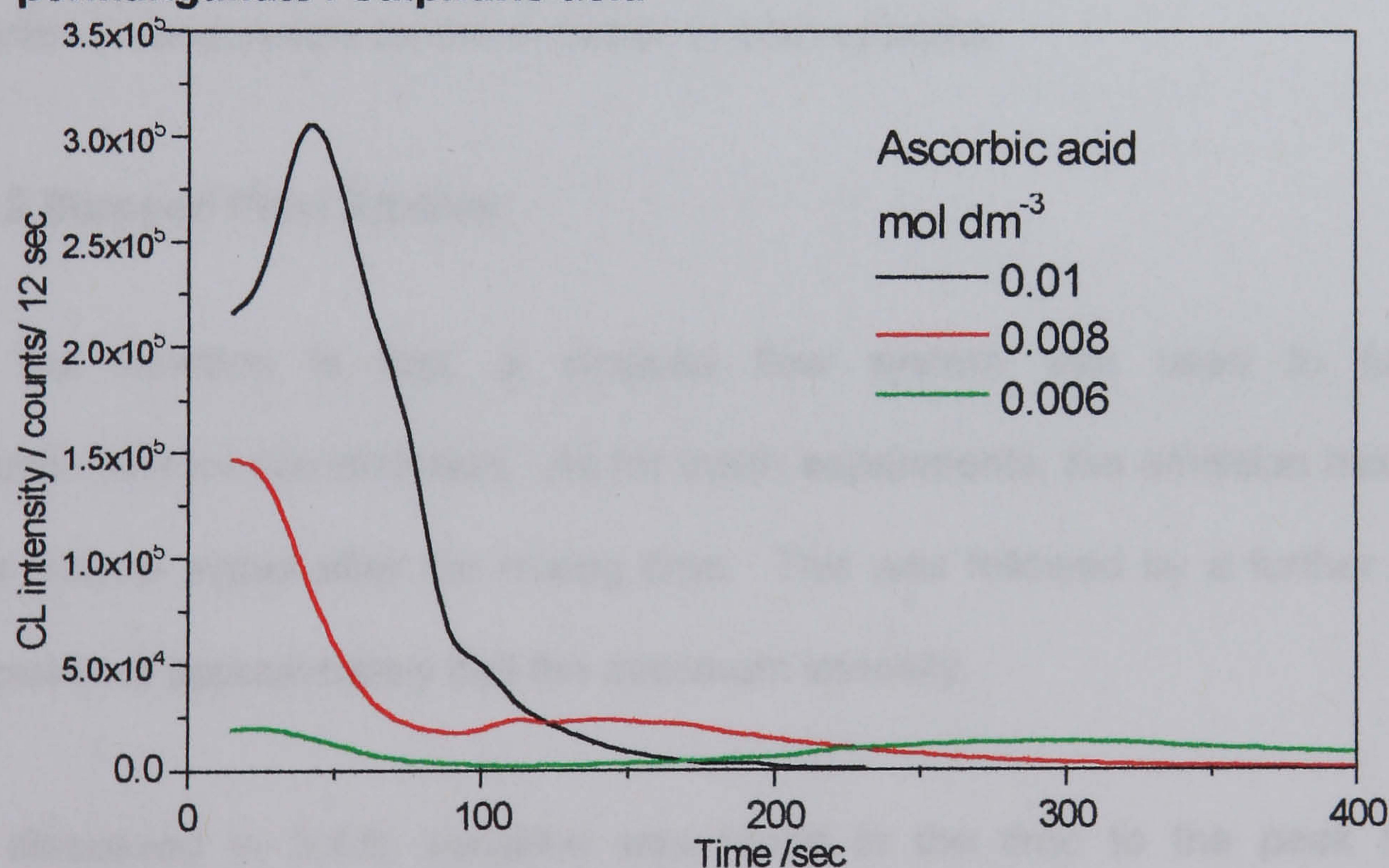
Other statistical tests were carried out including a principal component analysis which showed a high correlation between the three methods. The non-parametric Friedman test also showed no significant difference between the methods.



## 5.5 Batch Studies

It was apparent from the flow studies that the reaction between ascorbic acid and permanganate is very fast compared with the reaction between sugars and permanganate catalysed by manganese (II). The emission from the ascorbic acid/permanganate reaction was measured using the batch system. As for the carbohydrates, the reaction could only be investigated over a narrow range of reductant concentrations. At high concentrations the emission took place within the non-measuring period of the instrument. For low concentrations no emission was observed, although reduction of permanganate could be observed in the solution. The results are shown as Figure 5.6.

**Figure 5.6 Time course for Chemiluminescence from Ascorbic acid/permanganate / sulphuric acid**



2cm<sup>3</sup> sulphuric acid 2 mol dm<sup>-3</sup> mixed with 0.25cm<sup>3</sup> ascorbic acid to give the final concentration indicated. Reaction started by adding 0.1cm<sup>3</sup> 0.1 mol dm<sup>-3</sup> permanganate. CL measured after 15 sec then at 12 sec intervals

In each of the examples shown there appear to be two phases of the reaction, an initial intense emission followed by a second slow, low intensity emission, a similar pattern to that observed for carbohydrates reacting with manganese (IV) and manganese (III) solutions, which will be discussed in Chapter 7.



## 5.6 Spectroscopic Studies

### 5.6.1 Batch Studies

Initially both batch and semi-flow methods were used to collect spectra. Using the narrow range PMT, the spectra were very similar to those for carbohydrates using the same system. In a semi-flow experiment  $0.5\text{ cm}^3$   $0.5\text{ mol dm}^{-3}$  ascorbic acid in  $2\text{ mol dm}^{-3}$  was placed in a cuvette and  $0.1\text{ mol dm}^{-3}$  permanganate in water was pumped in at approximately  $1.8\text{ cm}^3\text{ min}^{-1}$ . Relative standard deviations were 0.3% for  $\lambda_{\text{max}}$ , 5.3% for bandwidth and 9.0% for peak height. The poorer repeatability for height was partly due to the changing concentrations of reactants as the mixing progressed. The similarity of the spectra of the emissions from sugar/permanganate/ Mn(II) and ascorbic acid/ permanganate suggests that the same species is responsible for the emission in both systems.

### 5.6.2 Stopped Flow Studies

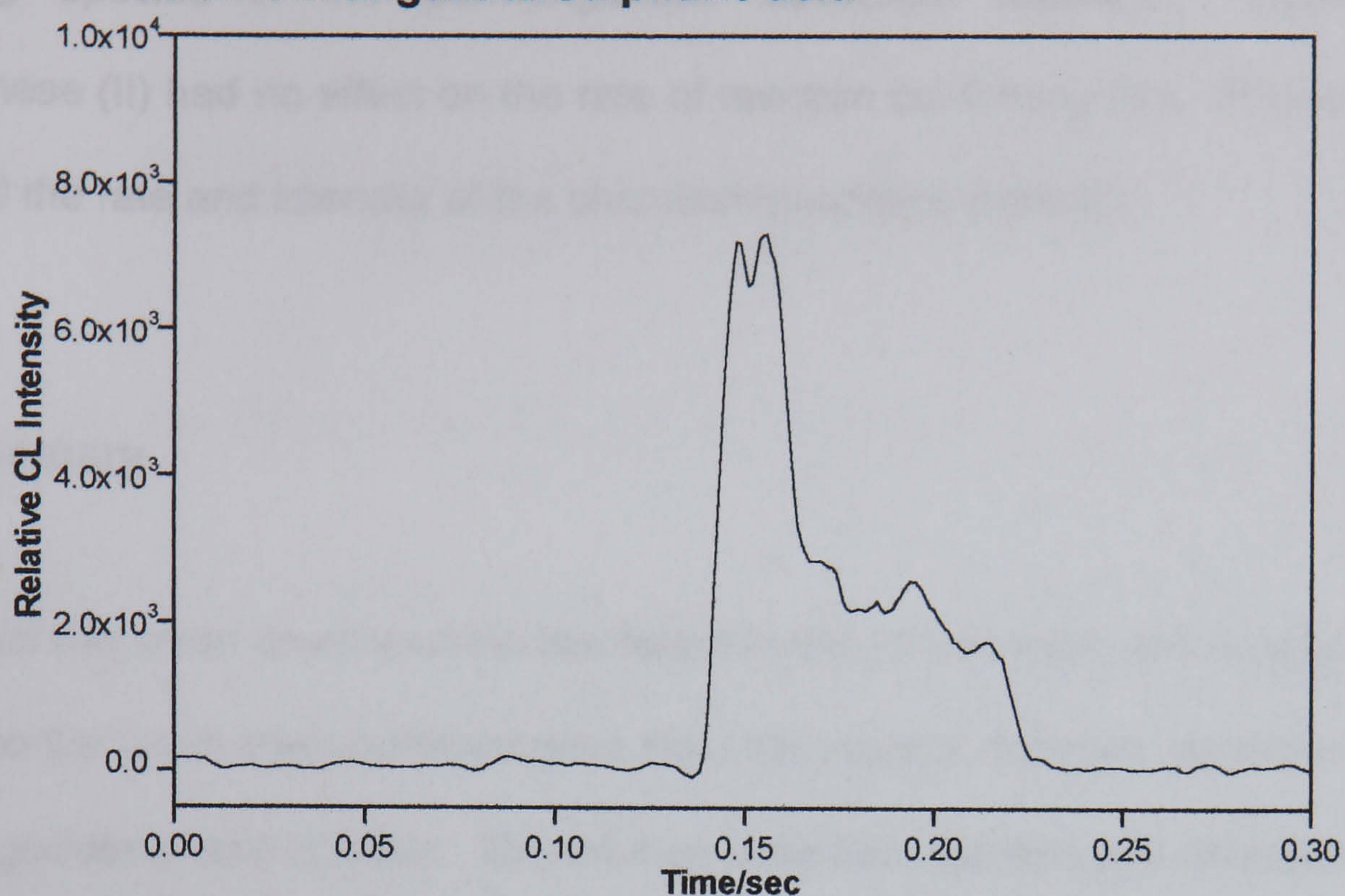
As the reaction is fast, a stopped flow system was used to follow the chemiluminescence emission. As for batch experiments, the emission has an initial high narrow signal after the mixing time. This was followed by a further period of emission of approximately half the maximum intensity.

As discussed in 3.5.6, variation was found in the time to the peak maximum depending on the position of the syringes. Mathematical smoothing using the Savitsky-Golay method was used to clarify the features. Twenty spectra were averaged and the result is shown in Figure 5.7.

The reaction is fast and even with the fast scanning capability only part of the spectrum could be collected and is shown in Figure 5.8.



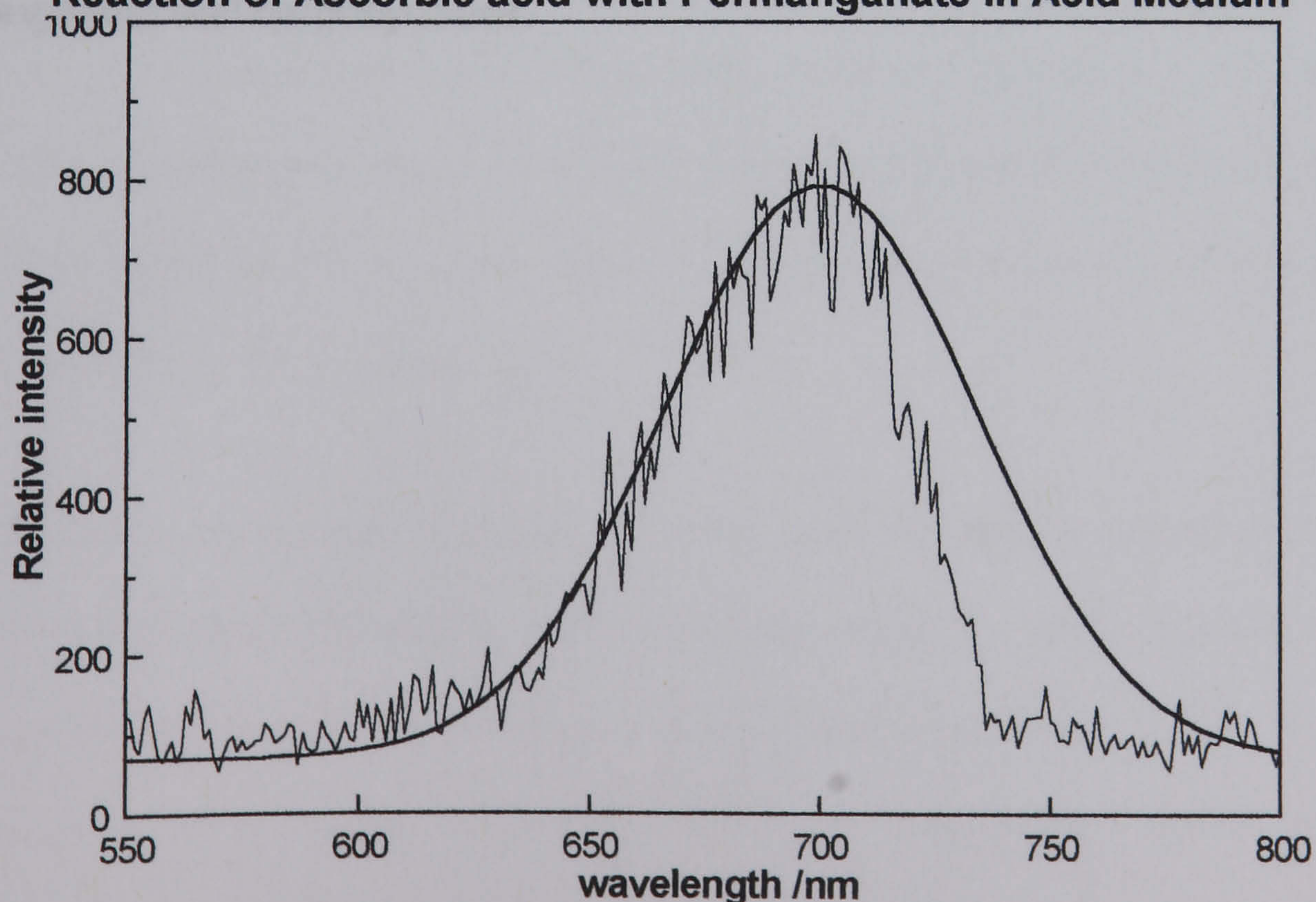
**Figure 5.7 Time-course of Chemiluminescence for Ascorbic acid/Permanganate/Sulphuric acid**



Emission at 700nm by stopped-flow, mixed solution contains  $1 \times 10^{-4} \text{ mol dm}^{-3}$  ascorbic acid  $2 \times 10^{-3} \text{ mol dm}^{-3}$  sulphuric acid  $1 \times 10^{-5} \text{ mol dm}^{-3}$  permanganate

The leading edge of the band fits well to a Gaussian function with  $\lambda_{\text{max}}$  at 700nm. As for the semi-flow method the results show that the emitting species is probably the same as that in carbohydrate permanganate reactions.

**Figure 5.8 Stopped-flow Chemiluminescence Spectrum for the Reaction of Ascorbic acid with Permanganate in Acid Medium**



Mixed solution contains  $1 \times 10^{-4} \text{ mol dm}^{-3}$  ascorbic acid  $2 \times 10^{-3} \text{ mol dm}^{-3}$  sulphuric acid  $1 \times 10^{-5} \text{ mol dm}^{-3}$



As shown in Scheme 2.9, manganese (VII)<sup>153</sup> has been proposed as the primary oxidising species in the permanganate/ ascorbate reaction. Fluoride and manganese (II) had no effect on the rate of reaction confirming this. Pyrophosphate reduced the rate and intensity of the chemiluminescence emission.

## 5.7 Summary

A method has been developed for the determination of ascorbic acid in solution. It is based on the direct chemiluminescence from the reaction between ascorbic acid and permanganate in acid solution. The method uses flow injection and detection using a red-sensitive photomultiplier.

The method is fast, simple and is not subject to interferences from levels of other components typically found in food supplements.

Spectroscopic studies have shown that the emitting species is probably the same as that responsible for the chemiluminescence emitted in the reaction between permanganate and carbohydrates.



## CHAPTER 6

### DEVELOPMENT OF A MANGANESE (III) REAGENT FOR CHEMILUMINESCENCE

#### 6.1 Reasons for Using Other Manganese Species

Manganese (VII) is a strong oxidising agent capable of oxidising a wide range of organic and inorganic compounds. Many of the oxidation reactions are autocatalytic, dependent on the initial production of manganese (II). The consequence is that without an initial concentration of manganese (II) the reactions have a characteristic lag time before the reaction occurs at significant rate. This can be seen as a slow initial reduction in the absorbance due to manganese (VII) at 500 to 600nm. As the reaction proceeds the rate increases with a faster decrease in absorbance. Figure 4.28 showed a typical profile for the decrease in absorbance due to manganese (VII) at its maximum of 545nm. This was in the absence of a catalyst.

Where such a reaction yields chemiluminescence, the emission of light starts only when most of the manganese (VII) has been reduced, whether or not a catalyst is present at the start of the reaction. It is clear therefore that the chemiluminescence is associated with a lower oxidation state of manganese, previous results suggesting manganese (III) or manganese (II).

Other manganese species, particularly manganese (III) and manganese (IV) have been used in organic oxidations, generally under neutral or acidic conditions. Their milder oxidising powers can result in more specific reactions. It was decided to investigate whether lower oxidation states of manganese would also give chemiluminescence, and to investigate its nature.



Manganese (IV) is generally used in heterogeneous reactions in the form of prepared manganese dioxide powder or as manganese dioxide sol. The sol can have good stability in neutral solution at concentrations up to  $1 \times 10^{-3}$ .

Manganese (III) is reasonably stable as complexes with ligands such as acetate, acetylacetonate and EDTA. However even these forms decompose slowly in solution. In some cases the ligand is itself oxidised by the manganese species. Manganese (III), can also be produced electrochemically<sup>262</sup> and this source has been used in oxidations.

## **6.2 Manganese (IV) Oxide**

Prepared manganese dioxide is used as a mild oxidising agent. Oxidation takes place on the solid surface, possibly by direct binding of organic species to manganese atoms. Oxidations of phenolic compounds and ascorbic acid, in neutral solutions have been described.<sup>263</sup> Polyhydroxy aliphatic alcohols such as glycerol and sorbitol, and simple aldehydes did not show significant reactions.

### **6.2.1 Studies with Prepared Manganese dioxide solid**

Commercially prepared manganese dioxide, a finely divided black powder, was shaken with excess acidified ascorbic acid. The solid was found to dissolve readily, but no light was observed. Acid solutions of sugars had no obvious effect on the solid even on prolonged standing.

### **6.2.2 Studies with Manganese dioxide Sol**

A stable manganese dioxide sol was produced by reducing permanganate with a stoichiometric amount of thiosulphate. The average size of the colloidal particles for a  $5 \times 10^{-4} \text{ mol dm}^{-3}$  preparation was reported to be 120nm.<sup>131</sup> A sol at this



concentration was found to be stable for several months at room temperature. More concentrated sols were also prepared using the stoichiometric amounts of permanganate and thiosulphate. At above  $2 \times 10^{-3} \text{ mol dm}^{-3}$  sol particles coagulated within 1-2 hours and solid manganese dioxide precipitated. The  $2 \times 10^{-3} \text{ mol dm}^{-3}$  sol was stable for several days, but gradually precipitated. The neutral sol reacted with ascorbic acid, the brown colour disappearing, indicating reduction of the manganese dioxide. In the absence of sulphuric acid no luminescence was observed. In the presence of dilute sulphuric acid low level luminescence was observed by batch counting. Some manganese dioxide precipitated as the sol was mixed with the acid.

### **6.2.3 Flow Studies with Manganese dioxide Sol**

As the addition of acid to the sol resulted in precipitation, prior to the reaction with the reductant, it was decided to use a flow system. This enabled the addition of acid to take place immediately before the injection of sample. In a flow system the coagulation of colloidal particles in the presence of acid should be reproducible. In the short time between mixing and reaction of sample the degree of coagulation was expected to be low. Any oxidation reaction would be in acid medium and the oxidising reagent would consist of manganese dioxide particles in the process of coagulation. Manifold 2 was used to mix the sol and sulphuric acid in a Y piece. Ascorbic acid solutions were injected through the loop injection valve.

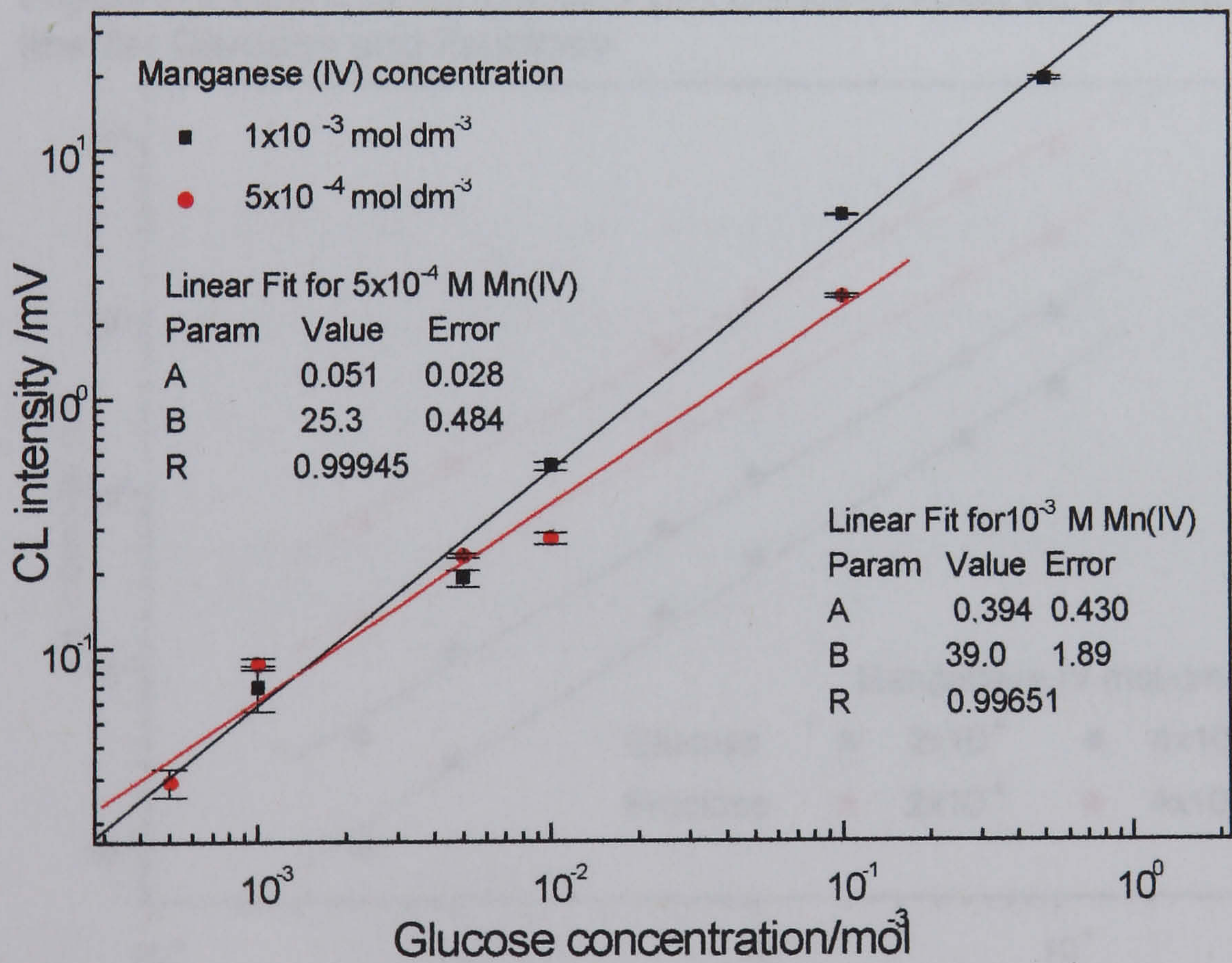
The signal was found to increase with increasing manganese (IV) concentration and increasing acid concentration. The signal was lower than that with permanganate and linearity and repeatability were not good. In the absence of injected ascorbic acid manganese dioxide precipitated in the manifold, coating the inside of the tubing. This was removed by injecting strong ascorbic acid.



Attempts to obtain signals for sugar solutions using this system were unsuccessful. It was found that the presence of additional manganese (II) gave a detectable signal.

Due to the problems of precipitation, Manifold 3 was used, with the sol added as a merging zone, via a T-piece, immediately before the detector. The sugar was injected into a carrier of 0.1mol dm<sup>-3</sup> manganese sulphate in 2 mol dm<sup>-3</sup> sulphuric acid. The chemiluminescent reaction with manganese dioxide sol was taking place in acid medium. As before, any coagulation of particles was expected to be reproducible and limited due to the short time between mixing and detection. Typical calibration plots for glucose are shown in Figure 6.1.

**Figure 6.1 Calibration for Glucose using Manganese dioxide Sol**



Manifold 3, carrier 0.1mol dm<sup>-3</sup> manganese sulphate in 2 mol dm<sup>-3</sup> sulphuric acid and 1x10<sup>-3</sup> mol dm<sup>-3</sup>, 2x10<sup>-3</sup> mol dm<sup>-3</sup> manganese dioxide sol, glucose concentrations as indicated

Linearity and repeatability were satisfactory, as shown by the parameters for linear fits. The signals achieved with, the maximum sol concentration, were poor in comparison with those with permanganate; additional manganese (II) was required.

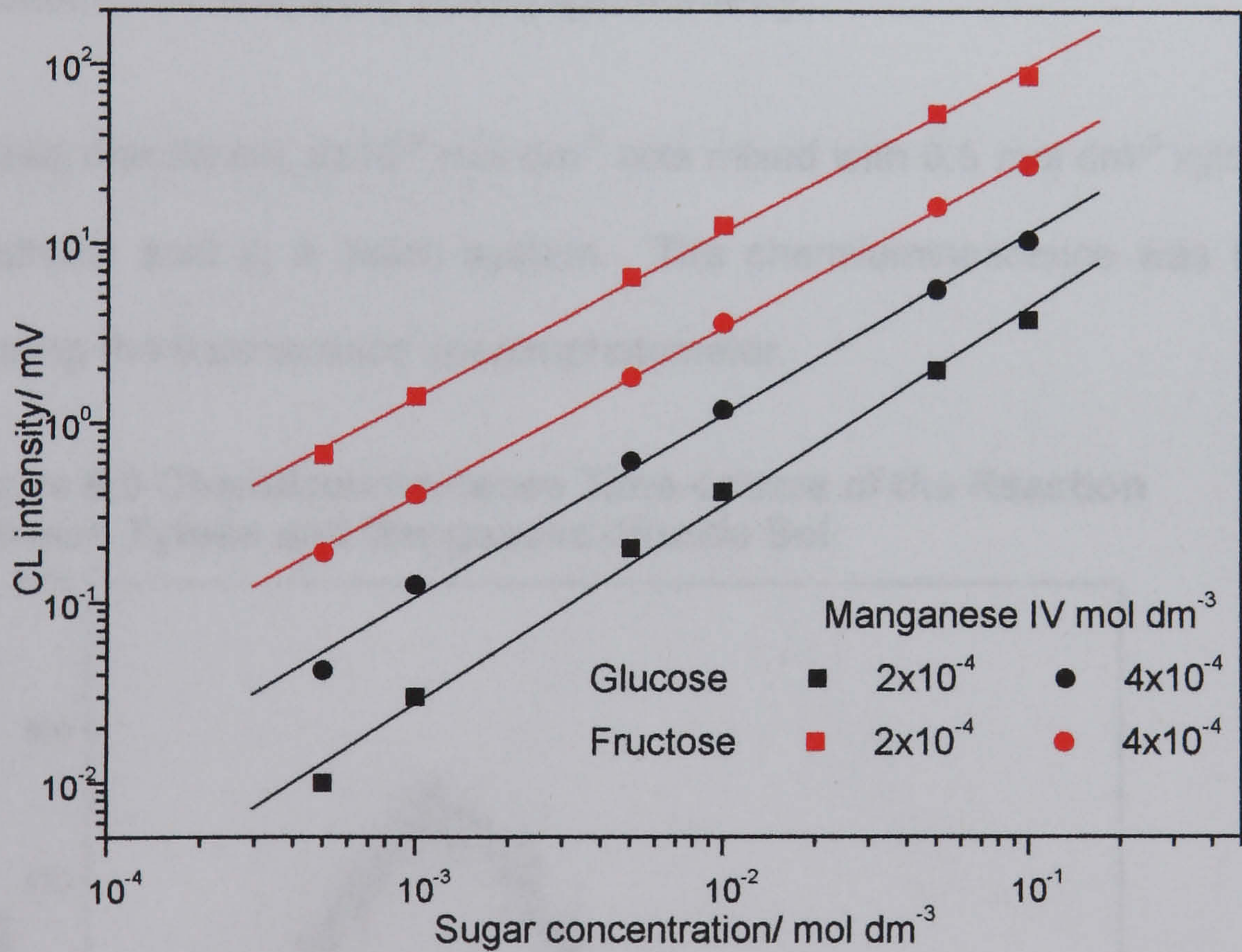


For some combinations of acid, manganese dioxide sol and manganese (II) sulphate concentrations, pink solutions were produced. For these mixtures manganese dioxide precipitated slowly after standing at room temperature. Absorbance spectra of these solutions were run and will be discussed in section 6.2.4.2.

A range of solutions containing different amounts of manganese dioxide sol and manganese (II) sulphate were prepared and used directly as carriers in a single line manifold. Solutions of glucose and fructose were injected.

Increasing the manganese (IV) concentration in the mixture had a marked effect on the chemiluminescence signal, up to the limit of stability. This is shown in Figure 6.2.

**Figure 6.2 Effect of Manganese (IV) Concentration on Calibration line for Glucose and Fructose**



Manifold 1 Concentrations as in legend

The concentration of manganese (II) in the FIA system did not appear as significant as that of manganese (IV). This can be seen from the slopes of the calibration lines in Table 6.1, which show little variation. A maximum was observed for fructose but not for glucose.



**Table 6.1 Calibration Parameters for Glucose and Fructose Varying Manganese (II) Concentrations**

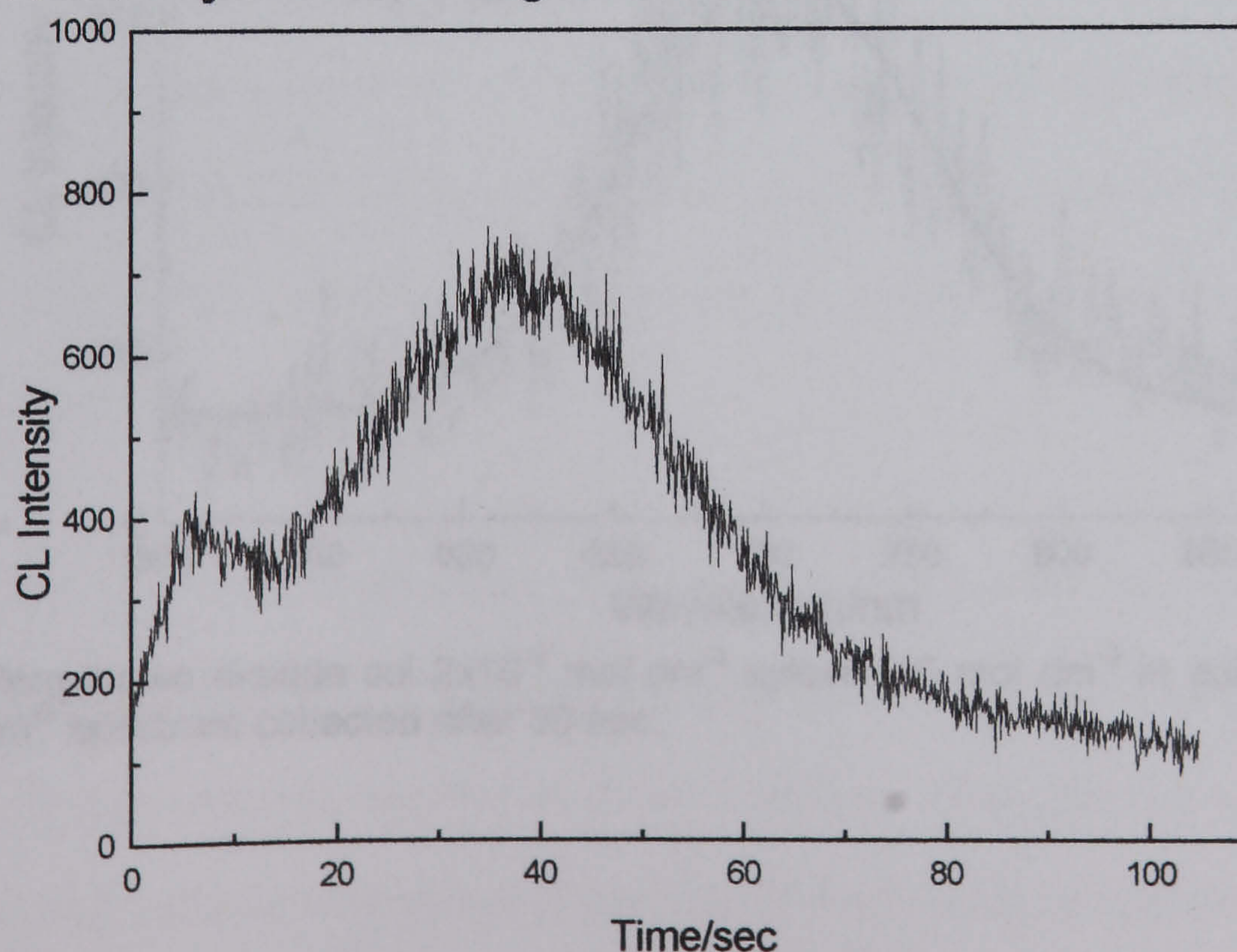
	Mn(II) /mol dm <sup>-3</sup>	Intercept /mV	Slope /mVmol <sup>-1</sup> dm <sup>3</sup>	R
Glucose	0.04	0.03	29.9	0.9996
	0.08	0.03	37.8	0.9998
	0.12	0.02	38.6	0.9999
	0.16	0.06	40.7	0.9996
Fructose	0.04	0.22	318	0.9994
	0.08	0.13	378	0.9998
	0.12	0.09	341	0.9984
	0.16	0.07	292	0.9999

## 6.2.4 Spectroscopic Studies with Manganese dioxide Sol

### 6.2.4.1 Chemiluminescence Spectrophotometry

Manganese dioxide sol,  $2 \times 10^{-3}$  mol dm<sup>-3</sup> was mixed with 0.5 mol dm<sup>-3</sup> xylose in 4mol dm<sup>-3</sup> sulphuric acid in a batch system. The chemiluminescence was followed at 700nm using the fluorescence spectrophotometer.

**Figure 6.3 Chemiluminescence Time-course of the Reaction between Xylose and Manganese dioxide Sol**



Manganese dioxide sol  $2 \times 10^{-3}$  mol dm<sup>-3</sup>, xylose 0.5 mol dm<sup>-3</sup> in sulphuric acid 4 mol dm<sup>-3</sup> at 700nm

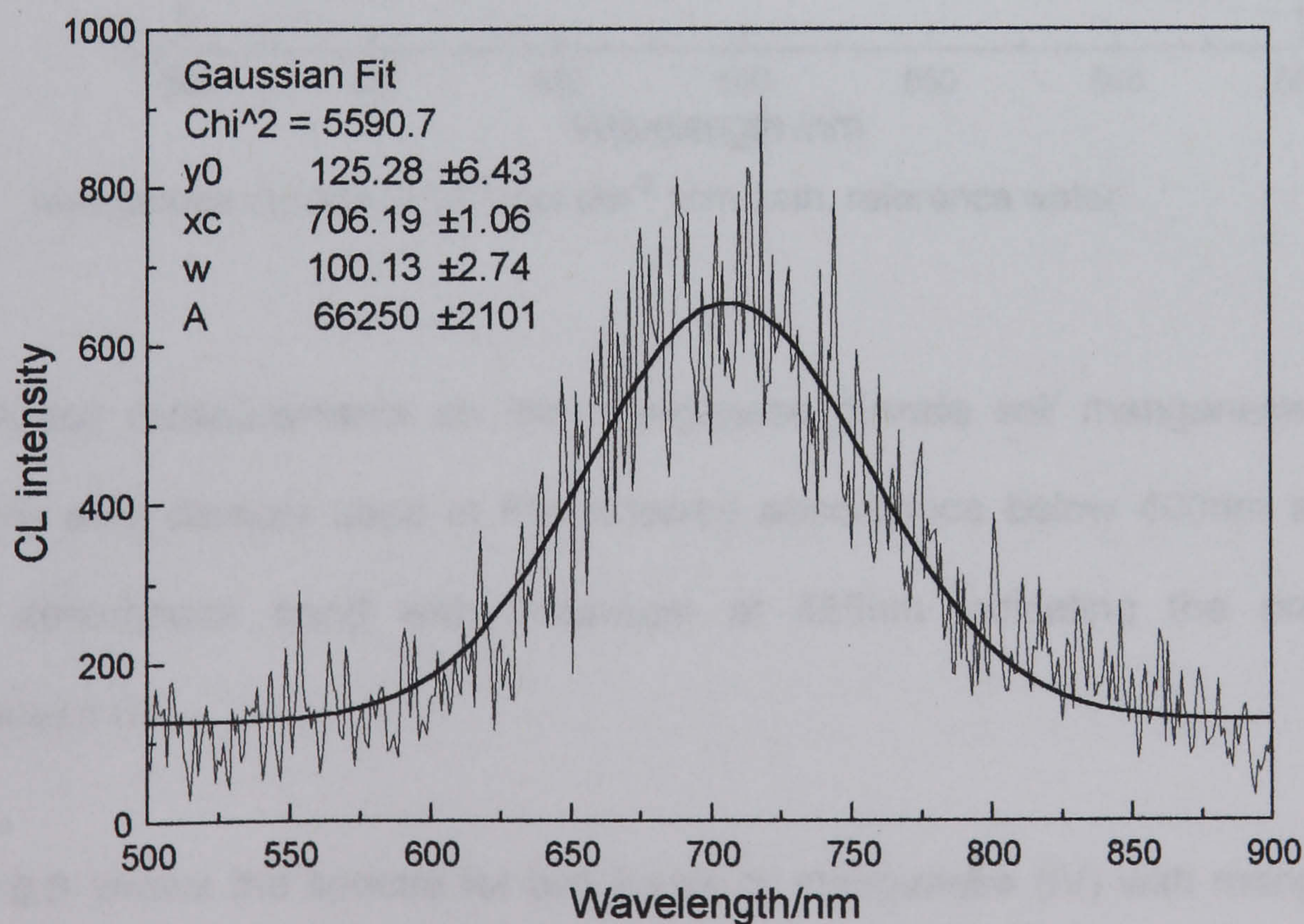


Xylose was selected as the response is higher than for glucose and is stable in acid solution. The time course of the reaction is shown in Figure 6.3.

Two maxima were observed, one at approximately 5 sec and a larger one at 35 sec. The intensity of the emission is low compared with the intensities obtained using permanganate solution with similar concentrations of sugars. It is believed that the first peak is due to the reaction with a small amount of manganese (III) in the solution. This is immediately reduced to manganese (II) resulting in the fast emission, followed by the slower reduction of manganese (IV) from the surface of the colloidal particles giving the gradual increase and decay of the luminescence.

The emission spectrum is shown in Figure 6.4. It is identical to that for permanganate oxidation indicating that the same excited species is responsible.

**Figure 6.4 Chemiluminescence Spectrum for the Reaction Between Xylose and Manganese dioxide Sol**



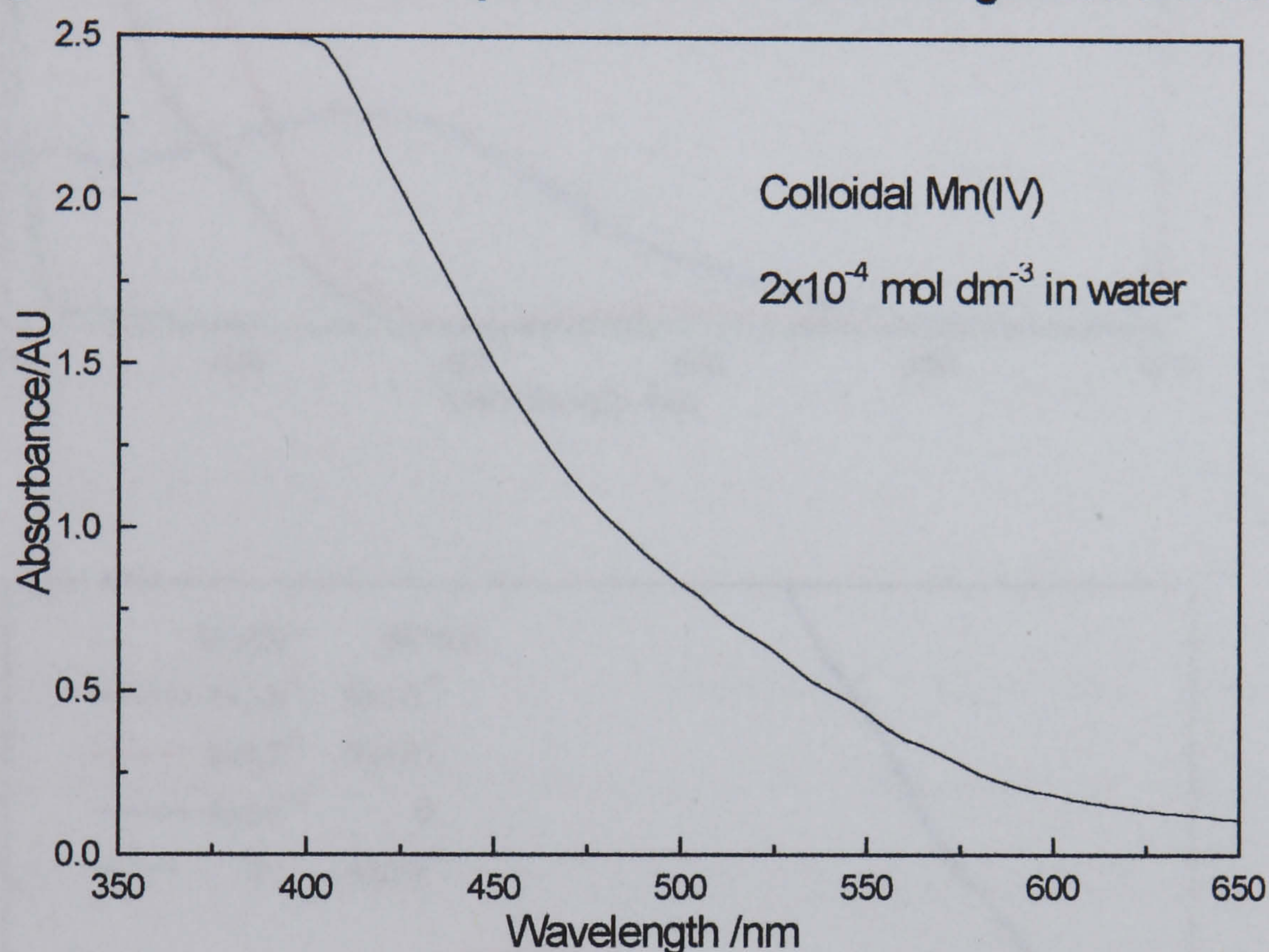
Manganese dioxide sol  $2 \times 10^{-3}$  mol dm<sup>-3</sup> xylose 0.5 mol dm<sup>-3</sup> in sulphuric acid 4 mol dm<sup>-3</sup> spectrum collected after 30 sec.



#### 6.2.4.2 Absorbance Spectrophotometry

The absorbance spectrum of the neutral manganese dioxide sol was measured and is shown in Figure 6.5. It is, as described in the literature, a broad absorbance decreasing towards 600nm.

**Figure 6.5 Absorbance Spectrum for Neutral Manganese dioxide Sol**



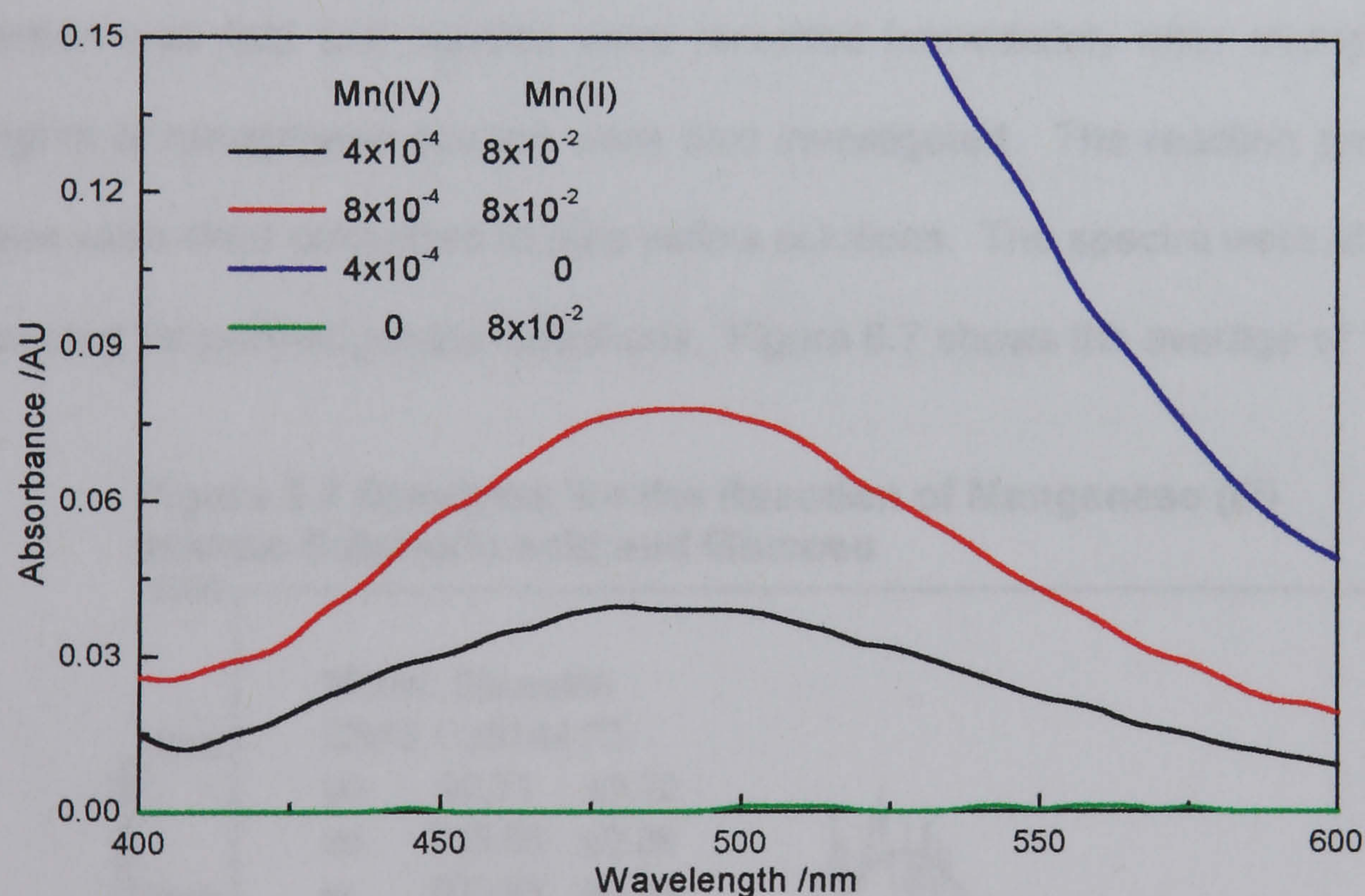
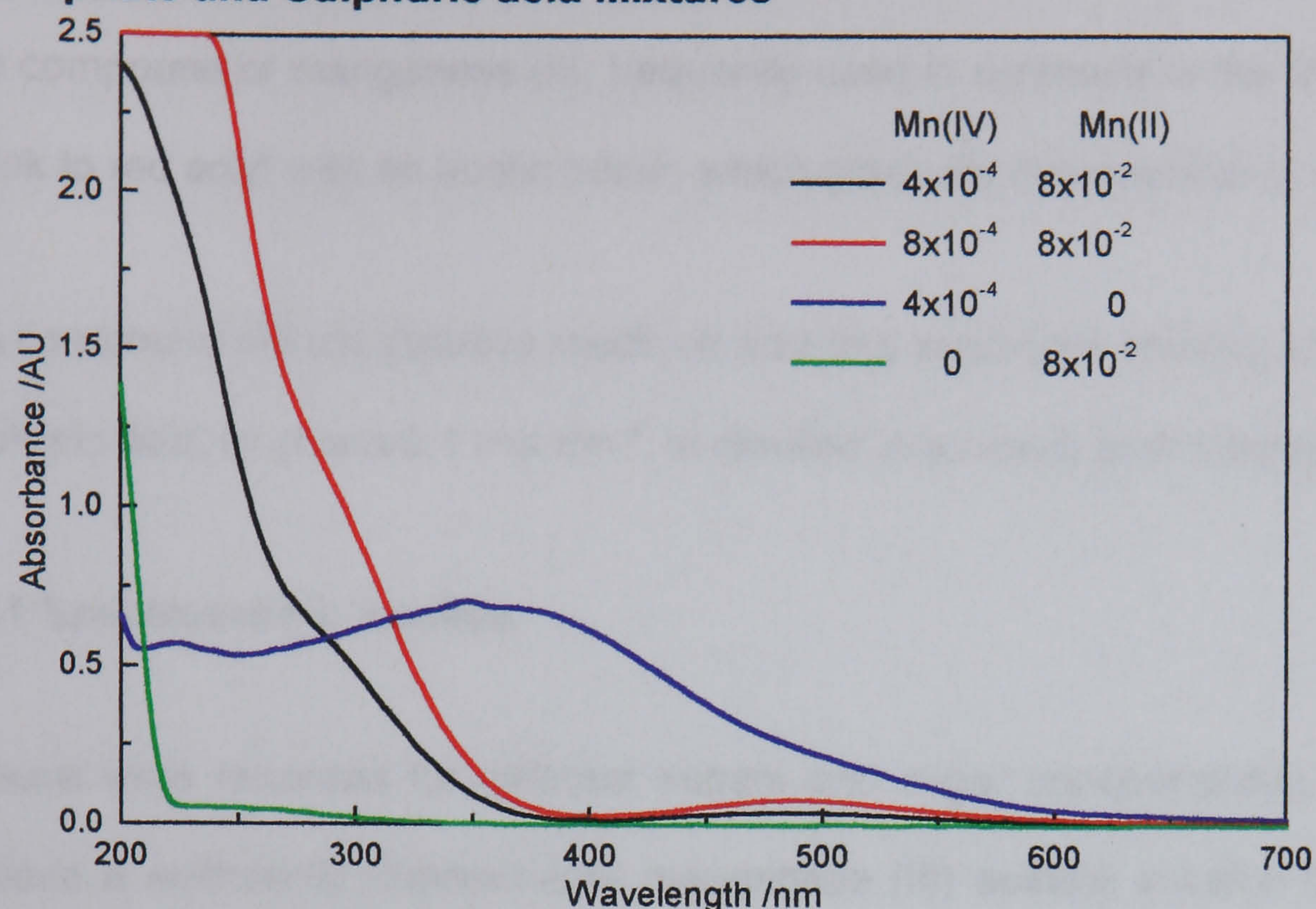
Manganese dioxide  $2 \times 10^{-4} \text{ mol dm}^{-3}$  1cm path, reference water

Absorbance measurements on the manganese dioxide sol/ manganese sulphate/ sulphuric acid carriers used in FIA showed absorbance below 400nm and a low, broad absorbance band with maximum at 485nm indicating the presence of manganese (III).

Figure 6.6 shows the spectra for two levels of manganese (IV) with manganese (II). Spectra for manganese (IV) sol and manganese (II) solution, acidified to the same extent as the mixtures, are shown for comparison. Re-scaling the wavelength range between 400 and 600nm shows a band, for the mixtures, at approximately 500nm.



**Figure 6.6 Absorbance Spectra for Manganese dioxide Sol, Manganese sulphate and Sulphuric acid Mixtures**



Manganese dioxide and manganese (II) mixtures, concentrations as show in 4 mol  $\text{dm}^{-3}$  sulphuric acid, reference 4mol  $\text{dm}^{-3}$  sulphuric acid. Lower figure shows expansion of 400 to 600 nm range

Addition of pyrophosphate to the manganese (IV)/ manganese (II) mixture resulted, as expected, in increased stabilisation of manganese (III). For the same concentrations of manganese, the absorbance band at around 500nm was approximately ten times larger in the presence of pyrophosphate.



## 6.3 Manganese (III) Acetate

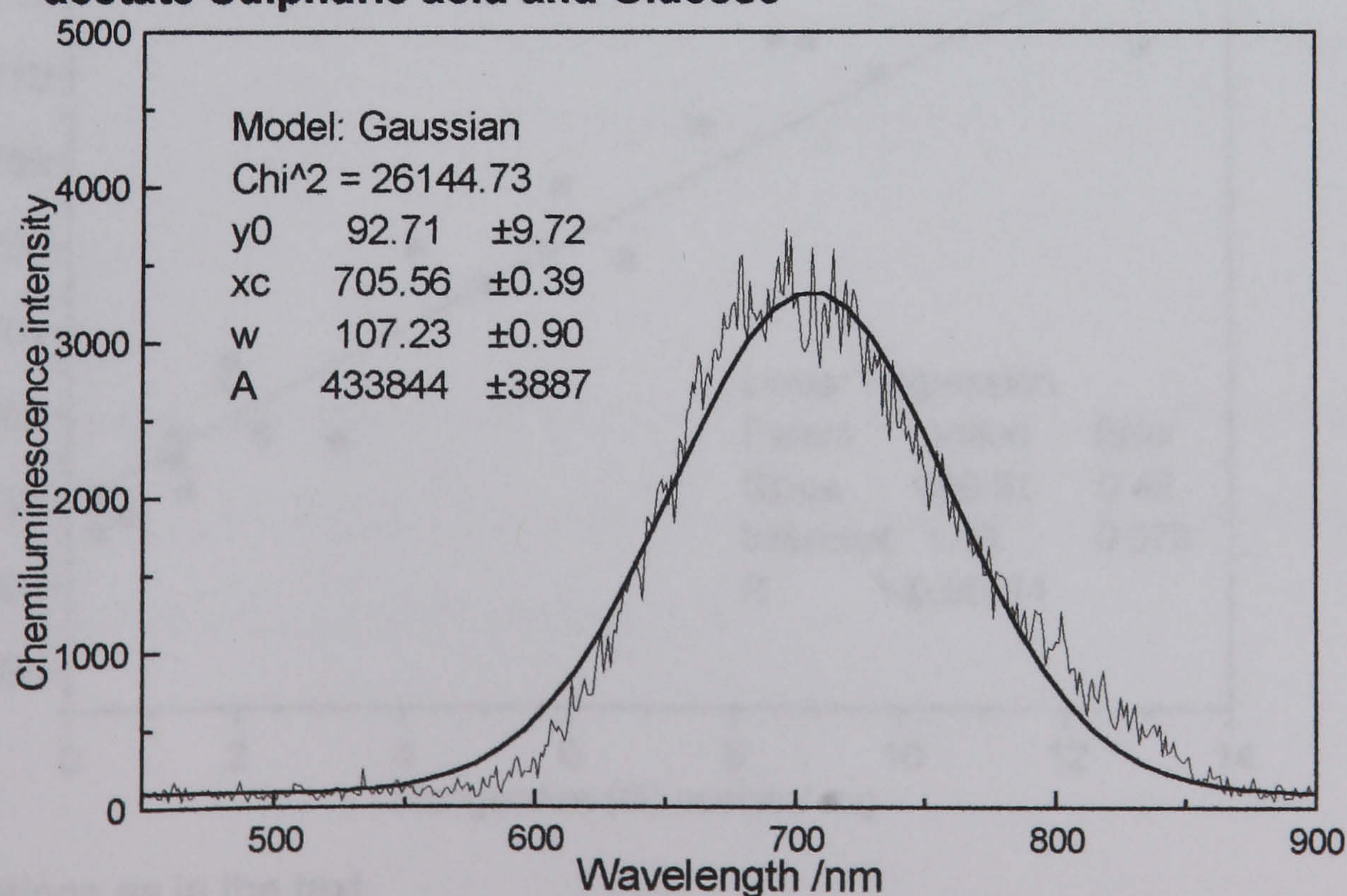
The compound of manganese (III) frequently used in synthesis is the triacetate. It is a pink to red solid with an acetic odour, which gradually decomposes in air.

The compound did not dissolve readily in acid and prolonged shaking with  $2 \text{ mol dm}^{-3}$  sulphuric acid, to give a  $0.1 \text{ mol dm}^{-3}$ , in resulted in a cloudy pink suspension.

### 6.3.1 Spectroscopic Studies

Spectra were recorded for different sugars and sugar concentrations. In order to achieve a sufficiently concentrated manganese (III) acetate solution the solid was shaken with sulphuric acid immediately before addition of sugar solution. The reaction was fast and spectra were recorded immediately after mixing. Different weights of manganese acetate were also investigated. The reaction products in all cases were clear colourless to pale yellow solutions. The spectra were all of the form expected for permanganate oxidations. Figure 6.7 shows the average of 10 spectra.

**Figure 6.7 Spectrum for the Reaction of Manganese (III) acetate Sulphuric acid and Glucose**



Saturated manganese (III) acetate in  $2 \text{ mol dm}^{-3}$  sulphuric acid mixed with  $1 \text{ mol dm}^{-1}$  glucose. Spectrum collected immediately



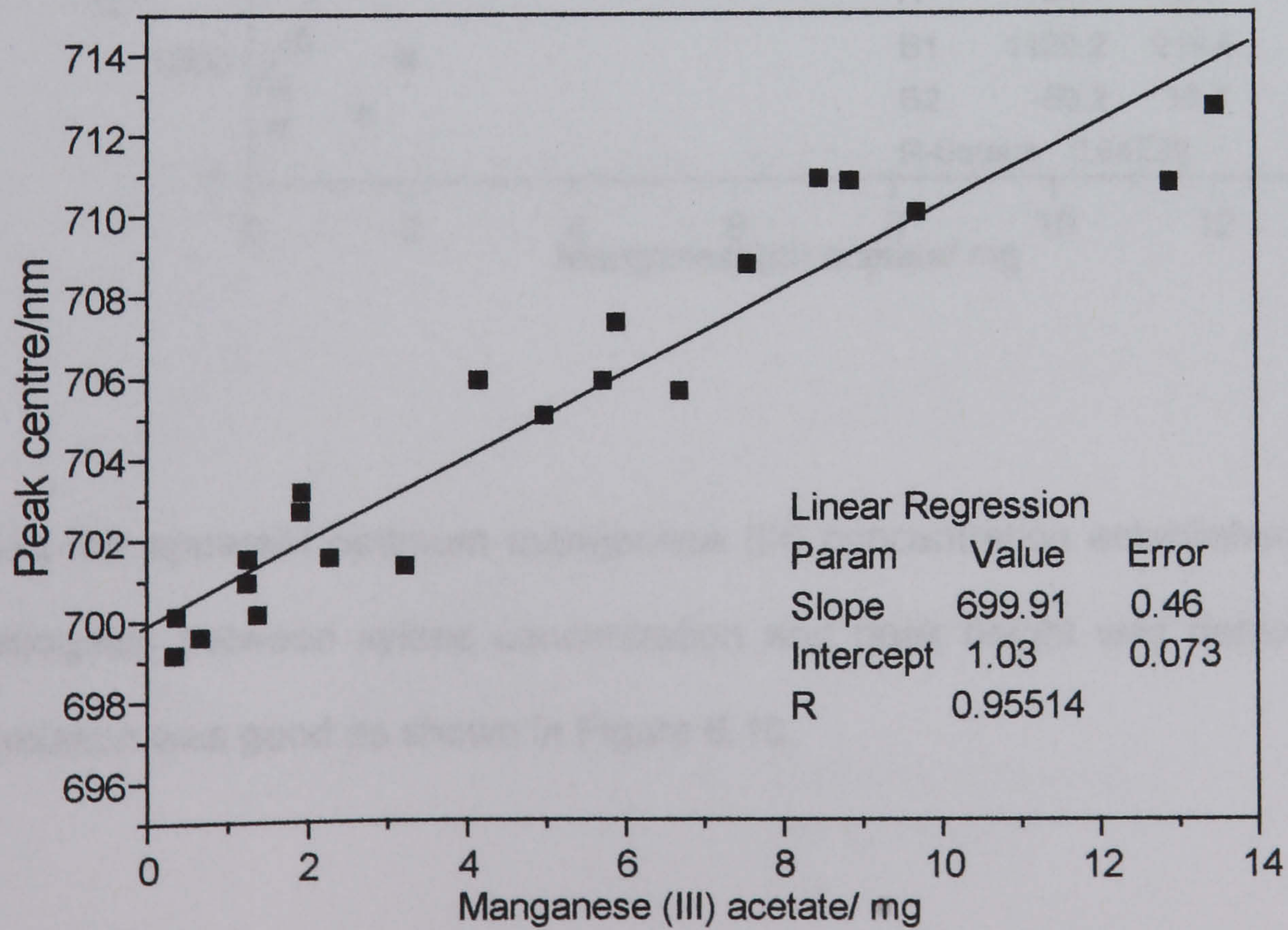
Four monosaccharides, three hexoses and a pentose, were treated with between 1 and 8mg of manganese (III) acetate. The molar ratio of sugar to manganese was in the range 20 to 50. Using Gaussian fits,  $\lambda_{\text{max}}$ , height at  $\lambda_{\text{max}}$ , and band-width were calculated for each spectrum. The results are shown in table 6.2.

**Table 6.2 Chemiluminescence Spectrum Parameters for Sugar/ Manganese (III) acetate Reactions**

Sugar	Centre nm	±	Width nm	±	Height Units	±
Glucose	705.36	1.83	106.45	3.20	3353	421
Galactose	703.50	1.66	106.21	3.07	3445	496
Fructose	706.25	1.56	104.54	4.63	9465	810
Xylose	704.56	0.92	106.12	4.18	3874	650

For xylose, the effect of varying the amount of manganese (III) acetate was investigated further. In all cases the peak maximum was in the same region but increased with increasing ratio of manganese (III) to xylose, as shown in Figure 6.8.

**Figure 6.8 Relationship between Chemiluminescence Spectral Maximum and Amount of Manganese (III) acetate**

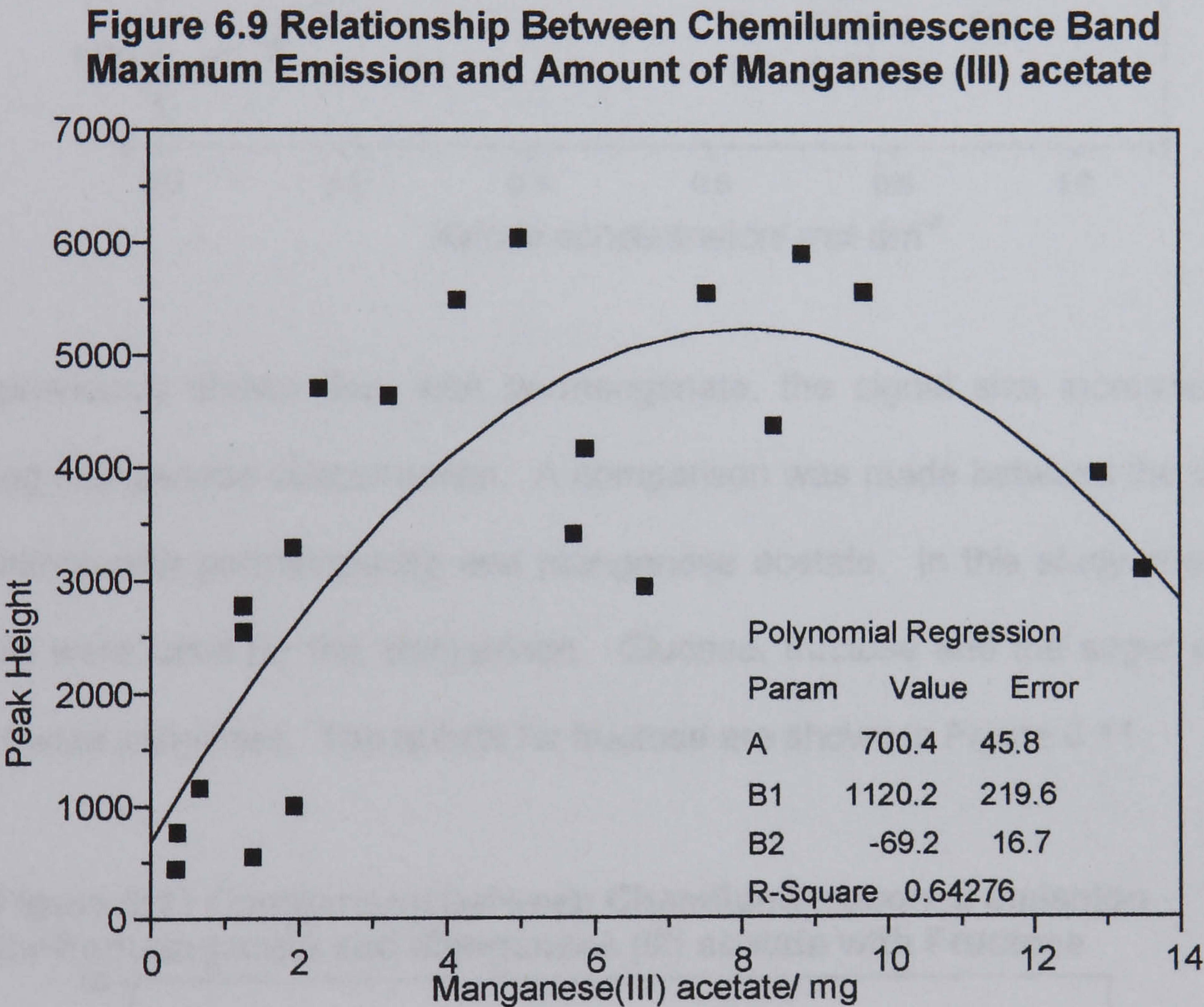


Conditions as in the text



The reason for the movement of the peak centre is probably due to the kinetics of the reaction. As the acetate is not completely dissolved before addition of the sugar the light emission continues as more acetate dissolves. No such correlation between  $\lambda_{\text{max}}$  and manganese concentration was seen for manganese (VII).

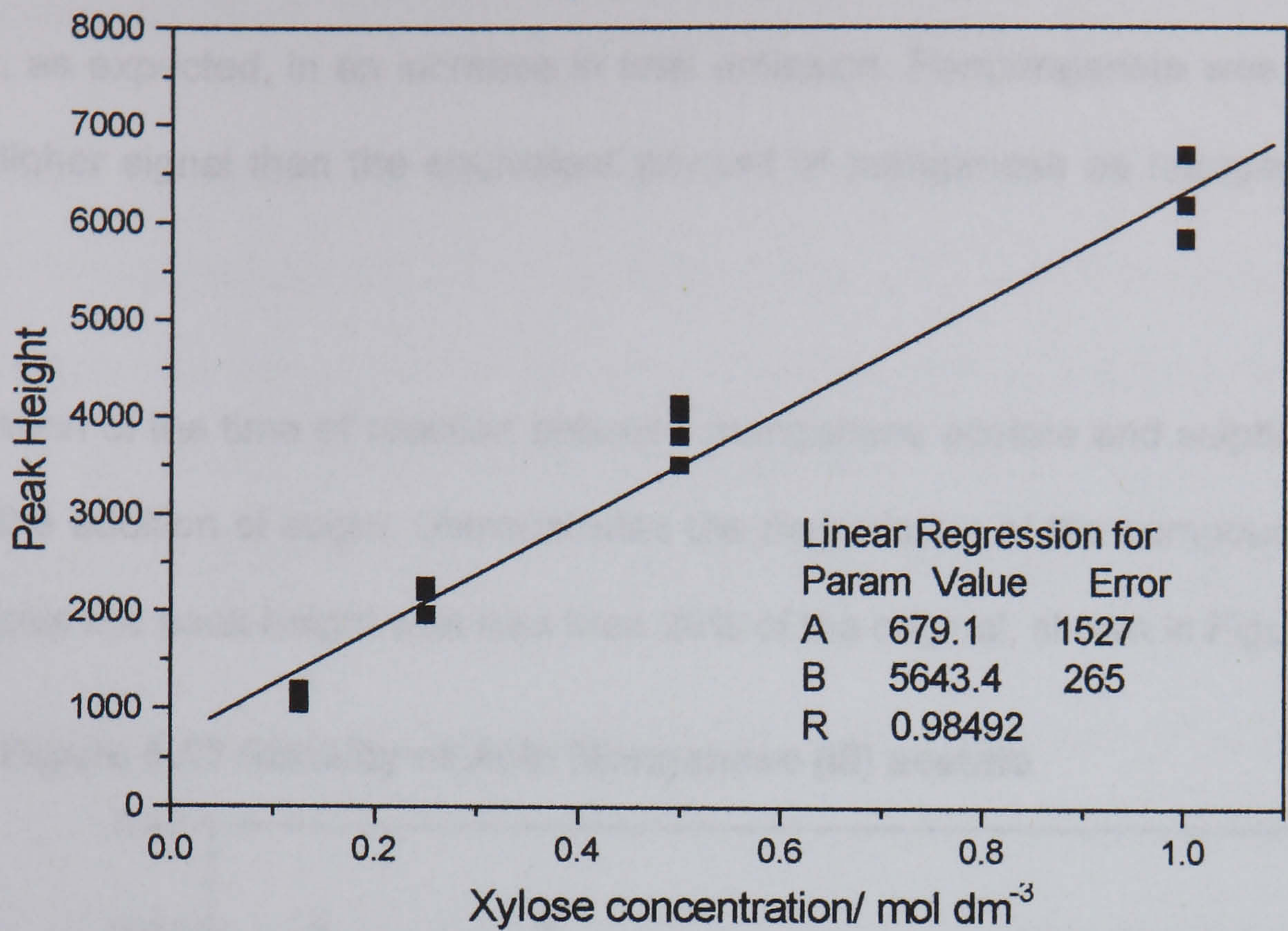
The results for peak height correlated less well but appeared to show a maximum as shown in Figure 6.9.



Using the apparent optimum manganese (III) concentration established above, the relationship between xylose concentration and peak height was determined. The correlation was good as shown in Figure 6.10.

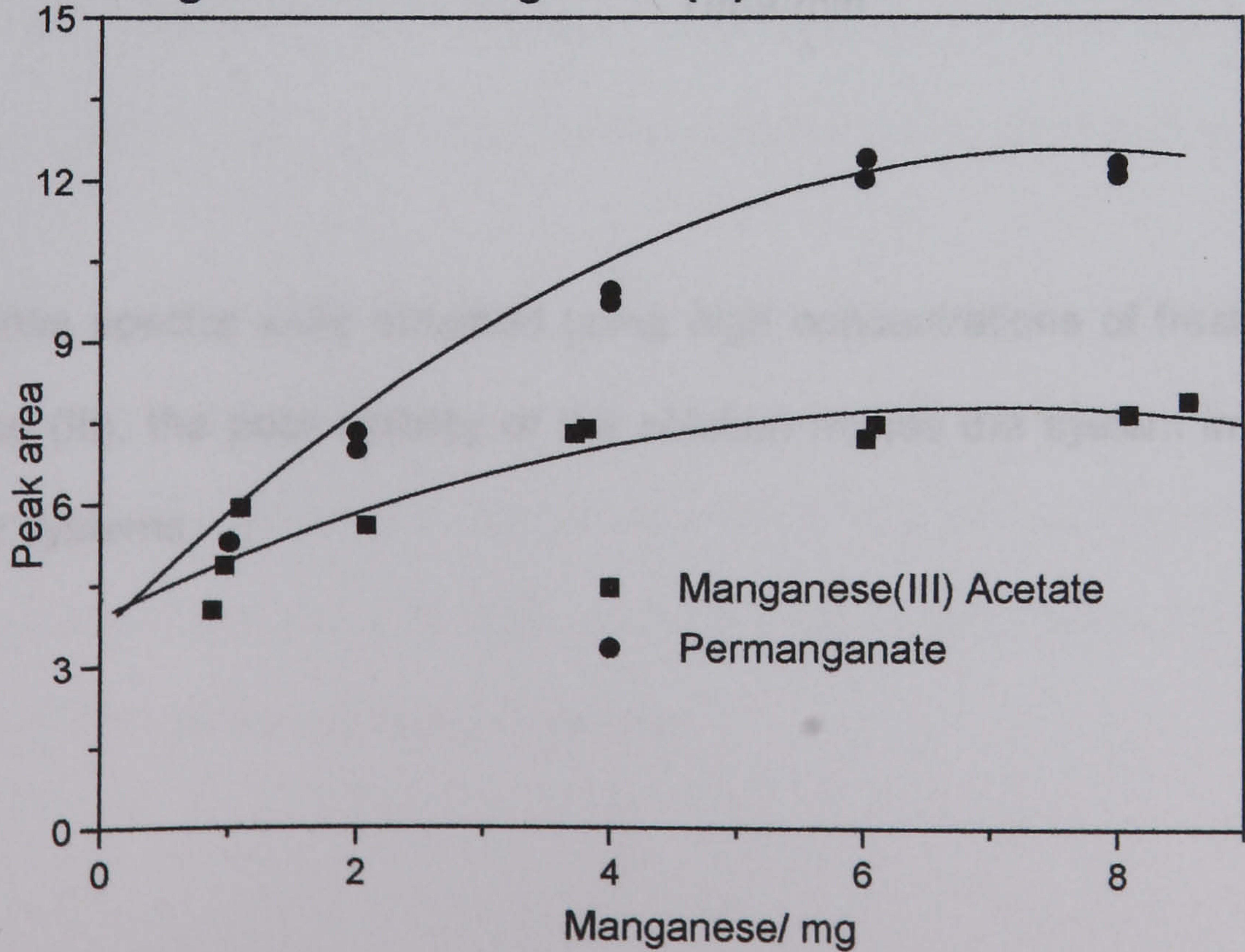


**Figure 6.10 Relationship Between Chemiluminescence Band Maximum Emission and Xylose Concentration**



It was previously shown that, with permanganate, the signal size increases with increasing manganese concentration. A comparison was made between the signals for oxidations with permanganate and manganese acetate. In this study integrated time plots were used for the comparison. Glucose, fructose and the sugar alcohol mannitol were examined. The results for fructose are shown in Figure 6.11.

**Figure 6.11 Comparison between Chemiluminescence emission for Permanganate and Manganese (III) acetate with Fructose**

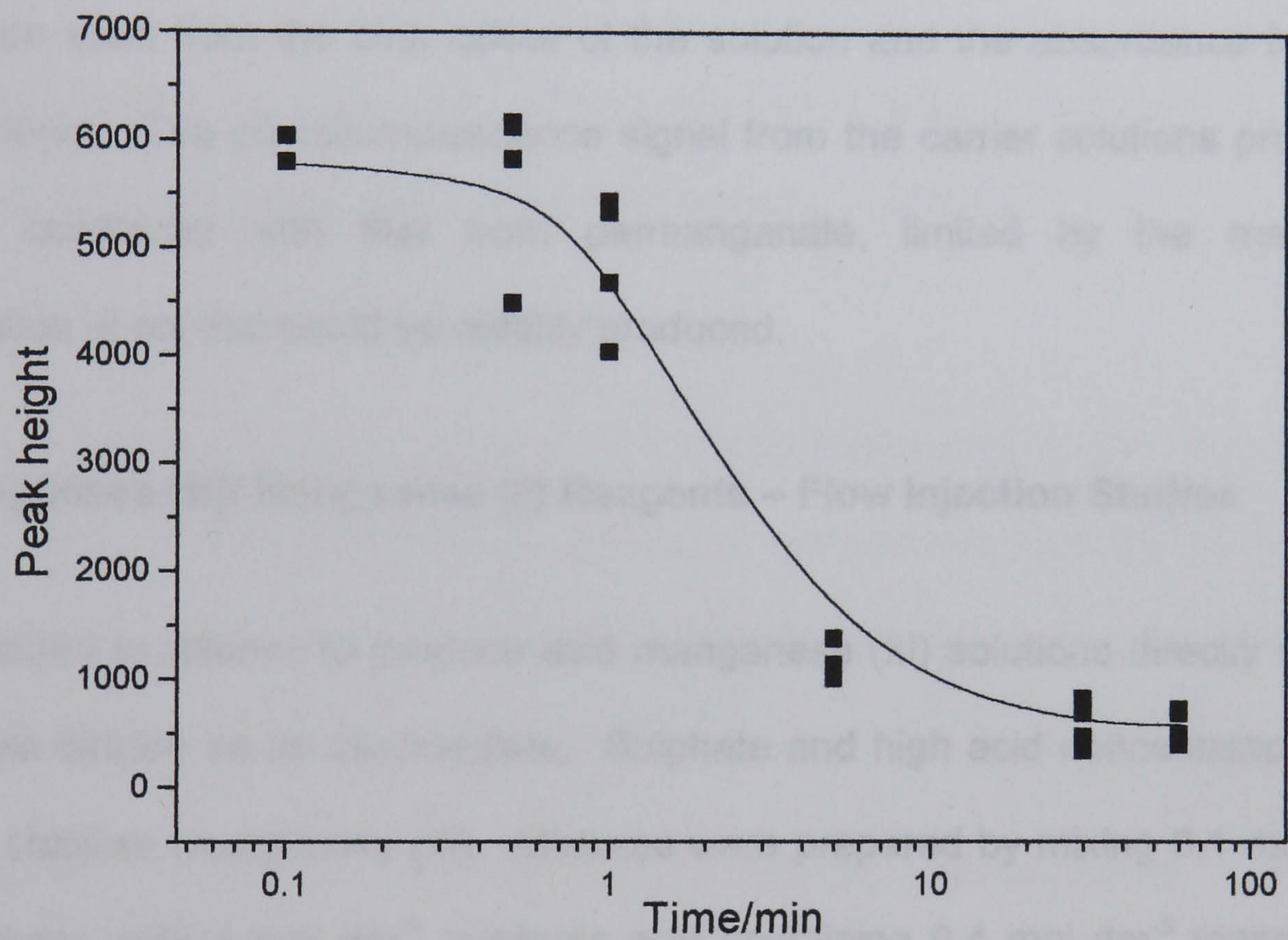




For all the sugars examined increasing the amount of manganese as permanganate, resulted, as expected, in an increase in total emission. Permanganate was found to give a higher signal than the equivalent amount of manganese as manganese (III) acetate.

Investigation of the time of reaction between manganese acetate and sulphuric acid, prior to the addition of sugar, demonstrates the degradation of the compound. After five minutes the peak height was less than 20% of the original, shown in Figure 6.12.

**Figure 6.12 Stability of Acid Manganese (III) acetate**



While intense spectra were obtained using high concentrations of freshly prepared manganese (III), the poor stability of the solution makes the system impractical for use in flow systems.



## **6.4 Manganese (III) Sulphate**

The reaction of manganese (III) acetate and sugars is fast compared with the reaction between sugars and permanganate. There is no lag time between mixing and the reaction reaching its maximum rate. This shows the potential for manganese acetate as an oxidant in the chemiluminescent reaction with sugars. The poor solubility and stability of the compound make it impractical for general use in FIA.

The studies on manganese dioxide sol show that some manganese (III) is produced, This can be seen from the pink colour of the solution and the absorbance band at around 500nm. The chemiluminescence signal from the carrier solutions produced was low compared with that from permanganate, limited by the maximum concentration of sol that could be reliably produced.

### **6.4.1 Manganese (III)/ Manganese (II) Reagents – Flow Injection Studies**

It was decided to attempt to produce acid manganese (III) solutions directly without manganese dioxide as an intermediate. Sulphate and high acid concentrations are known to stabilise manganese (III). Mixtures were prepared by mixing  $0.1 \text{ mol dm}^{-3}$  permanganate, with  $4 \text{ mol dm}^{-3}$  sulphuric acid containing  $0.4 \text{ mol dm}^{-3}$  manganese sulphate and water to give different ratios of manganese (II) and permanganate.

Each mixture was used as a carrier in a single line manifold and  $0.05 \text{ mol dm}^{-3}$  fructose in water was injected. The responses are shown in Table 6.3. The results show a significant increase in signal with increasing permanganate and hence increasing manganese (III). At high permanganate concentration the system was unstable and manganese dioxide precipitated

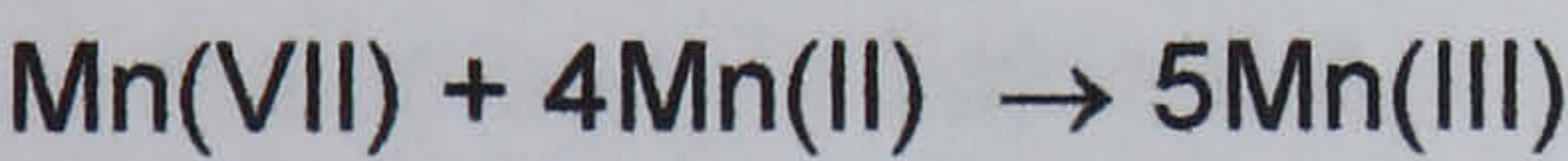


Table 6.3 Calibration slopes for Fructose with Increasing Concentrations of Manganese (II) and (VII)

	Manganese (VII)			
		1x10 <sup>-4</sup>	1x10 <sup>-3</sup>	1x10 <sup>-2</sup>
Manganese(II)	1x10 <sup>-3</sup>	4.27 ± 0.20	11.03 ± 0.21	2.60 ± 0.15
	1x10 <sup>-2</sup>	28.83 ± 0.34	343.50 ± 4.35	MnO <sub>2</sub> ↓
	1x10 <sup>-1</sup>	20.50 ± 0.35	342.08 ± 3.68	MnO <sub>2</sub> ↓

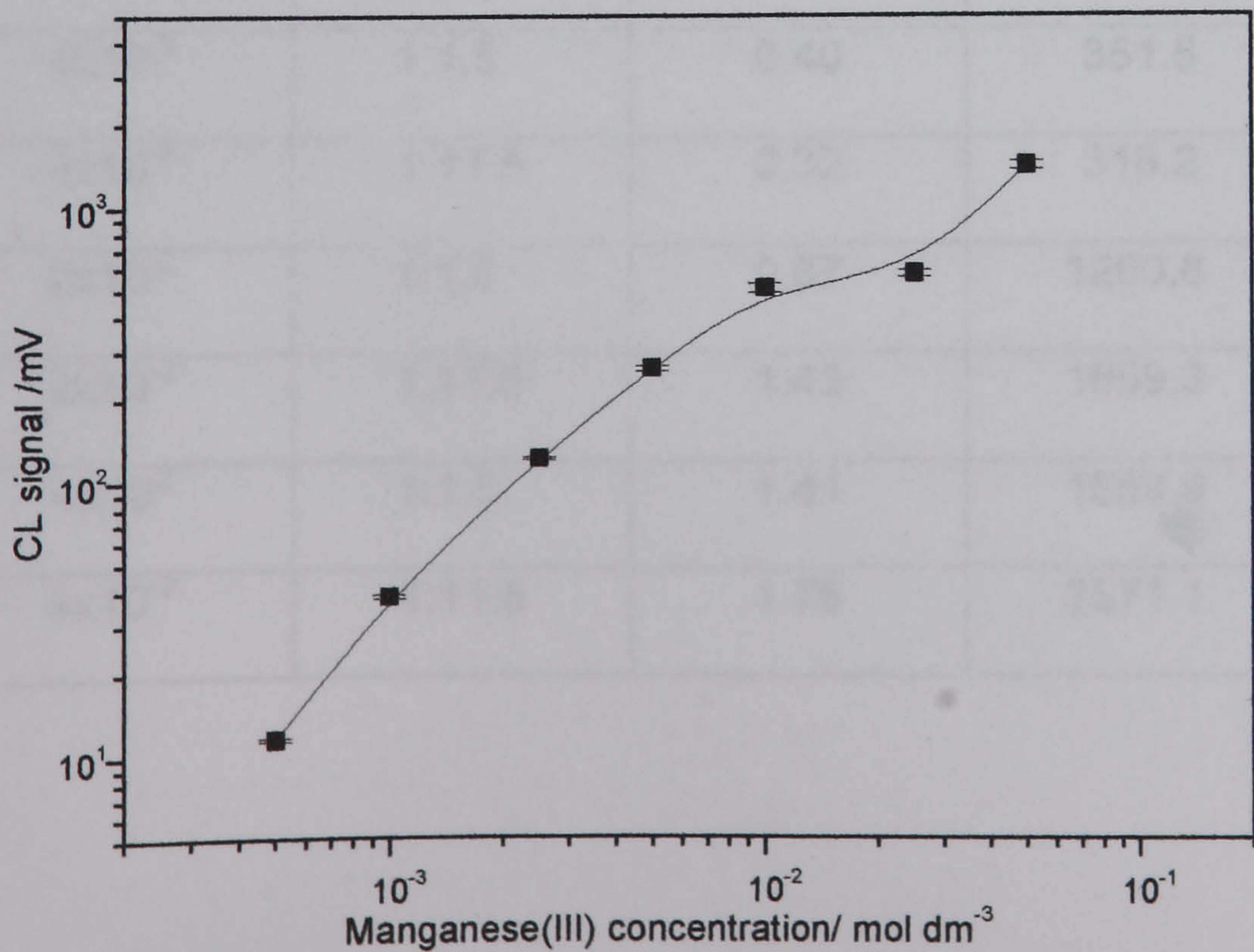
6.4.1.1 Effect of Manganese (III) Concentration

As no pemanganate could be seen in the absorbance spectra it was assumed that all the permanganate had been reduced to manganese (III) as follows:



The effect of increasing the manganese (III) concentration was further investigated. In each case the molar ratio of permanganate to manganese (II) in the mixture was constant at 1:20. Figure 6.13 shows the relationship between manganese (III) concentration and chemiluminescence signal

Figure 6.13 Relationship Between Manganese (III) Concentration and Chemiluminescence





At high concentrations of manganese (III), greater than  $1 \times 10^{-2}$ , the reagent had limited stability. A dark brown precipitate of manganese dioxide formed after a short time. The chemiluminescence signal was higher than had been observed for optimum concentrations of permanganate. For the most concentrated solution the absorbance at 500nm is nearly 1.0AU showing the high concentration of manganese (III) present.

A range of solutions was prepared with different concentrations of manganese (III) and different Mn(III) : Mn(II) ratios. A high acid concentration,  $4 \text{ mol dm}^{-3}$ , was used as this, as expected, stabilised the reagent. Calibrations for glucose, in the range  $1 \times 10^{-4}$  to  $1 \times 10^{-1} \text{ mol dm}^{-3}$ , were made using the manganese mixtures that gave stable solutions. The single line manifold was used. The parameters for the calibration lines are shown in Table 6.4.

Chemiluminescence increased with increasing manganese (III) concentration up to the point where the solution was unstable.

**Table 6.4 Calibration Line Parameters for Fructose with Varying Manganese (II) to Manganese (III) Ratios**

Manganese (III) /mol dm <sup>-3</sup>	Mn(II):Mn(III)	Intercept/ mV	Slope/ mV mol <sup>-1</sup> dm <sup>3</sup>	R
4x10 <sup>-3</sup>	1:0.25	0.37	382.7	0.9990
4x10 <sup>-3</sup>	1:1.5	0.40	351.5	0.9985
4x10 <sup>-3</sup>	1:11.5	0.32	318.2	0.9983
2x10 <sup>-2</sup>	1:1.5	0.87	1200.8	0.9995
2x10 <sup>-2</sup>	1:11.5	1.43	1659.3	0.9991
4x10 <sup>-2</sup>	1:1.5	1.41	1659.9	0.9991
4x10 <sup>-2</sup>	1:11.5	1.76	2571.1	0.9993



#### 6.4.1.2 Effect of Manganese (II) Concentration

In order to investigate the effect of manganese (II) a series of carriers was prepared to contain  $2 \times 10^{-3} \text{ mol dm}^{-3}$  manganese (III) and manganese (II) in the range  $1 \times 10^{-3}$  to  $0.5 \text{ mol dm}^{-3}$ .

Absorbance measurements on the solutions showed a slight increase with increasing manganese (II) from 0.995 to 1.138. The regression line for the relationship between manganese (II) and absorbance had the following parameters: R 0.9389, intercept 1.029 AU slope  $0.115 \text{ AU mol}^{-1} \text{ dm}^3$ .

The molar absorptivity of manganese (III) sulphate, prepared electrochemically, is reported to be in the order of  $120 \text{ dm}^3 \text{ cm}^{-1} \text{ mol}^{-1}$  and to vary with pH.<sup>262</sup> The high value is attributed to the presence of the hydrolysed species  $\text{Mn}(\text{OH})^{2+}$  the concentration of which decreases with increasing acid concentration. Further hydrolysis of this species to  $\text{Mn}(\text{OH})_2^+$  has also been suggested.

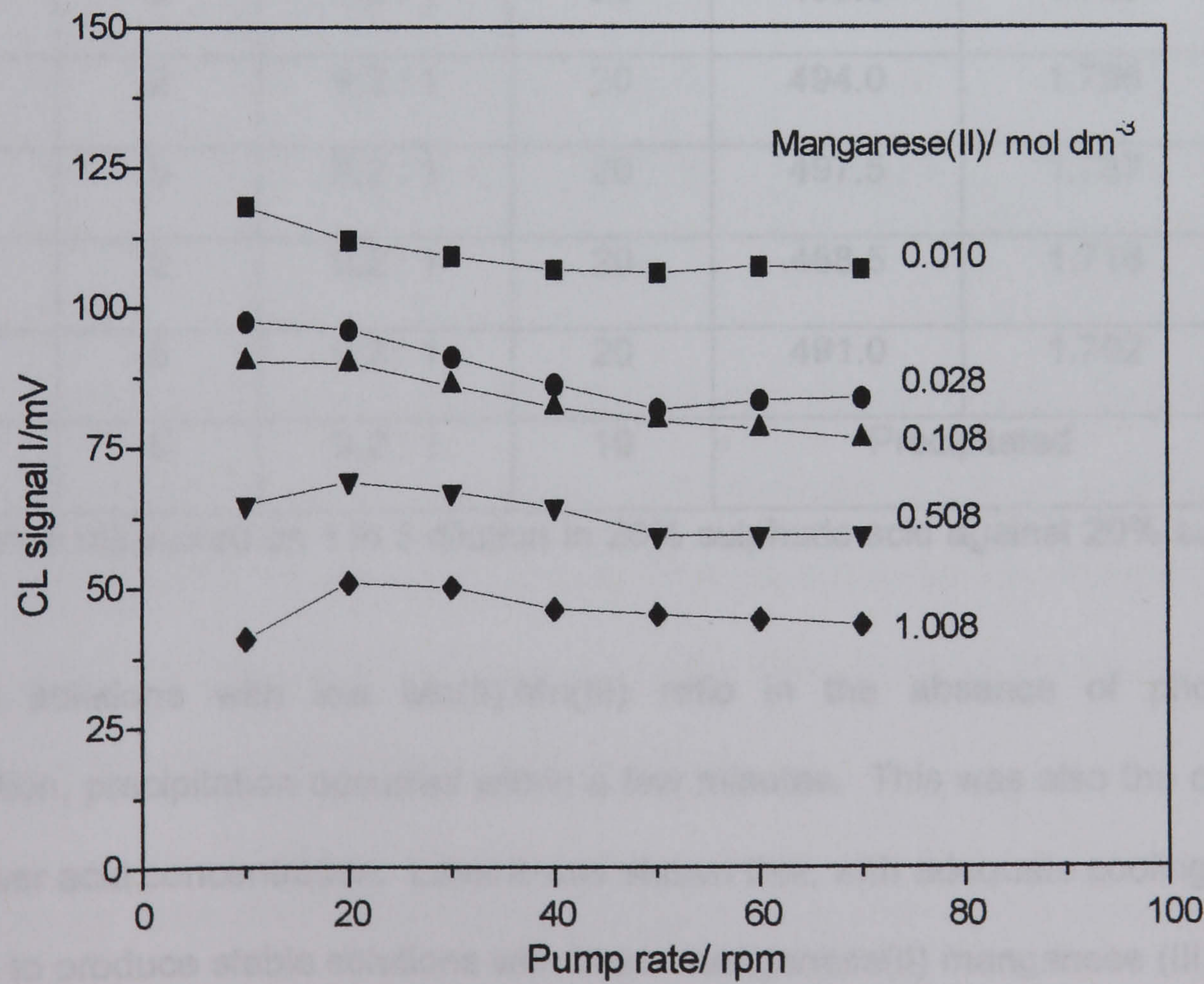
Calibration lines for glucose were constructed as above. For all the calibration lines regressions of the lines were good, at least 0.9999. There is marked reduction in signal with increasing manganese (II) content, shown by the slopes of the calibration lines in Table 6.5. The relationship is not linear; the maximum slope observed,  $1143 \text{ mV mol}^{-1} \text{ dm}^3$  is considerably higher than found for the permanganate system. For a  $0.1 \text{ mol dm}^{-3}$  solution changing the flow rate has a slight effect on the signal size. The variation of signal with the manganese (II) concentration is shown in Figure 6.14. This is considerably lower than the changes in signal with pump speed found for the permanganate system.



Table 6.5 Parameters for Fructose with Increasing Mn (II) Concentration

Mn(II)/mol dm <sup>-3</sup>	Intercept/ mV	Slope / mV mol <sup>-1</sup> dm <sup>3</sup>	R
0.010	0.49	1143.5	0.99994
0.013	0.532	1018.0	0.99994
0.018	0.534	1017.8	0.99996
0.028	0.41	893.9	0.99997
0.058	0.38	859.3	0.99995
0.108	0.37	838.2	0.99994
0.208	0.25	737.9	0.99997
0.508	0.29	637.6	0.99992
1.008	0.22	447.0	0.99993

Figure 6.14 Effect of Flow-rate on Chemiluminescence



0.1 mol dm<sup>-3</sup> fructose inject, carrier 2x10<sup>-3</sup> mol dm<sup>-3</sup> manganese (III) and manganese (II) as indicated



6.4.1.3 Effect of Phosphates

As discussed previously, the addition of phosphates has been reported to enhance the signal for some permanganate systems. It was thought that adding phosphate might allow lower acid concentrations to be used. A range of reagents was prepared to contain 0.05 mol dm<sup>-3</sup> manganese (III). Trisodium trimetaphosphate (TTMP) was added at 0, 2 and 5% w/v. In addition low and high Mn(II):Mn(III) ratios were prepared. The composition of the mixtures is as shown in Table 6.6.

Table 6.6 Preparation of Phosphate Manganese (III) Solutions

Carrier	TTMP/%	MnII:MnIII	Acid/%	Absorbance $\lambda_{\text{max}}$	Absorbance/ AU @491nm
1	0	9.2 : 1	20	488.5	1.763
2	0	1.2 : 1	20	Precipitated	
3	2	1.2 : 1	20	491.0	1.750
4	5	1.2 : 1	20	495.5	1.700
5	2	9.2 : 1	20	494.0	1.796
6	5	9.2 : 1	20	497.5	1.737
7	2	0.2 : 1	20	488.5	1.716
8	5	0.2 : 1	20	491.0	1.702
9	5	9.2 : 1	10	Precipitated	

Absorbance measured on 1 in 3 dilution in 20% sulphuric acid against 20% sulphuric acid

For the solutions with low Mn(II):Mn(III) ratio in the absence of phosphate stabilisation, precipitation occurred within a few minutes. This was also the case for h the lower acid concentration. Later it was shown that, with adequate cooling, it was possible to produce stable solutions with lower manganese(II) manganese (III) ratios. The absorbance values and wavelength maxima were consistent showing that the manganese (III) concentration was approximately the same in all the solutions.



Using the single line manifold, calibrations for glucose and fructose were carried out for the concentration range  $1 \times 10^{-4}$  to  $0.1 \text{ mol dm}^{-3}$ . The effect of flow rate was examined using  $0.1 \text{ mol dm}^{-3}$  glucose and fructose. A flow rate of  $1.3 \text{ cm}^3 \text{ min}^{-1}$  was selected to give reproducible peaks for both glucose and fructose and was a compromise rather than an optimum for either sugar. Regressions were calculated for each solution. The results are shown in table 6.7.

**Table 6.7 Calibration line parameters for Glucose and Fructose with varying Manganese (II) and Manganese (III) Concentrations**

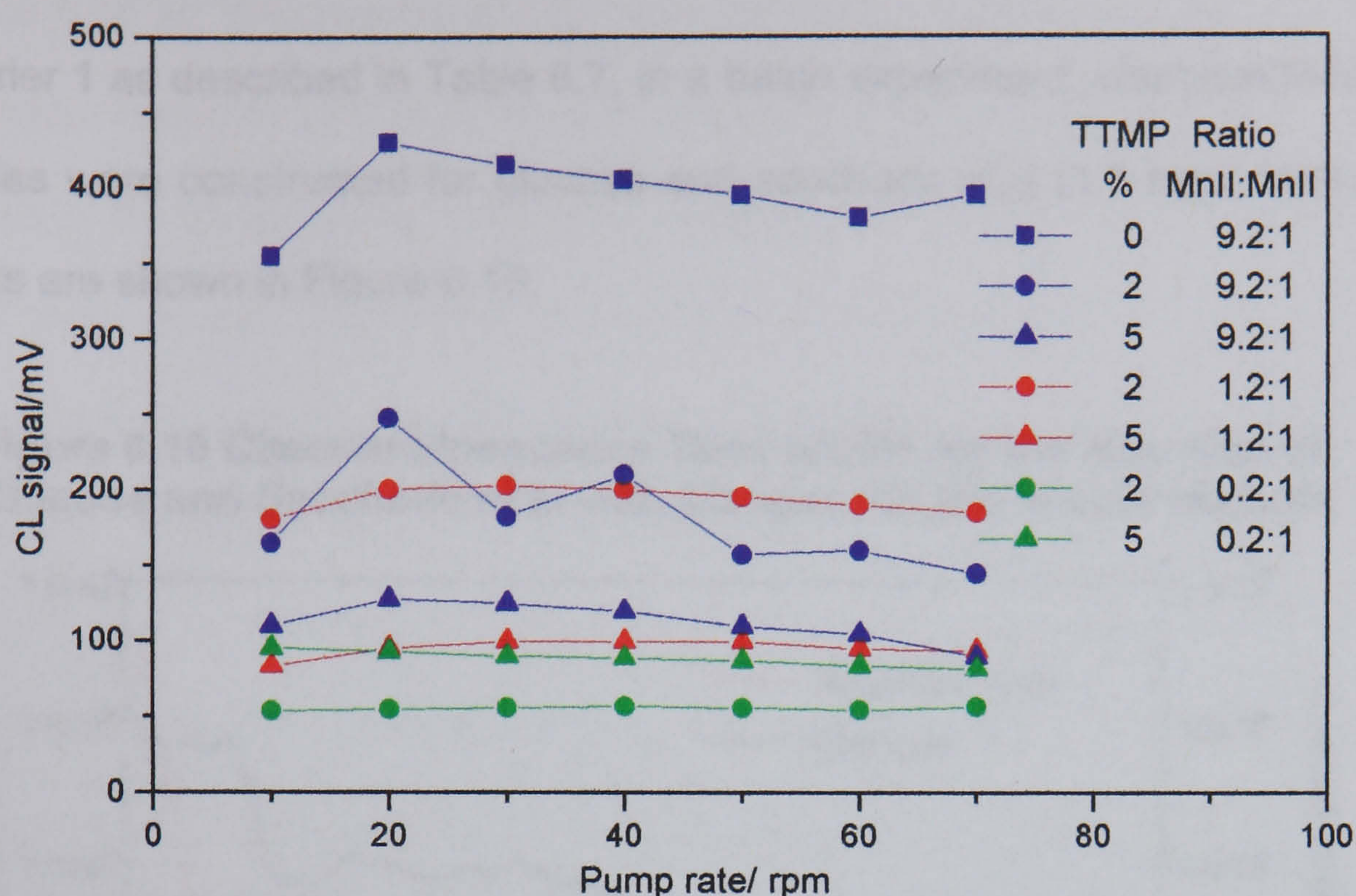
Carrier	Glucose			Fructose			Order	Ratio @ $0.05 \text{ mol dm}^{-3}$
	Intercept/ mV	Slope/ mV $\text{mol}^{-1} \text{ dm}^3$	R	Intercept/ mV	Slope/mV $\text{mol}^{-1} \text{ dm}^3$	R		
1	3.94	3553	0.99787	54.3	21510	0.99045	1	6.3
3	0.20	1995	0.99995	25.0	20753	0.99527	2	12.1
4	0.30	1068	0.99994	12.8	17592	0.99788	5	18.1
5	0.68	1918	0.99977	37.4	20011	0.99315	3	12.3
6	0.35	1240	0.99991	23.2	17808	0.99483	4	16.7
7	0.02	599	0.99994	-4.06	13046	0.99951	7	20.8
8	-0.08	924	0.99924	0.30	15815	0.99988	6	17.6

It can be seen from the values for slope that for both glucose and fructose the order in which the slope increased is the same. This is shown in column 8 of the table. The ratios of signal for fructose and glucose differ, as shown by the example for  $0.05 \text{ mol dm}^{-3}$  solutions shown in the final column of the table, however the ratio increases in almost the reverse order to the increase in slope.

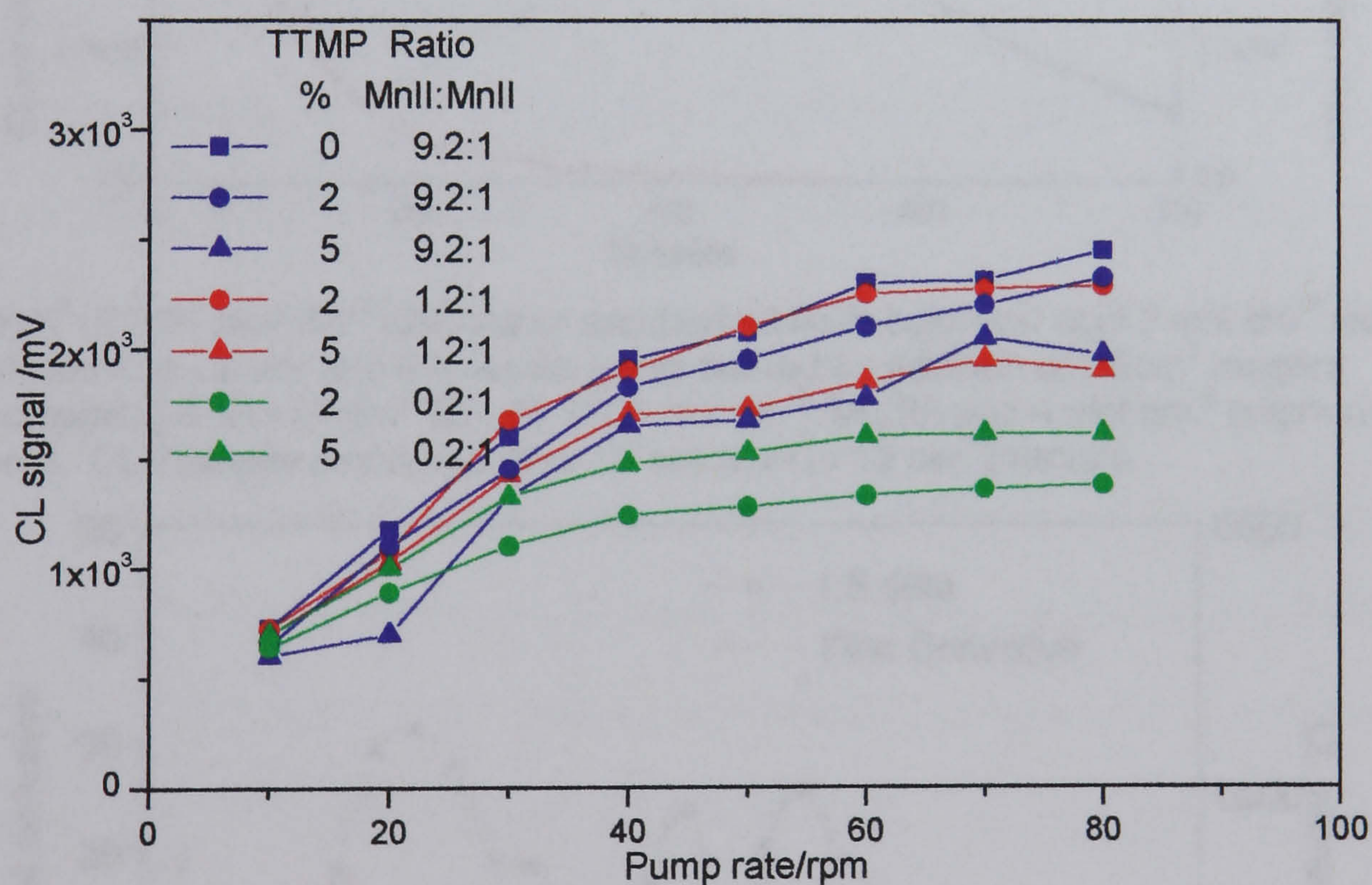
It can also be seen that the effect of phosphate is to reduce the signal and that increasing the manganese (II) to manganese (III) ratio results in an increased signal.



**Figure 6.15 A Effect of Flow-rate on Chemiluminescence for Glucose**



**Figure 6.15 B Effect of Flow-rate on Chemiluminescence for Fructose**



Figures 6.15 A and B show the effects of flow rate on the chemiluminescence signal. The reaction with fructose is faster than the reaction with glucose, and the effect of changing flow rate is more pronounced for fructose than for glucose. Phosphate may be useful for slowing the reaction in some circumstances but in FIA, where fast reactions are desirable, there is no advantage in its use.

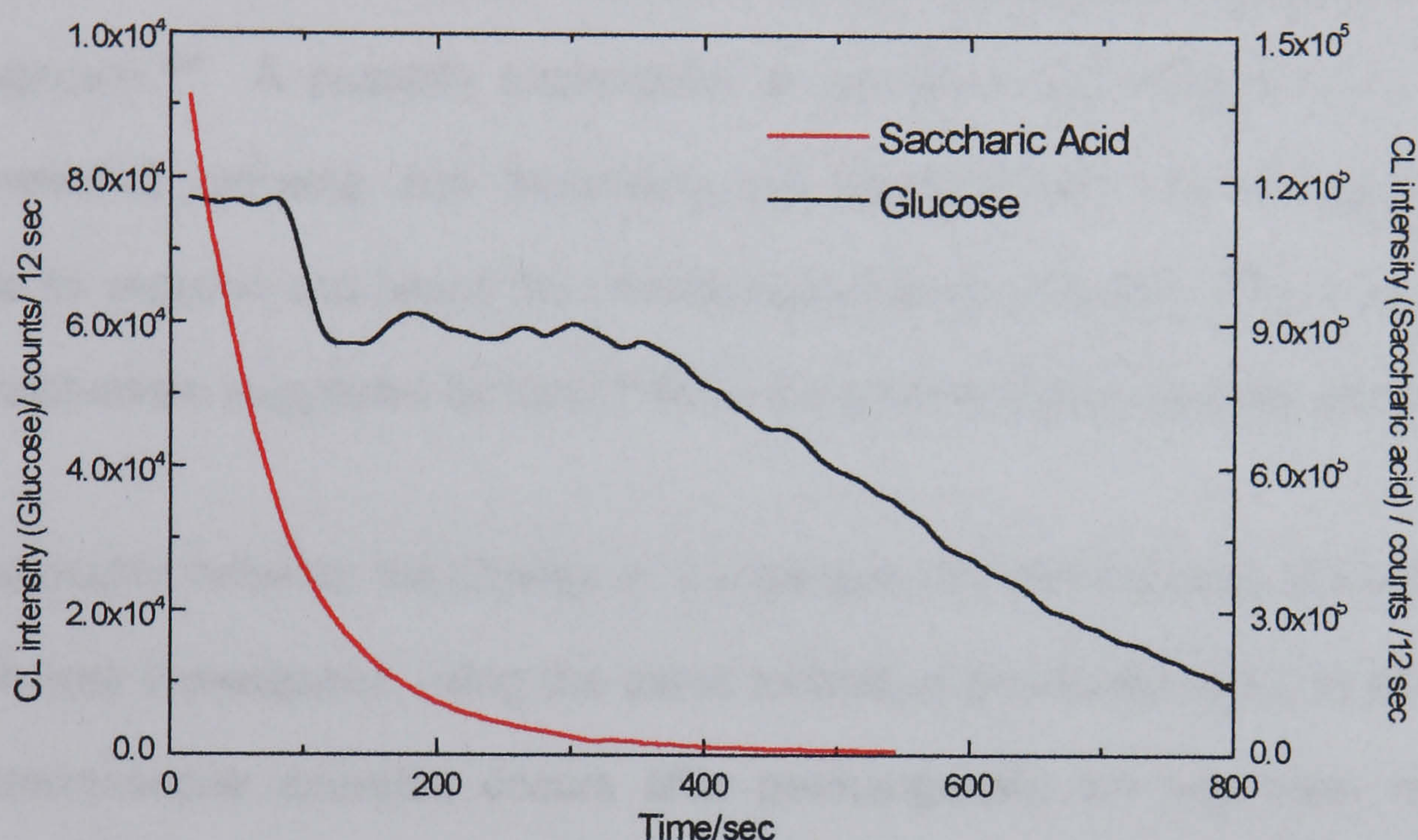


## 6.4.2 Spectroscopic Studies with Glucose

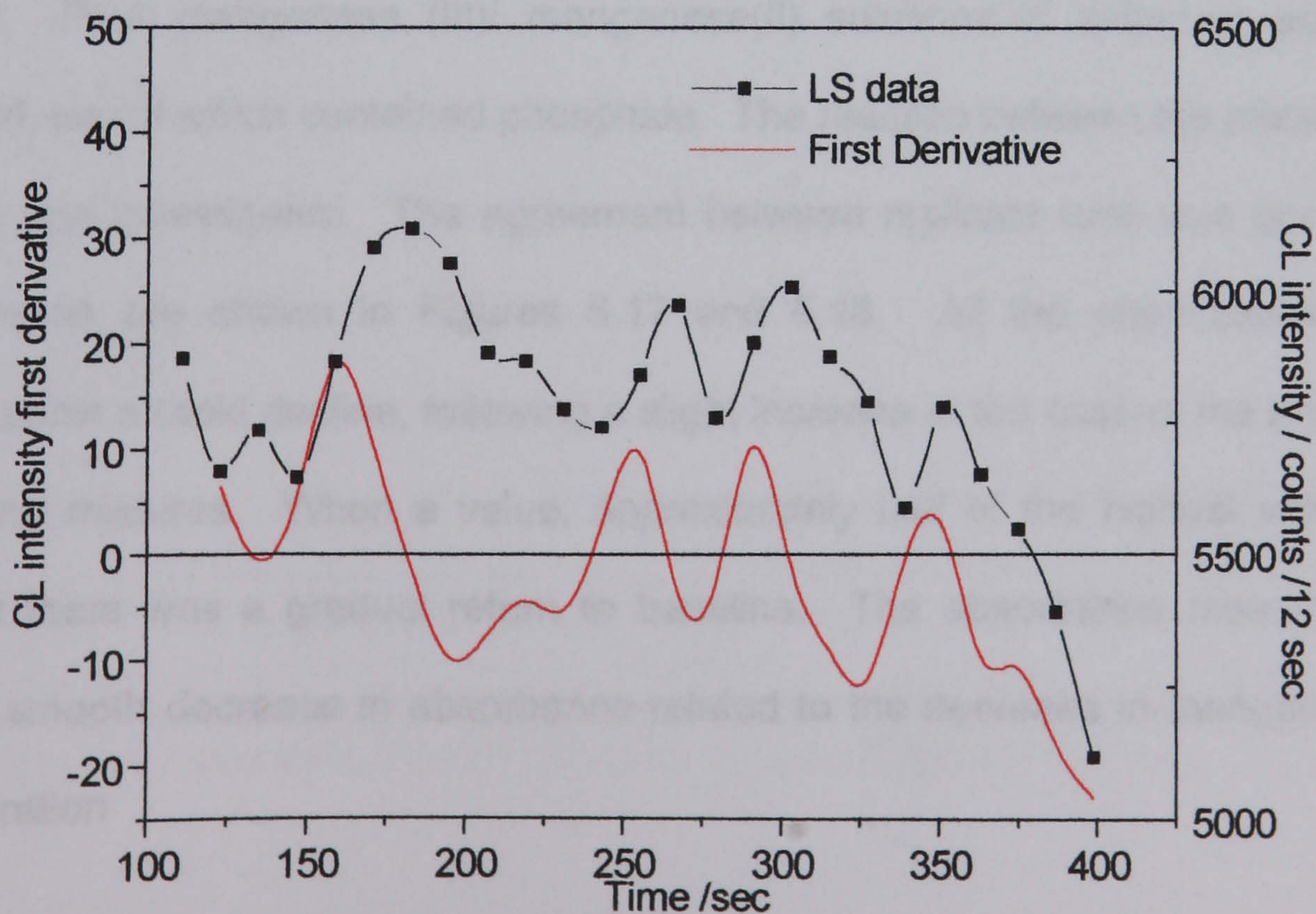
Using carrier 1 as described in Table 6.7, in a batch experiment, chemiluminescence time profiles were constructed for glucose and saccharic acid (1,6 hexandioic acid).

The results are shown in Figure 6.16.

**Figure 6.16 Chemiluminescence Time-profile for the Reaction of Glucose and Saccharic acid with Manganese (III) in acid medium**



2cm<sup>3</sup> of 0.01 mol dm<sup>-3</sup> glucose or saccharic acid in sulphuric acid 2 mol dm<sup>-3</sup> were placed in a LS vial and the reaction was started by addition of 0.5cm<sup>3</sup> reagent containing 0.46 mol dm<sup>-3</sup> Mn (II), 0.05 mol dm<sup>-3</sup> Mn(III) and 4 mol dm<sup>-3</sup> sulphuric acid. CL intensity monitored after 15 sec then at 12 sec intervals.



Area from 100 to 400 sec expanded and first derivative of the interval



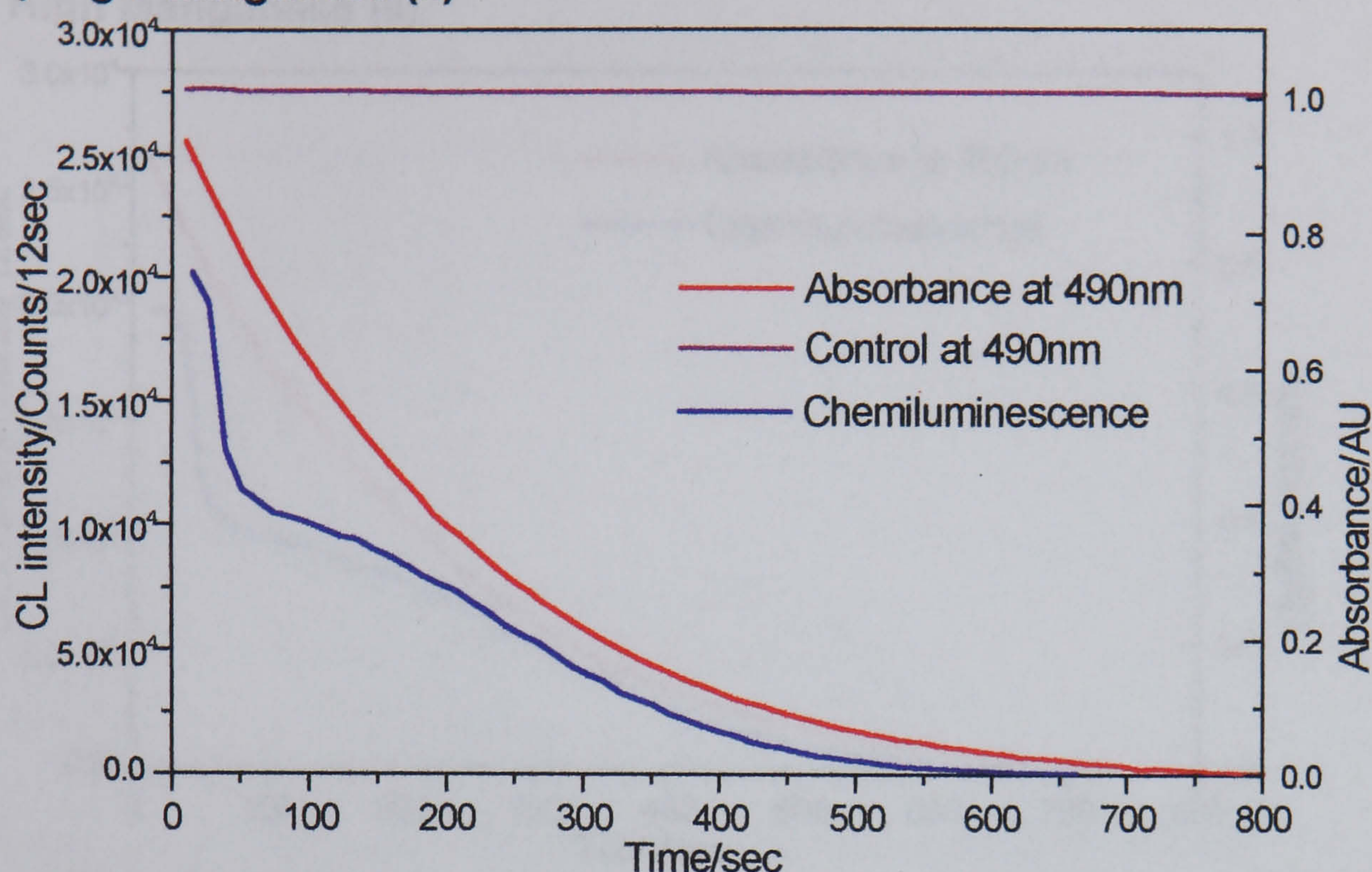
Saccharic acid gave a typical profile for a fast chemiluminescent reaction. The data agrees well with an exponential decay function. The profile for glucose shows an initial decrease followed by a fairly flat area and a final decrease to baseline. The flat area appears to show some oscillation; this can be seen more clearly in the expanded lower figure. The same degree of oscillation was not observed again in repeated attempts, nor in any UV studies. Oscillation has been reported in a permanganate oxalate system, shown by the change in absorbance of permanganate.<sup>134</sup> A possible explanation is formation and reduction of colloidal manganese(IV) reducing and increasing the concentration of manganese (III) available for reaction and hence the chemiluminescence emission. This is analogous to the mechanism suggested by Keki<sup>133</sup> for in the permanganate oxalate system.

The relationship between the change in manganese (III) and the chemiluminescence emission was investigated, using the same technique previously used, to show that chemiluminescence emission occurs after permanganate ion has been reduced. Manganese (III) concentration was monitored by absorbance at 490nm and chemiluminescence emission was monitored using the modified liquid scintillation counter. Four manganese (III)/ manganese(II) solutions in sulphuric acid were prepared, two of which contained phosphate. The reaction between the mixtures and glucose was investigated. The agreement between replicate runs was good. The comparisons are shown in Figures 6.17 and 6.18. All the chemiluminescence profiles show a rapid decline, following a slight increase in the case of the phosphate containing mixtures. When a value, approximately half of the highest value, was reached there was a gradual return to baseline. The absorbance measurements show a smooth decrease in absorbance related to the decrease in manganese (III) concentration



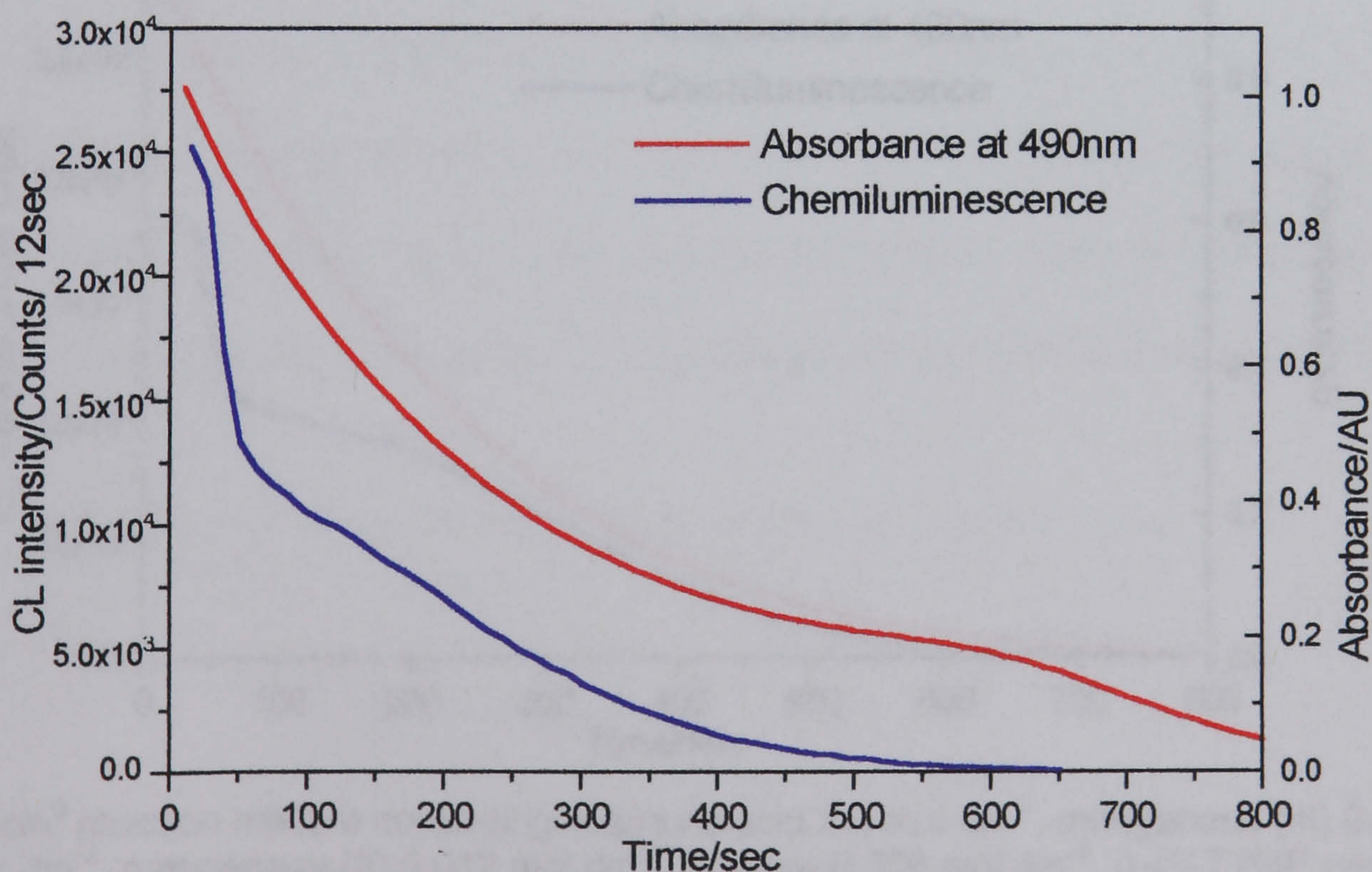
**Figure 6.17 Chemiluminescence and Absorbance Time-profiles for the Reaction of Glucose with Manganese (III) in acid medium**

**A) High Manganese (II)**



2.5cm<sup>3</sup> reaction mixture containing sulphuric acid 2.4 mol dm<sup>-3</sup>, manganese (III) 0.01 mol dm<sup>-3</sup>, manganese (II) 0.092 mol dm<sup>-3</sup>, glucose 0.008 mol dm<sup>-3</sup> in LS vial or UV cuvette. CL intensity monitored after 15 sec then at 12 sec intervals. Absorbance monitored after 10 sec and at 10 sec intervals. Control represents absorbance in the absence of glucose

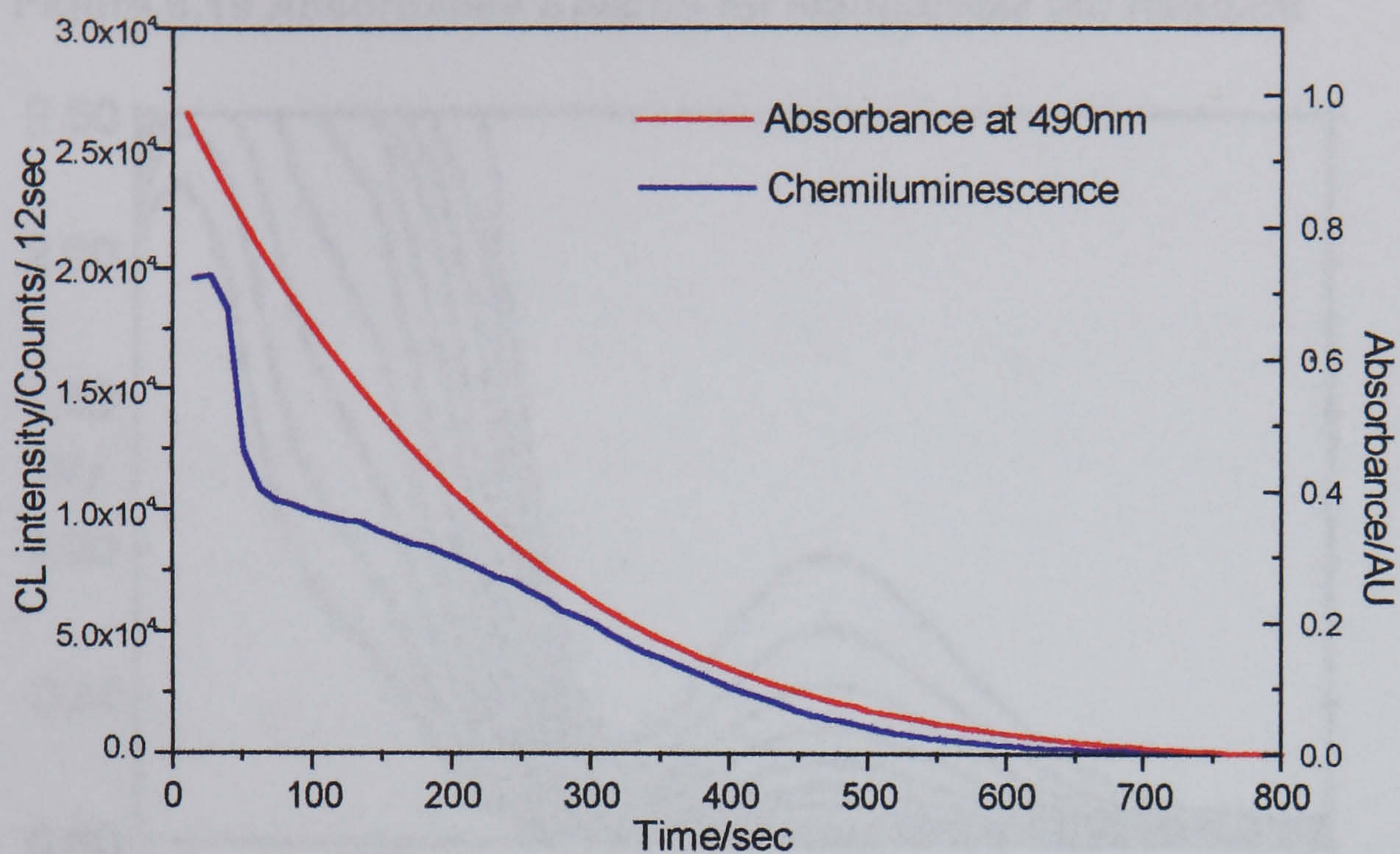
**B) Low Manganese (II)**



2.5cm<sup>3</sup> reaction mixture containing sulphuric acid 2.4 mol dm<sup>-3</sup>, manganese (III) 0.01 mol dm<sup>-3</sup>, manganese (II) 0.012 mol dm<sup>-3</sup>, glucose 0.008 mol dm<sup>-3</sup> treated as above

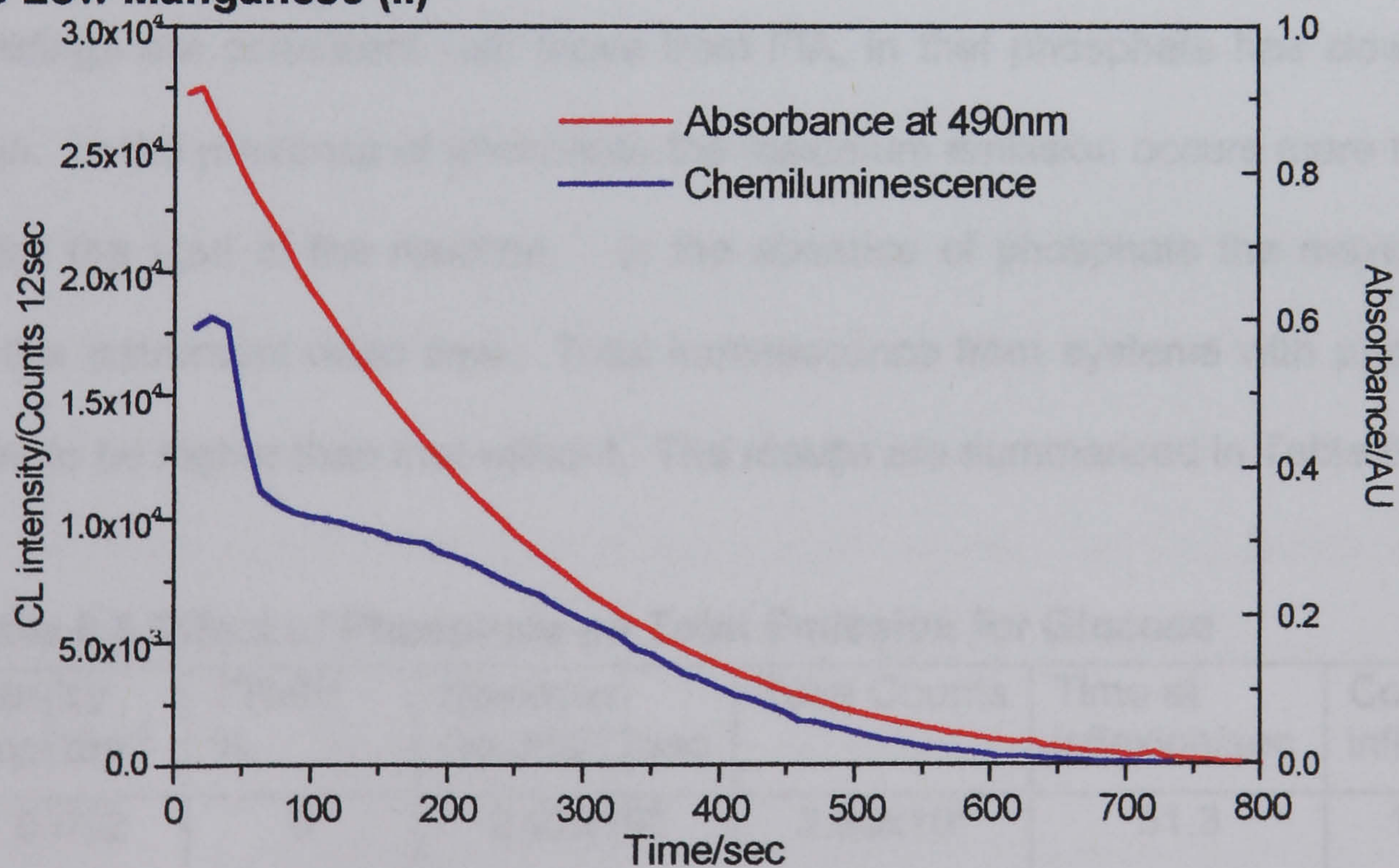


**Figure 6.18 Chemiluminescence and Absorbance Time-profiles for the Reaction of Glucose with Manganese (III) in acid Phosphate medium**  
**A) High Manganese (II)**



2.5cm<sup>3</sup> reaction mixture containing sulphuric acid 2.4 mol dm<sup>-3</sup>, manganese(III) 0.01 mol dm<sup>-3</sup>, manganese (II) 0.092 mol dm<sup>-3</sup>, glucose 0.008 mol dm<sup>-3</sup>, 0.4%TTMP in LS vial or UV cuvette. CL intensity monitored after 15 sec then at 12 sec intervals. Absorbance monitored after 10 sec and at 10 sec intervals.

**B Low Manganese (II)**

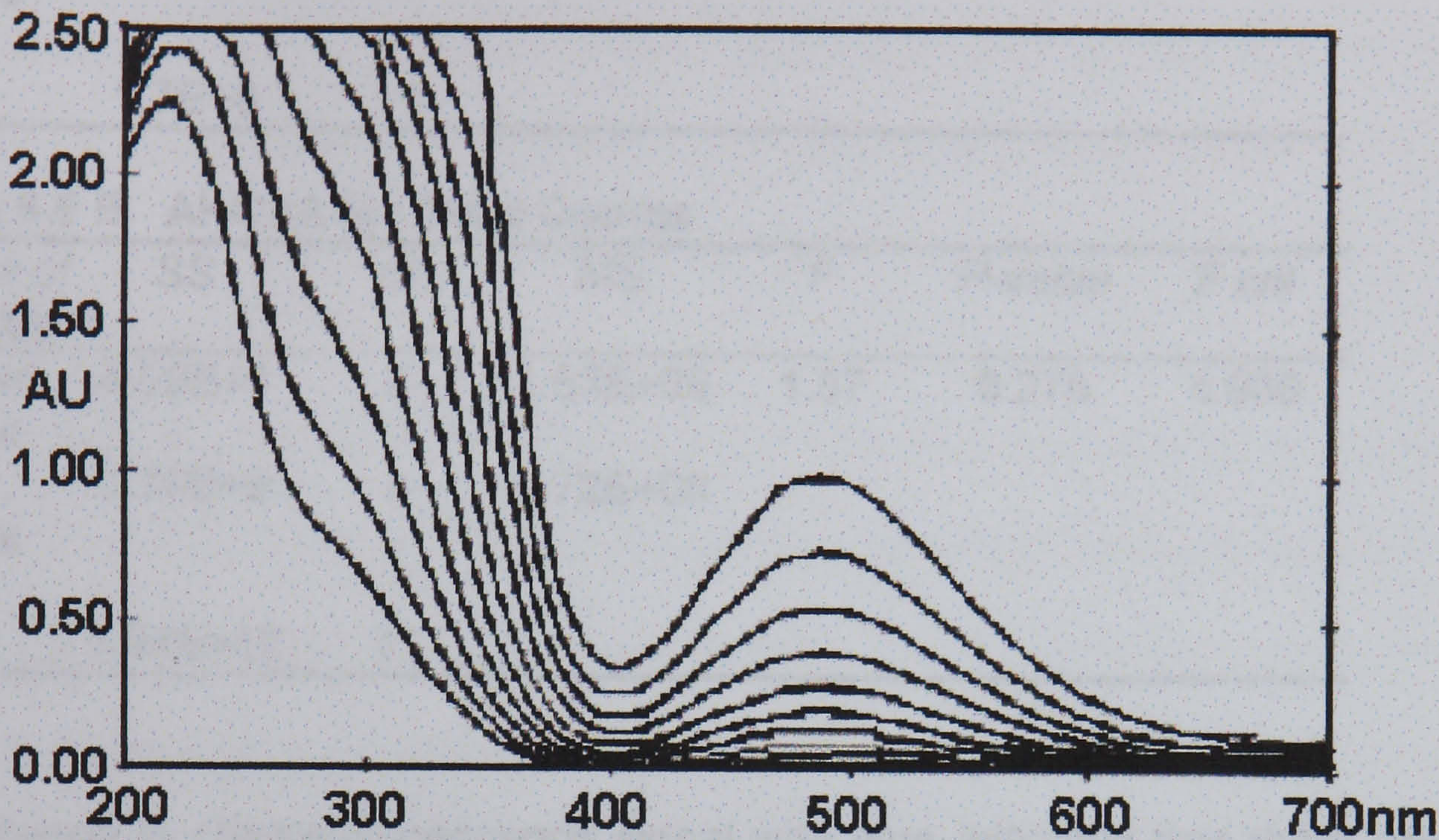


2.5cm<sup>3</sup> reaction mixture containing sulphuric acid 2.4 mol dm<sup>-3</sup>, manganese (III) 0.01 mol dm<sup>-3</sup>, manganese (II) 0.012 mol dm<sup>-3</sup>, glucose 0.008 mol dm<sup>-3</sup>, 0.4%TTMP treated as above



Multiple absorbance scans between 200 and 500nm showed a uniform collapse of the spectrum and no isosbestic points were observed. This is shown in Figure 6.19.

Figure 6.19 Absorbance Spectra for Manganese (III) Reagent



In the absence of glucose no luminescence was observed and no significant decrease in absorbance over 1000 sec. This is the control shown in Figure 6.17A. The findings are consistent with those from FIA, in that phosphate has slowed the reaction. In the presence of phosphate the maximum emission occurs more than 15 sec after the start of the reaction. In the absence of phosphate the maximum is within the instrument dead time. Total luminescence from systems with phosphate appears to be higher than that without. The results are summarised in Table 6.8.

Table 6.8 Effect of Phosphate on Total Emission for Glucose

Mn(II)/ mol dm <sup>-3</sup>	TTMP/ %	Maximum Counts/12sec	Total Counts	Time at inflexion/sec	Counts at inflexion
0.092	0	2.02x10 <sup>4</sup>	2.60x10 <sup>5</sup>	51.3	1.14x10 <sup>4</sup>
0.012	0	2.53x10 <sup>4</sup>	2.70x10 <sup>5</sup>	51.3	1.33 x10 <sup>4</sup>
0.092	0.4	1.97x10 <sup>4</sup>	2.96x10 <sup>6</sup>	63.0	1.10 x10 <sup>4</sup>
0.012	0.4	1.82x10 <sup>4</sup>	3.09x10 <sup>5</sup>	63.0	1.11x10 <sup>4</sup>

Statistical analysis shows that the differences between the signals are not significant.

The results of one way ANOVA are summarised in Tables 6.9 A and B.



**Table 6.9 A ANOVA for Maximum signal**

<i>Source of Variation</i>	<i>SS</i>	<i>df</i>	<i>MS</i>	<i>F</i>	<i>P-value</i>	<i>F crit</i>
Between Groups	8.39E+7	3	2.80E+7	2.59	0.125	4.066
Within Groups	8.62E+7	8	1.08E+8			
Total	1.7E+8	11				

**Table 6.9 B ANOVA for Total Counts**

<i>Source of Variation</i>	<i>SS</i>	<i>df</i>	<i>MS</i>	<i>F</i>	<i>P-value</i>	<i>F crit</i>
Between Groups	4.59E+9	3	1.53E+09	1.57	0.270	4.066
Within Groups	7.78E+9	8	9.72E+08			
Total	1.24E+10	11				

The change in chemiluminescence signal with time indicates that there are two or more phases to the emission. The time to the inflexion between the two parts of the curve was estimated from the second derivative and the size of the signal at this point was measured; the results are shown in the final column of Table 6.8. The shape is similar to that seen for the reaction with manganese dioxide sol, shown in Figure 6.3. The relative sizes of the peaks are reversed. The same mechanism is the probable explanation for this observation. The initial high peak is due to the reaction of glucose with manganese (III), which is in high concentration. At the same time, disproportionation of manganese (III) is taking place. The final, broad emission is due to the oxidation of analyte, which is in excess, by manganese (IV). The second phase of chemiluminescence continues for a longer time due to the colloidal nature of the species formed. Production of manganese dioxide might be expected during the reaction. This would be indicated by an increase in absorbance over a wide wavelength range. In particular the change in absorbance at 400nm would be expected to be slower than at 490nm; this was not observed.



6.4.3 Flow Studies with Phenolic Compounds

The chemiluminescence emitted on oxidation of polyphenolic compounds such as pyrogallol and gallic acid is well known, as discussed in section 2.9.1.2. Most of these reactions are in neutral or alkaline conditions and use hydrogen peroxide as the oxidant. There is a recent report on the permanganate oxidation<sup>171</sup> of pyrogallol. The optimum pH for this reaction was stated to be 1.0.

It was decided to compare any luminescence from the reaction of permanganate with dihydroxy benzoic acids with that for glucose. The single line manifold was used as before and 0.01 mol dm<sup>-3</sup> analyte was injected . The relatively low concentration was selected due to the low solubility of the aromatic acids. Table 6.10shows the results.

Table 6.10 Comparison of CL Signals for Glucose and Dihydroxy benzoic acids

	0% TTMP			2% TTMP		
Analyte	Peak height /mV	±	Relative to Glucose	Peak /mV	height ±	Relative to Glucose
Glucose	49.6	0.81	1.00	32.8	1.07	1.00
2,4 dihydroxy benzoic acid	1.73	0.036	0.04	1.43	0.017	0.04
2,5 dihydroxy benzoic acid	3.07	0.13	0.06	1.98	0.081	0.06
2,6 dihydroxy benzoic acid	18.8	0.31	0.38	18.9	0.52	0.57

Reagent contains 0.05 mol dm<sup>-3</sup> Mn(III), 0.06 mol dm<sup>-3</sup> (MnII), 3.6 mol dm<sup>-3</sup> sulphuric acid and trisodium trimetaphosphate as above

The chemiluminescence from the hydroxy benzoic acids was unexpectedly low. Only 2,6 dihydroxy benzoic acid (γ-resorcylic acid) gave a signal comparable with that for glucose. The signals for 2,4 dihydroxy benzoic (β- resorcylic) and 2,5 dihydroxy benzoic (genistic) acids were less than a tenth of that for glucose, with or without phosphate. The reactions are fast compared with permanganate oxidations of sugars.



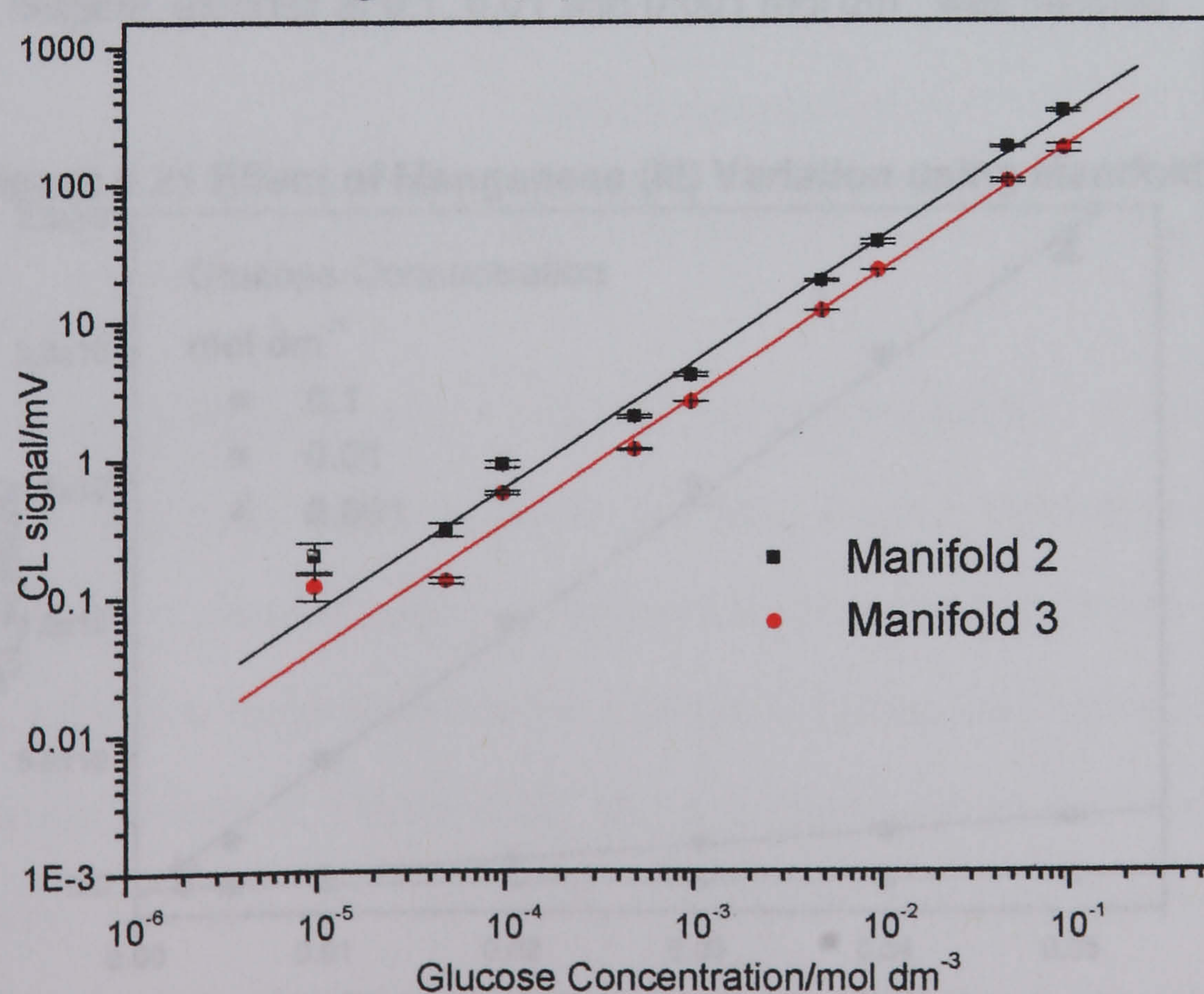
## 6.4.4 Further Flow Studies with Prepared Manganese (III) Reagents

### 6.4.4.1 Investigation of the Manganese (III) Reagent in a Post-column Format.

To investigate the potential use of the system in a post column format for use with a separation system a new manifold was set up. Sugar solution was injected into a water carrier and the reagent was added immediately before the detector via a T piece, manifold 3. This system was compared with the reverse FIA system, manifold 2. It was found that considerable precipitation of manganese dioxide occurred unless a high concentration of acid was present in the carrier stream. The results are shown in figure 6.20.

For both manifolds there was a significant blank signal. The results in figure 6.20 were corrected for the blank but still showed deviation from linearity for the  $10^{-5}$  mol  $\text{dm}^{-3}$  peaks.

**Figure 6.20 Comparison of Manifolds 2 and 3 for Calibration Lines with Glucose and Manganese (III) Reagent**



Reagent prepared from 16.9 g manganese sulphate, 0.158 g permanganate, 10  $\text{cm}^3$   $\text{H}_2\text{SO}_4$  in 100  $\text{cm}^3$ . Glucose concentration as indicated carrier 1.8 mol  $\text{dm}^{-3}$  acid.



Examination of the parameters for the linear fits demonstrates that manifold 2 gave considerably higher signals as shown in Table 6.11

**Table 6.11 Parameters for Glucose Calibration lines**

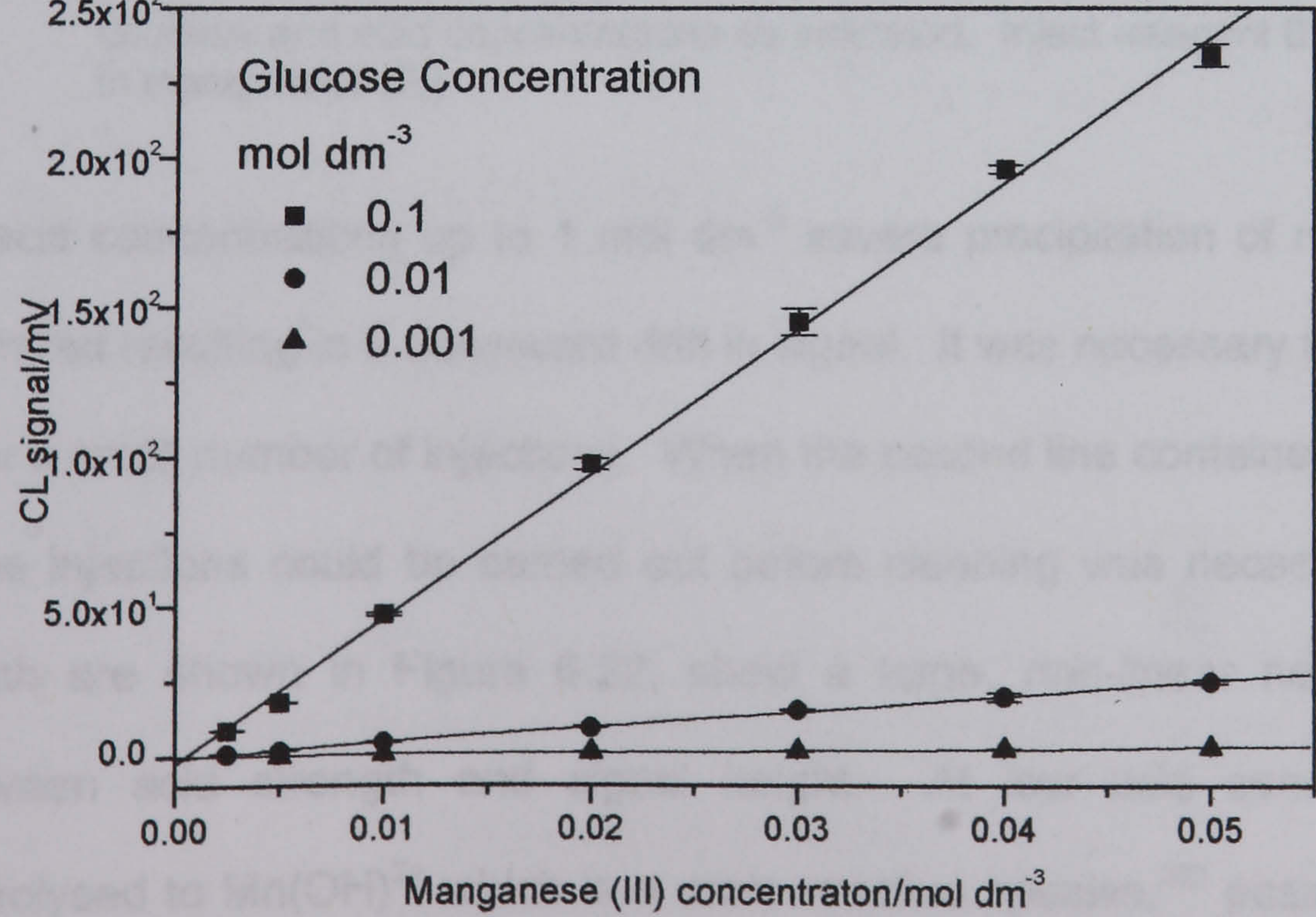
Manifold	Intercept/ mV	Slope / mV mol <sup>-1</sup> dm <sup>3</sup>	R
2	1.7	3292	0.9992
3	1.7	1776	0.9978

Results with manifold 3 demonstrated the reagent’s potential usefulness in a post column situation. The sensitivity was considerably better than with permanganate. Manifold 2 gave the higher signals and was used in further optimisation.

**6.4.4.2 Effect of Manganese (III) and acid Concentrations**

Strong manganese (III) reagent was prepared, as before, in 20% of concentrated sulphuric acid (3.6 mol dm<sup>-3</sup>). Dilutions were carried out using 20% sulphuric acid to give nominal manganese (III) concentrations between 0.0025 and 0.05 mol dm<sup>-3</sup>. For each reagent, glucose at 0.1, 0.01 and 0.001 mol dm<sup>-3</sup> was injected.

**Figure 6.21 Effect of Manganese (III) Variation using Manifold 2**



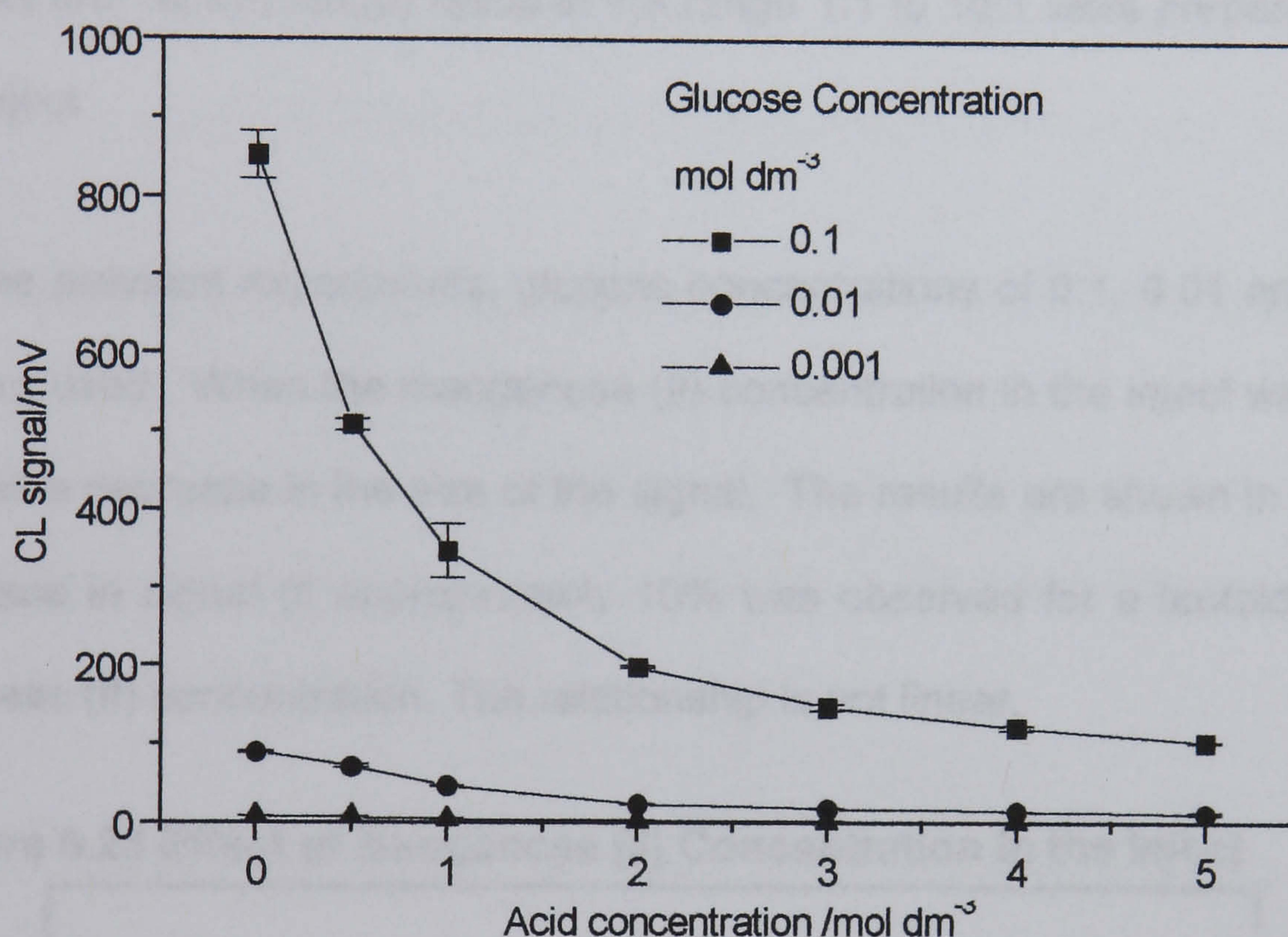
Glucose and manganese (III) concentrations as indicated carrier 2- 2 mol dm<sup>-3</sup> acid



An almost linear relationship between manganese (III) concentration and signal was observed as shown in Figure 6.21.

The effect of the acid concentration was also investigated further. Using the full strength reagent, nominal manganese (III)  $0.05 \text{ mol dm}^{-3}$ , the concentration of acid in the second line was varied between zero and  $5 \text{ mol dm}^{-3}$  giving a range of acid concentrations from zero to  $2.5 \text{ mol dm}^{-3}$  in the mixed acid/ glucose solution.

**Figure 6.22 Effect of Acid Variation using Manifold 2**



Glucose and acid concentrations as indicated. Inject -reagent  $0.05 \text{ mol dm}^{-3}$  in manganese (III)

At acid concentrations up to  $1 \text{ mol dm}^{-3}$  severe precipitation of manganese dioxide occurred resulting in a downward drift in signal. It was necessary to clean the system after a small number of injections. When the second line contained water only two or three injections could be carried out before cleaning was necessary. The results, which are shown in Figure 6.22, show a large, non-linear negative relationship between acid strength and signal height. At low acid concentration  $\text{Mn}^{3+}$  is hydrolysed to  $\text{Mn}(\text{OH})^{2+}$  which is a more reactive species,<sup>262</sup> possibly explaining the higher signal.

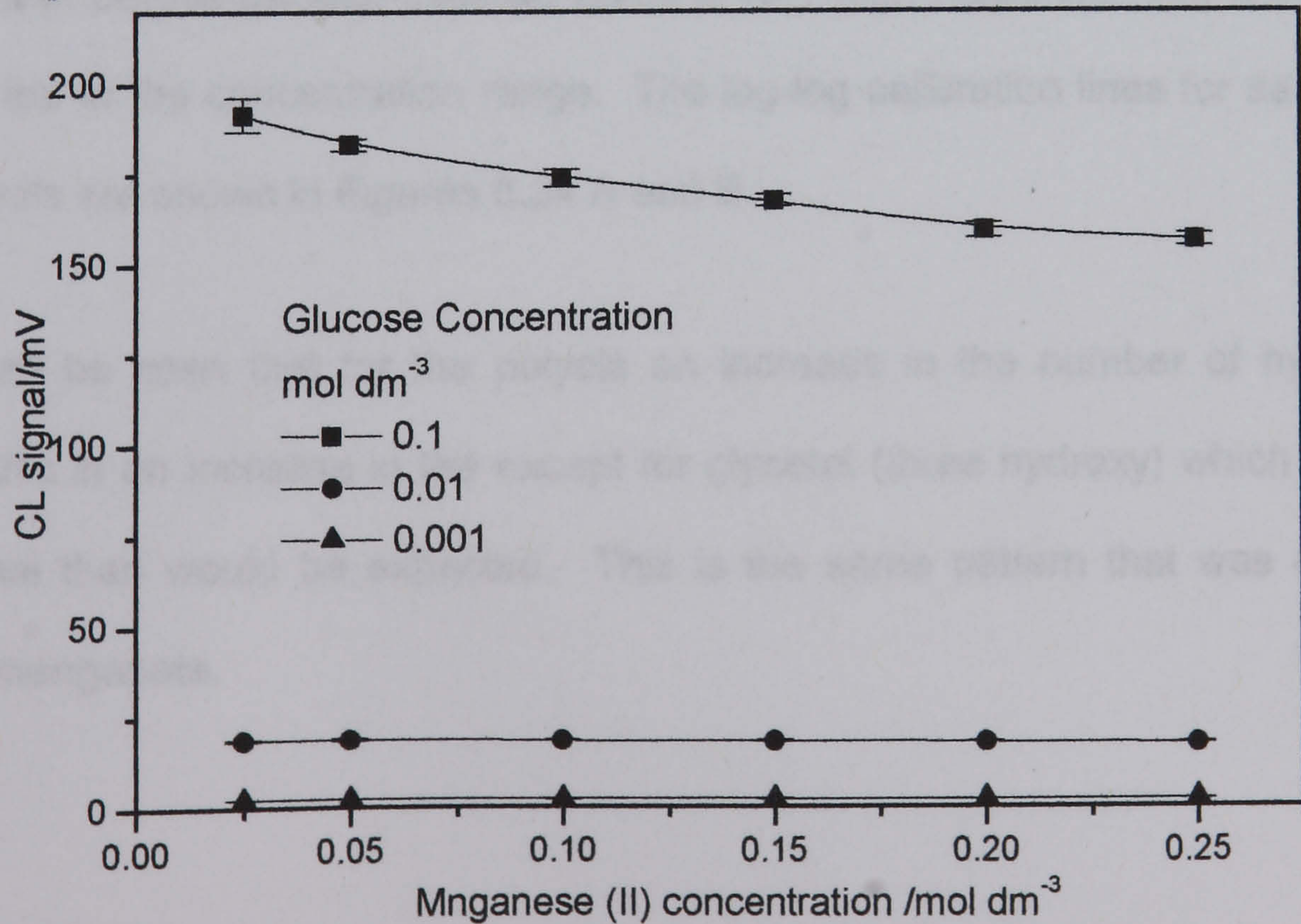


6.4.4.3 Effect of Manganese (II) Concentration

Continuing to use manifold 2 the effects of manganese (II) concentration in the carrier and in the inject were investigated. From previous work it was evident that, as expected, high levels of acid and high levels of manganese (II) stabilise the manganese(III) reagent. It was found that using 20% concentrated acid and cooling the reagent on ice during preparation and in use a reagent with a Mn(II):Mn(III) ratio of 1:1 could be reproducibly prepared. Using a nominal Mn(III) concentration of 0.025 mol dm<sup>-3</sup> Mn(II):Mn(III) ratios in the range 1:1 to 10:1 were prepared and used as the inject.

As for the previous experiments, glucose concentrations of 0.1, 0.01 and 0.001 mol dm<sup>-3</sup> were used. When the manganese (II) concentration in the inject was increased there was a decrease in the size of the signal. The results are shown in Figure 6.23. A decrease in signal of approximately 10% was observed for a tenfold increase in manganese (II) concentration. The relationship is not linear.

Figure 6.23 Effect of Manganese (II) Concentration in the Inject



Inject - manganese(III) 0.025 mol dm<sup>-3</sup>, acid 2mol dm<sup>-3</sup>, manganese(II) and glucose concentrations as shown



As for the previous experiments, glucose concentrations of 0.1, 0.01 and 0.001 mol dm<sup>-3</sup> were used. When the manganese (II) concentration in the inject was increased there was a decrease in the size of the signal. The results are shown in Figure 6.23. A decrease in signal of approximately 10% was observed for a tenfold increase in manganese (II) concentration. The relationship is not linear.

Finally, manganese (II) was added to the carrier so that glucose and manganese (II) were mixed before the manganese(III) was injected. The concentrations of glucose and acid were as for the previous experiment. In this there was little change in the chemiluminescence signal with increasing manganese (II) concentration.

#### **6.4.4.4 Comparisons for Different Saccharides and Related Compounds**

Calibration lines were run for a range of saccharides and related compounds using the conditions established above for manifold 2. The parameters for linear-linear plots are shown in table 6.12.

As with permanganate, fructose gives a very high response, and linearity is lost at the top of the concentration range. The log-log calibration lines for saccharides and polyols are shown in Figures 6.24 A and B.

It can be seen that for the polyols an increase in the number of hydroxy groups results in an increase in the except for glycerol (three hydroxy) which gives a lower signal than would be expected. This is the same pattern that was observed with permanganate.



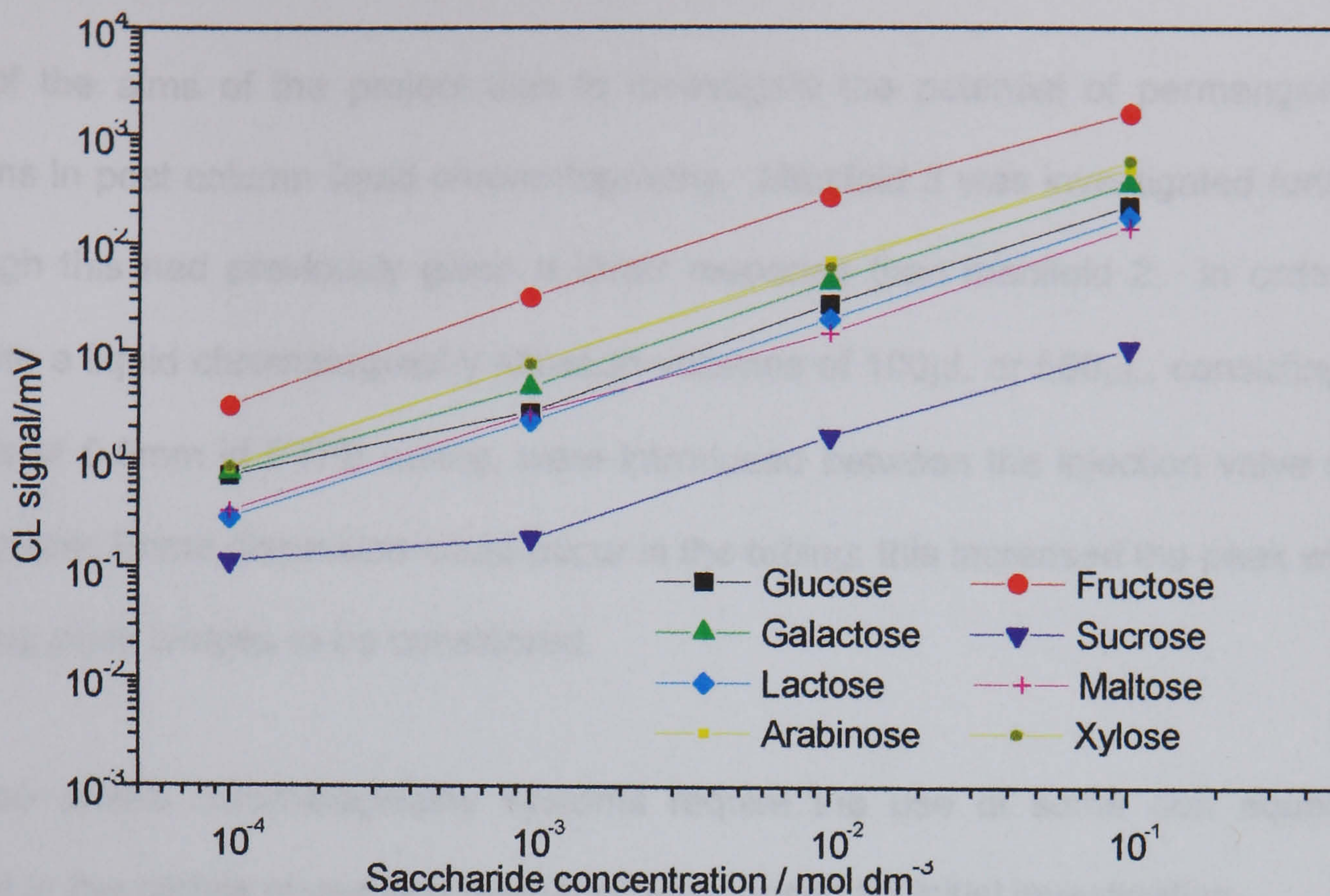
**Table 6.12 Parameters for Calibration lines for Saccharides and Related Compounds**

Compound	Slope /mV mol dm <sup>-3</sup>		Intercept /mV		R
	Value	sd ±	Value	sd ±	
Glucose	2389	28	1.5	1.5	0.99979
Galactose	3731	50	2.5	2.2	0.99973
Fructose 0.0001 to 0.01	16439	642	31	28	0.99772
	27898	334	2.1	1.9	0.99993
Arabinose	5128	107	5.2	4.8	0.99934
Xylose	6057	13	1.1	0.58	0.99999
Maltose	1487	6.4	0.62	0.29	0.99997
Sucrose	173	3.2	0.15	0.14	0.99876
Lactose	1886	12.4	0.78	0.56	0.99994
Mannitol	3717	738	37.8	33.2	0.94561
Sorbitol	8758	1628	87	73	0.95188
Glycerol	201	2.1	0.27	0.10	0.99983
Meso erythritol	2680	102	4.9	4.6	0.99785
1,2 Propandiol	1418	29	1.5	1.3	0.99936
Formaldehyde	16	1.2	0.13	0.05	0.99109
Glucosamine	13	1.2	0.10	0.05	0.99870

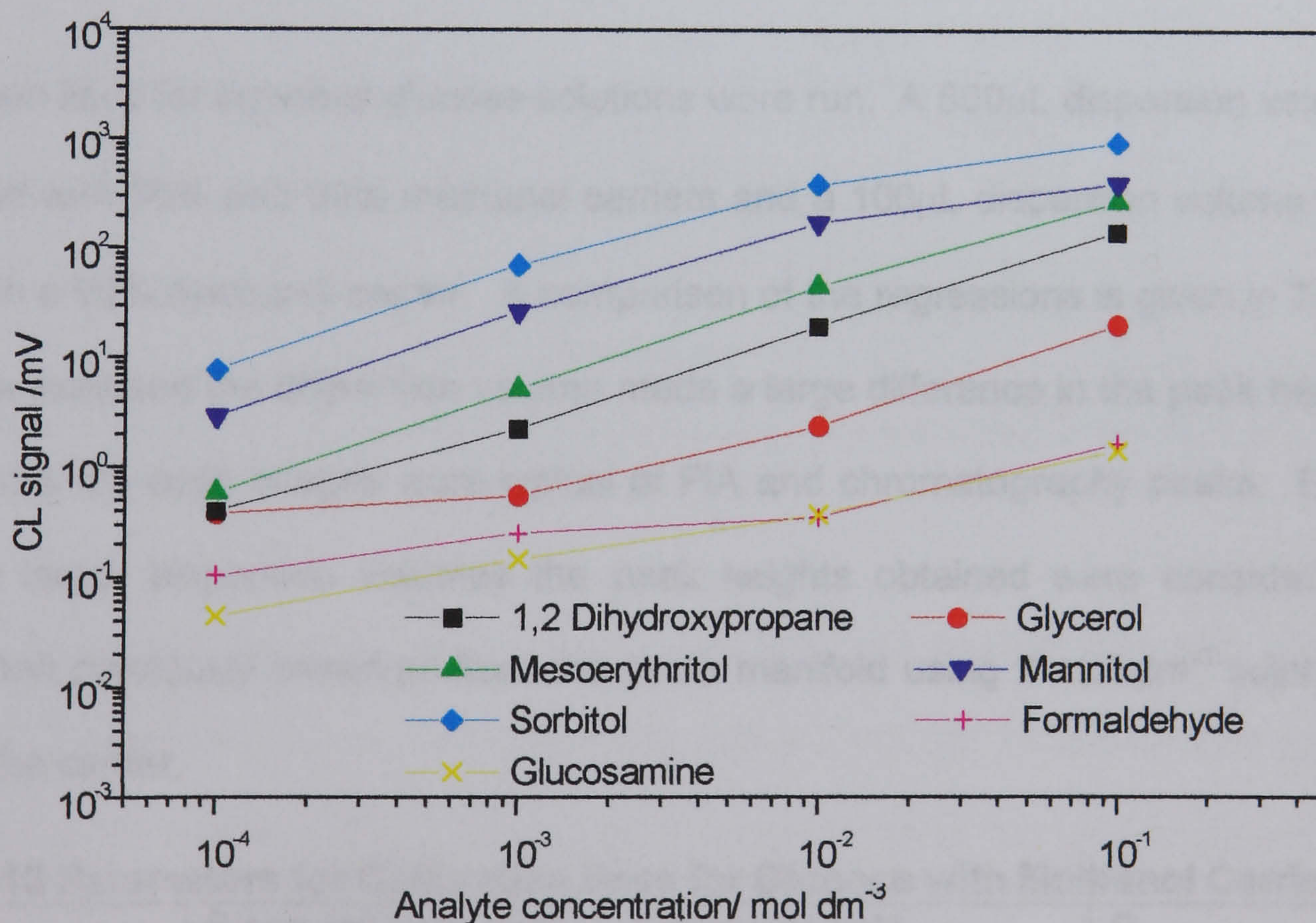
Concentration range 1x10<sup>-4</sup> to 0.1 mol dm<sup>-3</sup> unless otherwise indicated



**Figure 6.24 A Calibration lines for Mono- and Disaccharides**



**Figure 6.24 B Calibration lines for Polyols and Related Compounds**



Manifold 2 carrier sulphuric acid 2 mol dm<sup>-3</sup>, inject manganese reagent 0.05 mol dm<sup>-3</sup> Mn (III), analyte concentrations as shown



6.4.5 Effects of Organic Solvents on Chemiluminescence Signal

One of the aims of the project was to investigate the potential of permanganate systems in post column liquid chromatography. Manifold 3 was investigated further, although this had previously given a lower response than manifold 2. In order to simulate a liquid chromatography situation volumes of 100µL or 500µL, consisting of lengths of 0.8mm id PTFE tubing, were introduced between the injection valve and the T piece. Some dispersion could occur in the tubing; this increased the peak width enabling peak shapes to be considered.

Reverse phase chromatography systems require the use of some non aqueous solvent in the mobile phase and methanol was chosen for initial investigation.

6.4.5.1 Effect of Adding Methanol to the Carrier

Calibration lines for aqueous glucose solutions were run. A 500µL dispersion volume was used with 80% and 90% methanol carriers and a 100µL dispersion volume was used with a 90% methanol carrier. A comparison of the regressions is given in Table 6.13. As expected the dispersion volume made a large difference in the peak height. In all cases the peak shapes were typical of FIA and chromatography peaks. Even with the larger dispersion volumes the peak heights obtained were considerably higher than previously observed from the same manifold using 2 mol dm<sup>-3</sup> sulphuric acid as the carrier.

Table 6.13 Parameters for Calibration lines for Glucose with Methanol Carriers

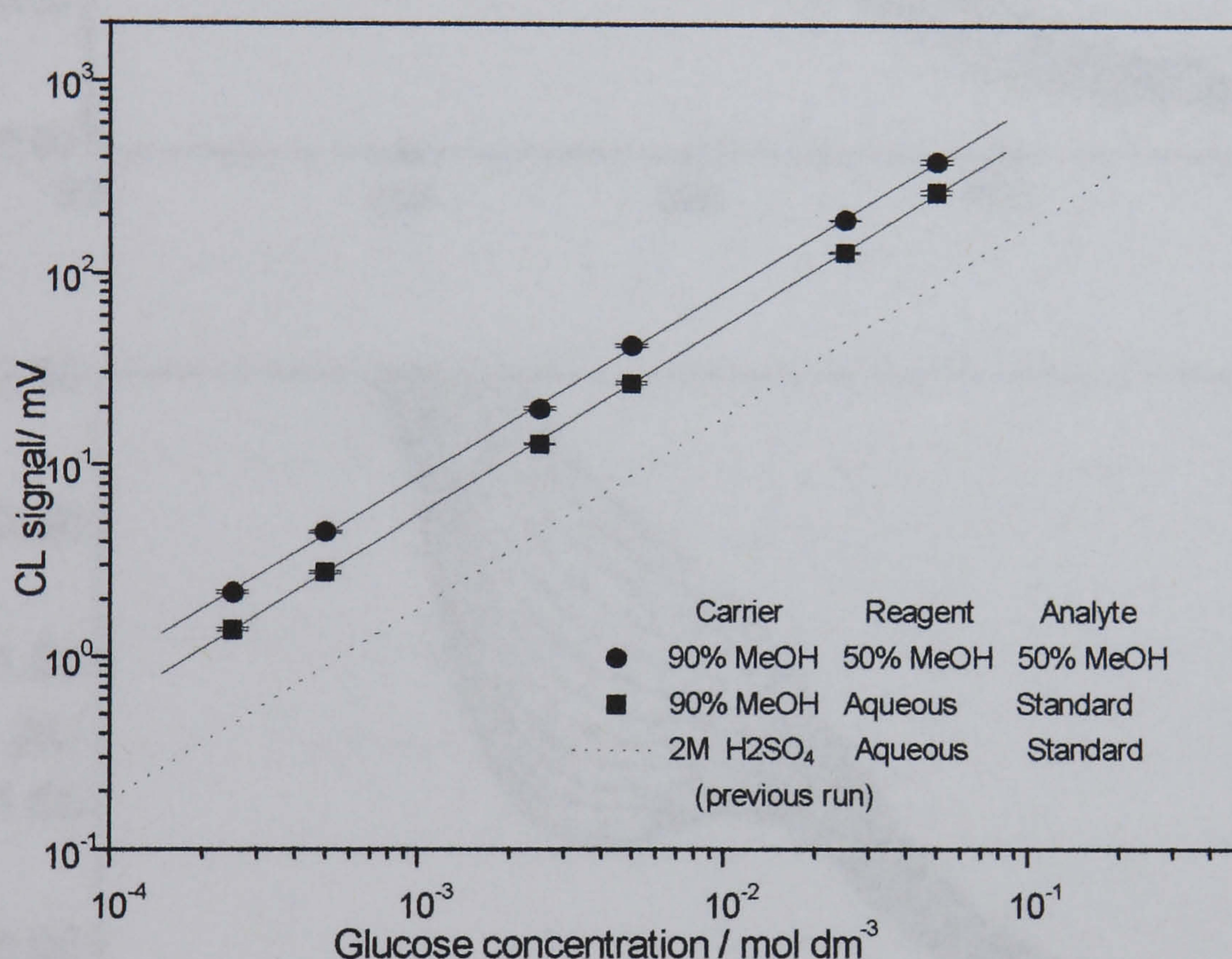
Carrier	Slope /mV mol dm <sup>-3</sup>		Intercept /mV		R
	Value	sd ±	Value	sd ±	
80% Methanol 500µL	3318	42	-0.3	0.8	0.99951
90% Methanol 500µL	3749	15	-0.5	0.6	0.99996
90% Methanol 100µL	5403	31	-0.002	0.6	0.99990



#### 6.4.5.2 Effect of Adding Methanol to the Reagent

To increase the percentage of methanol in the system the calibration was repeated using standards prepared in 50% methanol and diluting the reagent with an equal volume of methanol. Although the reagent concentration was reduced to half, the slope of the calibration line increased from 5403 to 7786 mV mol<sup>-1</sup> dm<sup>3</sup>.

**Figure 6.25 Effect of Methanol on the Calibration lines for Glucose**

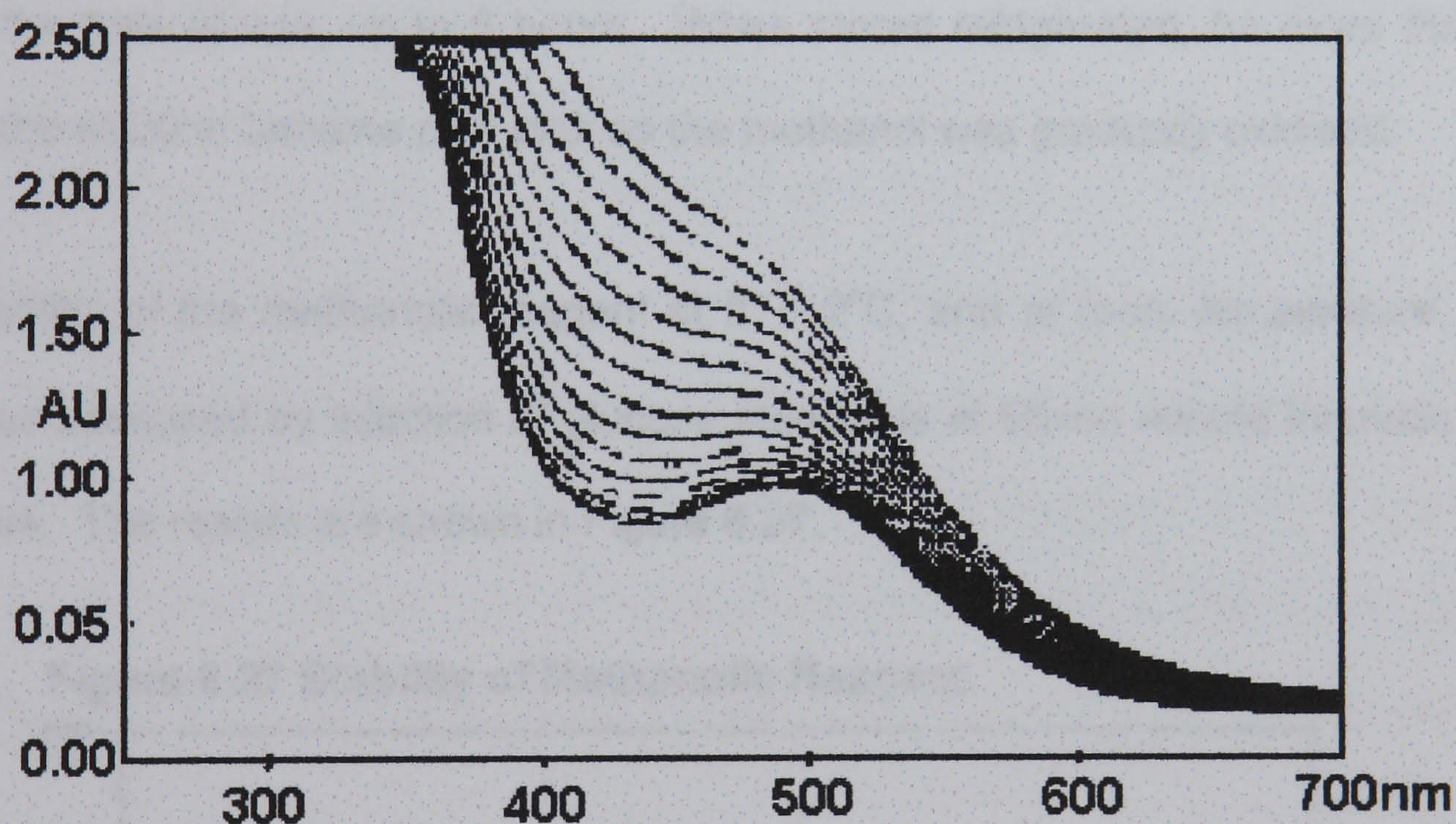
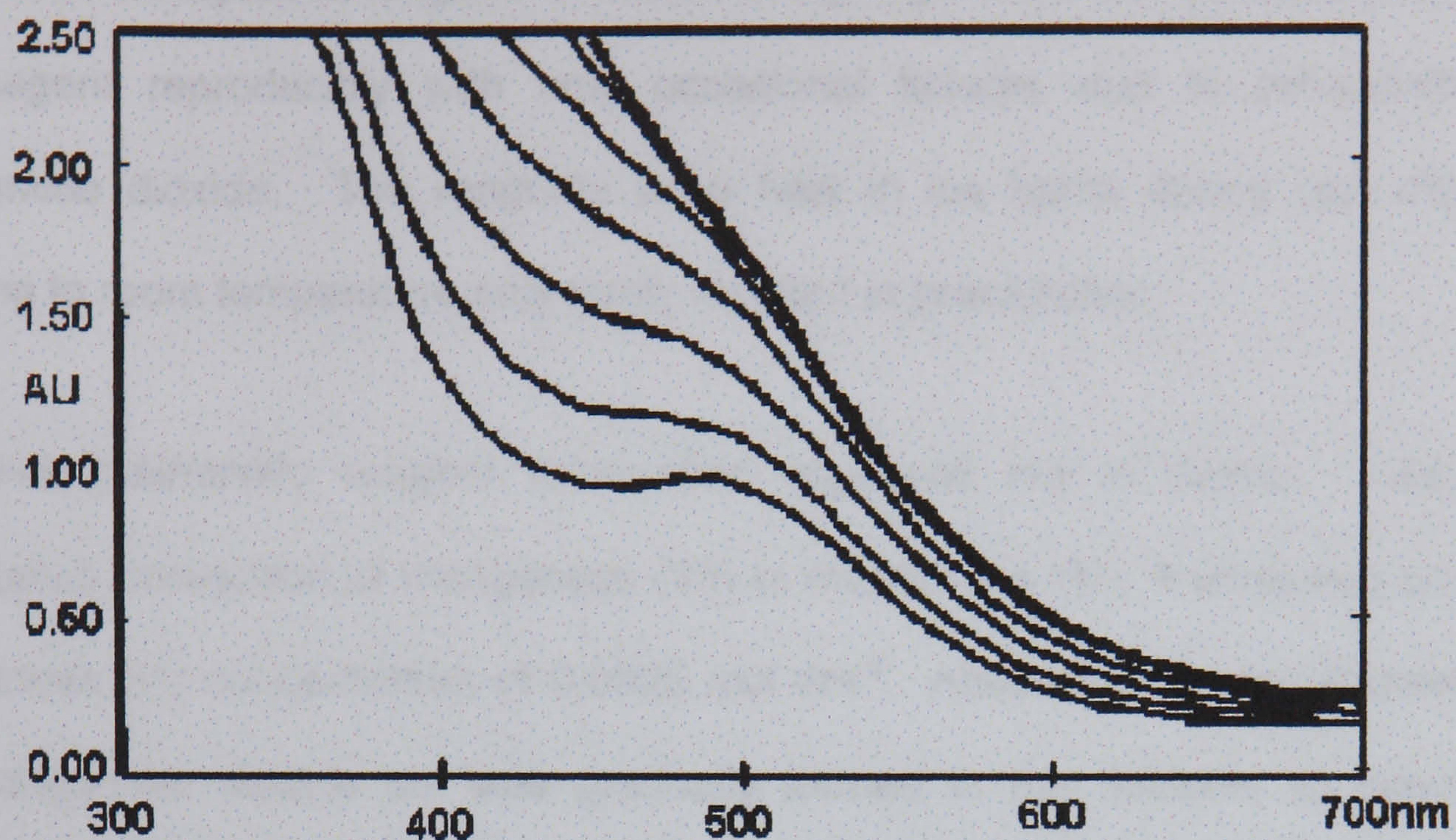


Concentrations as shown above, standard reagent 0.05 mol dm<sup>-3</sup> in Mn(III) 1.6 mol dm<sup>-3</sup> in sulphuric acid

Figure 6.25 shows the calibration lines for reagent and analyte with and without methanol. The position for the calibration line with a 2 mol dm<sup>-3</sup> sulphuric acid carrier is shown for comparison. The mixed reagent appeared clear but was orange/brown in colour, rather than the clear red of the aqueous reagent. The absorbance, scanned between 250 and 700nm, in a 2 mm path-length cuvette, showed a broad absorbance up to 600nm. A freshly prepared mixture showed a spectrum, shown in figure 6.26 typical of manganese (III) which over a period of 10 minutes disappeared leaving a spectrum typical of that of manganese dioxide sol.



**Figure 6.26 Absorbance Spectra for Manganese(III) Reagent with Methanol**



Reagent prepared from 1.5g manganese sulphate, 0.158g potassium permanganate in 160 cm<sup>3</sup> 50% methanol and 12.5% concentrated sulphuric acid. Scans at 1 minute intervals (top) and 30 sec intervals (bottom). First scan has lowest absorbance

#### 6.4.5.3 Preparation of an Improved Manganese (III) Reagent

Several attempts were made to prepare a reagent with high manganese (III) in methanol with a reduced acid content. Due to the oxidation of methanol by permanganate it was necessary to dissolve the permanganate in water, reducing the maximum concentration of methanol in the reagent. It was found that by careful

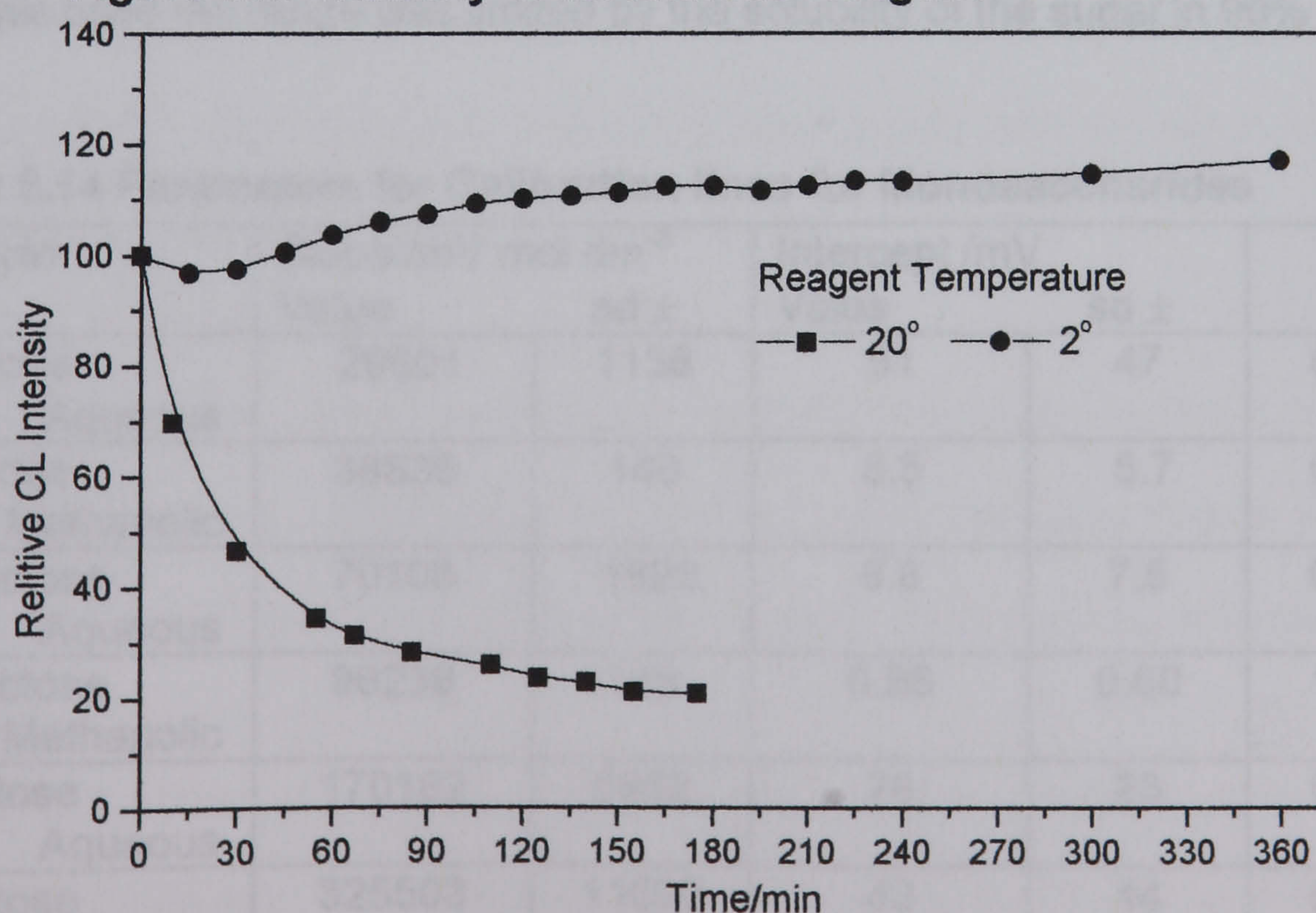


cooling during preparation, the acid concentration could be reduced to half that required for an aqueous reagent. A strict cooling regime made it possible to prepare the reagent reproducibly with only occasional failures due to precipitation of manganese dioxide. The reagents were held in ice baths during use although warming to room temperature only rarely resulted in precipitation.

The final methanolic reagent formulation appeared red in colour. Assuming quantitative conversion of manganese (VII) to manganese (III), it contained an initial manganese (III) concentration of  $0.0625 \text{ mol dm}^{-3}$ . Absorbance scans showed that the manganese dioxide sol was gradually formed in the solution, as previously described, however the colour and clarity of the reagent was visually unchanged during the time of use, up to 6 hours. When stored refrigerated, for more than 24 hours, the solution became pale pink as the methanol was gradually oxidised.

The stability of the methanolic reagent at  $2^\circ \pm 2^\circ\text{C}$ , and at room temperature,  $20^\circ \pm 2^\circ\text{C}$ , was assessed by injection of glucose standards at fifteen minute intervals over six hours. The results are shown in Figure 6.27.

**Figure 6.27 Stability of Methanolic Reagent**



Methanolic reagent, carrier 90% methanol,  $1 \times 10^{-3} \text{ mol dm}^{-3}$  glucose in 90% methanol



At room temperature there was a large decrease in signal size in the first hour, then gradual decrease. When kept cold, the reagent was stable for at least five hours.

#### 6.4.5.4 Effect of the Ratio of Carrier to Reagent

It had been found that the signal increased with increasing manganese (III) concentration. It also appeared that the rate at which the reagent was added was inversely related to the signal. This was studied further by modifying manifold 3 altering the ratio of flow rates by using a larger pump tube, 2mm id, to deliver the carrier and a smaller diameter pump tube 0.05mm id to deliver the reagent, changing the ratio of reagent to carrier from 1:1 to approximately 1:13. Both the aqueous and the standard reagent were used with a 90% methanol carrier and standards prepared in 90% methanol. The methanolic reagent gave higher signals than the aqueous and signals were considerably higher for the 1:13 ratio than the 1:1. The linear range for glucose was  $1 \times 10^{-6}$  to  $1 \times 10^{-1}$  mol dm<sup>-3</sup>. For fructose and galactose, which both give higher signals with the permanganate/ manganese (II) systems, the linear ranges were from  $2 \times 10^{-7}$  and  $5 \times 10^{-7}$  mol dm<sup>-3</sup> respectively. The upper end of the linear range for each was  $1 \times 10^{-2}$  mol dm<sup>-3</sup>. For fructose the calibration line curved at the top end. For galactose the range was limited by the solubility of the sugar in 90% methanol.

**Table 6.14 Parameters for Calibration lines for Monosaccharides**

Analyte	Slope /mV mol dm <sup>-3</sup>		Intercept /mV		R
	Value	sd ±	Value	sd ±	
Glucose Aqueous	29601	1136	51	47	0.99707
Glucose Methanolic	38836	140	8.5	5.7	0.99997
Galactose Aqueous	70103	1829	8.8	7.5	0.99864
Galactose Methanolic	96238	148	0.86	0.60	1.00000
Fructose Aqueous	170182	5952	26	23	0.99696
Fructose Methanolic	325503	11690	42	44	0.99679



As shown in Table 6.14, slopes for the lines using methanolic reagent are higher than those for the aqueous reagent. Considering the difference in flow rates between carrier and reagent, the differences in methanol concentration and acid concentration in the mixed stream are small. The difference must depend on chemistry within the reagent before it mixes with the dispersed analyte in the carrier stream.

The conditions in the methanolic reagent favour production of some manganese (IV) oxide sol. The sulphuric acid concentration, and hence both the acid strength and sulphate concentrations, are reduced. Hydrolysis of manganese (III) to  $\text{Mn}(\text{OH})^{2+}$  followed by disproportionation results in production of manganese (IV). Previous spectroscopic findings had suggested that both manganese (IV) and manganese (III) reactions result in chemiluminescence with the reactions taking place at different rates. The UV findings described above are also consistent with the presence of increased levels of manganese (IV) in the reagent, prior to mixing with the carrier analyte stream.

The slope for the glucose/ aqueous reagent system is considerably higher than previously seen for matched carrier-reagent flows. The reagent is mixing with the carrier stream in a much reduced ratio therefore the acid concentration and sulphate concentrations are reduced to a much greater extent than for matched flows, again favouring disproportionation of manganese (III).

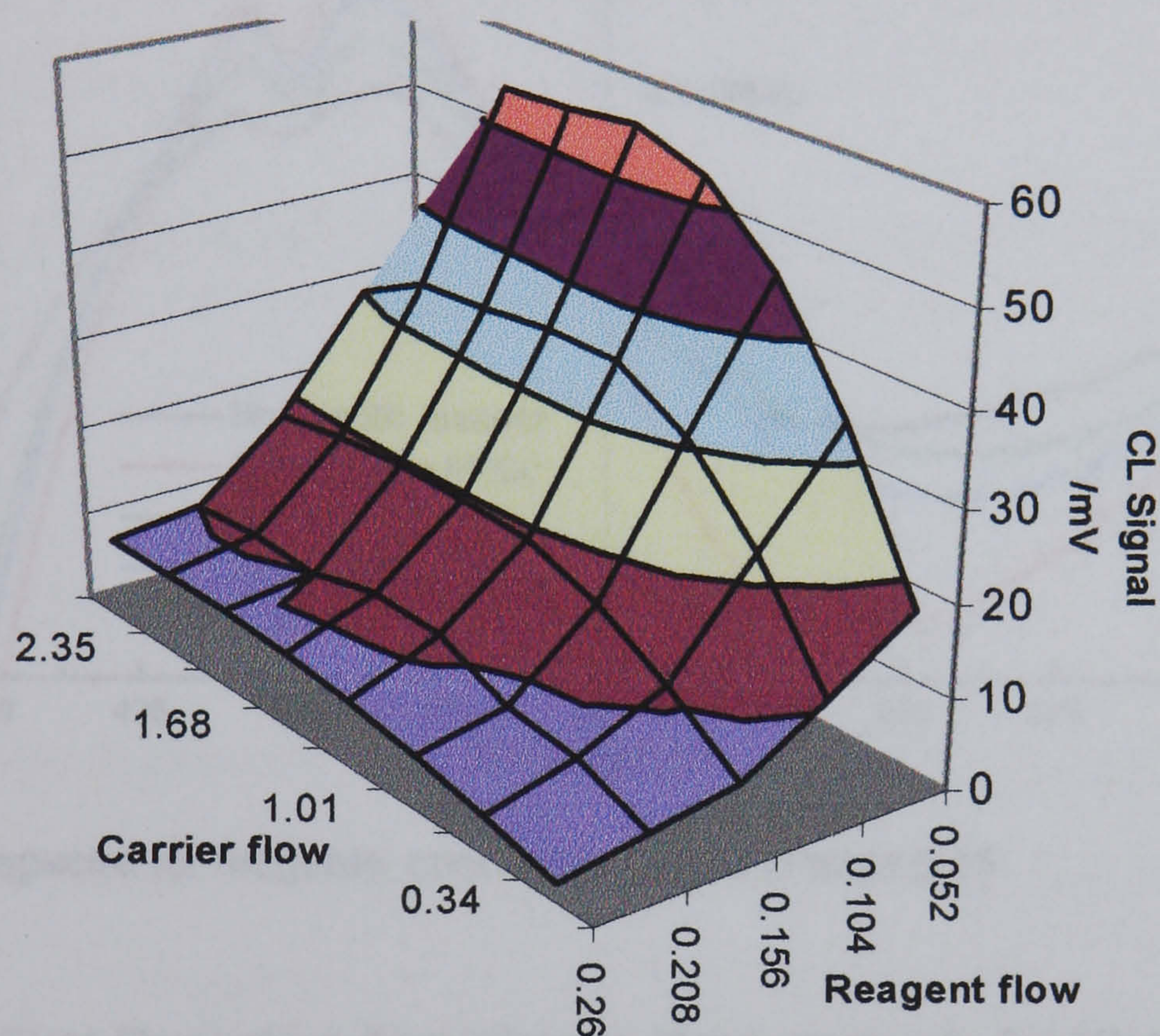
The effects of flow ratios were further investigated using separate pumps for the carrier and reagent. Methanolic reagent and 90% methanol carrier were used as before and  $1 \times 10^{-3}$ , glucose in 90% methanol was injected; pump speeds were varied.

Figure 6.28 shows the relationship between the peak height and the flow rates of carrier and reagent. The highest signal is obtained when the carrier flow rate is high and the reagent flow rate is low. The largest peaks were from a carrier to reagent



ratio of 32:1. This value was clearly still not the optimum, however higher carrier flow rates were impractical due to the increased back-pressure tending to cause leaks. The low reagent flow rates gave poorer repeatability for the peak heights.

**Figure 6.28 Effect of Carrier and Reagent Flow-rates on Chemiluminescence**



Further studies were carried out using a ratio of 13:1 using a single pump

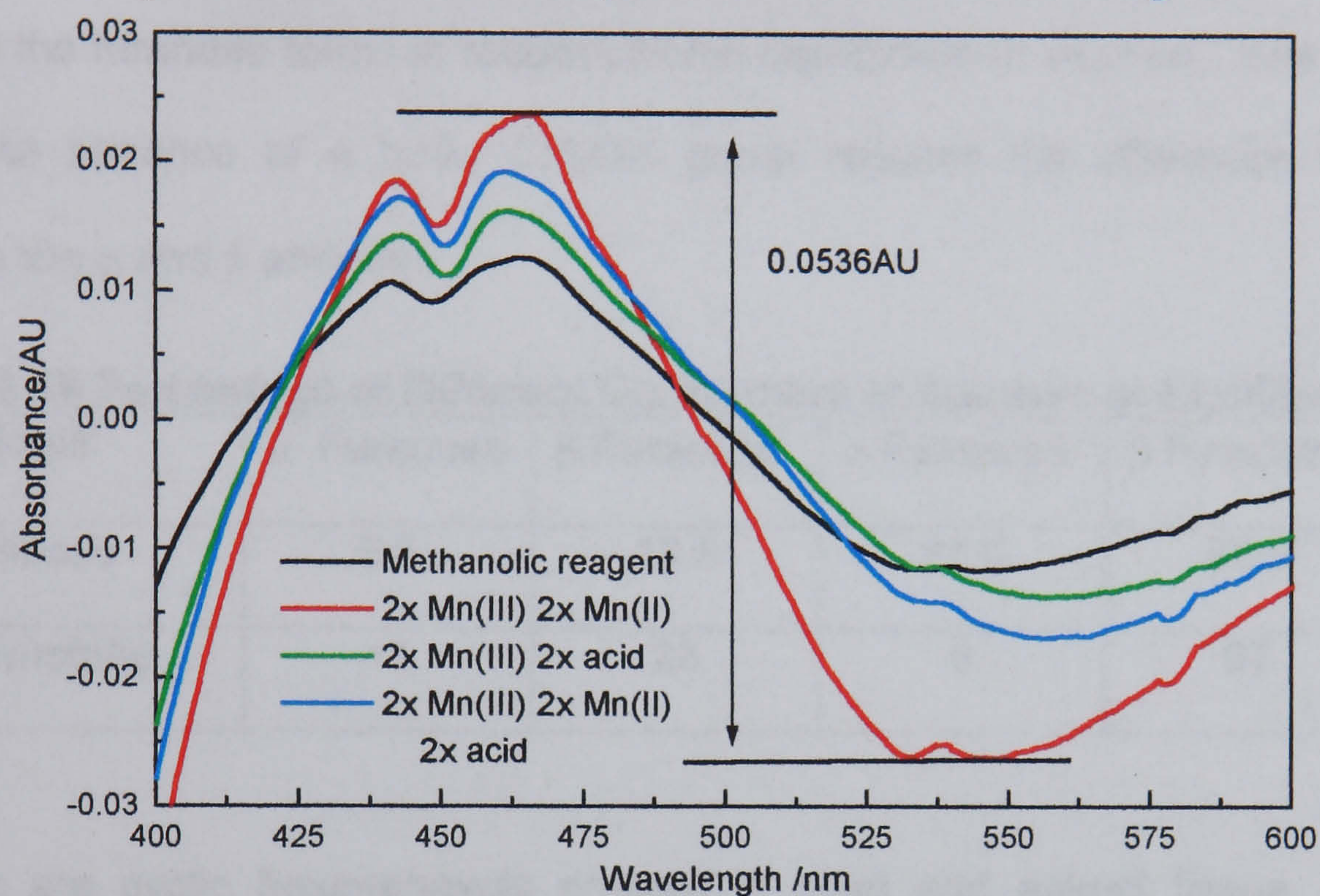
#### 6.4.5.5 Further Attempts to Prepare Stronger Reagents

Methanolic reagents were prepared using larger amounts of permanganate to contain double the concentration of manganese (III) and manganese (II). Limiting solubility of manganese sulphate in methanol limited the final concentration, in which case saturated solutions were prepared. Absorbance spectra were measured for the preparations and first derivatives were measured in order to estimate the relative concentrations of manganese (III). A preparation made using double the amount of permanganate, maintaining the ratio of manganese (III) gave a spectrum typical of



those for manganese dioxide sol, and showed no peaks on the first derivative. For the other solutions the derivative spectra are shown in figure 6.29 and the peak to peak data is shown in table 6.15.

Figure 6.29 Derivative Spectra for Methanolic Reagents



Derivative spectra for reagents, concentrations as in table 6.15

Table 6.15 First Derivative Absorbance Measurements for High-strength Manganese (III) Reagents

Potassium permanganate /g	Manganese sulphate /g	Sulphuric acid /cm <sup>3</sup>	Derivative absorbance /AU
0.158	1.5	10	0.0242
0.316	2.3	10	0.0063
0.316	3.0*	10	0.0296
0.316	2.1	20	0.0536
0.316	3.0*	20	0.0330

As expected, a higher manganese (II) to permanganate ratio resulted in a higher apparent manganese (III) content. Reagents at this concentration could not be reliably produced and the single strength reagents were used for further work.



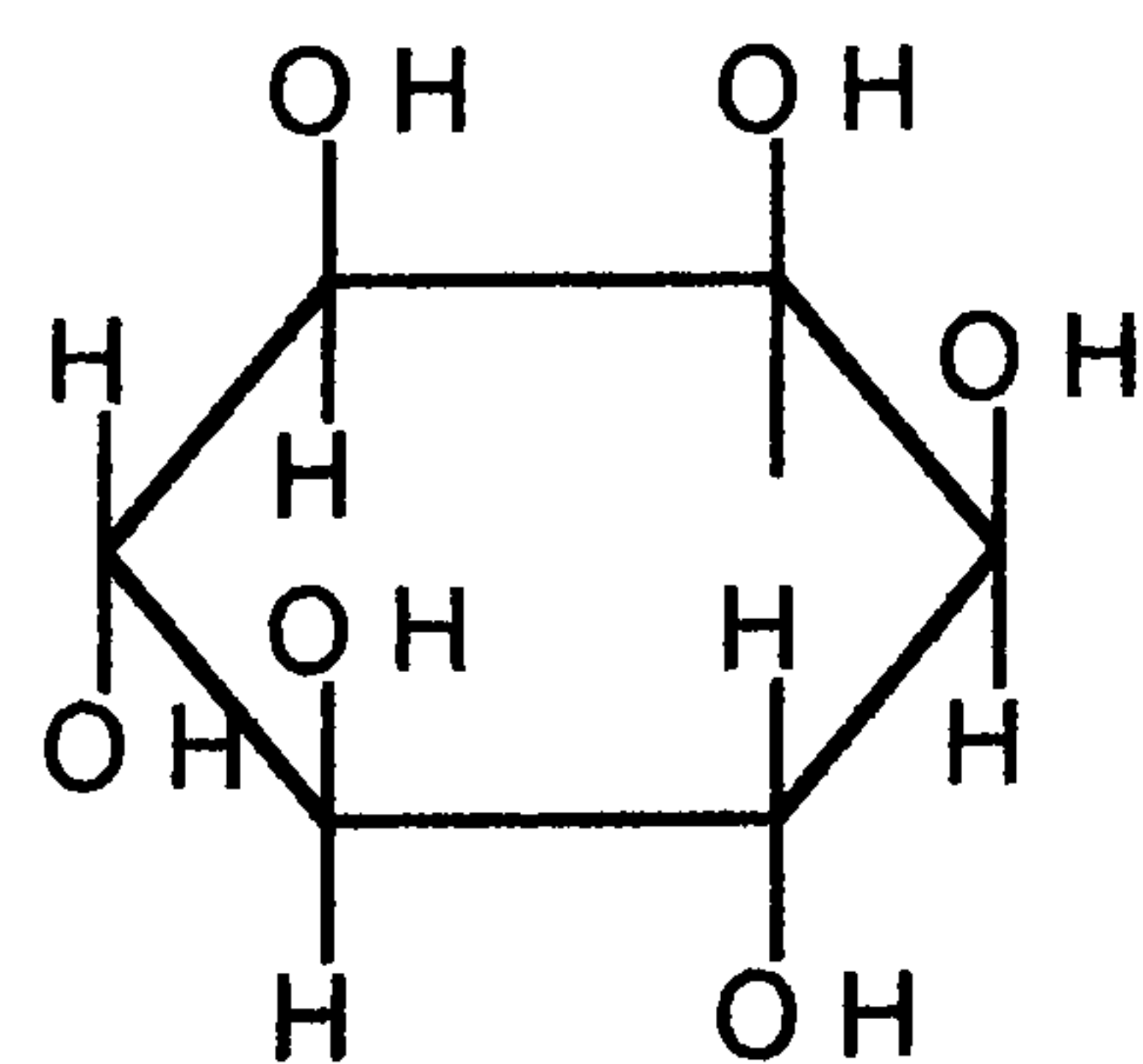
6.4.5 Flow Studies using Ribose and Inositol

In order to further investigate the relationships between sugar configuration and signal size an additional saccharide, ribose and a cyclic polyol, myo-inositol were compared with glucose. Ribose, like fructose, has a significant proportion of the sugar in the furanose forms in mutarotational equilibrium in solution. See also table 4.9. The absence of a bulky CH<sub>2</sub>OH group reduces the difference in stability between the α and β anomers.

Table 6.16 Percentage of Different Conformers in Solution at Equilibrium<sup>264</sup>

Sugar	α Furanose	β Furanose	α Pyranose	β Pyranose
Ribose	6.5	13.5	21.5	58.5
Fructose	<1	25	8	67

Inositols are cyclic hexanehexols present in plant and animal tissue, frequently combined with phosphate. The most widely distributed is myoinositol, which is a meso form, shown in Scheme 6.1.



Scheme 6.1  
myo-inositol

As with the saccharides the favoured conformation has the largest number of hydroxyls in equatorial positions.

Using manifold 3 with aqueous and methanolic reagents, methanolic carriers and a 13:1 carrier: reagent flow ratio, calibration lines were run for ribose and myo-inositol. Glucose, fructose and mannitol were run for comparison. A flow rate was selected to



give the maximum signal for  $1 \times 10^{-3} \text{ mol dm}^{-3}$  glucose and maintained throughout. The parameters for the calibration lines for saccharides and polyols are shown in Tables 6.17 A and B.

**Table 6.17 A Parameters for Calibration lines for Monosaccharides**

Analyte	Slope /mV mol dm <sup>-3</sup>		Intercept /mV		R
	Value	sd ±	Value	sd ±	
Aqueous					
Glucose	18977	79	0.66	0.32	0.99997
Ribose 1x10 <sup>-6</sup> to 1x10 <sup>-2</sup>	49931	3051	14	13	0.99261
Ribose 1x10 <sup>-6</sup> to 1x10 <sup>-3</sup>	112250	104	0.69	0.47	0.99987
Fructose 1x10 <sup>-6</sup> to 1x10 <sup>-2</sup>	149528	3452	15	14	0.99894
Fructose 1x10 <sup>-6</sup> to 1x10 <sup>-3</sup>	220060	87	0.65	0.39	0.99998
Methanolic					
Glucose	31720	90	0.71	0.40	0.99999
Ribose 1x10 <sup>-6</sup> to 1x10 <sup>-2</sup>	35278	900	4.4	4.0	0.99903

**Table 6.17 B Parameters for Calibration lines for Polyols**

Analyte	Slope /mV mol dm <sup>-3</sup>		Intercept /mV		R
	Value	sd ±	Value	sd ±	
Aqueous					
Mannitol 1x10 <sup>-6</sup> to 1x10 <sup>-2</sup>	25014	3326	15	14	0.96640
Mannitol 1x10 <sup>-6</sup> to 1x10 <sup>-3</sup>	92908	1864	1.13	0.84	0.99940
Myo Inositol 1x10 <sup>-6</sup> to 1x10 <sup>-2</sup>	220.5	9.8	0.28	0.04	0.99609
Methanolic					
Mannitol 1x10 <sup>-6</sup> to 1x10 <sup>-2</sup>	7185	1873	9.1	8.4	0.91143
Mannitol 1x10 <sup>-6</sup> to 1x10 <sup>-3</sup>	40852	596	0.33	0.30	0.99979
Myo Inositol 1x10 <sup>-6</sup> to 1x10 <sup>-2</sup>	282		0.16		a

a Average of highest and lowest concentrations only, intermediate concentrations gave no measurable signals

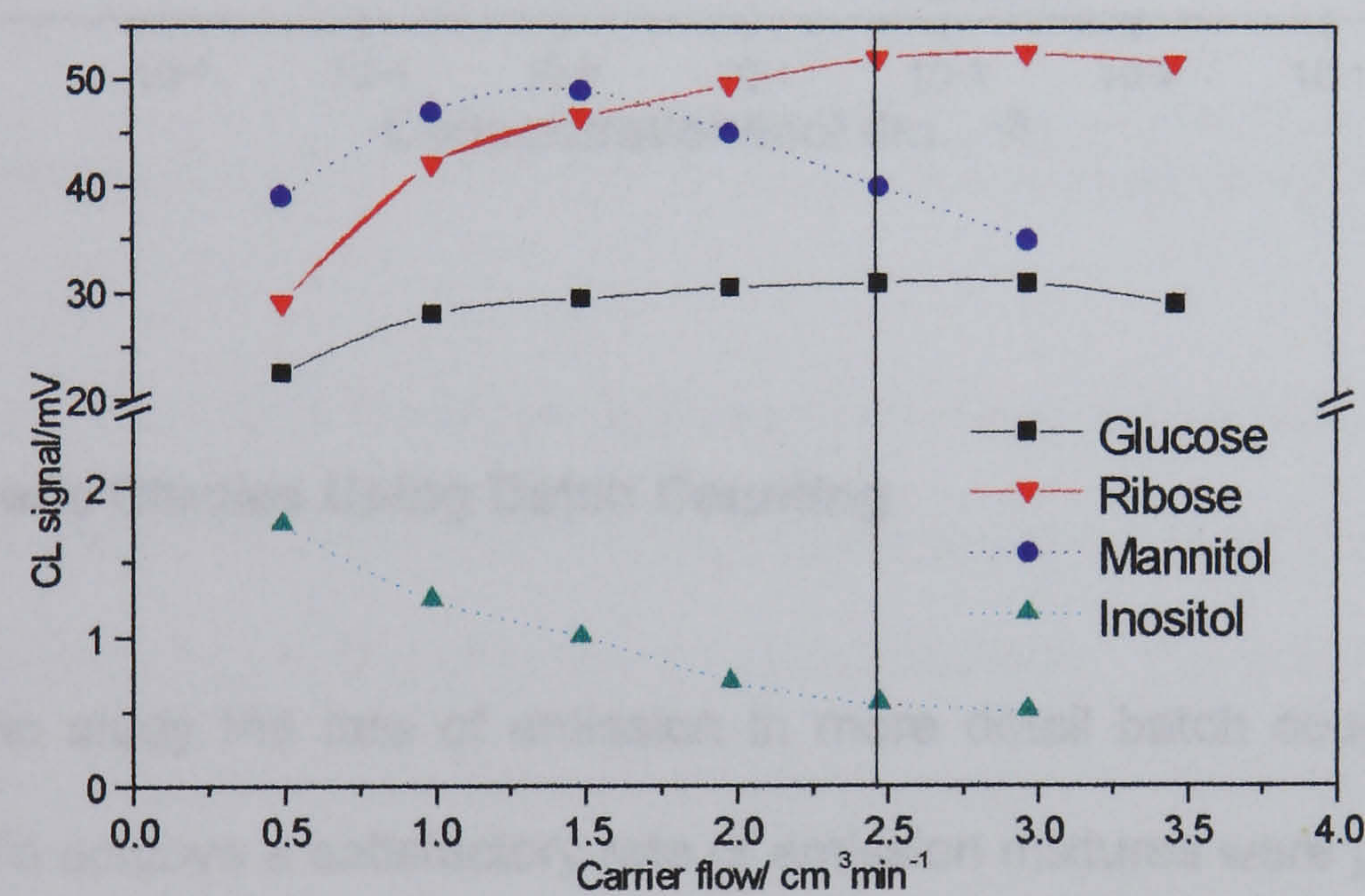
As anticipated, the response for ribose was higher than that for glucose. It was lower that that for fructose, showing that the proportion of furanose form in the equilibrium



mixture, 20:80 for ribose and 25:75 for fructose, is probably not the most significant factor for the intensity of signal from different saccharides.

The response for myo-inositol is very low, and the relationship is anomalous. This appears to be due to the slow rate of reaction. Plots of signal against flow rate using methanolic reagent for the saccharides and polyols are shown in Figure 6.30. As a single pump was used the carrier: reagent ratio was maintained.

**Figure 6.30 Effect of Flow-rate on Chemiluminescence for Saccharides and Polyols**



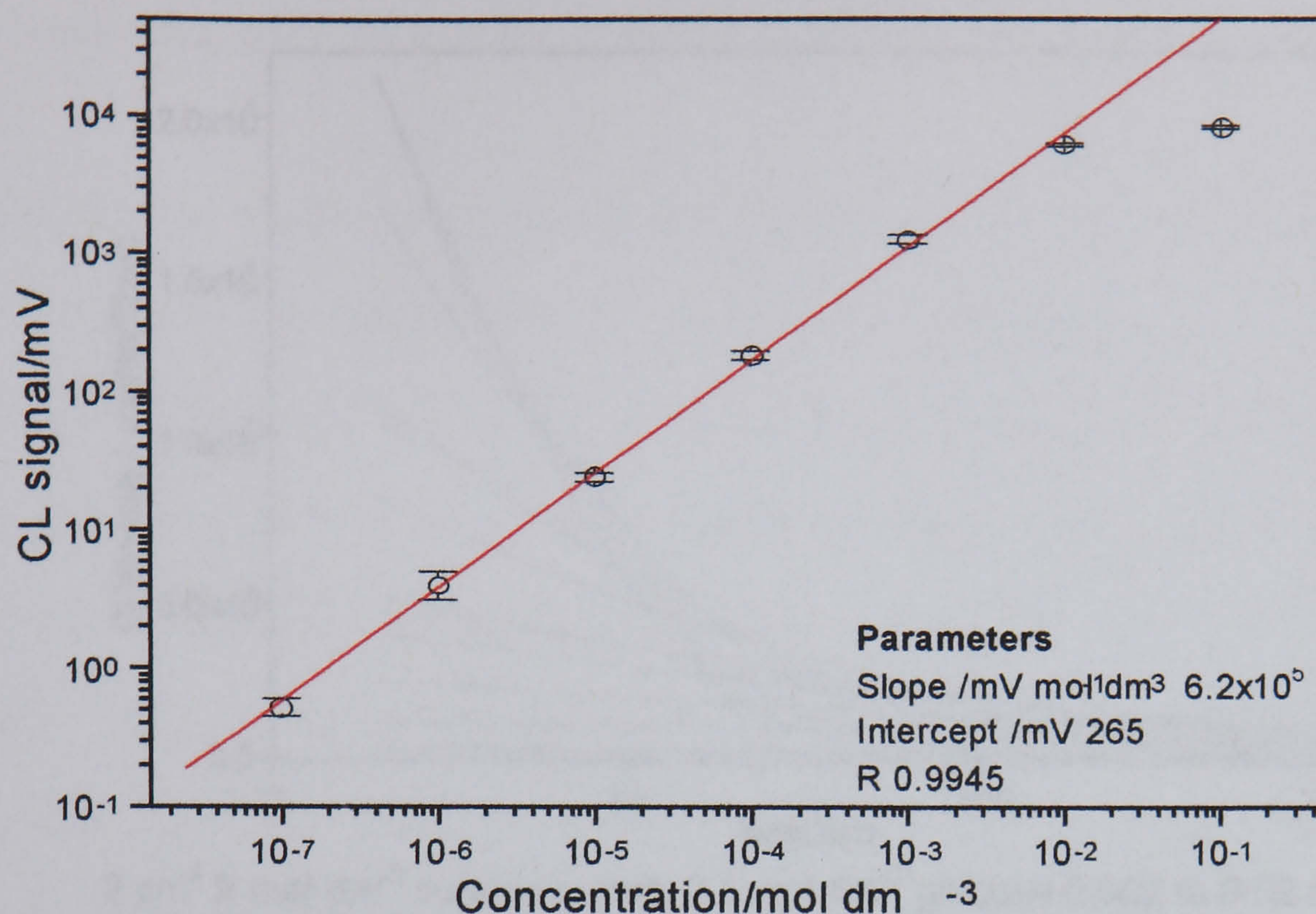
Methanolic manganese (III) reagent, analyte at  $1 \times 10^{-3}$  mol dm<sup>-3</sup>  
Vertical line shows the flow rate used in calibration lines

The highest signal for the saccharides is at approximately 2.5 cm<sup>3</sup> min<sup>-1</sup>, the flow rate used in constructing the calibration lines above. For the polyols the maximum for mannitol was 1.5 cm<sup>3</sup> min<sup>-1</sup> and that for inositol was below the range examined showing that the emission is essentially complete before the detector is reached.

As discussed previously, there was day to day variation in the signal due to the variability of the photomultiplier. Under optimum conditions the linear response for fructose was over the range  $1 \times 10^{-7}$  to  $1 \times 10^{-2}$  mol dm<sup>-3</sup>, as shown in Figure 6.31.



**Figure 6.31 Calibration line for Fructose in Methanol with Methanolic Manganese (III) Reagent**

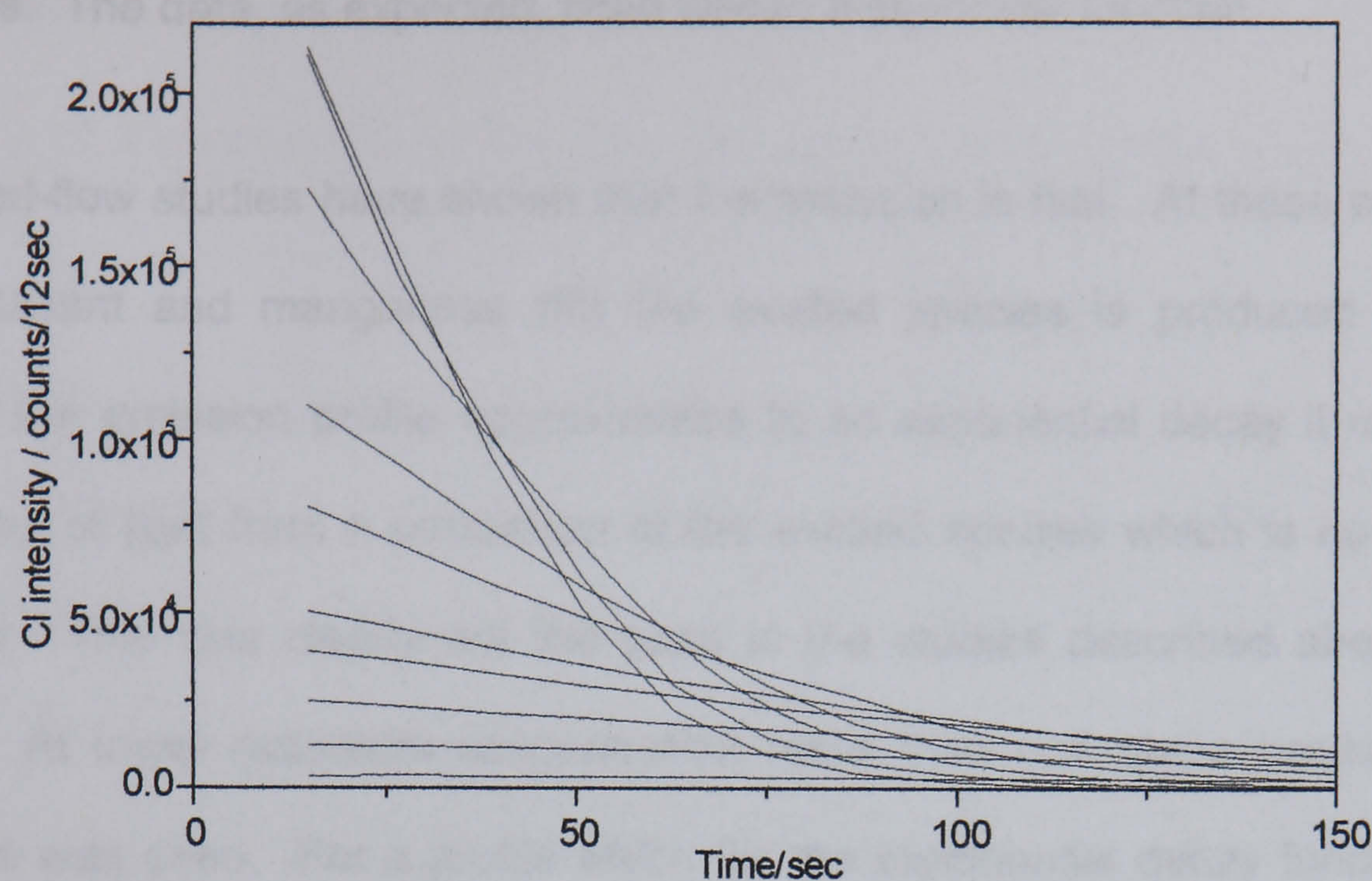


#### 6.4.6 Kinetic Studies Using Batch Counting

In order to study the rate of emission in more detail batch counting was used as before. To achieve a satisfactory rate of emission mixtures were prepared consisting of 2 cm<sup>3</sup> carrier, 2 mol dm<sup>-3</sup> sulphuric acid, and increasing volumes of 0.1 mol dm<sup>-3</sup> glucose to give between 0.002 and .02 mol dm<sup>-3</sup>. The reaction was started using 0.1 cm<sup>3</sup> methanolic reagent. In all experiments excess reductant was used, as confirmed by the colourless appearance of the solution at the end of the experiment. It was not possible to control the temperature of the reaction. Room temperature was recorded and is indicated in the corresponding tables. Manganese (III) reagents were stored on ice before use. As the mass of reagent was small compared with the mass of the vial and reaction solutions the difference in temperature due to the addition was small and reasonably consistent.



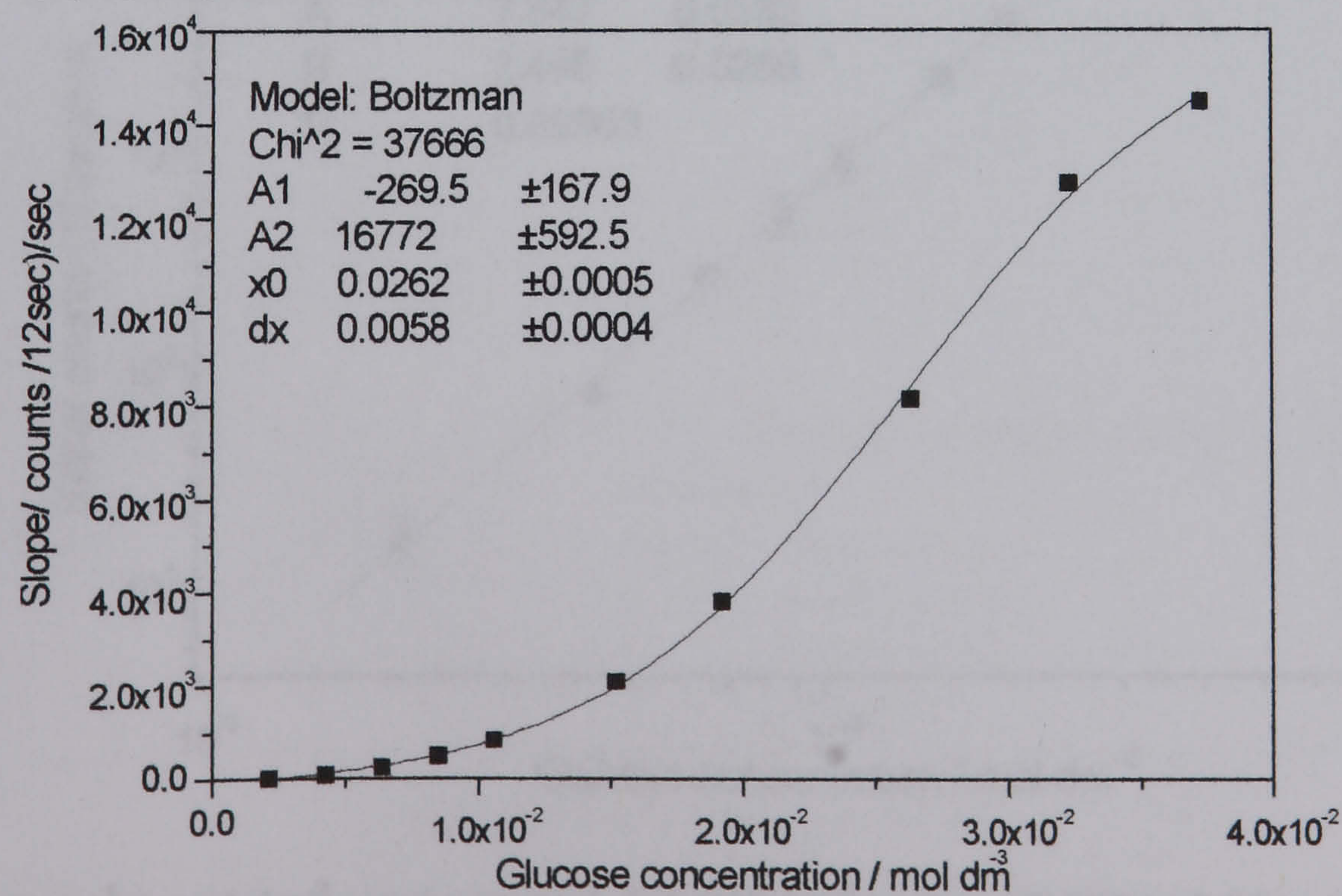
**Figure 6.33 Chemiluminescence Time-courses for Methanolic Manganese(III) Reagent with Glucose**



2 cm<sup>3</sup> 2 mol dm<sup>-3</sup> sulphuric acid, 0.1 mol dm<sup>-3</sup> glucose 0.002 to 0.02 mol dm<sup>-3</sup> 0.1 cm<sup>3</sup> methanolic reagent. Initial signal increases with increasing glucose concentration

The curves, which are averages for three runs are shown in Figure 6.33. The curve data fitted well to an exponential decay model and it was found that a run time of 7 minutes was sufficient to define the slope satisfactorily. Curves were fitted using the Solver fitting routine in the Excel software package.<sup>214</sup> The slope over the first 15 seconds was calculated in units of counts (12sec)<sup>-1</sup> sec<sup>-1</sup>.

**Figure 6.34 Relationship between the Initial Slope and Concentration of Glucose.**



2 cm<sup>3</sup> 2 mol dm<sup>-3</sup> sulphuric acid, 0.1 mol dm<sup>-3</sup> glucose 0.002 to 0.02 mol dm<sup>-3</sup> 0.1 cm<sup>3</sup> methanolic reagent. Slope measured over first 15 sec

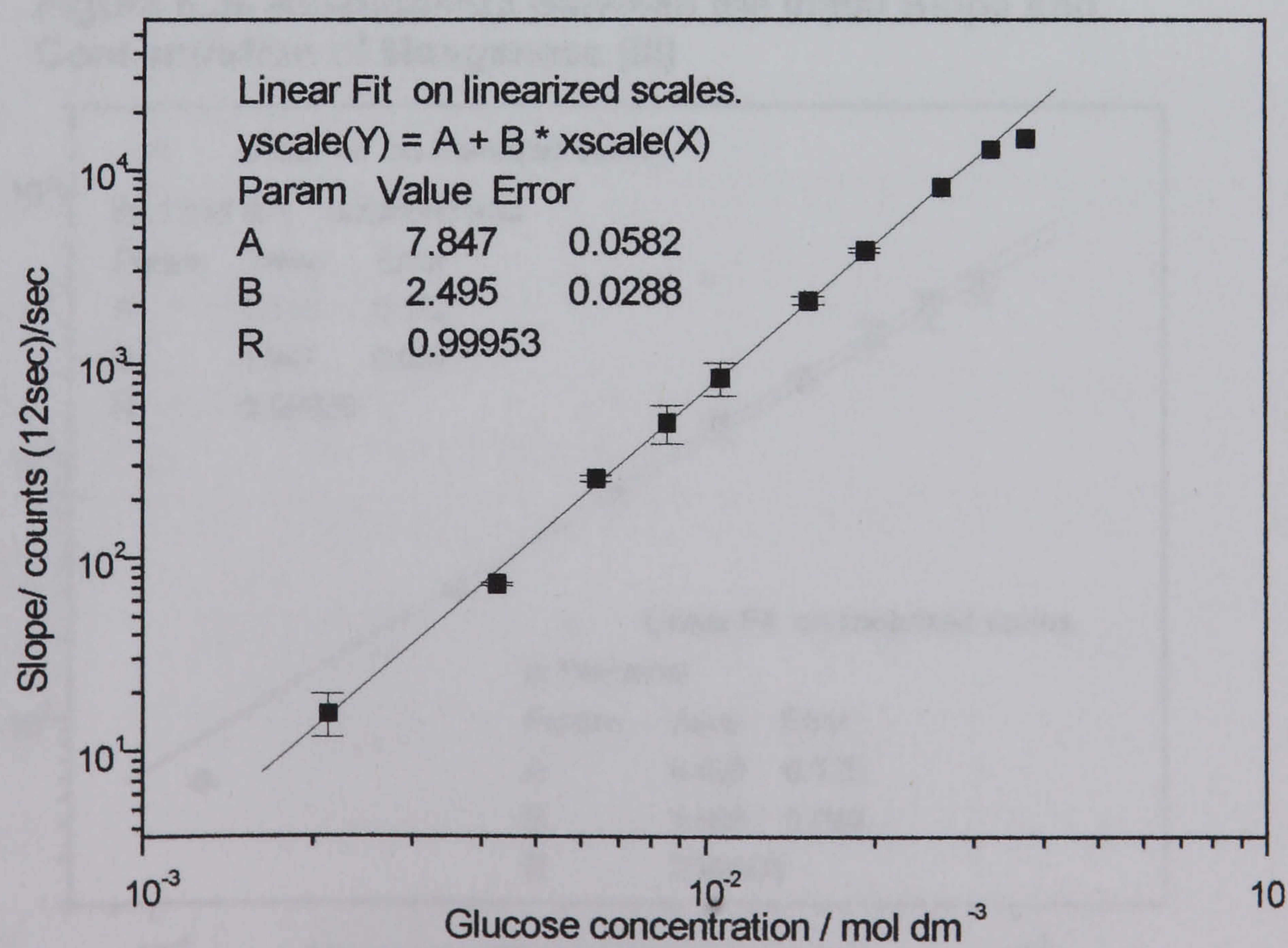


Figure 6.34 shows the relationship between the initial slope and concentration of glucose. The data, as expected, fitted well to a sigmoidal function.

Stopped-flow studies have shown that the emission is fast. At these concentrations of reductant and manganese (III) the excited species is produced very quickly. Where the emission profile approximates to an exponential decay it represents the emission of light from a population of the excited species which is no longer being formed. This was clearly not the case in the studies described above in section 6.4.2. At lower reductant concentration more than one stage producing emitting species was seen. For a profile which fits the exponential decay function the initial rate of decay of emission is proportional to the concentration of emitting species generated. This, in turn, depends on the rate of the reaction generating the species, allowing a comparison to be made between rates of reaction for different analytes

A log-log plot of the data in Figure 6.33 is shown as Figure 6.34.

**Figure 6.34 Relationship Between the Initial Slope and Concentration of Glucose.**



2 cm<sup>3</sup> 1 mol dm<sup>-3</sup> sulphuric acid, 0.1 mol dm<sup>-3</sup> glucose 0.002 to 0.02 mol dm<sup>-3</sup>  
0.1 cm<sup>3</sup> methanolic reagent. Slope measured over first 15 sec



It is a straight line with a slope of 2.5 and an intercept of 7.85. The results of repeat runs over ten days are shown in Table 6.18.

Table 6.18 Repeatability of Glucose Response Linear-Linear Calibration lines

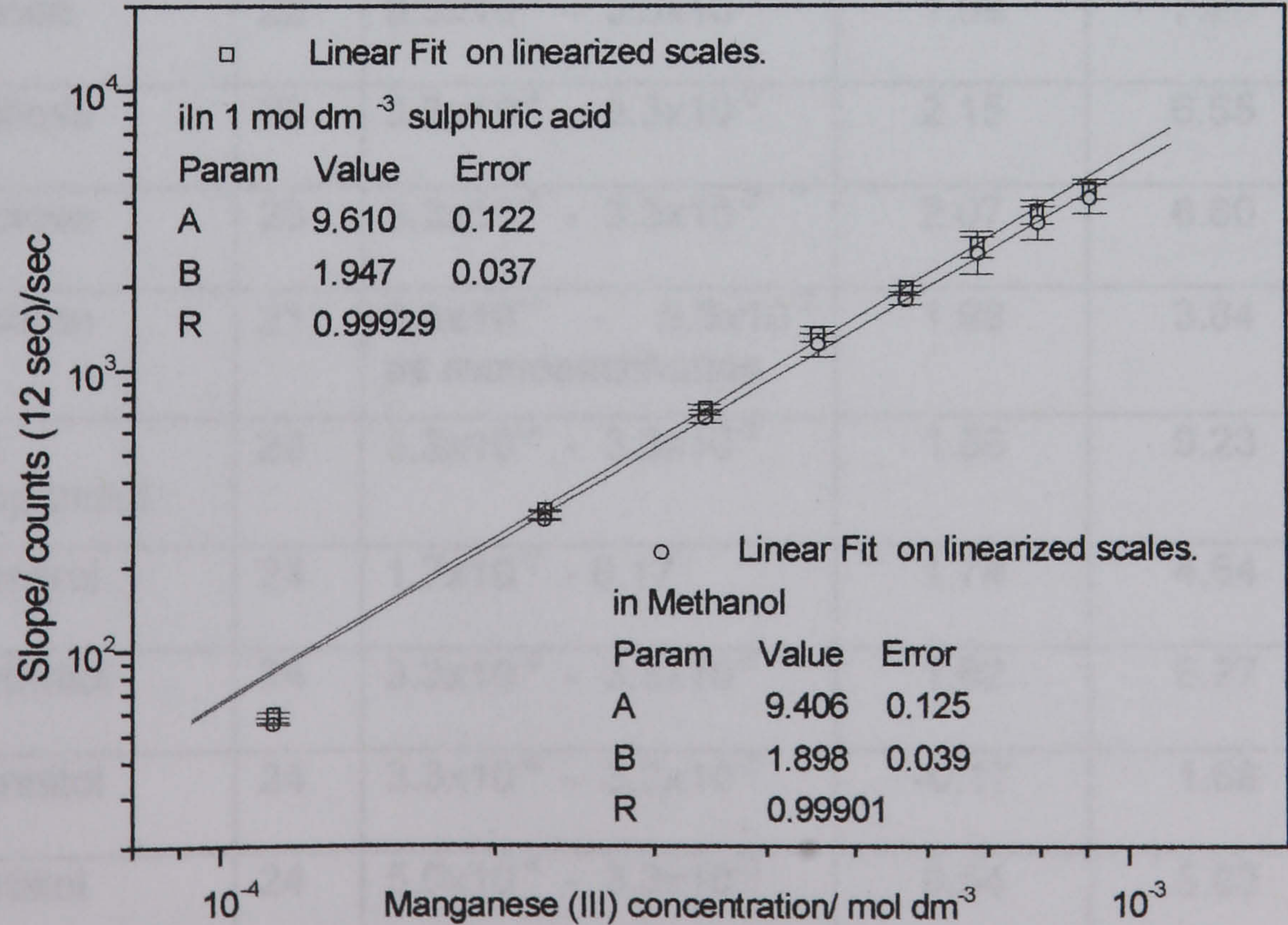
Date	T/ °C	Range	Slope	Intercept	R
16-03-98	22	$2.1 \times 10^{-3}$ - $3.7 \times 10^{-2}$	2.50	7.85	0.9995
19-03-98	21	$4.0 \times 10^{-3}$ - $3.2 \times 10^{-2}$	2.10	6.74	0.9982
20-03-98	23	$3.3 \times 10^{-4}$ - $3.3 \times 10^{-2}$	2.14	7.19	1.0000
23-03-98	22	$3.3 \times 10^{-4}$ - $3.3 \times 10^{-2}$	2.23	7.18	0.9974
24-03-98	23	$3.3 \times 10^{-4}$ - $3.3 \times 10^{-2}$	2.57	7.76	0.9992
25-03-98	24	$3.3 \times 10^{-4}$ - $3.3 \times 10^{-2}$	2.20	7.23	0.9968
Mean			2.29 ± 0.196*	7.325 ± 0.414*	

- 95% CI

Using the differential method to calculate the rate and order of the reaction shows that under the conditions used the reaction is approximately second order in glucose

The variation in rate does not correlate with the observed temperature differences

Figure 6.35 Relationship Between the Initial Slope and Concentration of Manganese (III)



2 cm<sup>3</sup> 1 mol dm<sup>-3</sup> sulphuric acid, glucose 0.02 mol dm<sup>-3</sup> 0.025 to 0.1 cm<sup>3</sup> methanolic reagent. Slope measured over first 15 sec



Figure 6.35 shows the relationship between initial slope and reagent concentration. Slope and intercept are very similar in sulphuric acid and methanol medium.

A range of saccharides and polyols was examined as above, using the sulphuric acid medium. The analyte concentration range was limited at the upper end by the linearity of the log-log plot. Additional points were established by doubling dilutions of analyte until the shape of the time course could no longer be represented by an exponential decay function. Glucose was run as a standard with each set. The parameters for the log-log plots are shown in Table 6.19

**Table 6.19 Parameters for Linear fits to Log- Log plots for Saccharides and Polyols**

Analyte	T/ °C	Range	Slope	Intercept	R
Glucose (from 7.18)			2.29 ± 0.196*	7.325 ± 0.414*	
Galactose	23	3.3x10 <sup>-4</sup> - 3.3x10 <sup>-2</sup>	2.26	7.24	0.9983
Fructose	23	2.0x10 <sup>-3</sup> - 3.3x10 <sup>-2</sup>	1.41	7.13	0.9925
Ribose	21	1.6x10 <sup>-3</sup> - 8.0x10 <sup>-3</sup>	2.11	8.48	0.9985
Arabinose	22	3.3x10 <sup>-4</sup> - 3.3x10 <sup>-2</sup>	2.29	8.31	0.9998
Xylose	22	3.3x10 <sup>-4</sup> - 3.3x10 <sup>-2</sup>	1.99	7.26	0.9988
Maltose	23	3.3x10 <sup>-4</sup> - 3.3x10 <sup>-2</sup>	2.15	6.55	0.9957
Lactose	23	3.3x10 <sup>-4</sup> - 3.3x10 <sup>-2</sup>	2.07	6.60	0.9992
Dextran	21	3.3x10 <sup>-4</sup> - 3.3x10 <sup>-2</sup> as monosaccharide	1.98	3.84	0.9866
1,2 Propandiol	23	3.3x10 <sup>-4</sup> - 3.3x10 <sup>-2</sup>	1.86	6.23	0.9964
Glycerol	24	1.7x10 <sup>-2</sup> - 0.17	1.74	4.64	0.9909
Erythritol	24	3.3x10 <sup>-4</sup> - 3.3x10 <sup>-2</sup>	1.82	6.27	0.9943
Mannitol	24	3.3x10 <sup>-4</sup> - 3.3x10 <sup>-2</sup>	-0.17	1.88	0.8677
Sorbitol	24	5.0x10 <sup>-4</sup> - 3.3x10 <sup>-2</sup>	0.54	5.03	0.9995

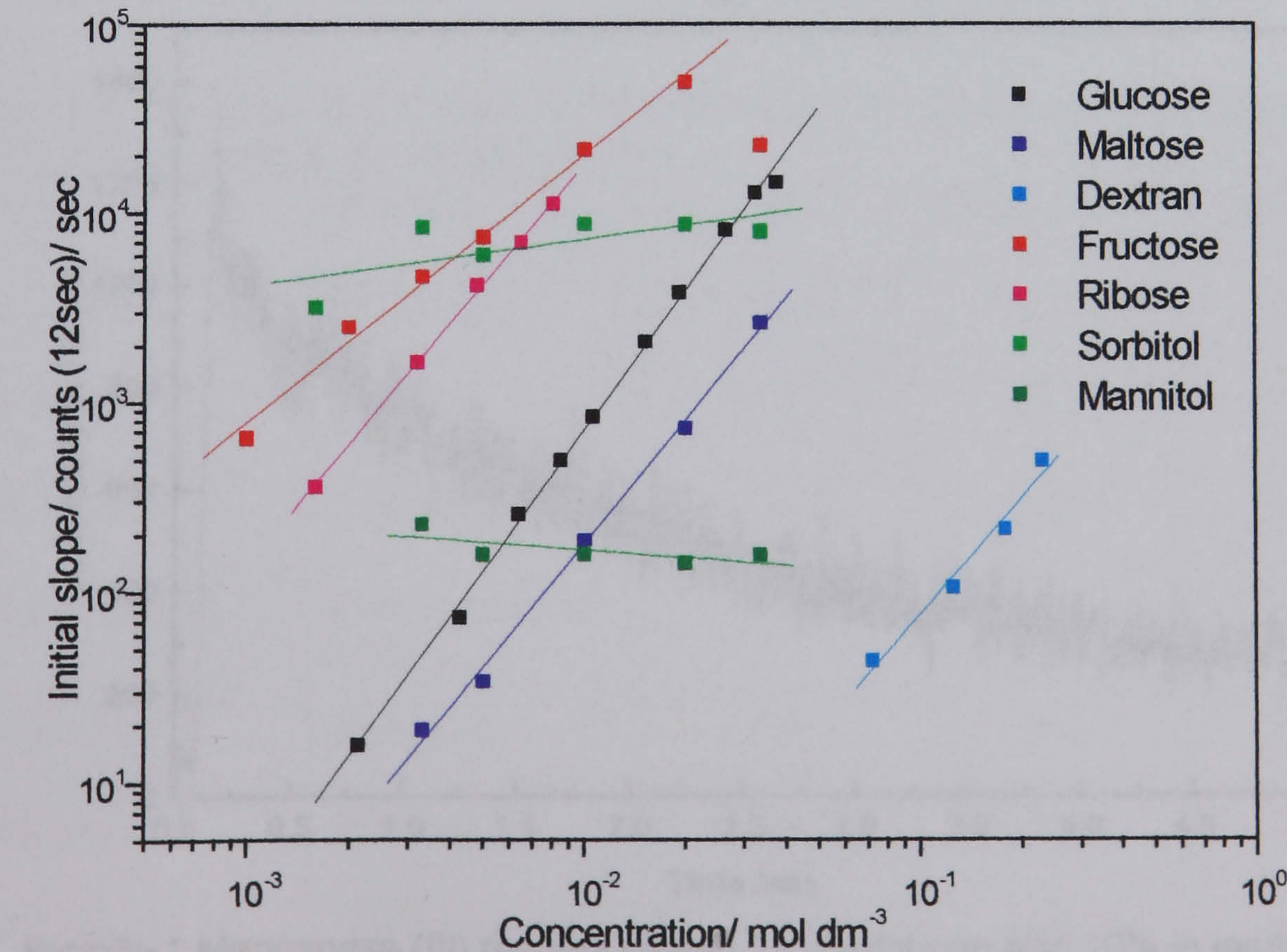
95% CI



The time course for sucrose showed a lag similar to those observed for permanganate reactions. This is due to the acid hydrolysis of sucrose followed by the reaction of fructose and glucose with manganese (III). No slopes could be calculated. Attempts to run myo-inositol were unsuccessful as the limit of solubility was reached before a significant signal was obtained. The reaction with ascorbic acid was too fast to measure; the reaction was complete within first 15 sec.

Using a t-test the values for slope and intercept were compared with the set of results for glucose. With the exception of fructose, the values for the saccharides are not significantly different from those for glucose. For the polyhydroxy compounds, however, only propan 1,2-diol and erythritol have slopes approaching 2. For sorbitol the dependence on the reductant concentration is fractional and for mannitol there is no apparent dependence on the reductant concentration, suggesting that a different mechanism is operating.

**Figure 6.36 Log- Log plots of Initial Slope against Concentration for a Representative Saccharides and Polyols**



Conditions as in the text

Figure 6.36 shows plots for a number of saccharides and polyols.



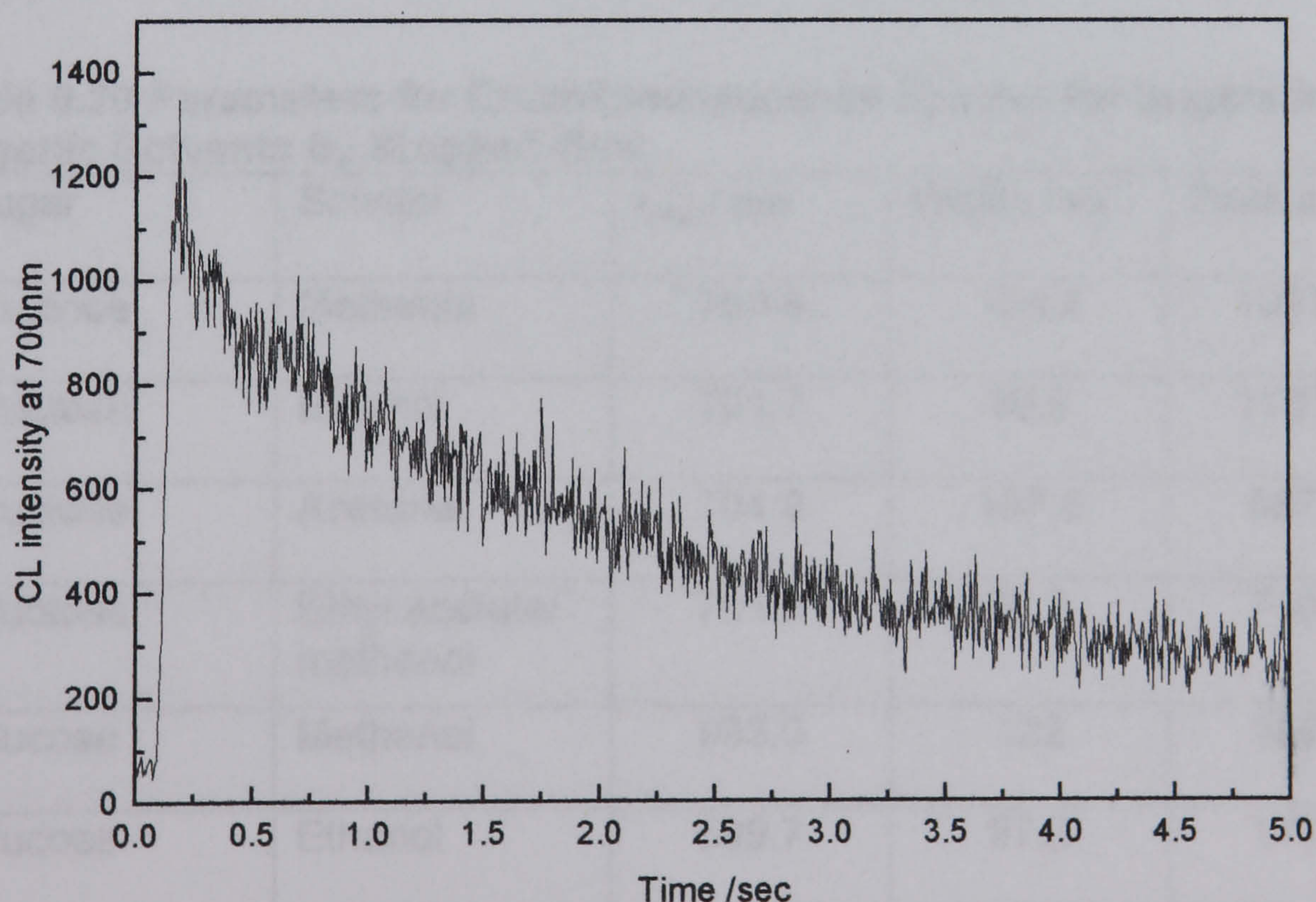
In order to assess the possibility of using the reagent in determination of polysaccharides, a dextran of average molecular weight  $2 \times 10^6$  was examined under the same conditions. The result is included in Table 6.19 with the concentration of dextran expressed as monosaccharide. The signal is considerably lower than those for the other materials but the slope not significantly different from those for mono- and disaccharides.

#### 6.4.7 Chemiluminescence Spectroscopy Using Stopped- Flow

Chemiluminescence spectra were run for fructose and glucose in a range of solvents. As the reactions are fast stopped-flow and continuous flow methods were used. The methanolic manganese (III) reagent was, diluted in 10% sulphuric acid in methanol.

A typical stopped-flow time course at 700nm is shown in Figure 6.37 it is the average of ten experiments.

**Figure 6.37 Chemiluminescence Time-course at 700nm for the Reaction of Fructose in methanol with Manganese (III) reagent – Stopped-flow**

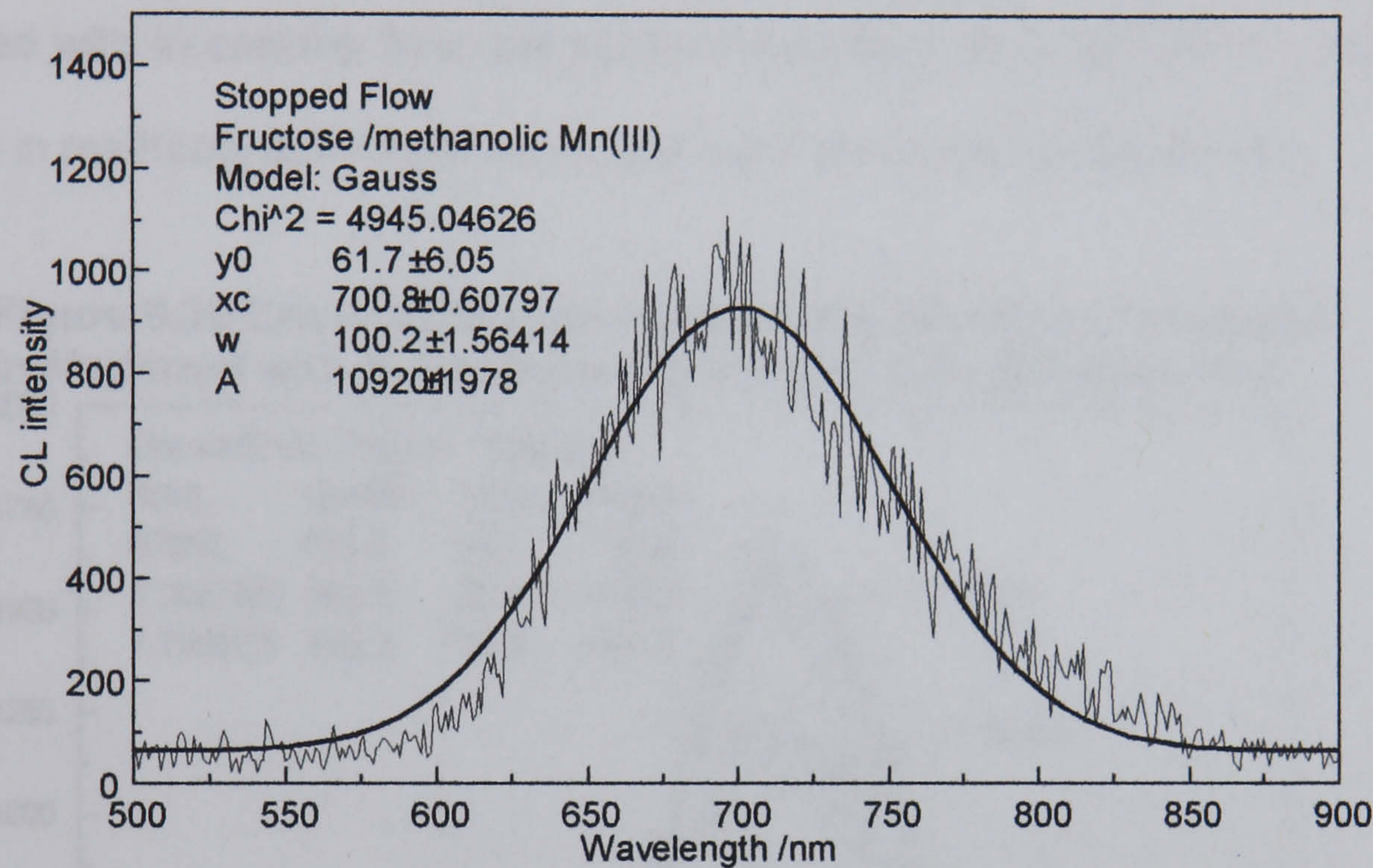


Syringe 1 Manganese (III) reagent diluted 1+ 4 sulphuric acid 10% in methanol  
 Syringe 2 Fructose  $0.01 \text{ mol dm}^{-3}$  in methanol Average of 10 runs



Figure 6.38 shows the spectrum for the same reaction. As the reaction is fast the scan was made immediately on mixing. Fitting a Gaussian curves to the data gave a peak maximum of  $700 \pm 10\text{nm}$ , irrespective of the solvent. The peak parameters for glucose and fructose in a range of solvents are shown in Table 6.20.

**Figure 6.38 Chemiluminescence from the Reaction of Fructose in Methanol with Manganese (III) Reagent – Stopped-flow**



Syringe 1 Manganese (III) reagent diluted 1+ 4 sulphuric acid 10% in methanol  
Syringe 2 Fructose  $0.01\text{mol dm}^{-3}$  in methanol

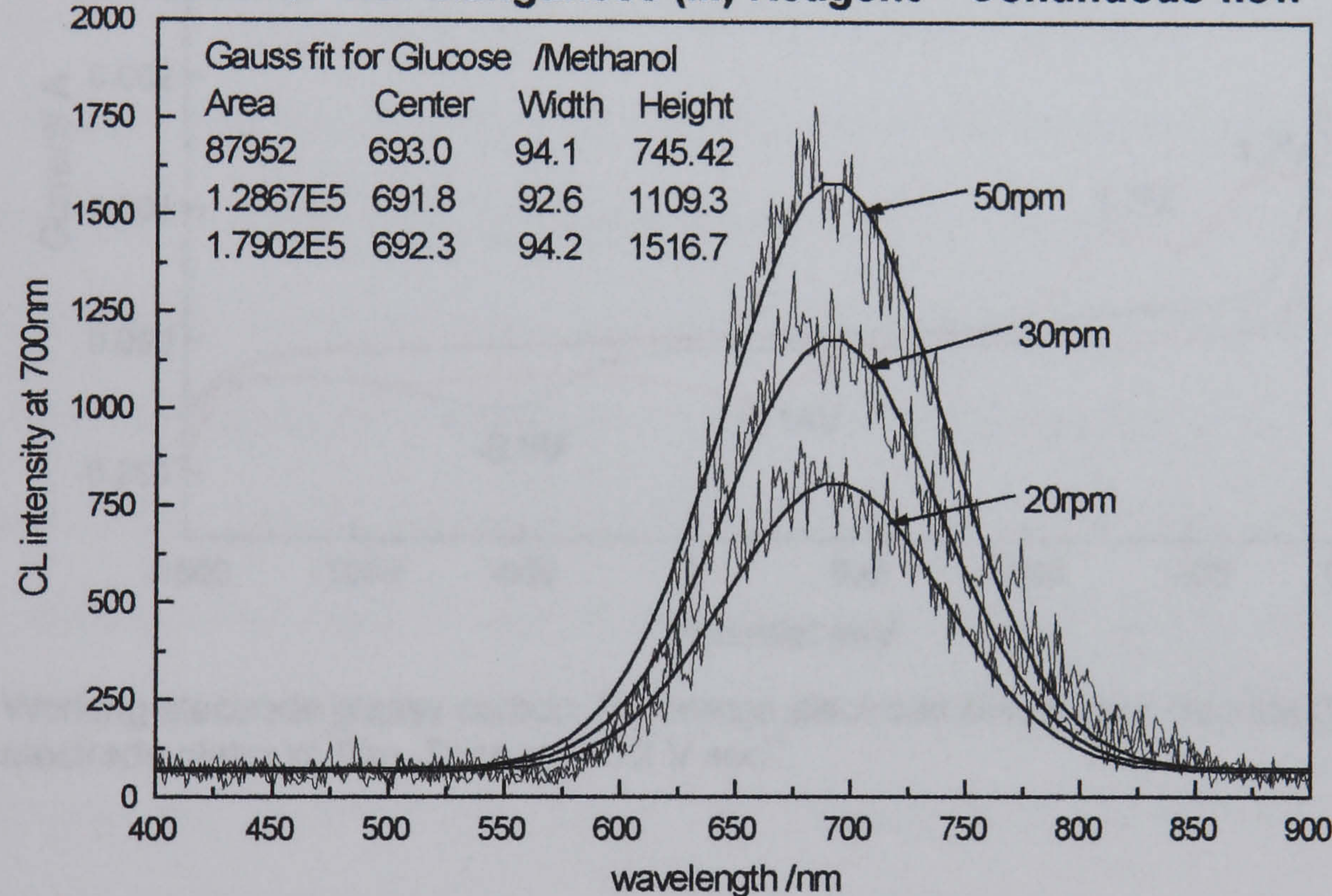
**Table 6.20 Parameters for Chemiluminescence Spectra for Sugars in Organic Solvents by Stopped-flow**

Sugar	Solvent	$\lambda_{\text{max}}/\text{nm}$	Width/ nm	Peak area
Fructose	Methanol	700.8	100.2	109781
Fructose	Ethanol	701.7	99.9	110746
Fructose	Acetone	704.9	107.6	58720
Fructose	Ethyl acetate/ methanol	701.9	98.7	74042
Glucose	Methanol	693.0	122	20867
Glucose	Ethanol	699.7	97.2	11167
Glucose	Ethyl acetate /methanol	704.5	102	11006



Spectra were also collected using continuous flow. Sugar solutions were prepared in methanol as before but the methanolic manganese (III) reagent was used without dilution. The required ratio of reagent to sample was established by using different pump tubes. To improve the signal to noise ratio multiple fast scans were averaged instrumentally using the computerised averaging for transients (CAT) facility. Again the wavelength maxima were  $700\pm 10\text{nm}$ . It was found that the signal intensity increased with increasing flow rate up to a maximum at  $7\text{ cm}^3\text{ min}^{-1}$ . Spectra for fructose in methanol at three different flow rates are shown in figure 6.39.

**Figure 6.39 Chemiluminescence from the Reaction of Fructose in Methanol with Manganese (III) Reagent – Continuous-flow**



Line 1 fructose  $0.01\text{ mol dm}^{-3}$  in methanol  $6.5\text{ cm}^3\text{ min}^{-1}$   
Line 2 methanolic manganese (III) reagent  $0.5\text{ cm}^3\text{ min}^{-1}$

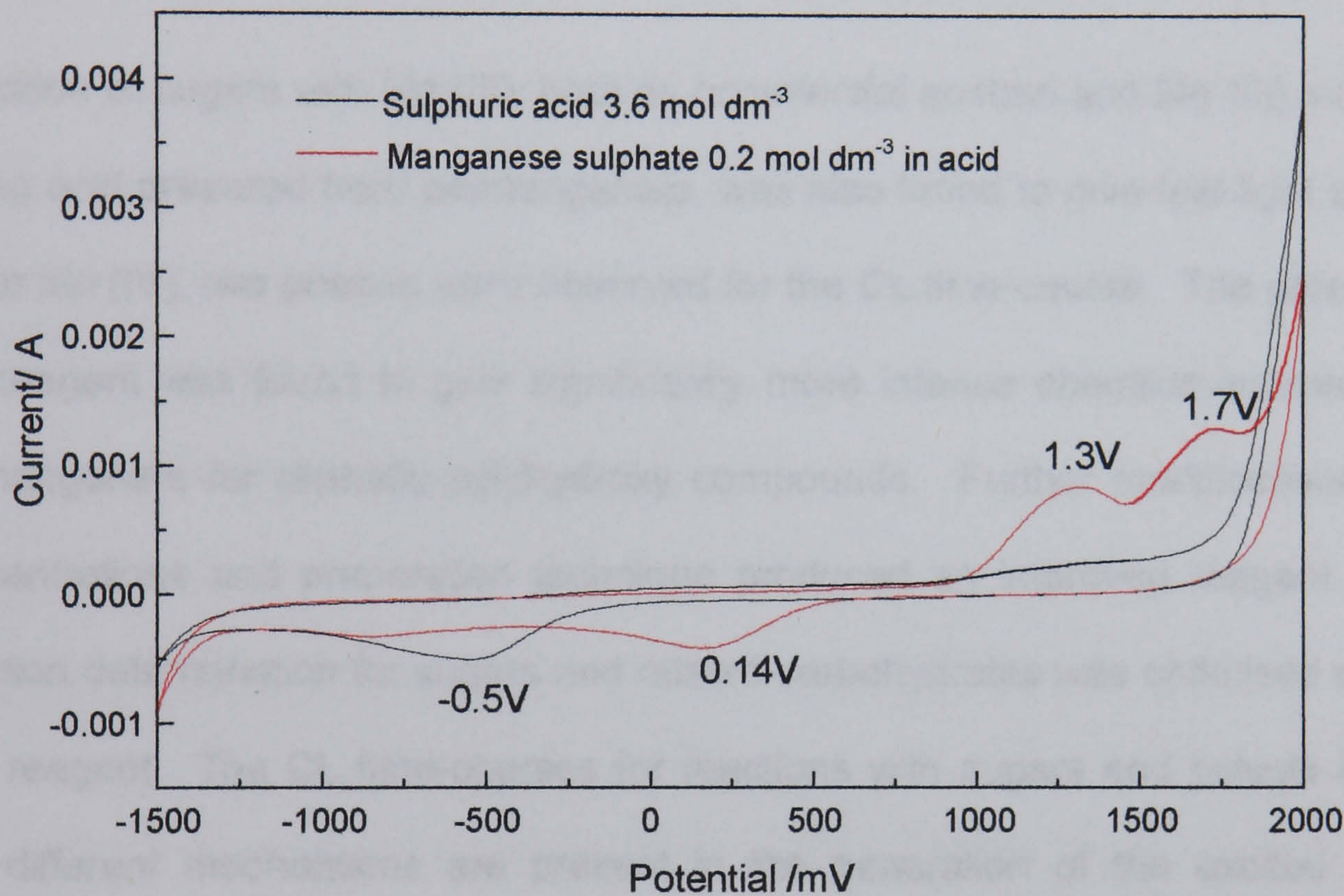
The spectral maxima are the same as for permanganate reactions, irrespective of the solvent mixture used, confirming that the same emitting species is probably involved in all the reactions and that it involves a manganese species.



6.5 Electrochemical generation of Manganese(III)

Several workers have produced manganese (III) electrochemically<sup>155,262</sup> for use in oxidation studies. In order to investigate the possibility of using electrogenerated manganese (III), cyclic voltammetry was undertaken on a solution of manganese sulphate in sulphuric acid..

Figure 6.40 Cyclic Voltammogram for Manganese (II) sulphate



Working electrode glassy carbon, Reference electrode silver/silver chloride Counter electrode platinum flag. Scan rate 0.2 V sec<sup>-1</sup>.

The voltammogram is shown in Figure 6.40. Two oxidation peaks were observed at 1.3 and 1.7V, suggesting that manganese (II) can be readily oxidised electrochemically for use as an oxidant.



## 6.6 Summary

The reaction of sugars with manganese (IV) dioxide sol was investigated and found to give CL in the presence of acid. The emission of light was faster than had been observed for permanganate. The intensity of emission was limited by the maximum concentration of sol that could be prepared. The CL time-course suggests the presence of two oxidising species, probably Mn (IV) and Mn (III).

Oxidation of sugars with Mn (III), both as commercial acetate and Mn (III) sulphate in strong acid prepared from permanganate, was also found to give fast light emission. As for Mn (IV), two phases were observed for the CL time-course. The prepared Mn (III) reagent was found to give significantly more intense chemiluminescence than permanganate for aliphatic polyhydroxy compounds. Further modifications in acid concentrations and preparation technique produced an improved reagent. A flow injection determination for sugars and related carbohydrates was optimised using the new reagent. The CL time-courses for reactions with sugars and polyols indicated that different mechanisms are present in the generation of the excited species. Methanol was found to significantly enhance the emission for the Mn (III) reagent, indicating the potential for use of the reagent for post-column detection in chromatographic systems using organic solvents.

Chemiluminescence spectra from the reactions of sugars and polyols compounds with Mn (IV) and Mn (III) species were the same as the from reactions with permanganate indicating that the same emitting species is probably generated in all the manganese oxidation reactions.

Initial investigations suggest that electrochemical generation of the manganese reagent is possible, with the potential of in-situ generation of the oxidant in the analytical flow injection, or post column system.



## **CHAPTER 7**

### **APPLICATIONS OF THE MANGANESE (III) REAGENT**

#### **HPLC WITH CHEMILUMINESCENCE DETECTION**

The determination of carbohydrates using the permanganate or manganese (III) reagents in flow injection systems is suitable for cases where individual carbohydrates are present. If the ratio of sugars in a mixture is known it is possible to prepare a suitable calibration mixture to determine total sugar. If the sugars are previously separated in a chromatographic system then it is possible to accurately determine levels of individual compounds.

#### **7.1 Chromatographic analysis of carbohydrates**

High performance liquid chromatography (HPLC) is the most used separation method for identification and determination of sugars in foods.<sup>265,266</sup>

##### **7.1.1 Choice of Chromatographic System**

Many phases have been used for the separation of carbohydrates, the choice depending on whether only mono and disaccharides are to be determined or if a determination of oligosaccharides is also required.

Of silica based phases the most frequently used is the aminopropyl-bonded phase with an acetonitrile/ water mobile phase. Octadecyl silica and diol bonded silica phases are also used. Unbonded silica phases can be used by modifying the mobile phase with amines, but these systems are not now often used. Cyclodextrine



bonded phases are also available and can separate anomeric forms of monosaccharides.<sup>231</sup> The other main type of separation used is ion chromatography, with both anion and cation systems based on polystyrene divinylbenzene. Ion chromatography columns have the advantage of a wide pH range but are expensive. For polysaccharides size exclusion systems can be used.

### **7.1.2 Detection Systems**

Sugars do not absorb UV light at analytically useful wavelengths therefore UV and fluorescence detectors cannot generally be used on the underivatised analytes. Wavelengths below 200nm have been used but, as most HPLC solvents also have significant absorbance at below 200nm, the system is only suitable for very high sugar concentrations.

Refractive index detectors are often used but are highly susceptible to changes in column temperature and solvent composition so in practice the limit of detection of sugar is 5 to 10µg. They are still commonly used for analysis of foods containing more than 1% of each sugar. The evaporative light scattering detector (ELS) is applicable to any non-volatile solute and has been used for detection of sugars.<sup>267</sup> Good sensitivity, in the region of 30ng on column, has been reported.<sup>268</sup> ELS detectors have poor linearity over the wide working ranges required in food analysis. As the detector measures a bulk property, like the refractive index detector, it is not selective.

For low levels of saccharides ion chromatography with pulsed amperometric detection is used. The system is very sensitive, capable of detecting ng amounts of sugars, and has been used to determine levels of sugars in authenticity studies.<sup>269 270</sup> The systems are expensive to buy and run.



In order to improve the sensitivity using normal or reverse phase HPLC pre-or post-column derivatisation is used to make UV absorbing or fluorescing products.<sup>271</sup> In general post column derivatisation is preferred, as derivatives may be unstable and reagents and secondary products could affect the chromatography. Post column methods for carbohydrates have been reviewed.<sup>272</sup> Several classical reactions have been adapted based on conversion of sugars to furfurals in strong mineral acid. Condensation with a reagent such as orcinol, anthrone or carbazole gives derivatives that absorb in the UV or visible regions. These systems have limits of detection of the order of 20ng, depending on the carbohydrate. Fluorescing and electroactive derivatives have been prepared by reaction with ethylenediamine, 2-cyanoacetamide and arginine. Limits of detection down to 4ng have been achieved. These reactions require long reaction times and/or heating to temperatures of more than 100°, necessitating the use of long post column reactors, some of several meters in length. Band broadening is considerable. Segmentation has been used to limit dispersion.

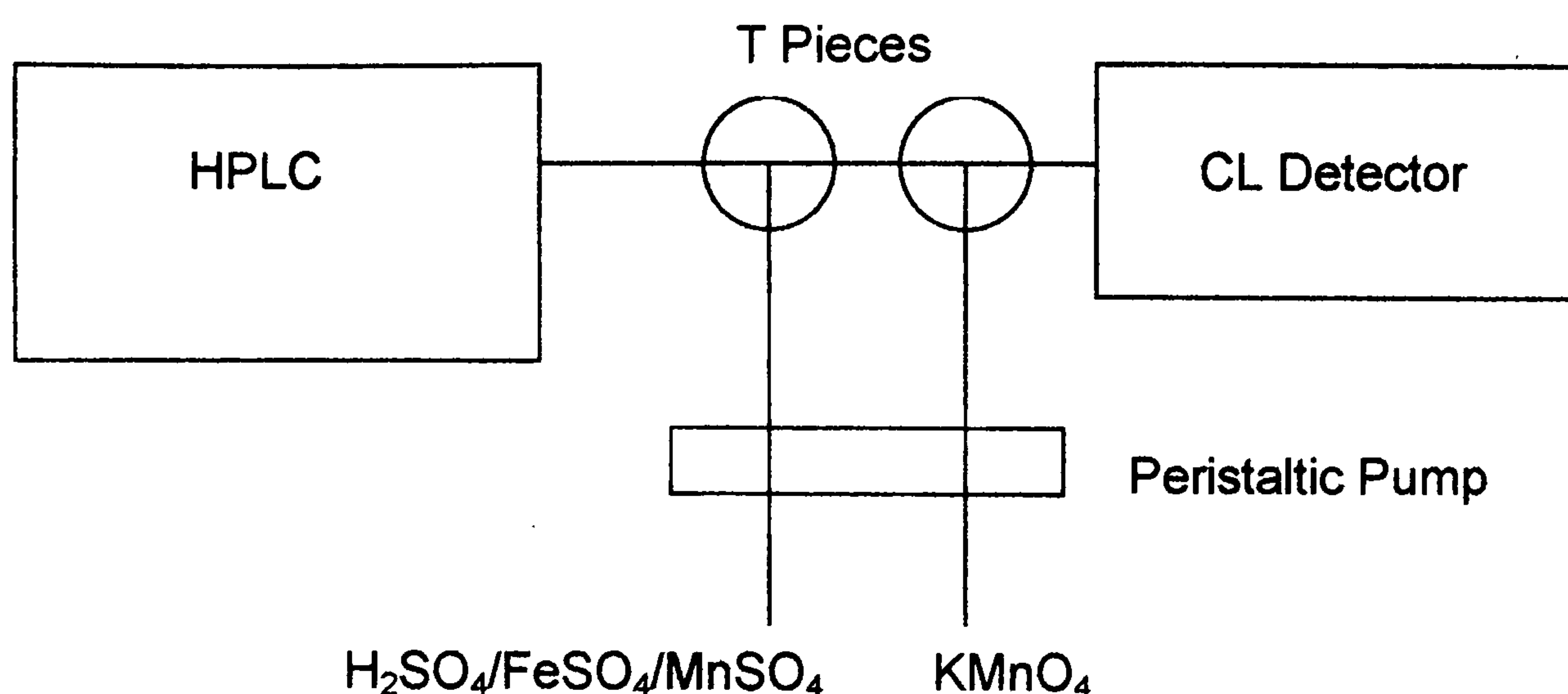
Chemiluminescence detection systems for HPLC have been proposed.<sup>273,274</sup> Systems based on luminol<sup>275,276</sup> and peroxyoxalate<sup>39,277,278</sup> are the most widely used. Permanganate chemiluminescence has been used for detection of morphine<sup>162 279</sup>. A detection system based on the manganese (III) chemiluminescent reaction would have the advantages of a rapid reaction with mild conditions.

Aminopropyl bonded silica was chosen as the chromatographic phase. Columns were readily available are the most widely used columns for sugar analysis.

## **7.2 Linking the Permanganate CL System to a Chromatograph**

Attempts were made to use permanganate directly, as in Figure 8.1. A standard chromatographic system with an acetonitrile/water mobile phase was set up.





**Figure 7.1 Post-Column Detection Manifold**

Acidic manganese sulphate/ ferrous sulphate was mixed with the column eluent and then aqueous permanganate was added immediately before the detector as in Figure 7.1. Problems were found with maintaining adequate flows of the two reagents using a peristaltic pump and no working system was obtained.

### 7.3 Linking the manganese (III) CL System to a Chromatograph

After the manganese (III) reagent was developed a simple single line post column system was set up as figure 7.2.

#### 7.3.1 Separation System

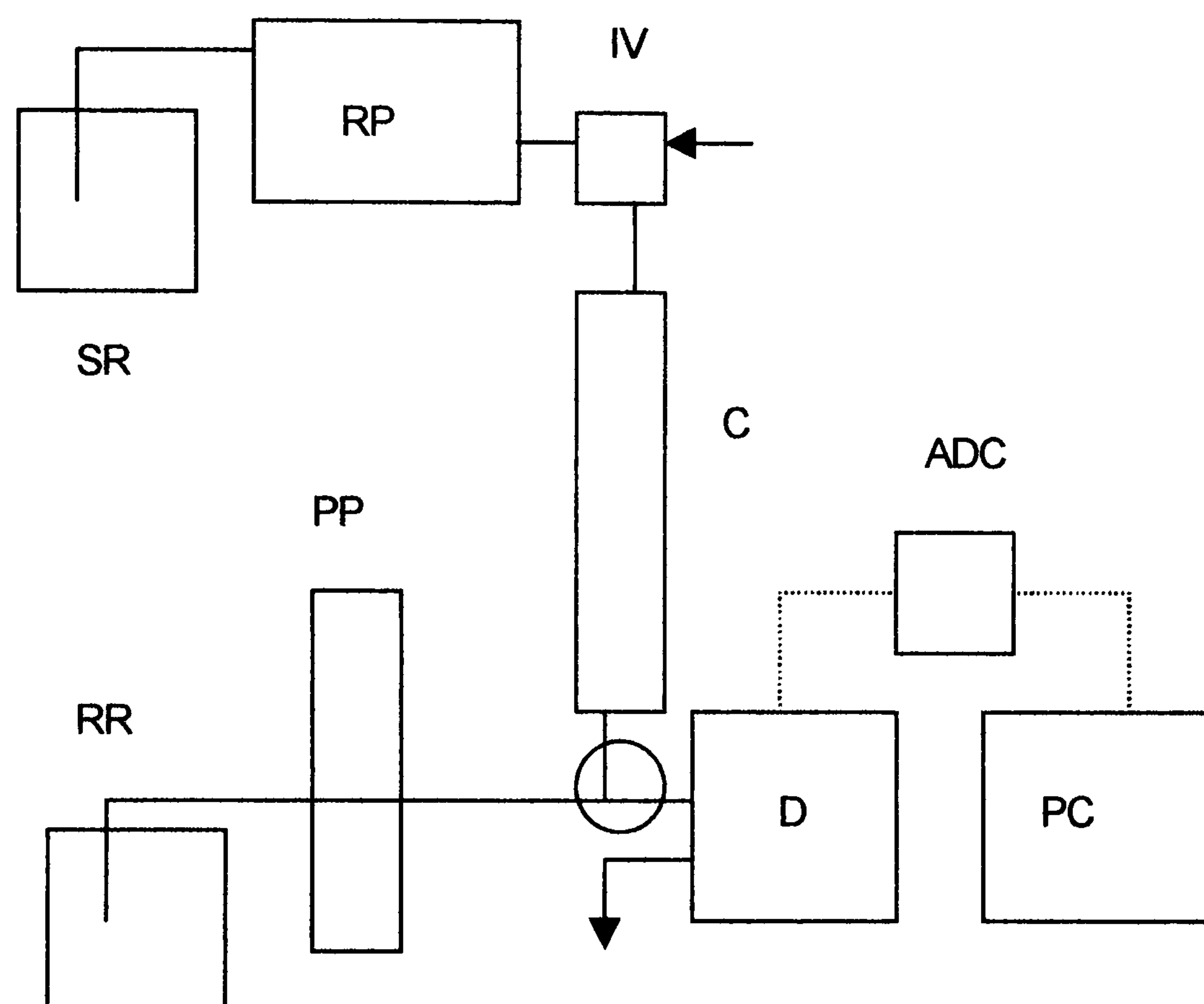
The glucose/cellobiose separation was taken as a model to assess the practicality of using the manganese (III) reagent in a post column detection system. The system was selected as of interest in enzyme studies in the formation of glucose oligomers. Typical sugar levels are below levels which can be measured using a refractive index detector.

The solvent most commonly used for the separation of sugars on aminopropyl columns is between 70 and 90% acetonitrile in water. It is known that acetonitrile



can quench some chemiluminescence systems and it was found that the permanganate chemiluminescence was strongly quenched. The standard chromatographic mobile phase was therefore unsuitable for use with the proposed post-column detection system.

**Figure 7.2 Post Column Chemiluminescence Detection System for Sugars**



SR- Solvent reservoir, RP- HPLC Pump, IV- Injection valve, C- HPLC column, RR- reagent reservoir, PP- Peristaltic pump, D- Detector, DC- Analog/digital converter  
PC-Computer

As discussed in Chapter 6.4.5.1, methanol enhances the chemiluminescence, this is believed to be by stabilising the intermediate manganese species manganese (IV) and manganese (III). Although methanol is widely used as a solvent in reverse-phase HPLC no satisfactory separation of sugars has been reported using a methanol/water system.

Few solvent systems other than acetonitrile/water or acetonitrile/ buffer have been reported, however ethanol/acetonitrile/water,<sup>280,281</sup> and acetone /ethyl acetate/water<sup>282</sup> have been reported to give adequate separation for small sugars.



A number of solvents were examined using a flow injection system to investigate the effect on the chemiluminescence signal. The chemiluminescence signals for glucose with the manganese (III) reagent using different solvents are shown in Table 7.1, Results are expressed relative to the signal with methanol.

**Table 7.1 Relative Signals for Glucose /Manganese (III)  
Chemiluminescence using Chromatography Solvents**

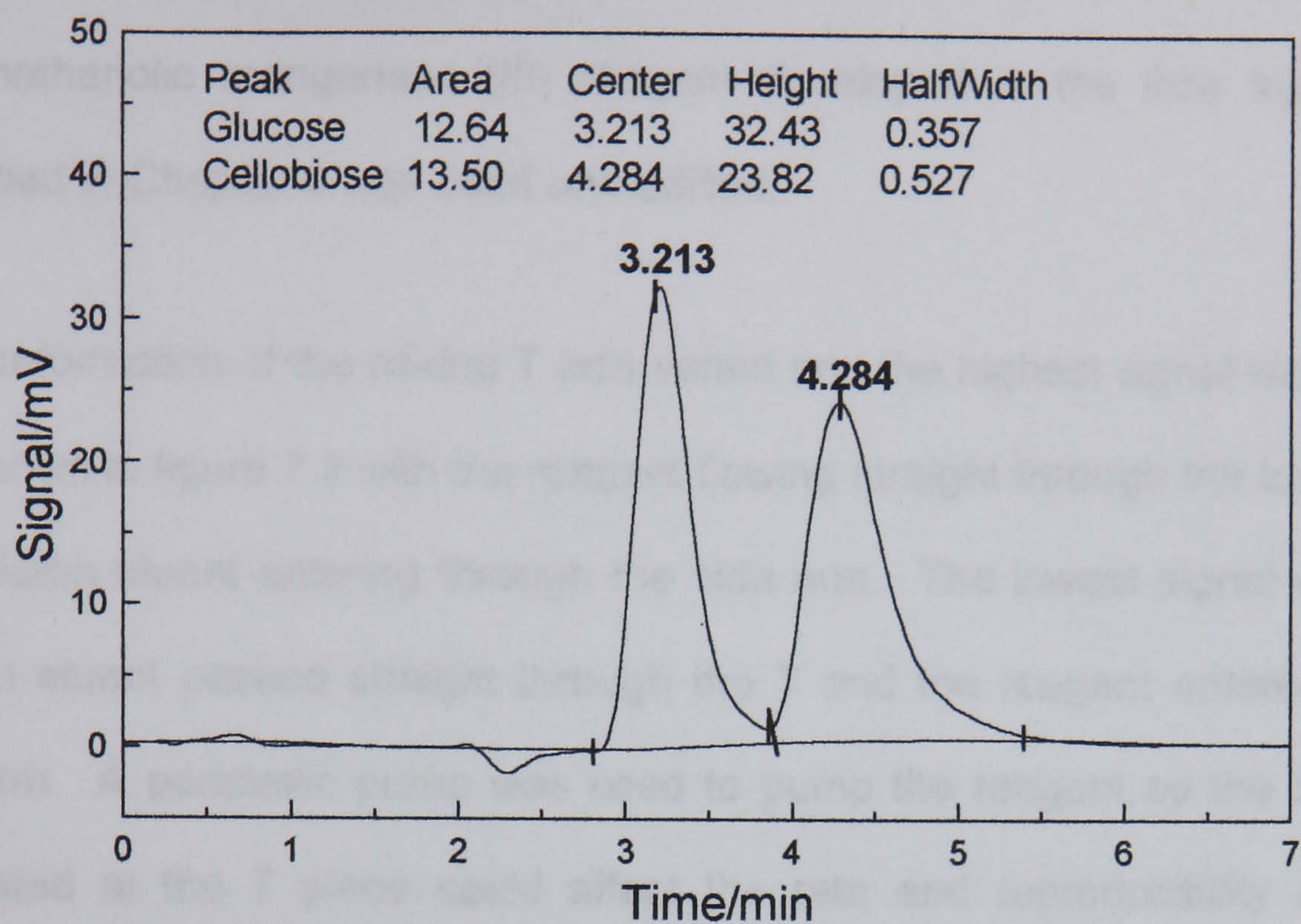
Solvent	Relative signal
Methanol	1.00
Ethanol	0.69
Tetrahydrofuran	0.46
Ethyl acetate	0.39
Acetone	0.20
Acetonitrile	0.03

It is clear any acetonitrile would seriously affect sensitivity and that acetone is also undesirable. Attempts were made to achieve separation with methanol/water, ethanol/water and ethanol/methanol/water and with methanol/tetrahydrofuran but no satisfactory separations were achieved for the model sugars.

Finally mixtures of ethyl acetate and methanol were investigated and near baseline separation of equimolar concentrations of glucose and cellobiose was achieved. The mobile phase was ethyl acetate/ methanol 55:45 and a typical chromatogram is shown in Figure 7.3. The mobile phase flow rate was optimised at 2 cm<sup>3</sup> min<sup>-1</sup> which gave a separation in 6 minutes with adequate resolution and peak shape.



**Figure 7.3 Chromatographic Separation of Glucose and Cellobiose using Manganese (III) Post-column Chemiluminescence Detection**



Mobile phase methanol/ethyl acetate 45:55 2.0cm<sup>3</sup> min<sup>-1</sup>  
Reagent 0.084 cm<sup>3</sup> min<sup>-1</sup> Glucose and cellobiose 1x10<sup>-3</sup> mol dm<sup>-3</sup>, 20μL

The chromatographic parameters for glucose and cellobiose at 1x10<sup>-3</sup> mol dm<sup>-3</sup> are shown in Table 7.2

**Table 7.2 Chromatographic Parameters for Glucose and Cellobiose**

Parameter	Glucose	Cellobiose
Resolution/%	96	
K'	6.5	8.9
Plates	440	370
Asymmetry	1.7	2.0

It can be seen that the efficiency of the column is poor, this could be due to an ageing column. The symmetry of the peaks is also poor but typical for sugars analysed on an amino column.



### 7.3.2 Optimisation of Post-column Parameters

The methanolic manganese (III) reagent developed in the flow injection studies described in Chapter 6 was used unmodified.

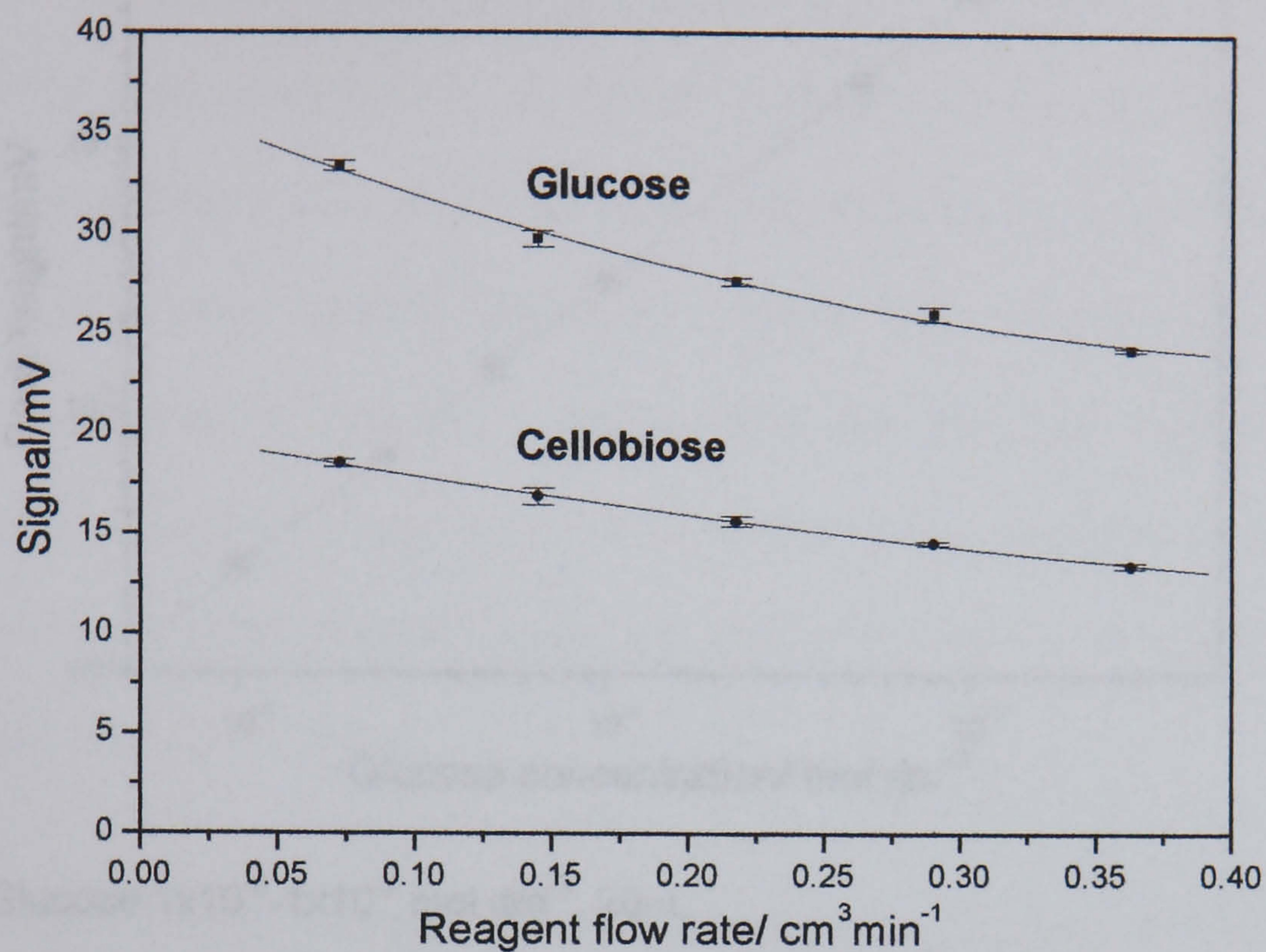
The conformation of the mixing T was varied and the highest signal was obtained for that shown in figure 7.2 with the reagent flowing straight through the top of the T and the column eluent entering through the side arm. The lowest signal was when the column eluent passed straight through the T and the reagent entered through the side arm. A peristaltic pump was used to pump the reagent so the back pressure generated at the T piece could affect the rate and reproducibility of pumping if reagent is added through the side arm. When, reagent is pumped straight the column eluent, which is pumped at a higher rate can aid the flow of reagent and improve the mixing efficiency resulting in a higher signal.

Increasing the eluent flow rate increased the signal. Above  $2.0 \text{ cm}^3 \text{ min}^{-1}$  the back pressure on the column was high therefore this flow rate was used for further studies. The effect of reagent flow rate was studied by varying both the pump speed and the tubing diameter. It was found that a low flow rate was required as shown in Figure 7.4. The results are consistent with those from the flow injection studies.

The use of more dilute reagent reduced the signal for a given flow rate showing that the decrease in signal at high flow rate is due to the increased dispersion at high flow rates and that a high concentration of manganese (III) is required in the reagent. A flow of  $0.08 \text{ cm}^3 \text{ min}^{-1}$  was selected. Below this the repeatability became poor. It is probable that with the use of a piston pump, capable of reliably delivering low flow rates, higher signals could be achieved.



**Figure 7.4 The Effect of Reagent Flow Rate on Peak Height**



Glucose, cellobiose  $1 \times 10^{-3} \text{ mol dm}^{-3}$ , Mobile phase  $2.0 \text{ cm}^3 \text{min}^{-1}$

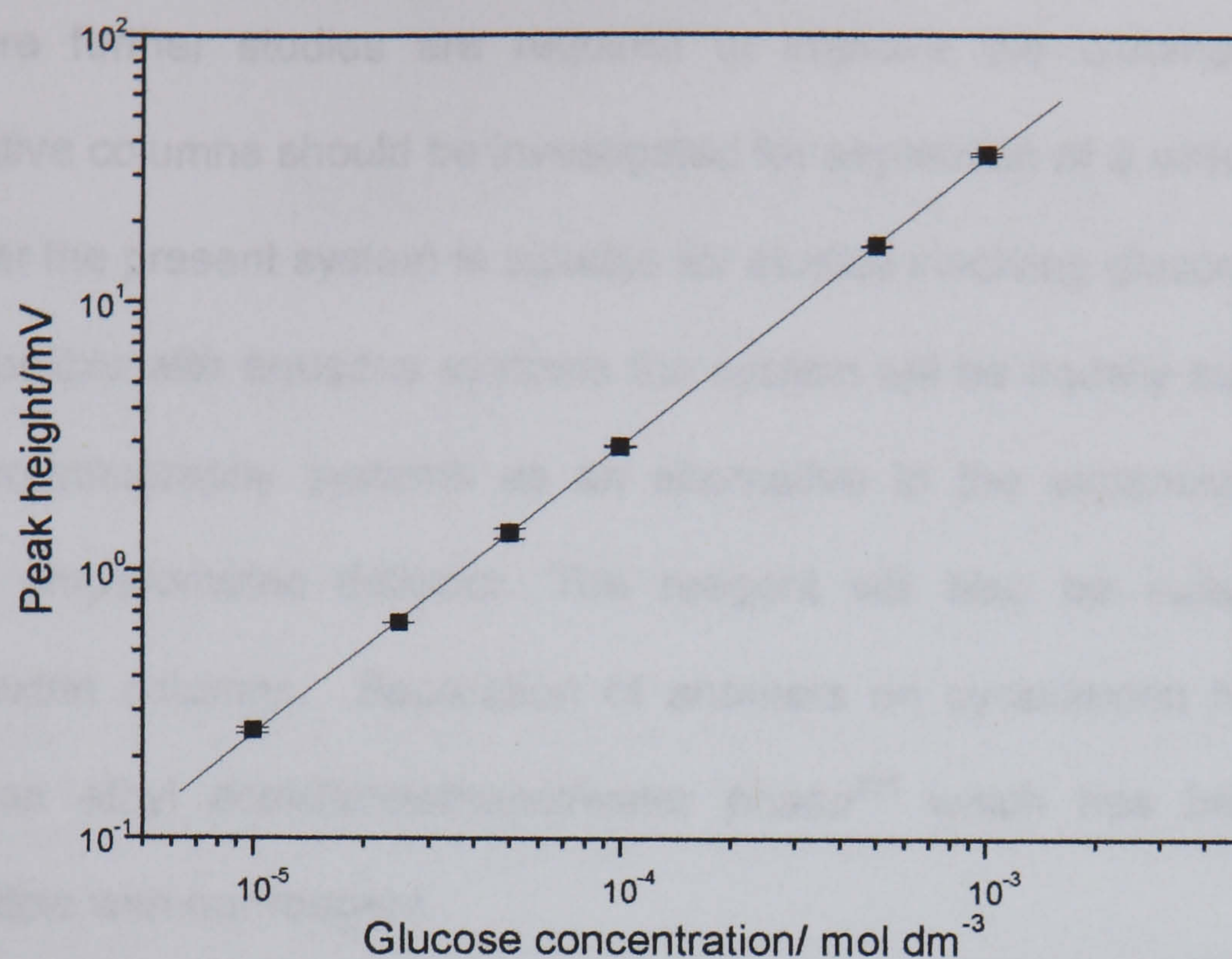
### 7.3.3 Calibration for Glucose

A calibration for glucose over the range  $1 \times 10^{-5}$  to  $1 \times 10^{-3} \text{ mol dm}^{-3}$  gave excellent linearity  $R=0.999$  and good reproducibility, RSDR of 3.86% for nine injections of  $1 \times 10^{-4} \text{ mol dm}^{-3}$  glucose.

A calibration line is shown in Figure 7.5. The limit of detection,<sup>217</sup> calculated over the range  $1 \times 10^{-5}$  to  $1 \times 10^{-4} \text{ mol dm}^{-3}$ , was found to be  $4 \times 10^{-6} \text{ mol dm}^{-3}$ , the equivalent of 15ng on column for a  $20 \mu\text{L}$  injection. The limit of detection is comparable to that quoted for light scattering detectors.



**Figure 7.5 Calibration line for Glucose**



Glucose  $1 \times 10^{-5}$ – $1 \times 10^{-3}$  mol dm<sup>-3</sup>, 20 μL

Mobile phase methanol/ethyl acetate 45:55 2.0 cm<sup>3</sup> min<sup>-1</sup>

Reagent 0.084 cm<sup>3</sup> min<sup>-1</sup>

## 7.4 Summary

A post column system for detection of sugars has been developed. The system shows linearity over two orders of magnitude and a limit of detection for glucose of 15 ng on column. This is better than detection of underivatized sugars by UV or refractive index and equivalent to that for evaporative light scattering. The limit of detection is of the same order as for the classical sugar reactions which have been adapted as post column systems and does not require prolonged heating in order to develop the detectable species. The fast reaction allows the chemiluminescent reagent to be added immediately before the detector limiting the amount of dispersion and minimising peak broadening. The low optimal flow rate of reagent, which is derived from inexpensive chemicals, makes the system economical to run.



The chromatographic parameters, plate number and asymmetry, were poor, therefore further studies are required to improve the chromatographic system. Alternative columns should be investigated for separation of a wider range of sugars, however the present system is suitable for studies involving glucose. As the reagent is compatible with aqueous systems the system will be equally suitable for use with ion chromatography systems as an alternative to the expensive, gold electrode, pulsed amperometric detector. The reagent will also be suitable for use with cyclodextrin columns. Separation of anomers on cyclodextrin has been reported using an ethyl acetate/methanol/water phase<sup>231</sup> which has been shown to be compatible with our reagent.

It was shown earlier, in section 6.4.6 that oligosaccharides give lower signals than monosaccharides, particularly in the case of non-reducing sugars such as sucrose. A large molecule such as dextran with an average molecular weight of  $2 \times 10^6$  can give a signal with the reagent. This shows the potential of the reagent as a post column detection system in polysaccharide chromatography, for example in glycobiology where, derivatisation methods are currently widely used<sup>283</sup>.



# CHAPTER 8

## SUMMARY AND CONCLUSIONS

### 8.1 Summary of the Project

#### 8.1.1 Permanganate Chemiluminescence

The utility of permanganate chemiluminescence in analysis of non-aromatic polyhydroxy compounds such as sugars and sugar alcohols has been demonstrated. The oxidation of polyhydroxy compounds by permanganate, catalysed by manganese (II) gives red chemiluminescence. The size of the signal is greatest for fructose and smaller for glucose and disaccharides. Non reducing sugars such as sucrose and trehalose giving the smallest signals.

For simple polyhydroxy compounds the trend in chemiluminescence response is for an increase in signal as the number of hydroxy groups increases. The emission of light has been shown to follow the reduction of manganese (VII) and to be related to the presence of manganese (III) in the reaction mixture.

#### 8.1.2 Manganese (III) Chemiluminescence

A reagent based on manganese (III) in sulphuric acid has been developed which gives significantly higher signals for aliphatic polyhydroxy compounds than acid permanganate. The system has a wide a linear range which, for fructose, is five orders of magnitude, from  $1 \times 10^{-7}$  to  $1 \times 10^{-2}$  mol dm<sup>-3</sup>.

The presence of alcohols enhances the signal and allows the use of less concentrated acids, making the reagent very compatible with chromatographic solvent systems.



### **8.1.3 Chemiluminescence spectroscopy**

Chemiluminescence spectroscopy has shown that the emitting species from permanganate and manganese (III) reagent are the same and involve a manganese species probably manganese (III) or manganese (II). A wide range of hydroxy compounds including saccharides, aliphatic polyols, ascorbic acid and some phenolic compounds have been shown to give the same chemiluminescence emission spectrum.

## **8.2 Analytical Applications**

Ascorbic acid has been determined in extracts of food supplements and fruit juices using direct permanganate chemiluminescence with flow injection.

A post column system has been developed for determination of sugars separated by HPLC. The system has sensitivity comparable with that of evaporative light scattering detectors and is linear over at least two orders of magnitude. The reaction is fast and requires no heat or delay coils minimising band broadening due to dispersion. The manganese (III) reagent, is prepared from inexpensive components making the system simple and economical to run.

## **8.3 Future Work**

Recent reports have described a range of compounds that give direct chemiluminescence with permanganate in acid medium. Many of these do not have any hydroxy groups and several include amino groups. Spectroscopic studies with some of these could give additional information regarding the nature of the manganese emitting species. Preliminary experiments with phenolic compounds showed that the chemiluminescent reaction with permanganate is much faster than



that for saccharides, even in the presence of manganese (II) catalyst. Further studies of these compounds should also give additional information about the emitting species.

Initial investigations have indicated that electrochemical generation of the manganese (III) reagent is possible, with the potential of in situ generation of the oxidant in the analytical system. This would overcome the requirement of cooling the reagent making it even more attractive for process control applications.

A limited data analysis has been carried out on flow injection measurements which has shown the potential for multiple component analysis. It may be possible to exploit the kinetic differences between reactions of permanganate or manganese (III) with the range of reducing compounds such as mixtures of sugars. The increasing availability of simple and rugged miniature photo diode detectors will enable sampling of chemiluminescence at several different times in the dispersion path, or after zone merging. Chemometric techniques can then be applied to the data sets generated.



# REFERENCES

- 
- <sup>1</sup>Bowie A.R., Sanders M.G., Worsfold P.J., *J. Biolumin. Chemilumin.*, 1996, **11**, 61-90, "Analytical applications of liquid phase chemiluminescence reactions-A review"
- <sup>2</sup>Cilento G., Adam W., *Photochemistry and Photobiology*, 1988, **48**, 361-368, "Photochemistry and photobiology without light"
- <sup>3</sup>Kricka L.J., Thorpe G.H.G., *Analyst*, 1983, **108**, 1274-1296, "Chemiluminescent and bioluminescent methods in analytical chemistry"
- <sup>4</sup>Robards K., Worsfold P.J., *Anal. Chim. Acta.*, 1992, **266**, 147-173, "Analytical applications of liquid phase chemiluminescence"
- <sup>5</sup>Seitz W.R., *CRC Critical Reviews in Analytical Chemistry*, 1981, 1-57, "Chemiluminescence and bioluminescence analysis; fundamentals and biomedical applications"
- <sup>6</sup>Townsend A., *Analyst*, 1990, **115**, 495-500, "Solution chemiluminescence -Some recent analytical developments"
- <sup>7</sup>Warner I.M., Soper S.A., McGown L.B., *Anal. Chem.*, 1996, **68**, R73-91, "Molecular fluorescence, phosphorescence and chemiluminescence spectrometry"
- <sup>8</sup>Barnett N.W., Lewis S.W., *Analysis Europa*, 1996, March, 29-33, "Tripping the light fantastic"
- <sup>9</sup>Lewis S.W., Price D., Worsfold P.J., *J Biolumin. Chemilumin.*, 1993, **8**, 183-199, "Flow injection assays with chemiluminescence and bioluminescence detection - A review"
- <sup>10</sup>Simpson J.S.A., Richardson A., *Bioluminescence and Chemiluminescence Proceedings*, Academic Press, 1981, pp673- 679, "Chemiluminescent labels in Immunoassay"
- <sup>11</sup>Rongen H.A.H., Hoetelmans R.M.W., Bult A., van Bennekom W.P., *J. Pharm. and Biomed. Analysis*, 1994, **12**, 433-462, "Chemiluminescence and Immunoassays"
- <sup>12</sup>Navas M.J., Jimenez A.M., *Food Chemistry*, 1996, **55**, 7-15, "Review of chemiluminescent methods in food analysis"
- <sup>13</sup>Harvey E.N., *A History of Luminescence from the Earliest Times until 1900*, 1957, American Philosophical Society, Philadelphia pp 470-474
- <sup>14</sup>Shadwell Thomas, "The Virtuoso" Regents Restoration Drama Series, Editors Nichlolson M.H., Rodes D.S., 1996, University of Nebraska Press
- <sup>15</sup>Turro N.J, *Modern Molecular Photochemistry*, 1991, University Science Books California
- <sup>16</sup>Usuki R., Kaneda T., Yamagichi A., Takyu C., Inaba., *J Food Sci*, 1979, **44**, 1573-1576, "Estimation of oxidative deterioration of oils and foods by Measurement of ultraweak CL"
- <sup>17</sup>Kaneda H., Kano Y., Kamimura M., Osawa T., Kawakishi S., *J. Food. Sci.*, 1990, **55**, 881-882, "Detection of chemiluminescence produced during beer oxidation"
- <sup>18</sup>Kaneda H., Kano Y., Kamimura M., Osawa T., Kawakishi S., *J. Food. Sci.*, 1990, **55**, 1361-1367, "Evaluation of beer deterioration by chemiluminescence"
- <sup>19</sup>Kaneda H., Kano Y., Kammimura M., Kawakishi S., Osawa T.A., *J.Inst.Brewing.*, 1991, **97**, 105-109, "A study of beer staling using chemiluminescence analysis"
- <sup>20</sup>Kaneda H., Kano Y., Osawa T., Kawakishi S., Koshino S., *J. Am. Soc. Brewing Chemists*, 1994, **52**, 70-75, "Role of beer components in chemiluminescence production during beer storage"
- <sup>21</sup>Gough T.A., Webb K.S., Eaton R.F.J., *J. Chromatog*, 1977, **137**, 293-303, "Simple Chemiluminescence detector for the screening of foods for the presence of volatile nitrosamines"



- 
- <sup>22</sup>Dressler M., *Selective Gas Chromatographic Detectors*, Journal of Chromatography Library Volume 36, 1986, Elsevier
- <sup>23</sup>Hutte R.S., Sievers R.E., Birks J.W., *J. Chromat. Sci.*, 1986, **24**, 499-505,  
"Gas chromatography detectors based on chemiluminescence"
- <sup>24</sup>Devore T.C., Gole J.L., *J. Phys. Chem.*, 1996, **100**, 5660-5667,  
"CL emission from the reaction of manganese vapour and halogen molecules"
- <sup>25</sup>Crowson A., Hiley R.W., Ingham T., McCreedy T., Pilgrim J., Townshend A.,  
*Anal Comm*, 1997, **34**, 213-216,  
"Investigation into the detection of nitrated organic compounds and explosives by direct chemiluminescent emission during thermally induced gas phase decomposition reactions"
- <sup>26</sup>Hopkins T.A., Seliger H.H., White E.H., Cass M.W., *J. Am. Chem. Soc.*, 1967, **89**, 7148-7150,  
"The chemiluminescence of firefly luciferin. A model for the bioluminescent reaction and identification of the product excited state"
- <sup>27</sup>Clerc S.D., *Thesis, University of Huddersfield*, 1996,  
"Analytical applications of bacterial bioluminescence"
- <sup>28</sup>Worsfold P.J., Nabi A., *Anal. Chim. Acta.*, 1986, **179**, 307-313,  
"Bioluminescent assays with immobilised firefly luciferase based on flow injection analysis"
- <sup>29</sup>Miller N.J., Nawari M.B., Burgess C., *Anal. Chim. Acta.*, 1992, **226**, 339-343,  
"Detection of bacterial ATP by reversed flow injection analysis with luminescence detection"
- <sup>30</sup>Easter M., *International Labmate*, 1998, **23**, 47-48,  
"Managing risk with rapid microbial testing systems."
- <sup>31</sup>Weller A. Zachariasse K., *Chem. Phys. Letters.*, 1971, **10**, 5902,  
"Chemiluminescence from radical ion recombination experimental evidence for the triplet triplet annihilation mechanism"
- <sup>32</sup>Lechtken P., Breslow R., Schmidt A.H., Turro N.J., *J. Am. Chem. Soc.*, 1973, **95**, 3025-3027,  
"Thermal rearrangement for dewar benzenes to benzene triplet states. Examples of spin-forbidden non-adiabatic pericyclic reactions"
- <sup>33</sup>Campbell A.K., "*Chemiluminescence Principles and Applications in Biology and Medicine*", 1988, Ellis Horwood, Chichester
- <sup>34</sup>Lind J., Merenyi G., Eriksen T.E., *J. Am. Chem. Soc.*, 1983, **105**, 7655-7661,  
"Chemiluminescence mechanism of cyclic hydrazines such as luminol in aqueous solutions"
- <sup>35</sup>Sasaki S., Arikawa Y., Shimomura M., Ikebukuro K., Karube I., *Anal. Comm.*, 1997, **34**, 299-302,  
"Measurement of sulphite using sulphate oxidase and luminol chemiluminescence"
- <sup>36</sup>Huang Y.L., Kim J.M., Schmid R.D., *Anal. Chim. Acta.*, 1992, **266**, 317-323,  
"Determination of sulphite in wine thorough flow injection analysis based on the suppression of luminol chemiluminescence"
- <sup>37</sup>Kearney N.J., *Thesis University of Huddersfield*, 1996,  
"Novel methods for the determination of analytes using luminescence"
- <sup>38</sup>Slavinska D., Lichszfeld K., Michalska T., *Pol. Jour. Chem.*, 1978, **32**, 1729,  
"Singlet oxygen and the chemiluminescence in the autoxidation of pyrogallol"
- <sup>39</sup>Hadd A.G., Birks J.W., "*Peroxyoxalate chemiluminescence Mechanism and Analytical Detection*".  
From "Selective Detectors Ed Sievers R.E., Chemical Analysis Series, 131, 1995, John Wiley and Sons
- <sup>40</sup>Rauhut M.M., *Acc. Chem. Res.*, 1969, **2**, 80-87,  
"Chemiluminescence from concerted decomposition reactions"



- 
- <sup>41</sup>Rauhut M.M., Bollyky B.G., Roberts B.G., Loy M., Whitman R.H., Lannotta A.V., Semsel A. M., Clarke R.A., *J. Am. Chem. Soc.*, 1967, **89**, 6515-6522,  
"Chemiluminescence from reactions of electronegatively substituted aryl oxalates with hydrogen peroxide and fluorescent compounds"
- <sup>42</sup>Schuster G.B., *Acc. Chem. Res.*, 1979, **12**, 366-373,  
"Chemiluminescence of organic peroxides. Conversion of ground state reactants to excited state products by the chemically initiated electron exchange luminescence mechanism."
- <sup>43</sup>McCapra F., *Prog. Org. Chem.*, 1973, **8**, 231-276, "Chemiluminescence of organic compounds"
- <sup>44</sup>Catherall C.L., Palmer T.F., Cundall R.B., *J., Chem. Soc. Faraday Trans.*, 1984, **80**, 837-849,  
"Chemiluminescence from reactions of bis(pentachlorophenyl)oxalate, hydrogen peroxide and fluorescent compounds"
- <sup>45</sup>Milofsky R.E., Birks J.W., *Anal. Chem.*, 1990, **62**, 1050-1055,  
"Photoinitiation of peroxyoxalate chemiluminescence: Application to flow injection analysis of chemilumophores"
- <sup>46</sup> Sigvardson J.M., Kennish J.M., Birks J.W., *Anal. Chem.*, 1984, **56**, 1096-1102, "Peroxyoxalate chemiluminescence detection of polycyclic aromatic amines in liquid chromatography"
- <sup>47</sup>Hanaoka N., Tanaka H., *J. Chromatog.*, 1992, **606**, 129-132,  
"Improvement of the peroxyoxalate chemiluminescence detection in liquid chromatography with gradient elution and long reaction time"
- <sup>48</sup>van Zoonen P., Bock H., Gooijer C., Velhorst H.H., Frei R.W., *Anal. Chim. Acta.*, 1987, **200**, 131-141,  
"Quenched peroxyoxalate chemiluminescence detection in aqueous liquid chromatography separations"
- <sup>49</sup> Hercules D.M., Lytle F.E., *J Am. Chem. Soc.*, 1966, **88**, 4745-4746,  
"Chemiluminescence from reduction reactions"
- <sup>50</sup>Barnett N.W., Hindson B.J., Lewis S.W., Purcell S.D., *Anal. Comm.*, 1998, **35**, 321-324,  
"Determination of Codeine, 6 Methoxy codeine and Thebaine using capillary electrophoresis with tris (2'2-bipyridyl)ruthenium(II) chemiluminescence detection"
- <sup>51</sup> Lee W.Y., *Mikrochimica Acta*, 1997, **127**, 19-39,  
"Tris (2,2'-bipyridyl)ruthenium(II) Electrogenerated chemiluminescence in analytical science"
- <sup>52</sup> Kearney N.J., Hall C.E., Jewsbury R.A., Timmis S.G., *Anal. Comm.*, 1996, **33**, 269-270,  
"Electrogenerated chemiluminescence using platinum electrodes with hydrogen peroxide pre-treatment"
- <sup>53</sup>Khan A.U., Kasha M., *J. Am. Chem. Soc.*, 1970, **92**, 3293-3300,  
"Chemiluminescence arising from simultaneous transitions in pairs of singlet oxygen molecules"
- <sup>54</sup>Lichszeld K., Kruk I., *Z. Phys. Chem.*, 1977, **108**, 167-175,  
"Singlet molecular oxygen in formaldehyde oxidation"
- <sup>55</sup>Ruzicka J., Hansen E.H., *Flow Injection Analysis*, 2<sup>nd</sup> Edition, 1988, John Wiley
- <sup>56</sup>Skeggs L.T., *Am. J Clin. Pathol.* 1957, **28**, 331-322,  
"Automatic method for colourimetric Analysis"
- <sup>57</sup>Skeggs L.T., *Automation in Analytical Chemistry*, 1966, Mediad NY
- <sup>58</sup>Stockwell P.B., Corns W.T., *Automatic Chemical Analysis*, 1996, Taylor and Francis
- <sup>59</sup>Wolf W.R., Stewart K.K., *Anal. Chem.*, 1979, **51**, 1201-1205,  
"Automated multiple flow injection analysis for flame atomic absorption spectroscopy"
- <sup>60</sup>Ruzicka J., Hansen E.H., Mosbeack H., *Anal. Chim. Acta.*, 1977, **92**, 235-249,  
"Flow injection analysis: A new approach to continuous flow titrations"
- <sup>61</sup>Reijn J.M., van der Linden W.E., Poppe H., *Anal. Chim. Acta.*, 1980, **114**, 105-118,  
"Some theoretical aspects of flow injection analysis"



- 
- <sup>62</sup>Stone D.C., Tyson J.F., *Analyst*, 1987, **112**, 515-521,  
"Models for dispersion in flow injection analysis. Part 1 Basic requirements and study of factors affecting dispersion"
- <sup>63</sup>Reijn J.M., van der Linden W.E., Poppe H., *Anal. Chim. Acta.*, 1981, **126**, 1-13,  
"Transport phenomena in flow injection analysis without chemical reaction"
- <sup>64</sup>Tyson J.F., *Analyst*, 1987, **112**, 523-526,  
"Analytical information from doublet peaks: 1 Basic equation and applications to flow injection titrations"
- <sup>65</sup>Chung H.K., Ingle J.D., *Anal. Chem.*, 1990, **62**, 2547-2552,  
"Kinetic data from individual peak profiles corrected for dispersion in flow injection analysis applied to the determination of Aluminium"
- <sup>66</sup>Tyson J.F., *Analyst*, 1987, **112**, 527-529,  
"Analytical information from doublet peaks: 2 Determination of stability constants"
- <sup>67</sup>Sahlestrom Y., Karlberg., *Anal. Chim. Acta.*, 1986, **179**, 315-323,  
"An unsegmented extraction system for flow injection analysis"
- <sup>68</sup>Masoom M., Townshend A., *Anal. Proc.*, 1985, **22**, 6-8,  
"Applications of immobilised enzymes in flow injection analysis"
- <sup>69</sup>Tryzell R., Karlberg B., *Anal. Chim. Acta.*, 1997, **343**, 183-190,  
"Calibration methods for determination of ammonia and excess acid in Kjeldahl digests by FIA"
- <sup>70</sup>Schothorst R.C., den Boef G., *Anal. Chim. Acta*, 1983, **153**, 133-139,  
"The application of strongly reducing agents in flow injection analysis: Part 2 Chromium"
- <sup>71</sup>Ruzicka J., Marshall G.D., *Anal. Chim. Acta.*, 1990, **237**, 329-343,  
"Sequential injection analysis a new concept for chemical sensors and process analysis"
- <sup>72</sup>Mas F., Cladera A., Estela J.M., Cerda V., *Analyst*, 1998, **123**, 1541-1546,  
"New approach to sequential injection analysis :Using the sample as carrier"
- <sup>73</sup>Cladera A., Tomas C., Gomez E., Estela J.M., Cerda V.,  
*Anal. Chim. Acta.*, 1995, **302**, 297-308,  
"A new instrumental implementation of sequential injection analysis"
- <sup>74</sup>Kakizake T., Imai K., Hasebe K., *Anal. Comm.*, 1996, **33**, 75-77,  
"Flow injection with diaphragm pump and amperometric detector"
- <sup>75</sup>Spatny N., Haswell S.J., Grasserbauer M., *Anal. Proc.*, 1995, **32**, 141-143,  
"FIA method for the determination of Vitamin A by Iodine"
- <sup>76</sup>Cladera A., Gomez E., Estela J.M., Cedra V. *Analyst*, 1991, **116**, 913,  
"Determination of Iron by flow injection based on the catalytic effect of the Iron EDTA complex on the oxidation of hydroxylamine by dissolved oxygen"
- <sup>77</sup>Reising J.A., Mottl M.J., *Anal. Chem.*, 1992, **64**, 2682-2687,  
"Determination of Manganese in sea- water using flow injection analysis with on-line pre-concentration and spectrophotometric detection"
- <sup>78</sup>Bergamin F.H., Medeiros J.X., Reis B.F., Zagatto E.A.G, *Anal. Chim. Acta.*, 1978, **101**, 9-16, "Solvent extraction in continuous flow injection analysis determination of Molybdenum in plant material"
- <sup>79</sup>Chen D.H., DeCastro M.L., Valcarcel M., *Analyst*, 1991, **116**, 1095-1111,  
"Determination of anions by flow injection analysis : A review"
- <sup>80</sup>Gine M.F., Bergamin H., Zagatto E.A.G., Reis B.F., *Anal. Chim. Acta.*, 1980, **114**, 191-197,  
"Simultaneous determination of nitrite and nitrate by flow injection analysis"
- <sup>81</sup>Shi R., Stein K., Schwedt G., *Z. Lebesm. Unters Forsch A*, 1977, **204**, 99-102,  
"Spectrophotometric determination of glucose in foods by flow injection analysis with an immobilised glucose oxidase reactor"



- 
- <sup>82</sup>Su X., Wei W., Nie I., Yao S., *Analyst*, 1998, **123**, 221-224,  
"Flow injection determination of sulphite in wines and fruit juices by using a bulk acoustic wave impedance sensor coupled to a membrane separation technique"
- <sup>83</sup>Sartini R.P., Oliviera C.C., Zagatto E.A.G., Bergamin Filho H., *Anal. Chim. Acta.*, 1998, **366**, 119-125,  
"Determination of reducing sugars by flow injection gravimetry"
- <sup>84</sup>Ruzicka J., *Analyst*, 1994, **119**, 1925-1934,  
"Discovering flow injection - From sample to a live cell and from solution to suspension"
- <sup>85</sup>Petersson B.A., *Anal Chim. Acta.*, 1988, **209**, 231-237,  
"Amperometric assay of glucose and lactic acid by flow injection analysis"
- <sup>86</sup>Hansen E.H., *Journal of Molecular Recognition*, 1996, **9**, 316-325,  
"Principles and applications of flow injection analysis in biosensors"
- <sup>87</sup>Burguera J.L., Townshend A., *Talanta*, 1981, **28**, 731-735,  
"Determination of manganese(II) by a chemiluminescence reaction"
- <sup>88</sup>Stanley P.E., *J. Biolum. Chemilum.*, 1992, **7**, 77-108,  
"Commercially available luminometers and imaging devices for low light level measurements of utilising and bioluminescence, including instruments for manual automatic and specialised operation for HPLC, LC, GLC and micro titre plates."
- <sup>89</sup>Stanley P.E., *J. Biolum. Chemilum.*, 1997, **12**, 61-78,  
"A survey of more than 90 commercially available luminometers and imaging devices for low light level measurements and kits and reagents utilising bioluminescence or bioluminescence Survey update 5"
- <sup>90</sup>Suppon P., *Chemistry and Light*, 1994, Royal Society of Chemistry
- <sup>91</sup>Horowitz P., Winfield H., *The Art of Electronics*, 1980, Cambridge University Press
- <sup>92</sup>Wright A. G., *Sources of Noise in Photomultipliers*,  
1985, Thorn EMI Electron Tubes Limited Photodetection Information Service Middlesex.
- <sup>93</sup>Marino D.F., Ingle J.D., *Anal. Chem.*, 1981, **53**, 645-650,  
"Microcomputer controlled diode array system for chemiluminescence spectra"
- <sup>94</sup>Wondrak G., Pier T., Tress R., *J. Biolum. Chemilum.*, 1995, **10**, 277-284,  
"Light form Maillard Reaction Photon Counting, Emission spectrum , Photography and Visual Perception"
- <sup>95</sup>Hunt D.J., Parkes H.C ., Lumley I.D., *Food Chemistry*, 1997, **60**, 437-442,  
"Identification of species of origin of raw and cooked meat products using oligonucleotide probes"
- <sup>96</sup>Slawinska D., Slawinski J., *J. Biolum. Chemilum.* 1998, **13**, 21-24,  
"Chemiluminescence of cereal products III :Two dimensional photocount imaging"
- <sup>97</sup>Chance B., *J. Franklin Inst.*, 1940, **229**, 613-640,  
"Accelerated flow method for rapid reactions: 1 analysis"
- <sup>98</sup>Chance B., *J. Franklin Inst.*, 1940, **229**, 737-766,  
"Accelerated flow method for rapid reactions 2 Design construction and tests"
- <sup>99</sup>Crouch S.R. Holler F.J. Notz P.K. Beckwith P.M., *Appl. Spectrosc. Rev.*, 1977, **13**, 165-259,  
"Automated stopped flow systems for fast reaction rate methods"
- <sup>100</sup>Gomez-Hens A., Perez-Bendito D., *Anal Chim Acta.* 1991, **242**, 147-177,  
"The stopped-flow technique in analytical chemistry"
- <sup>101</sup>Gibson , Q.H., *Discussions Faraday. Soc.*, 1954, **17**, 137-139,  
"Stopped-flow apparatus for the study of rapid reactions"
- <sup>102</sup>Gibson , Q.H. Roughton F.J.W., *Proc. Royal Soc. Lond.*, 1955, **143**, 310-334,  
"Kinetics of dissociation of the first oxygen molecule from fully saturated oxy-hemoglobin in sheep blood"



- 
- <sup>103</sup>Evans J.F., Bancroft E.E. Blount H.N., *Anal Chem*, 1981, **53**, 359-360,  
"Stopped flow syringes with teflon plunger tips and smooth bore glass barrels"
- <sup>104</sup>Lever S., Crooks J., *American Laboratory*, 1985, **17**, 106-117,  
"Study of fast chemical kinetics using stopped-flow spectrophotometry and the preparative quench technique"
- <sup>105</sup>Northrop D.B., Simpson F.B., *Bioorganic and Medicinal Chemistry*, 1997, **5**, 641-644, "Beyond enzyme kinetics : Direct determination of mechanisms by stopped-flow mass spectrometry"
- <sup>106</sup>Lorigullo A., Silva M., Perez-Bendito D., *Anal. Chim. Acta.*, 1987, **199**, 29-40,  
"Versatile automatic stopped-flow system for routine analysis"
- <sup>107</sup>Brzovic P.S., Dunn M.F., *Methods in Enzymology*, 1995, **246**, 168-201,  
"Rapid scanning ultraviolet/visible spectroscopy applied in stopped-flow studies"
- <sup>108</sup>Chance BE, Harvey N, Johnson F and Millikan N.,  
*J. Cellular. Comp. Physiol.*, 1940, **7**, 195-215, "The kinetics of bioluminescent flashes."
- <sup>109</sup>Gaikwad A., Silva M., Perez-Bendito D., *Anal. Chim. Acta.*, 1995, **302**, 275-282,  
"Selective stopped-flow determination of manganese with luminol in the absence of hydrogen peroxide"
- <sup>110</sup>Gonzales-Robledo D., Silva M., Perez-Bendito D., *Anal. Chim. Acta.*, 1989, **217**, 239-247,  
"Performance of the stopped-flow technique in chemiluminescence spectrometry based on direct rate measurements"
- <sup>111</sup>Gonzales-Robledo D., Silva M., Perez-Bendito D., *Anal. Chim. Acta.*, 1990, **228**, 123-128,  
"Determination of hypochlorite in waters by stopped-flow chemiluminescence spectroscopy"
- <sup>112</sup>Ventura S., Silva M., Perez-Bendito D., *Anal. Chim. Acta.*, 1992, **266**, 301-307,  
"Stopped-flow chemiluminescence spectrometry to improve the determination of penicillins based on the luminol-iodine reaction"
- <sup>113</sup>Ruzicka J., Hansen E.H., *Anal. Chim. Acta.*, 1979, **106**, 207-224,  
"Stopped flow and merging zones an new approach to enzymatic assay by flow injection analysis"
- <sup>114</sup>Christian G.D., Ruzicka J., *Anal. Chim. Acta.*, 1992, **231**, 11-21,  
"Exploiting stopped flow injection methods for quantitative analysis"
- <sup>115</sup>Hungeford J.M., Christian G.D., Ruzicka J., Giddings J.C., *Anal. Chem.* 1985, **57**, 1794-1798,  
"Reaction rate measurement by FIA using gradient stopped flow method"
- <sup>116</sup>Lazaro F, Luque de Castro M.D., Valcarcel M., *Anal. Chem.*, 1987, **59**, 950-954,  
"Doubly stopped flow a new alternative to simultaneous kinetic multi-determinations in unsegmented flow systems"
- <sup>117</sup>Pacey G.E., Hollowell D.A., Miller K.G., Straka M.R., Gordon G.  
*Anal. Chim. Acta.*, 1986, **179**, 259-267, "Selectivity enhancement by flow injection analysis"
- <sup>118</sup>Stewart R., *Oxidation in Organic Chemistry* Vol 5 Wilberg K.B and Trahanovsky W.S Ed.,  
1965, Academic Press pp1-68
- <sup>119</sup>Cotton A.F., Wilkinson G., *Advanced Inorganic Chemistry*, 3<sup>rd</sup> Edition, 1972, pp 845-855
- <sup>120</sup>Harcourt A.V. and Esson W., *Philos. Trans. Royal Soc. London*, 1866, **156**, 193-221,  
"On the laws of connexion between the conditions of a chemical change and its amount"
- <sup>121</sup>Powell R. T., Oskin T., Ganapathisubramanian N., *J. Phys. Chem.*, 1989, **93**, 2718-2721,  
"Permanganate oxidation of Mn(II) in aqueous acid solutions in the presence of oxalate and pyrophosphate"
- <sup>122</sup>Stauff J., Bergman U. Z., *Phys. Chem.*, 1972, **78**, 263-276,  
"Chemiluminescence from oxidation reactions : VII Carbonate radicals as sources of luminescence".



- 
- <sup>123</sup>Selim R.G., Lingane J.J., *Anal. Chim. Acta.*, 1959, **21**, 536-544,  
"Spectrophotometry of higher oxidation states of manganese. Coulometric titration of manganese (III)"
- <sup>124</sup>Launer H.F., *J. Am. Chem. Soc.*, 1932, **54**, 2597-2610,  
"Kinetics of reaction between permanganate and oxalic acid"
- <sup>125</sup>Belcher R., West T.S., *Anal. Chim. Acta.*, 1952, **6**, 322-332,  
"Trivalent manganese as an oxidimetric reagent"
- <sup>126</sup>Donganmoya H., Almeidaeves E., Coichev N., *Talanta*, 1997, **44**, 897-903,  
"The stabilisation of manganese (III) by azide ion in aqueous solution"
- <sup>127</sup>Alder S.J., Noyes R.M., *J. Am. Chem. Soc.*, 1955, **77**, 2036-2042,  
"The mechanism of the permanganate oxalate reaction"
- <sup>128</sup>Miles B., Nyaruk S.K., *J. Chem. Ed.*, 1990, **67**, 269-270,  
"The effects of crown ethers on the rate of oxidation of oxalic acid by the permanganate ion"
- <sup>129</sup>Koupparis M.A., Karyannis M.I., *Anal. Chim. Acta.*, 1982, **138**, 303-310,  
"Kinetic study of the permanganate oxalate reaction and kinetic determination of Mn(II)"
- <sup>130</sup>Lunge G., Smith J.H., *J. Soc. Chem. Ind.*, 1883, **2**, 463
- <sup>131</sup>PerezBendito J.F., Anas C., Amat E., *J. Colloid and Interface Science*, 1996, **177**, 288-297,  
"A kinetic study of the reduction of colloidal manganese dioxide by oxalic acid"
- <sup>132</sup>Pimenta V., Lavabre D., Levy G., Micheau J.C., *J. Phys. Chem.*, 1994, **98**, 13294-13299, "Reactivity of the Mn(II) and Mn(IV) intermediates in the permanganate oxalic acid sulphuric acid reaction - kinetic determination of the reducing species"
- <sup>133</sup>Keki S. Beck M.T., *Reaction Kinetics and Catalysis Letters*, 1991, **44**, 75-77,  
"Oscillatory kinetics of the permanganate oxidation of oxalic acid"
- <sup>134</sup>Fujiwara K., Kashima T., Tsubatoa B., Toyoshima T., Aihara M., Kiboki M.,  
*Chemistry Letters*, 1990, **8**, 1385-1386,  
"Oscillation found in the reaction between permanganate and oxalic acid"
- <sup>135</sup>Fazekas T., Mrakavrova M., Nagy A., Olexova A., *React. Kinet. Lett.*, 1990, **42**, 181-188,  
"Permanganate chemical oscillators in a CSTR"
- <sup>136</sup>Ansari M.A., Craig J.C., *Synthesis Comm.*, 1996, **26**, 1789-1792,  
"Homogeneous oxidation of alcohols by copper permanganate"
- <sup>137</sup>Mandal S.B., Achari B., Ghosh Dastidar P.P., *Tetrahedron Letters*, 1993, **34**, 1979-1980, "An unusual carbon carbon bond cleavage by KMnO<sub>4</sub>-CuSO<sub>4</sub> reagent"
- <sup>138</sup>Lee D.G., Moylan C.R., Hayashi T., Brauman J.I.,  
*J. Am. Chem. Soc.*, 1987, **109**, 3003-3010, "Photochemistry of aqueous permanganate ion"
- <sup>139</sup>*Water Quality, Determination of permanganate index*  
BS EN ISO 8467:1995, British Standards Institution
- <sup>140</sup>Research Committee on Analysis of Potable Spirits, *J. Assoc. Public Analysts*, 1977, **15**, 47-54,  
"The estimation of furfural, extract, permanganate time and pH in beverage spirits"
- <sup>141</sup>Boeseken J., *Rec. Trav. Chim.*, 1928, **47**, 683-693,  
"The configuration of  $\alpha$ -glycols formed by the oxidation of alkylenes"
- <sup>142</sup>Wiberg K.B., Sagebarth K.A., *J. Am. Chem. Soc.*, 1957, **79**, 2822-2824,  
"Mechanism of permanganate oxidation :IV Hydroxylation of olefins and related reactions"
- <sup>143</sup>Zahonyi-Budo E., Simandi L.I., *Inorg. Chim. Acta.*, 1995, **237**, 173-175,  
"Oxidations with unstable manganese(VI) in acidic solution"
- <sup>144</sup>Zahonyi-Budo E., Simandi L.I., *Inorg. Chim. Acta.*, 1996, **248**, 81-84,  
"Oxidation of propane 1,2 diol by acidic manganese V and manganese VI"



- 
- <sup>145</sup>Simandi L.I., Miklos J., *J. Am. Chem. Soc.*, 1976, **98**, 1995-1997,  
"Nature of the detectable intermediate in the permanganate oxidation of trans cinnamic acid"
- <sup>146</sup>Matsubara H., Nakayama S., *Water Research*, 1992, **26**, 1471-1478,  
"Stability of pre-methylated aromatic model compounds of constituents of humic substances towards KMnO<sub>4</sub> oxidation"
- <sup>147</sup>Jaky M., Szammer J., *J. Phys. Org. Chem.*, 1997, **10**, 420-426,  
"Oxidation of aldehydes with permanganate in acidic and alkaline media"
- <sup>148</sup>Insausti M.J., Alvarezmacho M.P., Mataperez F.,  
*Collection of Czech Chem. Comm.*, 1992, **57**, 2331-2336,  
"Oxidation of  $\alpha$ -amino acids by permanganate isokinetic reaction"
- <sup>149</sup>Lindroos-Heinonen R., Virtanen P.O.I., *Finnish Chem. Lett.*, 1988, **15**, 117-121,  
"Kinetics of the permanganate oxidation of monosaccharides and polyhydric alcohols"
- <sup>150</sup>Pande P.N., Gupta H.L., Ameta S.C., Sharma T.C., *Acta. Phys. Chem.*, 1981, **22**, 125-128,  
"Kinetics and mechanisms of the oxidation of glucose"
- <sup>151</sup>Sengupta K.K., Sanyal A., Tribendi P.S., Sengupta S., *J. Chem. Res. (S)*, 1993, 484-485,  
"Kinetic behaviour and relative reactivities of some aldoses amino sugars and methylated sugars towards permanganate in perchloric acid medium"
- <sup>152</sup>Ljunggren S., Olsson A., *Holzforschung*, 1984, **38**, 91-99,  
"The specificity in oxidation of some lignin and carbohydrate models and pine wood shavings with permanganate and pyridinium dichromate before the kraft pulping process"
- <sup>153</sup>Vekantishwer Rao G., Chinna Rajanna K., Saiprakash P.K.,  
*Z. Pys. Chemie Leipzig*, 1982, **3**, 622-627,  
"A kinetic and mechanistic study of reduction of KMnO<sub>4</sub> by L-ascorbic acid in sulphuric acid medium"
- <sup>154</sup>Bhat K.I., Sheringara B.S., Pinto I., *Indian J. Chem.*, 1994, **33A**, 42-46,  
"Kinetics of oxidation of pyridoxine by manganese (III) in pyrophosphate medium"
- <sup>155</sup>Chandraju S., Sheringara B.S., Made Gowda N.M., *Indian J. Chem. Kinetics*, 1994, 1105-1119,  
"Oxidation of arginine by manganese (III) in pyrophosphate and acetate media. A kinetic study"
- <sup>156</sup>Rangappa K.S., Chandraju S., Mahadevappa S., *Transition Metal Chemistry*, 1996, **21**, 519-523,  
"Kinetics of oxidation of L-lysine and L-phenylalanine by anodically generated manganese (III) in aqueous ethanoic acid"
- <sup>157</sup>AlTamrah S.A., Townshend A., Wheatley A.R., *Analyst*, 1987, **112**, 883-886,  
"Flow injection chemiluminescence determination of sulphite"
- <sup>158</sup>Psarellis I.M., Defteros N.T., Sarantonis E.G., Calokerinos A.C., *Anal. Chim. Acta.*, 1994, **294**, 27-34,  
"Flow injection chemiluminescence determination of some bile acids"
- <sup>159</sup>Zhang F., Lin Q.X., *Talanta*, 1993, **40**, 1557-1561, "New chemiluminescence system: MnO<sub>4</sub><sup>-</sup>-Na<sub>2</sub>CO<sub>3</sub>-KOH and its application in the determination of manganese"
- <sup>160</sup>Montalvo S.I., Ingle J.D., *Talanta*, 1993, **40**, 167-172,  
"Chemiluminescence during the oxidation of alcohols by permanganate application to the determination of ethanol in gin"
- <sup>161</sup>Zhu C.Q., Wang L., Wu J.L., *Fenxi Shiyanshi*, 1996, **15**, 49-51,  
"Determination of ascorbic acid by chemiluminescence in a new system of potassium permanganate/ascorbic acid"
- <sup>162</sup>Abbott R.W., Townshend A., *Anal. Proc.*, 1986, **23**, 25-26,  
"The chemiluminescence determination of drugs"
- <sup>163</sup>Abbott R.W., Townshend A., Gill R., *Analyst*, 1987, **112**, 397-406,  
"Determination of morphine in body fluids by HPLC with chemiluminescence detection"



- <sup>164</sup>Barnett N.W., Lewis S.W., Tucker D.J., *Fresenius J. Anal. Chem.*, 1996, **355**, 591-595, "Determination of morphine in process streams by sequential injection analysis with chemiluminescence detection"
- <sup>165</sup>Barnett N.W., Lenechan C.E., Lewis S.W., Tucker D.J., Essery K.M., *Analyst*, 1998, **423**, 601-605, "Determination of morphine in water immiscible process streams using sequential injection analysis coupled with acidic permanganate chemiluminescence detection"
- <sup>166</sup>Barnett N.W., Rolfe D.G., Bowser T.A., Paton T.W., *Anal. Chim. Acta.*, 1993, **282**, 551-557, "Determination of morphine in process streams using flow injection analysis with CL detection"
- <sup>167</sup>Tsaplev Y.B., *Zh. Fiz. Khim.*, 199, **65**, 799-802, "Chemiluminescence in acidic medium"
- <sup>168</sup>Christie T.J., Hanway R.H., Paulls D.A., Townshend A., *Anal. Proc.*, 1995, **32**, 91-93, "Chemiluminescence determination of codeine by permanganate oxidation"
- <sup>169</sup>Mitsana-Papazoglou A., Sarantonis E.G., Calokerinos A.C., *Biomedical Chromatography*, 1997, **11**, 67-68, "Chemiluminescence of organic molecules by the action of potassium permanganate"
- <sup>170</sup>Ikkai H., Nakagama T., Yamuda M., Hobo T., *Bull. Chem. Soc. Japan*, 1989, **62**, 1660-1662, "Flow chemiluminescence determination of catecholamines based on permanganate oxidation"
- <sup>171</sup>Evmeridis N.P., Thanasoulas N.K., Vlessidis A.G., *Talanta*, 1998, **46**, 179-196, "Chemiluminescence emission generated during oxidation of pyrogallol and its application in analytical chemistry. 1 Effect of oxidant compound"
- <sup>172</sup>Defteros N.T., Calokerinos A.C., Estathian C.E., *Analyst*, 1993, **118**, 627- 632, "Flow injection chemiluminescence determination of epinephrine, norepinephrine, dopamine and L-dopa"
- <sup>173</sup>Yang M.I., Li .L.Q., Feng M.L., Lu J.R., *Yaowu Fenxi Zazhi*, 1998, **18**, 41-45, "Study of a chemiluminescence system of  $\text{KmnO}_4$ /Levodopa in the assay of levodopa"
- <sup>174</sup>Qi H.Y., Yang M.I., Feng M.L., Lu J.R., *Chemical Journal of the Chinese Univeristies*, 1997, **13**, 229-234, "A new method for brucine analysis based on its chemiluminescence reaction with potassium permanganate"
- <sup>175</sup>Zhu L., Feng M.L., Wan X.Q., Lu J.R., *Chemical Journal of the Chinese Universities*, 1996, **17**, 1696-1696, "Chemiluminescence determination of brucine strychnine and ephedrine based on HPLC separation"
- <sup>176</sup>Zhang X.R., Baeyens W.R.G., Van der Weken G., Calokerinos A.C., Imai K., *Anal. Chim. Acta.*, 1995, **303**, 137-142, "Chemiluminescence determination of some local anaesthetics"
- <sup>177</sup>Marino D.F., Ingle J.D., *Anal. Chim. Acta.*, 1981, **124**, 23-30, "Determination of humic acid by chemiluminescence"
- <sup>178</sup>Ahmed T.E., Townshend A., *Anal. Chim. Acta.*, 1994, **292**, 169-174, "Flow injection chemiluminescence determination of the hydrazones of aromatic ketones"
- <sup>179</sup>Townshend A., Wheatly R.A., *Analyst*, 1998, **123**, 267-272, "Oxidative chemiluminescence of some nitrogen nucleophiles in the presence of formic acid as an ancillary reactant"
- <sup>180</sup>Townshend A., Wheatly R.A., *Analyst*, 1998, **123**, 1041-1046, "Oxidative chemiluminescence assay of 2, 4-dinitrophenyl hydrazine"
- <sup>181</sup>Townshend A., Wheatly R.A., *Analyst*, 1998, **123**, 1047-1051, "Determination of carbonyl compounds by the oxidative chemiluminescence of 2,4-dinitrophenyl hydrazine"
- <sup>182</sup>Li Z., Feng H.L., Lu J.T., Gong Z.L., Jiang H.L., *Anal. Lett.*, 1997, **30**, 797-80, "Flow injection CL determination of tetracyclines"



- 
- <sup>183</sup> LopezPaz J.L., Townshend A., *Anal. Comm.*, 1996, **33**, 31-34,  
"Flow injection chemiluminescence determination of imiprazine and chlorpromazine"
- <sup>184</sup> Barnett N.W., Hindson B.J., Lewis S.W., *Anal. Chim. Acta.*, 1998, **362**, 131-139, "Determination of 5 hydroxytryptamine (Serotonin) and related indoles by Flow injection analysis with acidic potassium permanganate chemiluminescence detection"
- <sup>185</sup> Li L.Q., Yang M.L., Feng M.L., Lu J.R., *Fenxi Shiyanshi*, 1998, **17**, 5-8,  
"Determination of vitamin B6 by a flow injection chemiluminescence method"
- <sup>186</sup> Li Z., Feng M.L., Lu J.R., *Microchem. J.*, 1998, **59**, 278-283,  
"KMnO<sub>4</sub> octylphenylpolyglycol ether chemiluminescence system for flow injection analysis of uric acid in urine"
- <sup>187</sup> Li L.Q., Yang M.L., Feng M.L., Lu J.R., *Fenxi Shiyanshi*, 1997, **16**, 33-35,  
"Study of the chemiluminescence system of potassium permanganate/ sodium dithionite /riboflavin"
- <sup>188</sup> Sultan S.M., Alumaibed A.M., Townshend A., *Fres. J. Anal. Chem.*, 1998, **362**, 167-169, "Flow injection chemiluminescence determination of madazepam"
- <sup>189</sup> Campaglio A., *Analyst*, 1998, **123**, 1053-1056,  
"Chemiluminescence determination of naltrexone based on potassium permanganate oxidation"
- <sup>190</sup> Fujimori K., Takenaka N., Bandow H, Maeda Y., *Anal. Comm.*, 1998., **3**, 307-308, "Continuous monitoring method for organic pollutants in water based on chemiluminescence reaction with potassium permanganate"
- <sup>191</sup> Food Safety Act, 1990, HMSO Publications
- <sup>192</sup> Kirk R.S., Sawyer R., *Pearson's Composition and Analysis of Foods*, 1991, 9th Edition, Longman Scientific and Technical
- <sup>193</sup> Crosby N.T., Patel I., *General Principles of Good Sampling Practice*, 1995, Royal Society of Chemistry
- <sup>194</sup> Pinche C., Billard J.P., Frasey A.M., Bargnoux H., Petit J., Berger J.A., Dang Vu B., Yonger J., *J. Chromatog.*, 1989, **463**, 201-206,  
"Separation and assay of N-nitroso compounds by high-performance liquid chromatography with chemiluminescence detection"
- <sup>195</sup> Escobar R., Lin Q., Guiraum A., de la Rosa F.F., *Analyst*, 1993, **118**, 643-647,  
"Flow injection chemiluminescence method for the selective determination of chromium (III)"
- <sup>196</sup> Koerner C.A., Neiman T.A., *Anal. Chem.*, 1986, **58**, 116-119,  
"Chemiluminescence flow injection determination of sucrose using enzymatic conversion"
- <sup>197</sup> Puchades R., Maquierra A., Toro L., *Analyst*, 1993, **118**, 855-858,  
"Enzymic flow-injection determination of lactose in milk with online dialysis"
- <sup>198</sup> Puchades R., Lemieux L., Simard R.E., *Food Science*, 1990, **55**, 285-289,  
"Determination of free amino acids in cheese by flow injection analysis with an enzymatic reactor and chemiluminescence detector"
- <sup>199</sup> Igarashi S., Hinze W.L., *Anal. Chim. Acta.*, 1989, **255**, 147-157,  
"Enzymatic assay with detection by enhanced luminol chemiluminescence in a reverse micellar system determination of amino acids and glucose"
- <sup>200</sup> Yamamoto Y., Brodsky M.H., Baker J.C., Ames B.N., *Anal. Chem.*, 1987, **160**, 7-13, "Detection and characterisation of hydroperoxides at picomole levels by high-performance liquid chromatography"
- <sup>201</sup> Boegl W., Heide L., *Radiation Phys. Chem.*, 1985, **25**, 173-185,  
"Chemiluminescence measurements as an identification method for gamma irradiated foodstuffs"
- <sup>202</sup> Anderle H., Steffan I., Wild E., Hille P., *Fresenius J. Anal. Chem.*, 1996, **354**, 925-928, "Radiolyo – chemiluminescence of bones and seafood shells a new promising method of detection of food irradiation"



- 
- <sup>203</sup>Montano L.A., Ingle J.D., *Anal. Chem.*, 1979, **51**, 926-930,  
"Determination of cobalt by lucigenin chemiluminescence"
- <sup>204</sup>Slawinska D., Slawinski J., *J. Biolumin. Chemilumin.*, 1998, **12**, 249-259, "Chemiluminescence of cereal products: I Kinetics activation energy and effect of solvents"
- <sup>205</sup>Katayama M., Takeuchi H., Taniguchi H., *Anal. Chim. Acta.*, 1993, **281**, 111-118, "Determination of amines by flow injection analysis based on aryloxalate sulphorodamine-101 chemiluminescence"
- <sup>206</sup>Grekas N., Calokerinos A.C., *Talanta*, 1990, **37**, 1043-1048,  
"Determination of thiamine by continuous flow chemiluminometric measurement"
- <sup>207</sup>Alwarthan A.A., *Anal. Sciences*, 1994, **10**, 919-922,  
"Flow injection chemiluminometric determination of folic acid in pharmaceutical materials"
- <sup>208</sup>PerezRuiz T., MartinezLozano C., Sanz A., Tomas V., *Analyst*, 1994, **119**, 1825-1828,  
"Photokinetic determination of riboflavin and FMN using flow injection analysis with chemiluminescence detection"
- <sup>209</sup>Weeks I., Boheshti I., McCapra F., Campbell A.K., Woodhead J.S.,  
*Clin. Chem.*, 1983, **29**, 1474-1479,  
"Acridinium esters as high specific activity labels in immunoassay"
- <sup>210</sup>Kricka J.L., *Pure and Applied Chemistry*, 1996, **68**, 10, 1825-1830, "Strategies for Immunoassay"
- <sup>211</sup>Woodhead S., *J. Clinical Ligand Assay*, 1995, **18**, 49-53,  
"Chemiluminescence immunoassay: A review"
- <sup>212</sup>LopezFernandez J.M., Rios A., Valcarcel M., *Analyst*, 1995, **120**, 2393-2400,  
"Assessment of quality of flow injection methods used in food analysis : A review"
- <sup>213</sup>Arthur C., *The Independent*, 24 June 1998,  
"Jellyfish genes are a biological recipe for a luminous lunch"
- <sup>214</sup>Diamond D., Hanratty V.C.A., *Spreadsheet Applications in Analytical Chemistry using Microsoft Excel*, 1997, Wiley Interscience
- <sup>215</sup>BS6108:1991 "Method of test for accuracy and precision of mechanical hand pipettes of capacity of 0.05mL and above"
- <sup>216</sup>van Staden J.F., Malan D., *Anal. Comm.*, 1996, **33**, 339-341,  
"Simple convenient method for measuring injection volumes in flow injection and sequential injection analysis"
- <sup>217</sup>Miller J.C., Miller J.N., *Statistics for Analytical Chemistry*, 3<sup>rd</sup> Ed, 1993,  
Ellis Horwood Series in Analytical Chemistry, pp 65-71
- <sup>218</sup>Leaback D.H., *Bioluminescence and Chemiluminescence : A Status Report*, 1993, 33-37,  
"Easy to use light standards as aids to luminometry", Ed Szalay A., Kricka L., Stanley P., Wiley  
Chichester
- <sup>219</sup>Burguera J.L., Townshend A. Greenfield S., *Anal. Chim. Acta.*, 1980, **114**, 209,  
"Flow injection analysis for monitoring chemiluminescence reactions"
- <sup>220</sup>Horwitz W., *Official Methods of the Association of Official Analytical Chemists*, 13<sup>th</sup> Ed, 1980, 43.056
- <sup>221</sup>Deutsh M.J., Weeks C.E., *J. Assoc. Off. Anal. Chem.*, 1965, **48**, 1248-1256, "Microfluorimetric Assay for Vitamin C"
- <sup>222</sup>Kaneda H., Kano Y., Osawa T., Kawakishi S., Kamimura M.,  
*Agric. Biol. Chem.*, 1990, **54**, 2165-2166,  
"Role of free radicals in chemiluminescence generation during the beer oxidation process"
- <sup>223</sup>Hardwick W.A., *Handbook of Brewing*, Hardwick W.A Editor,  
1995, Marcel Decker pp551-585, Chapter 19, "The properties of beer"



- 
- <sup>224</sup>Davies G., *Co-ordination Chemistry Reviews*, 1969, **4**, 199-224,  
"Some aspects of the chemistry of manganese (III) in aqueous solution"
- <sup>225</sup>Michalowski J., Koglo A., Trojanowicz M., Szosek B., Zagatto E.A.G.,  
*Anal. Chim. Acta.*, 1993, **271**, 239-246,  
"Simultaneous determination of sucrose and reducing sugars using indirect flow injection  
biamperometry"
- <sup>226</sup>Matsumoto K., Tsukatani T., Higuchi S., *Sensors and Materials*, 1995, **7**, 167-177,  
"Simultaneous sensing of five compounds in fruit by amperometric flow injection system with  
immobilised enzyme reactors"
- <sup>227</sup>Coultate T.P., *Food the Chemistry of its Components*, 1989 2<sup>nd</sup> Edition, RSC, London
- <sup>228</sup>Flood A.E., Johns M.R., White E.T., *Carbohydrate Research*, 1996, **288**, 45-56, "Mutarotation of d-  
fructose in aqueous -ethanolic solutions and its influence on crystallisation"
- <sup>229</sup>Angyal S.J., *Angew. Chem. Int. Ed.*, 1969, **8**, 157-166  
"Composition and conformation of sugars in solution"
- <sup>230</sup>Angyal S.J., *Carbohydrate Research*, 1994, **263**, 1-11,  
"The composition of reducing sugars in dimethyl sulphoxide"
- <sup>231</sup>Schumacher D., Kroh L.W., *Food Chemistry*, 1995, **54**, 353-356,  
"A rapid method for separation of anomeric saccharides using cyclodextrin bonded phases and for  
investigation of mutarotation"
- <sup>232</sup>Savitsky A., Golay M.E.J., *Anal. Chem.*, 1964, **36**, 1627-1639,  
"Smoothing and differentiation of data by simplified least squares procedures"
- <sup>233</sup>Lee J., Seliger H.H., *Photochem. Photobiol.*, 1972, **15**, 227,  
"Quantum yields of the luminol CL reaction in aqueous and aprotic solvents"
- <sup>234</sup>Christmann D.R., Crouch S.R., Holland J.F., Timnick A., *Anal. Chem.*, 1980, **52**, 291-295, "Correction  
of right angle molecular fluorescence measurements for absorbance of fluorescence reaction"
- <sup>235</sup>Ratzlaff E.H., Crouch S.R., *Anal. Chem.*, 1983, **55**, 384-352,  
"Absorption-corrected chemiluminescence measurements with a dual path spectrometer"
- <sup>236</sup>Hancox J.N., Miller J.N., Royal Society of Chemistry Research and Development Topics in Analytical  
Chemistry, Durham, 1998. Meeting Abstract,  
"Development of a near-infrared immunofluorimetric assay for the detection of sulfamethazine"
- <sup>237</sup>Ellingson A., Karned H.T., *Biomedical Chromatography*, 1998, **12**, 8-12,  
"Investigation of far red dyes for use in peroxyoxalate chemiluminescence detection and analysis of the  
CY5 derivative of amantadine hydrochloride in human plasma"
- <sup>38</sup>Simandi L.I., Jaky M., Savage C.R., Schelly Z.A., *J. Am. Chem. Soc.*, 1985, **107**, 4220-4224,  
"Kinetics and mechanism of the permanganate ion oxidation of sulphite in alkaline solutions the nature  
of short lived intermediates"
- <sup>239</sup>Weber P., Bendich A., Schalch W., *Int. J. for Vitamin and Nutrition Res.*, 1996, **66**, 19-30, "Vitamin C  
and human health - A review of recent data relevant to human requirements"
- <sup>240</sup>Pauling L., *Proc. Nat. Acad. Sci.*, 1970, **67**, 1643-1648, "Evolution and the need for ascorbic acid"
- <sup>241</sup>Klenner F.R., *J. Appl. Nutrition*, 1971, **23**, 61-88,  
"Observations on the Dose and Administration of ascorbic acid when employed beyond the range of a  
vitamin in human pathology"
- <sup>242</sup>Nakamoto Y., Motohashi S., Kasahara H., Numazawa K., *Nephrology Dialysis Transplantation*, 1988,  
**13**, 754-756,  
"Irreversible tubulointerstitial nephropathy associated with prolonged massive intake of  
vitamin C"



- 
- <sup>243</sup>Chamberlain N. from *Vitamin C: Ascorbic Acid*, 1981, Editors Counsell J.N., Hornig D.H., Applied Science Publishers
- <sup>244</sup>Karayannis M.I., *Anal. Chim. Acta.*, 1975, **76**, 121-130,  
"Kinetic determination of ascorbic acid by the 2,6-DCPIP reaction with a stopped-flow technique"
- <sup>245</sup>Lazaro F., Rios A., Luque de Castro M.D., Valcarel M., *Analyst*, 1986, **111**, 163-166, "Determination of vitamin C by flow injection analysis"
- <sup>246</sup>Nobrega J., Lopes G.S., *Talanta*, 1996, **73**, 971-976,  
"Flow injection spectrophotometric determination of ascorbic acid in pharmaceutical products with the Prussian blue reaction"
- <sup>247</sup>Garido E.M., Lima J.L.F.C., Delerue-Matos C., *Il Farmaco*, 1995, **50**, 881-884, "Determination of ascorbic acid in pharmaceutical products by flow injection analysis using an amperometric detector"
- <sup>248</sup>Janda P., Weber J., Dunsch L., Lever A.B.P., *Anal. Chem.*, 1996, **68**, 960-965,  
"Detection of ascorbic acid using a carbon fiber microelectrode coated with cobalt tetramethylpyridoporphyrzine"
- <sup>249</sup>Alwarthan A.A., *Analyst*, 1993, **118**, 640-642,  
"Determination of ascorbic acid by flow injection with chemiluminescence detection"
- <sup>250</sup>Zhang Z., Qin W., *Talanta*, 1996, **43**, 119-124,  
"Chemiluminescence flow sensor for the determination of ascorbic acid with immobilised reagents"
- <sup>251</sup>Bark L.S., Grime J.K., *Analyst*, 1974, **99**, 39-42, "The thermometric assay of ascorbic acid"
- <sup>252</sup>Mayers A.R., Taylor C.G., *Analyst*, 1987, **112**, 507-509,  
"Determination of ascorbic acid in multivit tablets by thermometric titrimetry with cerium (IV)"
- <sup>253</sup>Hammam A.M., Idrissi K.A., *J. Indian Chem. Soc.*, 1981, **48**, 140-142,  
"Macro- and microdetermination of ascorbic acid using potassium permanganate as an oxidant in fluoride medium"
- <sup>254</sup>Sengupta K.K., Tribendi P.S., *Indian Journal of Chemistry Section A*, 1996, **35**, 427-430,  
"Reactivities of some sugar phosphates towards pemanganate in perchloric acid"
- <sup>255</sup>van den Berg R., Peters J.A., van Bekkum H., *Carbohydrate Res.*, 1995, **267**, 65-77, "Selective alkaline oxidative degradation of mono and disaccharides by hydrogen peroxide. using borate as a catalyst and protecting group"
- <sup>256</sup>Grayeski M.L., Moritzen P.A., *Langmuir*, 1997, **13**, 2675-2680,  
"Chemiluminescence energy transfer processes and micellar effects"
- <sup>257</sup>Chen G.N., Duan D.P., Hu Q.F, *Anal. Chim. Acta.*, 1994, **282**, 159-167,  
"Study of the chemiluminescent characteristics of some xanthone dyes"
- <sup>258</sup>Suresh Ponraj D., Venkataraman R., Raghavan P.S., *J. Chem. Ed.*, 1990, **67**, 621, "Permanganate oxalic acid reaction: A modified approach using surfactant solutions"
- <sup>259</sup>Cooke J.R., Moxon R.E.D., from *Vitamin C: Ascorbic Acid*, 1981, Editors Counsell J.N., Hornig D.H., Applied Science Publishers
- <sup>260</sup>Holland B., Welch A.A., Unwin I.D., Buss D.H., Paul A.A., Southgate D.A.T., *McCance and Widdowson's The Composition of Foods*, 1991, 5<sup>th</sup> Edition, Royal Society of Chemistry.
- <sup>261</sup>Vandeslice J.T., Higgs D.J., *Am. J. Clin. Nutrition*, 1991, **54**, 1323-1327,  
"Vitamin C content of foods"
- <sup>262</sup>Pinto I., Sherigara B.S., Udupa H.V.K., *Analyst*, 1991, **116**, 286-289, "Electrolytically generated manganese(III) sulphate as a redox titrant : Potentiometric determination of thiosemicarbazide its metal complexes and thiosemicarbazones"



- <sup>263</sup>Stone A.T., Morgan J.J., *Environ. Sci. Technol.*, 1984, **18**, 617-624, "Reduction of manganese (III) and manganese(VI) oxides by organics 2: survey of the reactivity of organics"
- <sup>264</sup>Pigman W., Hopton D., *The Carbohydrates - Chemistry Biochemistry*, 1972, Vol IA 2nd Ed Academic Press, NY
- <sup>265</sup>Hanai T., *Advances in Chromatog.* 1986, **25**, 279-307, "Liquid chromatography of carbohydrates"
- <sup>266</sup>Verzele M., Simoens G., van Damme F., *Chromatographia*, 1987, **23**, 292-300, "A critical review of some liquid chromatography systems for the separation of sugars"
- <sup>267</sup>Lafosse M., Dreux M., Morin Allory L., *Journal of High Resolution Chromatography and Chromatography Communications*, 1985, **8**, 39-41, "Some applications of a commercial light scattering detector for liquid chromatography"
- <sup>268</sup>Herbreteau B., *Analusis*, 1992, **20**, 355-374, "Review and state of sugar analysis by HPLC"
- <sup>269</sup>Bernal J.J.L., Delnozal M.J., Toribo L., Delalmo M., *J. Agric. Food. Chem.*, 1996, **44**, 507-511, "HPLC analysis of carbohydrates in wines and instant coffees using anion exchange and pulsed amperometric detection"
- <sup>270</sup>Prodolliet J., Bruehlhart M., Lador F., Martinez C., Obert L., Mlanc M.B., Parchet J.M., *J. Ass. Off. Anal. Chem.*, 1995, **78**, 749-761, "Determination of free and total carbohydrate profile in soluble coffee"
- <sup>271</sup>Lingeman H., *Chromatographic Science*, 1990, pp1-50, "Derivatisation in liquid chromatography:"
- <sup>272</sup>Honda S., *J. Chromatography A*, 1996, **720**, 183-199, "Postcolumn derivatisation for chromatographic analysis of carbohydrates"
- <sup>273</sup>Dadoo R., Colon L.A., Zare R.N., *J. High Res. Chromatography*, 1992, **15**, 133-135, "Chemiluminescence detection in HPLC"
- <sup>274</sup>Miyawa J.H., Schulman S.G., Perrin J.H., *Biomedical Chromatography*, 1997, **11**, 224-229, "Post column chemiluminescence as a detection technique for liquid chromatography"
- <sup>275</sup>Kiba N., Saegusa K., Furusawa M., *J. Chromatog. B*, 1997, **689**, 393-398, "Post column enzyme reactors for chemiluminometric detection of glucose. 1, a anhydrioglucitol and 3-hydroxobutyrate in anion exchange chromatographic system"
- <sup>276</sup>Makinen M., Piironen V., Hopia A., *J. Chromatog. A*, 1996, **734**, 331-339, "Postcolumn chemiluminescence, ultraviolet and evaporative light-scattering detectors in high performance liquid chromatographic determination of triacylglycerol oxidation products"
- <sup>277</sup>Sigvardson K.W., Birks J.W., *Anal. Chem.*, 1983, **55**, 432-435, "Peroxyoxalate chemiluminescence detection of polycyclic aromatic hydrocarbons in LC"
- <sup>278</sup>Kwakmen P.J.M., Brinkman U.A.T., *Anal. Chim. Acta.*, 1992, **266**, 175-192, "Peroxyoxalate chemiluminescence detection in liquid chromatography"
- <sup>279</sup>Amiott E., Andrews A.R.J., *J. Liqu. Chrom. and Related Techniques*, 1997, **20**, 311-325, "Morphine determination by HPLC with improved chemiluminescence detection using a conventional silica based column"
- <sup>280</sup>Brandao S.C., Richmond M.L., Gray J.I., Morton I.D., Stine C.M., *J. Food Sci.*, 1980, **45**, 1492-1493, "Separation of mono-and di-saccharides and sorbitol by HPLC"
- <sup>281</sup>Richmond M.L., Brandao S.C.C., Gray J.I., Markakis P., Stine C.M., *Agric. Food Chem.*, 1981, **29**, 4-7, "Analysis of simple sugars and sorbitol in fruit by high performance liquid chromatography"
- <sup>282</sup>Gaub R., *Monatsschr. Brau.*, 1983, **36**, 125-128, "Determination of carbohydrates in drinks by high pressure liquid chromatography"
- <sup>283</sup>Lo-Guidice J.M., Lhermitte M., *Biomedical Chromatography*, 1996, **10**, 290-296, "HPLC of Oligosaccharides in Glycobiology"